S. V. Yepifanov, V. S. Chygryn

DESIGN
OF AIRCRAFT
GAS TURBINE ENGINES

2021

MINISTRY OF EDUCATION AND SCIENCE OF UKRAINE
National aerospace university
«Kharkiv Aviation Institute»

S. V. Yepifanov, V. S. Chygryn

DESIGN OF AIRCRAFT GAS TURBINE ENGINES

Textbook

Kharkiv «KhAI» 2021

УДК [621.452.3.03+621.452.3.03:539.4] (075.8)
Y-44

Розглянуто конструктивні схеми авіаційних ГТД, вимоги до них, викладено основи конструювання вузлів двигунів. Досліджено умови роботи основних деталей і визначення наявних навантажень. Описано деякі актуальні проблеми конструювання сучасних авіаційних ГТД.

Для студентів, які вивчають курси «Конструкція і робочі процеси АД та ЕУ», «Динаміка і міцність АД та ЕУ», «Конструкція і міцність авіаційних двигунів», «Двигуни літаків і вертольотів». Буде корисним під час курсового й дипломного проектування, а також інженерам і конструкторам, що займаються проектуванням авіаційних двигунів і силових установок.

Reviewers: Doctor of Engineering Science, Prof. A. Kachan,
Candidate of Engineering Science, Associate Prof. A. Lytvyak

Yepifanov, S. V.

Y-44 Design of Aircraft Turbine Engines [Text] : textbook / S. V. Yepifanov, V. S. Chygryn. — Kharkiv : National Aerospace University «Kharkiv Aviation Institute», 2021. — 320 p.

ISBN 978-966-662-794-3

Structural arrangements of aircraft gas turbine engines and engineering requirements to them are given. Bases of engine assemblies designing are considered. Conditions of the main component parts operation and main acting loads determining are studied. Some actual problems of the up-to-date aircraft engines designing are discussed.

For students studying the specialty «Aviation and Rocket-Space Engineering» for preparation to exam passing from the courses «Design and Strength of Aircraft Turbine Engines and Power Plants», «Design and Dynamics of Aircraft Turbine Engines and Power Plants», «Engines of Airplanes and Helicopters», and also for making course and diploma projects. It can be useful for the engineers and designers, which take part in aircraft engines and power plants designing.

Fig. 301. Tables 8. Bibliogr.: 53 names.

UDC [621.452.3.03+621.452.3.03:539.4] (075.8)

© Yepifanov S. V., Chygryn V. S., 2021
© National Aerospace University «Kharkiv Aviation Institute», 2021

ISBN 978-966-662-794-3

LIST OF DESIGNATIONS

b – chord
c – absolute velocity
D – diameter
F – area
G – mass flow
g – free fall acceleration
h – length
I – polar moment of inertia
L – length
M – Mach number; moment of force
m – mass
n – rotational speed
n_a – axial overload factor
n_c – centrifugal overload factor
n_r – radial (transversal) overload factor
P – force
p – pressure
p_H – atmospheric pressure
r – radius
t – time, temperature
u – circumferential velocity
v_f – flight velocity
w – relative velocity
Δ – deviation; radial clearance
δ – axial clearance
η – efficiency
λ – aspect ratio
μ – Poisson factor
π – pressure ratio
σ – stress
σ_{lt} – long-term stress
Ω, ω – angular velocity

LIST OF ABBREVIATIONS AND INDICES

a – axial

ABE – air-breathing engine

ACS – automatic control system

AIS – anti-icing system

APU – auxiliary power unit

ARCC – automatic radial clearance control

ATFE – afterburning turbofan engine

ATJE – afterburning turbojet engine

BPR – bypass ratio

bl – blade

C – compressor

CACS – clearance automatic control system

CC – combustion chamber

CPR – compressor pressure ratio

c – centrifugal

case – casing

cav – cavity

cool – cooling substance

cor – corrected parameter

d – disc

DP – draft proposal

dr – drain line

e – elastic

GTE – gas turbine engine

GV – guide vanes

g – gas

gyr – gyroscopic

HPC – high pressure compressor

HPT – high pressure turbine
in – inlet
IGV – inlet guide vanes
IPC – intermediate pressure compressor
IPT – intermediate pressure turbine
j – inertia
LPC – low pressure compressor
LPT – low pressure turbine
lock – locking part
m – mean
max – maximum
min – minimum
mount – mounting
OEI – one engine inoperative
OEM – original engine manufacturer
OPR – overall pressure ratio
TCL – throttle control lever
pr – pressure line
RCC – radial clearance control
r – radial
rot – rotor
SFC – specific fuel consumption
SV – straightening vanes
set – set value
st – stator
T – turbine
TBO – time between overhauls
TFE – turbofan engine
TIT – turbine inlet temperature

TJE – turbojet engine

TPE – turboprop engine

TPFE – turbo-prop-fan engine

TShE – turboshaft engine

t – tension

th – thermal

tor – torsion

UAV – unmanned aerial vehicle

VIGV – variable inlet guide vanes

VTOL – vertical take-off and landing

VSTOL – vertical/short take-off and landing

INTRODUCTION

Education discipline «Design and Strength of Aircraft Engines» is the profiling discipline in education of engineers on designing, manufacturing, maintenance and repairing of aircraft power plants. The goal of the discipline is to give a knowledge in design, strength, dynamics and reliability of the aircraft engines, their components and parts.

Problems of the engine design are considered taking into account technical requirements to the engines and components; methods of realization of these requirements are studied; a comparative analysis of different structural decisions of elements, components and parts is done.

Strength analysis is considered in application to the main highly loaded structural elements – rotor blades, discs, casing parts and shafts – which determine mainly the engine reliability and service life.

The aircraft power plants play the primary role in aviation development. Flights of first airplanes became possible only when the engines were designed with enough power, low mass and low size.

All the most important stages of the aviation development are related with new types of power plants or with radical improvement of already existing engines. The examples are appearance of piston engines, turbojets, afterburning turbojets, turbofans, afterburning turbofans, etc. The engines play so significant role in the modern aviation that many designers mean that the power plant seats the feed forward place in the aircraft designing. Designing, manufacturing and development of the modern aircraft engine needs 5–10 years; this often exceeds a term of designing, manufacturing and development of the aircraft.

The modern aircraft engine is a complex and expensive machine, which implements the up-to-date progress in science and engineering. By turn, development in aircraft engine engineering determines development of science and many branches of industry.

At modern level of aviation with high flight altitude (25 to 30 km) and ($M_П$ = 3 to 3.5), airplanes with new aerodynamic performances appear, which cannot maneuver with switched off engines, even for landing. The modern passenger aircraft transports some hundreds of passengers. In these conditions, requirements to the engine reliability become stronger. The level of reliability that is realized at designing must be supported in maintenance due to a deep knowledge of the engine and due to efficient service.

The scientific base of the education discipline «Design and Strength of Aircraft Engines» are special disciplines (Gas Dynamics, Theory of Impellor Machines, Theory of Air-breathing Engines) and general engineering disciplines (Mathematics, Physics, Chemistry, Engineering Graphics,

Thermodynamics, Heat transfer, Hydro-gas Dynamics, Engineering Mechanics, Material Science, Strength of Materials, Machine Elements, etc., which are a base of all engineering disciplines.

By turn, deep knowledge of aircraft engines design will help in studying of the engine systems, technology of manufacturing and repairing, maintenance, automatic control and health management.

This textbook is written based on the experience gained by the authors during teaching courses of design, dynamics and strength of aircraft gas turbine engines. It is the edited and updated translation of V. Chygryn's "Design and Strength of Aircraft Engines" lecture notes.

1. GENERAL PROBLEMS OF AERO ENGINE DESIGNING

1.1. Generations and main trends in designing of turbine engine

1.1.1. Turbine engine generations

Gas turbine engines are used for propulsion in various types of aircraft. These aircraft include airliners, military aircraft, business aircraft, trainer aircraft, helicopters and agricultural aircraft. During development of the gas turbine engine, the designers and engineers faced many challenges. Some of the concerns, which designers are constantly striving to improve the turbine engines, are performance, fuel efficiency, noise levels, reliability, manufacturability, maintainability and reparability.

The turbine engine dominates in aviation since 50-th of the XX century. Their development is subdivided conditionally into several stages.

1. 40–50-th of the XX century – stage of formation and development of engines of the first generation.

The idea to use the turbine engine as an aircraft propulsor was known at the beginning of XX century. But specialists declared the idea unworkable: the engine based on known that time technologies was fuel inefficient and bulky comparing to a piston engine, which allowed the aircraft to fly and was intensively developed at that time.

Theory of the air-breathing engine was published by Soviet Academician Boris Stechkin in 1929.

First operable engineering projects were implemented in three countries: Great Britain, Germany and Soviet Union. British engineer Frank Whittle proposed in 1929 and patented in 1930 a compound axial-centrifugal compressor and a single-stage axial turbine. The modified Whittle engine (designated WU for Whittle Unit) was successfully tested in 1937. Whittle's WU engine was composed of a double entry centrifugal compressor and a single stage axial turbine. After the Second World War, engines of Frank Whittle were produced in Soviet Union according to a license under names of RD-45 and RD-500.

Approximately six years after Whittle, Germany's Hans Pabst von Ohain put forth his ideas for a turbojet engine in 1935. It consisted of a compound axial-centrifugal compressor similar to Whittle's patent design and a radial turbine. H.P. von Ohain's designs were built by aircraft manufacturer Ernst Heinkel. August 24, 1939 marked the maiden flight of a turbojet aircraft, the He 178, powered by the HeS 3B engine. Just after the Second World War, German turbojets Jumo-004 and BMW-003 were used in first Soviet jet fighters MiG-9 and Yak-15 under names of RD-10 and RD-20.

Professor of Moscow Technical University Vladimir Uvarov in 1932 proposed a project of original turboprop engine, which was built and tested later.

Engineer of Kharkov Aviation Institute Archip Lyulka in 1935 proposed a project of turbojet engine with centrifugal compressor. In 1938, he patented the turbofan engine.

TR-1 was the first Soviet turbojet engine. It was designed by Archip Lyulka. Having thrust of 13.5 kN, it was equipped with the axial compressor, annual combustion chamber, single-stage turbine and fixed jet nozzle. This engine was the base for the following turbojets AL-3 and AL-5 with thrust 45 and 50 kN, respectively.

Vladimir Klimov, Chief Designer, headed a work on modification of Frank Whittle's NIN-1 engine, which was manufactured in Leningrad by license. The modification has been finished in 1948 and is known as VK-1 turbojet with thrust of 26.5 kN, centrifugal compressor, can combustors and single-spool turbine. The engine was the most mass-produced, reliable and long-living one. It was powering the MiG-15, MiG-17, Il-28 and other aircraft.

Engines of the first generation were of a single-spool single-flow diagram; they had low thrust (up to 30 kN), pressure ratio ($OPR \leq 7$) and turbine inlet temperature (TIT = 900 to 1100 K), high specific fuel consumption (SFC > 0.1 kg/(N hour)), were equipped with the axial or centrifugal compressor and turbine with non-cooled rotor blades. Turbine casings and discs were made of the thermal-resistant steel. Turbine rotor blades of some engines were made of the thermal resistant nickel-base alloy.

Mainly, these engines were for the military airplanes. But in 1949, the design bureau of Alexandr Mikulin designed the RD-3M-500 engine for the Tu-16 bomber, and upgraded version AM-3 of this engine was installed on the Tu-104 passenger airplane, which first commercial flight was in 1955 (Boeing 707 with turbojet engines – in 1958).

2. Engines of the second generation appeared in the 50-th – beginning of 60-th. This period is characterized by the large number of projects of the gas turbine engines. As before, these engines were mainly for the military airplanes.

The distinctions are usage of the two-spool rotors (the R11F-300), variable guide vanes (the AL-7F), turboprop engines (the AI-20, AI-24, and NK-12). Compressors were axial only (OPR=10 to 12), turbines (TIT = 1200 to 1275 K) were made of the nickel-based alloys with non-cooled blades, but the nozzle vanes were cooled in some engines. Comparing to the engines of the first generation, the second generation engines had higher thrust (60 to 100 kN), overall pressure ratio (9 to 10) and efficiency (SFC < 0.1 kg/N· hour).

At the beginning of 50-th, supersonic stages were applied in the compressor design (the engines AL-7F, RD-9B, VD-5, VD-7, and RD-7-M2). Due to the two-spool diagram and supersonic stages, the total number of compressor stages has been decreased. For example, the two-spool afterburner turbojet R11F-300 has two compressor cascades with three stages in each, and same American single-spool engine J-79 has 17-stage single-spool compressor).

At this time, a complex problem of a high-power gearbox for turboprop has been solved: the gearbox for the NK-12 engine having power of 15000 hp has been designed, which efficiency was 0.992. This gearbox for driving a double-row coaxial propeller is still a champion in power and long life.

3. The third generation (60-70-th) is characterized with further development of the turbojets and afterburning turbojets, but its distinction is development of turbofan engines – TFE and ATFE (the NK-8, D-20P, D-30P, D-30KU, D-30KP, AI-25, NK-144 and other engines). Efficiency was improved significantly. Bypass ratio (BPR) of the turbofans increased gradually from 0.9 (the D-20P) to 2.4 (the D-30KU), thus decreasing SFC from 0.068 kg/(N hour) (the D-20P) to 0.0494 kg/(N hour) (the D-30KU).

Compressors of the engines of the third generation are mainly two-cascade with OPR=15 to 20. Titanium and thermal-resistant alloys constitute significant part of the structural materials. Turbines are designed with cooled discs, nozzle vanes and rotor blades, TIT=1350 to 1450 K.

4.The engines of the fourth generation have been appeared at the end of the 70-th – beginning of the 80-th. That period is characterized with variety of diagrams, designs and parameters of two-spool and triple-spool turbofans. The fourth generation engines (the D-36, D-136, and D-18T designed in Zaporozhye, the PS-90 designed in Perm and other engines) had high OPR (up to 30) and TIT (1500 to 1700 K), medium BPR (4 to 6) and characteristic design features: modular structure, developed diagnostic system, radial clearance control, intensive cooling of hot parts, single-crystal and directly-solidified turbine rotor blades, smokeless combustion chambers. New methods of the numerical analysis were implemented during designing at that period of time.

The progressive maintenance system on on-condition base has been developed, digital electronic control systems were implemented. Transition to the condition-based maintenance stimulated researches in the analysis of the engine service life, which include analysis of thermal-stress condition of the engine parts, gas flow duct analysis, non-destructive testing, vibration diagnostics, etc.

5. Engines of the fifth generation have started experimental development since 1990-th. Now engines GE-90, GENx, GE9X, LEAP, PW-1100 and Trent are manufactured in series and powering the most efficient passenger aircraft.

The main trends in designing of the fifth generation engines are as follows:

a) increasing of OPR at relatively slow growth of the TIT, thus improving the fuel economy at the required high level of reliability within service life; this is characteristic for the passenger and transport aviation;

b) further increasing of the TIT in the engines for the military aviation, thus improving thrust-to-weight ratio; at the nearest time, the TIT value would exceed 2000 K.

Besides, engines of fifth generation have low specific weight ($\gamma \approx 0.01$ kg/N) due to light and strong materials, smaller number of the parts, implemented “blisk” and “bling” structures, wide-chord compressor blades. They also are characterized by the low maintenance expenses. One of directions of the engines of the fifth generation perfection is variable bypass ratio; this engine is efficient both at low subsonic and at supersonic flight velocity. Another direction is application of the alternative fuel, for example, liquid gas and hydrogen.

6. The engines of the sixth generation will be based on the technologies that are developed since the beginning of the XX-th century. It is difficult to imagine their detailed look now. We may only predict that they will be developed towards growth of the OPR (it will exceed 50 to 80) and the TIT growth up to the stoichiometric value (2200 to 2400 K). This will stimulate wide introduction of the ceramic and intermetallic parts in the engine hot portion, new methods of cooling and thrust augmentation. At that time, the engine thrust-to-weight ratio will reach 200 N/kg (the engines of the fourth generation have approximately 80). Combined power plants will appear, which integrate the turbo-compressor with the rocket gas generator, or use of two fuels: the hydrocarbon fuel is used at takeoff, climbing and landing, and the nuclear fuel is used during cruise, thus providing a long-distance durable flight without refueling.

1.1.2. Main trends in engine designing

Principle of a base gas generator. Designing of these engines is extremely expensive and durable. Therefore, the primary task is cost decreasing and time shortening of the engine development. To solve this task, one must change priorities in the methods of new engines development. The new methodology is based on the anticipatory development of the scientific and technical backlog in key technologies, assemblies, units, systems, base gas generators, etc. (Fig. 1.1).

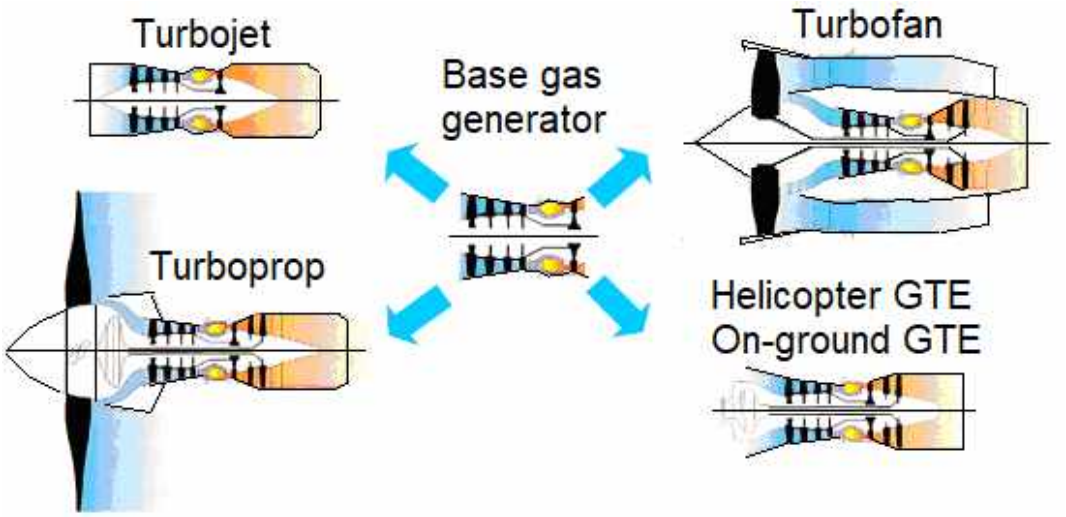


Fig. 1.1. Turbine engines development using base gas generator

One of the efficient directions in development of the modern GTE is the engine generations designing in wide range of thrust, using the base gas generator. The examples are families (the D36, D436T, D436T1, D436TP, and D436-148), RB211, CFM56, V2500, (GE90, GEnx, GE9X), Trent, PW4000, and PW2000.

Multi-level modelling and simulation. Demonstrator engines are designed and experimentally developed, numerical simulation methods are widely implemented. Place and role of the experimental research in the engine designing technology has been changed: volume of the experimental works on an experimental engine development has been decreased; experiments are preferably used to verify models and to approve the engine reliability in critical maintenance conditions, which are difficult to simulate.

Thus, the role of numerical simulation during the engine designing grows continuously. When designing the fourth generation engines, bases of the integrated tools were created, which include three categories of analysis:

– integration of some processes, disciplines and performance parameters (multi-disciplinary analysis); for example, thermal-stress condition of the turbine rotor blade analysis includes the blade external viscous streamlining calculation, the cooling air flow calculation, the heat exchange on the external and internal surfaces of the blade calculation, three-dimensional temperature and stress distribution calculation, the blade service life calculation and complex thermal-stress condition of rotor estimation;

– application of the integral models of the engine assemblies and structural members (for example, joint operation of the air intake duct, compressor, combustion chamber, turbine, and jet nozzle);

– rational combination of the simple and complex models; the simple models of elementary level are applied during the preliminary designing; the more complex models are applied at the detailed designing.

Scientific and technological advance. The role of scientific and technological advance in the engine development will be increased due to the following reasons:

– economic and technical risk must be decreased, because technical mistakes in designing become more and more expensive;
– the market conditions become more complicated and unpredictable;
– during the scientific and technological advance development, new unique technologies appear, which have own value in the market of science-intensive technology for application in other areas of engineering.

Technical solutions that are made during designing of new engines must be ahead of current achievements. Therefore, the developed structure must accumulate all modern achievements in the engine engineering and must be oriented at promising solutions in this area.

Traditional trend in development of the aircraft turbine engine is increasing of the turbine inlet temperature and overall pressure ratio.

Some most promising trends in the engine development are as follows:

– application of principles of system and service life designing during development of new engines;
– application of the turbo-prop-fan engines in aircraft with high subsonic velocity;
– application of the variable bypass engines in the multi-mode power plants;
– use of the passive and active radial clearance control in turbine and compressor;
– making design decisions, which decrease toxicity and noise levels;
– use of the structural members that facilitate the technical diagnostics and incorporation of the engine modular design.

Development of engine engineering in nearest decades will result in a new level of the engine perfection indices:

– service life and reliability growth in 1.5 to 2 times;
– economy growth by 10 to 15 %;
– reduction of the number of parts by 50 %;
– two times reduction of the maintenance labor content;
– power plant total noise reduction by 20 to 30 dB;
– 2 to 3 times reduction of harmful emission according to the current international norms.

Such engines will become a base for the competitive aircraft, which will be designed in 2030 to 2040 and will be in maintenance for nearest 50–60 years.

This work is done just now in some directions:

– fundamentally new class of the high-temperature thermal resistant materials has been developed on a base of the nickel and titanium structures, which have low density and high resistance to oxidation; for example, the alloy ВКНА-1В (Ni_3Al) for the turbine rotor blades and nozzle vanes, flaps of jet nozzle, internal parts of the flame tubes;

– protection of blade surface from the high-temperature oxidation by deposition of special thermal protection coatings by using the vapor and plasma flows, which provide high service life at working temperature of 1300 to 1500 K;

– development of the phase-reinforced materials for operating temperature of 1500 K and higher; matrix of these structure is nickel-base thermal resistant alloy and intermetallic structure, and the reinforcing phase is fiber of niobium or tantalum mono-carbide;

– development of the welded high-tech thermal resistant alloys for combustion chamber casings (for example, ВЖ-145, ВЖ-155, and ВЖ-159), which ultimate limit is higher than 1400 MPa at 20 °C.

Compressor. Trend in compressor design is high pressure ratio at low number of stages. The problem is solved using unshrouded wide-chord blades, which are streamlined by the air flow with Mach number up to 1.7. The rotor of such engine is high-speed, so it needs new bearings: magnetic bearings, sliding bearings, roller bearings with non-metallic rolling bodies. The shaft can be composite, the fan blades may be made hollow and of the metallic composite (for example, the titanium–silicon carbide composite decreases compressor weight approximately by 50 %, and structure “bling” of the same material decreases the weight by 70 %).

Turbine. Trend in designing of the gas turbine is a single-stage highly loaded turbine with high efficiency and turbine inlet temperature (150 to 300 K higher than the present-day turbines have). With this purpose, bliscs with single-crystal transpiration cooled blades are developed; this decreases turbine weight by 25 %. In 1997, the rotor blade with penetration transpiration cooling was tested at TIT = 2000 K, and in 2000 its modified sample was tested at TIT = 2200 K. The blade body is film-cooled, but indices of cooling (the air consumption and cooling efficiency) are close to the indices of the porous cooling.

The blade is cast and attached to the disc by a high-temperature brazing. Three-dimensional blade bodies are profiled and manufactured. Until now, the turbine blades were cast with rigid core inserts, which formed channels to supply the cooling air. Now, the new technology has been developed for the three-dimensional transpiration-cooled blades. In this technology, the flexible ceramic strips are used, which form “hot” and “cold” walls and additional channels in parallel to the blade airfoil section.

Combustion chamber. One more problem of the promising engine development is designing of the combustion chamber with high combustion efficiency (more than 0.99), high exhaust gas temperature (more than 2000 K), high service life of the flame tubes (20 to 30 thousand hours) and twice less consumption of the cooling air comparing to the up-to-date design structures. At the same time, the combustion chamber must have low toxic pollutions (2 to 2.5 times less comparing to the up-to-date design structures) and a high level of maintenance performance parameters: reliable on-ground and in-flight starting, uniform temperature field at the turbine inlet, controllability and reparability.

The diagram of the combustion chamber is now designed with the modular furnaces. Each of them has its own stable circulation zone and individual air supply for full combustion of the fuel. Mixers in side walls of the flame tube supply small amount of the air. The combustion efficiency is not less than 0.99 at decreased consumption of the cooling air (14 %). Walls of the flame tube are double-layer, perforated (with spraying). The “cold” wall is load-carrying, and the “hot” wall is designed of separate segments made of the thermal-resistant material. Dividing of hot wall on separate segments excludes thermal stress, which are inherent to a solid wall.

Pollutions of nitrogen oxides in this combustion chamber are 1.5 to 2 times less than in the best modern combustion chambers.

This combustion chamber can be a prototype of the new designed engines and also a base for upgrading of the serial engines.

Bypass ratio. The bypass ratio affects both the engine specific fuel consumption and the specific weight, diameter and aerodynamic drag. On one hand, when the BPR increases, the SFC will decrease. But at same time, the aircraft drag becomes more and the aircraft needs more thrust to overcome it. Therefore, rational values of the BPR are determined not only by the engine itself, but also by aerodynamic performance parameters of the aircraft and its flight profile (including velocity and altitude). Theoretical analysis predicts that characteristic BPR value for fighters will be 0.2 to 0.3, and for supersonic aircraft – up to 18. Engines for trainer jet airplanes possess intermediate place because, on one hand, they must provide durable flight with subsonic velocity during training; on other hand, they must be easy convertible in light combat airplanes that may fly with low supersonic velocity. The BPR of these engines may reach 1 or even more.

When the BPR is 10 and more, some new problems arise that need new structural transformations of the engine. High BPR affects adversely operation of the low pressure turbine (LPT), fan and booster stages of the compressor. At direct driving of the fan, the last determines low level of the rotational speed. Thus, the LPT and the booster become slow and multi-stage, thus increasing weight and dimensions of the engine, making distance between rotor supports

longer and rotor critical rotation speed less. To overcome this problem, the gear-driven fan may be designed. This engine has the high-speed low-stage LPT that drives directly the booster. The fan is driven through a planetary gearbox. The example is the PW-1100 turbofan.

The second problem of BPR increasing is subcritical operation of a secondary jet nozzle at cruise power ratings. In this case, the similarity conditions are not satisfied and the operation line of the fan performance is dislocated aside lower pressure ratio and higher air consumption, thus decreasing the fan efficiency. This efficiency drop may compensate the positive effect that is reached due to BPR increasing. To exclude this affect one must save conditions of the nozzle operation at all flight conditions. This is possible if a variable nozzle is used. So, the external wall of the bypass duct must be movable. If to remember that this engine must be equipped with a thrust reverser, we understand that the bypass duct of this engine must be equipped with a combined double-action device: in flight it is a variable nozzle, after landing it is thrust reverser.

Automatic Control System (ACS). The engine performance parameters in many respects depend on the ACS, which must be optimum at all operating conditions and reliable (mean time between failures must be not less than 10^6 hours). Up to the beginning of the 80-th the ACS of turbine engines were mainly hydromechanical. At the end of the 70-th, electronic limiters appeared. Due to development of electronic technologies, in the 80-th Full Authority Digital Electronic Control (FADEC) systems were designed and implemented. Their advantages are: perfect control quality, multiple functions, high reliability, simple maintenance, low cost. The new engine ACS is designed so that it is integrated into the aircraft control system, with thermal resistant circuitry, intellectual sensors (with built-in processors), which provide preliminary data processing and correction. This ASC provides optimum parameters at current operation power rating (adaptive control), faults detection and parrying (ACS reconfiguration using reserve information sources, indirect information sources and simulation results).

Health Management System. Efficient maintenance at high reliability has determining role in the upgrading of the up-to-date engines. Therefore, turbine engine diagnostics is one of intensively developed problems. Researches on creation of new on-board and on-the-ground diagnostic tools are done using parametrical diagnostics, tribological diagnostics, vibro-acoustical diagnostics, and decision making methods. The main directions of the engine diagnostics are improvement of the sensors and wide application of the engine, its systems and assemblies simulation.

Upgrading of series engines. Actual direction in engine designing is development of competitive upgradings on the base of series engines due to

application of new materials and new design and technological solutions. Single-crystal alloys, composite materials, ceramics, intermetallic materials are widely used. Engines of the fifth and sixth generations improve their parameters due to replacement of the titanium and nickel-base alloys with reinforced superalloys and composite materials with metallic and ceramic matrixes. For example, the blade alloy ЖС-47 is alloyed with rhenium up to 10 % (melting temperature of rhenium is 3170 °C, its total world production in 1990 was 900 kg per year). The long-term strength of the blade airfoil section (made of this alloy) at a temperature of 1300 K is $\sigma_{lt} = 350$ MPa. High-gradient technology of single-crystal casting has been developed (the gradient reaches 250 degrees per centimeter), which allows to make casting of strongly set crystallographic orientation. This casting may operate at TIT = 2200 K (for military airplanes) or at less temperature but high service life (for civil airplanes). At the same time, the air bleed for cooling decreases, the engine specific parameters become better, the engine dimensions and weight decrease.

Integrated designing. One of characteristic features of the up-to-date approach to the turbine engine designing is a complex (system) solution of the designing tasks. The systemacy in designing means considering of the engine as a component part of a complex that includes a power plant and an airframe. Considering of the engine operation in isolation from this complex results in irrational composition of the aircraft, partial realization of potential design decisions, and in some cases to significant deviations of implemented parameters from the declared values. Therefore, new engine must be designed taking into account its operation in real aircraft power plant.

The complex approach to the engine designing is implemented in six main functional areas:

1. Transport aircraft with M_f = 0.6 to 0.9, which are driven by the turbofan (TFE), turboprop (TPE) and turbopropfan (TPFE) engines.

2. Helicopters with v_f = 150 to 400 km/hour, which are driven by the turboshaft engines (preferably with free turbine).

3. Auxiliary power units (APU), including starting and lift engines (LE), which not influence directly aircraft flight velocity and serve auxiliary purposes: starting of thrust engines, aircraft conditioning, etc. The most applicable scheme of APU is turboshaft, the most applicable scheme of LE is turbojet (TJE).

4. Military aircraft with M_f = 3.0 to 3.5, which are based on the TJE or ATJE, TFE or ATFE, and turbo-ramjet engines (TRJE).

5. Air rockets and pilotless aircraft with $M_f = 0.6$ to 3.0, which are based on the TJE, TFE, TRJE and rocket-turbine engines (RTE).

6. Aerospace complexes (ASC) for flight with $M_f = 10$ to 25, which are based on the supersonic air-breathing engines, TRJE and aircraft engines with liquefaction of the atmospheric oxygen.

Besides aviation, the turbine engines are used in many on-the-ground units. In this case, aviation engines are converted or new engines are designed for on-the-ground or marine application.

Variety of functional areas of the turbine engine application determine wide range of their characteristics. So, the engine thrust varies from 300 N to 500 kN, the engine power – from 20 kW to 40 MW, the external diameter – from 0.3 m to 3.0 m.

Maximum technical efficiency of the system aircraft-engine may be reached if to take into account full interference of the power plant structural members and airframe. As maintenance experience shows, parameters of power plant are significantly influenced by the intake duct and exhaust system, which are mated with the airframe structure.

The intake duct is usually considered to be the aircraft component part, and so is not worked out in details at the stage of engine designing. However, for optimum designing of the operating process, the intake duct must be considered in common operation with the engine as the component part that provides minimum pressure losses at specified air consumption. The intake duct of supersonic aircraft is designed of variable geometry to decrease pressure losses and to prevent engine unstable operation. The intake ducts of a side type are widely used. They have less length of the air supplying channels and are less sensitive to variation of the attack angle and the aircraft sideslip. The experience shows that the engine designing taking into account the intake duct performance parameters provides for minimum thrust losses that are linked to non-uniformity of the air flow, which enters compressor.

In turn, designing of the exhaust system is closely related to a chosen type of the intake duct. This is determined at least by three reasons. First, the air consumption performance parameters must be coordinated with all structural members of the gas flow duct, including the exhaust system performance parameters. Second, structure of the exhaust system must be successfully composed with a tail part of the aircraft. Third, the exhaust system may provide such functions as thrust vectoring and thrust reversing to improve the aircraft maneuverability. All of these factors make necessary to consider the exhaust system structural design in complex with the engine features, its control diagram and the aircraft function.

The trend has been outlined in transition from traditional round shape of the exhaust system to a plane two-dimensional jet nozzle, which has a set of significant advantages comparing to the axisymmetric nozzle. The plane nozzle is more rationally combined with the airframe configuration, minimizes intensity of infrared radiation of the exhaust gas, thus decreasing a danger of the aircraft damage by the rockets with thermal self-directed heads, and helps for more flexible variation of thrust value and direction.

In promising, the engine will be automatically controlled by on-board computers in accordance with the special control program, which will be coordinated with the aircraft flight control system, i.e. all engine control systems will be naturally related with the aircraft control system.

Complex and systematic approach is efficient also at the stage of designing of the separate engine structural elements. So, efficiency of the gas generator depends on coordination between turbine and compressor, shape and structure of the engine gas flow duct. In turn, for example, the compressor efficiency depends on coordination between separate stages and between rotor and guide vanes at each stage.

Hence, efficiency of the assemblies is estimated using indices of the engine as a whole in the aircraft system, while efficiency of the parts design is estimated using functional indices of the assemblies, which include these parts, in the engine system.

The maximum complete analysis of all sides and interference of different factors in the engine development process is a main feature of the systematic approach to designing.

1.2. Types, main parameters and areas of application of air-breathing engines

Different classifications may be done, based on the most characteristic design features: for example, type of compressor, combustion chamber or turbine, the number of rotors, method of thrust producing, etc. All these features are present in the engine diagram. The jet engines are subdivided into two classes: air-breathing (ABE) and rocket (RE) engines. In turn, each of these classes is subdivided into separate types (Fig. 1.2).

At the first stage of engine development, the most expedient is classification by structural arrangement with separation of engine types that have specific structural differences. *Structural arrangement of engine* is coordinated arrangement of its component parts that meets the requirements. The structural arrangement is characterized with its design arrangement – simplified drawing that determines type of the engine, mutual arrangements and power interaction of the main component parts.

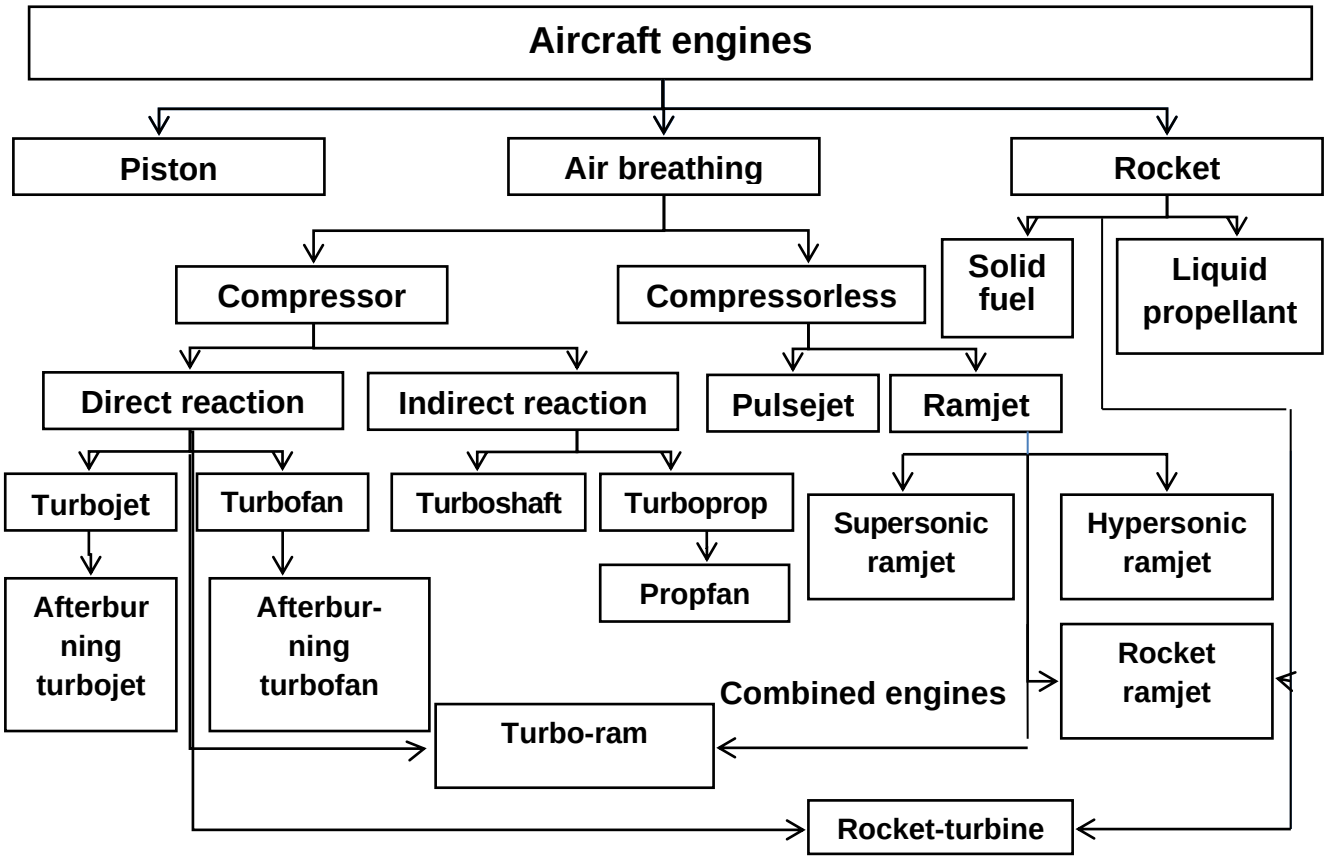


Fig. 1.2. Classification of aircraft engines

The structural arrangement is directly related to designing, drawing of parts and their links. Designing of new arrangements makes the engine designing process individual, logically closed and independent of foreign solutions. But the reverse is true: in case of absence of the structural arrangement designing stage, the designer needs in choosing prototypes and analogs among already designed engines that complicate a development of the original competitive engines.

The following types of turbine engines structural arrangement are differed:

– turbojet engine (TJE) and afterburner turbojet (ATJE);
– turbofan (TFE) and afterburner turbofan (ATF);
– turboprop (TPE) and turbopropfan (TPFE);
– free turbine helicopter (turboshaft) engines (TShE);
– turbojet for vertical and short takeoff and landing (VSTOL) aircraft;
– turbine engine of aircraft auxiliary power plant.

Each of the above mentioned types of engines has its own area of preferable application. Fig. 1.3 shows approximate ranges of altitude and

velocity that correspond to aircraft that are driven by the engines of different types.

Engines of different structural arrangement have not only different areas of application but also a number of design features.

Turbojet engines (TJE) are widely used in all types of the airplanes and unmanned aerial vehicles (UAV) and provide a flight velocity that corresponds to Mach number M_f = 1.35 to 1.40 at altitude 12 to 14 km. When afterburner is applied (ATJE) then velocity increases to M_f = 2.5 to 3.5 at altitude 22 to 25 km.

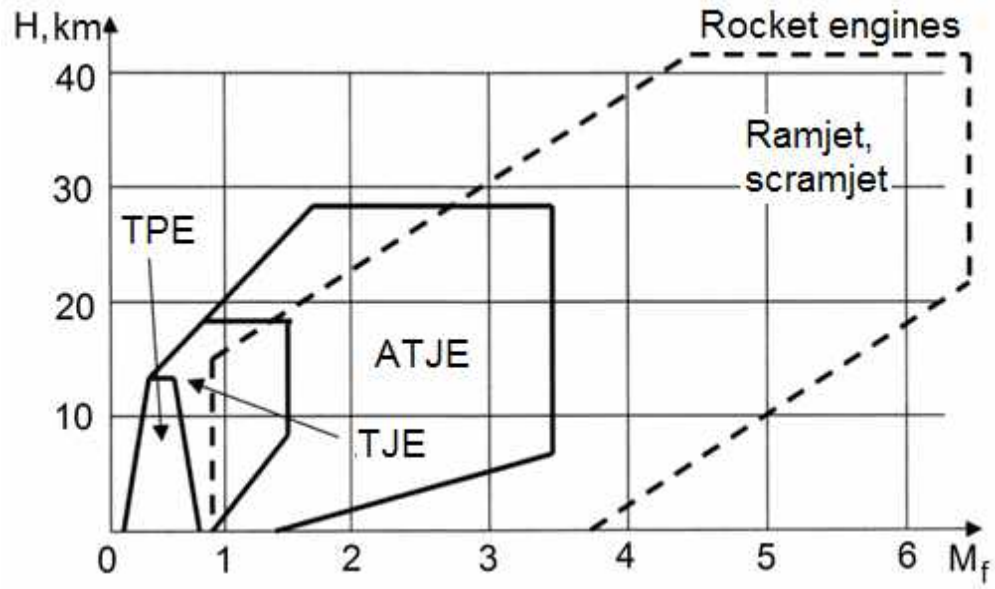


Fig. 1.3. Areas of application of air-breathing engines

Approximate values of the absolute and specific parameters of TJE and ATJE are shown in Table 1.1.

Table 1.1

Main parameters of the TJE and ATJE

Parameters	Type of engine		
	Low-size turbojets	TJE and ATJE	
		Mean thrust	High thrust
Thrust P/P_{AB}, kN	0.5...50	50... 100 70... 150	100...250 150...300
Specific thrust $P_{sp}/P_{sp\ AB}$, (kN·s)/kg	0.5...0.6	0.7...0.8 1.1...1.2	0.8...0.9 0.9...1.0
Specific fuel consumption $C_{sp}/C_{sp\ AB}$, kg/(N·hour)	0.10...0.13	0.08...0.10 0.20...0.22	0.09...0.10 0.17...0.19
Specific weight $\gamma_{sp}/\gamma_{sp\ AB}$, kg/N	0.01...0.05	0.020...0.025 0.015...0.020	0.025...0.035 0.020...0.022

The structural arrangements are differed by type of the compressor, combustion chamber, exhaust system, method of thrust augmentation, number of rotors and another design features.

Fig. 1.4 shows the structural arrangement of the TJE with centrifugal compressor. Engines VK-1, RD-45, and RD-500 of this arrangement were used in the MiG-15, MiG-17, and Il-28 aircraft.

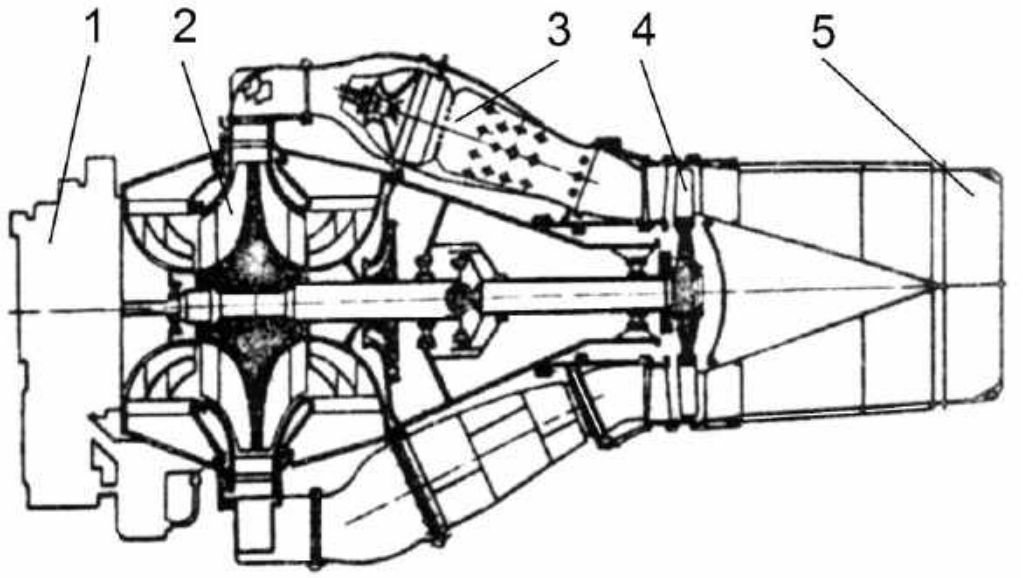


Fig. 1.4. Structural arrangement of TJE with centrifugal compressor:
1 – accessories; 2 – compressor; 3 – combustion chamber;
4 – turbine; 5 – jet nozzle

Centrifugal compressor of this engine has two intake ducts. This increases the air flow. The air is supplied radially by two intake pipes, in which the stationary inlet guide vanes are mounted. The compressed air flows to the combustion chamber by the outlet pipes, wherein the vanes of diffuser and the straightening guide vanes are located.

Individual can-type combustion chambers are dislocated around the engine casing. The number of cans may be from 6 to 16. They are united by common gas collector, which directs the gas to the turbine.

Turbine of the VK-1 turbojet is a single-stage, axial-flow, and reaction-type one. The gas flows from the turbine to the convergent non-controlled jet nozzle. The engine rotor has three supports. This engine was modified and equipped with the afterburner and variable jet nozzle.

Simple design structure, high reliability and survivability of the VK-1 affect its durable application. Now engine of the same arrangement Walter M-701 is used in the L-29 combat trainer aircraft.

Fig. 1.5 shows arrangement of the single-spool ATJE for high supersonic velocity. This arrangement has some design features. Axial-flow compressor

consumes not high power from a single-stage turbine. Afterburner is located downstream of the turbine; it contains diffuser with flame stabilizers and fuel manifold.

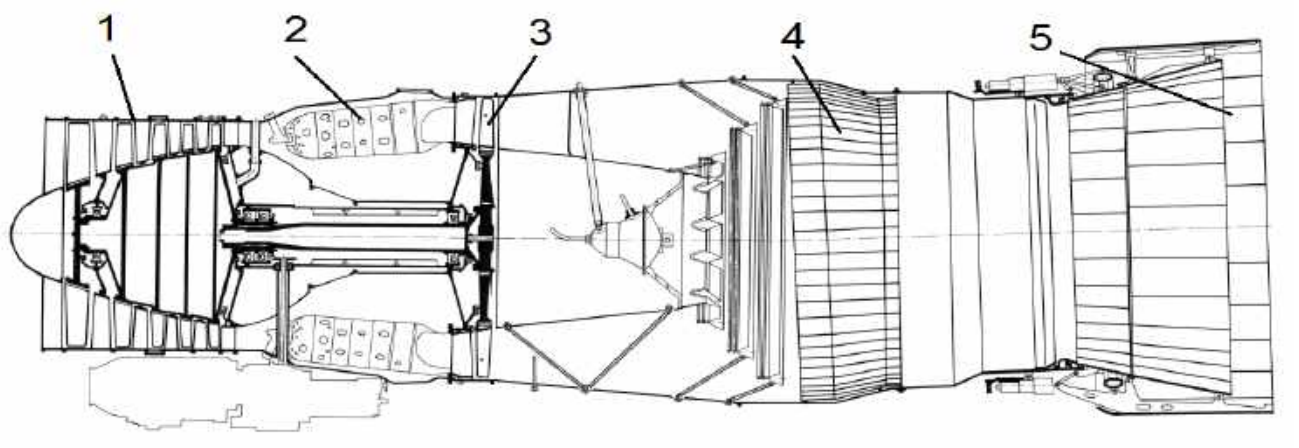


Fig. 1.5. Structural arrangement of single-shaft ATJE:
1 – compressor; 2 – combustion chamber; 3 – turbine; 4 – afterburner;
5 – variable jet nozzle

At high pressure ratio, compressor of the single-spool TJE (ATJE) needs in complex control system. Structural arrangement of the single-spool ATJE AL-21F-3 for the Su-24 aircraft with advanced compressor control system is shown in Fig. 1.6.

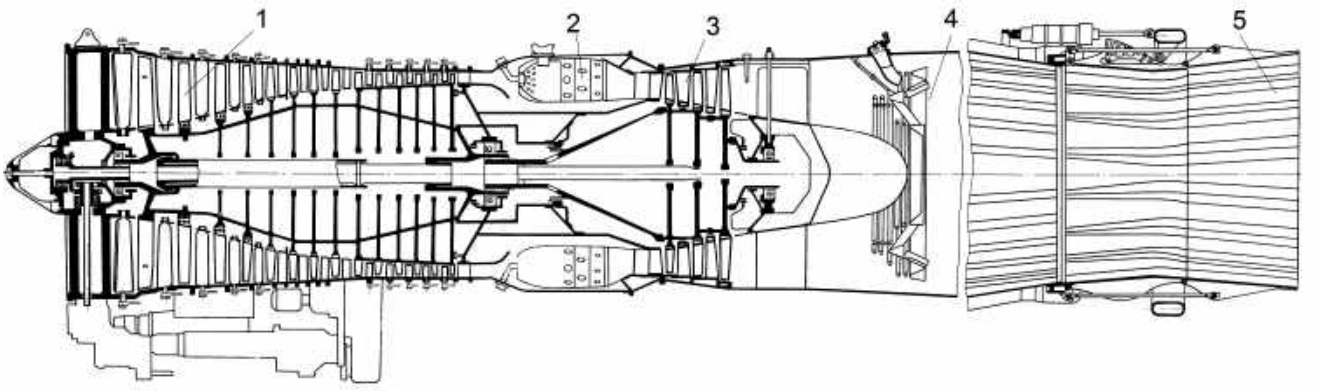


Fig. 1.6. Structural arrangement of single-spool ATJE with advanced compressor control system:
1 – compressor; 2 – combustion chamber; 3 – turbine; 4 – afterburner;
5 – variable jet nozzle

High-pressure compressor provides for stable operation in two-spool engines (Fig. 1.7). The examples are the RD-95Sh and R-195 turbojets for the Su-25 aircraft. The engine has high pressure and low pressure rotors that are not linked mechanically and rotate each other at optimum rotation speeds. The

rotors are driven by their own turbines. Shaft of the low pressure rotor is dislocated inside a hollow shaft of the high pressure rotor; therefore, the engine arrangement is more complex than in previously considered engines.

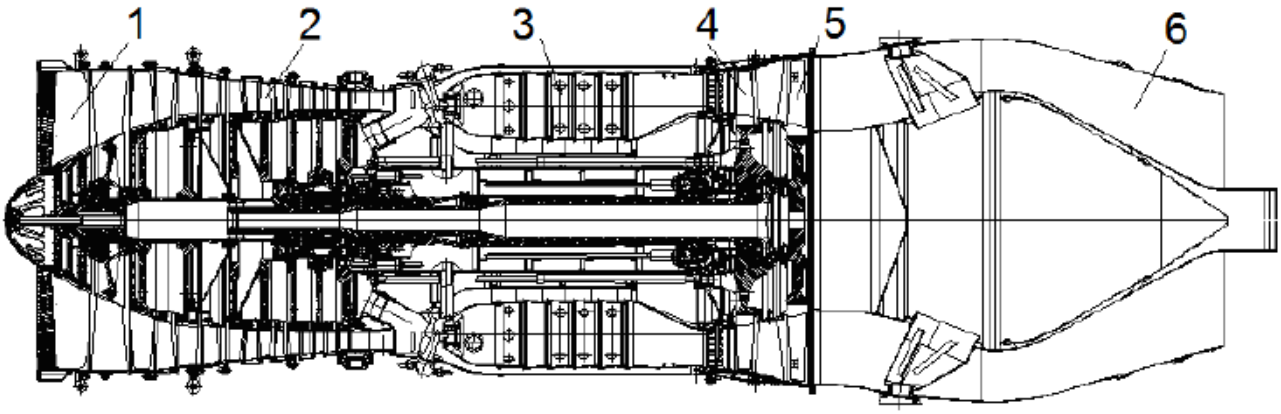


Fig. 1.7. Structural arrangement of two-spool TJE:
1 – low pressure compressor; 2 – high pressure compressor;
3 – combustion chamber; 4 – high pressure turbine;
5 – low pressure turbine; 6 – jet nozzle

Turbofan engines (TFE and ATFE) are the most widespread in aircraft of military and civil aviation.

In the turbofan engine, the air that flows from the intake duct is compressed in the front portion of the compressor, which is named as a fan, and then it is divided into two flows. The internal flow is compressed in the rear part of the compressor and enters the combustion chamber wherein it is heated. The external flow goes from the fan into the bypass duct and is expanded in a ring nozzle, thus increasing the engine thrust. Ratio of the air flow that flows through the bypass duct to the air flow in the internal duct is named as a bypass ratio m.

Turbofan engines have less fuel consumption comparing to the turbojets at subsonic velocity of flight (M_f = 0.7 to 0.9) and less noise level. Efficiency of the turbofan becomes better when bypass ratio m increases. The bypass ratio reaches 6 to 10 for subsonic passenger and transport airplanes. In the afterburner turbofans, the minimum specific fuel consumption is implemented at relatively low bypass ratio that is m = 0.3 to 2.1. At high degree of afterburning, these engines provide high supersonic velocities that reach M_f = 2.2 to 3.2 at acceptable efficiency. Therefore, the ATFE are now the main engines for the supersonic airplanes of various types.

Relatively low-cost small-size turbofans with low bypass ratio are used in the power plants of the combat trainers and unmanned aerial vehicles (UAV).

Approximate values of absolute and specific parameters of TFE and ATFE are given in Table 1.2.

Table 1.2

Main parameters of TFE and ATFE

Parameters	Engine type		
	Small-size TFE	TFE and ATFE	
		Mean thrust	High thrust
Thrust P/P_{AB}, kN	3...50	50...100 60... 150	100...250 150...300
Specific thrust $P_{sp}/P_{sp\ AB}$, (kN·s)/kg	0.4...0.5	0.3...0.5 0.7...0.8	0.4...0.6 0.80...0.85
Specific fuel consumption $C_{sp}/C_{sp\ AB}$, kg/(N·hour)	0.05...0.07	0.05...0.07 0.13...0.22	0.05...0.06 0.22...0.24
Specific weight $\gamma_{sp}/\gamma_{ysp\ AB}$, kg/N	0.02...0.03	0.015...0.025 0.012...0.014	0.015...0.025 0.012...0.016

The following structural arrangements of turbofans are differed:

– by the number of rotors – single-, double- and triple-spool;

– by location of fan – front and rear location;

– by method of the air and the gas exhausting from the ducts – with mixing flows and with separate flows;

– by method of thrust augmentation – burning additional fuel after the mixing chamber and burning of additional fuel in the bypass duct.

Characteristic structural arrangement of the TFE with low bypass ratio without mixing flows of the AI-25 engine for the Yak-40 airplane is shown in Fig. 1.8.

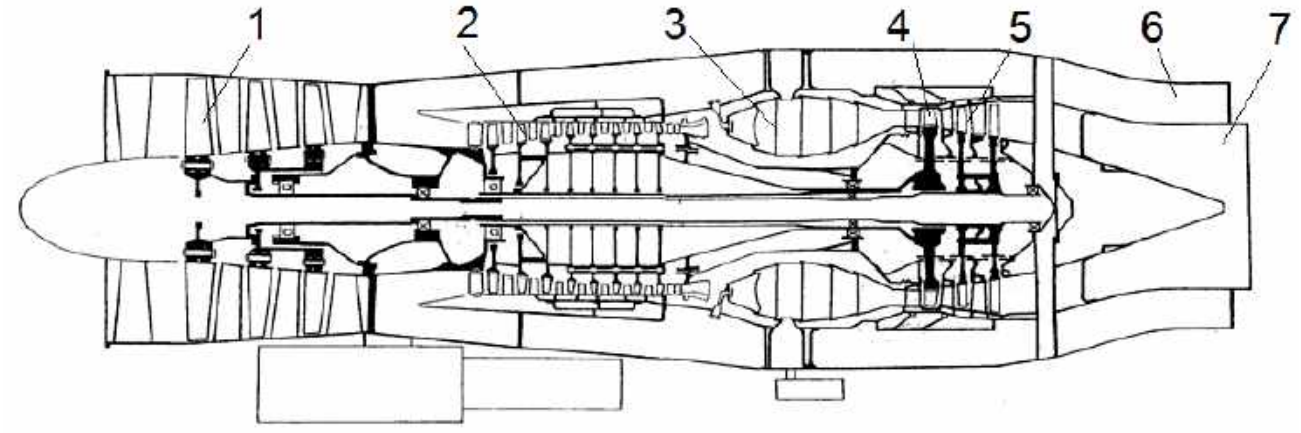


Fig. 1.8. Structural arrangement of two-spool TFE:
1 – fan; 2 – high pressure compressor; 3 – combustion chamber;
4 – high pressure turbine; 5 – low pressure turbine;
6 – nozzle of bypass duct; 7 – nozzle of primary duct

The engine has high and low pressure rotors that are rotated with different rotation speeds and are driven by their own turbines. Shaft of the low pressure rotor is located inside the shaft of the high pressure rotor. The air from the bypass duct and the hot gas from the primary duct enter jet nozzles that are dislocated downstream of the turbine. In the AI-25TL modified engine for the L-39 combat trainer, the air from the bypass duct and the hot gas from the primary duct are mixed downstream of the turbine. Then the mixed gas flows out through a common non-controlled jet nozzle.

Fig. 1.9 shows a structural arrangement of three-spool TFE with high bypass ratio – the D-18T engine for the An-124 “Ruslan” and An-225 “Mriya” airplanes.

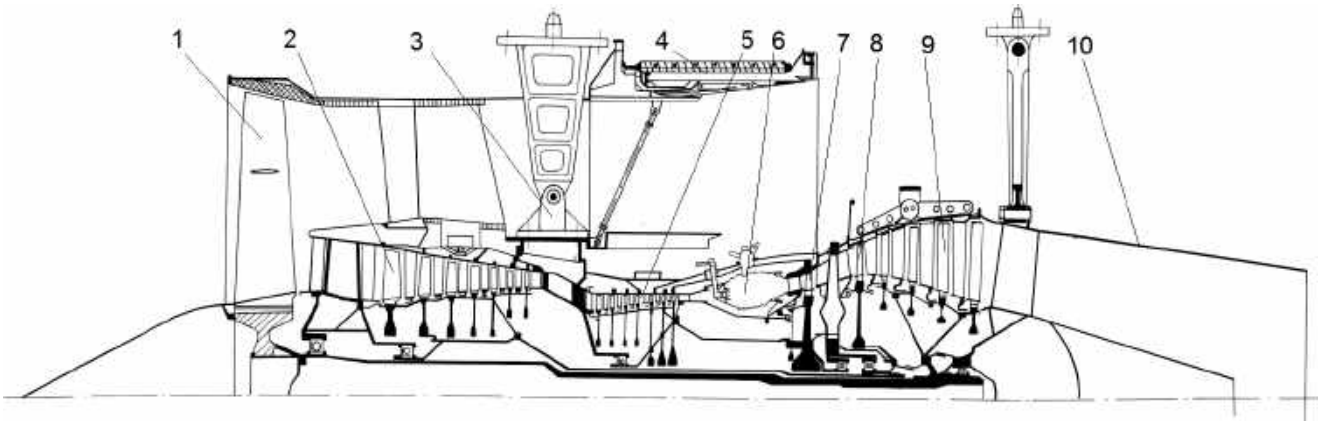


Fig. 1.9. Structural arrangement of three-spool TFE:
1 – fan; 2 – intermediate pressure compressor; 3 – separating casing;
4 – reversing system; 5 – high pressure compressor; 6 – combustion chamber;
7 – high pressure turbine; 8 – intermediate pressure turbine;
9 – low pressure turbine; 10 – jet nozzle

Single-stage fan is driven by a four-stage turbine. The air flows from the fan to the bypass and primary ducts. The IPC and HPC are driven by their own single-stage turbines. The flows are not mixed, the air of the bypass duct and the gas of the primary duct are exhausted through the non-controlled convergent nozzles.

Each rotor is supported by two bearings. The supports are equipped with elastic and damper structural members that prevent dangerous bending oscillations of rotors when the engine is running.

Fig. 1.10 shows structural arrangement of the ATJE with low bypass ratio for the supersonic aircraft. The engine has mixing flows arrangement; afterburner is placed downstream of the mixing chamber. Variable multi-mode jet nozzle provides full expansion of the gas with the minimum losses.

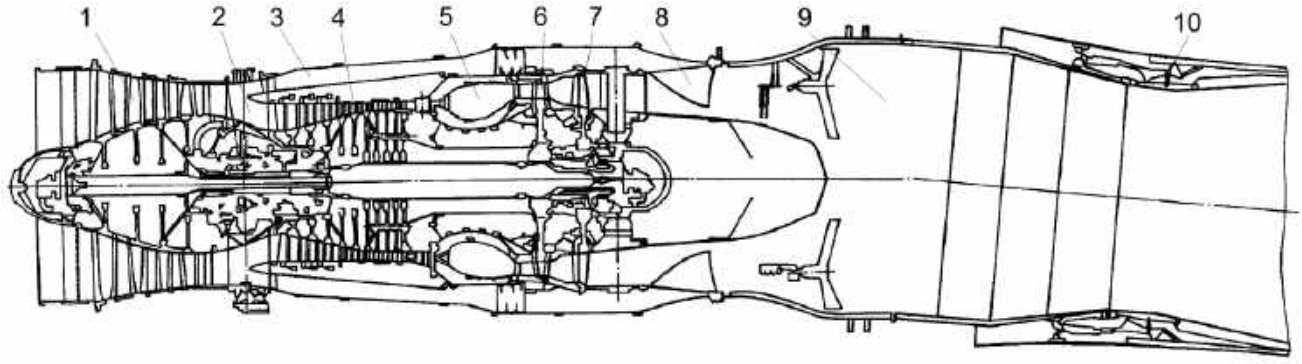


Fig. 1.10. Structural arrangement of two-spool ATJE with low bypass ratio:
1 – low pressure compressor; 2 – separation casing of compressor;
3 – bypass duct; 4 – high pressure compressor; 5 – combustion chamber;
6 – high pressure turbine; 7 – low pressure turbine; 8 – axial-flow mixer;
9 – afterburner; 10 – variable jet nozzle

Turboprop engines are the heat machines, in which the most part of effective heat power transforms into mechanical work in the turbine and drives the aircraft propeller.

The propulsor of the turboprop power plant is the air propeller that maintains high efficiency only at $M_f < 0.65$ to 0.86. At this low velocity, they are more efficient than gas turbine engines of other types. Flight altitude of airplane with the TPE not exceed 10 to 11 km.

TPE are widely used in the transport airplanes, long-distance strategic bombers and rocket-carriers, aircraft of the anti-submarine defense, and short-distance passenger airplanes. The major indices of these airplanes are the maximum specific payload, high flight distance and durability.

Power of TPE is varied from 250 kW to 11.0 MW. Specific power of modern TPE reaches 300 to 400 kW·s/kg, specific fuel consumption is 0.22 to 0.25 kg/(kW·hour), specific weight without propeller is 0.20 to 0.35 kg/kW. Presence of the propeller, hub for pitch control and gearbox complicates the engine design, automatic control and maintenance.

Structural arrangements of the TPE are differed by the following essential features: the number of rotors, displacement of gearbox and propeller, the number of propeller rows.

The most simple is arrangement of a single-spool TPE with coaxial built-in gearbox. Fig. 1.11 shows a structural arrangement of the AI-24 TPE for the An-26 airplane).

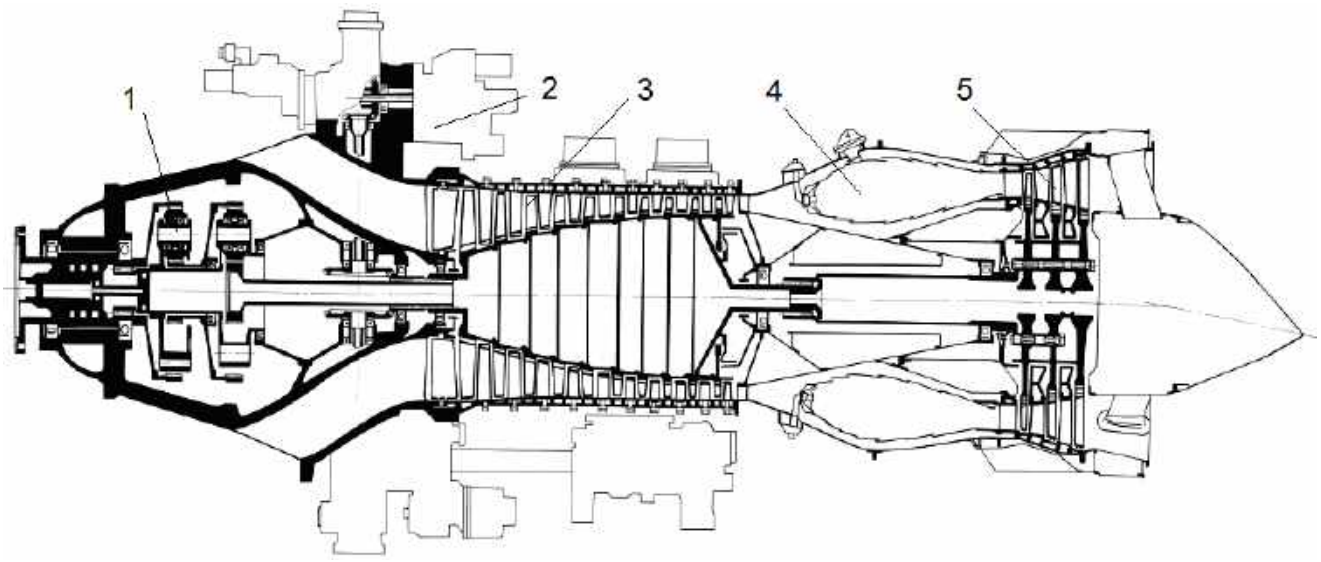


Fig. 1.11. Structural arrangement of single-spool TPE:
1 – planetary gearbox; 2 – accessory gearbox; 3 – axial compressor;
4 – combustion chamber; 5 – turbine

The advantage of a single-spool arrangement is its relative simplicity. The disadvantage is “inflexibility” of the engine control, which consists in that the required laws of control for the gas generator and propeller are essentially different and cannot be optimized in a full range of the flight conditions and power ratings. The TPE with a single-row propeller is usually used for power up to 3 500 to 5 000 kW, as at higher power the propeller is bulky and less efficient.

At higher power (up to 11 MW), arrangement with two-row coaxial propeller is used. Example of this arrangement for the NK-12 engine to power the Tu-95 and An-22 airplanes is shown in Fig. 1.12.

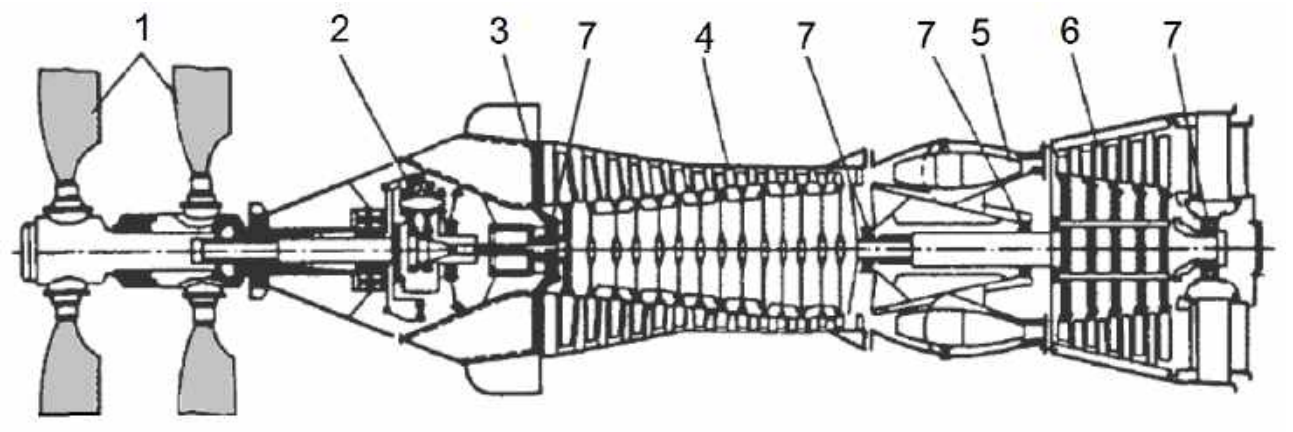


Fig. 1.12. Structural arrangement of a single-spool TPE with two-row propeller:
1 – double-row contra-rotating propeller; 2 – gearbox; 3 – air intake duct;
4 – compressor; 5 – combustion chamber; 6 – turbine;
7 – engine rotor bearings

The propeller rows are contra-rotating ones thus equalizing gyroscopic moments, which originate at the airplane evolutions, and improve blowing of engine nacelle by the air.

In this arrangement, the compressor is driven directly by a multistage turbine, and the propeller is driven through a gearbox. Front and coaxial to the engine arrangement of the gearbox complicates entry of the air into the compressor and increases external dimensions of the air intake duct.

To simplify the engine control and reduce weight of the gearbox, the TPEs with free turbine are used widely. Fig. 1.13 shows arrangement of the TV3-117-VMA-SBM1 TPE. In this arrangement, the compressor, combustion chamber and high pressure turbine compose the gas generator that supplies the hot gas to the turbine, which drives the propeller through the gearbox. The arrangement is simple in development, helps to use a low-speed free turbine that decreases a gear ratio and weight of the gearbox. This arrangement may be modified easily. At this modular design, the engine overhaul is simplified.

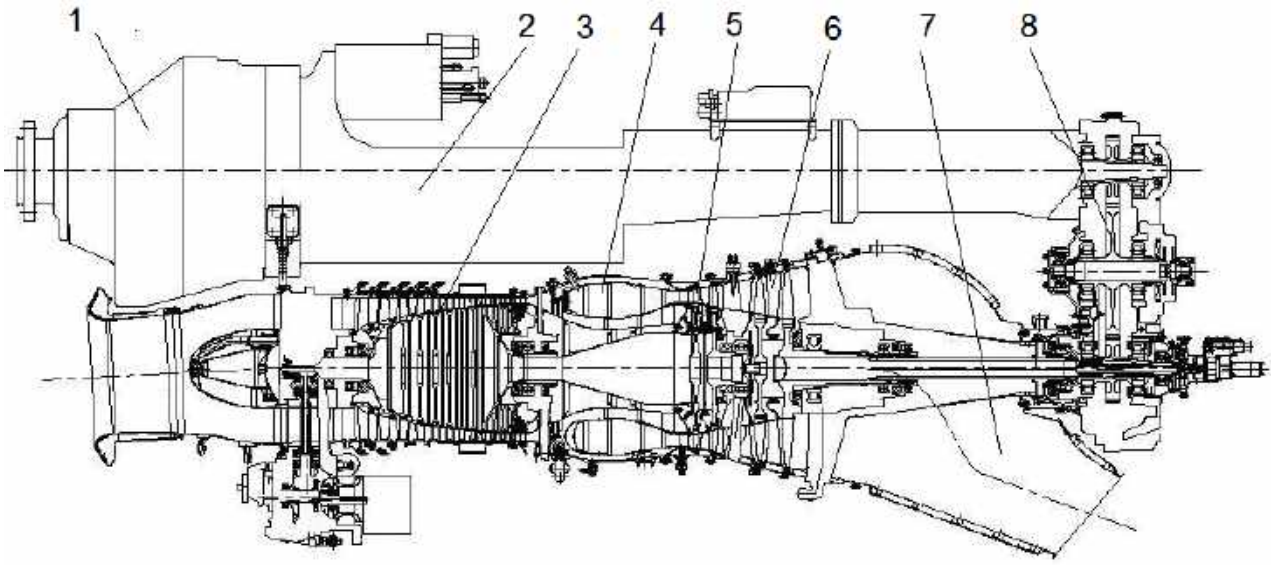


Fig. 1.13. Structural arrangement of a free-turbine TPE:
1 – main gearbox; 2 – shafting; 3 – compressor; 4 – combustion chamber;
5 – high pressure turbine; 6 – low pressure turbine; 7 – exhaust system;
8 – rear gearbox

Propeller generates the main thrust of the TPE, and a jet thrust is not more than 12 to 15 %; therefore, the non-controlled convergent nozzle is used as the TPE exhaust system.

Turbopropfan engine (TPFE) is a peculiar hybrid of the TFE with the high bypass ratio and the TPE. Fig. 1.14 shows structural arrangement of the NK-93 engine having power of 25 MW, which bypass ratio is 16. Its main difference

from the TPE is that the propeller blades are truncated and ducted. The number of the blades is twice more than the conventional propeller has.

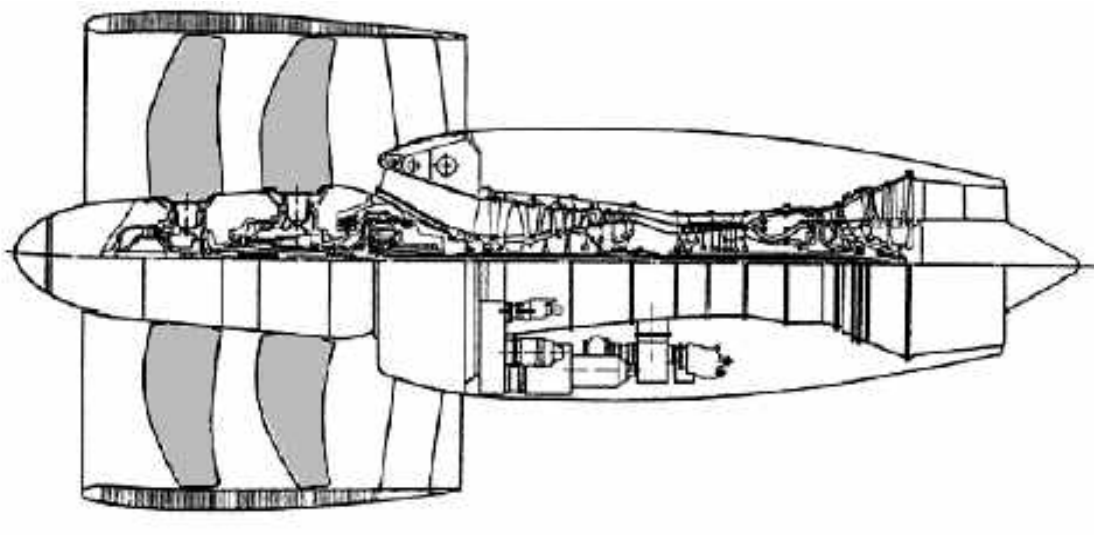


Fig. 1.14. Structural arrangement of the NK-93 TPFE

The main difference of the TPFE from the TFE with a built-in gearbox is that the propfan blades have a variable pitch that is automatically controlled. The NK-93 engine has the two-row propeller. It is driven by the free turbine, which shaft is joined to the gearbox. The differential gearbox has two output shafts, which are rotating in opposite directions.

The propfan of the TPFE is not to be ducted. For example, Fig. 1.15 shows external view of the D-27 engine. This TPFE features open-rotor propfan.

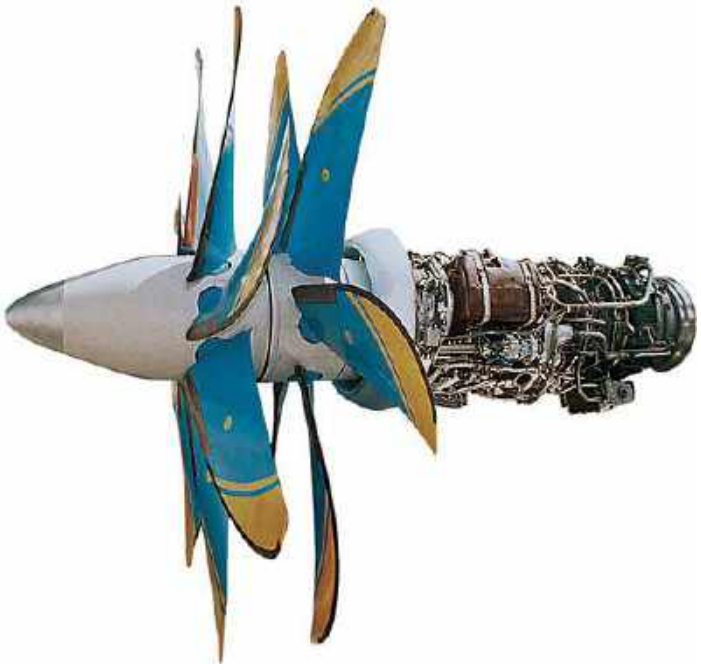


Fig. 1.15. External view of the D-27 TPFE

Turboshaft engines (TShE) are turbine engines that are powering the helicopters, operate in relatively low range of flight velocity and altitude (the velocity is 250 to 400 km/hour, and the altitude is not higher than 5000 to 6000 m). The helicopter engines have the following approximate values of parameters: power is 200 to 8 500 kW, specific weight is 0.11 to 0.55 kg/kW, specific fuel consumption is 0.22 to 0.40 kg/(kW·hour).

According to conditions of flight safety, the helicopter power plants are equipped with two turbine engines that drive a common gearbox. Design of transmission provides operation of the power plant with one engine when the second engine is inoperative.

The distinction of structural arrangement of the helicopter engines is a presence of free turbine that has not mechanical connection with the engine gas generator (Fig. 1.16 – the TV3-117V TShE to power the Mi-8MT, Mi-24, Ka-27 and other helicopters, Fig. 1.17 – the D-136 engine to power the Mi-26 helicopter). Engine is a double-shaft or triple-shaft. The gas generator contains compressor (low pressure and high pressure cascades), combustion chamber and compressor turbine (high pressure and intermediate pressure cascades). The independent rotor is the free turbine with the output shaft.

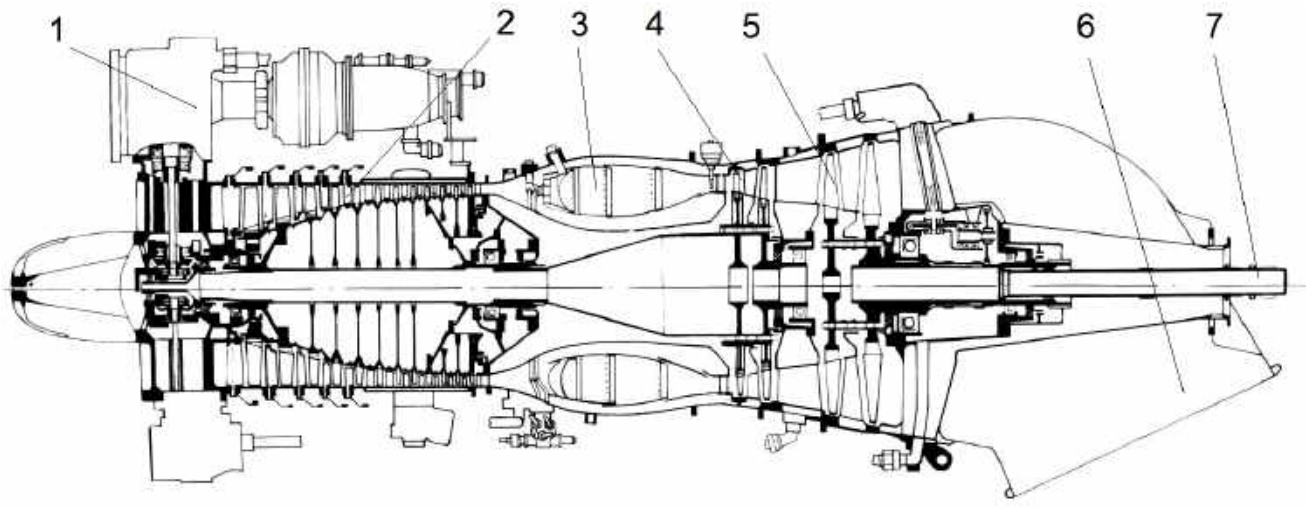


Fig. 1.16. Structural arrangement of turboshaft engine
with a single-cascade compressor:
1 – accessory drive gearbox; 2 – compressor; 3 – combustion chamber;
4 – compressor turbine; 5 – free turbine; 6 – exhaust duct; 7 – output shaft

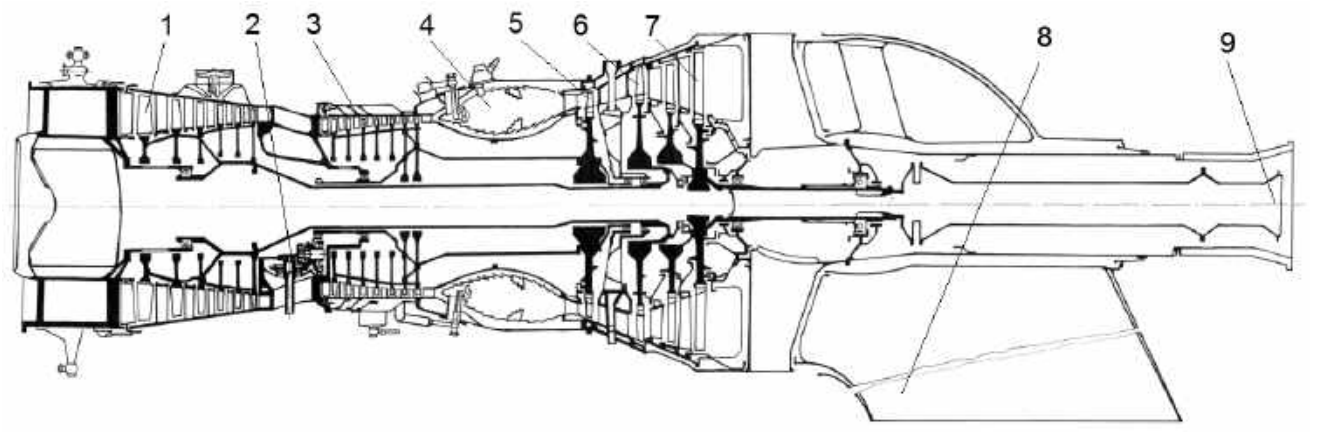


Fig. 1.17. Structural arrangement of turboshaft engine
with two-cascade compressor:
1 – low pressure compressor; 2 – accessory drives; 3 – high pressure compressor;
4 – combustion chamber; 5 – high pressure turbine;
6 – intermediate pressure turbine; 7 – free turbine; 8 – exhaust duct; 9 – output shaft

Output duct of the helicopter engine is designed as a divergent pipe that exhausts the gas from the free turbine into the atmosphere with turning of the gas flow.

Fig. 1.18 shows arrangement of the GTD-350 TShE of low power with the axial-centrifugal compressor and separate combustion chamber, which is used in the Mi-2 helicopter.

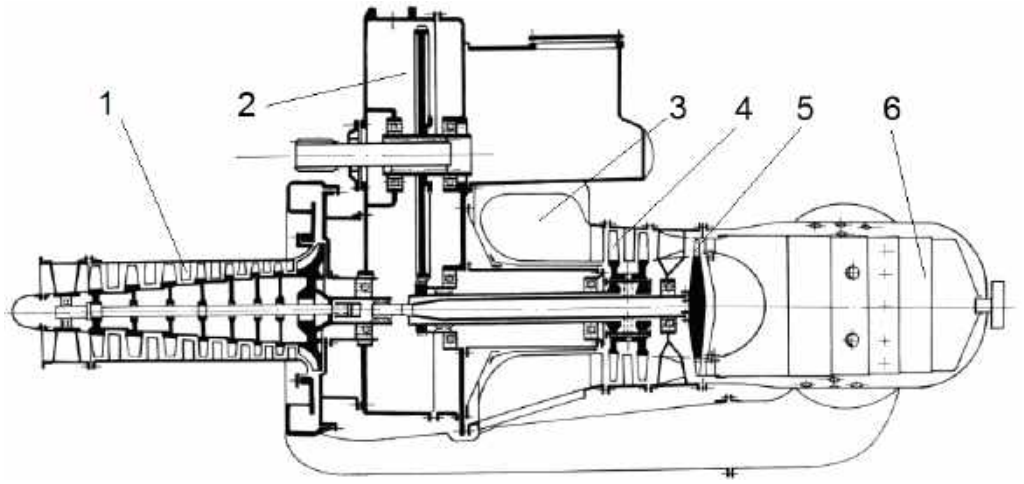


Fig. 1.18. Structural arrangement of turboshaft engine
with axial-centrifugal compressor:
1 – axial-centrifugal compressor; 2 – intermediate gearbox; 3 – exhaust duct;
4 – free turbine; 5 – compressor turbine; 6 – combustion chamber

The distinctive feature of this arrangement is the positional relationship of the compressor, combustion chamber, compressor turbine and free turbine. The air flows from the compressor through the external pipes to the individual

reverse-flow combustion chamber that is located in the rear part of the engine; the gas flows to the compressor turbine and then to the free turbine that is mounted downstream of the gearbox. High pressure shaft is located inside the free turbine shaft.

The exhaust gas is discharged with turning of the flow through the exhaust pipes that are mounted between the free turbine and gearbox.

Fig. 1.19 shows structural arrangement of engine with centrifugal compressor and loop-type combustion chamber.

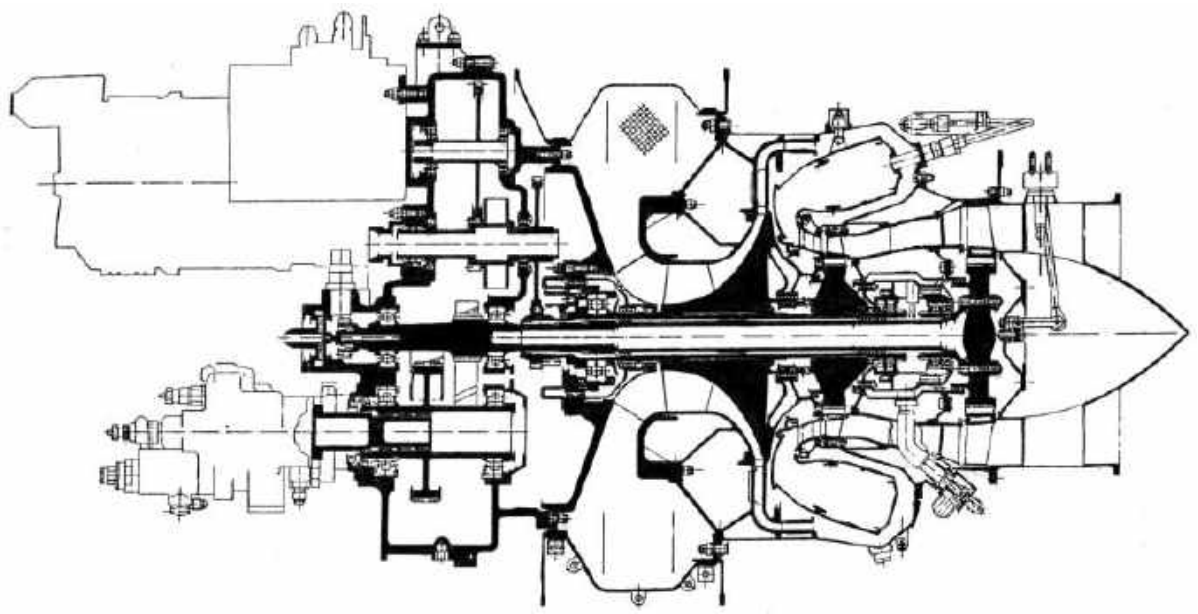


Fig. 1.19. Structural arrangement of turboshaft engine with centrifugal compressor

GTE for vertical/short takeoff and landing (VSTOL) airplanes. The aircraft that are able to vertically take-off and land (VTOL) have essential operation advantages. They are widely used in the carrier aviation. The aircraft with short takeoff at full load and vertical landing and with short takeoff and landing are also developed.

Vertical takeoff and required maneuverable characteristics of the aircraft need in engine thrust that is 15 to 20 % more than the takeoff weight of the aircraft. Therefore, the VTOL aircraft are equipped with engines having thrust vectoring or special lift engines that generate a vertical thrust at takeoff.

The lift-thrust engine generates vertical and horizontal thrust using a vectorable nozzle. The lift-thrust engine can be TJE, TFE, ATJE, ATFE. Structural arrangement of the lift-thrust TFE “Pegasus” for the “Harrier” VTOL aircraft is shown in Fig. 1.20. The engine is equipped with four vectorable nozzles. The front pair of the nozzles takes the air from the fan, while the rear pair takes the gas from the turbine.

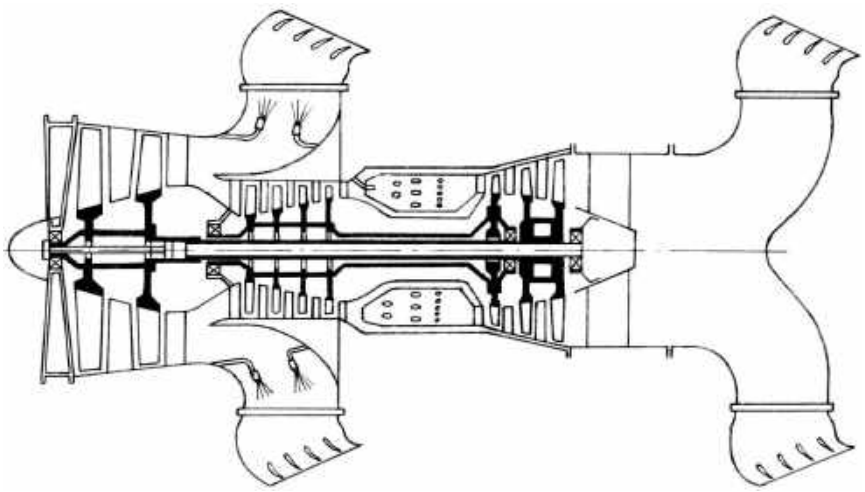
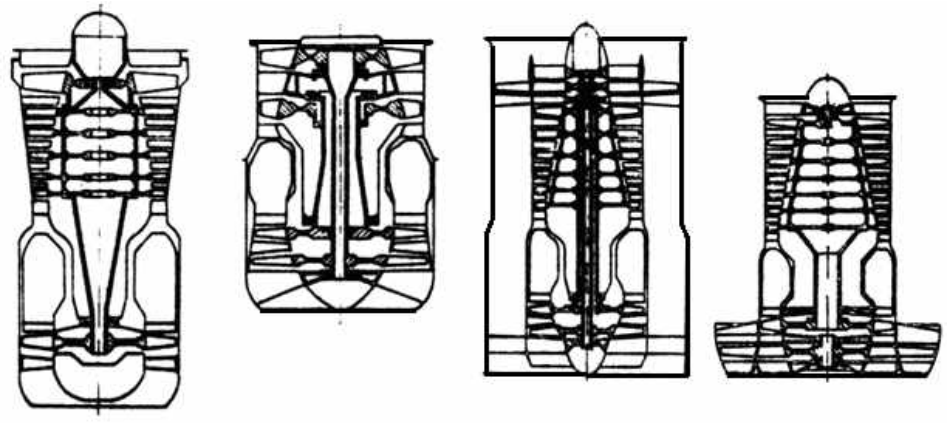


Fig. 1.20. Structural arrangement of lift-thrust TFE

Lift engines that generate only lift thrust at the aircraft takeoff are the TJE or TFE, which are mounted in the fuselage or in the wings of the aircraft. They have various structural arrangements.

The lift engines run for a short period of time, only at takeoff and landing; in flight, they are inoperative and in fact are the aircraft ballast. Therefore, their structural arrangement must meet specific requirements. The lift engines have a compressor with small number of stages, shortened combustion chamber and jet nozzle, two-support rotors, simplified lubrication and fuel supply systems. The engine starts reliably without starter by the hot air or the gas that is supplied directly to turbine. The structural parts have lowered safety factors and are made of the light materials (fiberglass plastic, titanium alloys, or composite materials).

The lift engines may be single-shaft or two-shaft TJE and TFE with front or rear displacement of the fan (Fig. 1.21).



a *b* *c* *d*

Fig. 1.21. Structural arrangements of the lift GTE:
a – single-shaft TJE; *b* – two-shaft TJE; *c* – TFE with front fan;
d – TFE with rear fan

Approximate parameters of the lift GTE are given in Table 1.3.

Table 1.3

Main parameters of the lift GTE

Parameters	Lift GTE	
	TJE	TFE
Thrust P, kN	10 to 50	10 to 50
Turbine inlet temperature T^*_g, K	1 400 to 1 600	1 400 to 1 600
Bypass ratio m	–	4 to 12
Specific thrust P_{sp}, kN·s/kg	0.80 to 0.95	0.18 to 0.35
Specific fuel consumption, kg/(N·hour)	0.110 to 0.125	0.04 to 0.06
Specific weight, kg/N	0.004 to 0.010	0.006 to 0.012

Auxiliary power units (APU) are widely used in aviation. They are designed based on the GTE having small dimensions. They do not generate thrust, but they are used as on-board sources of mechanical power, electric power, hot compressed air etc. The APU includes the following:

– gas turbine starters of thrust engines;

– electric turbine-generator power plants for supplying electric power of electric starters during starting of the main engines, of the on-board electric system supplying with direct and alternating current when the on-board systems checking and when preparing the aircraft for flights;

– generators of the compressed air for the air starters, air conditioning, warming of the main engines before starting in cold season.

The APU is featuring simple design and maintenance, low weight comparing to another types of the GTE. The APU run for a short period of time, so they don’t need to meet strong requirements to fuel efficiency, as a rule.

Centrifugal and diagonal compressors, annular combustion chambers, axial-flow and radial centripetal turbines, simplified lubrication, starting and fuel systems are used in the APU design. Application of these component parts and systems determines convenience of the engine arrangement, the minimum dimensions and weight, reliable operation and convenient maintenance at satisfactory indices of the operating process.

Fig. 1.22 shows a structural arrangement of the TA-8V auxiliary power plant with centrifugal compressor and radial centripetal turbine, which is a source of electricity and generator of the compressed air for the Mi-26 helicopter.

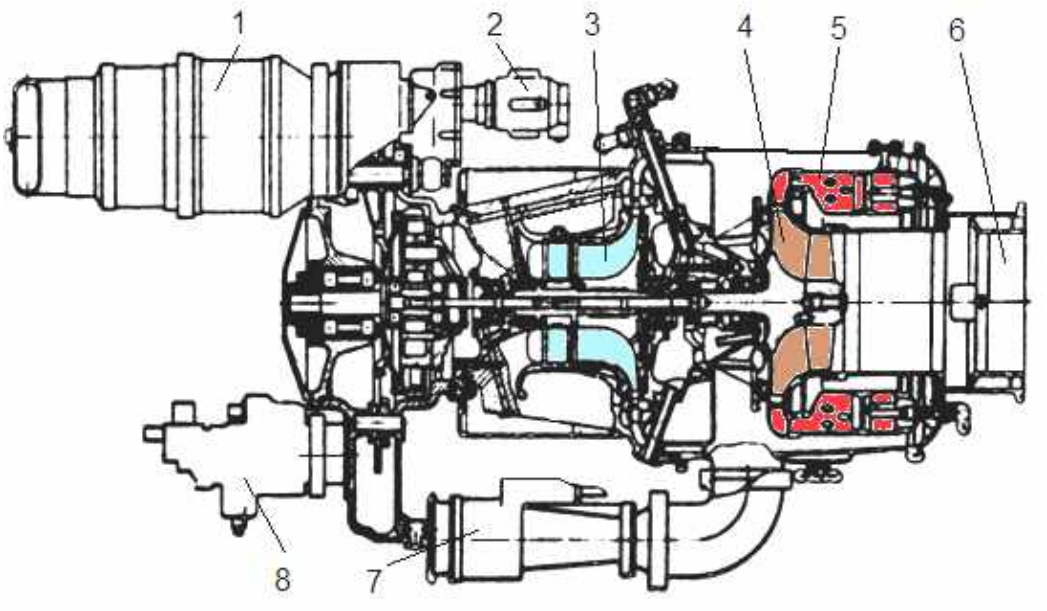


Fig. 1.22. Structural arrangement of the TA-8V auxiliary power unit:
1 – electric generator; 2 – tachometer generator; 3 – centrifugal compressor;
4 – centripetal turbine; 5 – loop-type combustion chamber; 6 – exhaust pipe;
7 – air bleeding pipe; 8 – fuel control pump

1.3. General engineering requirements to the aero engines

Engineering requirements to the aero engines include general requirements that summarize experience of application of different types of engines, and an engineering specification to the designed engine that take into account properties of the aircraft, in which the engine will be used. Maintenance conditions are also taken into account. Quantitative indices must provide the best qualities of the aircraft-engine complex.

Structure of the aero engine is defined by the requirements to it.

The requirements are conditionally subdivided into three groups:

– requirements of high engineering efficiency (type of power plant, the number of engines, efficiency, weight and geometric characteristics, reliability, service life);

– production and technological requirements (simple and technological structure, low production cost, high level of manufacturability);

– maintenance and repairing requirements (high maintainability and repairability, the minimum expenses of materials, labor, means and time for engine engineering service and repairing).

One of the main engineering requirements to the specific engine is the minimum environmental adverse effect.

Let’s consider in details the main requirements to the aero engines.

Reliability

Reliability is one of the main requirements, as it determines a flight safety and faultless achievement of goal. Level of reliability is one of the major criteria of the engine quality.

The reliability is a complex property of the engine, which includes faultness, durability, storegeability and repairability.

Level of the reliability is characterized with the quantitative indices that are determined by the statistical data and numerical analysis. It is specified in the engine designing, is ensured in its manufacturing and is supported in maintenance.

Example. Fighting readiness of the military aircraft must be not less than 95 %. When faultness of 60 attack planes of Great Britain Air Forces decreased from 95 to 83 %, they were need to buy additional twelve aircraft and increase maintenance expenses during 10 years at total cost that is 1.5 times higher than that of these 60 aircraft.

Methods of a required reliability ensuring are the following:

– easy access to the most damaged elements;

– application of on-board and on-ground inspection tools that estimate the engine state and predict its reliability;

– backing-up the most significant and the least reliable structural members;

– lowering of the number of joints with the rubber and other contact seals;

– application of the automatic control, safeguarding and limiting devices that exclude the engine operation at dangerous power ratings;

– use of the up-to-date production processes and non-destructive testing methods during manufacture;

– finding the least reliable structural members during maintenance and when carrying out respective preventive maintenance operations;

– accurate testing and upgrading of the engine as a whole.

Overall dimensions

Requirements to the overall dimensions of the engine are related with the convenience of its mounting on the aircraft. Overall diameter of the engine (maximum diameter of casing or flange) is a significant parameter, because it affects dimensions of the engine nacelle, hence its drag and weight. The design diameter of the compressor intake and the design shape of the engine gas flow duct affect the value of the overall diameter. All these parameters depend on the engine arrangement and also depend on the designer’s choice.

Small length of the engine is also a significant index of its quality, since it decreases a weight and volume of the engine and increases the aircraft payload.

The requirements to the overall dimensions are met at the designing stage. For example, the outline drawing is agreed with the aircraft designer. The drawing contains information about the maximum diameter and length, contours of accessories, and engine mounting assemblies.

Engine thrust

The engine thrust must be sufficient for required flight conditions at the specified climatic conditions. Perfect will be the engine that has higher specific thrust, i.e. generates required thrust at the minimum weight and fuel consumption.

Engine weight

Overall engine weight is a total weight of separate assemblies and parts. Values of the engine weight and weight of its assemblies and parts are presented in design documentation and are checked when manufacturing, assembling and delivering to the customer.

Engine weight affects the aircraft payload. For example, the practices showed that each excess 1 kg of the engine weight increases the aircraft weight 3 kg.

The engine weight can be decreased at the specified thrust by using some methods. One of them is a choice of a structural arrangement of the engine and its major assemblies. The second method is improvement of the applicable materials, introduction of new materials with higher strength-to-density ratio. Light-weight aluminum, magnesium and titanium alloys are widely used in low-temperature portion of the engine. The third method is a rational designing of all engine parts and their structural members with weight decreasing.

Specific weight

Specific weight of the designed engine should not exceed the specific weight of the best maintained engines of the same type. According to the preliminary estimations, the specific weight of the structurally similar engines, which have the same mechanical and thermal strength and differ by the absolute dimensions, is changed in accordance with the ratio of their inlet diameters in power from 2 to 3. Their thrusts are proportional to squares of diameters. Hence, if the engine dimensions decrease then the specific weight will be decreased. However, it is true only up to a known limit, when proportional decreasing of the dimensions and weight of all parts and accessories becomes impossible.

Specific fuel consumption

Requirement to the specific fuel consumption is of the same significance because it influences the engine efficiency and corresponding performance parameters of the aircraft, flight distance and flying time. The aircraft designer depending on the aircraft functions and assumed performance parameters establishes the values of specific fuel consumption.

Implementing of this requirement consists in corresponding choice of parameters of the operating process and design methods of engine components' efficiency increasing due to lowering of gas-dynamic and heat losses in the engine gas flow duct.

As usual, when the specific fuel consumption decreases due to complication of the engine structural design, the specific weight is increases. Weight of the engine, fuel and fuel tanks determines the weight of the power plant and aircraft. Therefore, the aircraft designer specifies requirements to the specific fuel consumption based on optimization of the general arrangement of the aircraft in cooperation with the engine designer.

Specific thrust

Requirement to the specific thrust at the specified absolute thrust determines the air consumption that is highly dependent on the engine overall dimensions. The fuel consumption affects not only dimensions and weight of the engine but it affects also the dimensions of the engine intake and power plant. The higher is the specific thrust, the less is the air consumption, weight and dimensions of the engine and power plant.

Manufacturability

Requirement of the engine manufacturability means lowering of its production cost by decreasing labour expenses of manufacturing, assembling and testing. Manual labor must be excluded, if possible. This requirement is significant alone and becomes even more significant in case of long-term series production.

The requirement of manufacturability is expressed in a value of permissible labour intensity of its production in man-hours and by a rate of the labour intensity decreasing in the following series production.

Implementation of this requirement begins from the engine designing and needs in continuous creative cooperation of the designers and process engineers.

The engine must have a simple structural arrangement that is oriented on the advanced methods of manufacture. Machining must be substituted with more productive technological processes – stamping, precise investment casting, rolling, powder metallurgy, and friction welding.

Application of the advanced technologies for the blanks production depends on a designed configuration of the part.

Stock utilization ratio (SUR) is a ratio between the weight of produced part and that of the blank. It is an important index of manufacturability. The values of SUR are specified in the drawings of the engine parts.

Cost of development

Cost of modern aircraft and engine development reaches huge values. For example, actual cost of supersonic bomber B-1 development in 1974 was 2.7 billion USD, and a cost of series aircraft in 1976 was 100 million USD. Cost of a series supersonic aircraft F-15A in 1982 was 19.3 million USD, expenses on its development exceed 1 billion USD. Cost of the engine development is about 18 to 35 % of the cost of aircraft development. In absolute values, the cost of aircraft engines development is about 200 to 800 million USD.

Company Lockheed Martin (USA) spent more than 60 billion USD on modern aircraft F-35 Lightning II. Currently, cost of one airplane is 160 million USD and is planned to be decreased to 100 million USD. Cost of Pratt&Whitney engine F-135 is 106 million USD, it is planned to be 19.9 million USD in series production.

Service life

The engine service life is its operating time with the specified performance parameters and required reliability. The service life is specified at designing stage taking into account the engine purpose. The service life of short-life engines is several hours; the service life of engines for passenger and transport airplanes is some thousands hours. Sometimes, the life is specified as the number of flight cycles (starting – operation – shutdown). The service life is approved by testing. The service life is increased slowly, step-by step. The designer determines it during strength analysis of all assemblies and parts. All OEM assemblies determine the life, including shafts, turbine blades and discs, bearings etc. There are differed assigned service lives: the first overhaul period, time between overhauls (TBO) (to the second overhaul, etc.), and assigned total service life that is a sum of the overhaul periods.

Maintainability

Requirement to the maintainability means the minimum labour expenses in man-hours for engine maintenance beginning form the engine mounting in the aircraft, accomplishment of all scheduled maintenance operations and engine removal. To satisfy this requirement, the engines are designed with due regard to the accessibility of the compressor and turbine blades for inspection and repair. This requirement also means easy access to the accessories for replacement and adjustment.

Implementation of this requirement begins at the stage of the GTE project and then it is tested on the mockups of the engine and aircraft and in the course of engine maintenance.

Vitality

Requirement of vitality means ensuring the engine ability to operate at most probable faults for helping the aircraft to execute the flight task. This requirement is implemented during engine designing by possible protection of the most vulnerable places, for example, servicing lines, and by designing standby systems (fuel, anti-surge, etc.).

Requirement of the minimum environmental impact

Requirement of the minimum environmental impact is first of all related to the engines of the civil aircraft and consists in limiting engine noise at takeoff and landing, harmful emissions (carbon monoxide, hydrocarbons, and nitrogen oxides) and smoke. This requirement is implemented during designing of the engine assemblies, noise suppression units, smokeless combustion chambers etc. Strong International Norms of ICAO are directed on flight safety improvement and harmful emissions decreasing that act the environment. According to the Norms, every new engine type is subject to checking tests, including stones, sand and bird ingestion; the designed casing parts should withstand impact of broken rotor blades, etc.

1.4. Role of strength analysis, experimental researches and similarity theory in engine development

Engine development process consists of two main stages:

– engine designing;

– engine manufacturing and introduction into a serial production.

Before designing, some problems must be solved:

– choosing structural arrangement, which is a basis of implementation of the chosen gas-dynamic arrangement with ensuring conditions of strength, vibration safety, reliability and maintainability;

– determining engine power diagram, transmission of forces and moments (for example, from the rotor to casing), joining major assemblies, and strength analysis;

– determining arrangement of the engine mounting in the aircraft, and main forces and moments affecting the mounts (these values are required according to the Norms of Aviation Rules AR-33 for the engine certification and are used by the aircraft designer);

– meeting main engine performance requirements (Draft Proposal, Airworthiness Standards, AR-33, FAR-33);

– implementation of modular design.

One of tasks of the GTE designing is ensuring the minimum cost of the engine life cycle.

The engine designer must also ensure a strength balance of the engine assemblies and structural elements at the specified reliability. In this case, the engine weight will be as minimum as possible.

This task is solved at the stage of strength analysis, which goal is determining of the optimum dimensions of the parts that meet Norms of Strength.

The strength analysis may be done in two ways:

– ***design analysis***, which determines geometric parameters (for example, cross-sectional areas) of the part by using chosen materials, specified safety factors, and applied loads;

– ***revise analysis***, which determines the applied stresses and safety factors, and one makes conclusion about the part operability, reliability and service life for the part with the specified geometrical dimensions with chosen design material (the revise analysis is reverse to the design analysis).

The revise analysis is usually performed for the parts, which geometry was already determined by previous calculations and is fixed (for example, for airfoils of the compressor and turbine rotor blades that are determined at the stage of aerodynamic designing).

The design analysis is usually performed for the parts, which geometry was not determined in previous calculations and may be varied within some limits, which depend upon conditions of assembling and adjacency (for example, rotors, discs, etc.).

The strength analysis is performed for the engine power ratings that are the most unfavorable ones (for example, for turbine this is the power rating that corresponds to the maximum gas temperature and maximum rotation speed of the rotor; for compressor this is the power rating with the maximum air flow, etc.). There is expedient to ensure the best indices of any engine at power ratings for its main application (for example, at cruise flight of the passenger airplane). Hence, the main power ratings may be not dangerous for the strength of the engine parts. Therefore, the strength analysis is performed for some main and high-duty power ratings.

Engine strength and functional limitations may limit conditions of the aircraft application. For example, the compressor outlet air pressure shall not exceed the maximum permissible one, which is limited by strength of the combustion chamber casing. These limitations may be required for the maximum duration of the engine continuous operation at take-off power rating, the maximum turbine inlet temperature, the gas load affecting the compressor rotor blades, the maximum rotation speed etc.

Fig. 1.23 shows a range of altitudes and flight velocities of the aircraft, and possible limitations of the aircraft flight performance parameters that constrained by the engine.

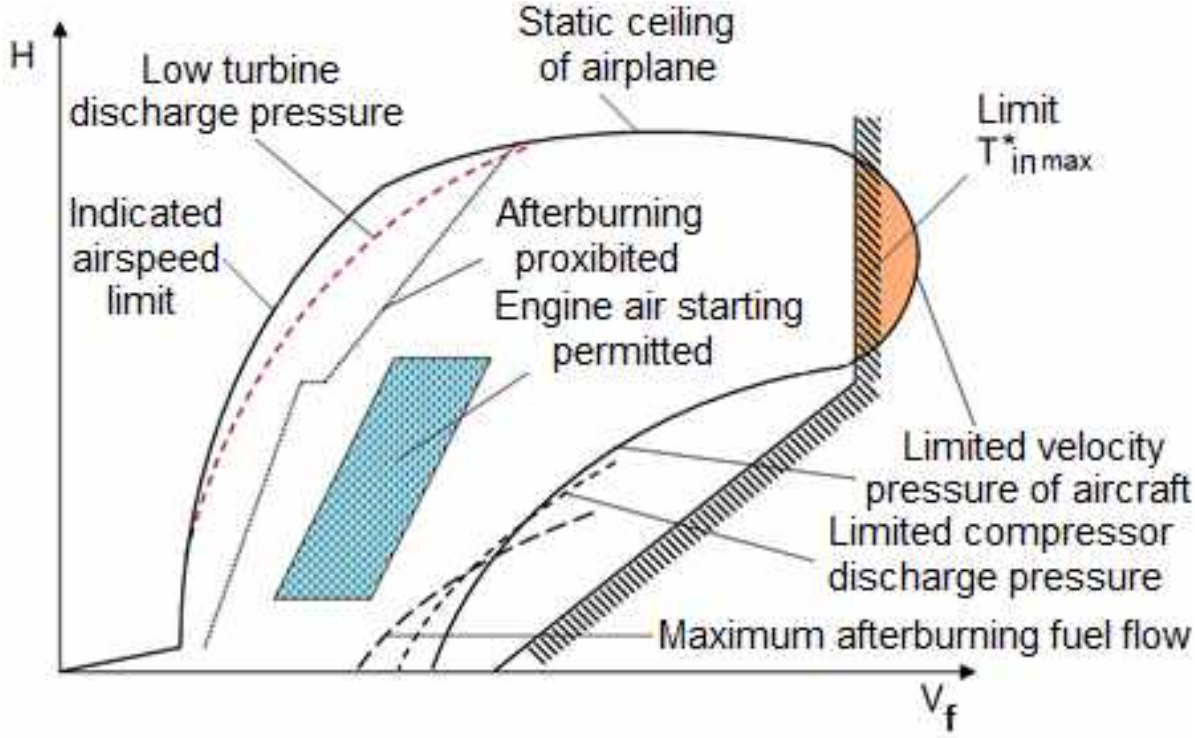


Fig. 1.23. Constraints of aircraft flight performance parameters that are imposed by the engine

Low turbine exhaust gas pressure limitation originates at low flight velocity, when the air pressure increases in the intake duct lightly by the ram air; hence, the compressor outlet air and turbine exhaust gas pressure will be also low. Naturally, actuation of the afterburner at this power rating will have no sense.

Velocity head limitation is related to heating of the aircraft structure and action of high gas loads on it. The air that enters the compressor is also highly heated. When the air is broken in the intake duct and is compressed in the compressor its temperature increases additionally and may exceed the permissible limit.

The air pressure and velocity head are the maximum ones at low altitude, maximum velocity and minimum atmospheric temperature. This is the mode of the maximum airflow through the engine. The compressor discharge pressure will be also high and may exceed strength limitations of the combustion chamber casing. At this mode, fuel flow may also exceed the maximum limit when the afterburner will be actuated.

The engine in-flight starting is performed at the windmilling mode. At high altitude, the air density is low. Therefore, the rotor will not reach a rotation speed that is required for starting. Deficiency of the oxygen and loose of stable ignition by the air/fuel ratio will complicate ignition of the combustion chamber. At high velocity, ignition of the combustion chamber will be complicated due to high velocity in its flameholder and it will result in flameout. Therefore, the in-flight starting in performed at indicator flight velocity v_{ind} = 550…650 km/hour at altitude up to 8 km (up to 10 to 11 km with oxygen replenishment). Starting is prohibited at altitude less than 2 km according to safety conditions (the crew must have reserve of altitude to leave the aircraft when starting is impossible).

It is impossible to take into account all factors that affect strength of many engine parts, especially under conditions of vibrations. Besides, many engine parts have intricate geometric shape. Therefore, precise strength analysis using analytical relations is impossible. It these cases, calculations are done using numerical methods (finite differences, finite elements methods, etc.). Comparative analysis and experiments with models and natural prototypes are helping the designer.

When carrying out the comparative analysis, the stresses in the designed engine are compared with those in the similar parts of the prototype engine, which showed itself perfect during maintenance.

At the stage of engine designing, the great help for the designer gives the Theory of Similarity that ensures preliminary estimation of parameters of the designed engine knowing information about the geometrically and gas-dynamically similar prototype engine.

The following relations are true for these engines:

– weight-to-weight ratio is proportional to a ratio of cubic value of their diameters;

– thrusts-to-thrust ratio is proportional to a ratio of square value of diameters;

– centrifugal forces of the rotor structural elements at similar points, which have the same circumferential velocities, are proportional to square value of their linear sizes: $P_{c1}/P_{c2} = D^2_{C1}/D^2_{C2}$, and stresses in similar points are equal; the same is related to the gas forces and stresses caused by them.

Theory of Similarity becomes especially significant in connection with introduction of designing of new engines based on the well-developed base gas generator.

Before the engine designing begins, the aircraft designer presents the Draft Proposal (DP).

DP contains the following information:

– engine purpose;

– its main performances;

– the major engineering requirements to the engine and quality indices;

– engineering, economic and social requirements that are related with the expected maintenance conditions of the designed engine.

The engine designing process includes the following stages:

1. ***Engineering proposal*** of the engine designer that is a collection of design documents, which contain engineering and engineering-and-economical grounding for designing of the new engine. It is developed based on analysis of the DP requirements, and taking into account the preliminary calculations and design studies.

2. ***Draft design*** is a more complete design of a chosen variant of the engine arrangement with all assemblies, which includes required calculations and choice of the optimum arrangement of the engine assemblies.

3. ***Engineering design*** is issued after approval of the draft design by the aircraft designer. This is a collection of the design documents representing final engineering solutions that are initial data for development and issue of the project documentation in full capacity.

4. Issue of the ***project documentation*** is the final stage of designing. It is done taking into account the specific production process to manufacture and testing of the engine, its assemblies and systems. Composition of the project documentation is determined by the branch standard and it includes the following:

– drawings (installation, component, detailed);

– engineering requirements to manufacture of the engine, its assemblies and parts;

– instructions;

– methods of testing;

– chemotological chart of the fuels and lubricants to be used;

– engine maintenance manual etc.

The engine full-size mock-up is manufactured and used for rational displacement of its accessories and servicing lines. It is also coordinated with the mock-up of the designed aircraft jointly with the customer.

The engine manufacturing begins from three to four experimental copies, which are subjected to the following tests:

– factory tests (on-the-ground and flight);

– some long-time benchmark tests for checking strength and reliability;

– special tests for approving engine compliance with the specified engineering requirements;

– climatic vacuum chamber tests;

– flight tests in the flying laboratory;
– flight tests in the aircraft;
– condition testing (on-ground and in-flight);
– maintenance testing.

Serial production of the engine begins after positive results of the condition testing. Sometimes, separate stages of different tests are overlapped for shortening of time-frame.

When a serial production begins, the service life of the engine for the civil aviation is usually at least 500 hours. With the purpose of establishing (approving) of assigned service life and overhaul periods, the engines are subjected to leader (accelerated) tests; running time of the leader engines 1.5 to 2 times advances the running time of engines in series maintenance. In further, the service life is increased based on the results of reliable operation of the leader engines. Every increasing of the service life needs drawing up of corresponding resolution, which shall be approved by the central governing body of the Ministry, by the Customer's representative, and by the Civil Aviation Research Institute.

Increase of service life of the vendor items, which are used as component parts of the engine is the necessary condition for increasing the engine service life (accessory units, having not sufficient service life, must be relocated).

The engines may be subjected to special testing to confirm efficiency of operations carried out at the engines (upgrading, improvement according to Service Bulletins, etc.).

Series engines are subjected to factory delivery routine check testing.

1.5. Forces and moments affecting assemblies of gas turbine engine

The main forces affecting the assemblies of the gas turbine engine when it is running may be subdivided into three groups:

- forces *caused by action of the gas loads*;

- *inertial forces originated by the rotor rotation, changing flight velocity, and aircraft evolutions*;

- *temperature loads caused by nonuniform heating of the engine parts and assemblies and engine as a whole.* Some of these forces and moments are compensated inside but some of them are transmitter to the neighboring assemblies and to the aircraft design structure via the engine mounts (for example, engine thrust tie rods).

The causes of origination of the forces and moments of various nature as well as resulting stresses in the engine structural members will be described in details in the respective chapters of the present course.

Resultant moment, transmitted to the mounting units, turns aircraft and needs compensation by moment of aerodynamic forces created by special construction or by aircraft controlling.

1.5.1. Classification of loads that affect the gas turbine engines

All loads that affect the gas turbine engines may be classified by several features. Given below, are the features presented in this classification.

On deformations behavior:
- ***tensile*** and ***compressive*** forces (caused by gas pressure or centrifugal forces of rotated weight);
- ***bending*** moments (caused by gas forces, weight or inertial forces);
- ***torsion*** moments (caused by action of gas on rotor blades and stator vanes).

On direction: – forces:
- ***axial***;
- ***radial***;
- ***circumferential.***

Moments:
- ***bending;***
- ***torsion.***

On reason of initiation:
- caused by action of propulsive ***mass*** (air and gas);
- caused by forces of ***inertia*** (of rotated rotor and aircraft overloads during maneuvers);
- ***thermal*** origin (caused by non-uniform heating or by difference in thermal expansion factors of joined components).

On variation in time:
- ***stationary;***
- ***dynamic.***

A part of these loads is localized inside the engine, another part is transmitted to the adjacent assemblies and to the aircraft through the engine mounts (for example the engine thrust).

The forces and moments of various nature and stresses in the engine structure that are originated by these loads will be considered in the respective chapters of this course.

1.5.2. Force of the gas static pressure

The force of gas static pressure P_{st} is a product of absolute or access pressure on area on which this pressure is affecting:

$$P_{st} = p\,F \text{ or } P_{st} = \Delta p\,F.$$

This force acts the wall of the casing. The example is the force affecting the outer casing of the combustion chamber of the TFE (Fig. 1.24). Outside pressure $p_{F\,II}$ is low, inside pressure p_C is high. Thus, the casing is pressurized from inside.

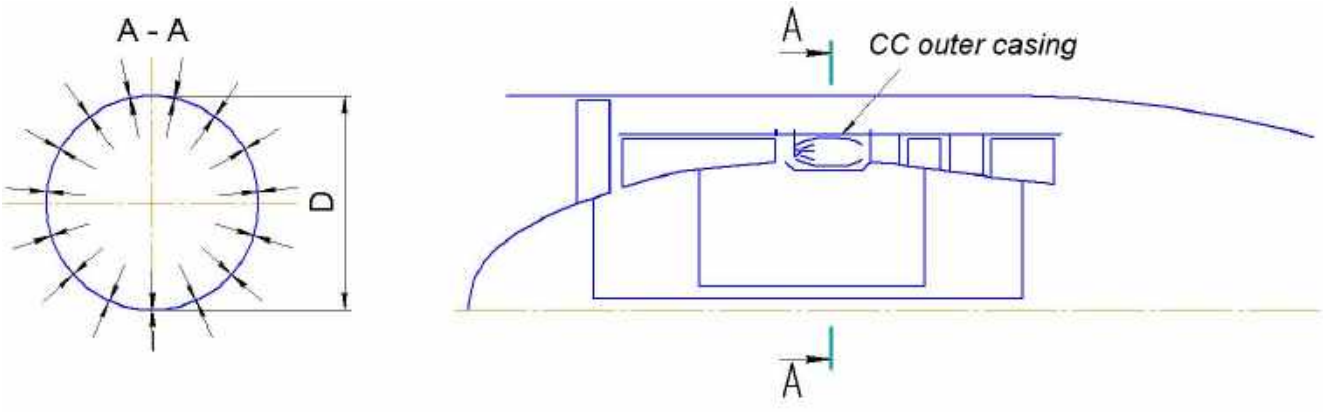


Fig. 1.24. Loads affecting the external casing of the combustion chamber

1.5.3. Force of the flowing gas dynamic action

This force is equal to a vector difference of momentums:

$$\vec{P}_d = G\vec{w}_2 - G\vec{w}_1.$$

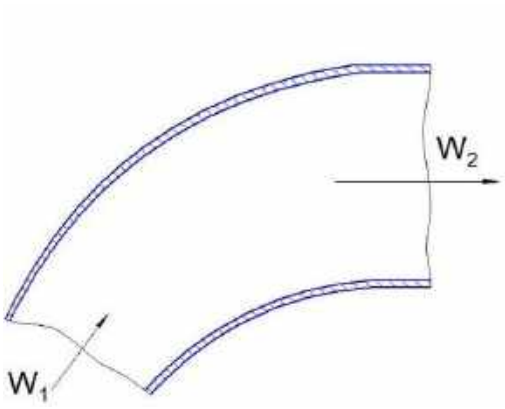


Fig. 1.25. Diagram of curved duct

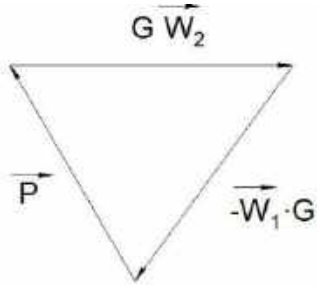


Fig. 1.26. Force affecting curved duct

In a direct duct, $P_d=G(w_2-w_1)$, so this formula gives the nozzle thrust at full expansion: $P=G(c_N - v_f)$.

1.5.4. Gas forces that affect the different assemblies of the gas turbine engine

Force affecting the intake duct

Let's consider the intake duct, which diagram is shown in Fig. 1.27. The output area is larger than the input one. Therefore, the air is decelerated in this duct and its static pressure builds up. So, $w_2 < w_1$ and $p_2 > p_1$.

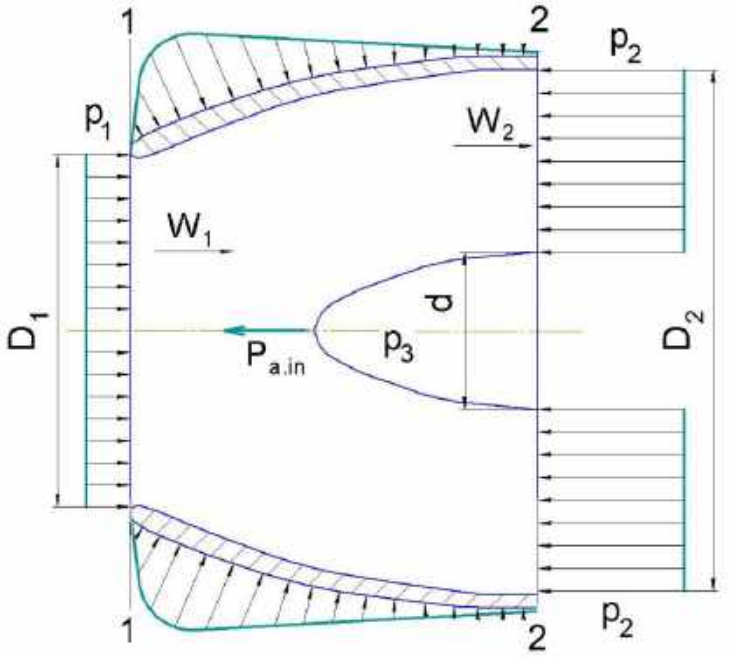


Fig. 1.27. Diagram of intake duct

Resultant axial force of static pressure:

$$P_{st} = p_2F_2 + p_3F_3 - p_1F_1,$$

where $F_1 = \frac{\pi D_1^2}{4}$; $F_2 = \frac{\pi(D_2^2 - d^2)}{4}$; $F_3 = \frac{\pi d^2}{4}$.

Dynamic force:

$$P_d = G(w_2 - w_1).$$

Total force:

$$P_{0\,in} = P_{st} + P_d = p_2F_2 + p_3F_3 - p_1F_1 + G(w_2 - w_1).$$

This force is affecting the internal wall of the duct and external wall of a cowl (these structural members are joined together by the radial aerodynamic struts). Total force affecting the flange, which joins the inlet duct with the compressor casing, is equal to internal force $P_{0\,in}$, plus external force, which is equal to the integral of the external gas pressure on the outer surface of intake duct.

Force affecting the inner surface of the curved pipe

In a curved pipe (Fig. 1.28), the flow changes its direction, thus generating a side reaction force. In general case, the flow velocity and pressure can also change their values, it the duct is of variable area.

The total force affecting the pipe is a sum of the static and dynamic components:

$$\vec{P} = \vec{P}_{st} + \vec{P}_d = \vec{p}_2 F_2 + \vec{p}_1 F_1 + G(\vec{w}_2 - \vec{w}_1) =$$

$$= (\vec{p}_2 F_2 + G\vec{w}_2) + (\vec{p}_1 F_1 - G\vec{w}_1) = \vec{P}_1 + \vec{P}_2.$$

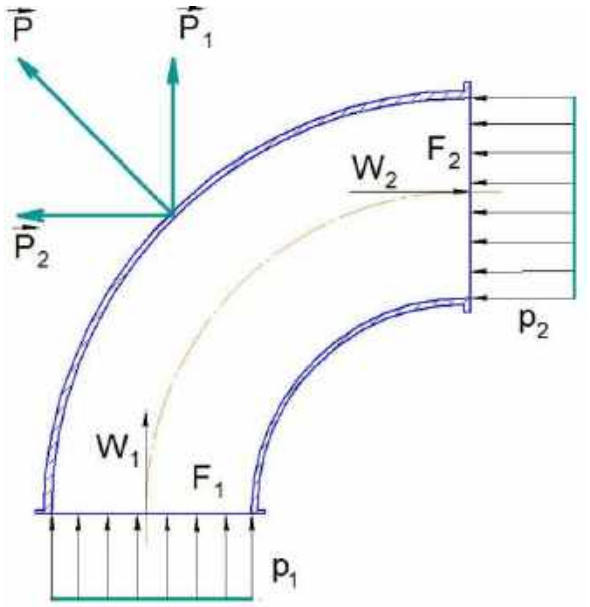


Fig. 1.28. Curved pipe

Force affecting the axial compressor rotor

Fig. 1.29 shows the example of the three-stage axial compressor. The air is compressed from inlet pressure p_{in} to outlet pressure p_C. The compressor is equipped with unloading pressure balance cambers that are sealed from the gas flow duct by the labyrinth seals. The front unloading camber is connected through the external pipe with the compressor outlet, while the rear unloading camber is communicated with the atmosphere, and pressure in this camber is p_0.

Radial shape of the compressor depends on its diameters:

- D_1 is diameter of the front seal;
- D_2 is inner diameter at the inlet;
- D_3 is diameter of the rear seal;
- D_4 is inner diameter at the outlet;
- D_5 is peripheral diameter (the considered is designed with constant peripheral diameter).

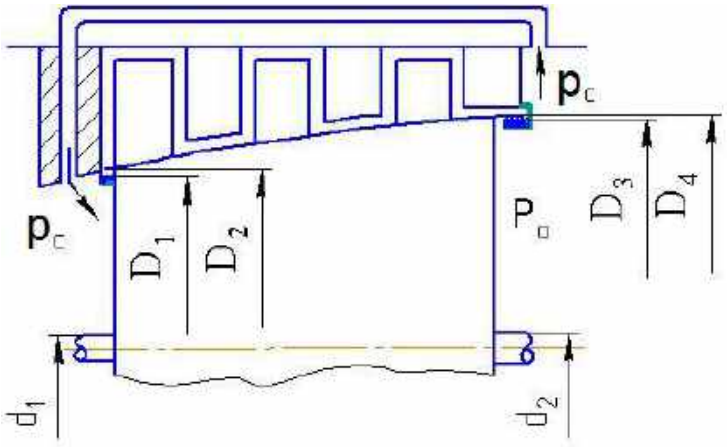


Fig. 1.29. Diagram of axial compressor

The resulting axial force Q affecting the compressor rotor is determined as

$$Q = Q_1 - Q_2 + Q_3,$$

where Q_1 – is force affecting gas flow duct,

$$Q_1 = \sum_{i=1}^{z} Q_{stage\ i},$$

$$Q_{stage\ i} = p_{2\,i} F_{2\,i} - p_{1\,i} F_{1\,i} + \frac{p_{1\,i} + p_{2\,i}}{2} \Delta F_{C\,i} + G \Delta c_{a\,C\,i},$$

where z is number of stages;

$F_{1\,i}$ and $F_{2\,i}$ are areas of inlet and outlet sections of the rotor wheel;

$\Delta F_{C\,i} = F_{2\,i} - F_{1\,i}$;

$\Delta c_{a\,C\,i}$ is increment of axial velocity, determining dynamic component of force.

Q_2 is force affecting rotor front flange (Fig. 1.30);

Q_3 is force affecting rotor rear flange.

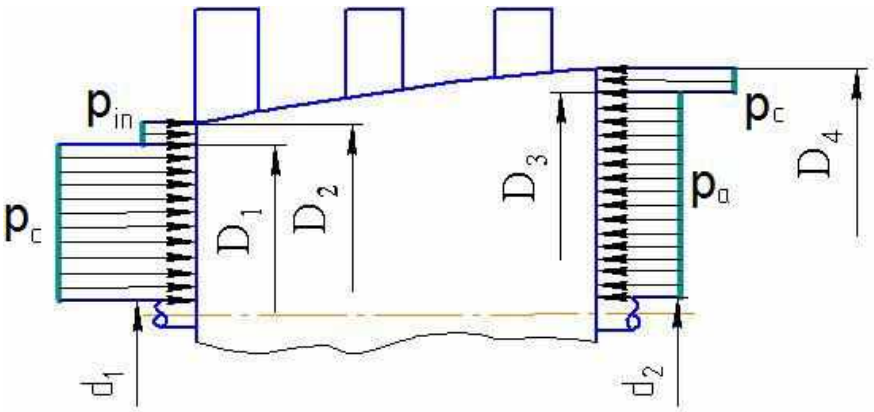


Fig. 1.30. Forces affecting faces of axial compressor

Force affecting the drum is as follows (Fig. 1.31):

$$P_{drum} = P_s \sin\alpha;$$

$$P_s = p_m S;\ p_m = \frac{p_{1i} + p_{2i}}{2};\ S = \frac{\Delta F_{Ci}}{\sin\alpha},\ \text{therefore,}\ P_{drum} = \frac{p_{1i} + p_{2i}}{2}\Delta F_{Ci}.$$

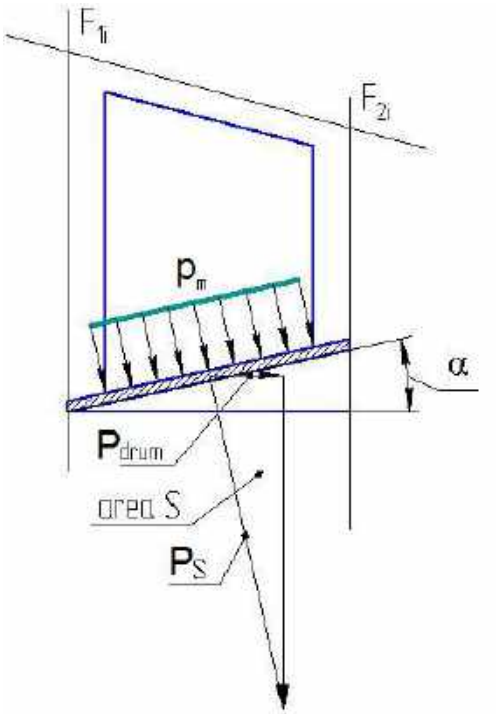


Fig. 1.31. Axial force affecting the drum

Axial force affecting the centrifugal compressor rotor

Let's consider the centrifugal compressor rotor wheel. Suppose that the pressure in the compressor changes from p_1 to p_2 (Fig. 1.32).

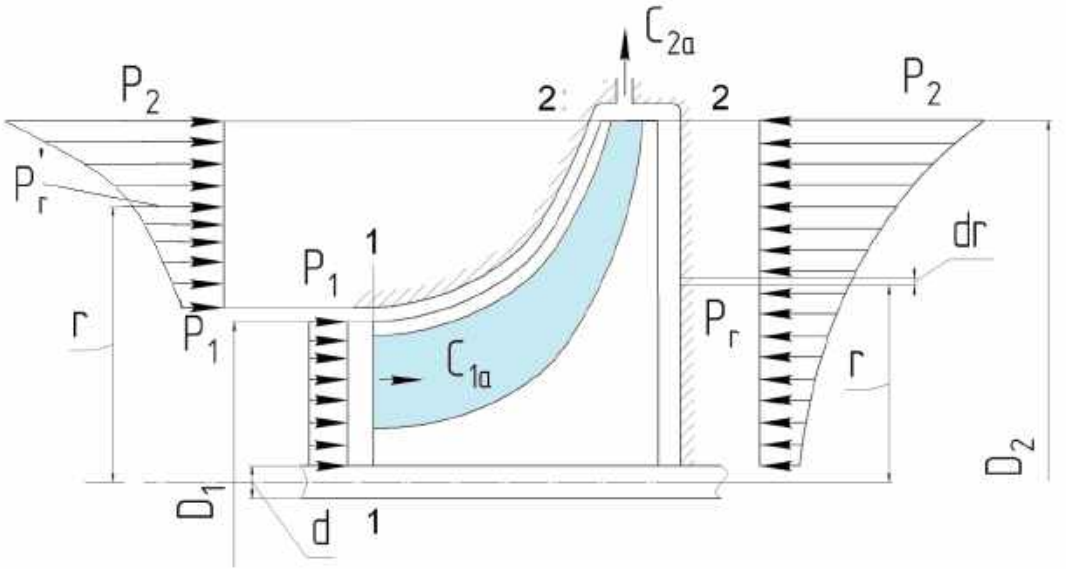


Fig. 1.32. Centrifugal compressor rotor

To calculate forces generated on the front and rear faces of the rotor wheel, we need to know corresponding distributions of the static pressure. The pressure distribution on the front face depends on a law of the blade profiling. The pressure distribution on the rear face depends on a clearance between the rotor and stator and on the presence and configuration of the seal, which is usually designed at the rear face for decreasing of the total axial force.

Force acting elemental ring area of width is dr on radius r:

$$P_r = p_r 2\pi\, r\, dr.$$

Then the axial force is:

$$P_a = p_1 \frac{\pi}{4}(D_1^2 - d_1^2) - \int_{d/2}^{D_1/2} p_r\ 2\pi r\ dr + \int_{D_1/2}^{D_2/2} p'_r\ 2\pi r\ dr\,.$$

This force is usually directed to the left – to the inlet.

Axial force affecting the turbine rotor

Initial data for determining the axial force are known from designing of the gas dynamic; they are static pressure and axial velocity at the rotor inlet and outlet: p_1, p_2, c_{1a}, c_{2a}. We also need to know a static pressure in the front camber. Let's suppose that the right camber is connected to the gas flow duct and pressure in it is p'_2 . This pressure is lower than pressure p_2 in the gas flow duct because of friction of the rear surface, which results in flow swirling directed to the disk center, thus decreasing the static pressure (Fig. 1.33).

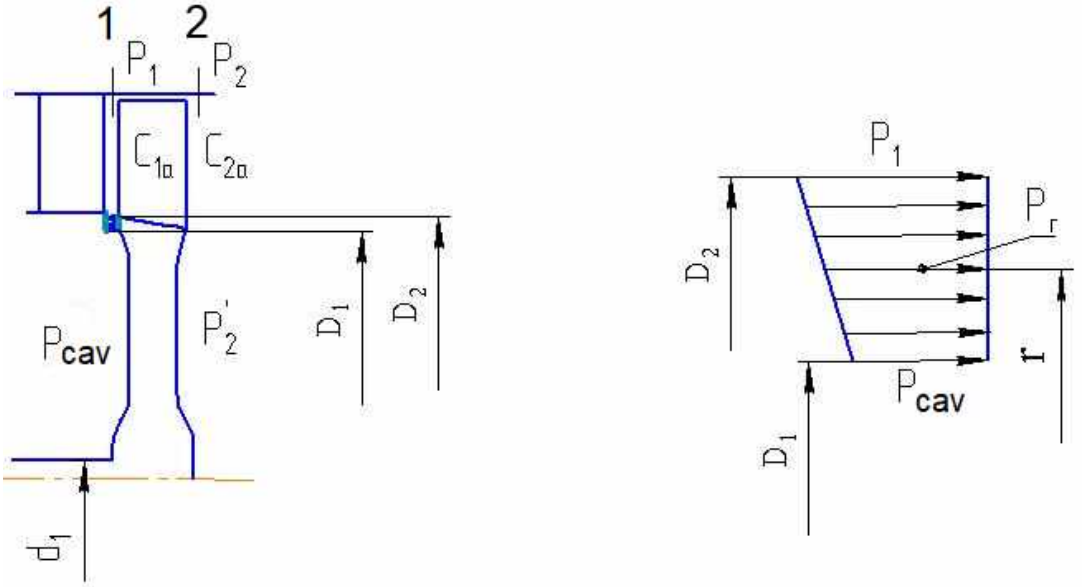


Fig. 1.33. Diagram of turbine rotor and pressure distribution in a seal

Axial force:

$$P_a = Q_1 + Q_2 + Q_3 - Q_4 - Q_5,$$

where Q_1 is a force affecting from the left side of the ring surface of the disc, limited by diameters d_1 and D_1,

$$Q_1 = p_{cav}\frac{\pi}{4}(D_1^2 - d_1^2);$$

Q_2 is a force affecting from the left side in area of the labyrinth seal, limited by diameters D_2 and D_1.

Supposing that the pressure in this area is varied linearly (see Fig. 1.33), we get

$$p_r = p_{cav} + \frac{p_1 - p_{cav}}{D_2/2 - D_1/2}(r - \frac{D_1}{2}).$$

Thus,

$$Q_2 = \int_{D_1/2}^{D_2/2} p_r \; 2\pi r \; dr - \int_{D_1/2}^{D_2/2} [p_{cav} + \frac{p_1 - p_{cav}}{D_2 - D_1}(2r - \frac{D_1}{2})] 2\pi r \; dr =$$

$$= \pi r^2 \Big|_{D_1/2}^{D_2/2} + \frac{p_1 - p_{cav}}{D_2 - D_1}\frac{4}{3}\pi r^3 \Big|_{D_1/2}^{D_2/2} - \frac{p_1 - p_{cav}}{D_2 - D_1} D_1 \pi r^2 \Big|_{D_1/2}^{D_2/2} =$$

$$= \frac{\pi}{4}(D_1^2 - D_2^2) + (p_1 - p_{cav})[\frac{\pi}{6}(D_2^2 + D_1 D_2 + D_1^2) - \frac{\pi}{4} D_1 (D_2 + D_1)].$$

Q_3 is a force affecting the rotor blades from the left side; it is determined by the pressure differential:

$$Q_3 = \frac{\pi}{4}(D_3^2 - D_2^2)(p_1 - p_2).$$

Q_4 is a dynamic force affecting from the right side:

$$Q_4 = G(c_{2a} - c_{1a}).$$

Q_5 is a force affecting from the rear surface of the disc; it is determined by pressure p_2' :

$$Q_5 = p_2' \; \frac{\pi}{4} D_2^2.$$

Axial force affecting the combustion chamber

Let's consider a simple configuration of the combustion chamber with external and internal casings having a cylindrical shape (Fig. 1.34).

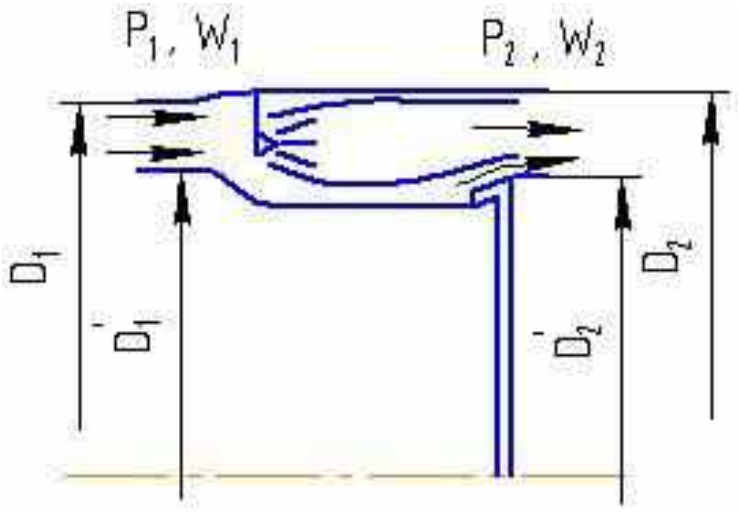


Fig. 1.34. Diagram of combustion chamber

Supposing that positive force is directed upstream, we get

$$P_{CC\,a} = G(w_1 - w_2) + \frac{\pi}{4}[p_1(D_1^2 - D_1'^2) - p_2(D_2^2 - D_2'^2)].$$

Axial force acting the jet nozzle

The jet nozzle consists of two shells: one is casing, the second one is internal cowl (Fig. 1.35). The shells are joined by the radial struts. Camber inside the cowl is usually not sealed, so the gas pressure in this camber is equal to turbine discharge static pressure p_1.

The gas is accelerated in the jet nozzle, so $w_2>w_1$ and $p_2<p_1$. At full expansion in the jet nozzle, the exhaust gas static pressure is equal to atmospheric pressure p_H. At partial expansion, $p_2>p_H$, at excessive expansion $p_2<p_H$.

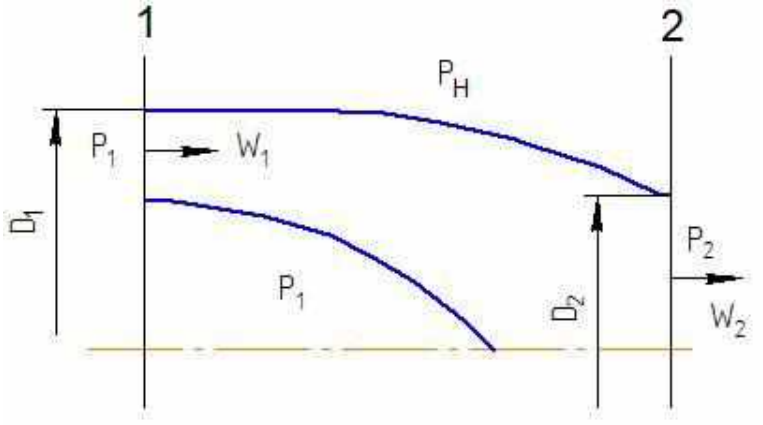


Fig. 1.35. Diagram of jet nozzle

Axial force affecting the jet nozzle consists of dynamic and static components:

$$P_{N\,a} = G(w_1 - w_2) + \frac{\pi}{4}(p_1 D_1^2 - p_2 D_1^2) - \frac{\pi}{4} p_H (D_1^2 - D_2^2).$$

1.5.5. Distribution of gas forces between engine assemblies

The engine thrust is a result of the axial gas forces affecting all engine assemblies. Fig. 1.36 shows an example of values and directions of the axial forces that affect in a single-spool turbojet. The forces are represented in percentage. The thrust force is considered to be equal 100 %.

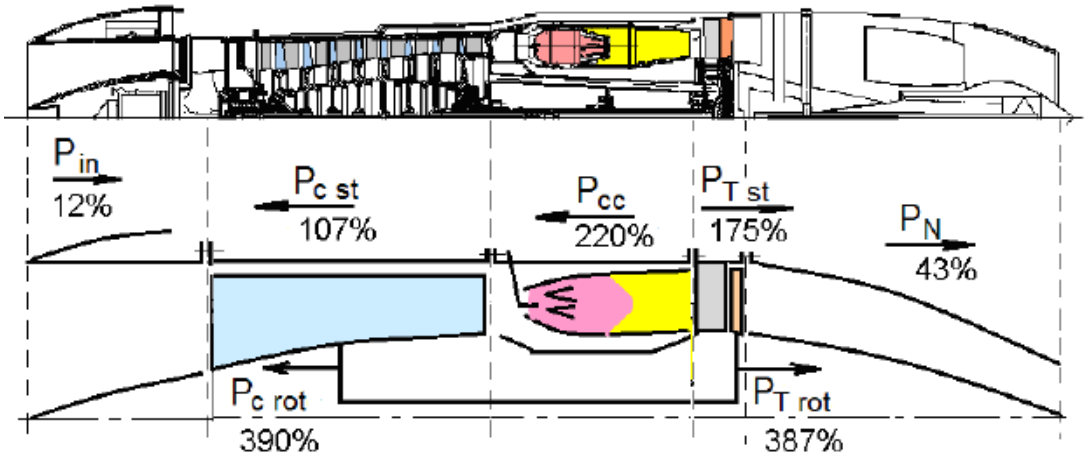


Fig. 1.36. Axial forces affecting structural members of turbojet engine

Total force that acts downstream is 617 %. Total force that acts upstream is 717 %. Resultant force is 100 %. This is thrust force.

Fig. 1.37 shows an example of values and directions of the axial forces that affect in a two-spool turbofan with mixed flows.

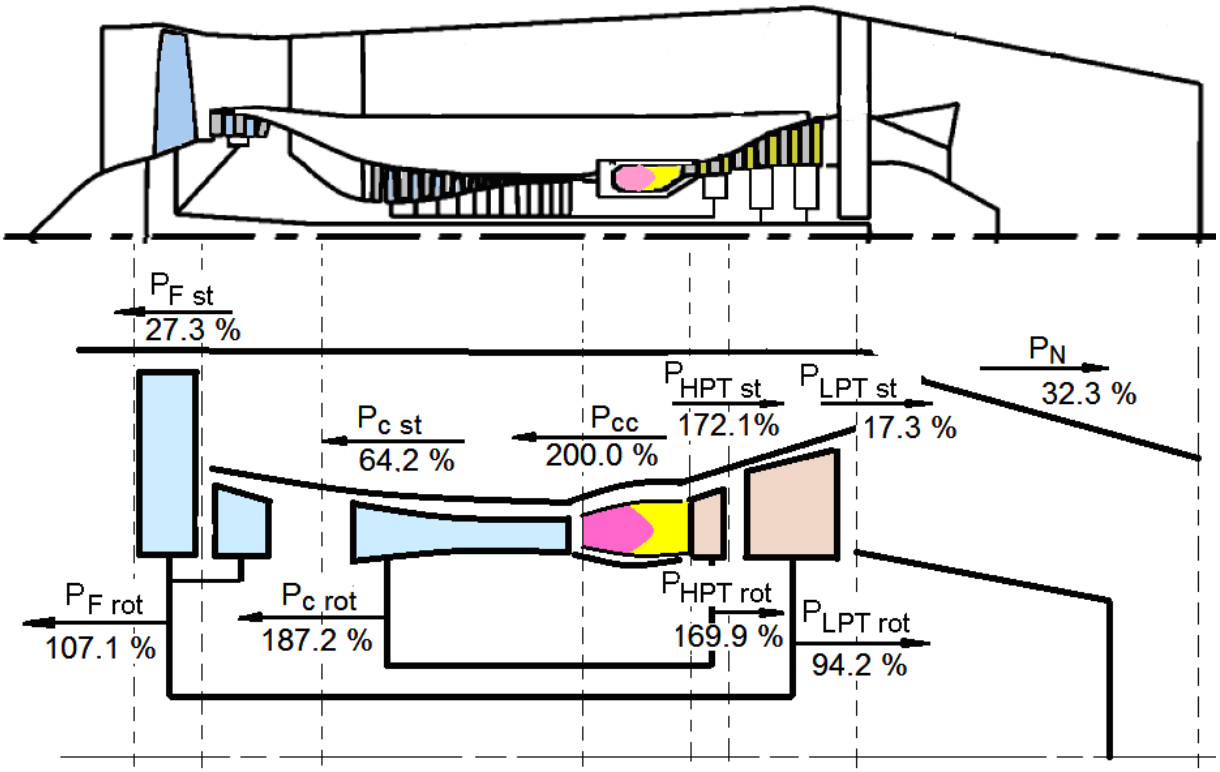


Fig. 1.37. Two-spool turbofan with mixed flows

Total force that acts downstream is 485.8 %. Total force that acts upstream is 585.8 %. Resultant force is 100 %. This is thrust force.

Fig. 1.38 shows an example of values and directions of the axial forces that affect in a three-spool turbofan with separate flows.

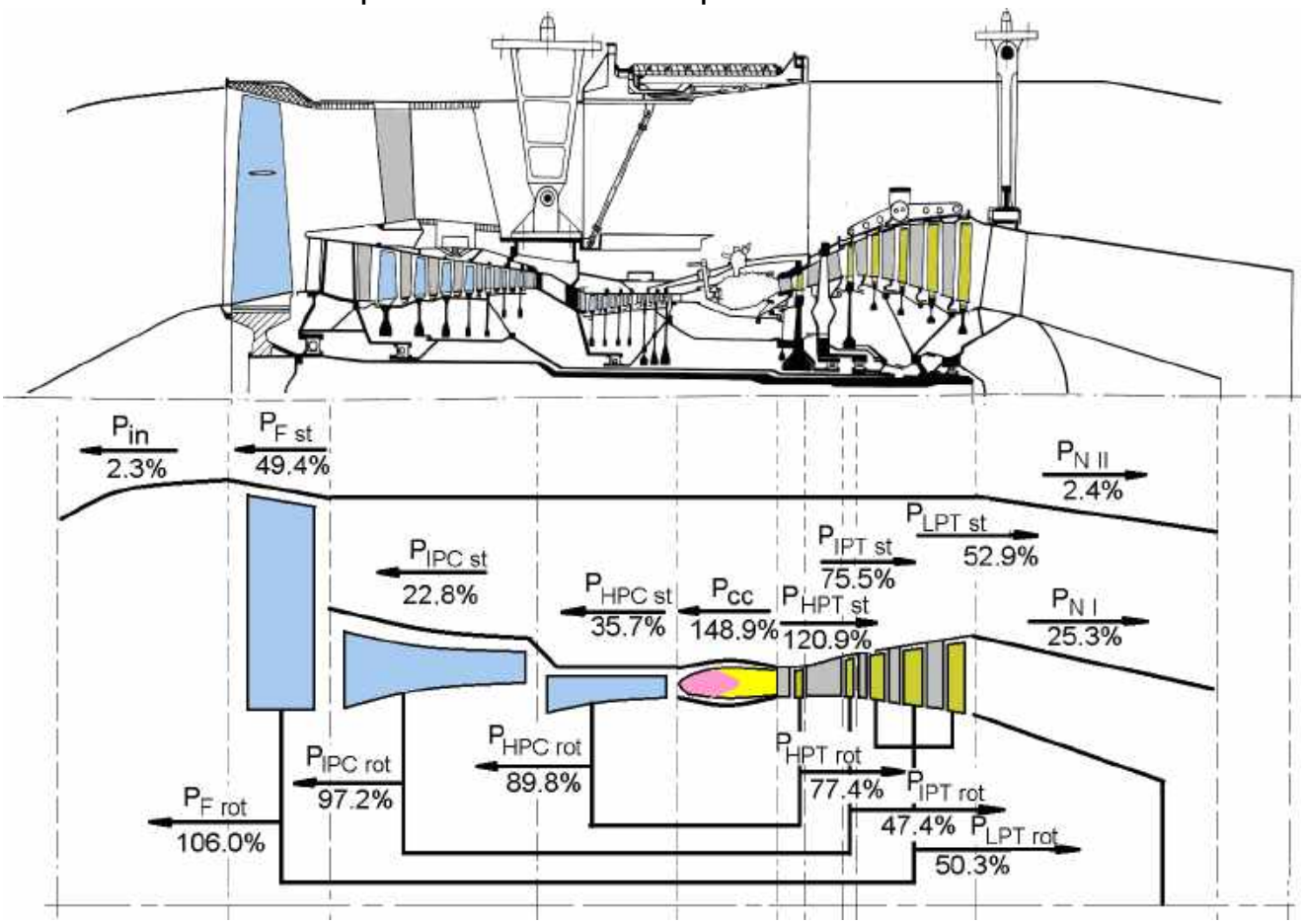


Fig. 1.38. Three-spool turbofan with separate flows

Total force that acts downstream is 452.1 %. Total force that acts upstream is 552.1 %. Resultant force is 100 %. This is thrust force.

1.5.6. Inertial forces and moments in the gas turbine engine

Inertial forces and moments are originated in the engine parts by three reasons:

- weight of the engine components;
- rotor rotation;
- maneuvers of the aircraft.

Stationary force affecting engine assemblies under all conditions is ***weight***.

Engine rotor rotation originates ***centrifugal forces***. They affect the rotary parts (rotor blades, discs and shafts) and cause tension, and sometimes bending and torsion.

The centrifugal force P_c affecting body of mass m, which trajectory has local radius r and centrifugal velocity ω, is

$$P_c = m\,\omega^2\,r.$$

This force is directed abaxially (from axis of rotation) and applied to the center of gravity. As the center of gravity moves, the centrifugal force also moves. For example, the center of gravity of the engine rotor has some small unbalance (displacement of the center of gravity to the axis of rotation). Therefore, the centrifugal force affecting the rotor is non-zero and rotates; its centrifugal velocity is equal to the rotor centrifugal velocity. Projection of this force on radial axis r is

$$P_r = P_c\sin(\omega t).$$

Thus, in accordance with this function, radial projection of the centrifugal force oscillates, and the rotor vibrates.

The non-equilibrated centrifugal forces are transmitted through bearings to the stator and engine mounts as radial alternating forces. Due to precise rotor balancing, they are small, but they have high frequency and may excite forced oscillations and fatigue damage to the engine parts.

Inertial forces that originate at the aircraft evolutions are shown in Fig. 1.39.

At the aircraft evolutions, different forces and moments are affecting the engine assemblies. These forces are inertial ones, and proportional to acceleration. Aircraft accelerations are usually expressed in terms of overloads. Value of the overload is specific and proportional to the gravitational acceleration:

$$n = \frac{a}{g},$$

where a is aircraft acceleration;

g is gravitational acceleration.

Thus, the value of overload shows how much the force of inertia related to the weight of considered object is. The maximum overload is normed:

- for maneuverable airplanes (fighters) is 8 to 9;
- for restricted-maneuverable aircraft (attack aircraft) is 4 to 6;
- for non-maneuverable airplanes (passenger and cargo airplanes) is 2 to 3.

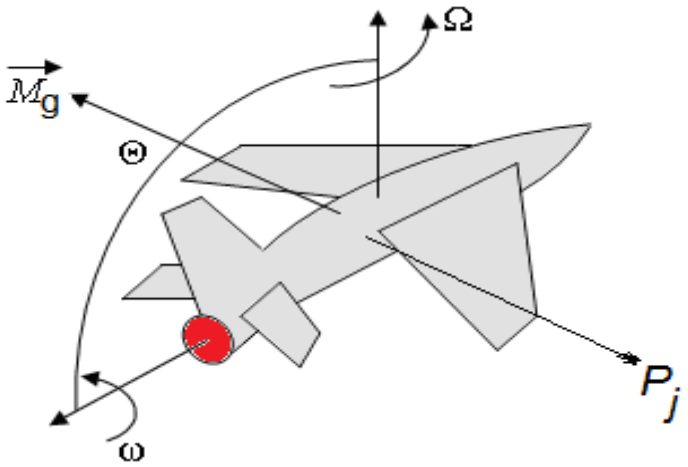


Fig. 1.39. Forces and moments originating at aircraft evolutions

At the aircraft turning (spiral, U-turn), the overload is 3 to 5, at spin is 2 to 3, at rolling is 4 to 5.

The inertia force is directed from the center of rotation along the radius of curvature of trajectory at the aircraft evolutions.

When the engine is running, its rotor is rotating at higher angular rotational speed ω. In addition to the inertia forces, rotated rotor is affected by ***gyroscopic moment:***

$$M_g = I_p \cdot \omega \cdot \Omega \cdot \sin\Theta,$$

where I_p is rotor polar moment of inertia with respect to its axis of rotation;

ω is angular velocity of rotor rotation;

Ω is angular velocity of aircraft motion, $\Omega = \frac{v}{R}$;

Θ is angle between vectors $\vec{\Omega}$ and $\vec{\omega}$ (as usual, the worst case is considered when Θ=π/2 and sinΘ = 1);

R is radius of flight trajectory;

v is flight velocity.

Direction of the gyroscopic moment is determined by using such rule: it always tries to turn vector $\vec{\omega}$ to vector $\vec{\Omega}$. Plane in which the gyroscopic moment affects, is perpendicular to the plane in which the aircraft makes turn.

The gyroscopic moment originates in each disc. It is the most significant load affecting the engine rotor. It causes rotor sagging and is equilibrated by responses in the rotor bearing supports.

1.6. Check questions

1. Generations in development of the gas turbine engine. Name the distinctive features between the engines of various generations.

2. Types of the GTE design arrangement. GTE classification by the design arrangement.

3. Application areas of GTE of various types.

4. Main requirements to the aircraft GTE.

5. What system approach to the GTE designing consists in?

6. Name the promising directions of improvement of the GTE design.

7. Constraints of aircraft flight performance parameters that are imposed by the engine.

8. Main stages of the engine designing process.

9. Classification of main loads affecting the GTE assemblies.

10. Axial gas forces affecting the GTE assemblies.

11. Inertial forces affecting the GTE assemblies. Gyroscopic moment.

2. COMPRESSOR DESIGN

2.1. GTE compressor purpose and main design parameters

The GTE compressor is designed to compress the air and to supply it into the combustion chamber.

As it is known from education course “Air-Breathing Engines Theory”, the air plays three roles in a turbojet engine:

1) is working fluid of the thermodynamic cycle;
2) is propulsive mass for generation of the thrust;
3) is a source of oxidizer for combustion.

Therefore, the compressor as the air consumer may be considered as a major unit of the engine.

From the theory it is also known that the engine cannot operate without air compression. Just compressor helps engine to generate thrust when the aircraft stays on the ground. In addition, the value of the compressor pressure ratio is one of the main thermodynamic parameters determining the engine performance.

The compressor as a bladed machine is characterized by a variety of parameters, which may be conditionally subdivided into two groups – gas-dynamic and design parameters.

The ***gas-dynamic parameters*** are:

– compressor ***overall pressure ratio*** OPR $\pi_C^* = \frac{p_C^*}{p_{in}^*}$ (OPR in the up-to-date GTE is 30 to 50 and for some engines exceeds 70);

– the ***air flow*** (from some kilograms per second for small-dimensioned GTE to 600 to 800 kg/s for super-high bypass ratio turbofans, which thrust is several hundred kilonewtons);

– ***efficiency*** η_C^* (the efficiency of modern compressors is 0.80 to 0.88) and other parameters, which are considered in the educational course “Theory of Air-Breathing Engines”.

The design parameters are not only parameters that characterize the compressor as the bladed machine, by also parameters that determine its shape, geometric dimensions, loads and stresses, which are acting in the compressor parts. They are:

1. ***Relative bush diameter*** (Fig. 2.1) is relation of compressor duct inner diameter to its outer diameter: $\bar{d} = \frac{D_{int}}{D_{ext}}$.

First stages of the axial compressors are designed with the following proportions:

- in the TJE $\bar{d} \geq$ 0.35 to 0.45;
- in the TPE and TShE $\bar{d} \geq$ 0.5 to 0.7;
- in the TFE $\bar{d} \geq$ 0.3 to 0.4.

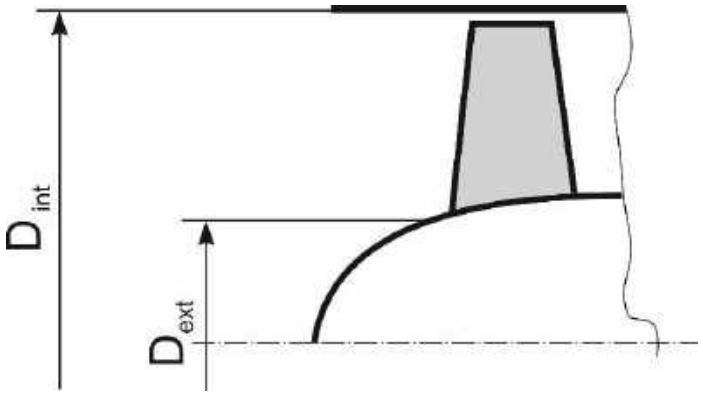


Fig. 2.1. Determination of relative bush diameter

The last stages of the axial compressors have $\bar{d} \approx 0.8$ to 0.9; larger values are not recommended because the rotor blades become too short (less than 15 to 30 mm), that significantly increases spilling and friction losses, thus efficiency falls down.

Increased values of $\bar{d}$ for the turboshaft engines are explained by the presence of a built-in gearbox placed in the front of the compressor inlet.

2. ***Circumferential velocity*** u_2 at the rotor peripheral diameter. When this velocity increases, then a head of the compressor stages is increased (because the head is proportional to u_2); thus it is possible to decrease the number of stages, compressor weight and dimensions at given π_C^*.

The maximum value of u_2 is limited by two reasons:

- permissible Mach number M_w at the tip of the airfoil portion of the rotor blade;
- conditions of the rotor blade strength at chosen $\bar{d}$. For the first subsonic stages u_2 is 280 to 330 m/s, herewith $\pi_{stage}^* = 1.2$ to 1.35. For the transonic and hypersonic stages $u_2 = 350 \ldots 470$ m/s and $\pi_{stage}^* = 1.8$ to 2.1.

3. ***Blade length*** $l = \frac{D_2 - D_1}{2} = \frac{D_2}{2}(1 - \bar{d})$. First stages of the TJE and TPE have $l = 250$ to 400 mm; fan blades of turbofans have 1000 mm length and more. The length of the last stages of the compressor is 15 to 40 mm.

4. ***Blade aspect ratio*** $\lambda = \dfrac{l}{b_m}$ is a relation of the blade length to the chord on mean diameter of the rotor wheel or ring of the guide vanes.

Axial compressor rotor blades have $\lambda = 1.2$ to 3.0; the guide vanes have $\lambda = 1.0$ to 3.0.

Blades with the aspect ratio $\lambda \geq 3.0$ (up to 5.0) may be used for the subsonic compressors. In this case, the length and weight of stage are decreased, but it becomes difficult to fit the required number of blades in the disc, blades stresses are increased and stage head is decreased.

5. ***Airfoil chord/space ratio*** $\left(\dfrac{b}{t}\right)_m$ usually is specified on the mean radius. This parameter is defined from the aerodynamic calculation and in the designed structures of the rotor wheels $\left(\dfrac{b}{t}\right)_m = 0.6$ to 1.7. The blades of the first stages have smaller values. For the guide vanes $\left(\dfrac{b}{t}\right)_m = 0.8$ to 1.8.

The chord/space ratio is used to determine airfoil pitch and blade chord on the mean radius; it means that if the number of blades is known, it is possible to find the conditions of arrangement of the blades on the rotor wheel:

$$b_m = \frac{l}{\lambda}; \quad t_m = \frac{b_m}{(b/t)_m}.$$

6. ***Number of blades***

$$z = \frac{\pi D_m}{t_m}. \qquad (2.1)$$

On the other hand, the number of blades may be defined by other parameters:

$$D_m = \frac{D_2 + D_1}{2}; \qquad t_m = \frac{b_m}{(b/t)_m}; \qquad b_m = \frac{l}{\lambda}; \qquad l = \frac{D_2}{2}(1 - \bar{d}).$$

After substitution of these formulas in (2.1), we get

$$z = \pi\lambda\left(\frac{b}{t}\right)_m \frac{1 + \bar{d}}{1 - \bar{d}}.$$

This relation allows analyzing the influence of various parameters on the number of blades in the blades rim.

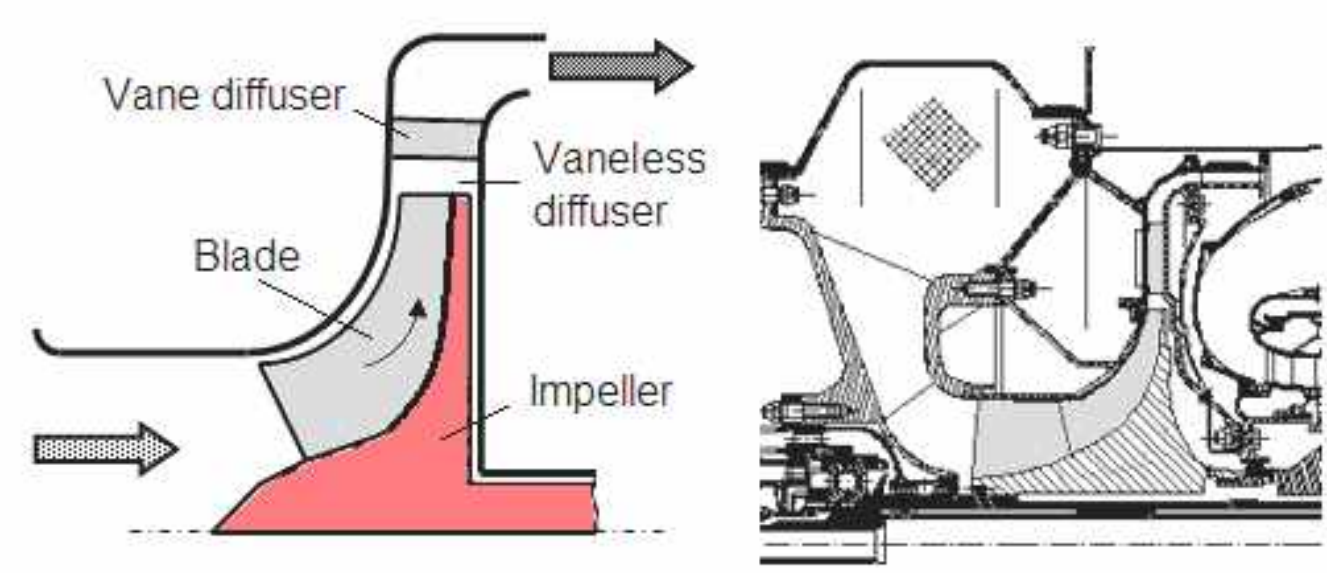
7. ***Compressor specific weight*** $\gamma_C = \dfrac{G_C}{G_E}$ is relation of the compressor weight to the engine weight. For the TJE, $\gamma_C = 0.3$ to 0.4; for the TPE, $\gamma_C = 0.2$

to 0.3, i.e. the compressor weight is significant part of the engine overall weight (30 to 40 %); 18 to 23 % of this weight is rotor, the remaining weight is stator. At a given diameter of a stage, its weight may be decreased due to the length of stage decreasing (by chord decreasing), using materials with high specific strength, choosing rational shape of a gas flow duct and power structure of the rotor and stator.

2.2. Compressors classification by a type of bladed machine

Compressors classification is based on the type of the bladed machine:

1. ***Centrifugal (radial) compressors*** with single-inlet (Fig. 2.2) or double-inlet (Fig. 2.3) impeller.



a *b*

Fig. 2.2. Diagram (*a*) and design (*b*) of centrifugal compressor with a single-inlet impeller

The centrifugal compressors have simple structure (it means low labor content and cost), high reliability (low sensitivity to foreign matter ingestion and to erosion), and wide range of stable operation, low length and low weight ($\gamma_c \leq 0.3$). Disadvantages are low efficiency ($\eta_c \leq 0.78$), limited air flow (up to 70 kg/s for double-side impeller), low pressure ratio (5 to 6, for modern compressors it is 8 to 12), complicated arrangement in combination with the combustion chamber.

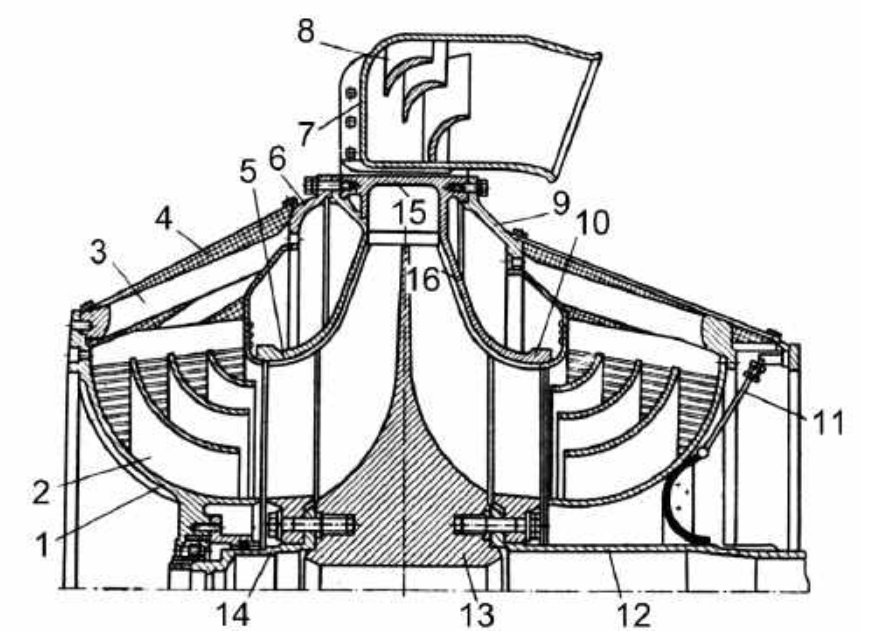


Fig. 2.3. Centrifugal compressor with double-side rotor wheel (VK-1 turbojet):
1 – casing of front bearing; 2 – guide cones; 3 – guide vanes; 4 – protective grid;
5 – case cover; 6, 9 – front and rear trusses; 7 – output branch pipe;
8 – duct vanes; 10 – casing; 11 – bracing rod; 12, 14 – rear and front hubs;
13 – compressor rotor wheel; 15 – cylinder wall of casing;
16 – rear wall of casing

2. ***Axial compressors*** are widely used in the up-to-date GTE; their characteristics will be described later.

3. ***Combined axial-centrifugal compressors*** (Fig. 2.4) are used in the small-dimensioned engines with high pressure ratio (for example GTD-3F) and in modern medium-dimensioned engines with high pressure ratio (for example D-27 which pressure ratio is higher than 40).

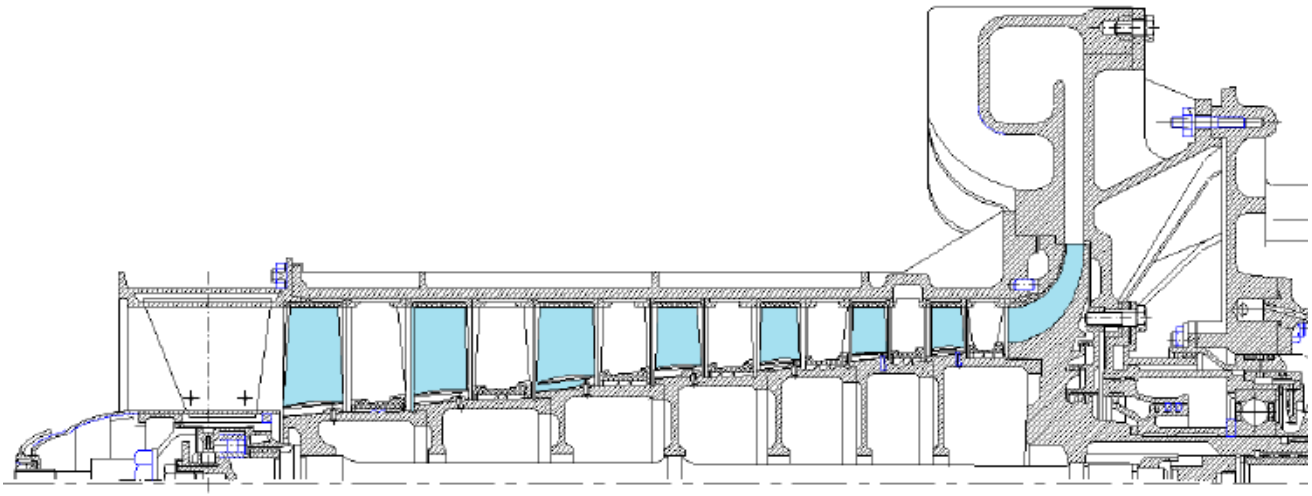


Fig. 2.4. Axial-centrifugal compressor (GTD-350 turboshaft)

4. ***Diagonal compressors*** (Fig. 2.5) possess the intermediate place between the axial compressors and the centrifugal ones. They compress the air both under the action of the centrifugal forces and due to a diffuser shape of the interblade channels (as in the axial compressors). The diagonal compressor stages are usually used in the fans of the turbofan engines with the low bypass ratio (for example the AL-41F, VD-7 and DV-2).

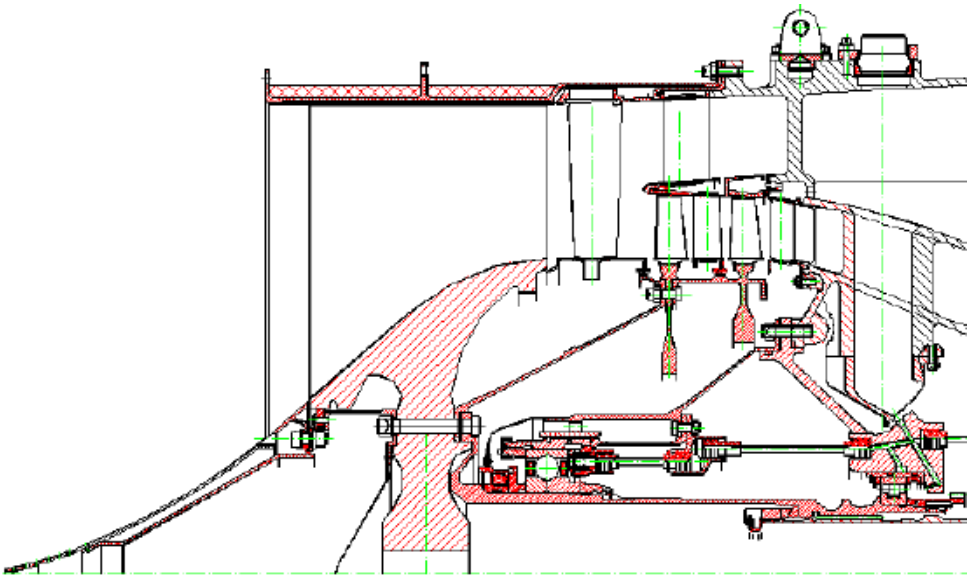


Fig. 2.5. Diagonal fan (the DV-2 turbofan to power the L-59 aircraft)

5. ***Axial-diagonal compressors*** are a combination of the axial and diagonal compressors, used for the auxiliary power units and for the low-thrust and low-power engines (Fig. 2.6).



Fig. 2.6. Diagonal fan and axial-diagonal compressor
of the low-thrust turbofan

2.3. Axial compressor design arrangement

Design and layout arrangement of the compressor depends on its type, layout, shape of the gas flow duct and power structures of rotor and stator.

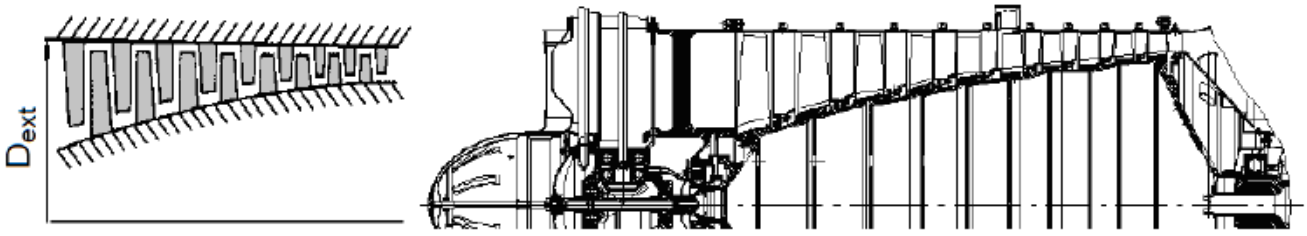
Compressor structure consists of two parts: rotor and stator. Compressor arrangement may be classified:

1. ***By the number of rotors***: single-rotor (one-spool), twin-rotor (two-spool), triple-rotor (three-spool). The multi-spool diagram expands a range of compressor stable operation, simplifies engine starting and increases compressor efficiency at off-design power ratings. Otherwise, its structure is more complicated than that of a single-rotor diagram.

2. ***By the air velocity*** in the gas flow duct: subsonic, supersonic, and transonic. Usually the first stages are supersonic ones, thus a pressure ratio is increased comparing to the subsonic stages, but the efficiency and range of stability are smaller.

3. ***By the shape of the gas flow duct***. This is significant design property of the axial compressor. Gas path area in the axial compressor decreases from the first to the last stages, because the pressure and density are increased. This decreasing of the area is provided by a special profiling of the compressor gas flow duct, which may be of the following shapes: constant external diameter; constant bushing diameter; constant mean diameter; combined gas flow duct.

Casing of the compressor with ***constant external diameter*** $D_{ext} = \text{const}$ (Fig. 2.7) is cylinder, its manufacturing is simple.

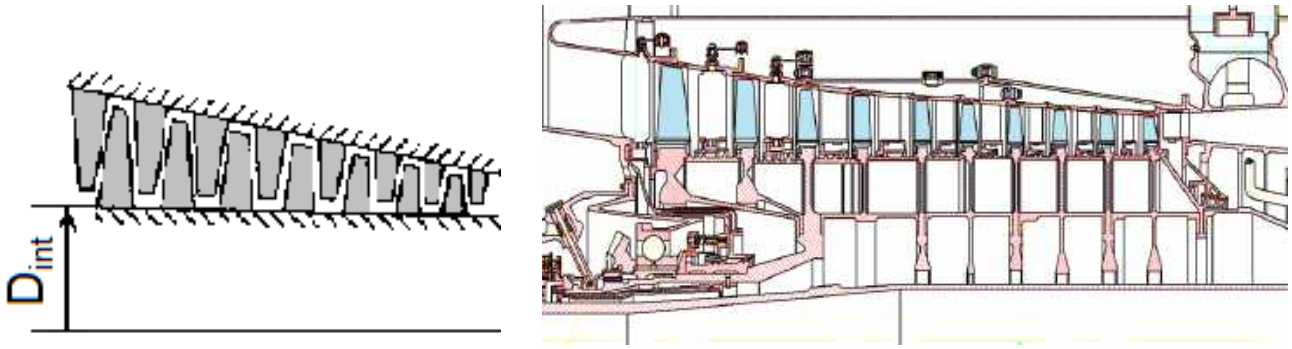


a *b*

Fig. 2.7. Diagram (*a*) and example (*b*) of axial compressor with constant external diameter (the RD-9B turbojet)

The head of the last stages increases because mean diameter D_m and circumferential velocity on mean diameter u_m are increased. However, the blades of the last stages may become too short (less than 15 to 20 mm), relative radial clearance between the blade and casing is increased, spilling losses are also increased and the efficiency falls down.

In the gas flow duct with ***constant bushing diameter*** ($D_{int} = \text{const}$), length of the blades of the last stages is increased (Fig. 2.8). However, the compressor head goes down, as D_m and u_m are decreased.

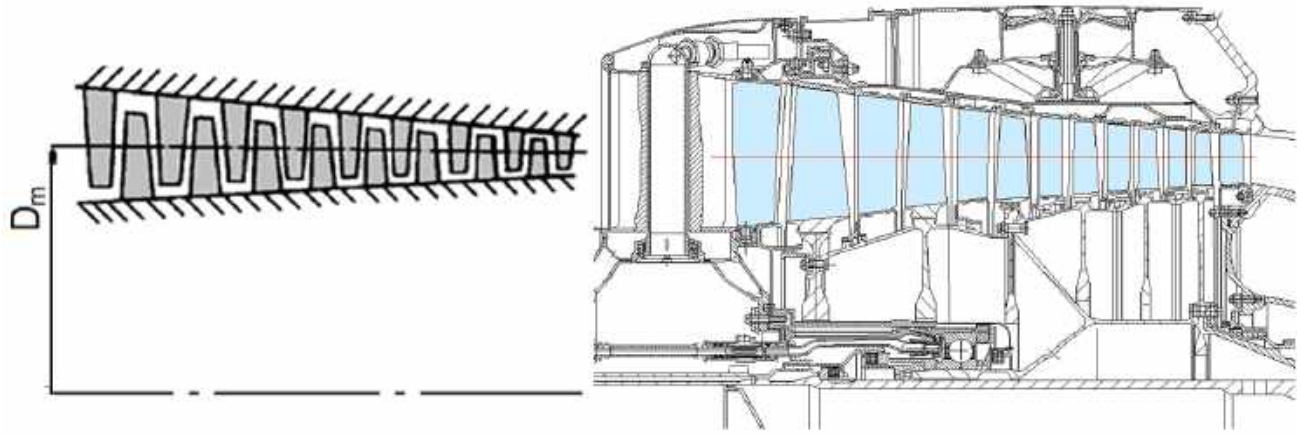


a *b*

Fig. 2.8. Diagram (*a*) and example (*b*) of axial compressor
with constant internal diameter (HPC of F-100-PW-100 turbofan)

This shape of the gas flow duct simplifies arrangement of the accessories with the central drive in the intermediate support area without significant increasing in diameters. It is possible to decrease a weight of the stator and the compressor as a whole. But in this case, the distance between the rotor supports is increased and sealing of the blade tips is complicated because of possible axial displacement of the rotor.

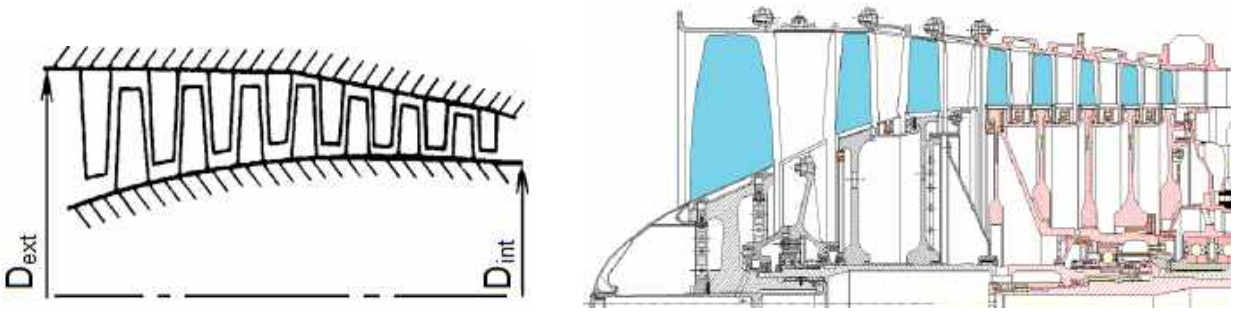
Diagram of the gas flow duct with ***constant mean diameter*** ($D_m = \text{const}$) is a compromise, is has both positive and negative features comparing to two previous diagrams (Fig. 2.9). This diagram is widely used in the turbofan engines for coordination between the fan outlet and HPC inlet (to optimize the **S**-shape duct between the fan and HPC).



a *b*

Fig. 2.9. Diagram (*a*) and example (*b*) of axial compressor
with constant mean diameter (compressor of the D-36 turbofan)

Diagrams with the ***combined gas flow duct*** (Fig. 2.10) are used to reach the maximum effect of all above-mentioned diagrams without increasing their disadvantages. These diagrams are more complicated by design as compared with diagrams D_{ext} = const, D_{int} = const, and D_m = const.



a *b*

Fig. 2.10. Diagram (*a*) and example (*b*) of axial compressor with combined gas path (the R-25F-300)

2.4. Requirements to compressor design and their implementation

Compressor is one of the main engine component parts that define the engine absolute and specific parameters.

Basic requirements to the compressors are:

- the minimum weight and overall dimensions at specified air flow G_{air} and pressure ratio π_C^*;
- the maximum efficiency at the design power ratings;
- wide range of stable operation;
- high maintenance reliability;
- low cost of manufacture and overhaul.

The first requirement is implemented by increasing the head of stages, the air velocity in the gas flow duct, by increasing the blades aspect ratio and permissible stresses in the design structures, by using materials with high specific strength (titanium alloys and composite materials), by rational designing of shape of the parts and power diagrams, etc.

The compressor efficiency is increased due to implementation of the variable guide vanes, by decreasing the number of struts, by decreasing radial clearances in the gas flow duct, which reduce adverse spilling of the air, etc.

Wide range of the compressor stable operation is provided by using compressor control system (variable guide vanes, valves, shuttles and bands to bypass partially the air into the atmosphere or to the engine secondary duct), by using intra-stage ring bypass, and by using two-spool and three-spool rotors.

High operational reliability may be achieved by design improvement, by using high-strength corrosion resistant materials, by using protection against entry of foreign matter, by improving blades vibration properties, and by increasing maintenance culture. The operational reliability of the axial compressors is always in the centre of attention. Experience in maintenance shows large number of unscheduled removals of engines caused by compressor faults such as damage and deterioration of the blades and vanes as a result of entry of foreign matter, contamination and corrosion of the blades, initiation of the cracks in the design structures as a result of vibration, air leakage, clearance increasing, and rotor unbalance.

Axial compressor manufacture and overhaul are expensive, which is explained by the large number of blades (up to 1000 pcs or more), which require high precision when manufacturing and assembling them. Designing and introducing of new production processes (precise forming, extrusion, rolling, forge rolling etc.), improving of design engineering, using of comparatively low-cost materials, as well as modular design decrease the cost of manufacture and overhaul of the compressor assembly.

2.5. Design of rotors of axial compressors

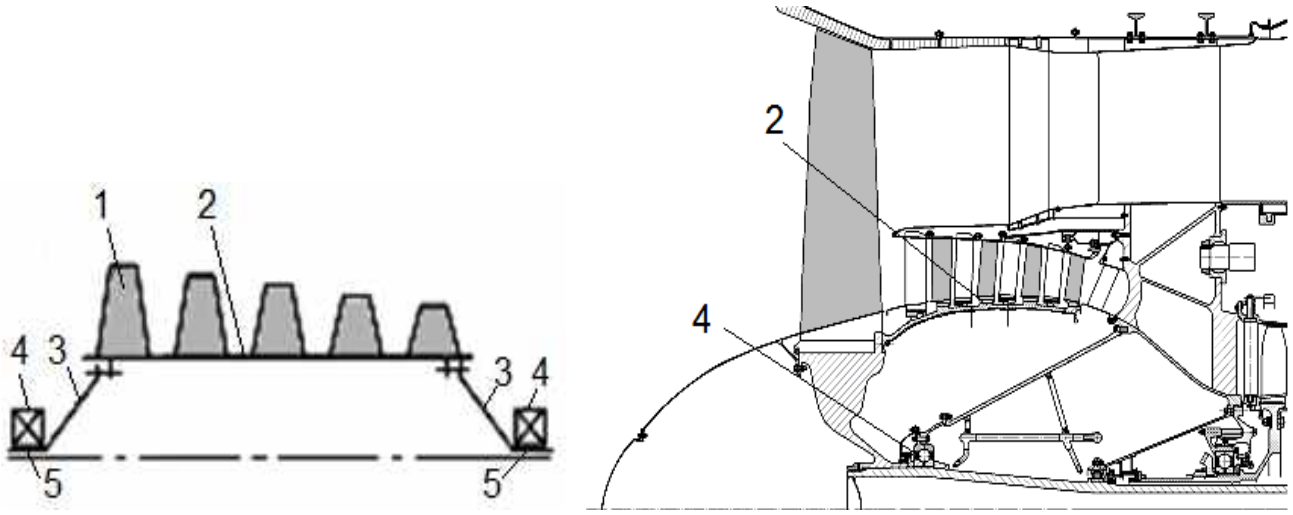
The main members of the rotor are as follows: rotor blades, discs (or drum) that carry rotor blades, shafts and journals, which support shaft on the stator by using bearings.

Rotor design members make a load-carrying structure, which is a body of revolution. This structure must be rigid and strong at the minimum weight, because it is highly loaded during engine operation by high centrifugal forces of mass of the rotor blades and its own weight and mass inertial forces that occur during evolutions of the aircraft, as well as gas forces, thermal and vibration loads.

Depending on the load-carrying structure, the rotors are subdivided into the following types: drum-type, disc-type, and drum-and-disc-type.

2.5.1. Drum-type rotors

The drum-type rotors (Fig. 2.11) have a shape of cylinder or truncated cone. External surface of the drum has ring-shaped or longitudinal slots for attachment of the blades. The faces of the drum are attached to the flanges with supporting journals. The drum transmits torque.



a *b*

Fig. 2.11. Diagram (*a*) and design (*b*) of drum-type rotor:
1 – rotor blade; 2 – drum; 3 – flange; 4 – bearing; 5 – supporting journal

Ring-shaped slots are preferable because they help to attach more blades stage-wise, thus increasing compressor efficiency. Ring-shaped slots also reduce the strength of the drum less than the longitudinal ones.

The drums may be solid or composed. The length of the drum is decreased when the journals are located inside the drum; in this case, the first and the last compressor stages are arranged in a cantilever type (Fig. 2.11, *b*).

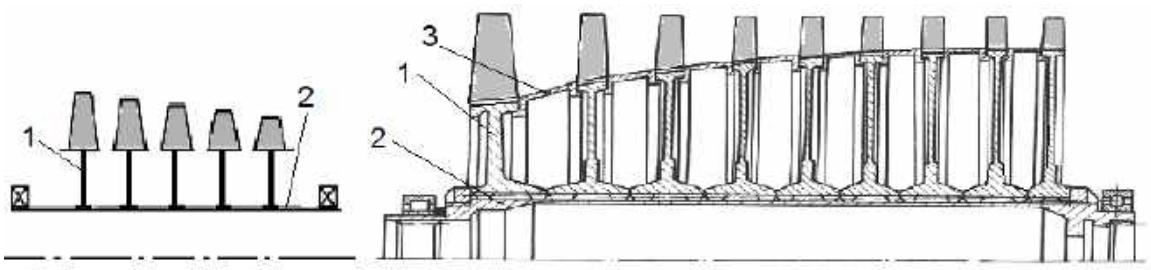
Advantages of the drum-type rotor are high bending rigidity, simple design and manufacturing, and low cost.

Disadvantages are low limited circumferential velocity (due to the drum strength conditions, the circumferential velocity of the drum is not higher than 180 to 220 m/s) and low transversal rigidity because the drum operates for rupture under the action of centrifugal forces caused by rotating weight of the rotor blades and the drum itself).

The example is the TR-1 turbojet. These rotors are also applied in low-sized GTE and in booster stages of turbofans (see Fig. 2.11, *b*).

2.5.2. Disc-type rotors

Disc-type rotor (Fig. 2.12) has not drum elements. Actually, it is a set of separate discs attached to the common shaft. The shaft is usually hollow. It is designed to transmit the torque and to align the discs.

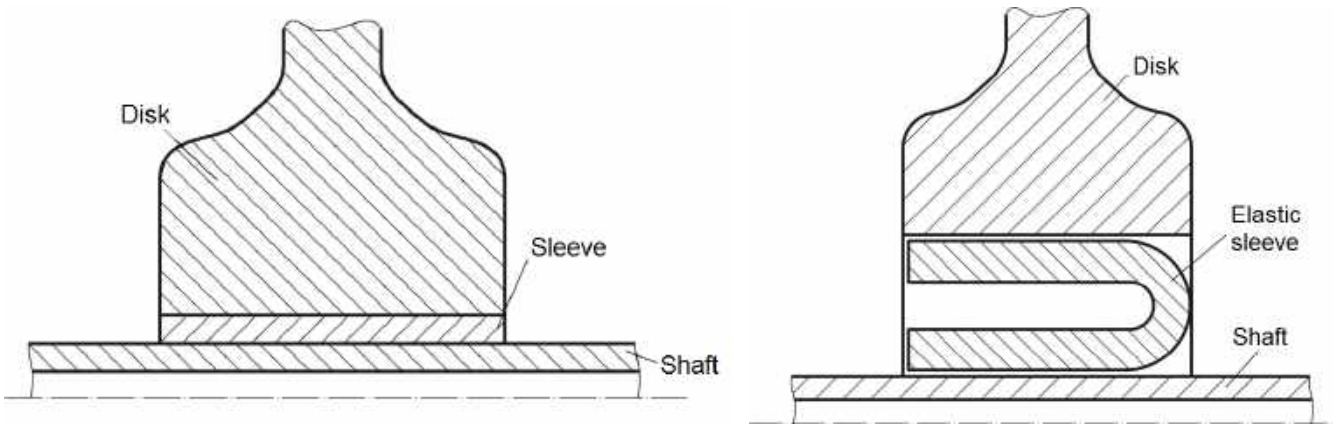


a *b*

Fig. 2.12. Diagram (*a*) and design (*b*) of disc-type rotor (the D-25V turboshaft):
1 – disc; 2 – shaft; 3 – duct ring

To transmit the torque, the disc is attached to the shaft by press-fitting (Fig. 2.13), by splines (Fig. 2.14, *a*, *b*), by the bolts that join the discs with the shaft flanges (Fig. 2.14, *c*). In case of press-fitting, the tightness is chosen based on transmission of torque at operating condition, when the disc is heated and extended by the centrifugal forces. Probably, the tightness in cold condition (when assembling the rotor) is very high (for example, the disc is pressed with a force of 14 to 15 tons to transmit the torque 350 to 400 Nm). To prevent disc damage during press-fitting, the intermediate sleeves are mounted between the disc and shaft (Fig. 2.13, *a*). These sleeves are deformed and the disc turns relative to the shaft during a long-time operation. To prevent this turning, the sleeve may be designed as elastic one (Fig. 2.13, *b*).

The disc-type rotor with press junction has been used in the Jumo-004 (the RD-20) turbojet.



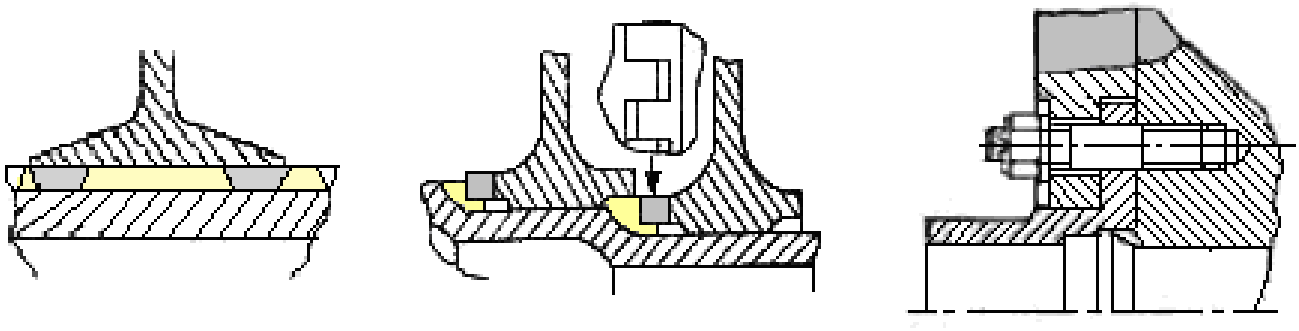
a *b*

Fig. 2.13. Disc-to-shaft attachment by press-fitting:
a – through normal sleeve; *b* – through elastic sleeve

In case of splined joint, a slight interference is required for the disc-to-shaft alignment. Involute, triangle or square splines may be used. If the disc is

made of aluminum alloy, then its sleeve expands strongly at heating. Therefore, when this disc is joined to the shaft made of steel then the preload interference is not enough for alignment. In this case, the so-called heat-resistant splines are used (Fig. 2.14, *a*, *b*), whose side faces are arranged radially. They allow keeping tight connection during engine operation. The discs with the elastic sleeve also may be used.

In case of flanged joint (see Fig. 2.14, *c*), the template bolts are used.



a *b* *c*

Fig. 2.14. Methods of disc-to-shaft joining:
a – splines on cylindrical surface; *b* – face splines; *c* – flange-and-bolt joint

The high circumferential velocities at the peripheral diameter (350 to 450 m/s) are allowed for the disc-type rotors.

Disadvantages of the disc-type rotors are:

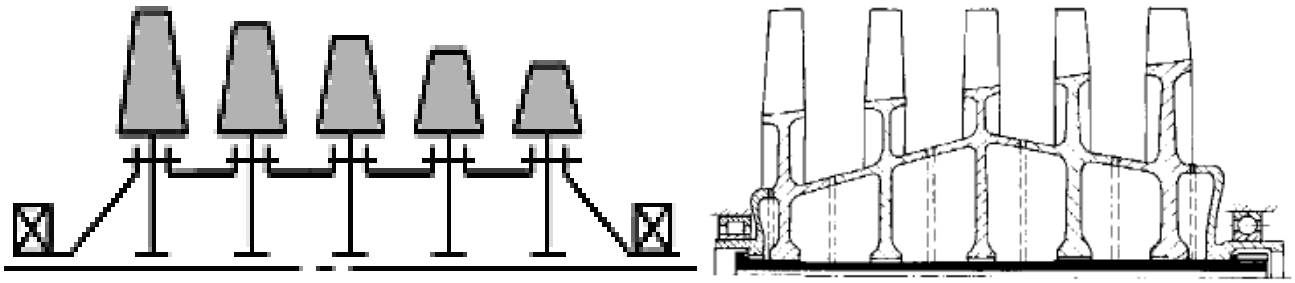
- low bending rigidity due to small diameter of the shaft;
- possible vibration of the disc;
- complicated assembling and disassembling procedures;
- high cost of manufacture and overhaul.

Bending rigidity of the disc-type rotor may be improved by increasing shaft diameter and by mounting peripheral duct rings (inter-stage spacers) (see Fig. 2.12, *b*), which name is explained by their function of being part of the engine gas flow duct. This method allows avoiding disc vibration. One more function of the duct rings is axial retaining of the rotor blades.

The disc-type rotors are used to wide extent in some types of engines (the D-25V, HPC D-20P, D-30, etc.).

2.5.3. Drum-and disc rotors

Drum-and-disc rotors (Fig. 2.15) constitute a package of discs with axial collars that make a drum portion of the rotor after joining. They may be as disassembled or not disassembled structures.



a *b*

Fig. 2.15. Diagram (*a*) and design (*b*) of drum-and-disc rotor

The ***not disassembled rotor*** is assembled of separate sections that may be joined by the following methods:

1. ***Press-fitting and pinning***. The disc collar has a retaining shoulder, which is aligned and pressed into the rim of the next disc. The female rim is heated by 50 to 100 °C higher than the operating temperature. The joint is additionally restrained after pressing by the radial pins (Fig. 2.16), which are inserted with interference into the holes drilled in the slots for blades retaining (the R-11F-300, RD-9B, R-25F, R-95Sh, R-29F-300, AM-3, AI-20 etc.). The blades cover the pins and restrain them against radial displacement by the centrifugal forces.

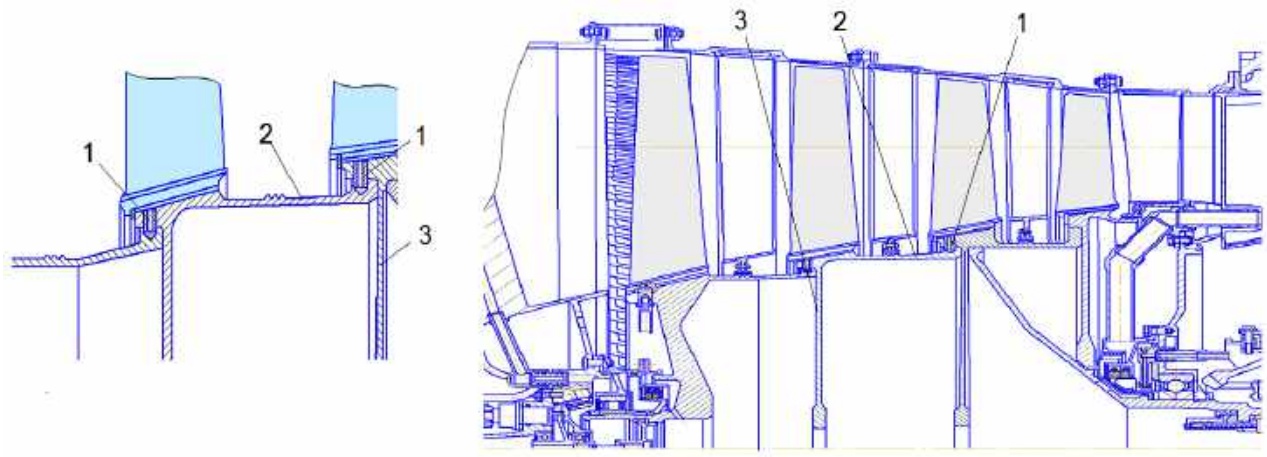


Fig. 2.16. Joining by press-fitting and pinning (LPC of the RD-33 turbofan):
1 – pin; 2 – drum area; 3 – disc

2. ***Welding*** (electron beam, friction). These welding operations provide the minimum decrease of the strength in a weld comparing to the main material (approximately 2 %). The examples are compressors of the TV3-117 turboshaft engine (Fig. 2.17), D-36 turbofan, and D-136 turboshaft, made of titanium alloys.

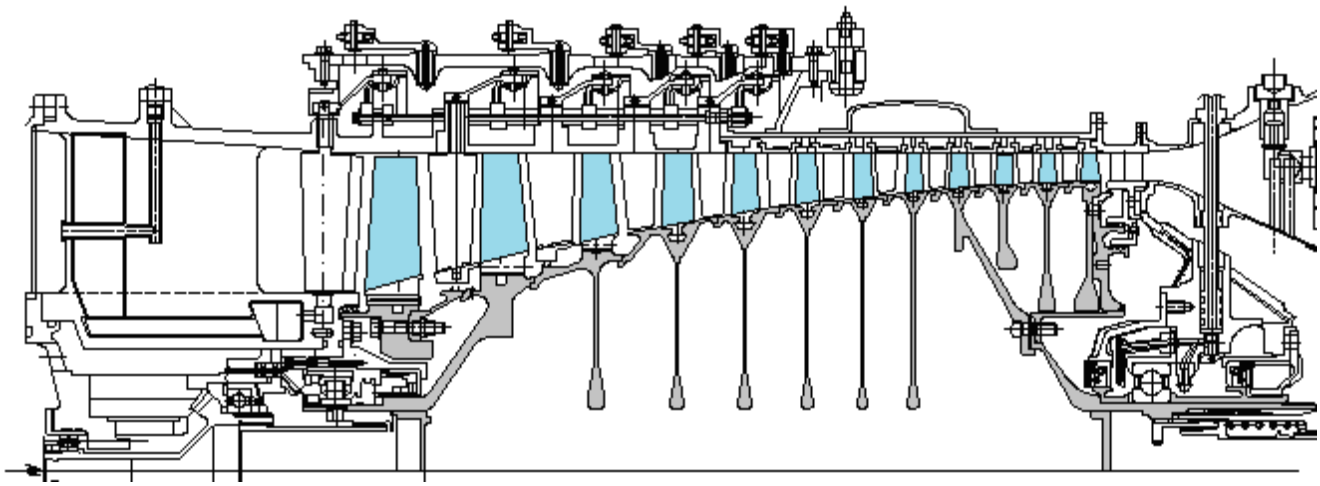


Fig. 2.17. Compressor of the TV3-117 turboshaft. Discs are joined by electron beam welding (except for the first stage)

Junction of the ***disassebled rotors*** is implemented as follows:

1. ***Flange-and-bolt joint*** (Fig. 2.18). Template bolts are used for transmission of torque and alignment of the discs to each other.

The examples are compressor of the NK-12 turboprop, HPC of the NK-8 turbofan, fan of the AI-25 turbofan, joining of welded sections of compressor in the D-36 turbofan.

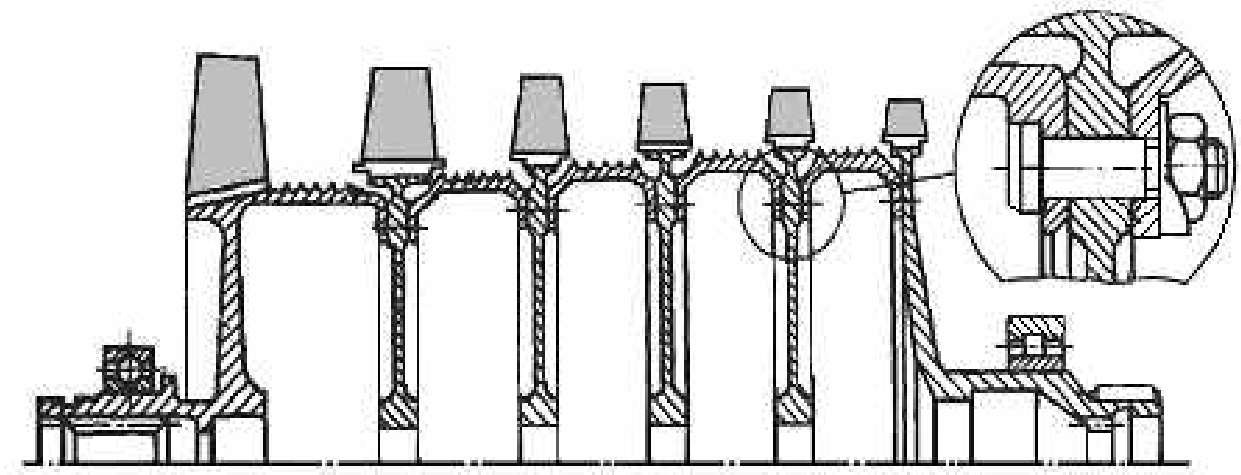


Fig. 2.18. Flange-and-bolt joint of the NK-8 HPC rotor

2. ***Joining by peripheral turnbuckle bolts*** (Fig. 2.19). The joined parts are aligned by retaining shoulders or sleeves; torque is transmitted by friction. For joining compressor rotor, a long bolt is needed. It may be damaged by torsion when tightening a nut. To prevent its torsion, the bolt is retained by special mounting key through the plate surfaces on a square head of the bolt end.

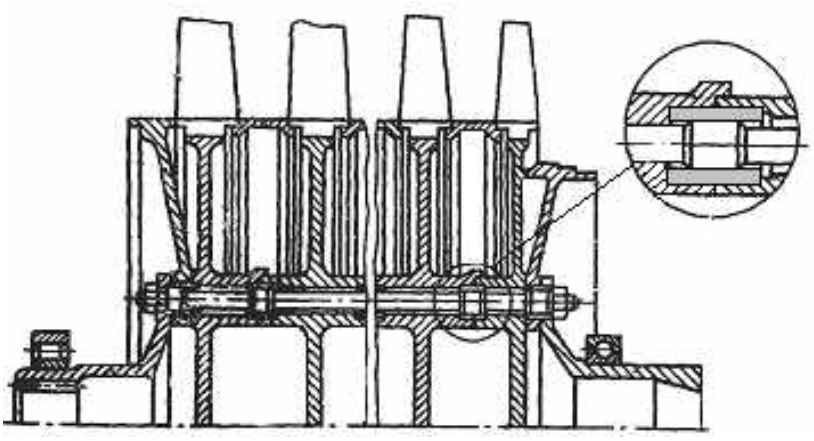
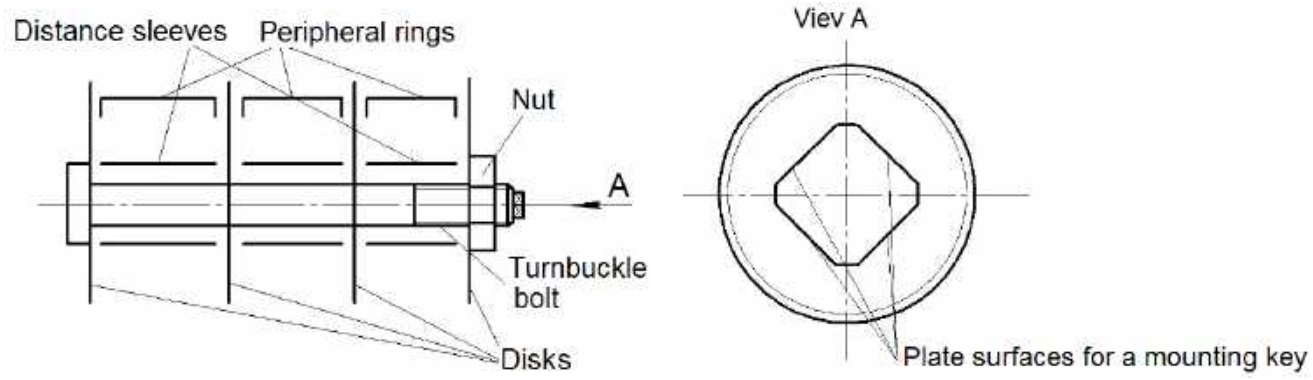


Fig. 2.19. Joining by peripheral turnbuckle bolts with aligning sleeves

Peripheral rings (Figs 2.19, 2.20, *a*) separate the internal chamber of the rotor from a gas flow duct. Distance sleeves (see Fig. 2.20, *a*) prevent discs from bending when the joint is tightened.

The bolt is peripheral, so it is loaded by the centrifugal force that bends it. For decreasing a bending flexure, it is necessary to increase rigidity of the bolt. This is done due to a special shape of the bolt, which has some fillets for hardening. The bolt head is equipped with the plate surfaces for a mounting key (Fig. 2.20, *b*). This is done to prevent the bolt breakage at threading.

The examples are high pressure compressors of the AI-25, AL-31 and RD-33 turbofans.



a *b*

Fig. 2.20. Joining by peripheral turnbuckle bolts with distance sleeves:
a – diagram of joint; *b* – bolt head

3. ***Joining by central turnbuckle bolt*** (Fig. 2.21). In most of designs, torque transmission and alignment may be performed by the face splines (the AL-7F, AL-21F, fan of the D-20P, fan of the D-30P, etc.).

In some designs, the parts are aligned by retaining shoulders and the torque is transmitted by friction in the joint (the GTD-3F). Tightening force provides such friction moment between the parts, which exceeds the torque under all operating conditions.

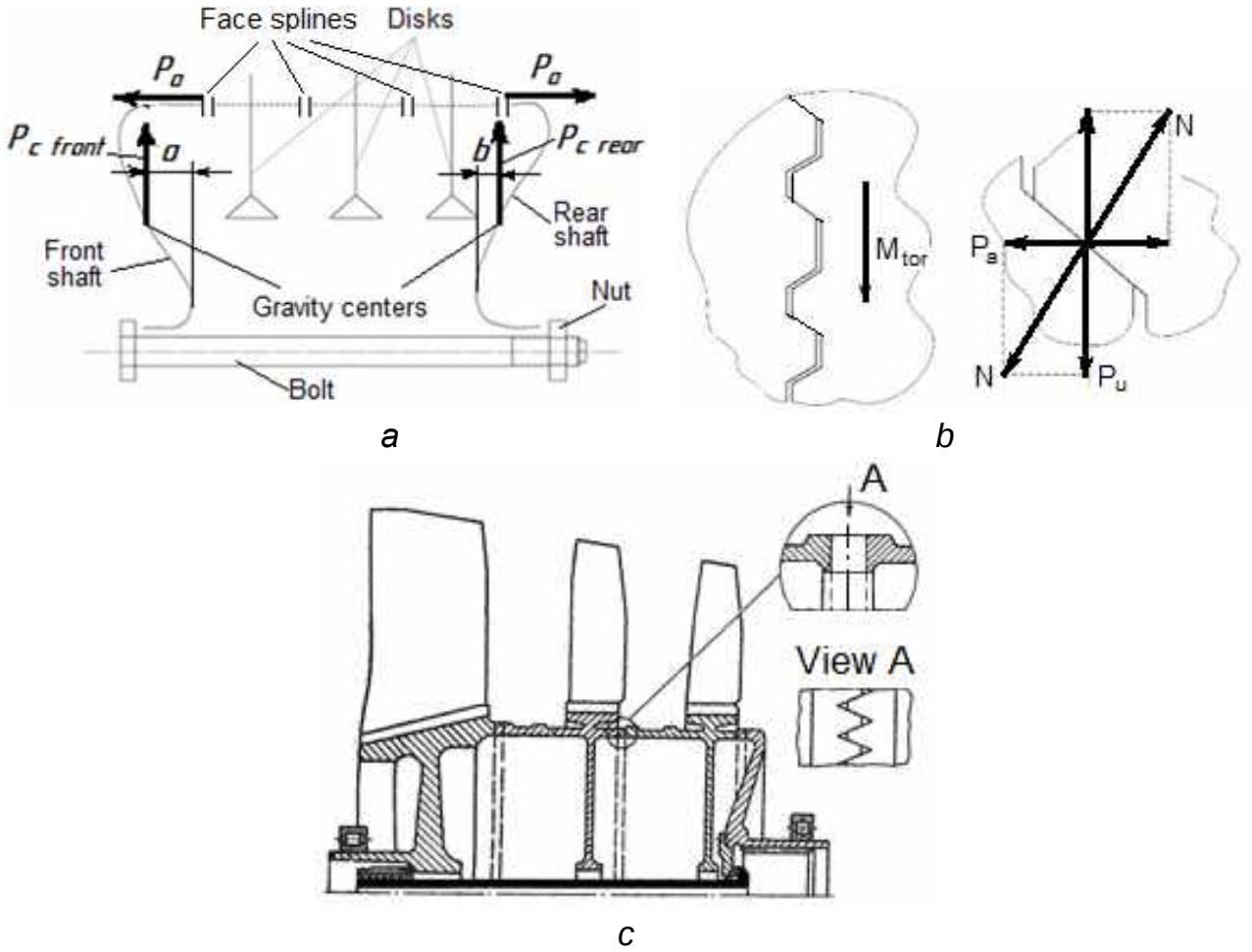


Fig. 2.21. Joining by central turnbuckle bolt:
a – diagram of joint; *b* – forces that affect in face splines;
c – design (fan of the D-20P turbofan)

When the torque is transmitted, the normal force N originates between the splines of the adjacent drum segments (Fig. 2.21, *b*). Its circumferential component P_u generates the torque. The axial component P_a tends to draw the drum segments apart, thus opening the joint. The tightening bolt prevents this opening, but the required tightening force is very high.

To decrease the bolt tightening and its weight, the rotor is designed with the declined front and rear shafts (Fig. 2.21, *a*, *c*). Due to declination of the shafts, their gravity centers are dislocated in relation to the end points of the shaft journals (at distances *a* and *b* in Fig. 2.21, *a*), and centrifugal forces $P_{c\,front}$ and $P_{c\ rear}$ of the shafts generate bending moments $M_{b\,front} = P_{c\,front} \cdot a$ and $M_{b\,front} = P_{c\ rear} \cdot b$. These moments help to overcome the moment of forces P_a that act splines of the front and rear shafts. The second effect of the shafts declination is decreasing of the rotor internal axial dimensions, because supports become closer to each other.

When the rotor sags, the peripheral bolts are loaded non-uniformly. Thus, the drum segments must be widened in bolting spots. Design with the central bolt has less weight and is simpler in manufacturing; its drum portion may be made as a beam of uniform strength (the AL-7F, AL-21F). Therefore, the design with the central turnbuckle bolt is preferable comparing to that with the peripheral bolts. This design is not applicable if another rotor goes through the considered rotor.

Disadvantages of the drum-type rotors are relatively high complexity of the manufacture and high cost.

2.6. Rotor blades. Design and attachment to rotor

2.6.1. Blade structure and requirements

Rotor blades are the major components of the compressor rotor. The airfoils create interblade channels, in which the work of rotor rotation is transformed into kinetic energy of the air motion and simultaneously into potential energy of its pressure. All other rotor parts transmit mechanical energy to the rotor blades and provide required rotational speed.

Requirements to the rotor blade

The compressor rotor blade must meet the following requirements:

1. High aerodynamic performances of the airfoil – high lift force, low drag, smooth streamlining without stall in wide range of attack angles.

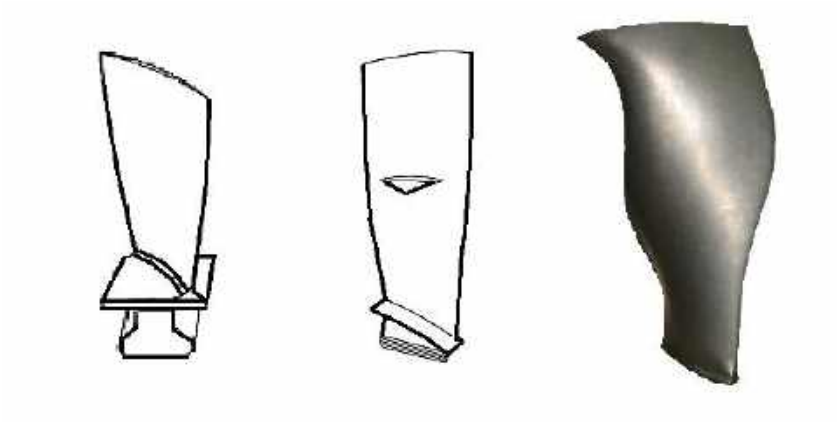
2. High accuracy of manufacturing, which influences both strength and aerodynamic performances. Deviation of the linear dimensions must be not more than 0.05 to 0.15 mm, angular dimension – 15 angular minutes. The blades of one rotor wheel must have same weight; this simplifies rotor balancing. The difference in the weight must not exceed 5 to 6 grams.

3. High strength and vibration resistance. One rotor wheel must be equipped with the blades, which variation of the natural oscillation frequency is not higher than 3 to 4 %.

4. Low weight, low cost and possibility of mass production.

Structure

The compressor rotor blade (Fig. 2.22) consists of the airfoil portion and blade root, which restrains the blade in the disc or drum. These members are connected by a smooth fillet to decrease stress concentration. The blade may be equipped with the inner shroud that forms internal surface of the gas flow duct.



a *b* *c*

Fig. 2.22. Compressor rotor blade:
a – unshrouded; *b* – with mid-span shroud; *c* – 3D-profiled

The blade body is streamlined by the air. So its aerodynamic performances define the compressor pressure ratio and efficiency.

In the turbofan engines with high bypass ratio, the **fan blades** may be equipped with the mid-span shrouds (snubbers) that are located at a distance from the root, which is approximately equal to 2/3 of the blade length (Fig. 2.22, *b*). The main purpose of the mid-span shroud is to avoid a danger of bending and torsional resonant oscillations. Therefore, it is named as the antivibration shroud (the AL-21F, NK-8, D-30, and D-36).

The disadvantage of this design concept is the snubber is located in the supersonic flow where pressure losses are the greatest, resulting in reduction of efficiency and airflow. The shrouds complicate the blade manufacturing significantly, decrease the strength; mid-span shrouds increase hydraulic losses.

This disadvantage has been overcome with implementation of the wide chord fan blade. The blade oscillation stability is provided by the increased chord of the blade, thus avoiding the need in snubber. So, modern fans are equipped with the unshrouded blades (Fig. 2.22, *c*). These blades may be hollow or composite, with metallic titanium or carbonic rod. They must be rigid, because the chord is increased by radius. Chambers of the hollow blades may be filled with the polymer or other honeycomb fillers to damp oscillations.

The rotor blade is highly loaded by the centrifugal and gas forces that cause significant tensile, bending and torsion stresses in the blade body. The magnitude of the centrifugal force that affects the blade depends on the magnitude of circumferential velocity, structural material, and the blade dimensions and reaches 7 to 60 kN. The magnitude of the gas force depends on a stage head and the blade dimensions and is usually by one order less than the centrifugal force.

2.6.2. Blades retaining

As usual, the compressor rotor wheel is made disassembled; the blades are attached to the disc by using a blade attachment, which simplifies overhaul.

The blade attachment must satisfy the following requirements:

- displacement of the specified number of blades;
- high strength and service life;
- precise blade positioning;
- easy assembling and disassembling;
- simple manufacturing;
- low weight.

The blades and disc may be made as a single component part; it is named “blisk” (bladed disc). Usually the blades are manufactured separately and then welded to the disc by friction welding. This procedure allows producing the blades and disc by using different alloys, providing the best properties of each of them. The merit of this design is absence of a vulnerable part (attachment); the disadvantages are complicated manufacturing and necessity of replacement the whole rotor wheel when separate blades are non-operable.

Design of the attachment for a small-sized engine may be non-demountable, when a shaft is made all-in-one with discs and blades. This design is named as “bling”.

When the retaining attachment is used, the blades are restrained in the ring-shaped, longitudinal or sweep slots (Fig. 2.23).

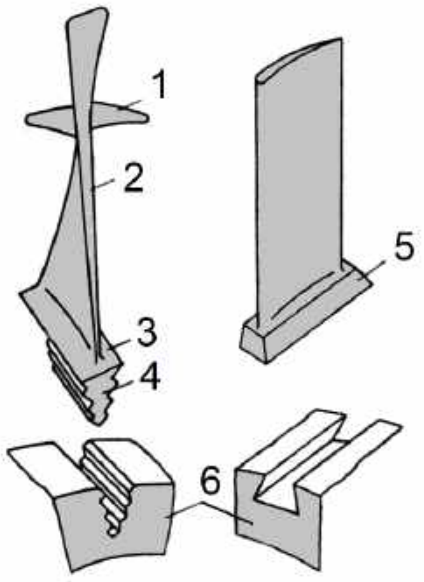


Fig. 2.23. Blades retaining in sweep slots of dovetail and fir-tree shape:
1 – snubber; 2 – blade body; 3 – inner shroud;
4 – fir-tree root attachment; 5 – dovetail root attachment; 6 – disc

The following types of attachments are used:

- trapezoidal (dovetail);
- fir-tree;
- pin;
- hinge (fork-pin).

Trapezoidal (dovetail root) attachment is most widely used.

This attachment is simple in manufacturing because it has only two working surfaces. The standards provide the use of the root with apex angle $\alpha = 40°$, 60°, and 90°. Possible types of the blade body mating with the dovetail root attachment are shown in Fig. 2.24. The first two types are regulated by the branch standard.

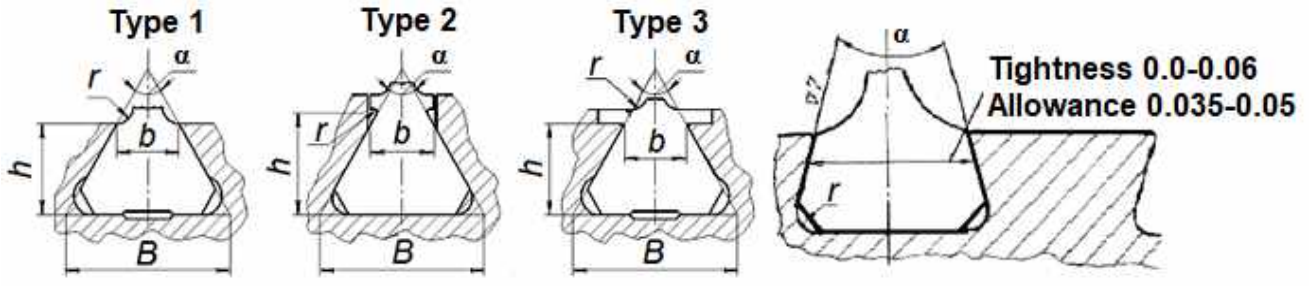


Fig. 2.24. Types of the trapezoidal attachment

The shape of the attachment is a right-angular trapezoid with a base angle 45 to 70° (if the angle decreases then the attachment height becomes less but at the same time the strength of joint is decreased). The maximum strength corresponds to $\alpha \approx 60°$.

The values of dimensions B, b, h, r are given in the branch standards. This decreases the nomenclature of the cutting tools.

The blade may be restrained with interference (it improves rigidity of the retaining joint but it complicates assembling/disassembling) or with positive allowance (this improves assembling/disassembling and helps to damp the blade oscillations). The root faces are usually made in parallel to a chord of the blade root cross-section. So the slots in the disc are arranged at an angle to the rotor axis that is close to the stagger angle of the blade root cross-section. This decreases a weight of the blade transition member between the body and the root and also decreases a specific pressure on the mating surface, thus improving strength of the joint. The blade root may have 3 to 5 μm thick layer of copper or silver electroplated coating, which facilitates assembling due to its “lubrication” effect.

“Fir-tree” attachment is not widely used in the GTE compressors. It provides increased contact surface between the blade and disc. Therefore, it

has improved bearing capacity comparing to other attachment types and allows joining more blades to the disc rim. Therefore, it is used at high loads or when one of the joined parts is made of soft material (for example, aluminum alloy).

Heavy blades of fans are restrained in sweep slots by “fir-tree” attachments.

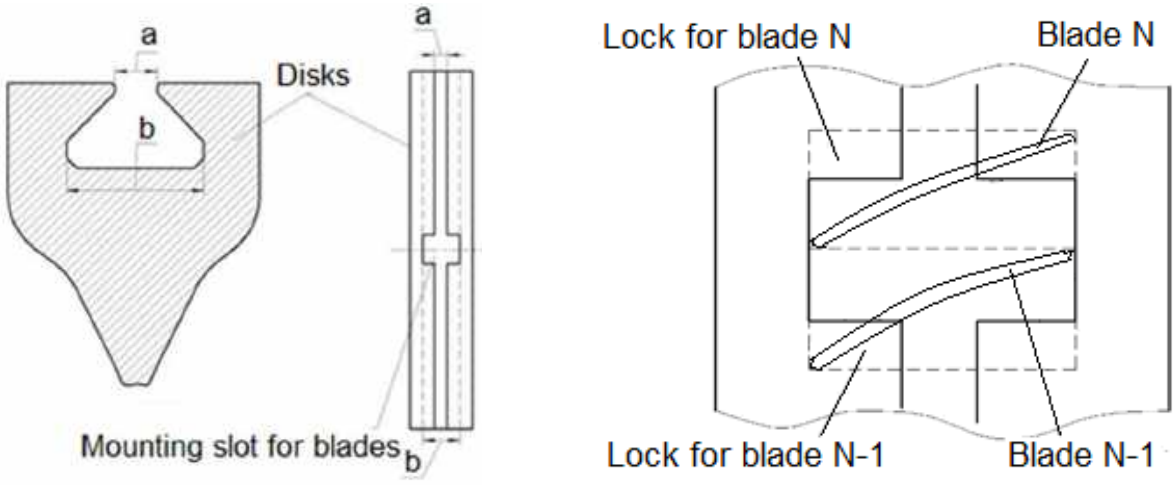
Examples are fan blades of the D-36 turbofan and compressor blades of the AM-3 and TR-1 turbojets. Disadvantages of the “fir-tree” attachment are complicated, labor-consuming and expensive manufacturing, also this attachment has a lot of intensive stress concentrators.

Blades retaining in a ring slot

Peripheral retaining portion of the disc may have a circular slot with cross-section of dovetail or “fir-tree” shape (Fig. 2.25, *a*).

Each blade is fit radially into a disc retaining ring slot through a special mounting slot and then is dislocated to its operating position on a circle (Fig. 2.25, *b*).

The last two blades are arranged in such a way that a boundary between their attachments is located at a center of the mounting slot, thus blades have radial retaining. The examples are the TV3-117 turboshaft, HPC of the AL-31F turbofan.



a *b*

Fig. 2.25. Blades securing to disc in a ring slot:
a – ring slot; *b* – mounting slot with contours of two last blades

Hinge retaining (Fig. 2.26) is applied for long blades, for example, in the fans of the turbofans with low bypass ratio. Two ears of such blades are located in two ring slots of the disc rim between three rim collars. A pin locks the ears; this pin is pressed in the rim collars and locked by the retaining washer and rivet. The pin is fitted in the ears with clearance, thus allowing free turning of the blade around axis of the pin; the turning angle is limited by the inner shroud touching rim collars.

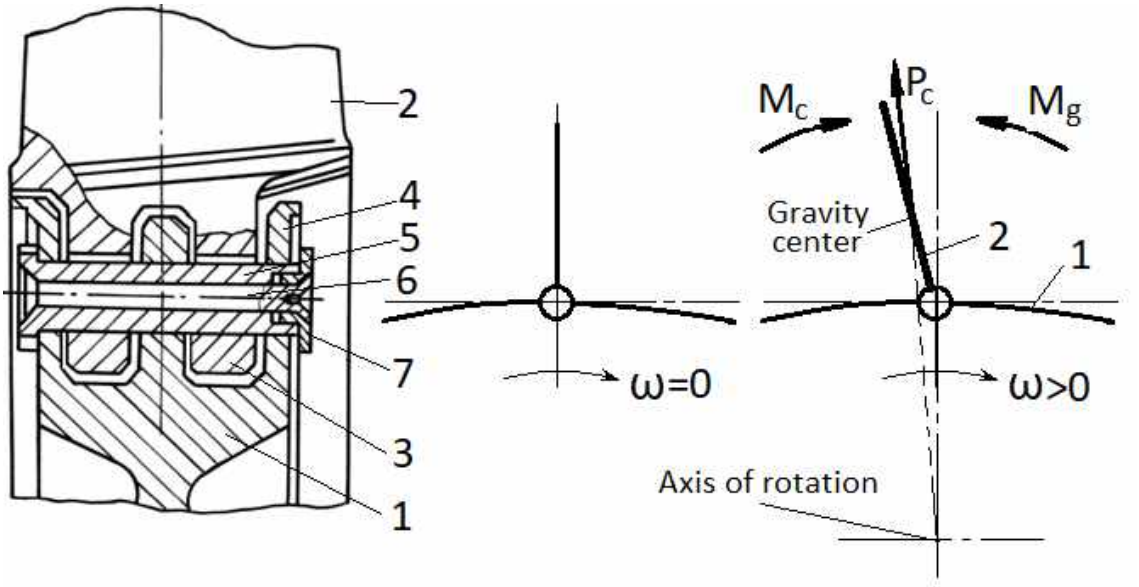


Fig. 2.26. Blade hinge locking:
1 – disc; 2 – blade; 3 – ear; 4 – disc collar; 5 – pin; 6 – rivet; retaining washer

This joint allows blade turning under the action of gas forces. Thus, the blade center of gravity is dislocated from the radius going through the center of the hinge, and bending moment of centrifugal force M_c initiates the effect opposite to the bending moment of gas forces M_g. This moment fully or partially compensates for the moment of gas forces, thus decreasing blade bending.

Essential friction forces originate in a hinge when the blade oscillates; these forces damp oscillations intensively. To prevent wearing of the joined members, their surfaces are smeared with grease, based on ***molybdenum disulfide MoS_2***.

The disadvantages of the hinge joint are complicated manufacturing and high weight of the joint.

2.6.3. Blade axial retaining

During operation, the compressor blades are affected by the high axial forces, which may exceed a friction force and dispose blades in the disc slots. The axial gas force is directed forward (to the compressor inlet); axial component of the centrifugal force, which is initiated due to declination of the blade retaining portion to the disc axis, acts in opposite direction (upwards). So, the blade attached in individual sweep slot needs axial retaining. This is done by special retainers.

The blades can be retained individually or in a group.

Methods of individual retaining:

1. ***Radial pin*** (Fig. 2.27). The disadvantage is necessity to retain the pin from withdrawal.

The pins may be provided with heads of various dimensions and used as rotor balancing weights. To remove the blade from the disc, it is necessary to drill or to cut pins off, and then drive the blade from the slot.

The examples are the R-11F-300 and R-29 turbojets.

2. ***Mill cog*** (Fig. 2.28). The mill cog is made in rear part of the blade attachment. It bears on the disc rear flange and prevents the blade displacement against flow.

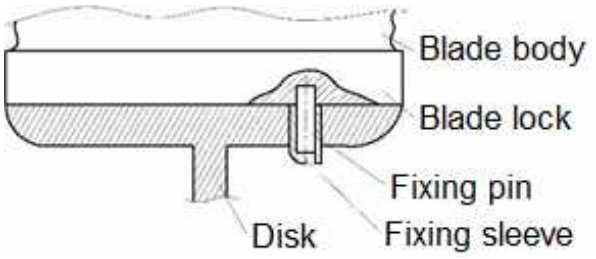


Fig. 2.27. Blade axial retaining by radial pin

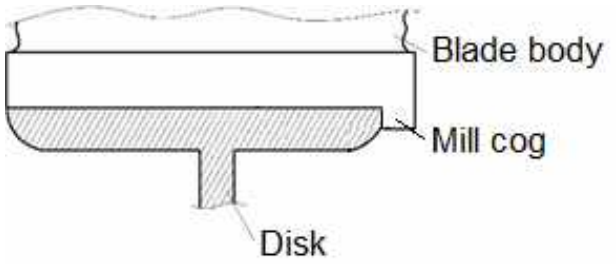


Fig. 2.28. Blade axial retaining by mill cog

3. ***Retaining plate***. Different types of the retaining plates are shown in Fig. 2.29.

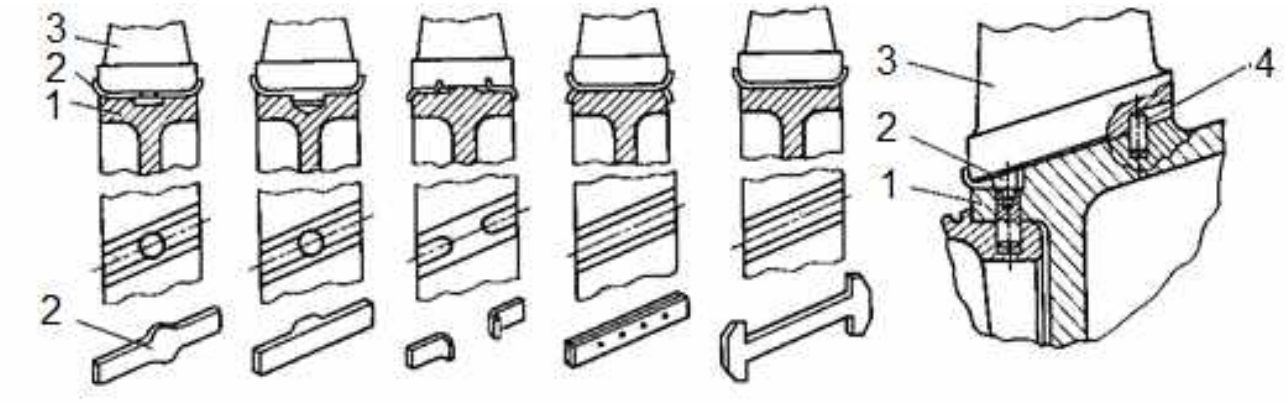


Fig. 2.29. Blade axial retaining by retaining plate:
1 – disc; 2 – retaining plate; 3 – blade; 4 – pin

Methods of grouped retaining:

1. ***Inter-stage spacers*** or duct rings (see Fig. 2.12, *b*) located between discs; the examples are the D-25V turboshaft, D-30P and PS-90A turbofans.

2. ***Split spring ring*** (Fig. 2.30). The ring is located in a ring slot provided in the blade tail. The inner portion of side surface of the ring bears on the disc, thus preventing displacement of the blade. The example is the R-11F-300 turbojet.

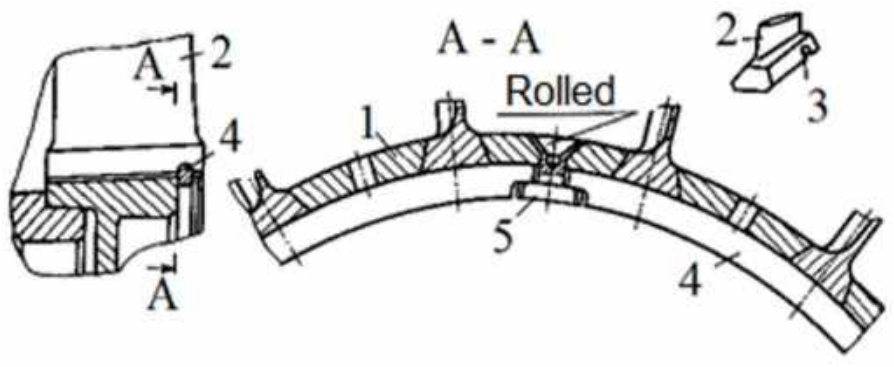


Fig. 2.30. Blades axial retaining by split spring ring:
1 – disc; 2 – blade; 3 – ring slot; 4 – split spring ring; 5 – ring holder

To facilitate a rotor balancing, the blades are selected by mass before assembling. Mass difference of opposite blades must be no more than 1–2 g.

2.7. Loads that affect axial compressor rotor

2.7.1. Forces and moments

Great number of loads affect the axial compressor rotor in service.

1. ***Centrifugal forces*** P_c of the rotated parts. These forces cause tensile stresses in the drum and discs.

Centrifugal forces, which originate due to imbalance, are not localized in the rotor parts and are transmitted to the engine casing, and then through engine mounts to the aircraft. Thus, the rotor must be balanced both statically and dynamically.

2. ***Rotor weight*** G causes bending. The bending moment is the maximum one in middle area between the supports. The smaller the distance between supports, the smaller is bending moment at the same weight.

In a disc-type rotor, the bending moment is taken by the shaft; in a drum and drum-and-disc rotor it is taken by the drum.

3. ***Forces of inertia*** P_j originate when vector of aircraft velocity is changed. It may be when the aircraft is accelerated/decelerated or when it moves by the curved trajectory.

When the aircraft accelerates, the axial inertia force originates

$$P_{j\,a} = m_r g n_a ,$$

which is transmitted from the rotor to the engine casing through a radial-thrust bearing.

When a flight trajectory is curved, the centrifugal inertia force originates

$$P_{j\,c} = m_r r \Omega^2 = m_r g n_c ,$$

where m_r is mass of rotor;

n_a and n_c are axial and centrifugal overload factors;

r is radius of flight trajectory curvature;

Ω is aircraft angular velocity.

Permissive values of overload factors are specified in the Norms of Strength for various flight conditions (see Subsection 1.5.6).

4. ***Gyroscopic moment*** originates when a flight trajectory is curved. It results in rotor sagging:

$$M_{gyr} = I_r \omega \Omega \sin\theta,$$

where I_r is rotor polar moment of inertia;

ω is rotor angular velocity;

θ is angle between $\vec{\omega}$ and $\vec{\Omega}$ vectors.

In the worst case $\theta = 90°$, then $M_{gyr\,max} = I_r \omega \Omega$.

The gyroscopic moment additionally loads the bearings of the rotor supports and through the bearings is transmitted to the casing. It causes sagging of the rotor and casing. The gyroscopic moment decreases if a distance between the rotor supports shortens.

5. ***Torque*** M_{tor} is transmitted from the turbine to compressor and causes torsion stresses in the shaft or in the drum.

6. ***Forces of external and internal pressure*** (Fig. 2.31):

– force $P_{gas\,path} = p_{gas\,path} F_{gas\,path}$ acts the rotor from the compressor gas flow duct;

– force $P_{int} = p_{int} F_{int}$ affects the rotor from its internal chamber.

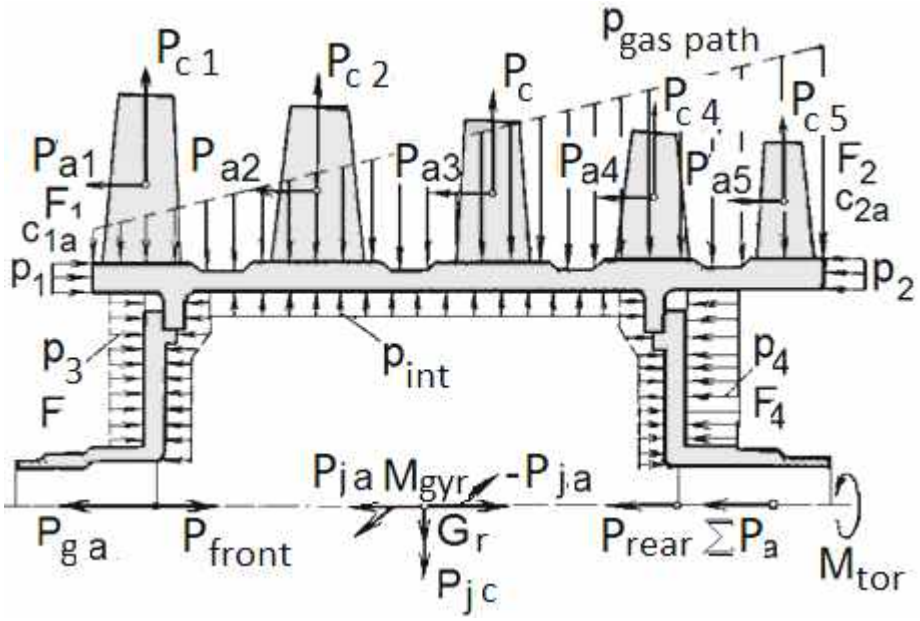


Fig. 2.31. Forces that affect a compressor rotor

7. ***Axial gas-dynamic forces*** are axial components of the aerodynamic forces that affect the rotor blades and pressure forces that affect the rotor drum and faces (Fig. 2.32).

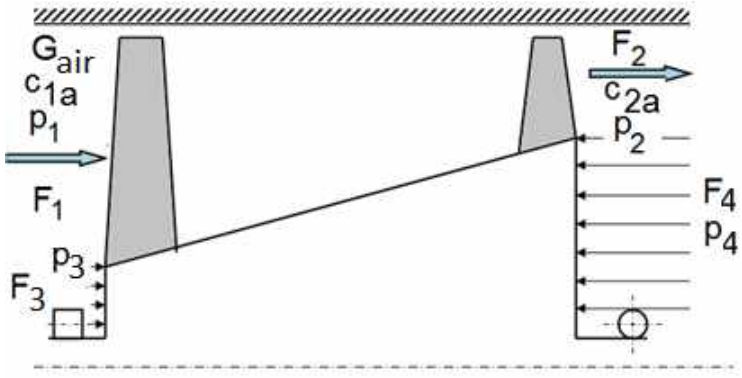


Fig. 2.32. Axial gas forces that affect axial compressor rotor

Total gas-dynamic force that affects compressor consists of two components. The first component affects from the gas flow duct and may be defined using Euler's equation:

$$P_{g\,1} = G_{air}\left(c_{2\,a} - c_{1\,a}\right) + p_2F_2 - p_1F_1,$$

where G_{air} is air mass flow;

p_1, p_2 are inlet and discharge static pressures;

$c_{2\,a}$, $c_{1\,a}$ are inlet and discharge axial velocities;

F_1, F_2 are input and output areas of the compressor duct.

The second component is resultant of pressure forces that affect the rotor face planes:

$$P_{g\,2} = p_4F_4 - p_3F_3,$$

where p_3, p_4 are static pressures in front and rear cambers;

F_3, F_4 are areas of front and rear faces of the rotor.

The total gas-dynamic force affecting the compressor is as follows:

$$P_{g\,a} = G_{air}\left(c_{2\,a} - c_{1\,a}\right) + p_2F_2 - p_1F_1 + p_4F_4 - p_3F_3.$$

The total axial force $P_{g\,a}$ may exceed the engine thrust in 5 to 6 times.

2.7.2. Compressor rotor axial unloading

The rotor as a whole includes compressor and turbine and has only one radial-thrust bearing support, which is usually included into the compressor arrangement. All other supports are radial ones. Rotors of the compressor and turbine are joined by a coupling, which transmits from the turbine to the compressor not only a torque but also the axial force that affects the turbine rotor. The axial forces of the compressor and turbine have opposite signs and

are added one to another. The total axial force $P_{a\Sigma}$ is transmitted to the compressor stator through the radial-thrust bearing. Since the axial force of compressor is always significantly more than the axial force of the turbine, so the total force is high and the bearing is overloaded.

The total force is decreased due to a special design of the compressor: the rear and front chambers are sealed from the gas flow duct and become the unloading chambers (Fig. 2.33).

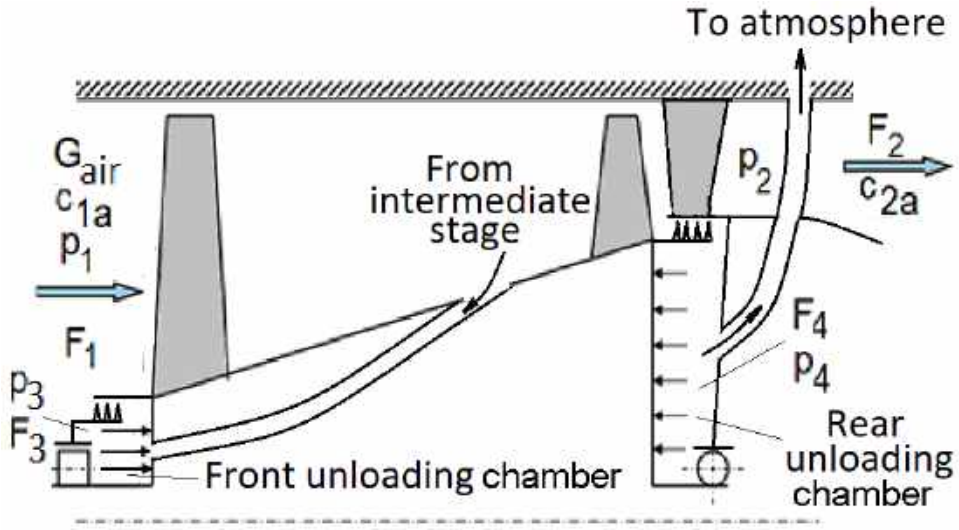


Fig. 2.33. Unloading chambers of compressor

The front unloading chamber is separated from the compressor inlet by the labyrinth seal and pressurized by the high-pressure air coming from the compressor intermediate stage: $p_3 > p_1$.

The rear unloading chamber is separated from the compressor outlet by another labyrinth seal and communicates with the atmosphere (or with the bypass duct in the turbofan) through the air jet. Thus, $p_4 < p_2$, but the pressure in the rear unloading chamber is somewhat higher than the atmospheric one; that allows pressurizing of the oil chambers, which pressure is atmospheric one:

$$p_4 = p_н + \Delta p,$$

where $p_н$ is atmospheric pressure;

Δp is gauge pressure, which at the on-ground conditions is 40 to 90 kPa.

The pressure in the rear chamber p_4 is designed to pressurize the oil chamber of the rear bearing. Then area of the air jet is determined taking into account this pressure and the air escape through the rear labyrinth seal, which separates the rear chamber from the compressor duct, and the air escape through the seal, which separates the rear chamber from the bearing chamber.

The required pressure p_3 in the front chamber depends from the known specified value of p_4, total axial force $P_{a\Sigma}$ and load capacity of bearing $P_{a\,specif}$ as

$$p_3 = \frac{P_{a\,specif} + p_4 F_4 - P_{a\,\Sigma}}{F_3}.$$

Then, knowing the pressure p_3, the compressor stage is chosen for the air bleeding to the front chamber.

2.8. Stators of axial compressors

Stator together with the rotor makes the compressor gas flow duct. The stator also is one of the engine load-carrying members.

2.8.1. Main components of compressor casing

The main members of a compressor stator are:

- supporting casings (frames);
- compressor casing;
- inlet guide vanes, guide vanes and straightening vanes.

The compressor stator is one of the major structural elements of the engine power structure. It carries the compressor vanes (IGV, GV, SV) and the rotor supports. Outer side of the casing contains the engine-to-aircraft mounts, accessory drive gearboxes, engine accessories and other structural members.

Requirements to the compressor stator:

- high strength;
- required rigidity;
- air proofness;
- low weight;
- simple manufacturing and overhauling, especially easy assembling and disassembling of the stationary vanes and rotor;
- possibility of visual inspection of the gas flow duct during maintenance.

The axial-flow compressor stator consists of three components (Fig. 2.34):

- front frame with IGV;
- casing of guide vanes (intermediate casing) with GV;
- rear frame with SV.

This is the commonly used composition. In partial designs, the front frame may be absent (the R-11F-300 turbojet).

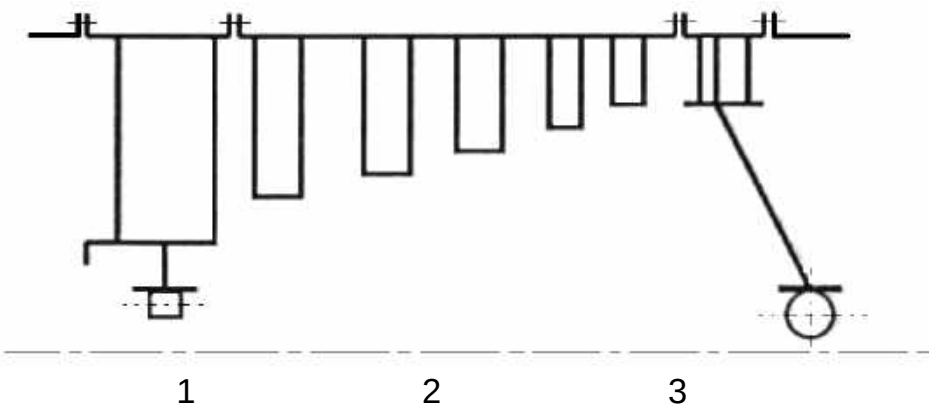


Fig. 2.34. Casing of a single -shaft turbojet:
1 – front frame; 2 – casing of guide vanes; 3 – rear frame

2.8.2. Front frame

The front frame (Fig. 2.35) is the engine load-carrying element. It keeps a front bearing and inlet guide vanes. The front frame of the turboprop engine also keeps a front carter and a gearbox. The front frame is a cast or welded structure, which consists of two concentric rings, joined by the aerodynamic struts or by the inlet guide vanes (IGV). The struts or vanes are power links between the front bearing and the engine casing.

The front frames of some engines have support units for mounting the engine to the aircraft (for example, the TV3-117 turboshaft). The engine accessory units are mounted on the front frame.



Fig. 2.35. Front frame

The IGV are located before the first stage of the compressor to swirl preliminary the air and to increase the thermodynamic work of the first stage. The IGV may be variable for providing the compressor stable operation (Fig. 2.36). The rotary vanes have hubs, which are supported by the sliding or rolling bearings. The sliding bearings are preferable. They have bronze or glass-teflon inserts. The vanes are turned simultaneously by a gear mechanism (the AM-3) or by a ring with levers joined to the upper hubs of the vanes (the TV3-117, AL-7, AI-25, D-36, etc.).

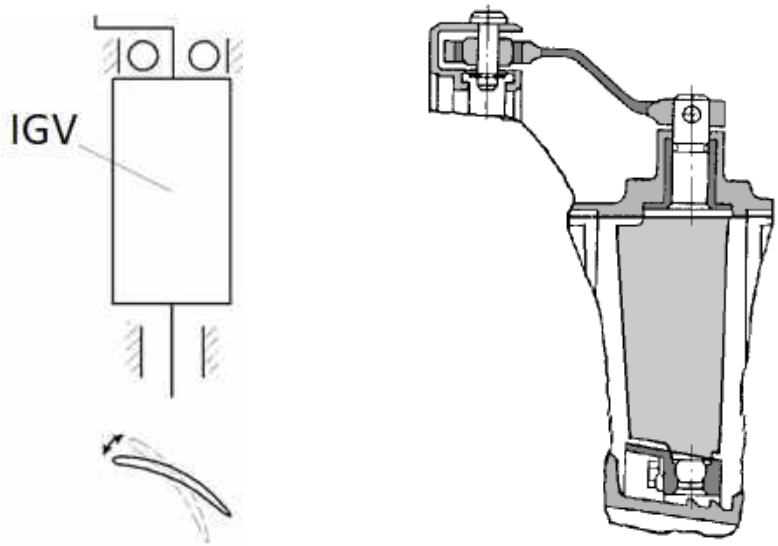


Fig. 2.36. Variable inlet guide vanes

The struts of the front frame and IGV may be covered with ice. To prevent ice formation, the struts, IGV and spinner are covered with the hydrophobic varnish and heated. The vanes are hollow or are equipped with external deflector (Fig. 2.37).



Fig. 2.37. Vanes with ice protection

Compressed air, oil or electricity may be used as a heater. The hot air is preferable (Fig. 2.38).

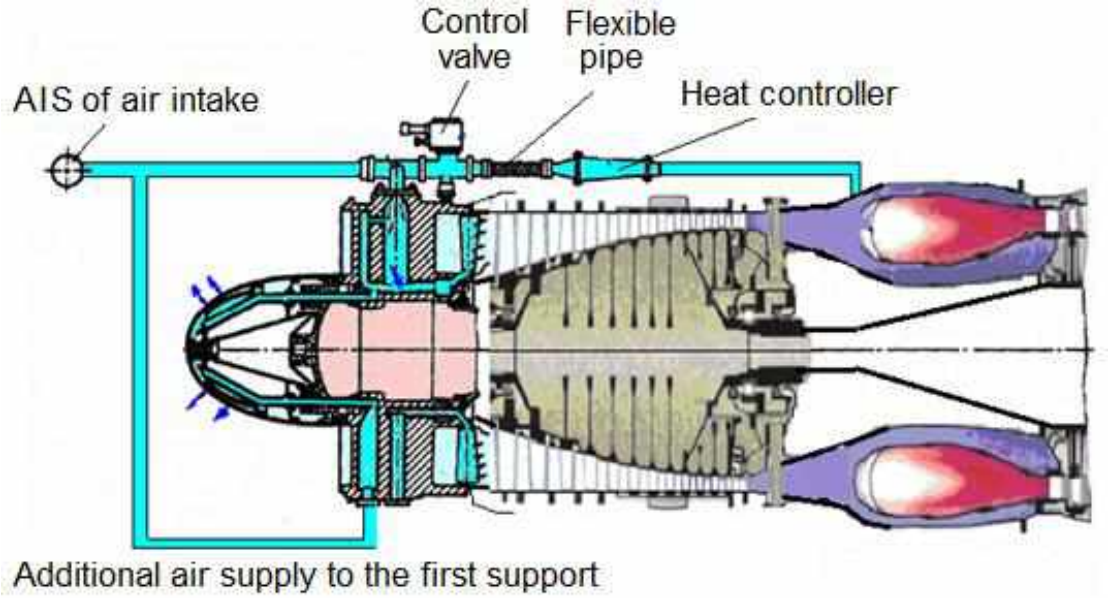


Fig. 2.38. Anti-icing system of TV3-117 turboshaft

2.8.3. Casing of guide vanes

Casing of guide vanes usually forms the compressor gas flow duct. It keeps guide vanes. It is an intermediate load-carrying element, which transmits loads from the front rotor support to the engine mounting units located on the rear frame.

The casing may be casted or welded, disassembled or not disassembled. Rigidity of welded thin-walled casing is improved by welded structural sections, which are transversal and longitudinal reinforcing ribs. As usual, the casing keeps structural members of compressor control system.

Disassembled casing (Fig. 2.39) facilitates compressor assembling and vanes inspection during maintenance, but has increased weight, less strength and rigidity. It may be split longwise or crosswise, or have both splits. The casing parts must be aligned at assembling. This is done by pins (in longwise split) and by seat collars or precise bolts (in crosswise split).

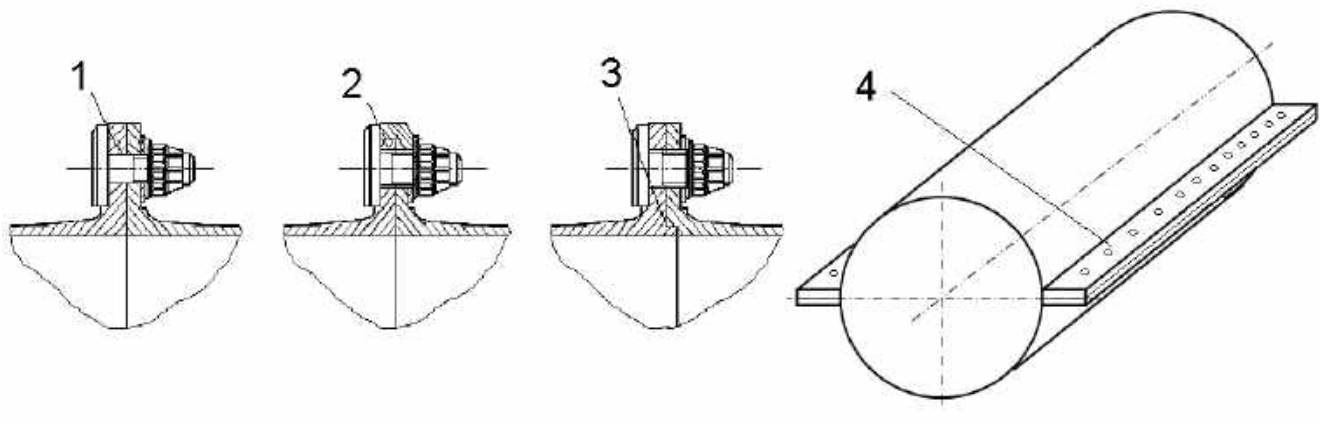


Fig. 2.39. Disassembled casings of axial compressor:
1 – alignment by template bolts (pins); 2 – alignment by outer seat collar;
3 – alignment by inner seat collar; 4 – casing with longwise split

The transversal split with alignment by the inner seat collar is used in the first stages where heating is low (item. 3 in Fig. 2.39). Axial clearance allows components tightening to prevent the air escape. If the split is located in hot zone, the outer seat collar is used (pos. 2 in Fig. 2.39).

The radial deformation of the flange in hot zone is increased. In this case, flanges are aligned by template bolts inserted into the out-of-roundness holes (Fig. 2.40). The example is the TV3-117 turboshaft.

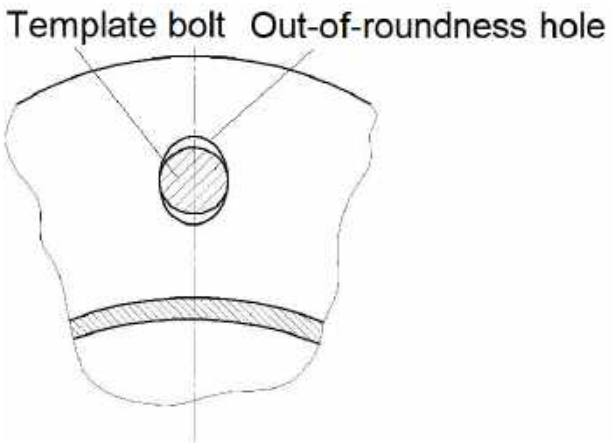


Fig. 2.40. Alignment of highly heated casing

Guide vanes are the end portion of the compressor stage. They turn the air flowing from the rotor blades at a specified angle and also transform the part of a kinetic energy of the air flow into the potential energy, thus increasing the pressure.

Design of the guide vanes depends on the used type of casing (disassembled or not) and rotor.

Attachment of the guide vanes may be classified according to its load-carrying structure as cantilever, two-support and frame attachment (Fig. 2.41).

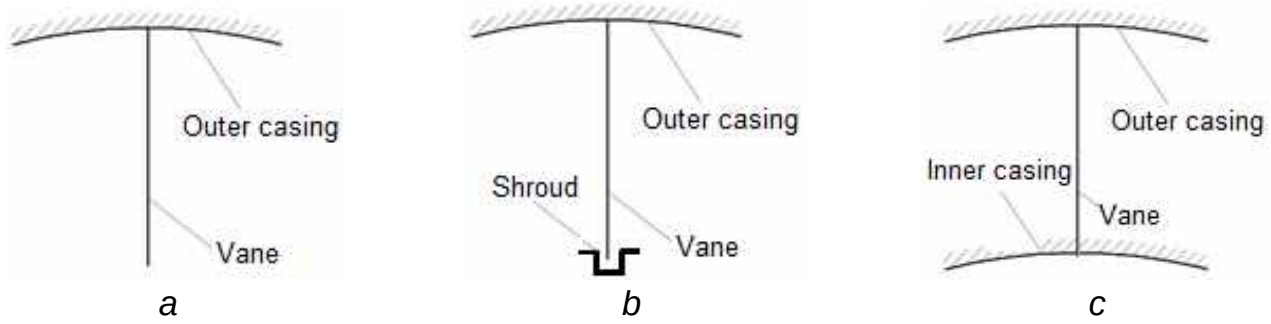


Fig. 2.41. Types of guide vanes attachment:
a – cantilever; *b* – half-frame; *c* – frame

The vanes are ***attached in cantilever*** if internal diameter of gas flow duct is formed by the rotor and vanes are short (the HPC of the D-30P turbofan, D-25V turboshaft, TV3-117 turboshaft, etc.).

For long vanes, the ***half-frame*** attachment is applied (Fig. 2.42). Free end of the vane is joined to the shroud, which supports all vanes, takes their loads and increases rigidity of the airfoil.

The shroud may be of a split-type or solid. In the last case, the vanes have hubs, which allow radial displacement of the vanes relative to the stator caused by the non-uniform heating.

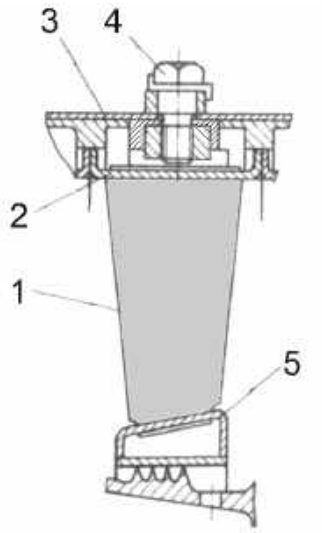


Fig. 2.42. Guide vanes with rigid attachment to outer half-ring
and free attachment to inner ring:
1 – vane; 2 – outer half-ring; 3 – casing; 4 – screw; 5 – inner half-ring

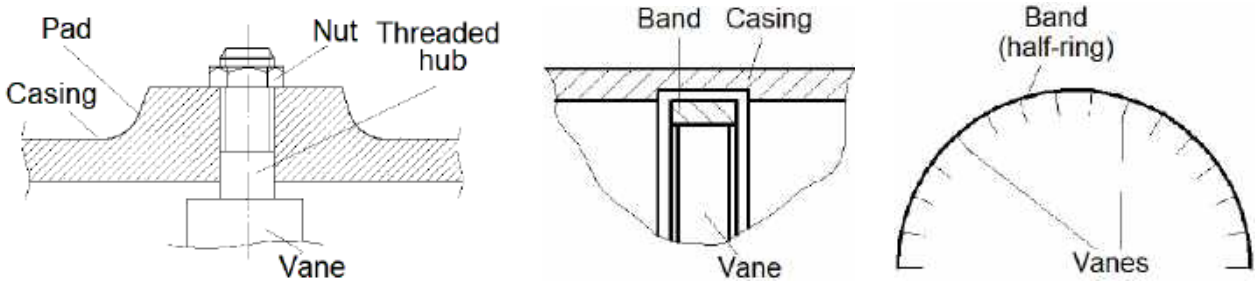
Frame attachment is implemented if vanes are included into the casing power structure and transmit load from the support to the engine casing. This concerns mainly straightening vanes of the compressor last stage.

The joint between the guide vanes and casing can be not-disassembled (by welding or brazing) or disassembled.

The non-disassembled joint is used in the engines with small life time (for example, the R-15B turbojet, Fig. 2.43).

In case of disassembled casing, the vanes can be locked by the threaded journals. However, the strength of the casing is decreased due to a large number of holes.

The band is joined to the casing by pins or screws (the number of joints must be not less than 6 to 8).



a *b* *c*

Fig. 2.43. Joining guide vanes with casing:
a – individual; *b*, *c* – grouped using a band

2.8.4. Rear frame

Rear frame of compressor is usually the main engine load-carrying member (Fig. 2.44). It contains the engine mounts and the casing of the rear

compressor support (housing of the engine intermediate bearing) that are usually included into a load-carrying system. The power link of the bearing with the casing is usually implemented by the compressor straightening vanes. In this case, the frame mounting of vanes is applied.

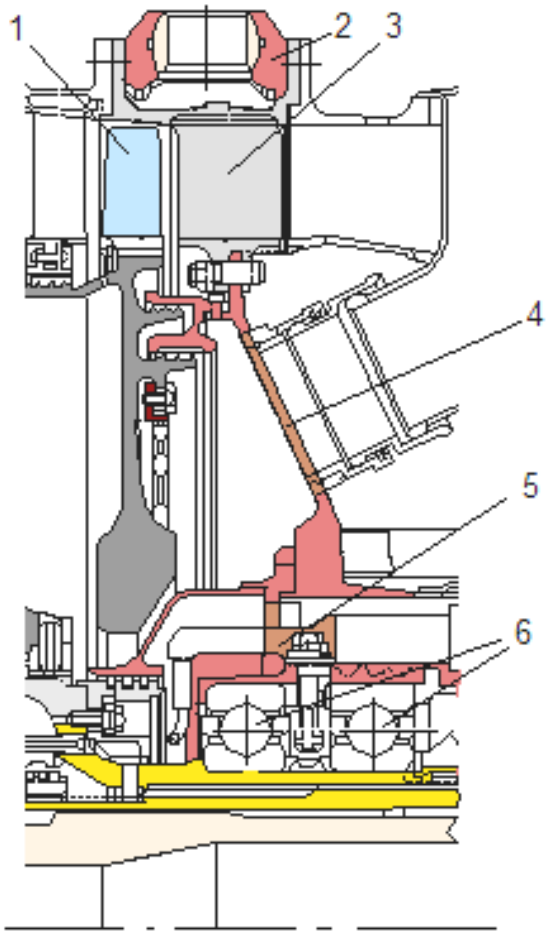


Fig. 2.44. Rear frame of the R-95Sh turbojet compressor:
1 – rotor blade; 2 – thrust transmission unit; 3 – straightening vane;
4 – diaphragm; 5 – bearing housing; 6 – radial-thrust bearings

The main load-carrying member of the turbofan engine is a compressor intermediate casing, which is a rear casing of the LPC and simultaneously a front casing of the HPC.

2.9. Clearances between rotor and stator

Radial and axial clearances between the rotor and stator (Fig. 2.45) exclude touching of the rotor blades to the stator at all power ratings. Clearances at power ratings significantly differ from those of cold engine, because when the engine operates, the parts of rotor and casing are deformed under the effect of heating and various mechanical loads.

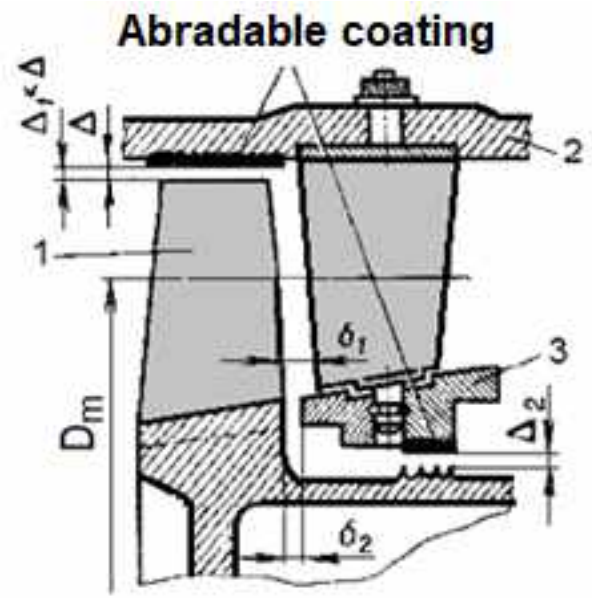


Fig. 2.45. Radial and axial clearances in a compressor stage:
1 – rotor blade; 2 – casing; 3 – inner ring of guide vanes

Clearances in a gas flow duct influence compressor performance significantly, thus influencing overall engine performance. For example, increasing of the radial clearance on 1 % decreases compressor efficiency by 1 % and increases the specific fuel consumption on 0.65 to 0.95 %.

When specifying the radial clearances Δ, it is necessary to take into account their variation due to heating, action of centrifugal forces on the rotor components, and also due to action of the pressure forces on the stator. Permissible values of the relative radial clearance in the engine cold state are $\bar{\Delta}_1 = \frac{\Delta_1}{l} = 0.002$ to 0.007 for the first stages and $\bar{\Delta}_1 = 0.015$ to 0.04 for the last stages. This value may be decreased by using soft wearable (abradable) coatings on the casing upstream of the tips of the rotor blades if the coatings are made of graphite, talk or composite materials.

Another method to decrease danger of blades touching the casing is cutting the tip of the blade.

Radial clearance Δ_2 between guide vanes shroud and ribs of the labyrinth seal under cold condition is $\Delta_2 = 0.2$ to 2 mm. The axial clearances shall be the minimum for decreasing the compressor length and weight. But it is known that each airfoil portion streamlined by the gas is followed by the Carman's track. This track contains turbulent vortex, which decreases intensity at a distance from the trailing edge. Hence, small axial clearance provokes oscillations of the rotor blades. Therefore, axial clearances in the compressor are compromise between the compressor length and its efficiency.

Usually, on the mean radius $\bar{\delta} = \frac{\delta}{b_m} = 0.15$ to 0.25, where b_m is a mean chord; in the fan stages of high bypass ratio, $\bar{\delta} = 1.7$ to 2.0.

2.10. Sealing of compressor gas flow duct and oil chambers

Seals in the compressor are used to separate the air and oil chambers; in the gas flow duct of each stage they prevent the air spilling from the chambers with high pressure (stage outlet) to the chambers with low pressure (stage inlet).

Negative results of oil entering gas flow duct are not only the oil leakage that increases necessary oil storage in the tank. Toxic oil vapor may be contained in the air, which is bled from the compressor for the air conditioning in the crew and passengers cabins.

Two types of seals are used:

- contact (dispensable) seal;
- non-contact (non-dispensable) seal.

Typical sealing assembly (Fig. 2.46) includes an oil chamber, which is separated by the contact seals. The contact seals are pressurized from the outside by higher pressure in the pressurizing chamber. The last is separated from the gas chamber by the non-contact labyrinth seals. Pressure in this chamber may be higher than in the gas chamber.

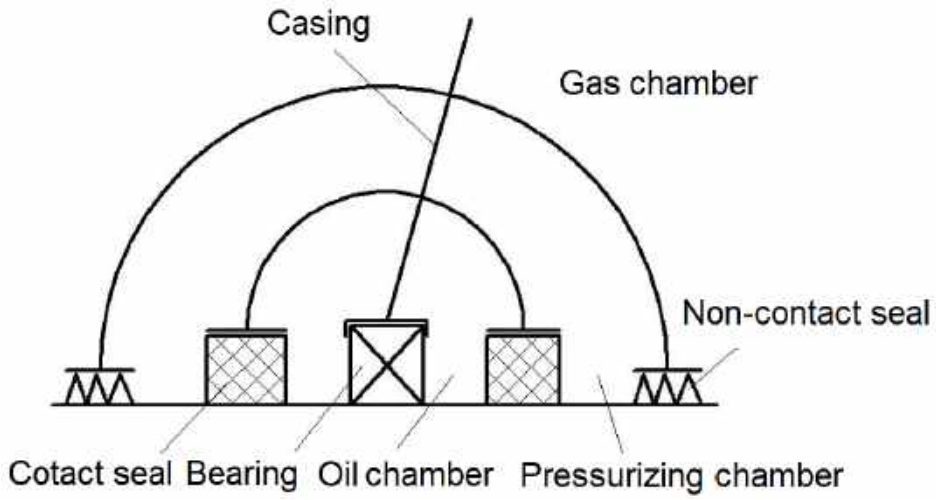


Fig. 2.46. Typical sealing assembly

2.10.1. Contact seals

Contact seals (ring, face, and radial-face) separate the chamber of bearing (oil chamber) and prevent the oil leakage from this chamber to the engine gas flow duct.

The ***ring seal*** is used at velocity less than 100 m/s and pressure difference of 0.2 to 0.3 MPa (for example, the front support of the R11F-300 turbojet, Fig. 2.47, *a*). They contain 2 or 3 split rings made of chromium cast iron with porous chromium coating of the end faces or of tin bronze. The ring elasticity is specially chosen in such a way that when a shaft rotates, the ring stays almost stationary and slightly nutates.

The ***face contact seal*** operates due to a spring, which presses the stationary sealing sleeve to a graphite sealing ring (the F-100-PW-100 turbofan). The pressing force depends on the spring tightness and pressure difference between both sides of the seal (Fig. 2.47, *b*). The graphite, casted iron, bronze of composite material are used as the antifriction material.

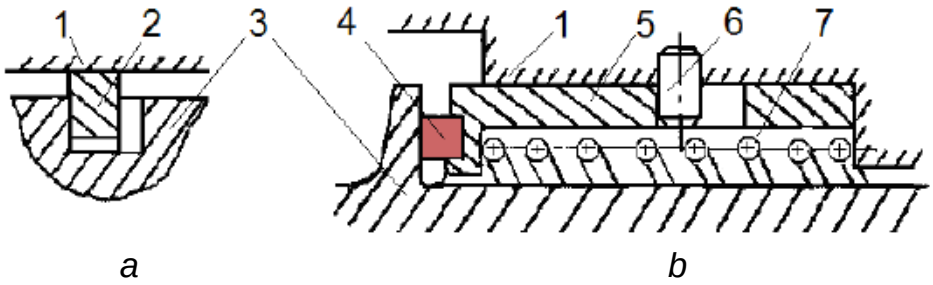


Fig. 2.47. Ring (*a*) and face (*b*) contact seals:
1 – stator; 2 – elastic ring; 3 – shaft; 4 – ring made of antifriction material;
5 – movable sleeve; 6 – pin; 7 – spring

The ***radial-face seal*** (Fig. 2.48) contains a graphite ring located between two end face rings. This ring is split; thus, it is pressed to the inner wall of the casing. Pressure in the air chamber presses this ring to one of the end face rings (at the right in the figure).

All supports of the D-36, D-436, D-136 engines are equipped with the duplicate radial-end face seals.

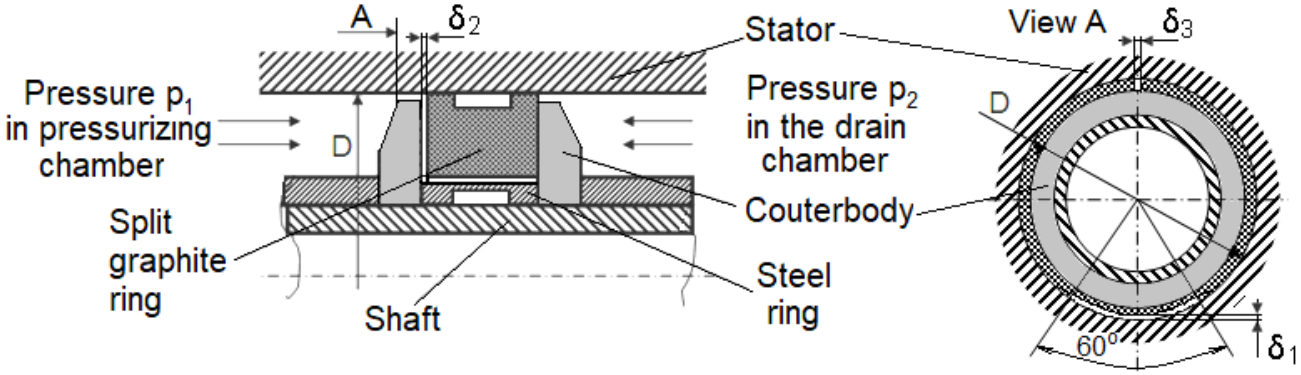


Fig. 2.48. Graphite radial end face contact seal

Efficiency of the radial end face seal is defined by consumption of the air escape from the pressurizing chamber to the drain chamber. Pressure p_1 in the

pressurizing chamber is higher than pressure p_2 in the bearing (drain) chamber; so the oil from the drain chamber not enters the pressurizing chamber, and the air from the pressurizing chamber flows to the drain chamber.

Leakage through the radial and face seal is calculated by using formula of Khristianovych:

$$G_{seal} = \frac{m\, A\, p_1^* f\, q(\lambda)}{\sqrt{T_1^*}},$$

where $m = 0.03965$ is flow factor;

$A = 0.6$ is empirical coefficient for this type of seal;

p_1^* and T_1^* are stagnation pressure and temperature in pressuring chamber, respectively;

f is cross-sectional area of the seal;

$q(\lambda)$ is gas-dynamic function, corrected mass flow.

Parameters p_1^* and T_1^* of the air before the seal (in the pressurizing chamber) are defined by using results of the pressurizing numerical analysis. The cross-sectional area consists of several components is as follows:

$$f = \frac{\pi D \delta_1}{6} + \pi D \delta_2 + \delta_3^2,$$

where δ_1 is gap at arc 60° at the external diameter of the graphite ring ($\delta_1 \approx 0.1\ldots0.3$ mm);

δ_2 is clearance between the graphite ring and counterbody under operating condition of the radial end face seal when the engine is running ($\delta_2 \approx 0.2\ldots0.4$ mm);

δ_3^2 is area clearance in slot of the graphite ring, which projects above the counterbody ($\delta_3 \approx 0\ldots0.2$ mm).

The gas-dynamic function $q(\lambda) = \left(\frac{k+1}{k}\right)^{\frac{k}{k-1}} \lambda \left(1 - \frac{k-1}{k+1}\lambda^2\right)^{\frac{1}{k-1}}$; parameter λ is a ratio of the air velocity at adiabatic flow to a critical velocity. Value λ is determined by ratio of a pressure p_1 in the pressurizing chamber to a pressure p_2 in the drain chamber:

$$\lambda = \sqrt{\frac{k+1}{k-1}\left[1 - \left(\frac{p_1}{p_2}\right)^{\frac{k-1}{k}}\right]},$$

where $k = 1.4$ is adiabatic factor of the air.

The air temperature at the seal outlet is determined by the equation

$$T_2 = \frac{T_1}{(p_1 / p_2)^{\frac{k-1}{k}}} .$$

2.10.2. Non-contact seals

The labyrinth, slot-type and brush non-contact seals are applied.

Labyrinth seals (Fig. 2.49) provide multiple throttling of the air following through the passages with abruptly changing cross-sectional areas (via narrow slot into large chamber).

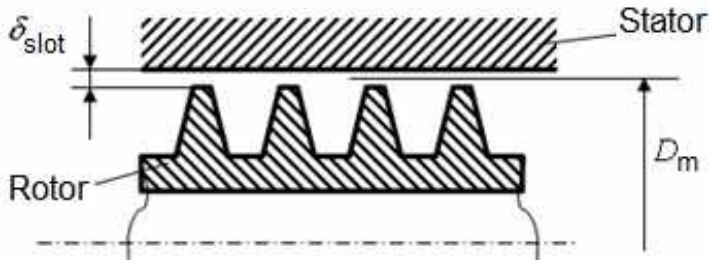


Fig. 2.49. Labyrinth seal

The air escape in the labyrinth seal takes place through the clearances (slots) between the labyrinth seal fins and stator.

Efficiency of functioning of the labyrinth seal depends on the number of fins, their configuration, pressure difference between the chambers and the value of radial clearance. This efficiency is defined as the value of the air escape through a seal (kg/s):

$$G_{seal} = K\, f_{slot} \sqrt{\frac{p_1^2 - p_2^2}{zRT_1}} ,$$

where K is flow factor that takes into account specifics of expansion in the clearance and non-complete breaking in the labyrinth chamber (depends on the labyrinth type and shape of the fins);

$f_{slot} = \pi D_m \delta$ is slot area;

p_1 and p_2 –are pressures at both sides of the labyrinth, respectively;

R is gas constant (for the air, $R = 287$ J/(kg·K);

z is the number of fins.

In case of necessity, the air temperature at the labyrinth seal outlet may be defined in the same way as for the contact seal.

Recommended permissible value of the air escape through the labyrinth seal shall not exceed 0.5 to 1 % of the total air flow.

Fig. 2.50 shows various types of the labyrinth seals.

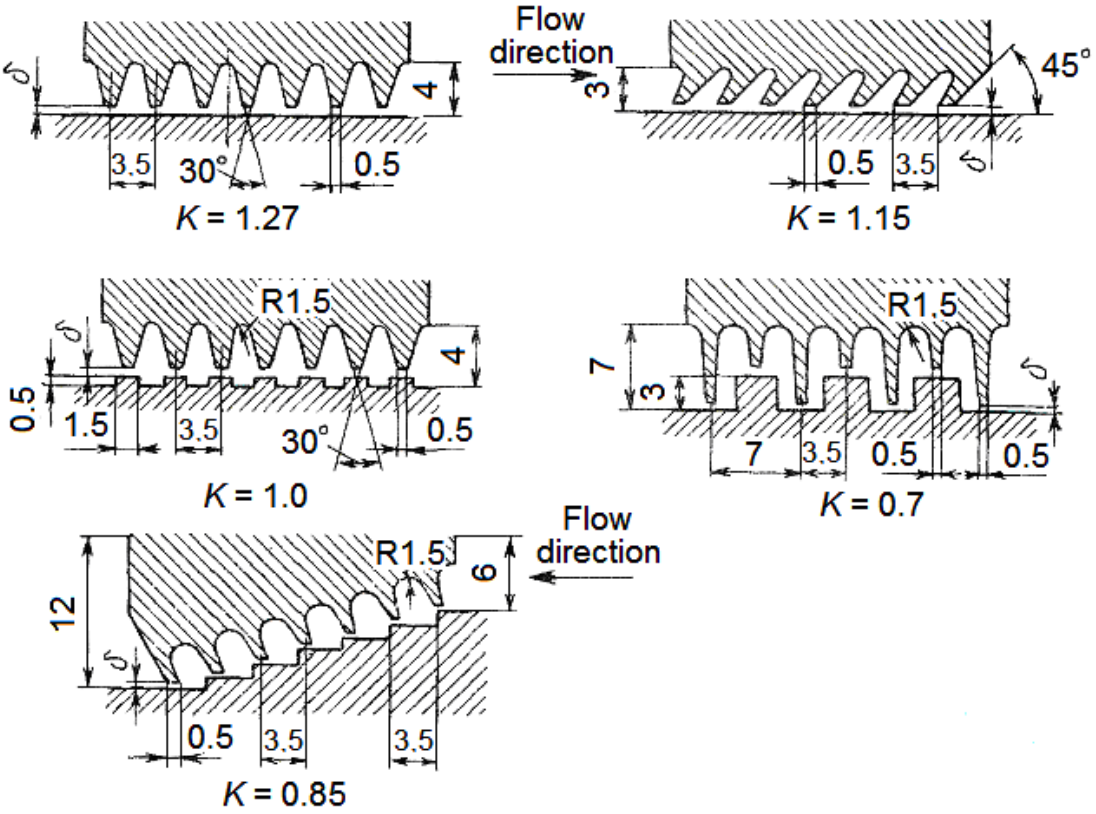


Fig. 2.50. Types of labyrinth seals and respective flow factors

It was shown by the experiments that if the number of fins exceeds 6 to 8, addition of a new fin increases efficiency slightly. Therefore, if it is necessary to use more fins or if the length of the labyrinth is strongly limited, then the labyrinth seal is designed as a double-row or a triple-row structure (Fig. 2.51).

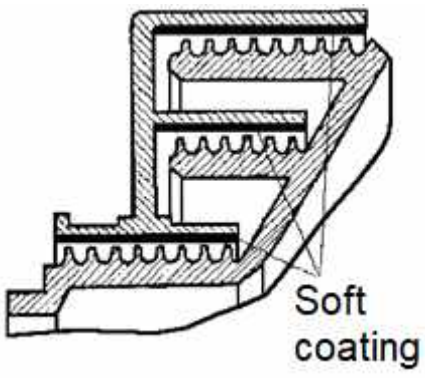


Fig. 2.51. Triple-row labyrinth seal

Besides the type and number of the fins, the labyrinth seal efficiency depends on the shape of the edges. It was shown by the experiments that even small rounding of the edges decreases functioning of the labyrinth seal significantly.

Axial and radial **slot seals** are partial versions of the labyrinth seal.

In design of the labyrinth and slot seals, usually wearable coatings are used for covering surface, which contacts with the fins. The coating may be made of talk, graphite, honeycomb, or abradable ceramics.

2.10.3. Brush seals

Brush seal is a labyrinth-contact seal, which flexible brush touches continuously (at an angle of approximately 45°) the rotating part of the seal. The brush is made of cobalt alloy wires, which diameter is 0.025 to 0.1 mm. The diagram of a two-row brush seal is shown in Fig. 2.52. Each row consists of brushes that are pressed between small and large plate rings. In case of brush breaking, the large rings with clearance δ operate like a labyrinth seal. The brushes are positioned with respect to the slots with clearance δ, thus decreasing the air escape on 20 to 40 %.

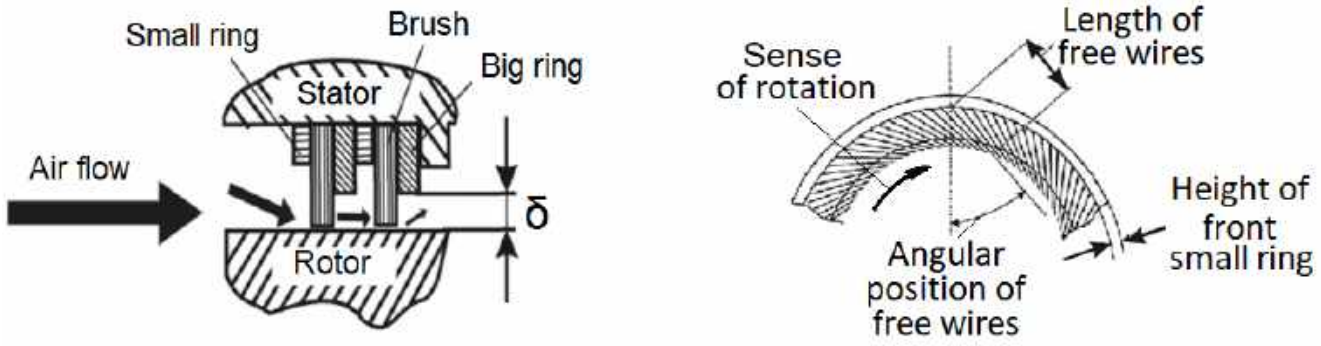


Fig. 2.52. Brush seal

2.11. Compressor controls

Off-design operating conditions unbalance stages of the axial compressor and change attack angles of the rotor blades and guide vanes. This changes conditions of the blades and vanes streamlining and can provoke stall and surge.

To prevent unbalance operation of the axial compressor at the off-design operating conditions, various devices are used. These devices make it possible to change partially geometrical characteristics of the gas flow duct or to bleed the air partially into the atmosphere.

Designing of a multi-stage axial compressor that operates stably within a wide range of operating conditions is one of the most difficult problems. To expand the range of compressor stable operation, the following methods may be used:

– by choosing of two- or three-spool arrangement of compressor instead of a single-spool arrangement with a gas dynamic connection between the spools;

– by varying compressor airflow by variable IGV and guide vanes, which turn according to a predefined program (e.g. corrected rotational speed), which forms commands basing on information received from the sensors;

– by using the air bleeding to the atmosphere (in the TFE into the bypass duct) from the intermediate compressor stages during starting and low operating power ratings through the ports in the compressor casing.

Heavy loaded single-spool compressors need in the airflow control to provide the required gas dynamic stability margin in the whole range of operating conditions. The control may be ensured by ***variable inlet guide vanes and guide vanes*** of some other succeeding stages. When the compressor decelerates from its design value, these variable guide vanes are gradually closed in order to keep an acceptable attack angle on the adjacent rotor blades. The examples are the TV3-117 turboshaft, AL-21F turbojet, D-30 turbofan, etc.

Additionally, or alternatively an inter-stage ***air bleeding*** may be provided through the air bleed valves or the air bleed strips (which are known as the anti-surge devices). The air bleeding (Fig. 2.53) is performed through the ports, uniformly and circumferentially located on the external wall of the casing.

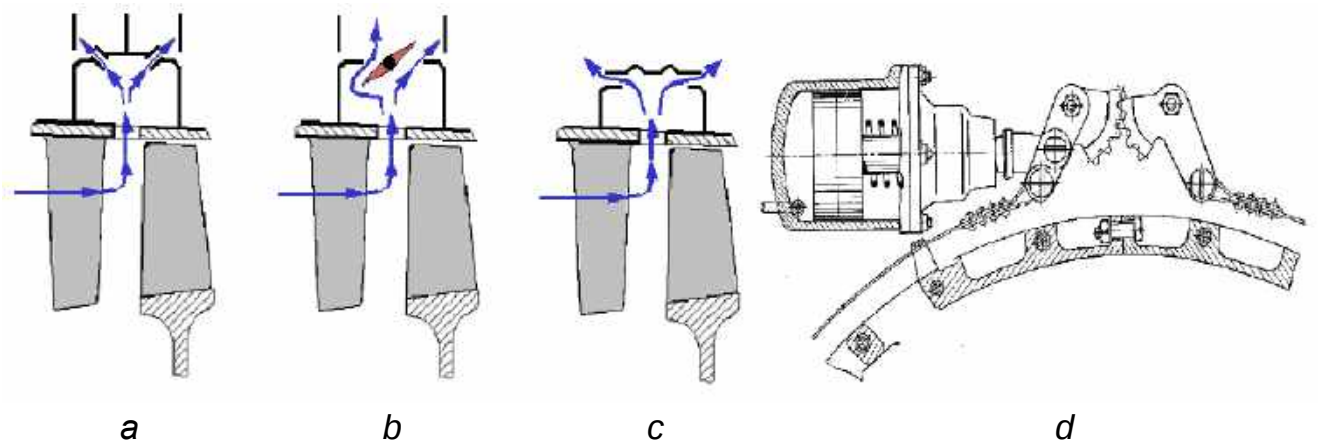


Fig. 2.53. Air bypassing systems:
a – valve; *b* – shuttle; *c* – strip; *d* – bypass strip control mechanism

Thus, the air from the gas flow duct enters through these ports to the ring manifold, isolated from the atmosphere (or from the bypass duct) by bypassing structural members, which may be valves, strips or throttle flaps. These members are automatically controlled by pneumatic system (the AI-25, and D-36) or by hydraulic one (the AI-20, D-30, and NK-12), which receive

information about the rotor rotational speed from the sensors. The working fluid, which is used in hydraulic systems, usually is kerosene or oil.

The valves, shuttles and strips are usually mounted on the compressor intermediate casing downstream of the unstably operating stages. The number of sections where the air is bled usually does not exceed two. When the engine is running at design power ratings and at power ratings that are close to them, the bleeding is not used. When the engine power rating is reduced, the air bleeding shall be switched on first from the front stages, and then from the rear ones. The bleeding must be designed so that the flow non-uniformity in the gas flow duct must be the minimum one. From this point of view, the bypass strips are preferable but they have low vibration resistance.

When the engine operates at low and off-design power ratings, the ring air bypassing may be used (Fig. 2.54). The bypassing unit consists of the П-shape ring chamber and the vanes that are restrained in the slots of the ring.

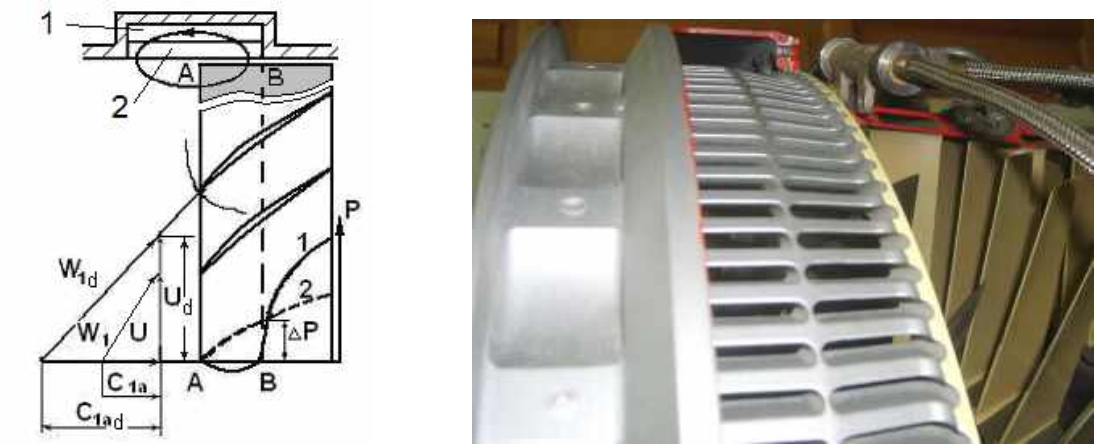


Fig. 2.54. Ring bypassing:
1 – П-shape ring camber; 2 – vanes

When the engine power rating is reduced, the axial velocity at the inlet to the first compressor stage decreases faster than the circumferential velocity. Therefore, the velocity triangles ($\vec{c}_{1a\,d} + \vec{u}_d = \vec{w}_{1\,d}$) become not similar, the blade attack angle increases, and the flow stall can originate at the convex sides of the blades. This is the reason of the compressor unstable operation. The ring bypassing system prevents origination of this phenomenon at peripheral area of the blade.

When the engine with supersonic compressor operates at the design power rating, the normal shock waves seat the leading edges of the rotor blades of the first stage. Static pressure in the interblade channels before the shock wave decreases due to the flow acceleration, and the pressure increases rapidly after the shock (curve 1). The air pressure above the rotor blades (point B) becomes equal to the pressure at the inlet to the interblade channel (point A), and the air not flows through the bypassing chamber.

When the engine power rating reduces, the first stage operates as the subsonic one, and the pressure in the interblade channel increases (curve 2).

The pressure difference initiates the ring vortex in the bypassing chamber, which decreases the flow area, thus increasing the axial velocity at the inlet to the first stage. The velocity triangles become similar to the design triangles, and the flow stall not happens.

2.12. Compressor structural materials

Choice of material for manufacture of the compressor parts mainly depends on their temperature condition during engine operation (Table 2.1).

Table 2.1

Properties of compressor structural materials

t	Materials	Density, kg/m^3	Ultimate strength, MPa
$t < 250°C$	Al and Mg alloys	2700	270
$250 < t < 500°C$	Ti alloys	4500	800…1000
$t > 500°C$	Heat-resistant steels	7800	1000

Examples of materials used for manufacture of the rotor blades and discs are given in Table 2.2.

Table 2.2

Materials for compressor blades and discs

Name of part	Titanium-base alloys	Heat resistant steels and alloys
Rotor blades of fan and compressor first stages	ВТ3-1	
Rotor blades of compressor last stages	ВТ5, ВТ9, ВТ9Л, ВТ18, ВТ18У, ВТ25	ЭИ268, ЭИ696М, ЭИ736, ЭИ961, ЭИ962
Compressor discs	ВТ3-1, ВТ8, ВТ9, ВТ9Л, ВТ18, ВТ18У, ВТ25	ЭИ268, ЭИ961, ЭИ962
Compressor rotor drum	ВТ8	
Guide vanes	ОТ4, ОТ4-1, ВТ9, ВТ9Л, ВТ18, ВТ18У, ВТ25	

Rotor blades are made of aluminum alloys АК2, АК4, АК4-1, ВД-17, titanium alloys ВТ3-1, ВТ8, ВТ10, ВТ18, steels 40ХНМА, 40ХН3МА, ЭИ-736, ЭИ-961, Х17Н2, 18ХНВА, 30ХГСА, etc. They are manufactured by pressing, stamping, cold forge-rolling of the wrought high-strength material. In some cases, they are made by precision casting. Finishing is made by milling, grinding, mechanical or electrochemical polishing.

The blades of the first stages are usually made of steel because this material demonstrates good resistance in case of entry of the foreign matter. In this case, discs must also be made of steel.

The material used for the ***fan blades*** is a titanium alloy (the D-36, D-18T, and CFM-56). Some companies use the hollow wide-chord swept fan blades of titanium alloy made by the super-plastic extrusion attached to the titanium disc by the diffusion welding (the Trent 500) or friction welding (the F119). Some other designs contain a fan made as the ***blisk*** with solid blades of titanium alloy (the PW6000). The weight of the wide-chord fan blades makes less by fabricating the blade from skins of titanium incorporating a honeycomb core. If a structural material of a fan blade is a composition of fibrous material (high-fill, boron-fill), which has high damping characteristic, then there is no need to use the anti-vibration snubber.

Compressor discs and drums are made of aluminum alloys АК2, АК4, АК6, ВД-17; titanium alloys ВТ3-1, ВТ-8, ВТ-10; steels 30ХГСА, 40ХН3М, 18ХНВА, 40 ХНМА, 12Х2Н4А, 13х14НВФРА (usually for the last stages of the high-pressure compressors).

Shafts and tightening bolts are made of steels 40ХНМА, 18ХНВА, 12Х2Н4А, 30ХГСА.

The parts of the ***labyrinth seals*** are made of steel 10 or aluminum alloy.

Casing parts are made of aluminum or magnesium alloys АЛ4, АЛ5, МЛ5, steel 10, titanium alloys.

If titanium alloys are used in the compressor design, there is necessary to take into account some specific features:

– these alloys are the most corrosion resistant;

– they have high friction factor and low erosion wear resistance; therefore, the blades need in chromium coating or titanium nitride spraying (not nitride coating because the nitrogen hardens a surface but also decreases its plasticity);

– heat conductivity of titanium alloys is 15 times less than that of the aluminum alloys and 5 times less than that of steel; therefore, the residual stresses are originated in welds;

– at temperature higher than 500 ºС, the titanium reacts actively with the oxygen, in case of friction of titanium with titanium, the contact area is fast heated, thus initiating a titanium fire; therefore, if the rotor blades are made of the titanium alloy, the rings above them must be made of steel; if the rotor is made of titanium alloy, the guide vanes must be made of steel.

2.13. Centrifugal compressors

2.13.1. Classification of centrifugal compressors

The first gas turbine engines were designed with the centrifugal compressors. That was mainly because these machines were already well-known and widely used in the mechanical engineering. Then the centrifugal compressors were substituted by the axial ones. Now they returned and are used when small axial dimensions is required.

The centrifugal compressors are classified according to the following features (Fig. 2.55):

– according to design of the blades – compressors with radial blades and with blades that are arranged at the angle to the radius of counter rotation, which makes it possible to increase the compressor head without increasing circumferential velocity, and diameter (the so-called active blades);

– according to design of the inlet and rotor wheel – there are single-inlet and double-inlet compressors; the first are used at low consumption of the air, the second – at high consumption;

– according to the type of the rotor wheel – compressors with open, semi-open and closed rotor wheel;

– according to the number of stages – there are single-stage, two-stage and multi-stage compressors (application of multi-stage compressors significantly complicates the engine design structure).

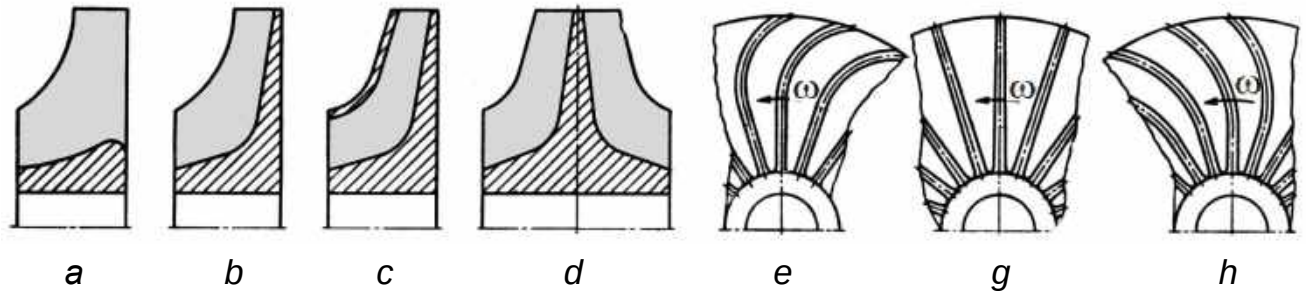


Fig. 2.55. Types of centrifugal compressor rotor wheel:
a – opened single-side rotor wheel; *b* – semi-opened rotor wheel;
c – closed rotor wheel; *d* – double-side rotor wheel; *e* – rotor wheel with blades curved in counter rotation; *g* – rotor wheel with radial blades;
h – rotor wheel with blades curved in normal rotation

According to the strength conditions, the maximum permissible circumferential velocity of the rotor wheel (impeller) is 450 to 500 m/s. In this case, the compressor pressure ratio is 4.0 to 4.5. When the supersonic diffuser or active impeller is used, then the pressure ratio can reach 6 to 12.

Overall dimensions of the centrifugal compressor depend upon the required air flow and axial velocity of the air at the impeller inlet.

The maximum velocity at the inlet must not exceed 120 to 150 m/s, because further increasing of the axial velocity increases losses at the inlet. Under this condition, the specific air flow (i.e., ratio of the air second mass flow to the compressor frontal area) is 15 to 30 кg/(s·m^2). Implementation of the double-side impeller of the same diameter increases the air flow on 80 to 85 % comparing to a single-side impeller.

2.13.2. Design of centrifugal compressors

Compressors with the open-type impeller has low weight, good manufacturability but low efficiency because of high hydraulic losses. They may be used as the second stage in the double-stage compressors because aluminum alloys are not applicable due to a high temperature of the air, and the titanium or steel impeller of semi-opened or closed type is not efficient from the point of view of manufacture. Such rotor wheel has low weight and satisfactory manufacturability, but it has high hydraulic losses.

The hydraulic losses of the closed-type impeller are low; the clearance between the casing and rotor wheel not influence the losses. But this impeller is difficult in manufacturing and has not sufficient strength at high circumferential velocity because the upper covering wall increases centrifugal force that affects blades and disc, thus decreasing strength of the impeller.

Centrifugal compressors with the semi-opened impeller are the most applicable in the up-to-date gas turbine engines. Their blades are made as one piece with the disc, which makes the impeller rigid and strong. Shape of the interblade channel in this impeller is more perfect as compared with the open impeller and simpler as compared with the closed impeller. The semi-open impellers are made of the heat resistant aluminum alloys by using press forming with subsequent machining and polishing of the external surface. After polishing, the surface is anodized. This coating prevents corrosion, increases surface hardness, decreases erosion wear and improves roughness, thus decreasing hydraulic losses.

The rotor wheel may be attached to the shaft by using several methods:

– splined joint is used for small compressors with low torque; joined components are aligned by the fit shoulder or by side surfaces of the teeth;

– flange-and-bolt joint with torque transmission by the friction forces and by shear forces in the template bolts or studs is applied in the case of high torque.

2.13.3. Design of rotor wheel

Dimensions of the rotor wheel at first are chosen approximately on the basis of results of the gas dynamic calculation and then they are corrected when calculating the rotor wheel strength.

Diameters D_1, D_2 and blade widths b_1, b_2 (Fig. 2.56) are knows from the gas dynamic analysis. All other dimensions are to be chosen by the designer:

- disc peripheral width $\Delta = 3$ to 5 mm;
- taper angle $\theta = 2°$ to 5°;
- the width of the rotor wheel hub is defined by structural design and is corrected after the strength analysis;
- the wall of the impeller is manufactured by milling; it is better to choose the milling radius as high as possible for providing smooth profile of the gas flow duct; usually $R_m \approx 1.5 b_1$ or $R_m \approx 0.25\, D_2$;
- the blade thickness is defined after calculation of its oscillation.

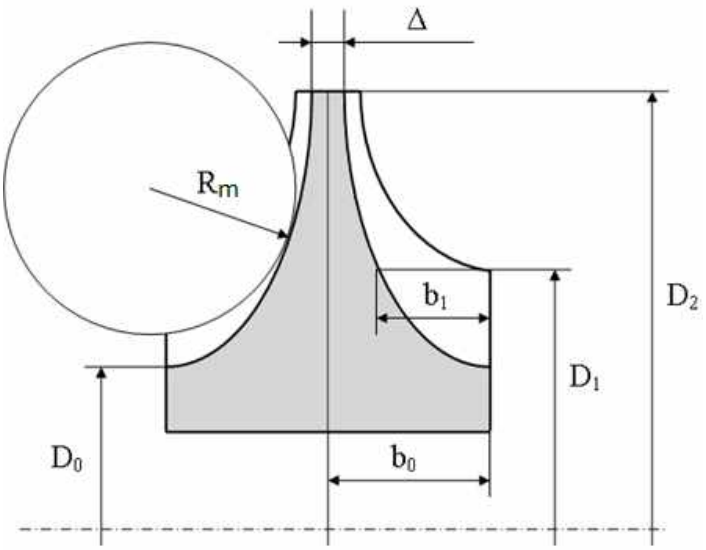


Fig. 2.56. Geometry of the centrifugal compressor rotor wheel

The inlet guide vanes are mounted in front of the rotor wheel. They may be stationary (SGV) or rotating (RGV), joined to the rotor wheel.

The SGV is used for preliminary twisting of the air flow aside rotation of the rotor wheel, thus decreasing specific velocity M_w at the rotor wheel inlet.

The VGV is designed to provide entry of the air into the rotor wheel with the minimum losses. It is, as a rule, separate component part that includes a set of profiled blades and is joined to the rotor wheel by the flange-and-bolt joint. The blades stagger angles are defined at the stage of the gas dynamic analysis. The diffuser angle of the VGV is less than 6° to 12° to prevent a stall.

2.13.4. Design of casing

Casing of the centrifugal compressor consists of the diffuser and bearing supports housing. They have transversal splits that are perpendicular to the shaft and are joined by the bolts or studs with alignment through the fit shoulders or pins.

The rotor wheel outlet is furnished with the vane diffuser, which is a disc with vanes. The vanes convert the air kinetic energy into pressure.

The velocity at the impeller outlet in the aero engine centrifugal compressors is a supersonic one. Therefore, the vane-less (slot) diffuser is located between the rotor wheel and the vane diffuser, which provides a shock-less braking of the flow from supersonic velocity to the subsonic one. Its efficiency is less than that of the vane diffuser, but the vane-less diffuser has no shocks, which prevents a stall flow at the inlet to the vane diffuser.

The diffuser casing is a load-carrying member. The intake pipes are attached to the casing. They may contain protective grids to prevent suction of the foreign matter into the compressor.

The rotor wheel, shaft and IGV may be joined together as it is shown in Fig. 2.57.

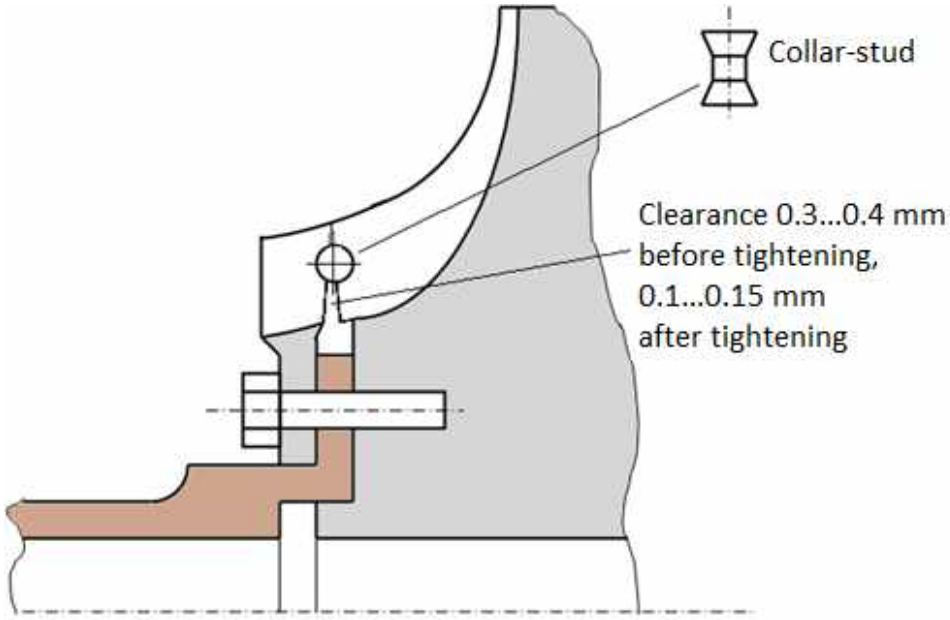


Fig. 2.57. Joining of RGV, impeller and shaft

Fig. 2.58 shows the impeller of promising centrifugal compressor, which contains splitter blades. Parameters of the compressor: pressure ratio 9.6; air flow $G_{air} = 3.3$ kg/s; peripheral circumferential velocity $u_2 = 628$ m/s; rotational speed $n = 40\,000$ rpm; efficiency $\eta_C = 0.8$.



Fig. 2.58. Triple-row impeller of promising centrifugal compressor

2.13.5. Materials for centrifugal compressors

Impeller and IGV are usually made by press forming of aluminum alloys AK2 or AK4 with subsequent machining. High-speed impellers are made of the titanium alloys (BT3) or steels.

Stationary guide vanes are made of sheet duralumin Д1.

Compressor casing and diffuser are made of silumin АЛ4 or АЛ5.

Shafts are made of steel (40ХНМА, 18ХНВА, 12Х2Н4А).

2.14. Compressor rotor balancing

Assembled compressor rotor is balanced, making a sum of inertia forces and a sum of moments of inertia forces of rotated weight zero in relation to the axis of rotation. This is done by removal of metal at the predetermined places, by mounting balancing weights, by replacement of the rotor blades, by fitting shims, etc. The imbalance is a cause of appearance of critical rotational speed in the engine operating range that results in the rotor vibrations.

The dynamic balancing of the rotor is carried out in the factory conditions by using special balancing machines, which make it possible to determine a value and direction of the non-balanced moment.

Practically it is impossible to balance the rotor completely. The residual imbalance must be less than the permissible value. The ***imbalance*** is a static moment of a weight , which should be located in a plane of the rotor support and makes the rotor to be balanced completely (to be in a state of indifferent equilibrium). Fig. 2.59 shows the front and rear balancing collars of the low pressure compressor with attached balancing weights.

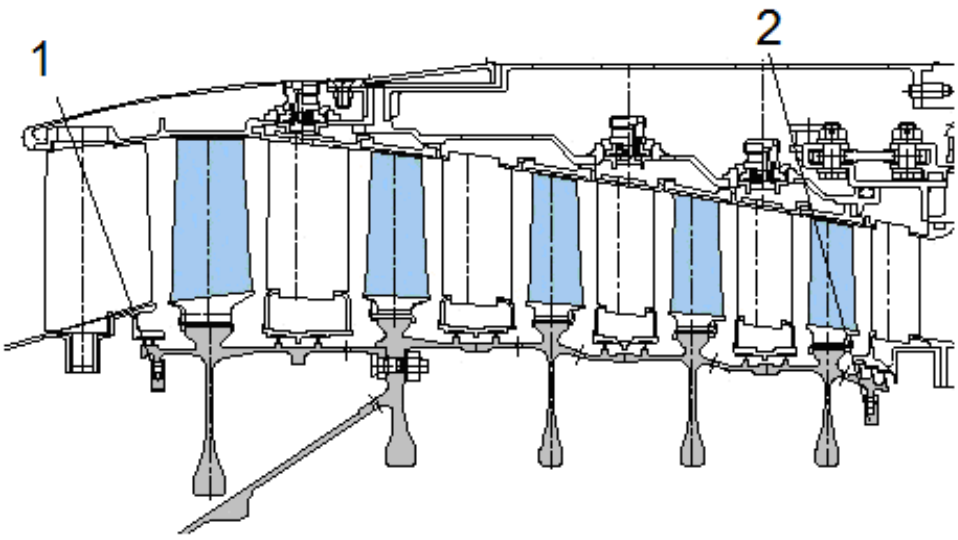


Fig. 2.59. Low pressure compressor:
1 – front balancing collar; 2 – rear balancing collar

2.15. Check questions

1. Functions of compressors in the gas turbine engines and requirements to their design.
2. Classification of gas turbine engine compressors.
3. Advantages, disadvantages and fields of application of the axial compressors.
4. Classification of the axial compressors.
5. Give examples of engines with different shape of the axial compressor gas flow duct.
6. Main structural members of the axial compressor and their functions.
7. Purpose of the inlet guide vanes, guide vanes and strengthening vanes of the axial compressor.
8. What is the reason of application of the inlet guide vanes? Describe their design.
9. What is the reason of application of the variable inlet guide vanes?
10. What is the reason of heating of the inlet guide vanes? How is it done?
11. Methods of mounting of the axial compressor stator vanes.
12. Compressor rotor blade design and its main structural members.
13. Requirements to mounting members of the rotor blades.
14. Types of blade attachment, their advantages and disadvantages. Retaining of blades against axial displacement.
15. What loads affect axial compressor blades?
16. What loads affect axial compressor rotor?
17. What loads affect axial compressor stator?

18. Name types of the axial compressor rotors, give their comparison.

19. How is the torque transmitted from stage to stage in drum, disc and drum-and-disc rotors?

20. Purpose and methods of compressor rotors balancing.

21. Compressor rotors axial unloading.

22. Casings of the axial compressors and their main functions. Types of the casings, their advantages and disadvantages.

23. Methods of joining of main parts of the compressors detachable casings.

24. Compressor radial and axial clearances, their influence on the compressor performances. Methods of decreasing of the radial clearances.

25. Labyrinth seals: functions, design and operation.

26. Means to expand a range of compressor stable operation at power ratings.

27. Purpose, design and operation of the compressor air bleeding systems.

28. Advantages, disadvantages and fields of application of the centrifugal compressors.

29. Centrifugal compressors classification.

30. Does the axial force affect a centrifugal compressor rotor? If yes, what side is it directed?

31. What loads affect a centrifugal compressor stator?

32. How the rotor wheel and shaft of the centrifugal compressor are joined? Torque and axial force transmission, alignment, axial clearance providing.

33. Requirements to materials used in structural members of the blades, rotor wheels and other structural members of the compressor rotors. Give examples.

34. Requirements to materials used in structural members of the compressor stator. Give examples.

35. What structural elements of a rotor help for its balancing?

3. DESIGN OF GAS TURBINE

3.1. Gas turbine purpose and operating conditions. Main requirements to the gas turbine structure and their implementation

GTE turbine of the GTE intends to transform a portion of enthalpy (heat content) of the hot gas into mechanical work, which is spent for driving of the compressor and accessory units, and in turboprop and turboshaft engines for driving of the propeller or rotor.

GTE turbines of GTE have high power generated by one component part at small weight and dimensions and relatively simple design. The power of aircraft turbine of the aero engine reaches 30 000 to 100 000 kW and higher, the weight of the turbine assembly is from several tens of kilograms to 700 to 900 kg. Such high power at small weight and dimensions is possible due to a high turbine inlet temperature (TIT). The TIT increasing provides increment of the engine specific thrust (approximately by 10 to 15 % per each 100 °C). When the TIT increases, the gas-dynamic and heat processes become more intensive. This increases loads that affect the turbine parts and limits the turbine life time and engine service life. Therefore, the turbine is a component part that determines the engine reliability.

Operating conditions of the gas turbines of the up-to-date aero engines may be characterized by the following indices:

– high turbine inlet temperature (experimental turbines operate at TIT = 1900 to 2000 K);

– high dynamic (due to a non-uniform gas flow) and static (due to centrifugal forces) loads that for a rotor blade can reach 10 to 12 tons;

– erosion and corrosion action of the chemically active gas on the turbine component parts;

– temperature non-uniformity that reaches 100 °C for blades and 150 to 250 °C for discs;

– high velocity of the gas flow (M = 0.4 to 0.9) accompanied by the presence of solid particles in the gas flow.

Such combination of adverse operating conditions of the gas turbine assembly limits the engine service life and decreases its reliability. Therefore, due to a significance of the turbine assembly in the engine design during its designing stage, the turbine must satisfy strong requirements:

1. *High efficiency* (for the up-to-data turbines it is 0.88 to 0.93). This is provided by the following:

– by the optimum choice of the number of stages and gas parameters;

– by careful profiling (including 3D-analysis) of the rotor blades and nozzle vanes, high quality of machining of the working surfaces, which reduces hydraulic losses;

– by decreasing of the gas escape in the axial and radial clearances by using labyrinth seals that work in combination with the abradable honeycomb inserts, which allows to ensure assembling of the seals without axial and radial clearances;

– by cutting the fins of the labyrinth seals on the shroud platforms along periphery of airfoil portion of the rotor blades so as to prevent both radial and axial spillover of the gas;

– by controlling the radial clearance between the rotor blade and casing according to the engine power rating;

– by preventing the flow stall from the blades by using the blades with jet flaps and tandem-type (split-type) blades (both methods allow to effect the boundary layer, thus preventing its stall and to increase the blade load; it is recommended to use the blades with the jet flaps in designs with cooled blades when the cooling air is discharged through the slots provided in the trailing edge; the split-type blades don't need supply the secondary air);

– by using variable nozzle vanes.

2. *Required power at the least weight and dimensions*. This is provided by the following:

– by increasing TIT;

– by increasing heat differential at turbine stage with simultaneous increasing circumferential velocity at the mean radius of the rotor wheel.

Decrease in the turbine overall dimensions and weight at the specified power by increasing load to the rotor blade and the turbine stage as a whole will result in increase in the blade airfoil lift factor C_y and in increase in the pressure differential between the blade convex and concave surfaces. In its turn, this causes intensive breaking of a flow on the airfoil surface, stall and high losses, thus decreasing efficiency and power.

To maintain high efficiency when the stage load increases, a boundary layer control is applied, the blade shape and manufacturing technology is improved. To provide the minimum weight, some parts are made of light high-strength materials (for example titanium alloys or composite materials), and the parts are designed with equal safety factor in all sections, which meets the Norms of Strength.

3. High reliability and high service life. This requirement is met by the following:

– by using heat-resistant and high-temperature alloys;

– by high-quality manufacturing of the turbine parts with perfect and multiple quality checking during manufacture;

– by intensifying cooling for decreasing temperature and temperature stress in the most heated parts;

– by damping dangerous oscillations in the turbine parts (especially in the rotor blades as the most subjected to oscillations) or by decreasing vibration stresses to a safe level by using shrouding and variable pitch in the nozzle box and rotor blades;

– by using a rigid load-carrying turbine casing, which is not broken through in case of breakage of the rotor blades and provides stable clearances in the turbine assembly and reliable operation of bearings.

In addition, it is necessary to take into account the fact that the turbine reliability and service life to a greater extent depends on the number of loading cycles and heating removals, which are related more to the engine starting, shutdown and variation of the power ratings than to the total engine operating hours.

4. Repairability – possibility of repair of the turbine assembly and its simplicity. This index is very important because the cost of the turbine accounts 35 to 45 % of the engine total cost. In the up-to-date gas turbine engines, this requirement is met by a modular design, which allows to replace the turbine assembly at relative by low labor expenditures.

5. Inspectability – ability for visual inspection and checking of the most loaded parts.

Correct choice of the turbine parameters is based on a comprehensive analysis of various factors and accumulated experience of the world engine engineering. The main trends in the turbine engineering are:

- increasing the number of stages by implementing the double- and triple-rotor diagrams, which is reasoned by the overall pressure ratio growth and velocity on the mean radius limitation (300 to 350 m/s);
- intensification of the air cooling of the turbine parts because of TIT growth, with wake swirling when supplying the cooling air (deflectors at the discs and wake swirling when supplying the cooling air; the use of the intermediate area between the airfoil portion and rotor blade root that decreases a heat removal to the disc; convective, penetrative and barrier cooling of the blades; preliminary cooling of the cooling air; automatic control of the cooling air flow depending on the engine power rating);
- wide application of the rotor blades shrouding in combination with the labyrinth seals;
- fitting of two blades in one slot as means for damping of vibrations and making possible to increase the number of blades with maintaining disc strength;
- close control over a temperature circumferential non-uniformity at the turbine inlet to prevent an overheating and to decrease thermal cyclic stress;

- radial clearance control;
- development of the new types of seals (for example brush seals).

3.2. Design diagrams and parameters of aircraft gas turbines

3.2.1. Design diagrams

Structures of turbines are differed by such features:

– *By a direction of the gas flow*: axial-flow and radial-flow turbines. The radial-flow turbines may be centrifugal-flow or radial-inflow ones. The axial-flow turbines are widely used in aircraft GTE. The radial-inflow (centripetal) turbines are used in small-dimensioned GTE and auxiliary power inits (for example, the APU TA-8V of Mi-26 helicopter, Fig. 3.1).

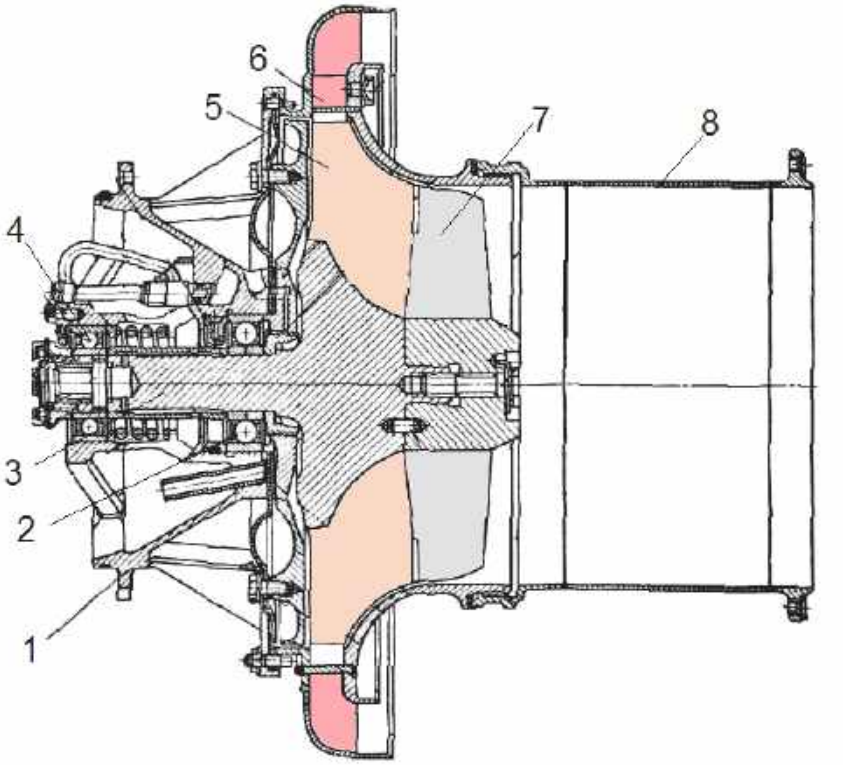


Fig. 3.1. Centripetal gas turbine:
1 – casing; 2 – radial-thrust bearing; 3 – turbine shaft;
4 – radial ball bearing; 5 – turbine rotor wheel; 6 – nozzle box;
7 – rotating nozzle box; 8 – exhaust pipe

– *By degree of reaction*: reactive and pulse-flow turbines. In the reactive turbines, some part of the gas expansion takes place in the nozzle box, another part − in the rotor. In the pulse-flow turbines, the rotor does not expand the gas; it only changes direction of its velocity. The pulse-flow turbines have less weight but less efficiency.

Hereinafter, we shall consider design of the axial-flow reactive turbines. The stage of this turbine consists of the nozzle box and rotor wheel (Fig.3.2).

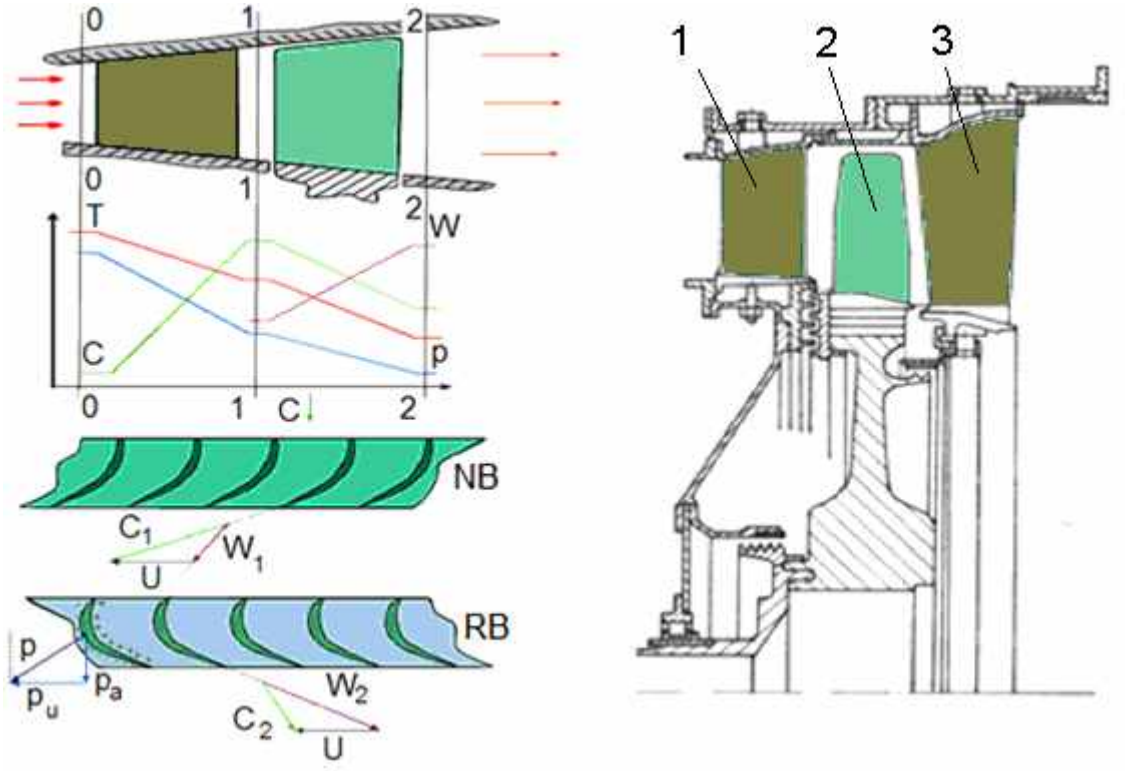
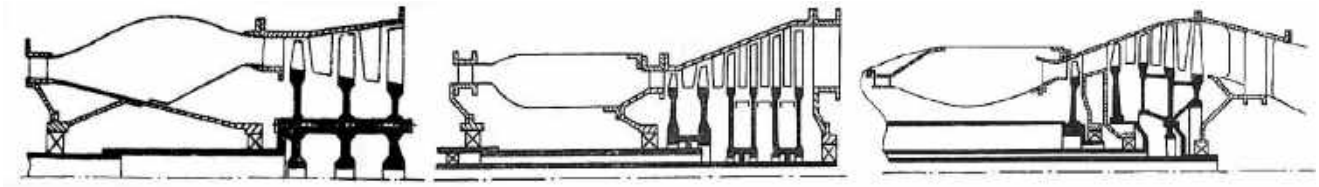


Fig. 3.2. Stage of axial-flow turbine:
1 – nozzle vanes; 2 – rotor blade; 3 – nozzle vanes of the consequent stage

– *By the number of stages*, there are single-stage and multistage turbines (up to 9 stages). In its turn, the multistage turbines may be single-, double- and triple-shaft ones (Fig. 3.3).



a *b* *c*

Fig. 3.3. Examples of multistage and multi-rotor turbines:
a – three-stage single-shaft turbine; *b* – six-stage double-shaft turbine (2 + 4);
c – five-stage triple-shaft turbine (1 + 1 + 3)

3.2.2. Parameters of gas turbines

The main parameters characterizing the turbine can be subdivided into three groups.

The first group contains parameters that characterize the turbine as a turbomachine:

– turbine inlet temperature (TIT);

– turbine pressure ratio (is within 2.5 to 5.0 for the TJE, and within 8 to 15 for the TPE and TShE);

– turbine efficiency;

– specific work of turbine stage, which is done by one kilogram of the working fluid (gas) L_{st} = (15 to 30)·10^4 J/kg.

The second group contains parameters that characterize the turbine structural perfection:

1. Bushing relative diameter $\bar{d}_B$ = 0.5 to 0.8. At low $\bar{d}_B$, the blade becomes too long; this decreases its vibration strength and complicates displacement of required number of blades on a disk rim. Therefore, as usual, $\bar{d}_B$ less than 0.5 is not applied.

2. Blade length h_t is determined by taking into consideration the following factors: the blade length shall not be too long in order not to worsen the strength and vibration characteristics; but the blade length shall not be too short in order not to worsen the gas-dynamic characteristics. Therefore, the relative blade length $\bar{h}_{bl} = \frac{h_{bl}}{D_m}$ in first stages of known turbines is 1/6…1/8 (sometimes up to 1/12); and up to 1/5 in the last stages. The length of the nozzle vane is by 1 to 2 % less than that of the rotor blade; this is done taking into account thermal expansion of the disc for providing equal internal diameter of rotor and stator after heating when the engine is running.

3. Blade aspect ratio $\lambda = h_{bl}/b_m$, where h_{bl} is the blade length on a trailing edge; b_m is the mean chord on the mean diameter. The rotor blades of known engines have λ = 2 to 5, the nozzle vanes have λ = 1.2 to 3.0 (smaller values are chosen for the first stages, and the higher values – for the last stages).

The aspect ratio is closely related to another specific parameter of the turbine – space/chord ratio on the mean diameter t_m. For the rotor blades it is 1.1 to 1.6, for the nozzle guide vanes – 1.3 to 2.0.

4. The number of the rotor blades for the first stages is 90 to 150, and for the last stages – 75 to 85. This number must be corrected taking into account oscillation properties of the turbine, to avoid dangerous resonant oscillations.

5. Shape of the gas flow duct. The gas flow duct with constant external diameter D_{ext} = const (Fig. 3.4) features simple design of the stator, perfect coordination between flow lines in the turbine and exhaust nozzle, and simple providing constant radial clearance. Nevertheless, the blades of the turbine last stages may be too long, which decreases their strength and vibration stability. If an angular expansion of the gas flow duct exceeds 18 to 20°, then stall is possible. Besides, in case of this shape of the gas flow duct the turbine has the maximum number of stages because the mean radius of the last stages

decreases, thus decreasing circumferential velocity u_m, and the value of the specific work is reduced from the first stages to the last ones.

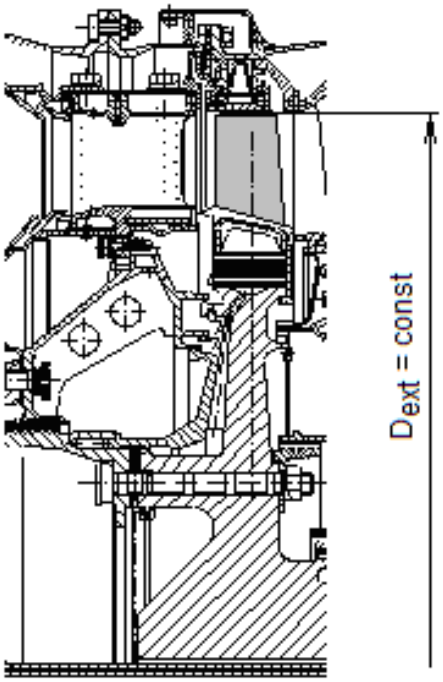


Fig. 3.4. Turbine gas flow duct with constant external diameter

Gas flow duct with constant hub diameter D_{int} = const (Fig. 3.5) provides increasing of specific work from the first stages to the last ones; therefore, the number of stages is the minimum one. The last stages have relatively short blades, which improves their strength and oscillation stability. Disadvantages of this gas flow duct type are complicated design of the stator, increased diameter and bad coordination of flow lines in the turbine and exhaust nozzle.

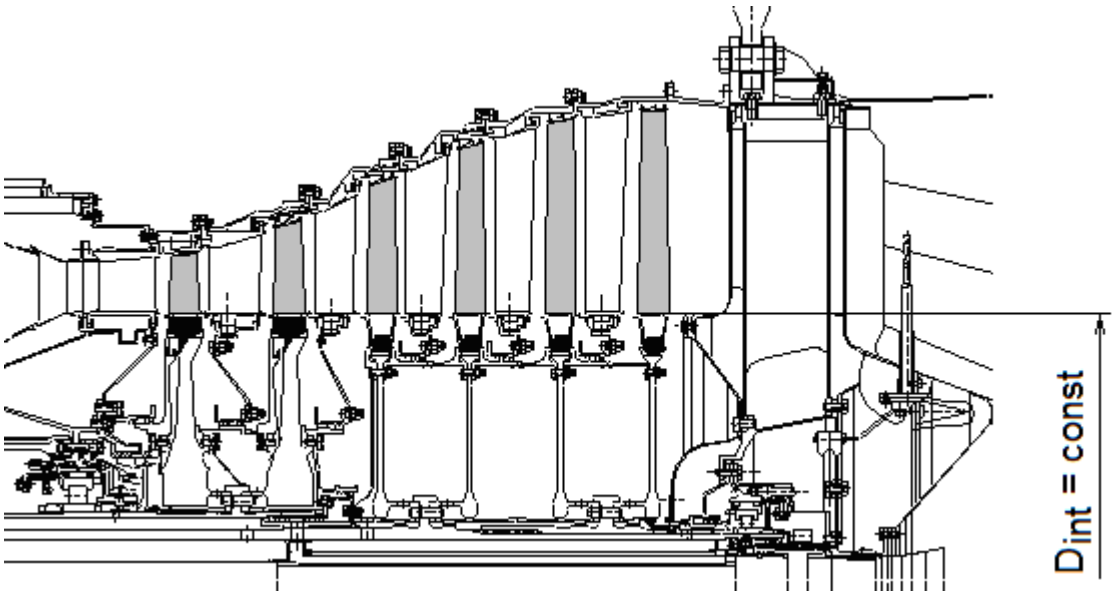


Fig. 3.5. Turbine gas flow duct with constant hub diameter

Gas flow duct with constant mean diameter D_m = const (Fig. 3.6) is a compromise scheme. Specific work is constant at all stages; the blades of the last stages are somewhat longer than in the second diagram, but shorter than in the first diagram. The angular expansion of the gas flow duct does not exceeds the limit one (not more than 15 to 18°). Coordination of flow lines in the turbine and exhaust nozzle is satisfactory. Disadvantages of this diagram are complex design of the stator and somewhat increased diameter.

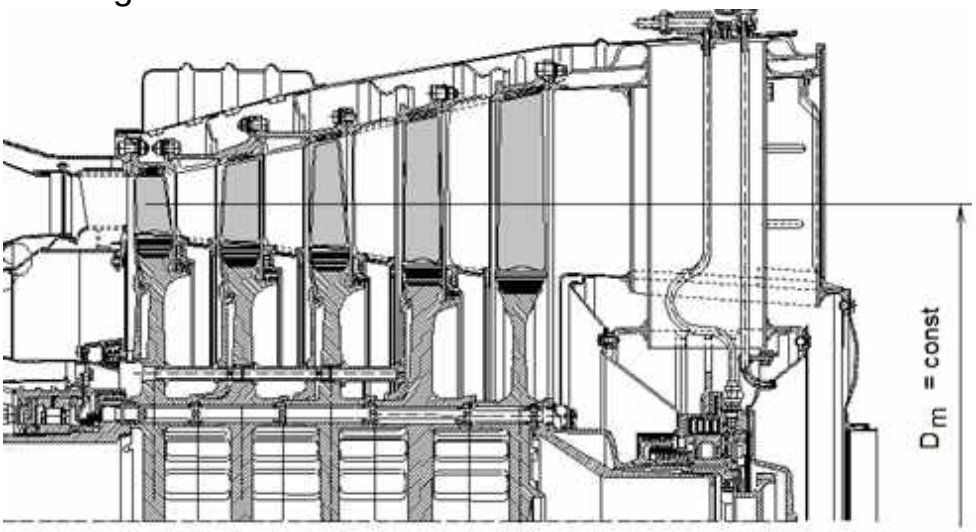


Fig. 3.6. Turbine gas flow duct with constant mean diameter

6. Turbine specific weight is a relation of turbine weight and its developed power; the specific weight of the up-to-date turbines is 0.01 to 0.04 kg/kW.

7. Turbine relative weight is a relation between the turbine weight and the engine weight; for the turbojet engines, it is 0.2 to 0.35, for the TPE and TFE – 0.3 to 0.45.

The weight of the turbine rotor is approximately 55 % of the turbine total weight; the weight of the nozzle box is 25 to 30 %, and the weight of the casing with supports is 10 to 12 %.

The third group includes parameters, which characterize the turbine as an object of maintenance and repair (maintainability, repairability). These parameters are provided at the stage of turbine designing.

3.3. Rotor blades

3.3.1. Design of turbine rotor blades

Rotor blades convert the energy of the gas flow into mechanical work.

The following loads affect the rotor blade:

– centrifugal force of the weight of the blade airfoil portion that causes tension stress;

– axial and circumferential gas forces that cause bending stress in the blade airfoil portion;

– non-uniform temperature field that causes thermal stresses.

Besides, the turbine rotor blade is affected by vibration, corrosion and erosion from the gas flow.

Requirements to the turbine rotor blades are the same as to the compressor rotor blades, but they are stricter because the turbine rotor blades operate at harder conditions as a result of effect of high temperature of the exhaust gas flow.

The turbine blades have the same structural members as compressor blades have (airfoil, root) but other geometric proportions: more thick and curved airfoils, larger transition portions and roots. The additional structural members of the turbine blade may include the inner and peripheral shrouds, shank of the retaining portion, passages and orifices for the cooling air (Fig. 3.7).

The **blade airfoil portion** has a tapered shape for providing uniform strength, with more intensive decreasing of sectional area than compressor blades have.

The inner shroud (shroud platform) is provided between the blade airfoil portion and root, which forms the inner shape of the gas flow duct and protects the blade root and disc rim from overheating by the hot gas.

The blade shank (transient portion) is an intermediate zone between the inner shroud and root (its length may reach 50 % of blade length). It allows to locate the blade root to the center of the disc, which load carrying capabilities of the root and to make the disc thinner because the disc rim is operating at lower temperatures as compared with the temperatures existing in the gas flow duct.

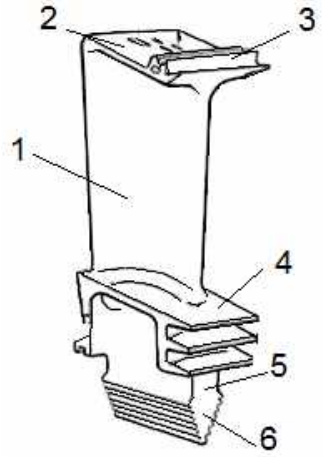
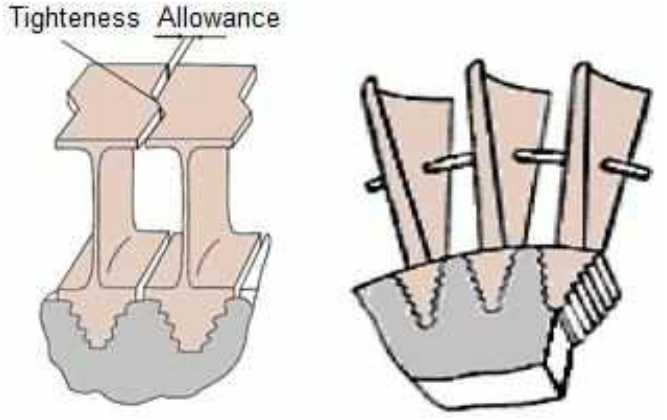


Fig. 3.7. Turbine rotor blade:
1 – blade airfoil portion; 2 – peripheral shroud; 3 – labyrinth seal fins;
4 – inner shroud; 5 – shank (elongated foot); 6 – “fir-tree” root

The turbine blade is usually bound using lashing wires, bushing or peripheral shroud to improve its oscillation properties (Fig. 3.8). The **peripheral shroud** constitutes a ring structure, which reduces spillover losses; the turbine

efficiency is increased by 1.5 to 2 %. The tips of the shrouds have fins of the labyrinth seals, which operate in combination with the easy abradable metal-ceramic (made of the iron-nickel-graphite) or honeycomb inserts attached on the turbine case. The shrouds of the blades may be mounted closely one to another in cold condition (with small interference) or may have clearance between themselves approximately 0.2 mm.



a *b*

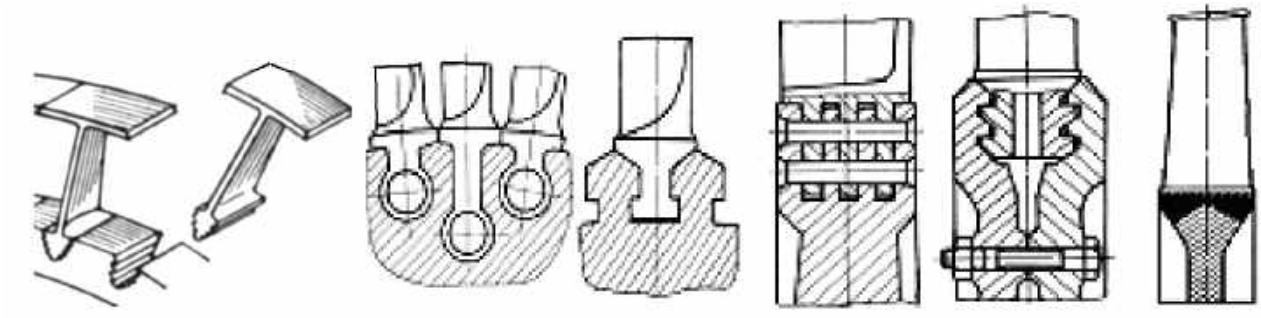
Fig. 3.8. Rotor blades with shroud (*a*) and wire (*b*) binding

If the blade has not shroud, its tip may be sharpened (chamfered) to facilitate its running in to the abradable coating and to prevent damage of the blade when touching a coating.

A set of the rotor blades of one rotor wheel is selected by the weight (weight deviation in one set shall not exceed 3 to 5 grams) to facilitate rotor balancing, and also by the first tone of frequency of natural bending oscillation (tolerance shall not exceed 3 %).

3.3.2. Rotor blades attachment

All types of the root joints that are used for attachment of the compressor blades may be used in the turbine (Fig. 3.9).



a *b* *c* *d* *e* *f*

Fig. 3.9. Methods of turbine blades locking:
a – “fir-tree” lock; *b* – cylindrical type; *c* – T-shape; *d* – comber-type;
e –”fir-tree” ring slots; *f* – welding

The most operable in turbine conditions is **“fir-tree” root,** which takes high centrifugal loads (approximately 2 to 3 tons on each pair of serrations) at small weight and dimensions. It also allows providing intensive cooling of the blades by heat transfer to the disc and by blowing root clearances with the air.

The “fir tree” root has some *disadvantages*:

– stress concentrators in the root serrations may initiate fatigue cracks in the serrations;

– complicated and expensive manufacturing because it is necessary to provide high precision of the serrations to receive uniform distribution of a load between them.

In **double roots,** two blades are fitted in one slot (Fig. 3.10). These roots are applied to mount increased number of blades. Such mounting improves damping of blades oscillations because in this case the damping is provided not only by friction of the blade in the disc slot but also by friction of the roots of blades between themselves.

Blades are usually mounted into the longitudinal slots, but in some cases they may be mounted in the circumferential slots (pin and serrations roots are the most acceptable in this case).

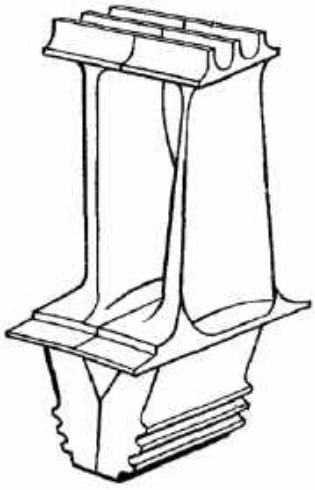


Fig. 3.10. Fitting two blades in one fir-tree slot

The blades may be retained individually or in group (Fig. 3.11).

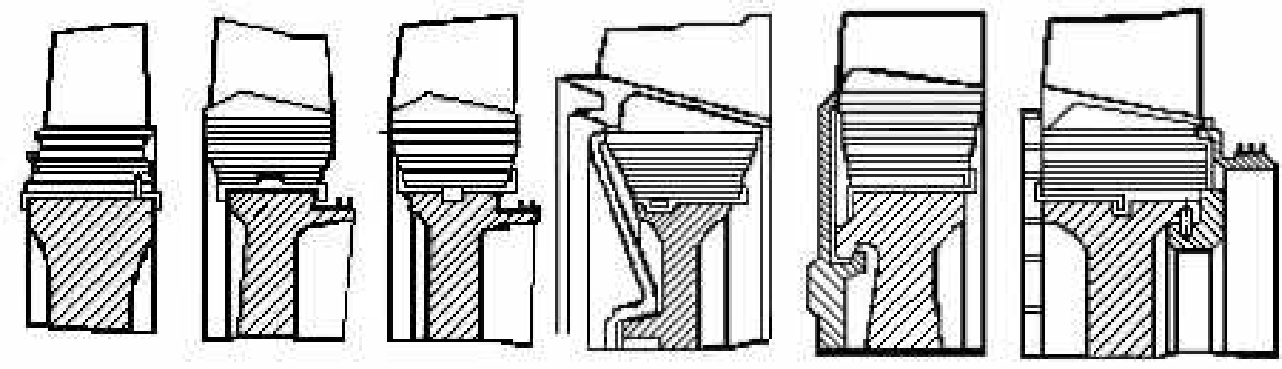


Fig. 3.11. Methods of axial retaining of rotor blades

The **group retaining** is made by deflectors, spacing rings, split spring rings, plate retaining sectors (RD-33 turbofan).

The **individual fixing** is made by rest serrations, plate locks, and dowels (the AL-7 turbojet).

The possibility to use simple and light retainers is provided by the fact that the gas force affecting one blade does not exceed 1000 N while the friction force, which prevents axial displacement of the blade, is 10 to 20 times higher.

In low-power turbines, the blades may be made with a disc as one part (the **blisk design**). The examples are turbine of the AI-9 APU (Fig. 3.12) and low pressure turbine of the RD-36MT turbofan.



Fig. 3.12. Turbine of the AI-9 APU

3.4. Turbine disks

3.4.1. Structure of turbine disk

Turbine discs are designed to mount the rotor blades and to transmit the torque and axial force from them to the shaft.

Loads that affect the turbine disc:

– high pulling centrifugal forces of the disc weight and weight of the blades with the roots and retainers;

– bending moments caused by the pressure difference on the disc side surfaces;

– dynamic stresses caused by the disc oscillation;

– thermal stresses caused by the temperature gradients at the disc radius and width.

The disc shape depends on the stress distribution and methods by which the discs are interconnected and connected to the shaft. Generally, the disc consists of a rim, web, and hub (Fig. 3.13).

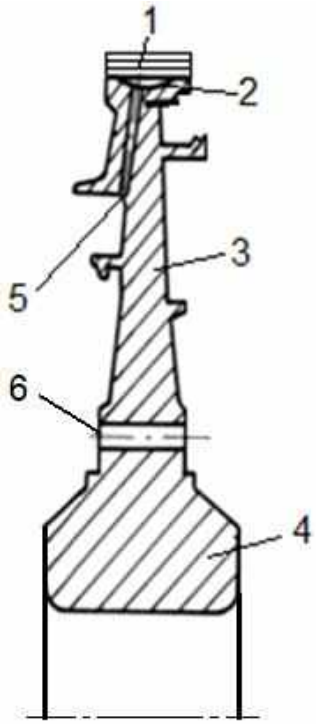


Fig. 3.13. Turbine disk:
1 – slot for blades fitting; 2 – rim; 3 – web; 4 – hub; 5 – orifices for supplying the cooling air to the rotor blades; 6 – hole for the joining disc and shaft

The **disc rim** (widened peripheral part) keeps rotor blades.

Width of the **web** (central part) is decreased from the center to the periphery for providing uniform strength. Following technological needs, the web profile by design usually has simple shape – conical or plate with conical sectors.

The **hub** is the widest sector. This is due to a strength conditions, as the hub is affected by the centrifugal forces that originate in the disc itself and are transmitted to the disc from the blades.

3.4.2. Joint of the turbine discs interconnected and connected with the shaft

The joint of the turbine discs interconnected and connected with the shaft must have high strength at small weight. It must transmit the torque, align reliably the component parts, must have required bending rigidity to prevent opening of the joint. It must be assembled and disassembled easily.

The discs-to-shaft joint must contain structural members, which decrease heat transfer from the disc to the shaft and bearing.

The method to be used for joining discs with the shaft depends on the number of discs, loads, method of cooling of the turbine component parts, conditions of assembling and disassembling, technologies succession, etc.

The joint of the turbine discs interconnected and connected with the shaft may be detachable or non-detachable.

Detachable joints (Fig. 3.14):

– *splined joint* (the IPT and LPT of the D-36 turbofan);

– *flange-and-bolt joint* (the HPT of the D-36 turbofan, the LPT of the D-30P turbofan, and the APU AI-8);

– *joining by long peripheral studs or bolts* (the NK-12 turboprop, and the TV3-117 turboshaft);

– *joining by central tightening bolt*.

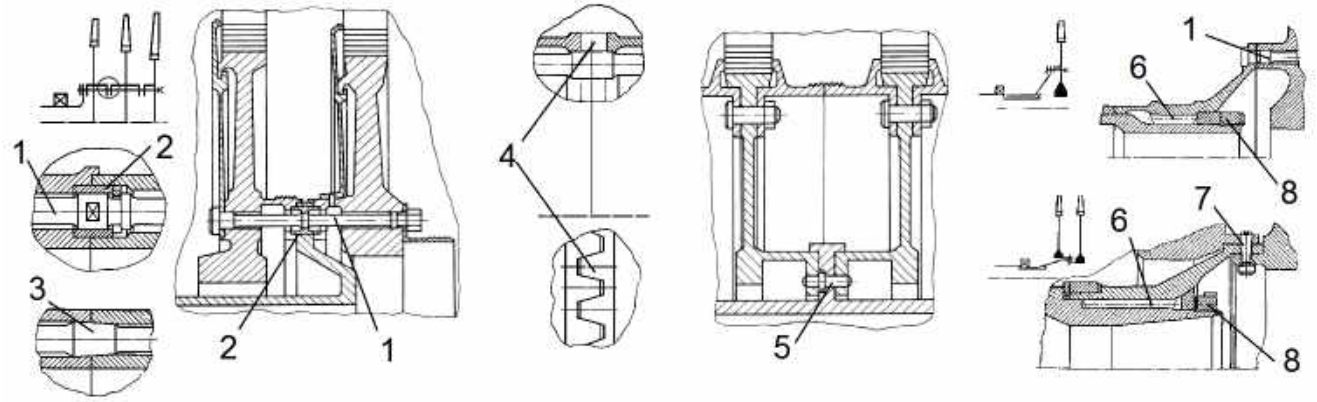
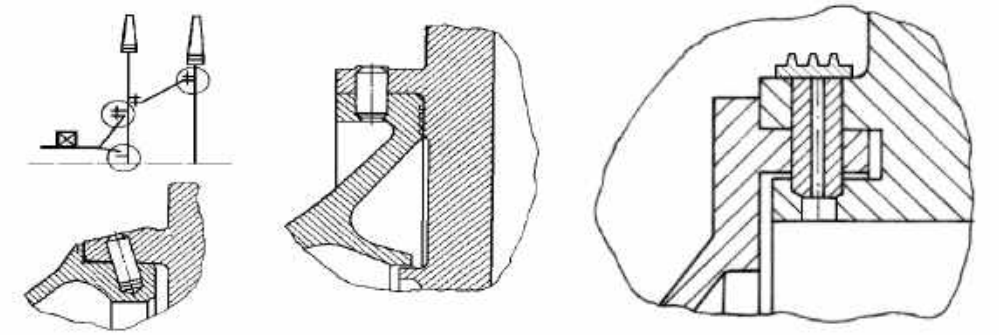


Fig. 3.14. Detachable joints between turbine disk and a shaft:
1 – coupling bolt; 2 – prisoner bushing; 3 – taper; 4 – end face splines;
5 – axial pin; 6 – axial splines; 7 – radial pin; 8 – nut

Non-detachable joints (Fig. 3.15):

– flange-and-pin junction of the disc with the shaft (the R11-F300 turbojet, D-20P and D-30P turbofans);

– joining of discs to each other by intermediate load-carrying ring and radial pins (th eAM-3, AL-7, and RD-9B turbojets);



a *b* *c*

Fig. 3.15. Joining of disc with shaft by press-fitting and pining:
a – joining of disc with spacer ring; *b* – pressing by shoulder;
c – fork-shaped press-fitting

– the disk and shaft may be manufactured as one part (for example, the second stage of free turbine of the TV3-117 turboshaft, Fig. 3.16).

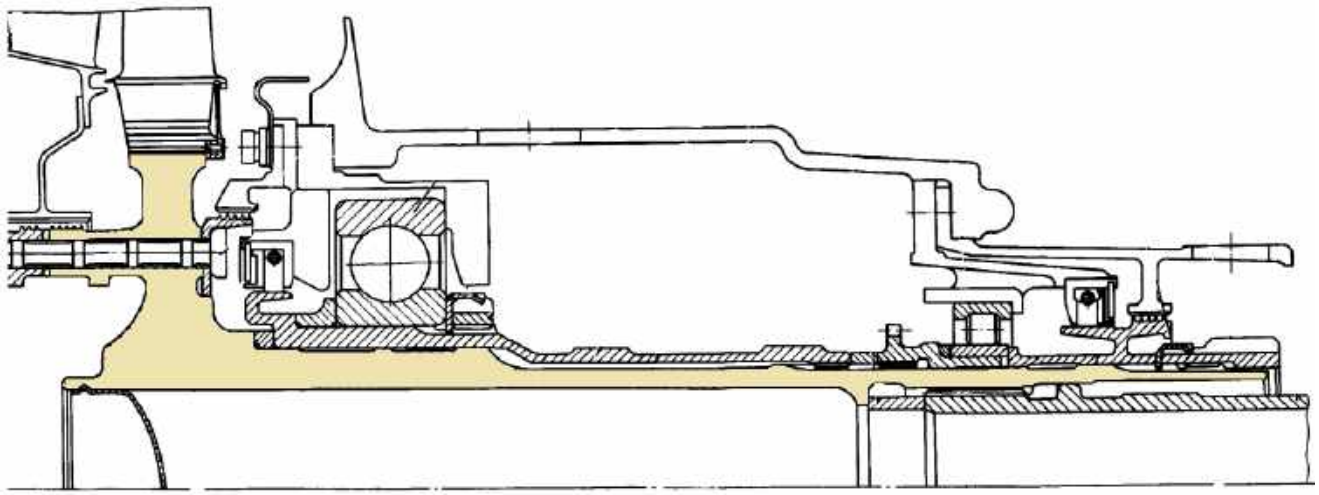


Fig. 3.16. Second stage of free turbine of the TV3-117 TShE

The detachable joints simplify assembling and disassembling of the turbine and decrease repair expenditures. It provides for separate rejection of the faulty component parts. Nevertheless, this type of joint is difficult for providing required rotor rigidity.

The non-detachable joints are made by press-fitting of the rotor component parts by cylindrical shoulders with negative interference 0.2 to 0.5 mm and additional retaining by plane pins.

3.5. Axial force that affects turbine rotor

The value of the axial gas-dynamic force that affects the turbine rotor is necessary for designing discs interconnection and connection with the shaft, and also for strength analysis of the turbine shaft, of the radial-thrust bearing and joint coupling of the turbine and compressor shafts. The design diagram is shown in Fig. 3.17.

The front side of the turbine rotor wheel is affected by pressure p_g, at the rotor wheel inlet; by air pressure p_A, in chamber A; pressure p_{lab} in the inter-labyrinth chambers, and pressure p_{sh} in the shaft chamber. The rear side of the turbine rotor wheel is affected by turbine discharge pressure p_T.

Axial force P_a that affects the turbine rotor is determined as a sum of the forces that are affecting separate stages:

$$P_a = \sum_{i=1}^{n} P_{st\,i}\,.$$

In its turn, the axial gas force of one stage is a result of force P_{bl}, which affects the airfoil, and force P_d, which affects the disc:

$$P_{st} = P_{bl} + P_d.$$

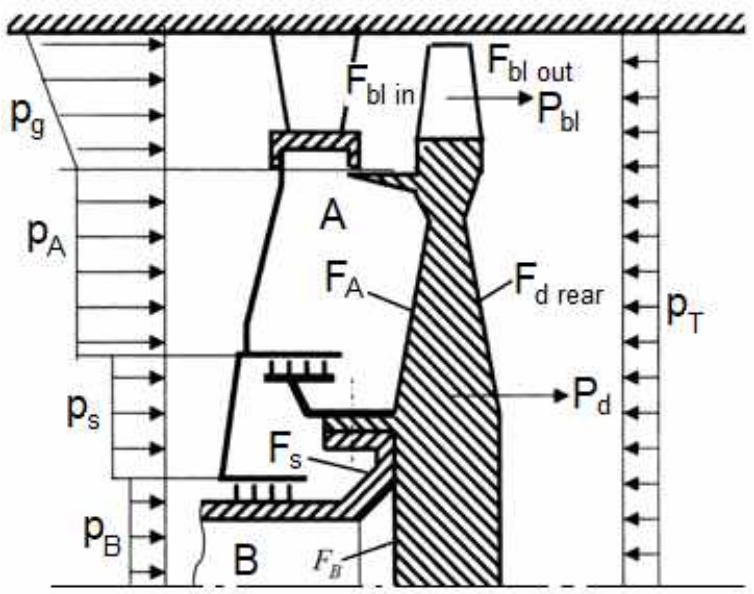


Fig. 3.17. Design diagram for determining axial force that affects turbine rotor

The axial force that affects airfoil is a total of the gas flow static and dynamic forces:

$$P_{bl} = G_g\,(c_{a\,T} - c_{a\,g}) + p_T\,F_{bl\ out} - p_m\,F_{bl\ in},$$

where $p_m = \dfrac{p_g + p_A}{2}$; $F_{bl\ out}$ and $F_{bl\ in}$ are areas of the airfoil ring at the outlet and inlet of the rotor wheel, respectively.

Force P_d is determined as static action of the gas flow on side surfaces of the disc:

$$P_d = p_T F_{d\ rear} - p_A F_A - p_s F_s - p_B F_B,$$

where $F_{d\ rear}$, F_A, F_s and F_B are areas of a disc from rear side, surface in chamber “A”, surface in a seal chamber and surface in a shaft inner chamber respectively.

The gas axial forces of the rotors of the modern gas turbines may reach 20 to 40 tons; they are directed downstream.

Knowing axial force P_{st}, it is possible to estimate the strength of the disc-to-shaft joint by using methods of strength of materials taking into account overload factors during engine operation.

Rotors of the turbine and compressor are joined by a special joining coupling; therefore, the axial force affecting the radial-thrust bearing is equal to a difference between the forces affecting the compressor and turbine rotors. This force (difference) is directed forward (if looking forward) and is taken into account when selecting and designing a radial-thrust bearing.

3.6. Gas turbine stators

The turbine stator consists of nozzle boxes, casings, and structure of the turbine bearing supports.

3.6.1. Gas turbine casings

Turbine casing (Fig. 3.18) is cylindrical or conical envelope (depending on a shape of the gas flow duct) with flanges, which connect the turbine casing with the outer casing of the combustion chamber and on the other side – with the casing of the afterburner or exhaust system. The gas turbine casing consists of the following:

– casings of the nozzle guide vanes;
– casing (cover) of the turbine shaft;
– casing of the turbine bearing support (if the support is available before the turbine);
– rear casing (if the support is available after the turbine).

Requirements to the turbine casing:

– high bending rigidity to prevent touching of the rotor against stator during engine bending deformation;
– reliable alignment of structural members of the casing at the point of their joining;
– the minimum heating of the casing walls and aircraft design structures;
– possibility of convenient inspection of the turbine members in service.

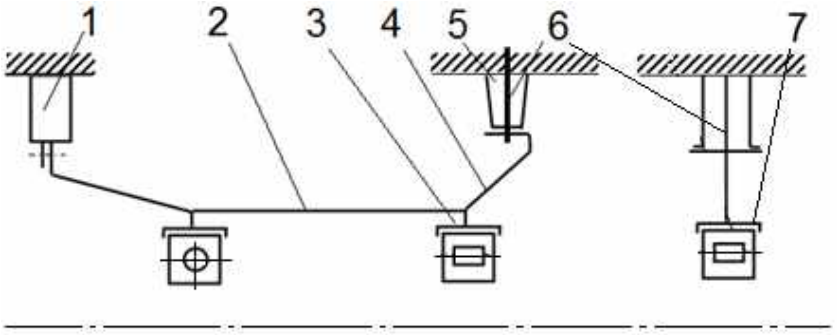


Fig. 3.18. Power diagram of turbine casing:
1 – compressor straightening vanes; 2 – housing of shaft; 3 – casing of front bearing support; 4 – diaphragm; 5 – casing of nozzle box with nozzle vanes; 6 – radial load-carrying elements; 7 – casing of rear bearing support

Casing of the nozzle guide vanes assemblies is used for allocation and attachment of the turbine nozzle guide vanes assemblies. They may have both longitudinal and transversal splits. The longitudinal split simplifies turbine mounting and inspection. But casing with such split has non-symmetrical thermal deformations; which results in non-uniform radial clearances and increase oscillations of rotor blades and causes a danger of rotor touching

against stator. Therefore, the longitudinal split is never used in turbines of the aero engines. This split may be used in relatively low-temperature stages of industrial turbines.

Transversal flange joints of casing parts are most widely used.

Centering shoulders are used for centering parts of the casing (prevention of their radial displacement). Pins or template bolts prevent circumferential displacement.

Tight joining in the splits is provided by precise machining and fitting of joining surfaces, and due to small pitch between attachment bolts or studs.

Structural members of the casing are heated non-uniformly: the inner surfaces that contact with the hot gas are heated to a temperature of 1000 ^{o}C to 1050 ^{o}C, the outer surfaces that are streamlined by the cold air may have a temperature of 550 ^{o}C to 600 ^{o}C. Thus, thermal expansion of the inner layers of the flange is limited by the outer cold layers. Therefore, compressing tensions appear in the inner layers and tensile stresses appear in the outer layers. The compressive stresses in the inner layers may exceed the yield stress, which results in appearance of the residual strains in the component parts of the casing. In flanged joint, it results in flange shrinkage, which complicates disassembling and finally may cause flange welding.

The flange shrinkage is prevented by using the following methods:

– cuts are made in a flange between the attachment bolts;

– design materials with low and similar thermal expansion factors are used for the flanges; if the thermal expansion is different, then the intermediate flange with intermediate thermal expansion is placed between the joining flanges;

– the inner layers of the flange are cooled by the air that flows through the multiple orifices of small diameter or through the slots equi-spaced circumferentially on the casing.

Housing of the turbine bearing support is usually made as a rigid frame. It includes support housing, load-carrying diaphragm, outer casing and inner support of the nozzle guide vanes assembly of the first turbine stage. These component parts are joined by the load-carrying rods passed through the hollow vanes assembly (the example is the RD-9B turbojet) or by diaphragms arranged between the flame tubes of the combustion chamber (the example is the D-30P turbofan).

In some cases, the power link in the area of the nozzle guide vanes assembly may be absent; in this case, the rigid housing of the shaft is functioning as the turbine support casing (the NK-12, AI-20).

Housing of the turbine shaft bears front support of the turbine rotor, support of the compressor and turbine stage one nozzle guide vanes assembly. Housing of shaft is protected against heating by the heat-reflecting shields

cooled by the air. This housing limits the volume of the tubular-type or tube-annular type combustion chamber.

Turbine rear casing (the NK-12, AL-21, D-36, etc.) bears a rear support, which load-carrying members cross a gas flow duct. The load-carrying members (rods, struts, frames) are protected against heating by shields of the streamlined shape. Chambers between the load-carrying members and shields are blown with the air.

3.6.2. Nozzle boxes: operating conditions, load-carrying structures and methods of vanes-to-casing attachment

The nozzle guide vanes assembly converts a portion of the gas potential energy into kinetic energy; it also directs the gas flow to the rotor wheel blades at the required angle.

The main structural members of the nozzle box are nozzle vanes assembly, inner and outer shroud rings (Fig. 3.19).

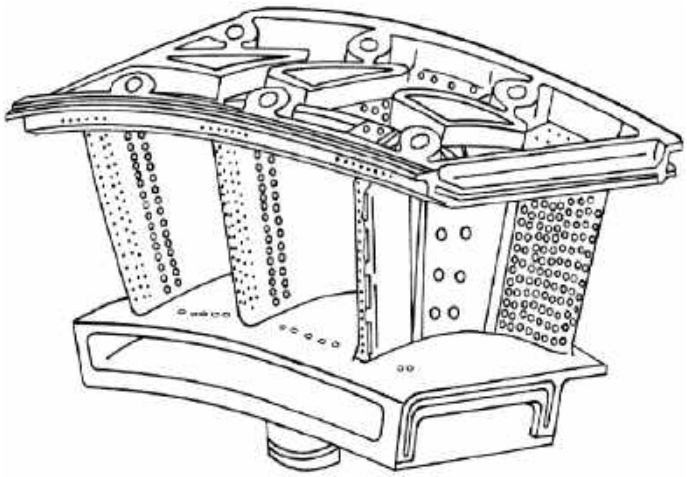


Fig. 3.19. Segment of nozzle guide vanes

The gas flow passes through the nozzle guide vanes at high velocity (500 to 600 m/s) and loads the vanes by the high axial and circumferential forces. The gas, which flows over the component parts of the nozzle guide vanes assembly, has high temperature (1200 to 1800 K) and contains excess oxygen, which causes corrosion. The nozzle guide vanes assembly must meet the following requirements:

– sufficient rigidity during operation to maintain optimum angular setting of the vanes and to take affecting loads;

– low thermal stresses;

– minimum hydraulic resistance and the gas escape through the clearances.

The nozzle guide vanes are characterized by same parameters as the rotor blades but they have other geometric proportions. The length of the

nozzle guide vane is chosen 1 to 2 % less than that of the rotor blade; this takes into account thermal elongation of the component parts and prevents the gas flow from the nozzle guide vanes assembly to a turbine disc rim in hot condition of the turbine component parts with subsequent shock and additional losses. Chord of the nozzle vane is more than that of the rotor blade because the flow turn angle in the nozzle guide vanes assembly is more than that in the rotor blade. The number of the nozzle guide vanes shall not be equal to or multiple to the number of the rotor blades to prevent dangerous resonant oscillations of the rotor blades.

Non-uniform heating of the component parts of the nozzle guide vanes assembly requires freedom of their thermal expansion. This is provided either by “floating” fit of the blades or by their mounting only to one of the shroud rings.

The nozzle vanes are made with end shroud platforms or without them, which depends on the peculiarities of their mounting. The shroud platforms form a gas flow duct of the nozzle box and are used for attachment of the nozzle guide vanes to them.

In case of two-support mounting, the airfoil cross-section along the vane length has a constant chord. In case of cantilever mounting, the chord and the vane thickness are decreased to the vane end for providing its full strength.

Depending on method of vanes mounting, there are the following power diagrams (Fig. 3.20):

– two-support mounting;
– cantilever or half-frame mounting;
– frame mounting.

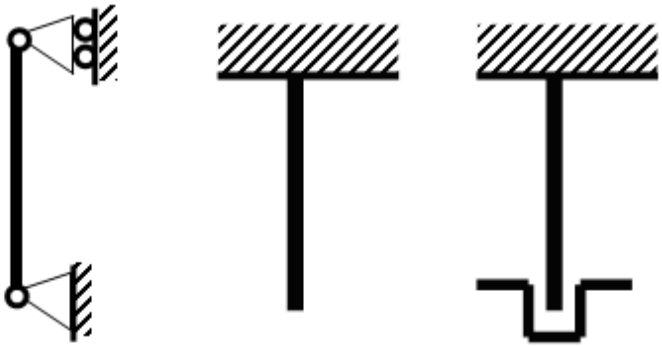


Fig. 3.20. Methods of mounting of nozzle vanes

The two-support mounting is usually used in the first stages. This type of mounting of the nozzle guide vanes assembly is rigid and strong; the nozzle vanes have freedom for thermal expansion. The nozzle vanes of the first turbine stages are not included into a power structure of the stator because they are highly heated and difficult to provide the required rigidity and strength. The load-carrying elements, which transmit forces from the bearing housings to

the turbine external casing (rods, bolts, spokes), are mounted inside the hollow vanes (the R-11F-300, AM-3, RD-9B, and R-29F-300 turbojets, Fig. 3.21) or between the flame tubes of the combustion chamber (the D-20P, D-30P turbofans, and D-25V turboshaft).

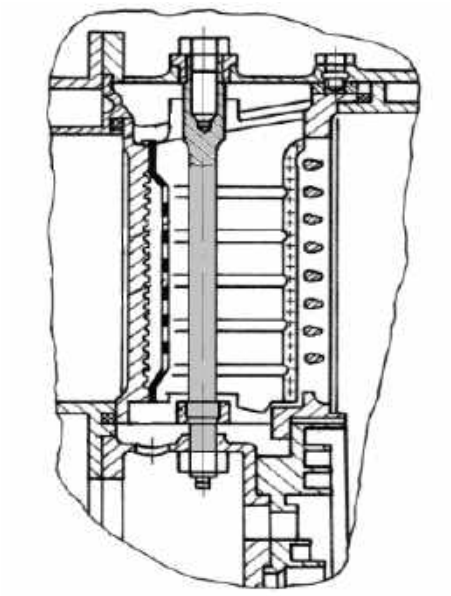


Fig. 3.21. Power link from the bearing housing through the load-carrying rod, which is mounted inside a hollow nozzle vane

The strength analysis of this mount is similar to that of two-support beam.

The cantilever mounting of the nozzle vanes is usually used in the second and subsequent turbine stages. The inner tips of the vanes may be joined by a shroud thereby increasing rigidity of the nozzle guide vanes assembly. This joint may be fixed or movable. The shroud of fixed joint has cuts in some places for decreasing thermal stresses (Fig. 3.22).

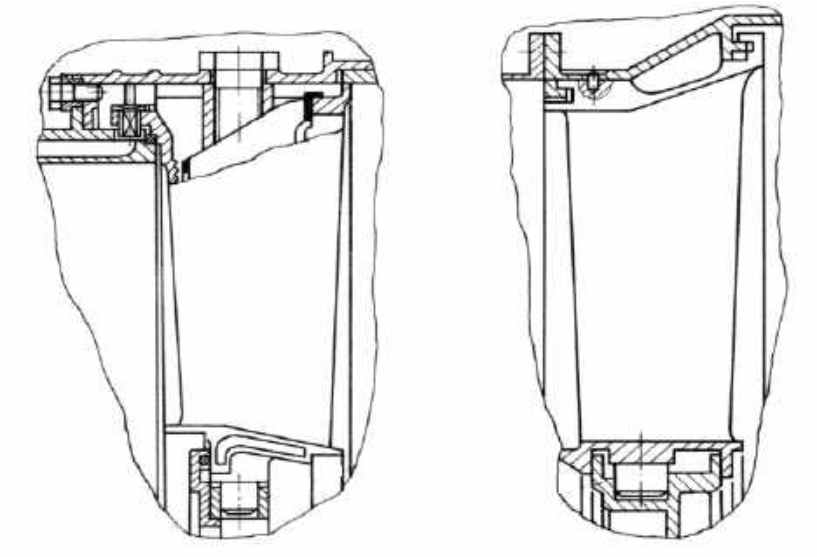


Fig. 3.22. Half-frame mount of the nozzle vanes

The vanes of the movable joint have smooth pins in the end portions; these pins are inserted in the radial holes provided in the shroud. This is a half-frame mounting. This mounting allows free thermal expansion of the vanes and shroud.

The shroud of such mounting does not take and does not transmit external the external loads; it only redistributes some loads (for example bending moments) between the vanes of one rim.

The strength analysis of this mounting diagram is similar to that of the cantilever beam without a shroud (the presence of the shroud increases strength margin of this structural member).

Frame mount of the nozzle vanes (Fig. 3.23) is used in rear cases (the examples are free turbines of the TV2-117 and TV3-117 turboshafts). They have relatively low temperature, which allows using them as load-carrying elements that transmit a force from the free turbine support to the engine casing.

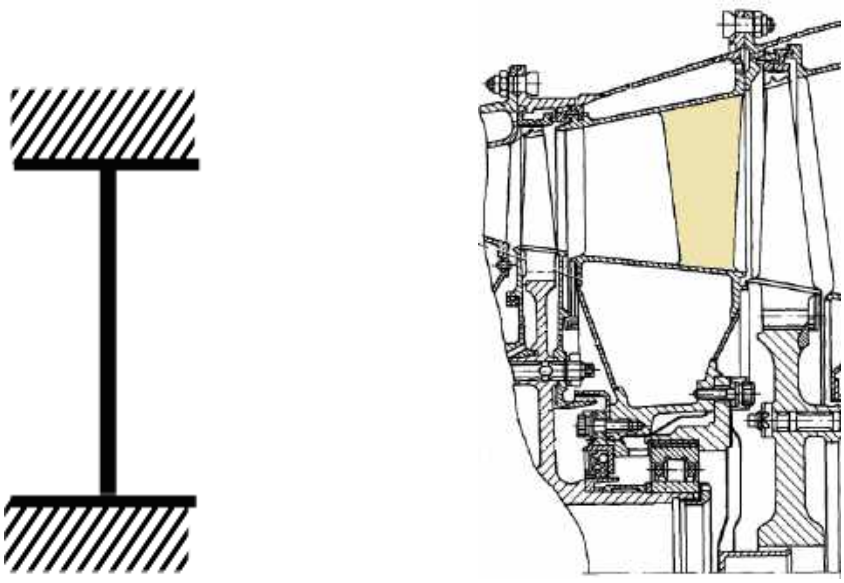


Fig. 3.23. Frame mount of the nozzle vanes

The nozzle vanes may be attached to the casing by the following methods:

– by welding (the AI-20, and NK-12);
– by bolts and screws (the R-15B, R-11F-300, and R-29F-300 turbojets);
– by special roots (the D-25V);
– by placing them into the ring groves made in the casing (the D-36, and D-136);
– by placing them into the slots punched in the shroud rings (the first stages of the NK-12 turboprop and TV3-117 turboshaft, and AI-20 turboprop).

The nozzle vanes are manufactured by pressing, milling and precision casting. The vanes of the first stage usually are hollow ones. This decreases material utilization and allows cooling them with low temperature non-uniformity.

3.7. Clearances between rotor and stator. Sealing of turbine gas flow duct

Radial and axial clearances prevent touching rotor against stator.

The **radial clearances** are clearances between tips of the rotor blades and casing (Δ_1) and clearances in the sealing labyrinths (Δ_2).

Let's consider variation of the radial clearances between the rotor blades and casing at various power ratings (Fig. 3.24).

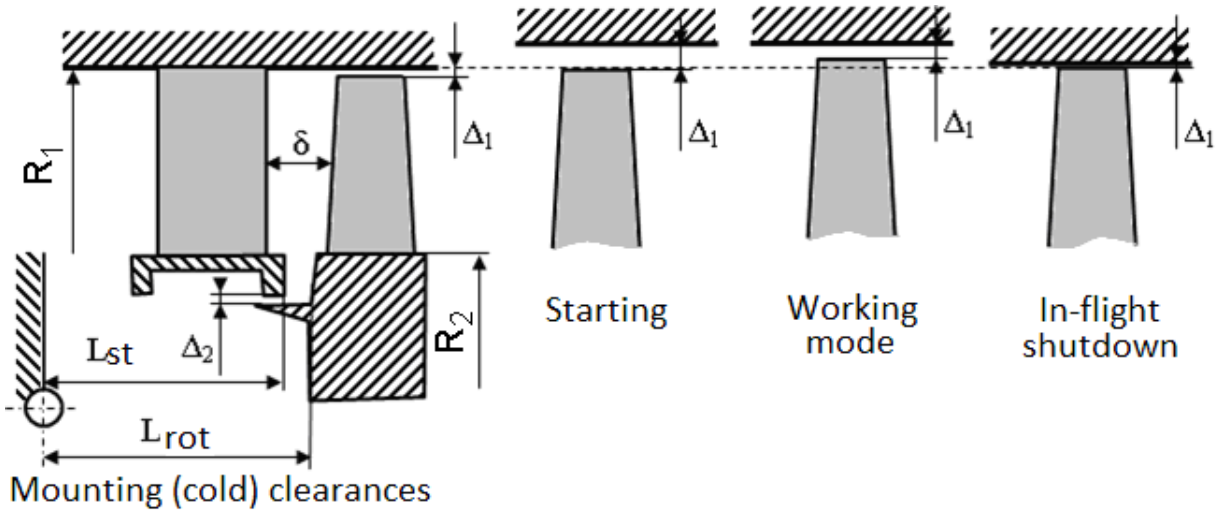


Fig. 3.24. Variation of the radial clearances depending on the engine power rating

The radial clearances affect significantly the turbine efficiency and specific fuel consumption. The clearance value in cold condition (mounting clearance) is determined to prevent touching a casing by the rotating parts after engine shutdown; when the engine is warmed up the "hot" clearance must be the minimum one. The value of the mounting clearance includes elastic and residual deformation of the blades, disc and casing, elongation of the blades and disc due to creep, rotor swash, etc.

Typical value of the radial clearance is 1.5 to 3 % of the blade length. The relative change of the radial clearance during turbine heating may be expressed by using the geometric parameters and temperature of the turbine parts:

$$\Delta_{1\,hot} = R_2(1 + \alpha_{case}\Delta t_{case}) - R_1(1 + \alpha_d\Delta t_d) - h_{bl}(1 + \alpha_{bl}\Delta t_{bl}),$$

where α_{case}, α_d, α_{bl} – are the linear thermal expansion factors of metal of the casing, disc and blade, respectively;

Δt_{case}, Δt_d, Δt_{bl} – are the increase in temperature of the casing, disc and blade comparing to the cold condition, respectively.

During engine starting, the casing is heated faster than the rotor is. Therefore, the **axial clearance** at disc front side decreases, and increases at

the disc rear side. After engine shutdown, vice versa – because the stator is cooling faster.

The relative axial clearance under the real designs is as follows:

$$\overline{\varphi} = \frac{\varphi_{cold} - \varphi_{hot}}{L} \approx 0.3...0.4\ \%, \text{ where } L = \frac{L_{rot} + L_{st}}{2}.$$

Axial interblade clearance δ in known designs is 10…40 % of the blade mean chord.

Such methods are used to decrease the radial clearance and to prevent damage of the blades when they are touching against casing:

– soft metal-ceramic inserts are mounted in the inner surface of the casing; they consist of two layers: the hard iron-nickel-graphite layer is a base and the soft nickel-graphite layer is a working surface;

– ring honeycomb inserts are mounted in the same places, the shroud platforms of the rotor blades are equipped with labyrinth fins;

– if the rotor blade has not shroud platform, then its peripheral tip is sharpened (chamfered).

The radial clearance is decreased gradually during the engine operation (the blades and discs are elongated due to residual strains and creep).

The gas spilling in the axial clearances is decreased due to the radial and axial labyrinth seals.

The labyrinths provided on the peripheral shroud platforms of the turbine blades are usually combined with the honeycomb inserts that are mounted on the stator. The labyrinth fins can cut into the thin metallic honeycombs, thus providing operation with the minimum radial clearance between the rotor and stator (Fig. 3.25).

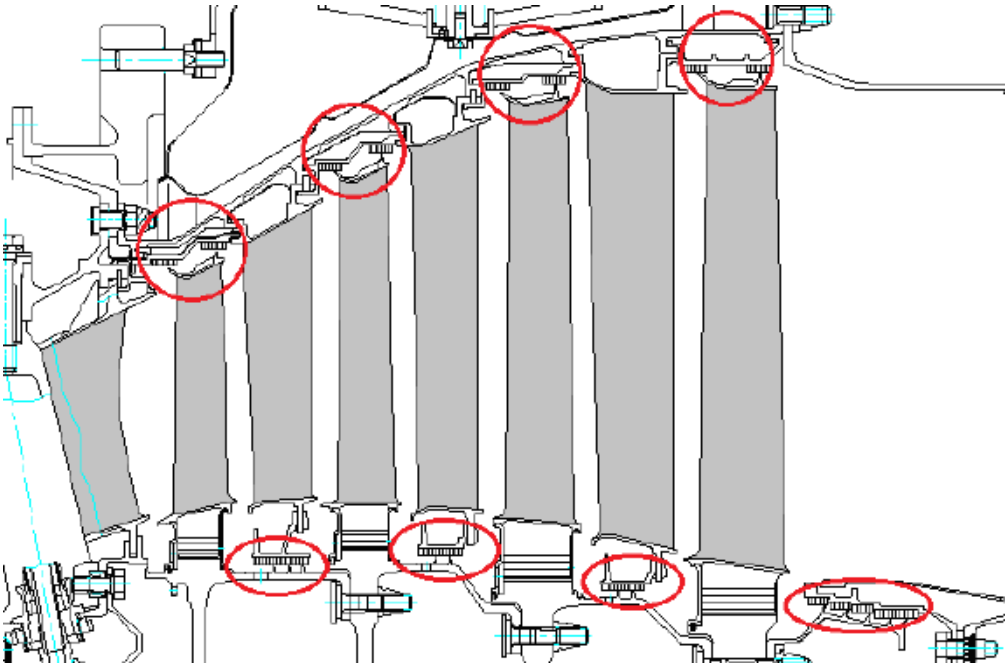


Fig. 3.25. Labyrinth seal with honeycomb inserts

The equation given in subchapter 2.10 for determining gas spillover through the labyrinth seal has satisfactory precision in case when the radial clearance is between the labyrinth seal fins and smooth wall of the stator. In case of application of the honeycomb insert, the equation is to be modified by some corrections, which were proposed by professor Ye. Bogomolov.

Let's consider the gas spillover through a cell above the fin at zero clearance between the fin and design of the honeycomb insert (Fig. 3.26).

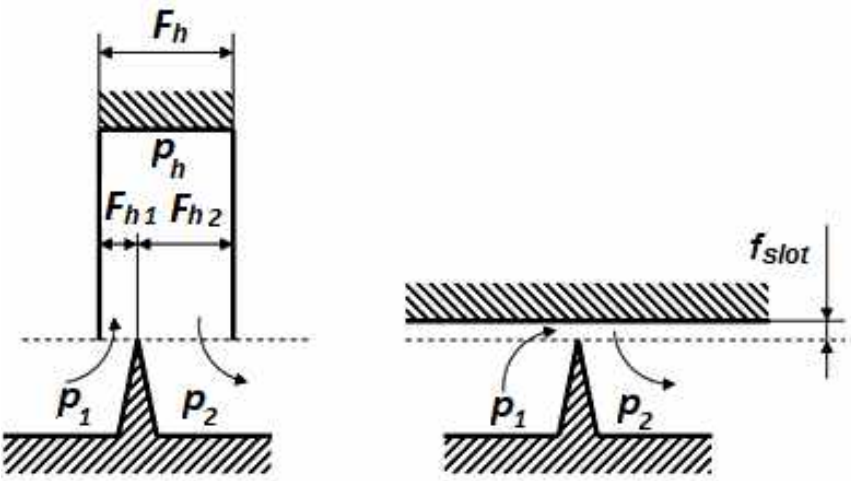


Fig. 3.26. Design diagram of spillover through the labyrinth with honeycomb insert

The gas consumption G_h through the honeycomb chamber is

$$G_h = v_{h1}\rho_{h1}F_{h1} = v_{h2}\rho_{h2}F_{h2},$$

where v_h, ρ_h are the gas velocity and density at the inlet to the honeycomb chamber (index 1) and at the outlet of the chamber (index 2);

F_{h1}, F_{h2} are the inlet and outlet areas of the chamber that are depended on the position of the rim and the cross-sectional area of the chamber ($F_{h1} + F_{h2} = F_h$).

According to the Bernoulli's equation for an incompressible fluid, we have the following:

$$v_{h1} = \sqrt{2\frac{p_1 - p_h}{p_{h1}}}; \quad v_{h2} = \sqrt{2\frac{p_h - p_2}{p_{h2}}},$$

where p_1 and p_2 are the pressures upstream and downstream of the fin, respectively;

p_h is stagnation pressure in the honeycomb chamber.

Average density of the gas is as follows:

$$\rho_{h1} = \frac{p_1 + p_h}{2}\frac{1}{RT}; \quad \rho_{h2} = \frac{p_h + p_2}{2}\frac{1}{RT},$$

where R is the gas constant;

T is the gas temperature.

The above equations give the following:

$$\sqrt{\frac{(p_1-p_h)(p_1+p_h)}{(p_h-p_2)(p_1+p_h)}}=\frac{F_{h\,2}}{F_{h\,1}},$$

wherefrom

$$\frac{p_h^2}{p_1^2}=\left(1+\frac{F_{h\,2}^2}{F_{h\,1}^2}\frac{p_2^2}{p_1^2}\right)/\left(1+\frac{F_{h\,2}^2}{F_{h\,1}^2}\right).$$

Thus, the gas flow through the honeycomb chamber is as follows:

$$G_h=\frac{p_1}{\sqrt{RT}}\sqrt{1-\left(\frac{p_h}{p_1}\right)^2}F_{h\,1}.$$

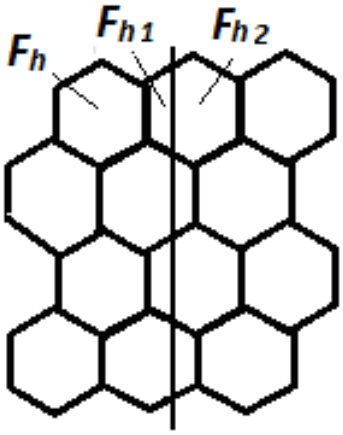


Рис. 3.27. Honeycomb areas

Taking into account the real character of the flow through the honeycomb, and the average ratio of the areas (Fig. 3.27), we may determine the flow through the seal on analogy to the Chapter 2.10.3:

$$G_{seal}=K\,F_{d\,eq}\sqrt{\frac{p_1^2-p_2^2}{zRT_1}}=0.2372Kf_{slot}\sqrt{\frac{p_1^2-p_2^2}{zRT_1}},$$

where K is flow factor that takes into account specifics of expansion in the clearance and non-complete breaking in the labyrinth chamber (depends on the labyrinth type and shape of collars).

3.8. Gas turbine cooling

Besides in 30-th of the previous century professor V. Uvarov demonstrated experimental gas turbine engine with turbine inlet temperature 1870 K, majority of manufactured and maintained turbine engines have 1600 to 1700 K and new technologies provide 1900 to 2000 K. The TIT increasing gives a lot of improvements:

– the gas output velocity increases, thus increasing the engine specific thrust;

– the specific and frontal thrust of the TJE and TFE increases;

– the specific power and fuel efficiency of the TPE, and TShE for the helicopter, on-ground and marine power plants increases;

– the specific mass of all the engine types decreases.

Turbine inlet temperature can be increased by two ways:

– by turbine materials improvement;

– by turbine parts cooling improvement.

The turbine cooling system provides maximum tolerant temperature of the turbine parts. At this temperature, the turbine parts have enough strength and required reliability (preset life).

The major turbine elements that need cooling are rotor blades and nozzle vanes, discs and casings of nozzle vanes.

For the first time, convex cooling of rotor blades has been implemented by German designers in the BMW-003 turbojet, which was also manufactured in Soviet Union under the name RD-20.

Classification of turbine parts cooling methods is shown in Fig. 3.28.

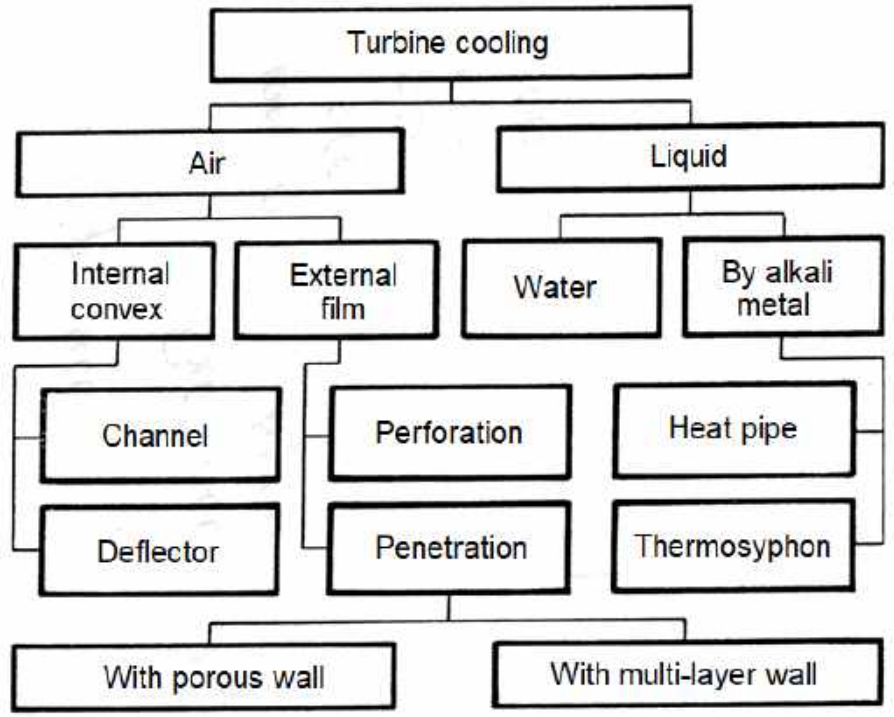


Fig. 3.28. Classification of methods for cooling of turbine parts

In up-to-date engines, the open-type cooling systems are used: the cooling air after cooling is discharged into the engine gas flow duct. The air for cooling the first turbine stages is taken from the compressor outlet (high pressure air); the air for cooling the subsequent stages and casing is taken from the intermediate stages of the compressor, from the bypass duct, from the engine cowl, from external fan (in the helicopter gas turbine engines).

3.8.1. Cooling of turbine rotor blades

Turbine rotor blades are protected against overheating by using the following methods:

– covering by the thermal protection enamels;
– heat transfer to the disc;
– blowing of clearances in the blade root and elongated blade shank by the air;
– convex cooling (longitudinal, transversal, combined);
– convex-film (obstructive) cooling;
– porous cooling;
– combined cooling;
– liquid cooling;
– vaporizing cooling;
– cooling by using liquid metals.

Special **heat protective enamels** are used for covering airfoil portion of the rotor blades. They are based on chromium oxide, zirconium oxide, silicon-oxide or special ceramics and decrease the blade temperature on 40 to 120 ºC as compared with the non-protected blade.

Rotor blade **cooling by heat transfer to the disc** is used at TIT value of 1150 to 1200 K. In this case, the maximum heated cross-section is located on 2/3 of the airfoil portion length from the root, its temperature is 140 to 160 K less than TIT (Fig. 3.29).

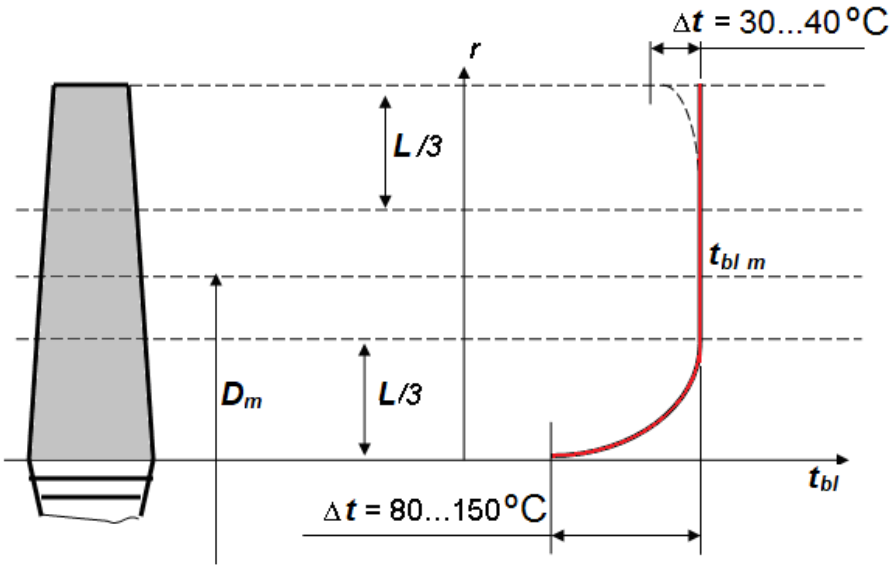


Fig. 3.29. Temperature distribution along blade length during heat transfer to the disc

Due to heat transfer to the disc, the temperature of 1/3 of the airfoil portion length from the root by 80 to 150 K lower than that of the non-cooled blade; this improves blade strength in the critical cross-section of the root.

The blade root clearances and elongated blade shank may be blown by the air. This method of cooling may be used at TIT = 1250 to 1300 K.

At higher TIT, special methods for cooling of the rotor blades, nozzle vanes, discs, and casings are used (Fig. 3.30).

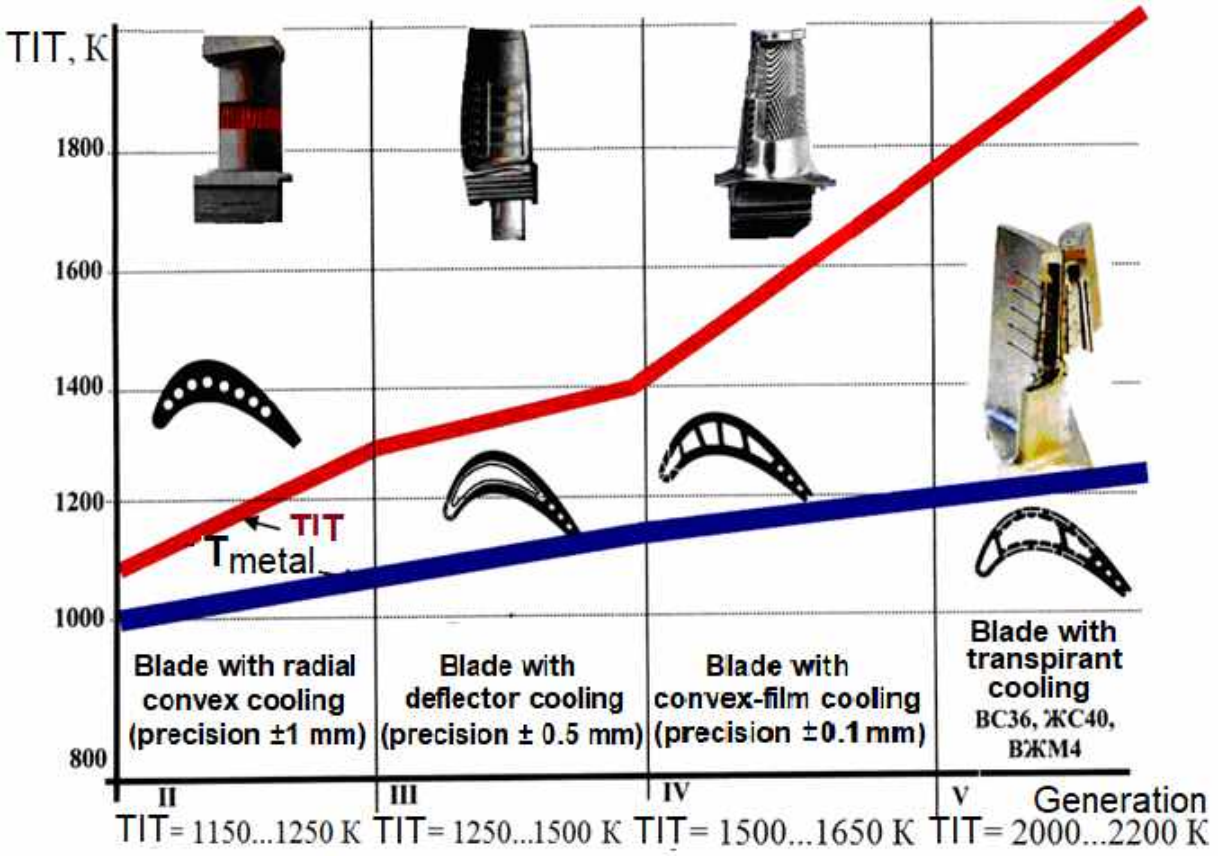


Fig. 3.30. Methods for cooling of rotor blades at various gas temperatures

In case of **convex (internal) cooling**, the cooling air enters the blade airfoil portion through the orifices provided in the root, wherein it flows by cooling channels, takes the heat from the blade walls and escapes into the turbine gas flow duct. This method of cooling may be used at TIT = 1400 to 1500 K, which depends on the design version.

Depending on the diagram of flow of the cooling air, there are longitudinal, transversal and combined (longitudinal and transversal) convex cooling methods.

In a blade with the **longitudinal (radial) flow**, the air flows along the blade in radial direction from the root to the periphery and escapes to the turbine gas flow duct through the orifices provided in the blade end face (the DV-2, HPT D-36, and D-136). The blade design is simple, but there is difficult to arrange the output channel in thin peripheral section, which is not cooled sufficiently because the air is heated when it flows from the root to the periphery of the blade (Fig. 3.31).

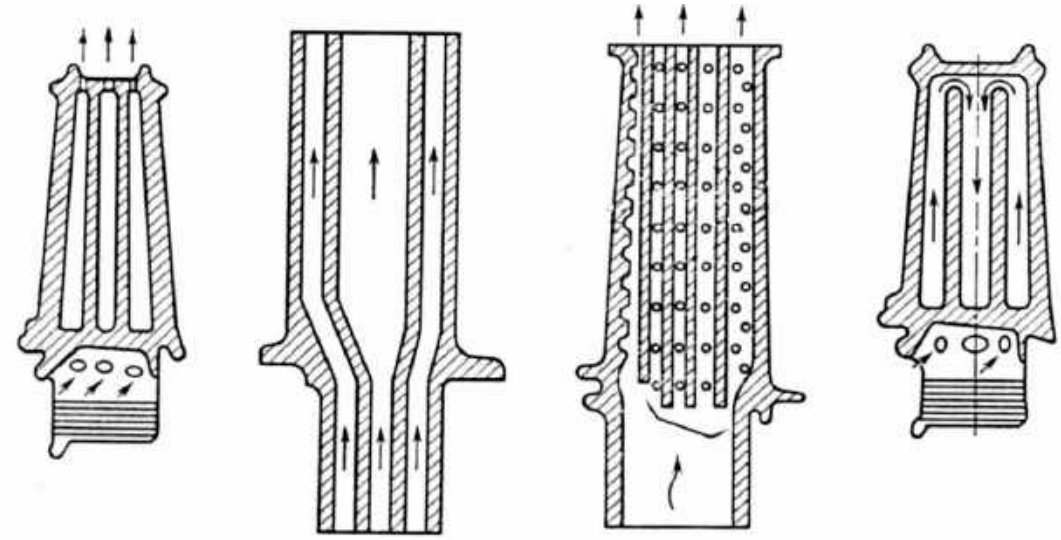


Fig. 3.31. Diagrams of rotor blades with longitudinal convective cooling

The cooling intensity is increased at the **transversal flowing of the cooling air**. Such blade is equipped with the deflector – thin-wall insert placed inside a hollow portion of the blade airfoil (Fig. 3.32).

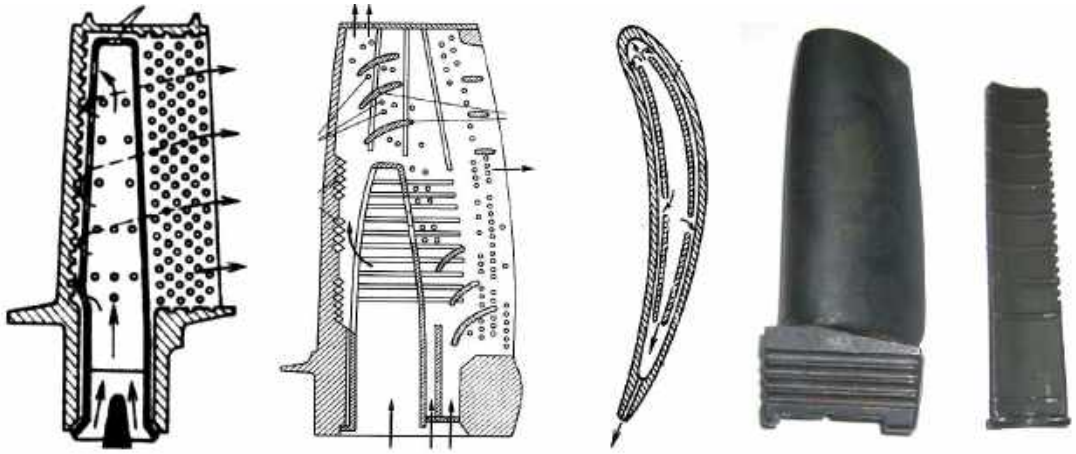


Fig. 3.32. Rotor blades with transversal (deflector) cooling

The cooling air enters inside the deflector and through a row of orifices provided in the front edge of the deflector flows to the inner side of the blade front edge. In this case, the temperature of the cooling air remains almost constant along the whole length of the blade airfoil portion. Then the air flows through a clearance between the deflector and the blade wall and is discharged into the turbine gas flow duct through a slot provided in a rear edge of the blade airfoil portion. Cooling is intensified if small ribs and burbling hillocks are made on the inner surface of the blade wall. This method of cooling gives TIT increase by 30 to 50 K comparing to the longitudinal convex cooling (the R-25F-300, and P-29F-300 turbojets).

Blade with **combined motion of the cooling air** is not provided with deflector; the internal channels are designed to provide flow of one portion of

the air along the blade airfoil portion from the root to the periphery, and other one flows transversally along the blade chord. The bulkheads, bridges and burbling fins direct the air and make turbulence, thus increasing a heat transfer from the hot wall to the cooling air. These blades are manufactured by the vacuum investment casting (the AL-21F afterburning turbojet).

Cyclone-vortex cooling is one of convex cooling methods. The blade is equipped with a special matrix with inclined channels and sharp turns of the cooling air flow (Fig. 3.33).

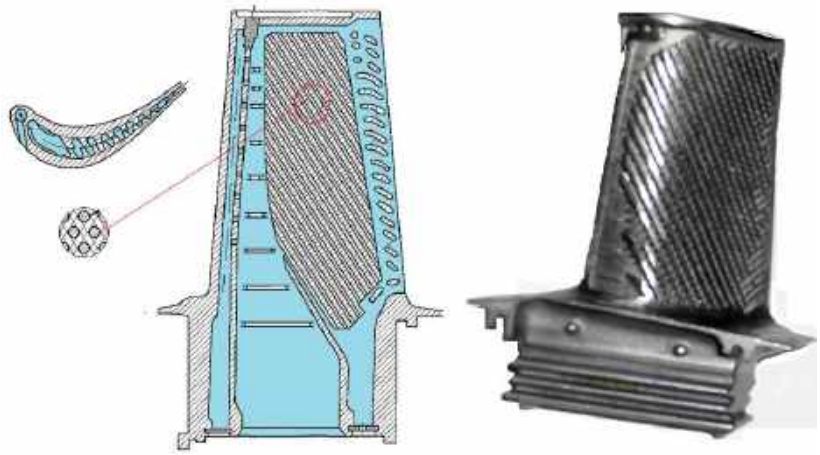


Fig. 3.33. Rotor blade with a vortex matrix

The cyclone-vortex cooling combined with a single-crystal blade may be used at TIT 1650 to 1700 K, but it needs the cooling air with higher pressure, because the complex internal channels have high hydraulic resistance (the RD-33).

In case of **convex-film (obstructive) cooling** (Fig. 3.34), the air flows by the internal channels, and then some portion of this air flows through the slots or rows of orifices to a blade surface thereby making a thin protective air film between the hot gas and the blade surface surface.

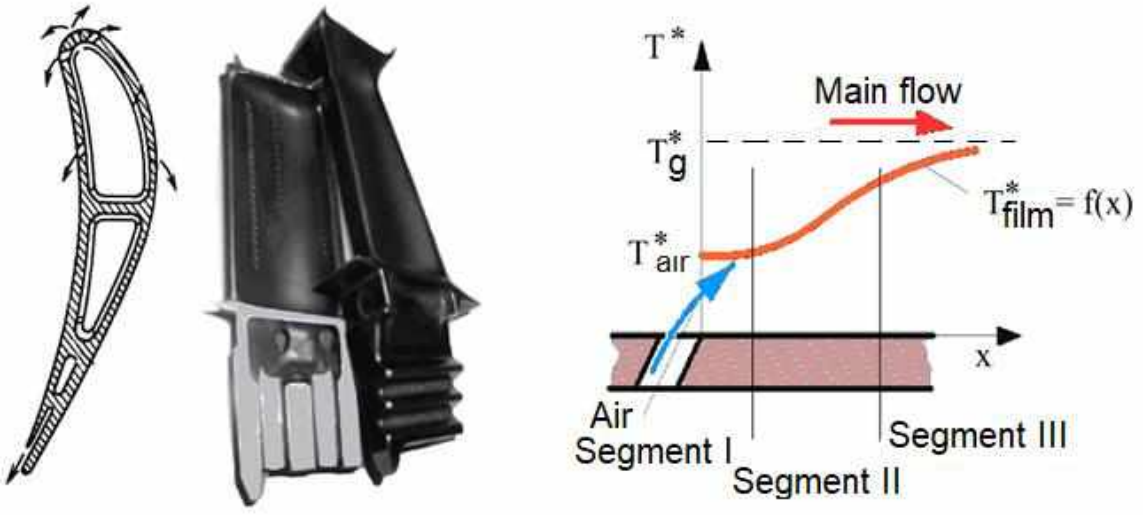


Fig. 3.34. Rotor blade with a convex-film (obstructive) cooling

Since the air veil is diffused by the flow of hot gas, the pitch between the rows of orifices has a value, which prevents destruction of the air streams before they reach the next row of the orifices. Diameter of the orifices is 0.3 to 0.4 mm. This cooling is effective at TIT = 1550 to 1650 K, and if it is combined with the single-crystal blade, it may be used at TIT up to 1700 K. Nevertheless, this type of cooling needs high pressure of the cooling air, and the cooling orifices are the concentrators of stresses in the blade airfoil portion (the D-30F6, and D-18T turbofans).

Porous cooling is promising if TIT exceeds 1600 to 1800 K. Wall of the blade is permeable (porous). It is manufactured by using powder metallurgy method. When the cooling air flows inside a hollow blade, it takes heat from the wall by convection; then it goes through the pores to the external surface and forms a thin cooling layer adjacent to the blade airfoil portion (Fig. 3.35).

This type of cooling is efficient; at TIT=1800 K the blade surface temperature is not higher than 1200 K at cooling air bleeds of 3 to 4 %.

There are differed porous and multi-layer permeable walls of the blade. Porous materials for hollow shells are made by sintering of the wire nets or of the fine-dispersed powder of the heat-resistant alloy. The porous materials have low load-carrying capacity. Therefore, the blades with this type of cooling are designed by the so called “sleeve” diagram. According to this diagram, the main load from the centrifugal forces is perceived by a load-carrying core, and a porous shell forms the blade airfoil portion and provides the blade cooling by the air that flows through the channels.

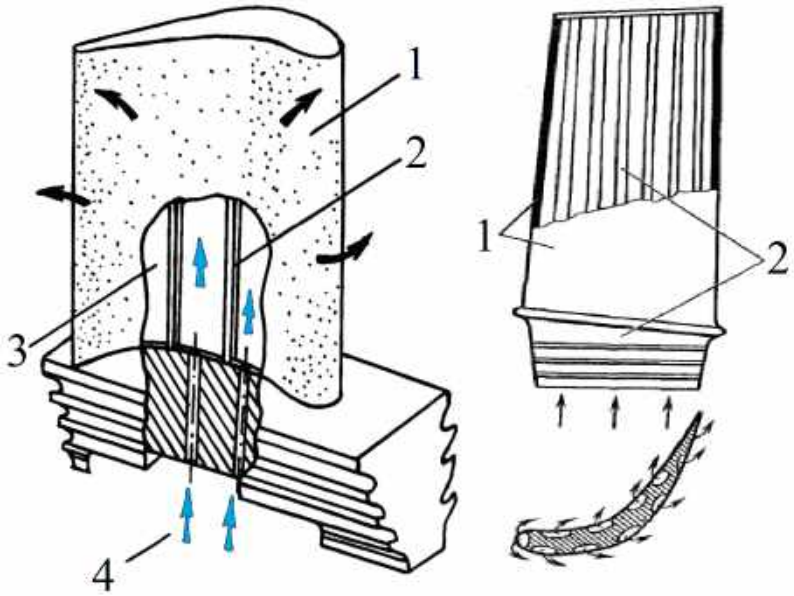


Fig. 3.35. Blade with porous cooling:
1 – porous shell; 2 – load-carrying rods; 3 – cavities for the air;
4 – air supplying channels

Disadvantage of porous cooling is tendency of porous materials to decreasing of permeability caused by oxidation and fluxing of the pores.

Taking into account these disadvantages of the sintering porous materials, leading companies are trying to develop sheet permeable materials with the regular inner structure. Allison Company proposed the multilayer shell of the rotor blade with penetrating air cooling that is named as the Lamilloy structure. The shell is formed by the outer layer, two intermediate layers and inner layer. Each layer has through holes that are arranged in different places of the shell and are interconnected by the grooves. The cooling air flows by these grooves to holes of the next row, until it reaches the outer layer (Fig. 3.36).

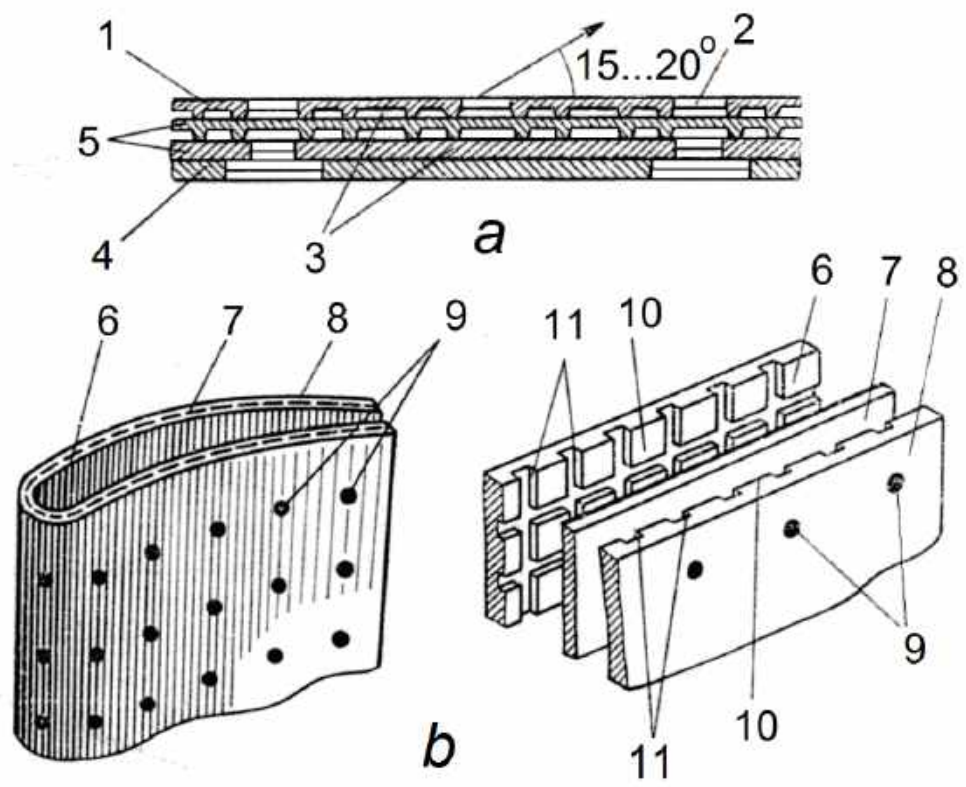


Fig. 3.36. Multilayer permeable material:
a – multilayer shell of Allison Company;
b – three-layered shell of Rolls-Royce company:
1, 8 – outer layer; 2, 9 – through holes, diameter is 0.4 to 0.6 mm;
3, 11 – connecting grooves of 0.125 mm deep; 4, 6 – inner layer;
5, 7 – intermediate layer, thickness is 0.25 mm

Transpiration cooling is the intermediate between the convex-film and porous cooling. The blade with such cooling is two-layer one with a lot of small skew holes on all surface of the airfoil portion (Fig. 3.37).

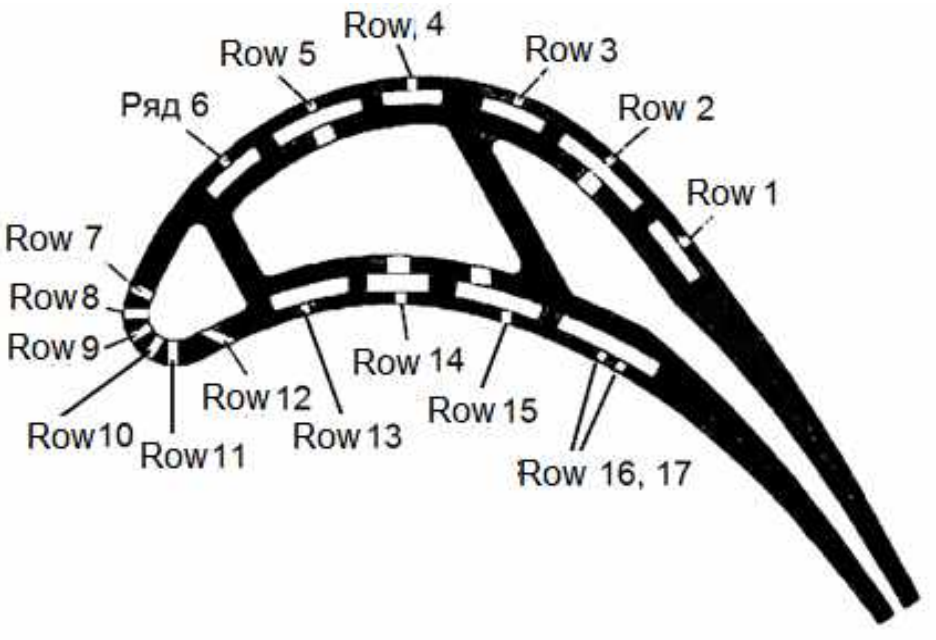


Fig. 3.37. Blade with transpiration cooling (“flexible rods” technology)

The single-crystal blades with transpiration cooling made of alloy ЖС-47 (alloyed by rhenium to 10 %) operate at TIT = 2000 K.

Fig. 3.38 shows the relation between cooling efficiency and the cooling air flow at various methods of cooling.

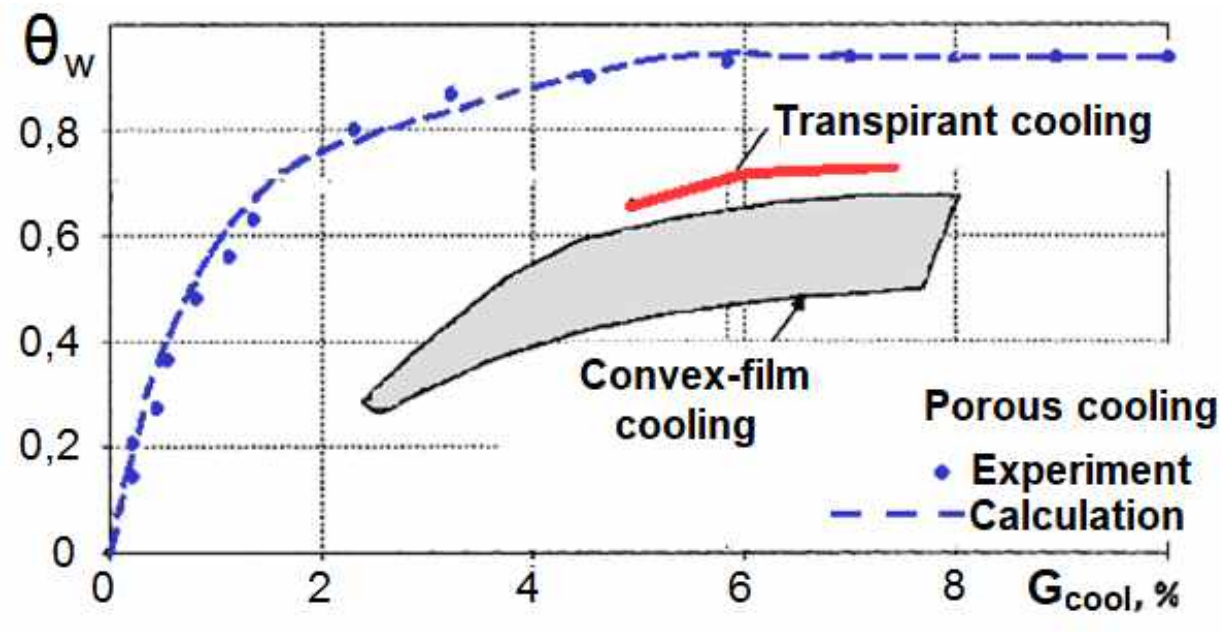


Fig. 3.38. Comparison of efficiency of transpiration, porous and convex-film cooling

The efficiency of the above described methods of cooling may be increased by using the air, which is preliminary cooled in special heat exchangers arranged in the bypass duct of the turbofan (the AL-31, Fig. 3.39).

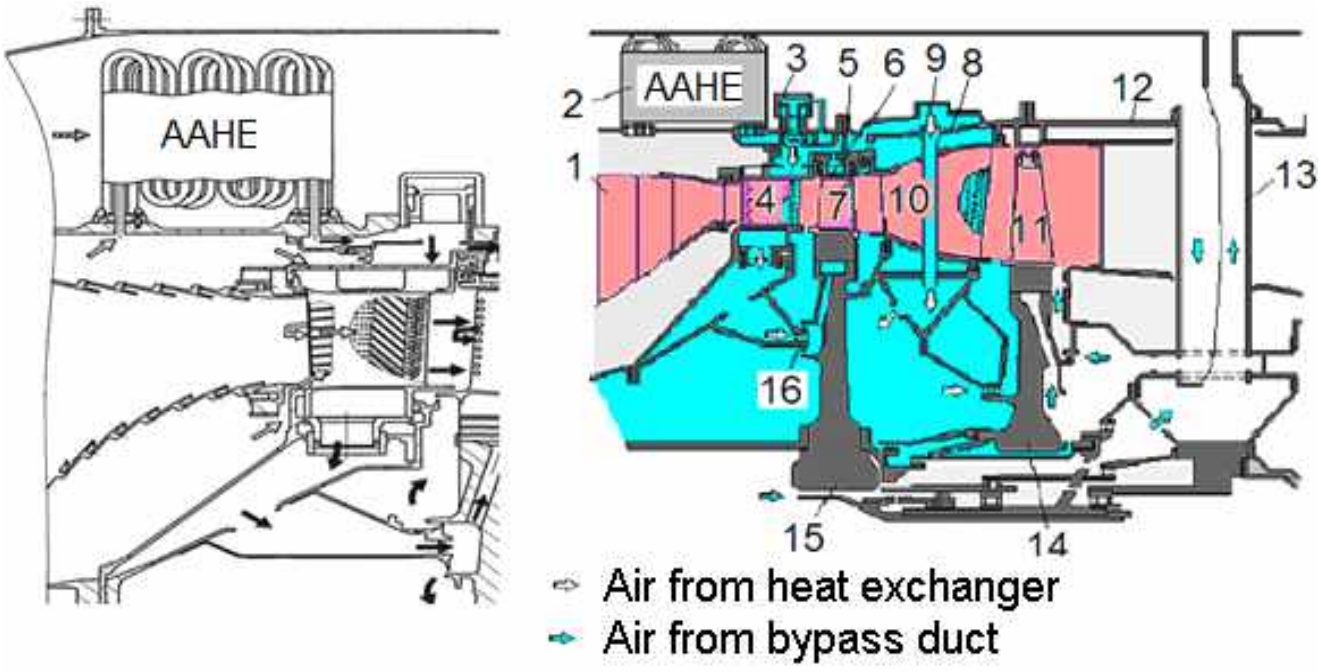


Fig. 3.39. Heat exchanger in bypass duct of afterburning turbofan:
1 – combustion chamber; 2 – air-air heat exchanger; 3 – valve;
4 – HPT nozzle vane; 5 – outer ring; 6 – honeycomb insert; 7 – HPT rotor blade;
8 – rim; 9 – bypass pipe; 10 – LPT nozzle guide vane; 11 – LPT rotor blade;
12 – turbine support housing; 13 – load-carrying strut; 14 – LPT disc;
15 – HPT disc; 16 – inducer vanes

Though heat exchangers in this case hydraulic resistance of secondary duct is increased and specific fuel consumption is increased too. Besides, the cold air entering hot surface initiates significant thermal stresses because of high temperature gradients.

Liquid cooling by vaporizing was designed and tested in 30-th of previous century by prof. V. Uvarov. Cooling by liquid low-melted metals (lithium, sodium, potassium) are developed now. They provide increasing TIT up to stoichiometric values (2200 to 2300 K).

Cooling by dry overheated saturated water steam is effective. Specific heat of the dry saturated water steam is 3560 J/kg·K; it is three times more than that of the air. Besides, viscosity of the dry water steam is three times less than that of the air. The overheated steam may be generated by bleeding small amount of heat at the turbine outlet. So, it is possible to obtain effective cooling at low consumption of the coolant and small areas of cooling channels. Disadvantage of this cooling method is necessity to carry onboard aircraft additional water tank. Therefore, in the nearest future this type of cooling is possible in the GTE for ground engines (Fig. 3.40).

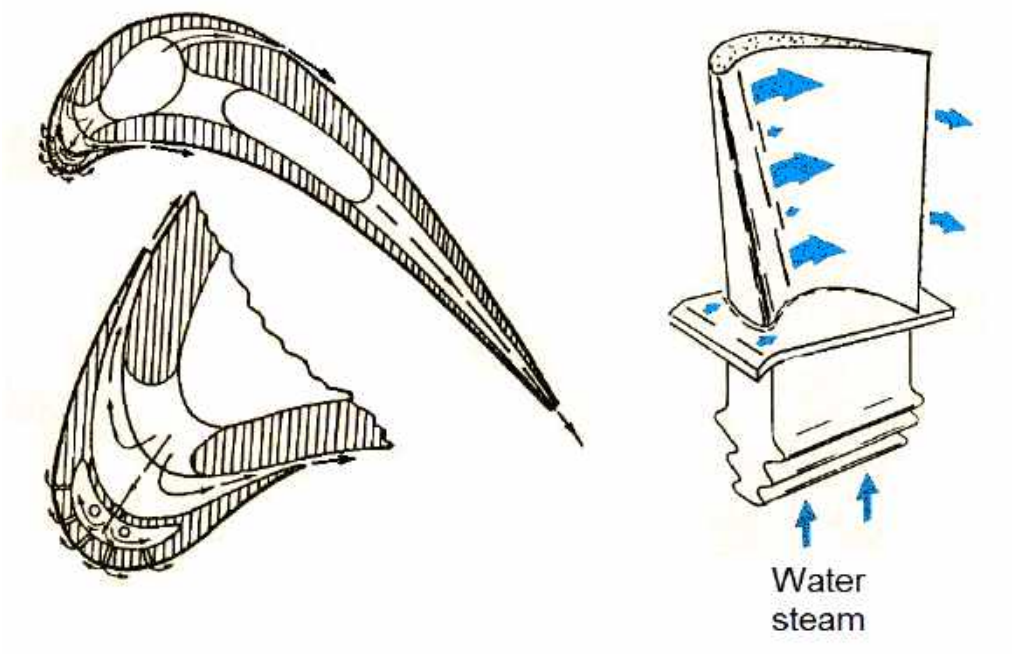


Fig. 3.40. Design of HPT nozzle vane and rotor blade with steam cooling

According to the load-carrying diagram, the cooled blades may be designed by using the following structural members:

– load-carrying wall;

– load-carrying rod.

In the first diagram, all loads are taken by a wall, which creates the blade airfoil portion and is manufactured as one piece with the root. If the blade is equipped with deflector, the latter is loaded by the centrifugal force and loads additionally the blade wall.

In the second diagram, the load-carrying rod is made as one piece with the root and takes all forces that affect the blade. The outer shell, which forms the blade airfoil portion, takes the gas forces and transmits them to the load-carrying rod.

Cooling of the nozzle vanes is the same as of the rotor blades.

To intensify the cooling efficiency, the ***water vapor*** may be used. Its pressure is chosen to be 0.020 to 0.035 MPa more than the pressure of the gas flow. The engine efficiency increases, because we not bleed the cooling air from the compressor.

3.8.2. Cooling of turbine discs and casings

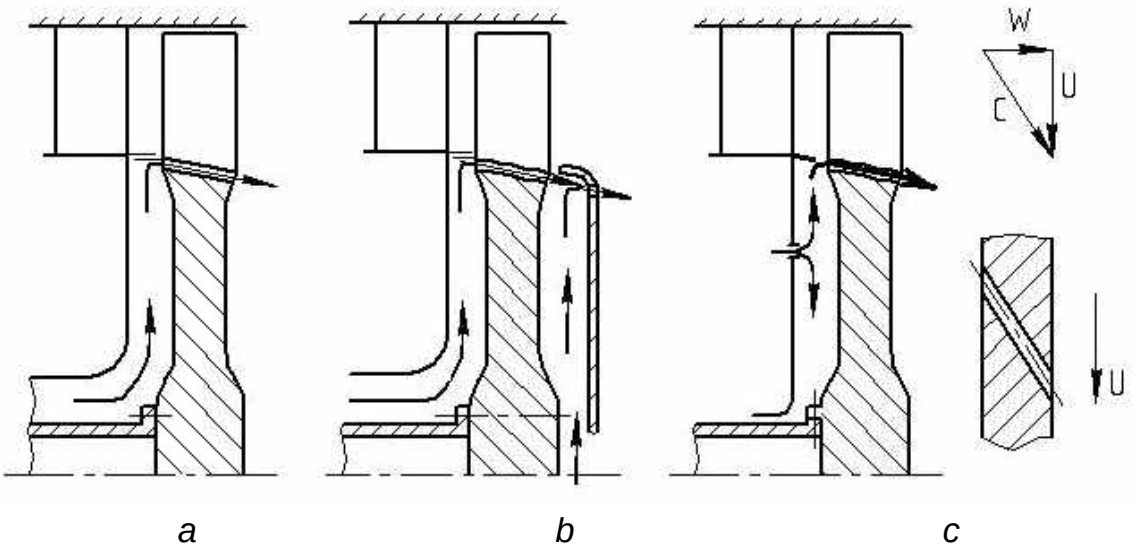
Turbine discs are cooled to decrease their temperature and to improve radial temperature uniformity at steady-state engine power ratings and,

especially, at transient power ratings (starting, acceleration and deceleration). The discs may be cooled by the following methods (Fig. 3.41):

– radial blowing of side surfaces;

– jet (transversal) blowing of side surfaces;

– disc rim blowing by air with blowing the air through the mounting clearances in the roots of the rotor blades.



a *b* *c*

Fig. 3.41. Methods of turbine discs cooling:
a – radial blowing; *b* – transversal blowing; *c* – blowing of a disc periphery with preliminary swirling of the air flow

In case of **radial blowing**, the air goes to the central portion of the disc and then it is radially directed by the deflector, or also flows radially without deflector along the side surfaces of the disc. In this case, the central less heated portion of the disc is cooled intensively. The cooling air is heated and goes to more heated peripheral area of the disc; therefore, this area is cooled worse.

Deflector decreases consumption of the cooling air, but the disc structural design is more complicated.

The **jet blowing** decreases temperature difference between the disc rim and hub if the cooling air is supplied closer to the rim.

The **disc rim blowing by the air and blowing air through the mounting clearances in the roots of the blades** decreases temperature difference comparing to two first cases, because in this case the most heated area of the disc is cooled in the first order. The cooling air is supplied to the disc rim through inclined holes (the D-36, and D-136) or vanes (the R-29F-300, and RB-211, Fig. 3.42). This is done for providing perpendicular flow of the air relatively to the disc, thus decreasing breaking losses. This design is named TOBI – Tangential on-Board Injection.

The air bleed for the disc cooling is approximately 0.5 to 0.8 % of the total air flow.

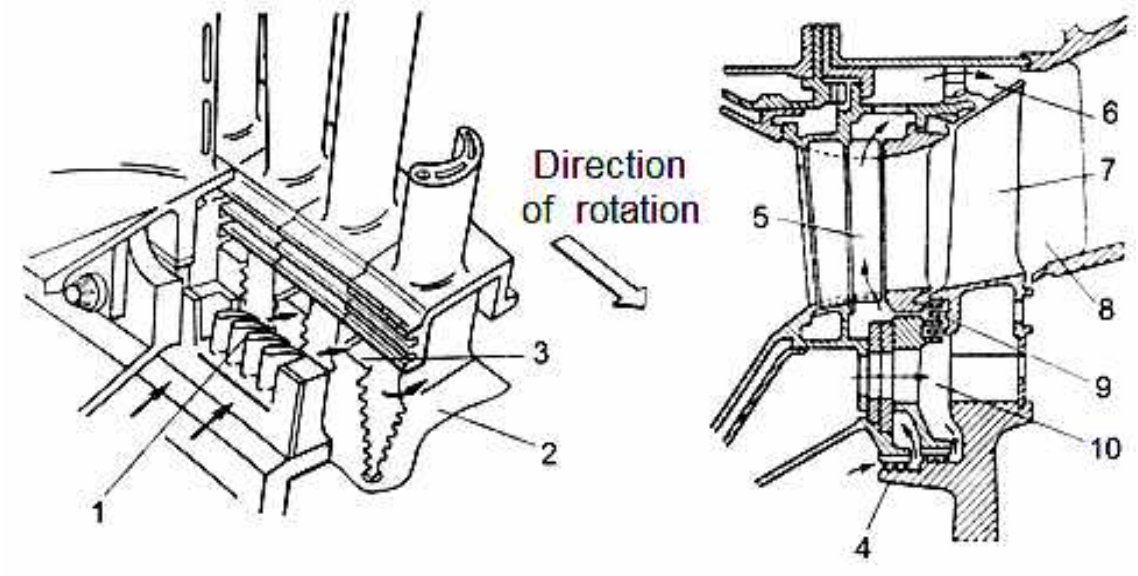


Fig. 3.42. Air supply to disc rim with preliminary swirling:
1 – swirling fixed vanes; 2 – turbine disc; 3 – receiving holes; 4, 9 – labyrinth seals;
5 – hollow nozzle vane; 6 – channel; 8, 10 – chambers; 7 – rotor blade

Turbine casings are cooled by blowing the air to the outer or inner surface through a system of small orifices.

Total air flow for turbine cooling is 5 to 12 % of the total air flow. This air bleed decreases specific thrust or power on 0.7 to 1.5 % and increases specific fuel consumption on 0.3 to 0.5 %. Therefore, some engines are equipped with control of the air bleeding for cooling (the R-29F-300, AL-21F turbojets, and AL-31F turbofan). The automatic control system decreases or switches off the cooling air flow at lower engine power ratings.

Fig. 3.43 shows the cooling air controlling mechanism of the AL-21F afterburning turbojet.

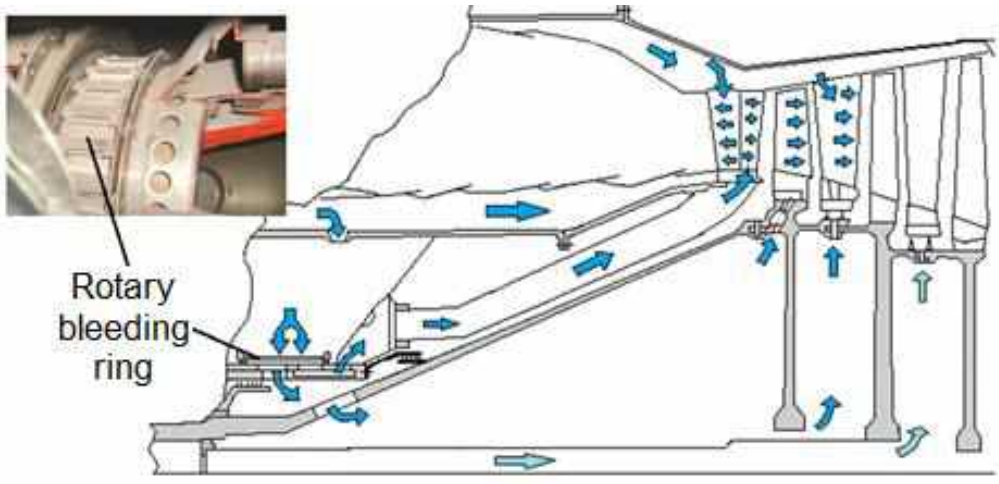


Fig. 3.43. Cooling air controlling mechanism

3.9. Structural materials for turbine parts

The most typical structural materials for turbine parts manufacturing are presented in Table 3.1.

Table 3.1

Structural materials for turbine parts

Rotor blades	ЭП220, ЭИ388, ЭИ437Б, ЭИ696, ЭИ827, ЭИ867, ЭИ867А, ЭИ893, ВЖЛ8, ВЖЛ12У, ЖС6К, ЖС6У, ЖС6Ф, ЖС30-ВИ, ВЖЛ14Н, ВКНА-4У, ВКНА-1В, ЖС26 ВКНС, ЖС36-ВНК, ЖС32ВНК МОНО, ВКЛС-20
Turbine discs	ЭИ388, ЭИ437Б, ЭИ481, ЭИ696М, ЭИ698, ЭИ736
Nozzle vanes	ЭИ388, ЭИ417, ЭИ435, ЭИ618, ЭИ652, ЭИ696, ЭИ696М, ЭИ893, ВЖЛ8, ЖС6К, ЖС6У, ЖС6Ф, ЖС-3

Turbine rotor blades operate at hard conditions. They take centrifugal and bending loads, vibrations, have non-uniform temperature field at average temperature 1000 to 1250 K. Therefore, the high-quality heat-resistant alloys are used for manufacture of the blades. Basis metal for these alloys is nickel. Non-cooled rotor blades for TIT = 1100 K may be made of alloy ЭИ-437Б or ЭИ-617; for TIT = 1150 K – alloy ЭИ-598; for TIT = 1180…1200 K – alloys ЭИ-822 and ЭИ-868. Cooled blades for TIT = 1250 K and higher are made of alloys ЖС6-КП (wrought alloy), ЖС-4 (cast alloy), ЖС6-КУ (enhanced); molybdenum or niobium-base alloys also may be used. Special alloys are designed for single-crystal blades, for example ВКНА-1В.

Fig. 3.44 demonstrates a working temperature of cast heat-resistant alloys that are used for manufacture of the turbine rotor blades and nozzle guide vanes.

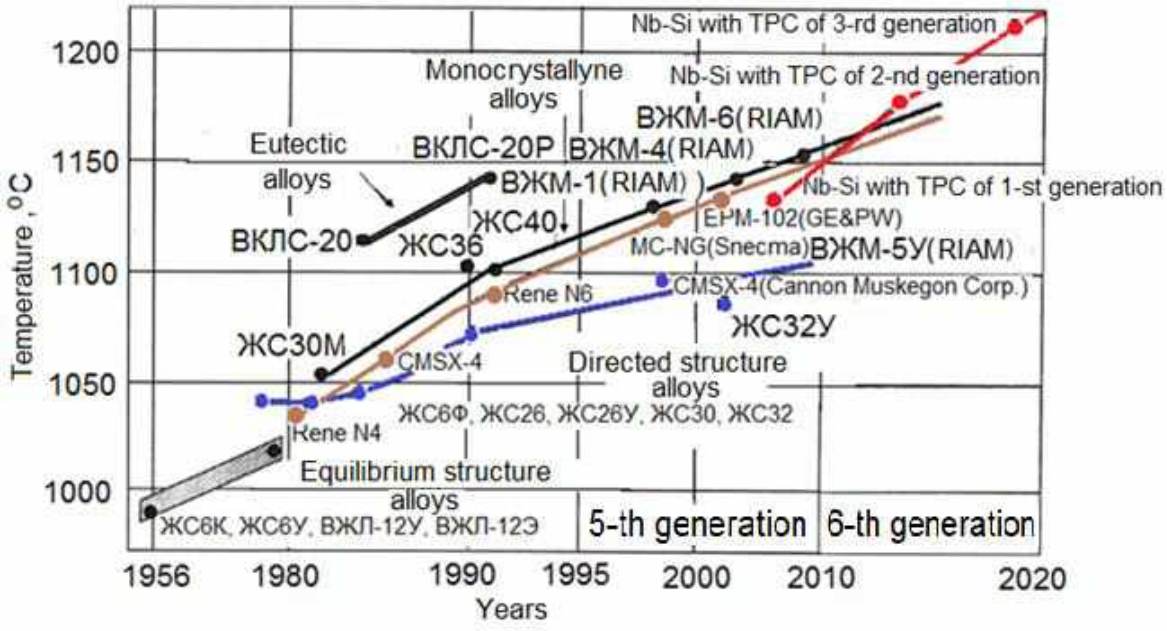


Fig. 3.44. Working temperature of cast heat-resistant alloys

Composite phase-reinforced materials for working temperature higher than 1500 K are designed. Matrix of these materials is nickel-base heat-resistant alloy or intermetallic nickel-base or titanium-base composition, for example Ni_3Al; reinforcing phase is made of niobium or tantalum carbides fiber.

In multistage turbines of the turboprop and turboshaft engines, the rotor blades of the last stages operate at low temperatures. Therefore, they may be made of heat-resistant steel ЭИ-696 or ЭИ-696М.

Nozzle vanes of first stages are made of cast alloys ЖС-3, АНВ-300ЖС6, and ЛК-4 (this alloy contains up to 60 % of cobalt); the vanes of the next stages are less loaded and made of alloys ЭИ-437А, ЭИ-437Б, ВЛ-745. The vanes of the last stages may be made of heat-resistant steel ЭИ-417 (Х23Н18).

The outer and inner casings of the nozzle box and casing parts are made of steel ЭИ-417 or ЭЯ1Т (Х18Н9Т). Bolts and nuts that attach the nozzle guide vanes are made of steel ЭИ388; the thread is copper plated to prevent sticking.

The turbine discs, which operate at temperature less than 900 К, are made of steel ЭИ-481, at higher temperature – of nickel-chromium alloy ЭИ-437Б.

The turbine shafts are made of steel 18ХНВА, 40ХНМА, ЭИ-736 (13Х14НВФРА); for temperature up to 780…800 К – of steel ЭИ-415.

3.10. Check questions

1. Functions of the GTE turbines and requirements to their design.
2. Major structural members of turbine.
3. Classification of the GTE turbines.
4. Structural arrangements of the turbines.
5. Design and main structural members of the turbine rotor blade.
6. Advantages of the dual rotor blades.
7. Requirements to the root of the turbine rotor blade.
8. Kinds of the blade roots, their advantages and disadvantages. Retaining of the blades against axial displacement.
9. What loads affect the turbine blades?
10. Advantages and disadvantages of the film cooling.
11. What loads affect the turbine rotor?
12. Design of the turbine disc.
13. Design of the turbine shaft. What loads affect the turbine shaft?
14. How are the turbine discs interconnected and conected to the shaft?

15. What loads affect the turbine stator?

16. Specifics of designing and manufacturing the nozzle guide vanes.

17. Why the nozzle guide vanes are not included into the load-carrying system of the turbine casing? How are they attached to the casing?

18. Casings of the turbines: requirements and main functions. Casing of the nozzle guide vanes, bearing supports housing of the turbine rotor, turbine shaft casing.

19. Methods of joining of the main parts of the turbine casings.

20. Radial and axial clearances in the turbine, their influence on the turbine performances. Methods of decreasing the radial clearances. Active and passive clearance control.

21. The turbine labyrinth sealing: functions, design and operation.

22. Why the cooling air before entering the cooled rotor blades is preliminary swirled? Which structural members provide this?

23. What factors are to be taken into account when choosing a place for bleeding of the cooling air from the compressor?

24. Requirements to materials used for blades, discs and other structural members of the turbine rotors. Give examples.

25. Requirements to materials used for the structural members of the turbine stator. Give examples.

4. DESIGN OF MAIN COMBUSTION CHAMBERS

4.1. Particular features of the combustion process in gas turbine engines

Combustion chamber (combustor) is the engine component part that is designed to supply heat to the working fluid by converting chemical energy of the fuel into the heat energy. Parameters of the combustion chamber significantly influence engine fuel economy, reliability and environmental properties.

Design of the combustion chamber shall meet a lot of requirements. For better understanding these requirements and design of the combustion chamber, we must familiarize with the bases of a combustion process in the gas turbine engines.

4.1.1. Requirements to the fuel

The fuel for the aero engine must meet the following requirements:

- low cost;
- high energy capacity;
- high density;
- stability;
- the optimum vaporizing ability.

In the nearest future, the least cost will have a fuel made of the natural petrol.

The energetic capacity of the fuel is expressed as the **least heat capacity** H_u. This is the amount of heat that is obtained at complete combustion of 1 kg of the fuel and further cooling of the combustion products to the initial temperature of the fuel and the air 293 K, not taking into account a heat of the water vapour condensation.

To meet the requirement of high density, the fuel must be liquid. It also helps for the fuel supplying, which in this case may be provided by the fuel hydraulic pumps.

High stability of the fuel allows to store it for a long time and to transport it easily.

The vaporizing ability must be not too high and not too low. The lower level of the vaporizing ability is limited by conditions of the fuel vaporization after spraying into the combustion chamber. Before ignition, the fuel must be sprayed, vaporized and mixed with the air within very short period of time.

Thus, the vaporizing ability must be as high as possible. The upper limit of the vaporizing ability is limited by conditions in the aircraft fuel tanks that are usually communicating with the atmosphere. Therefore, at high vaporizing ability, the liquid fuel trends to vaporize at increasing of flight altitude. The vaporizing will be prevented if it is possible to close and pressurize the fuel tanks. But in this case the tanks will be thick-walled and too heavy. Hence, the vaporizing ability must be not very high.

The above-mentioned requirements are satisfied in the best way by the liquid hydrocarbon fuels received by refining of the mineral earth oil. The best fuel for the gas turbine engines is kerosene. Its density is approximately 800 kg/m^3. Depending on composition of the raw mineral earth oil, the composition of the kerosene and its density, heat capacity and other properties may vary. It will influence the engine fuel performances (for example, the specific fuel consumption).

Therefore, for presentation of the thermodynamic analysis and engine performances, the Standard Hydrocarbon Fuel is taken into consideration. Mass of this fuel contains 85 % of the carbon and 15 % of the hydrogen and has the following properties: H_u = 42900 kJ/kg; L_0 = 14.8 (what is L_0 ref. below).

4.1.2. Stoichiometric, rich and lean mixture

One of the major parameters of the fuel is its **stoichiometric coefficient** L_0. It is the amount of the air, which is required for complete combustion of 1 kg of the fuel.

Before combustion, the fuel must be mixed with the air. Composition of the mixture is characterized by the **excess air/fuel ratio** α. It is a ratio of the actual air flow G_{air}, which really passes through the combustion chamber, to stoichiometric air flow $G_{air\ st}$, which is required for complete combustion of the consumed fuel. The stoichiometric fuel flow is related with the fuel flow G_f as $G_{air\ st} = G_f \cdot L_0$. So $\alpha = \dfrac{G_{air}}{G_f L_0}$, where the fuel flow is considered in kg/s.

At $\alpha = 1$, the **mixture is stoichiometric**: all of fuel is burnt and all of oxygen is used for the burning.

At $\alpha < 1$, the air consumption is less than required to combust all of the fuel. The mixture is named as a **rich mixture**. Due to insufficiency of oxygen, some part of the fuel is not burnt and is discharged.

At $\alpha > 1$, the air consumption is more than required to combust all of the fuel. The mixture is named as a **lean mixture**. All of fuel is burnt, and some amount of oxygen does not take part in combustion and is left in the gas composition.

4.1.3. Temperature of combustion

Combustion is the exothermal chemical reaction. It means that the combustion temperature depends on the excess air/fuel ratio α. By the theory, it is the maximum value for the stoichiometric mixture, which decreases at $\alpha < 1$ or $\alpha > 1$ when the combustion products are mixed with cool fuel when the mixture is rich or with cool air when the mixture is lean.

The elementary estimation of the combustion temperature may be done using the heat balance equation:

$$Q_{gas} = Q_{air} + Q_f + Q_{comb},$$

where Q_{gas} is heat energy of the gas after combustion;

Q_{air} is heat energy of the air that enters the combustion chamber;

Q_f is heat energy of the fuel that enters the combustion chamber (in the first approximation, we can neglect it and set $Q_f = 0$);

Q_{comb} is heat that is generated after combustion.

After relating the heat energies with the temperatures and consumptions, we get

$$C_{p\,gas}(G_{air} + G_f)T_{gas} = C_{p\,air}G_{air}T_{air} + G_{f\,comb}H_u\eta_{comb},$$

where η_{comb} is combustion efficiency;

C_p is specific heat capacity at constant pressure;

$G_{f\,comb}$ is flow of the fuel that is combusted.

In case of the lean mixture, $G_{f\,comb} = G_f$. Thus, neglecting the difference in heat capacities and setting $C_{p\,gas} = C_{p\,air} = C_p$ we get (taking into account that $L_0 \approx 15$ and $\alpha > 1$) the following:

$$T_{gas} = \frac{G_{air}}{G_{air}+G_f}T_{air} + \frac{G_f}{G_{air}+G_f}\frac{H_u\eta_{comb}}{C_p} = \frac{\alpha L_0}{1+\alpha L_0}\left(T_{air} + \frac{H_u\eta_{comb}}{\alpha L_0 C_p}\right) \approx T_{air} + \frac{H_u\eta_{comb}}{\alpha L_0 C_p}.$$

In case the mixture is rich, $G_{f\,comb} = \frac{G_{air}}{L_0}$ and

$$T_{gas} = \frac{G_{air}}{G_{air}+G_f}T_{air} + \frac{\frac{G_{air}}{L_0}}{G_{air}+G_f}\frac{H_u\eta_{comb}}{C_p} = \frac{\alpha L_0}{1+\alpha L_0}\left(T_{air} + \frac{H_u\eta_{comb}}{\alpha L_0 C_p}\right).$$

Fig. 4.1 shows the relation between the air/fuel ratio and the temperature of combustion at compressor discharge temperature of 700 K.

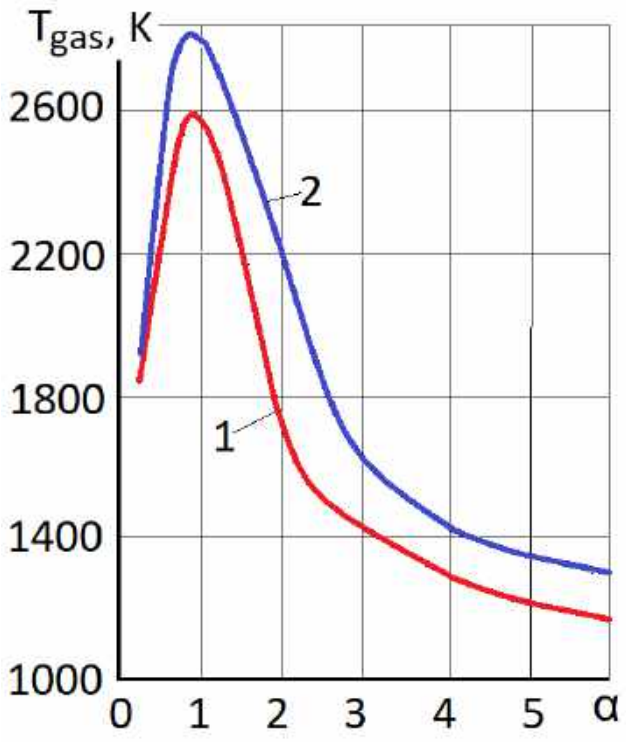


Fig. 4.1. Gas temperature vs air/fuel ratio:
1 – T_{air} = 700 K; 2 – T_{air} = 900 K

As the diagrams shows, the temperature reaches the maximum value not at stoichiometric conditions but when α is some less than 1.

4.1.4. Physical aspects of the combustion in flow

Combustion in the gas turbine engine is significantly different from that in the piston engine or in the industrial furnace. The main factor that determines this difference is that the fuel in the gas turbine engine is combusted in a very intensive flow. Remember that the air velocity at the compressor outlet is approximately 120 m/s. As different from the piston engine, the volume of the combustion chamber is not closed during combustion, the air flows continuously and the fuel is supplied continuously.

Therefore, for better understanding of the combustion chamber we must understand physical aspects of the burning in flow.

Before burning, complicated high-velocity processes are running in the combustion chamber (Fig. 4.2): fuel spraying, dispersion and vaporizing of droplets that are streamlined by the fuel, mixing of the fuel vapor with the air, ignition and combustion.

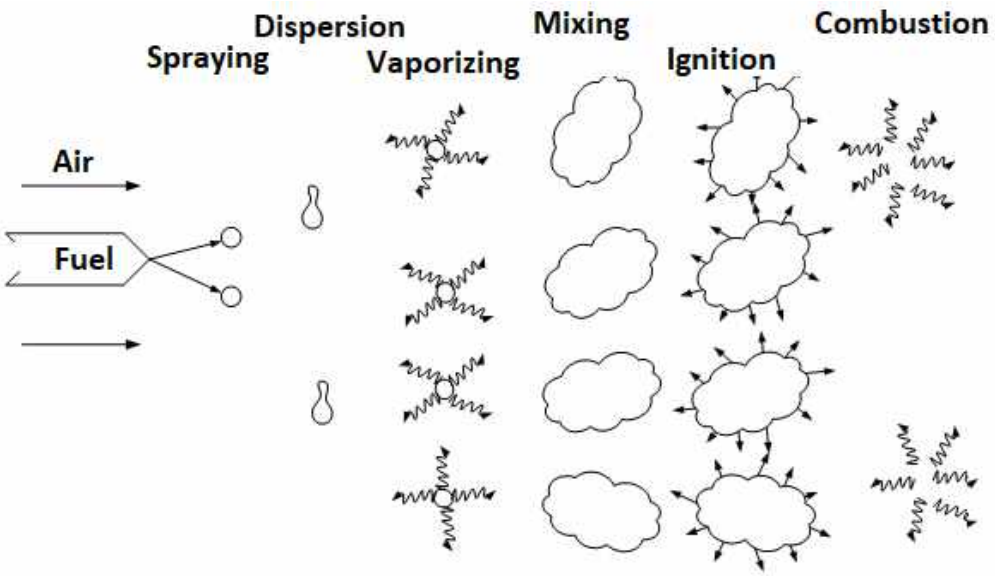


Fig. 4.2. Diagram of the processes in combustion chamber

A series of physical and chemical processes takes place during combustion. The combustion is an exothermal chemical reaction. It was proven that the combustion is a chain reaction, during which a lot of intermediate chemical compositions originate.

Progress of this reaction depends on properties of the fuel/air mixture and its flow. We will use the following *classification of the combustible mixtures*:

– by the values of local air/fuel ratio we will differ uniform and non-uniform mixtures;

– by the presence of burning droplets we will differ homogenous (that not contain the burning droplets) and heterogenous.

In laboratory conditions, the uniform homogenous mixtures are studied. In real engines, non-uniform heterogeneous mixtures are burnt.

In its turn, the flow in the combustion chamber may be laminar or turbulent. This also influences conditions of the combustion.

Burning of uniform homogenous mixture in a laminar flow

If to ignite an unmovable mixture in a point, then the flame front will propagate as a sphere of thickness δ~1 mm with velocity u_{fl} = 0.5 to 2.0 m/s. Hence, the combustion is fast and its durability is δ/u_{fl} = 0.001/1 s = 10^{-3} s.

The hydrocarbon fuel that we use is not self-inflammable. It means that the mixture needs in external energy to initialize burning. This energy depends on initial temperature of the mixture.

Analysis of these information results in the following conclusions:

1. Velocity of the flame propagation is approximately 100 times less than the velocity of the air flow at the compressor outlet (this velocity is approximately 120 m/s).

2. Fig. 4.1 shows that the margins of the component's concentration exist that separate the concentration range, out of which the temperature of combustion is too low and not enough to ignite a fresh mixture (in the considered example, $0.6 < \alpha_z < 1.7$).

3. If the mixture moves with velocity $c > u_{fl}$, then it takes the flame front away; therefore, for the fresh mixture ignition the external stationary source of energy is required.

Fig. 4.3 shows a disposition of the flame front when the external source of energy is used.

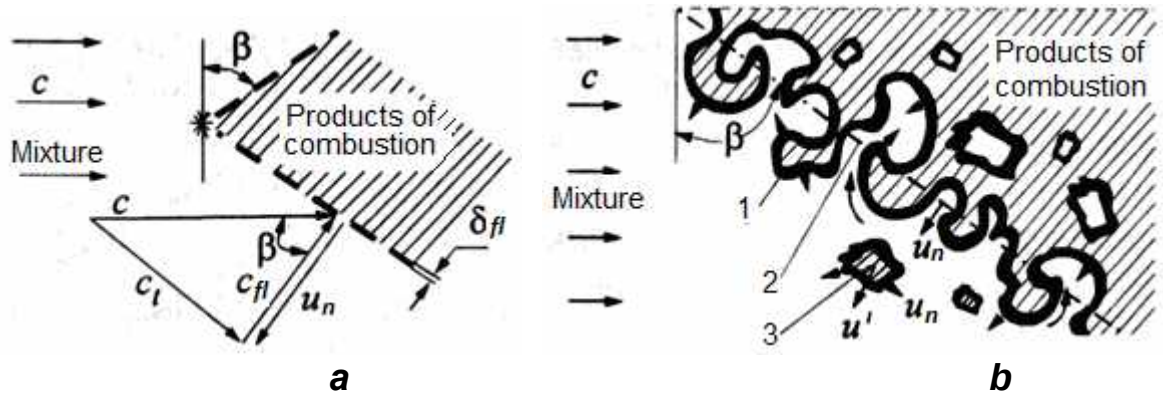


Fig. 4.3. Disposition of the flame front (_ _ _ _) in a laminar (*a*) and turbulent (*b*) flows at $c > u_{fl}$:
∗ – point source of ignition

The angle β of the flame front inclination is related with the values of flame and flow velocities: $u_{fl} = c\cos\beta$. This relation is known as the Mikhelson's law and is widely used for experimental determining of the flame propagation velocity.

Burning of heterogenous non-uniform mixture in a turbulent flow

In this case, the combustion process is more complicated. The flow is characterized not only by the velocity c but also by the turbulence scale l_T (characteristic dimensions of turbulent vortexes), by a mean square velocity of turbulent pulsations u' or by a turbulence intensity $\varepsilon = u'/c$. The turbulent pulsations strongly curve the flame front and make it discontinuous.

The flow in real combustion chambers is highly turbulent and non-uniform: $u' >> u_{fl}$, $l_T > \delta$, $\alpha_z \neq \alpha_{mean}$.

Therefore, the flame propagation velocity in the turbulent flow is significantly more than in a laminar flow: u_T = 15 to 30 m/s. This may be explained as the area of the flame front in this flow is approximately 10 times higher.

Types and modes of burning

The following ***types of burning*** are differed:

– burning of fuel vapor around separate droplets;

– burning of fuel vapor around groups of closely disposed droplets;

– burning of fuel vapor in a space between the droplets.

Combustion chambers of the gas turbine engines have all of these types of burning.

Numerical analysis of burning is based on modelling. The model of burning significantly depends on a choice of physical ***mechanism (mode) of burning***. There are differed the diffusion and the kinetic modes of burning.

Diffusion mode of burning is implemented at a low velocity of a flow, and the flame propagation velocity is determined by a motion of the fuel vapor to the flame.

Kinetic mode of burning is implemented at a high velocity of vaporization and mixing and low velocity of chemical reactions; therefore, namely velocity of chemical reactions determines the flame propagation velocity.

Concentration margins of combustion

Stable combustion of heterogeneous mixture is realized in a range $0.4 < \alpha_z < 2.2$, which depends on the temperature, pressure and velocity of the flow at the inlet to the combustion zone.

4.2. Combustion chambers purpose. Operation conditions and requirements to combustion chambers

The combustion chamber operates in complicated conditions:

– high gas temperature (temperature in burning zone reaches 2300 to 2600 K);

– high temperature of combustion chamber design structures (casings – up to 600 to 650 K, flame tubes – up to 1000 to 1200 K) at significant non-uniformity of temperature field (the gas flow temperature non-uniformity reaches 75 to 100 K on a circle and 40 to 70 K on a radius);

– combustion chamber design structures, especially flame tubes and mixers, are streamlined by the chemically active gases having increased pressure (up to 2.5 to 4.0 MPa) and essential velocity.

Combustion chamber design structures are non-uniformly heated, and the gas flow is divided into separate streams by the vortex generators, fuel nozzles and mixers. This cause their warping and burning through, which results in further buckling of the gas flow, local overheating and destruction of the design structure.

There is possible oscillatory combustion with periodic pressure variation with amplitude of 0.05 to 0.10 MPa and frequency of 1000 to 5000 Hz. It may destroy not only the combustion chamber component parts, but also aircraft design structures, affecting adversely normal operation of the engine and aircraft systems.

Processes in the combustion chamber are difficult for theoretical analysis; therefore, combustion chamber design needs a lot of experiments with further continuous and labor-consuming development using special test cells.

Requirements to combustion chambers

Combustion chamber is one of the engine component parts. Therefore, it must satisfy the general engineering requirements to the engine. They are low weight, low cost, reliability, manufacturability, repairability, maintainability, etc.

In addition to the general requirements, the combustion chambers must satisfy some special requirements:

– stable combustion at all power ratings and flight conditions;

– high combustion efficiency (modern combustion chambers have η_{CC} = 0.98 to 0.995) at the minimum heating of the engine and aircraft design structures and the minimum heat losses into the atmosphere;

– low hydraulic losses (pressure loss factor of up-to-date combustion chambers is σ_{CC} = 0.95…0.97);

– short flame torch to decrease axial dimensions of the combustion chamber and to prevent getting of flame onto the nozzle vanes and rotor blades;

– uniform distribution of velocity, temperature and velocity at combustion chamber outlet because non-uniform distribution of temperature may cause local overheating and burning of the vanes and blades, while the non-uniform distribution of pressure and velocity may cause vibration and fatigue failure of the rotor blades;

– reliable initiation of operation (inflaming) of the combustion chamber at any operating conditions; the on-the-ground starting must be ensured within a temperature range of minus 50 ºC to plus 50 ºC and within the altitude range of 0 to 4.5 km; the in-flight restart for the civil aircraft must be ensured at altitude up to 9 km;

– environmental purity.

Combustion chamber perfection by the overall dimensions is assessed by its heat intensity, which means the amount of heat generated by combustion of fuel in 1 m^3 of volume per one hour, related to one unit of air pressure in the combustion chamber:

$$Q_{CC} = \frac{G_f H_u \eta_{comb}}{V_{CC} p_{CC}},$$

where G_f is hour fuel flow;

H_u is fuel heat capacity (for kerosene, H_u = 43000 J/kg);

V_{CC} is volume of the combustion chamber;

p_{CC} is pressure in the combustion chamber.

The heat intensity of modern combustion chambers is expressed as:

$$Q_{CC} = (3.5...6.5) \cdot 10^6 \frac{J}{m^3 \cdot hour \cdot Pa}.$$

4.3. Design diagrams of the main combustion chambers and problems that are to be solved when designing combustion chamber

The main combustion chambers are classified by some features:

– ***by direction of flow*** – direct-flow (the D-36, AM-3, R-11F-300, etc.), reverse-flow (the GTD-350) and mixed-flow (loop – the AI-9, AI-450 and semi-loop – the GTD-3F);

– ***by method of fuel supplying*** into a combustion zone: vaporizing combustors (fuel is supplied in vapor phase – the TA-6 auxiliary power unit, the T-700-GE-700 turboshaft engine of General Electric, USA) and spray-jet combustors (fuel is supplied in liquid phase – the AL-7F, AI-25, etc.);

– ***by design and arrangement in engine*** (can or tubular – the VK-1, RD-45, RD-500, Walter M-701, tube-annular (cannular) – the R-11F-300, AM-3, D-30, AL-21F and annular – the AL-7F, AI-25, D-36, RD-33, and AL-31).

Direct-flow axial combustors are widespread as they have minimum hydraulic losses. Their diameter usually does not exceed compressor and turbine diameters.

Disadvantage of these combustors is increased axial dimensions that increases the engine length. Distance between the rotor supports is also increased; therefore, the engine design becomes complicated and heavy.

It is possible to decrease the axial dimensions by using **loop** or **semi-loop** chambers, but they have increased hydraulic losses comparing to the axial combustors.

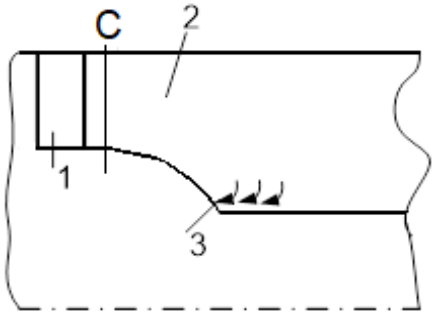


Fig. 4.4. Diagram of combustion chamber diffuser:
1 — compressor straightening vanes; 2 — non-stall diffuser; 3 — stall diffuser

Reverse-flow combustors have less length; therefore, a distance between the supports is decreased. They are used in the low-power GTE or auxiliary power units; thus, they are used in cases when the weight and dimensions decreasing is the most significant requirement, even if it results in increasing of the hydraulic losses.

Other features of the combustion chambers classification are considered below.

The main problems that are to be solved when designing combustion chamber are directly related to the above-considered particular features of the combustion in flow:

- decreasing of velocity at the inlet to the combustion zone;
- ensuring stable combustion;
- stabilizing combustion zone;
- supplying fuel;
- cooling combustion products;
- ensuring operability of design structures;
- ignition (initiation of combustion);
- ensuring environmental indices.

Let's consider methods of designing that solve these problems.

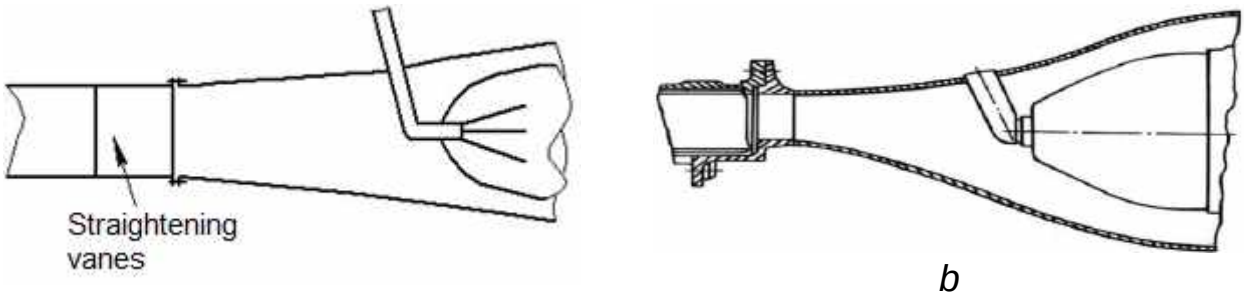
4.4. Decreasing velocity at the inlet to the combustion zone in relation to the compressor outlet flow velocity. Diffuser

The compressor outlet air flow velocity is approximately $c_C = 120$ to 150 m/s, and the combustion velocity (velocity of a flame propagation) is $u_T = 15$ to 30 m/s. So, the flow velocity must be decreased significantly. This task is solved by the ***diffuser*** (Fig. 4.4), which is a divergent channel that is placed directly after the compressor straightening vanes.

The **diffuser** is mounted at the inlet to the combustion chamber; it decreases the air flow velocity from (120 to 180) m/s to (30 to 50) m/s to provide stable combustion. The diffusers provide main part of the hydraulic losses in the combustion chambers, so they are carefully profiled.

There are differed some types of the diffusers: non-stall, with flows separation, and with predetermined stall.

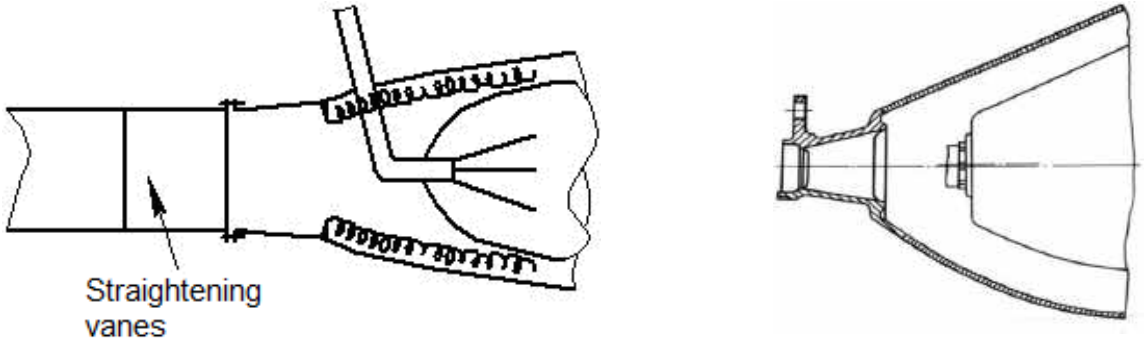
The non-stall diffuser (Fig. 4.5) is a smooth channel with angle of backing off 18º to 25º; it provides the air flow without stall and low hydraulic losses. Otherwise, it has high length that increases a distance between the supports and engine length.



a *b*

Fig. 4.5. Non-stall diffuser:
a – chart; *b* – design

Length of the diffuser becomes less if it is finished by a rapid increasing of the area (Fig. 4.6) with predetermined stall (the AL-21, TV3-117, and R-29). The place of the rapid increasing of the area may be equipped with special collars, which provoke the stall.



a *b*

Fig. 4.6. Stall diffuser:
a – chart; *b* – design

The non-stall diffuser may have significant angle of backing off (up to 35º to 40^0). The airflow in this diffuser is divided into two or three channels by bulkheads; each channel has small angle of backing off (Fig. 4.7).

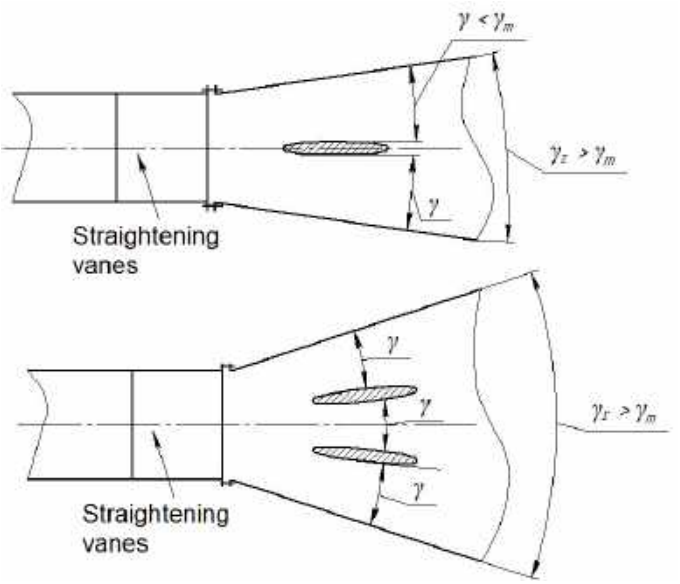


Fig. 4.7. Multi-channel diffuser with bulkheads

4.5. Ensuring stable combustion. Flame tube

As it was shown above, the margin of a stable combustion exists and corresponds approximately to a range of $0.6 < \alpha < 1.7$. Approximately, we can say that the combustion is stable when the air/fuel ratio is close to one. But this ratio cannot be close to one at the combustion chamber discharge, as in this case (see Fig. 4.1) the temperature is very high (higher than 2500 K). The turbine will be operable if this temperature is decreased, then at steady-state power ratings α = 3 to 5, and at acceleration and deceleration α = 2 to 12.

Stable operation of the combustion chamber under these conditions is impossible. Therefore, ***to ensure stable combustion, the air flow is divided into two parts*:**

– *the primary air* is supplied to a burning zone and takes part in a fuel inflammation;

– *the secondary air* bypasses the burning zone and is supplied to the combustion products at the turbine inlet and decreases their temperature.

The burning zone is separated from the secondary air by the **flame tubes**.

4.5.1. Structural arrangements of flame tubes

The design arrangement of the flame tubes is a primary structural member of classification of the combustion chambers and gives a name to the combustion chamber.

Depending on arrangement, there are differed individual (tube or can), tub-annular (can-annular) and annular combustion chambers (Fig. 4.8).

Can (individual) combustor is a separate component that consist of the flame tube placed inside the casing. The number of such chambers in the engine is 6 to 22. The chambers are arranged uniformly on circle. Separate chambers are connected by the flame propagation tubes to transmit the flame to the chambers from the igniters or from adjacent operating chambers. These combustors are well combined with the centrifugal compressor. Volume of one chamber is small; this simplifies combustor's development. Individual chambers improve the engine vitality and are handy in maintenance and repair.

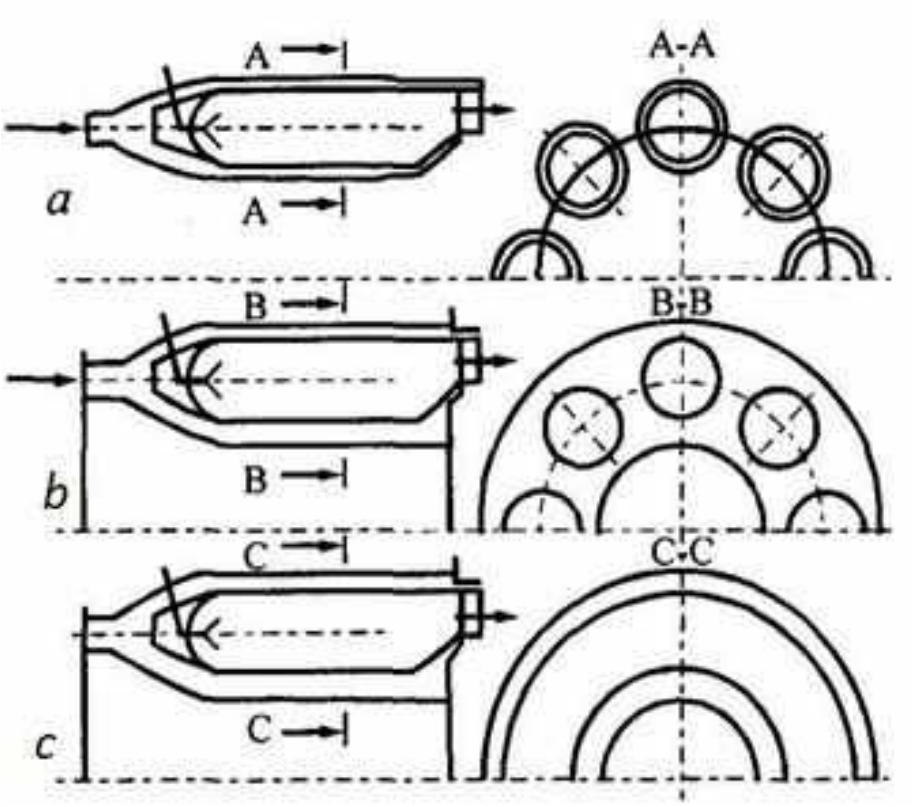


Fig. 4.8. Design schemes of combustion chambers:
a – can; *b* – can-annular; *c* – annular

Disadvantages of can combustors are heavy weight (up to 12 to 15 % of the engine weight), necessity of gas collector, large number of joints that need sealing, increased hydraulic resistance. Besides, the can combustors are not included into the power structure of the engine stator; therefore, the stator needs in additional load-carrying structures.

Annular combustor consists of a single flame tube of circular cross-section, the outer and inner casings, which usually are load-carrying design structures of the engine stator. These combustors are low-dimensions, because a volume of the combustion chamber is used the most rationally. Their weight is 6 to 8 % of the engine total weight.

The temperature field, velocity and gas pressure at the outlet of the annular combustor is most uniform comparing to other types of the combustors. This combustor has low hydraulic losses; problem of its sealing is simpler.

Disadvantages of the annular combustors:

– difficult development on stable combustion, especially at large dimensions of the flame tubes and high air consumption at high pressure;

– complicated maintenance inspection and repairing of the flame tube in service.

Tube-annular combustors combine some advantages of the can and annular combustors. They consist of separate flame tubes (from 9 to 14), located in the annular cavity that is created by the outer and inner casings of the combustion chamber; these casings are load-carrying design structures of the engine stator. Diameter of the outer casing usually does not exceeds diameters of the compressor and turbine. The flame tubes are interconnected by the flame propagation tubes.

These combustors have intermediate performances between the can and annular combustors by the weight, simplicity of repair and maintenance and development.

At the present time, the annular combustion chambers are the most widespread, because they have the minimum weight, more uniform temperature distribution and more reliable fuel inflammation.

4.5.2. Relation between secondary and primary flows in the combustion chamber

As it was mentioned above, combustion chambers can be classified taking into account relation between the directions of the secondary air flow around the flame tube and the primary airflow and the burnt gas flow inside the flame tube. By this feature, there are differed direct-flow, reverse-flow and mixed-flow (loop-type and semi-loop-type) combustion chambers.

In the ***direct-flow combustion chamber*** (Fig. 4.9), the air and the gas are flowing in parallel. These combustion chambers are the most widespread as they have the minimum losses. Their diametric dimensions usually does not exceed the dimensions of the compressor and turbine.

The disadvantage of this structure is increased axial dimensions that increases a total length of the engine, and a distance between the rotor supports. Hence, the engine design is complicated and its weight is increased.

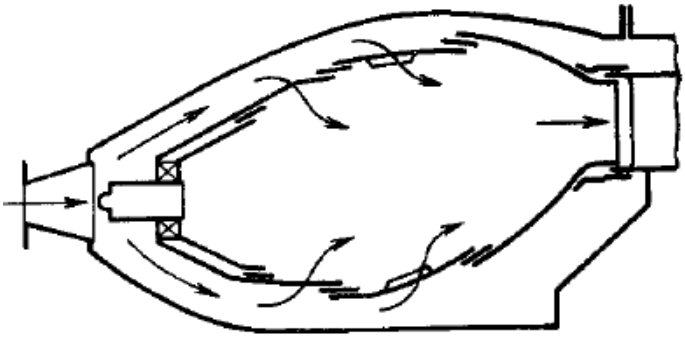


Fig. 4.9. Structure of the direct-flow combustion chamber

In ***loop*** (Fig. 4.10) and ***semi-loop*** (Fig. 4.11) ***combustion chambers***, the entire primary air or significand amount of it turns through 180° before entering the flame tube and burning zone. Due to this arrangement, the axial dimensions is decreased significantly comparing to a direct-flow arrangement. However, hydraulic losses grow.

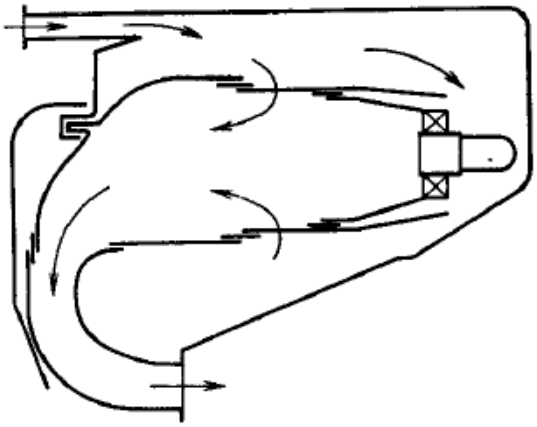


Fig. 4.10. Loop-type combustion chamber

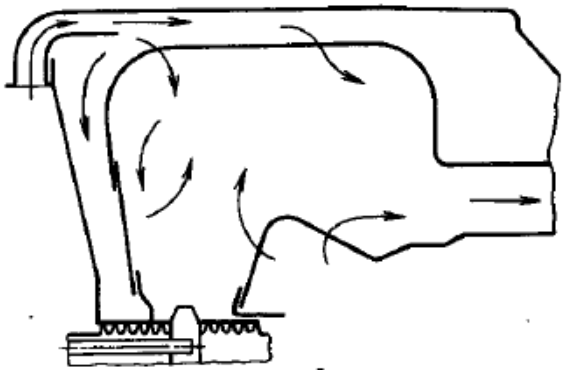


Fig. 4.11. Semi-loop-type combustion chamber

Reverse flow combustion chambers (Fig. 4.12) decrease a distance between the supports significantly. They are used in low-dimensions GTE and auxiliary power units, as they are expedient when the primary is requirement of

the engine low weight and dimensions, even if this causes increased losses in the combustion chamber.

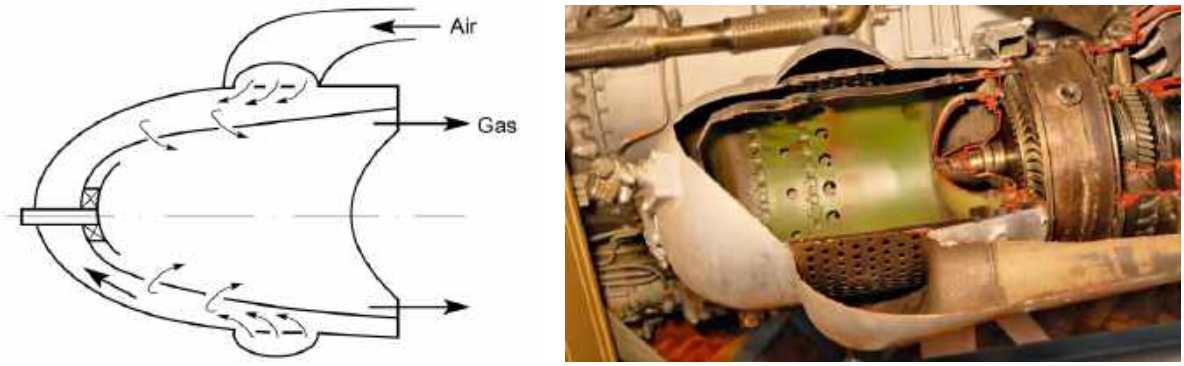


Fig. 4.12. Reverse flow combustion chamber

4.6. Stabilizing combustion zone. Combustor dome

Velocity of the flame propagation is low comparing to velocity of flow, even downstream of the diffuser. Stable combustion under these conditions is impossible, and complete combustion is possible in a very long chamber, which length is more that the length of the other part of the engine. We will overcome this problem and shorten the combustion zone, if increase a residence time of the fuel (air-fuel mixture) in the flame tube and if stabilize a burning zone so that it will “stand still” and ignite a fresh air-fuel mixture without the external source of energy for ignition.

This problem is solved due to a combustor dome (flameholder) (Fig. 4.13).

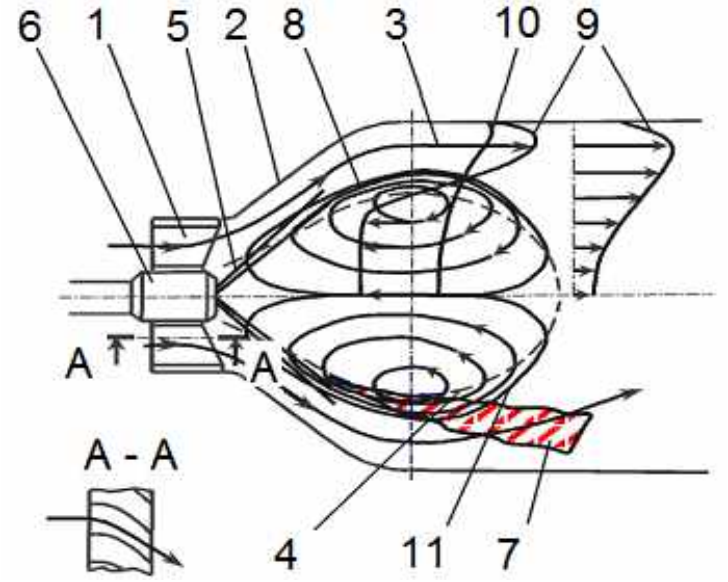
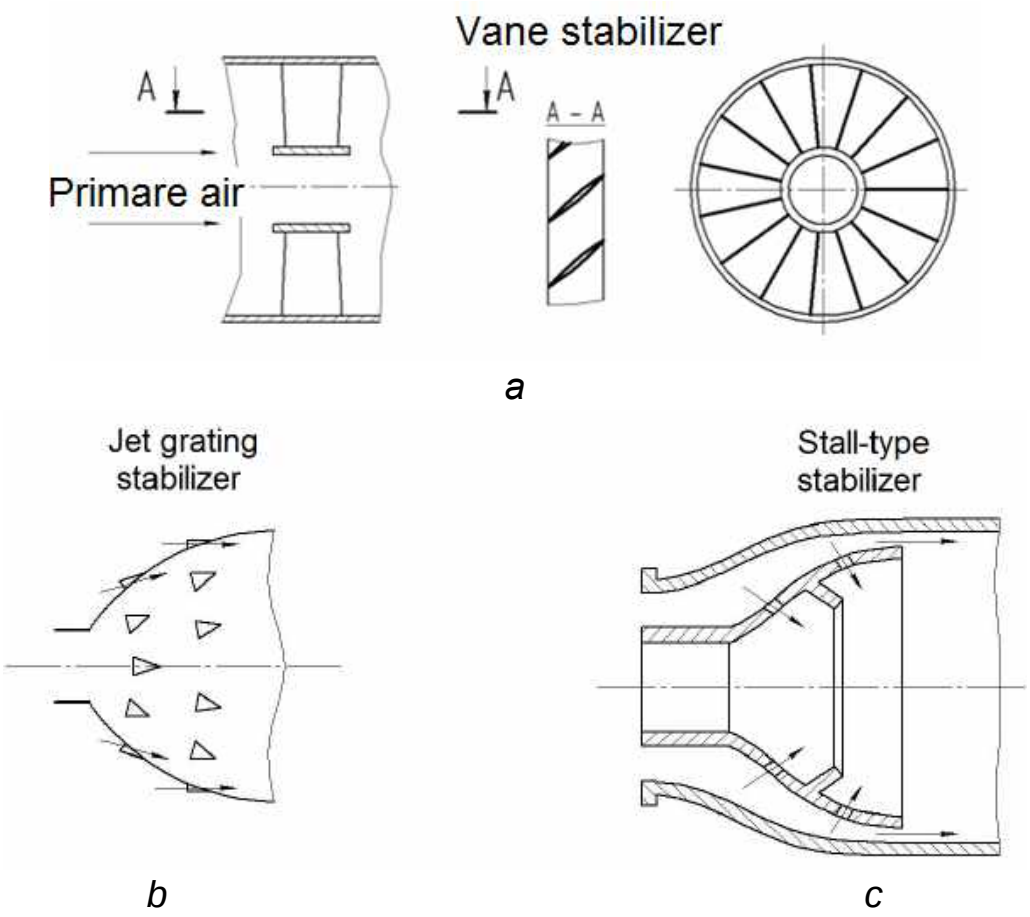


Fig. 4.13. Flow structure and flame stabilization in a flameholder:
1 – vane swirler; 2 – transition cone; 3 – conical air jet; 4 – zone of reverse flows;
5 – fuel cone; 6 – fuel nozzle; 7 – flame stabilization zone; 8 – reverse flows margin;
9 – diagram of axial velocity; 10 – pressure diagram; 11 – streamlines

The air enters the flame tube through the flameholder, which is equipped with the swirlers. Due to action of the centrifugal forces, a vacuum originates in the center of a burning zone, which stimulates reverse flows (Ref. diagram of pressure in Fig. 4.13). These flows return a flame towards the fresh mixture, thus increasing the residence time multiply.

The stabilizing effect is sometimes improved by using jet stabilizers (radial air jets that enter the burning zone through the walls of the flame tube in radial direction).

Vane (the R11F-300), jet (slot and grating) (the D-20P, D-30P) and stall (the AI-20, AI-25) stabilizers and their combinations are used (Fig. 4.14).



a

b *c*

Fig. 4.14. Stabilizers of different types:
a – vane stabilizer; *b* – jet-grating stabilizer; *c* – stall-type stabilizer

4.7. Fuel supplying. Fuel nozzles

Besides the flame stabilizing, stable and efficient combustion is ensured by thorough preparing of the air-fuel mixture: fast dispersion of the fuel droplets, their vaporizing, mixing with the air and heating to ignition temperature.

The fuel is supplied through the **fuel nozzles**.

The fuel nozzles and the combustor dome ensure the fuel supplying and stable combustion within the whole range of the engine power ratings.

The fuel may be delivered to the burning zone by two methods: injection and vaporizing.

Injection of the dispersed fuel through the jet fuel nozzles is the most widespread. High-quality dispersion is ensured by the centrifugal nozzles (Fig. 4.15) with tangential holes. Some of the nozzles are equipped with the air channels for better mixing of the fuel with the air (Fig. 4.16). For dispersion, the fuel flow must be stable with high velocity. Therefore, the jet fuel nozzles need in high pressure difference.

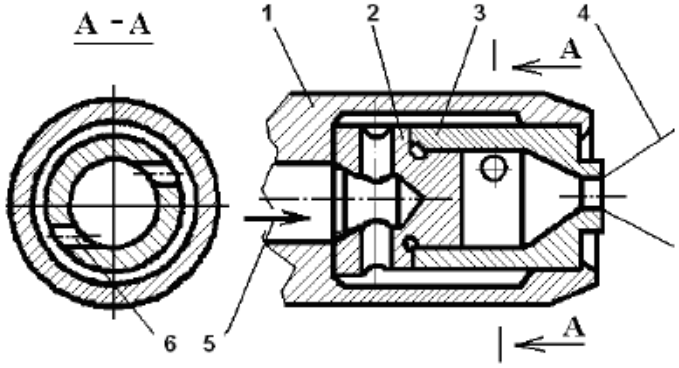


Fig. 4.15. Centrifugal fuel nozzle:
1 — casing; 2 — end cap;
3 — swirler nozzle; 4 — fuel cone;
5 — fuel inlet; 6 — tangential hole

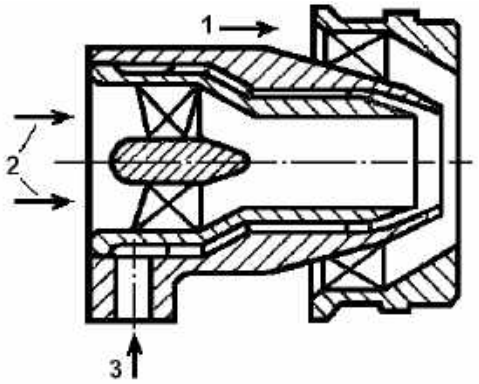


Fig. 4.16. Fuel nozzle with aerodynamic dispersion:
1 — air flow through external swirler;
2 — air flow through internal swirler;
3 — fuel flow

Combustion chambers with the jet fuel nozzles are most applicable in the up-to-date aero engines (Fig. 4.17). The fuel is sprayed by the flow with diameter of droplets 40 to 100 μm. In early designs of the gas turbine engines, when the mixture formation was not completely studied, the fuel was supplied oppositely to the air flow for better dispersion and mixing. This method of fuel supplying stimulated intensive heating of the nozzles and carbonization of the fuel.

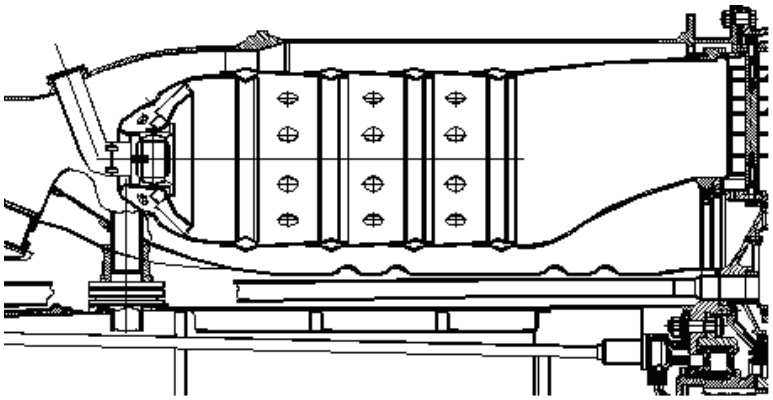


Fig. 4.17. Combustion chamber with the jet dispersion fuel supply system

In modern engines (beginning from the D-36, D-136, NK-8, NK-22 et. al.), the fuel from the centrifugal nozzle is sprayed not directly into a burning zone but under a cap, where it is intensively mixed with the hot air that goes from a compressor outlet. Approximately 75 % of the fuel is vaporized under the cap, and not only the fuel-air mixture but also the vapor-air mixture goes to the burning zone (Fig. 4.18). This method of fuel supplying improves combustion efficiency and environmental performances of the combustion chamber.

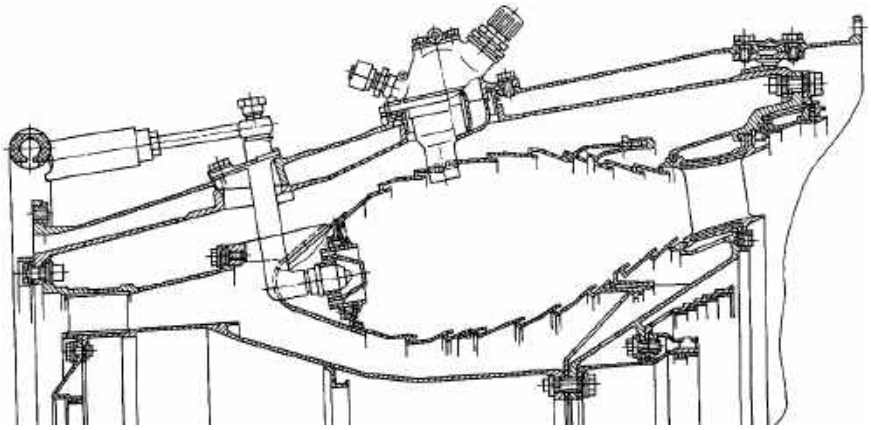


Fig. 4.18. Combustion chamber with fuel supply under the fuel nozzle cap

When the *vaporizing method* is applied, the fuel is sprayed from the feed line into the vaporizing tubes. The tubes are heated from outside by a heat flow from the burning zone. Due to heating, the fuel is vaporized, and the fuel-air mixture goes to the burning zone.

The vaporizing method ensures high combustion efficiency and environmental perfection of the engine (Fig. 4.19). But they are not widespread due to very complicated vaporizing system, which contains a series of pipes that are located in a burning zone. Inside the pipes, the fuel is vaporized and partially thermally decomposed (this process is named as ***cracking***) that can result in cocking of heavy fractions of the fuel in pipes, overheating and burnout of the pipes. When the pipe burns out, the rich fuel-air mixture may be formed with the air/fuel ratio $\alpha \approx 0.25$ to 0.30; this can result in the engine explosion.

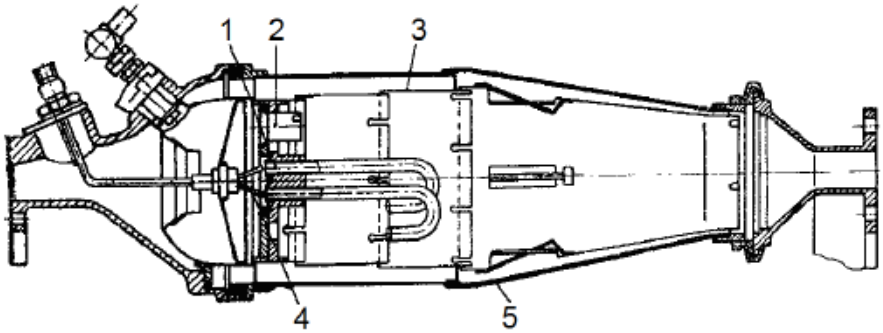


Fig. 4.19. Combustion chamber with vaporizing system:
1 – pipe-vaporizer; 2 – air supplying pipe; 3 – flame tube;
4 – fuel nozzle; 5 – external casing

4.8. Cooling of combustion products. Dilution zone

Temperature in the burning zone is more than 2500 K (see Fig. 4.1), and the turbine inlet temperature is 1400 to 1800 K. Besides, temperature distribution in the burning zone is significantly non-uniform, so local temperatures are very high. Therefore, it is necessary:

– to decrease the gas average temperature;

– to make the temperature distribution uniform or to provide its required shape.

The above-mentioned tasks are solved by designing a **dilution zone** at the combustion chamber outlet that has special slots, pipes or holes for the secondary air supplying into the flame tube.

Mixers supply the secondary air into the flame tube to decrease the gas temperature to the specified value. The cold secondary air shall not enter the zone of reverse flows, because in this case it will overcool the burning zone and thus discontinue burning. To prevent this, the secondary air is supplied inside the flame tube gradually through a system of holes or mixing pipes of different cross-sectional area (Fig. 4.20). Jets of the secondary air must have a high depth of penetration into the hot gas flow to decrease temperature not only near the walls but also in the flow core.

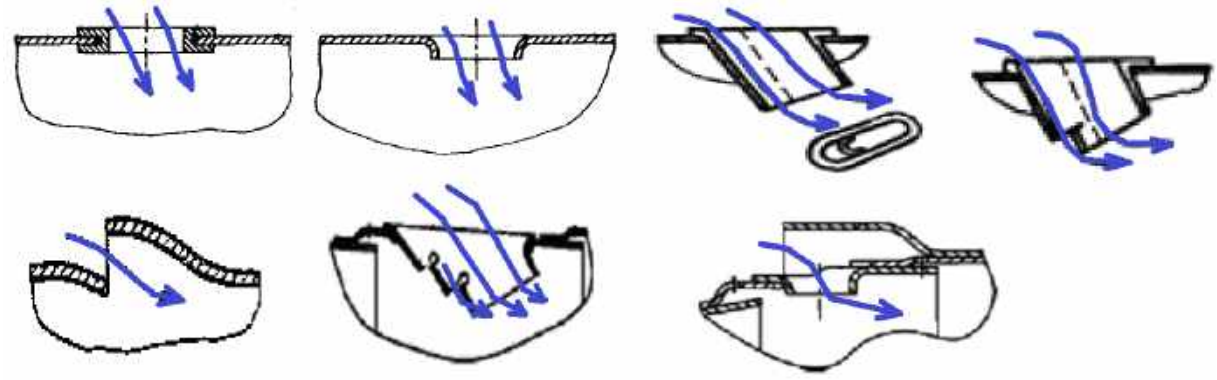


Fig. 4.20. Mixers of different types

The depth of the secondary air jets penetration into the flame tube (Fig. 4.21) is determines as

$$H = d\left(0.3 + 0.415\frac{w_0}{w_g}\right)\left(\frac{L}{d}\right)^{0.63},$$

where *d* is diameter of a hole;

w_0 and w_g are velocity of the secondary air in the hole and velocity of the gas flow, respectively;

L is current coordinate of the flame tube.

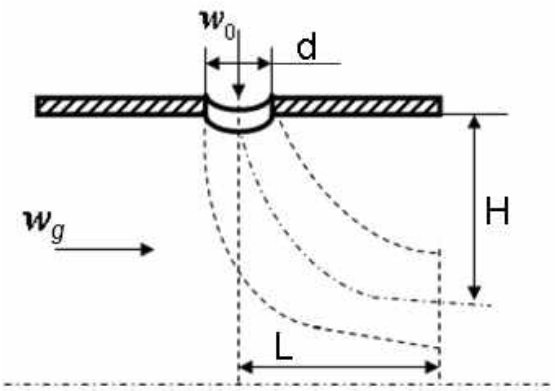


Fig. 4.21. Diagram of analysis of the secondary air penetration depth

4.9. Ensuring operability of design structures

Parts of the combustion chamber operate at high pressure and temperature. The external casing is affected by the pressure from the inside. Its temperature corresponds to the compressor outlet temperature. The internal chamber in many engines is separated from the gas flow duct by a seal and is used as a rear unloading chamber. In this case, the internal casing of the combustion chamber is loaded by the air pressure from the outside and must be prevented from buckling.

The most heated element of the combustion chamber is the flame tube. Its walls take heat from the hot gas, and a radiant heat flow from the burning zone. Operation temperature of the heat resistant alloys that are used for the flame tubes manufacturing is 1000 to 1100 °C. Therefore, the flame tubes need in thermal protection coating and intensive film cooling.

The flame tube is cooled from the outside by a secondary air. Thermal protection coating (enamel) decreases temperature of the flame tube on 40 to 100 °C. The film cooling takes up to 40 % of the secondary air.

Fig. 4.22 shows different methods of cooling of the flame tube wall.

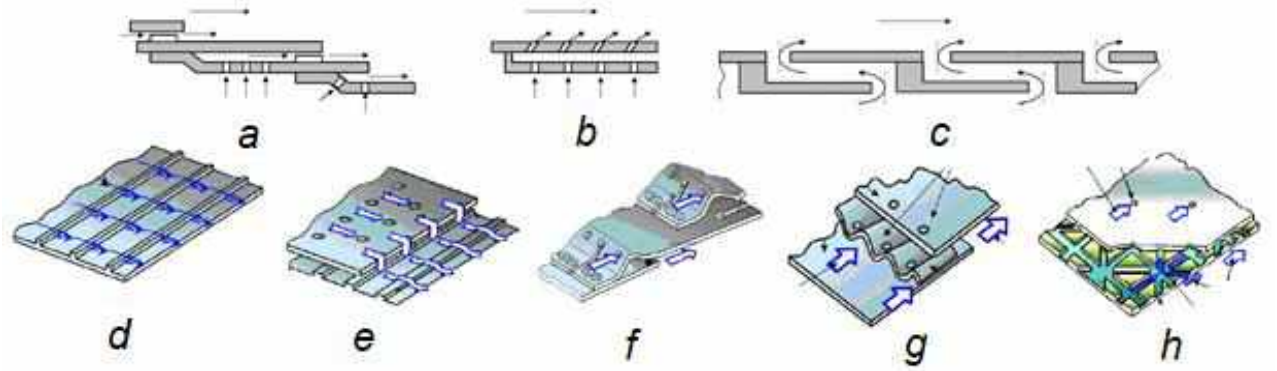


Fig. 4.22. Methods of the flame tube cooling:
a – film cooling with impingement; *b* – perforation cooling with impingement; *c* – convex-film cooling; *d* – single-layer convex cooling system; *e* – double-layer convex cooling system; *f* – film system; *g* – film system with goffered ring; *h* – transpiration cooling system

One more problem of ensuring the flame tube operability is decreasing of thermal stresses. Modern flame tubes are manufactured by forge-rolling, welding and thin-walled rings riveting; all these methods decrease thermal stresses in design (Fig. 4.23).

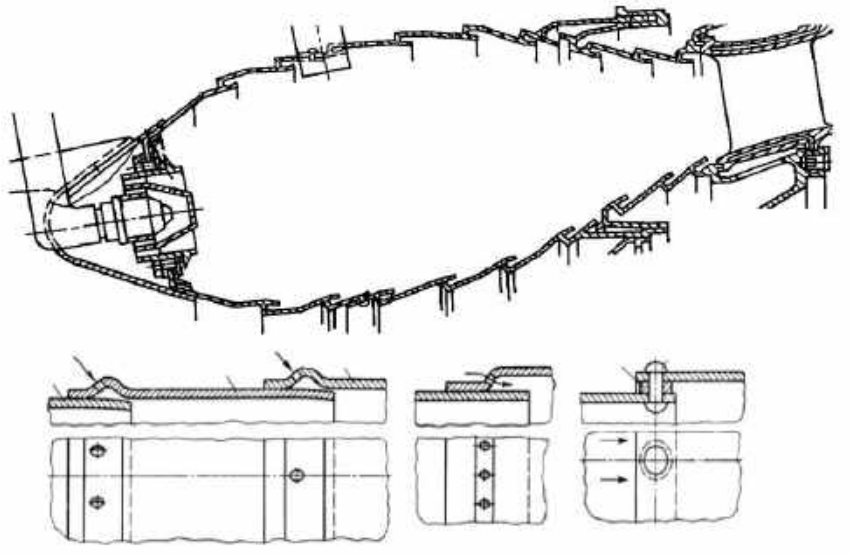
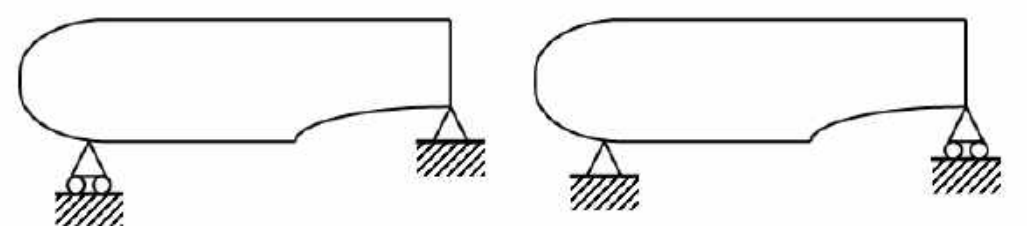


Fig. 4.23. Flame tube and methods of joining its design structures

The flame tube is fixed in a casing as a two-support beam (Fig. 4.24); it is retained in one support and has a freedom of thermal deformation in the other support.



a *b*

Fig. 4.24. Schemes of flame tube restraining:
a – fixing in rear area; *b* – fixing in front area

Designs that implement diagrams of Fig. 4.24, *a*, *b* are shown in Fig. 4.25 and Fig. 4.26, respectively.

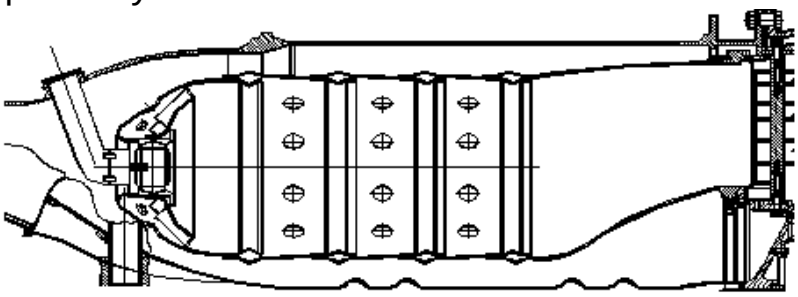
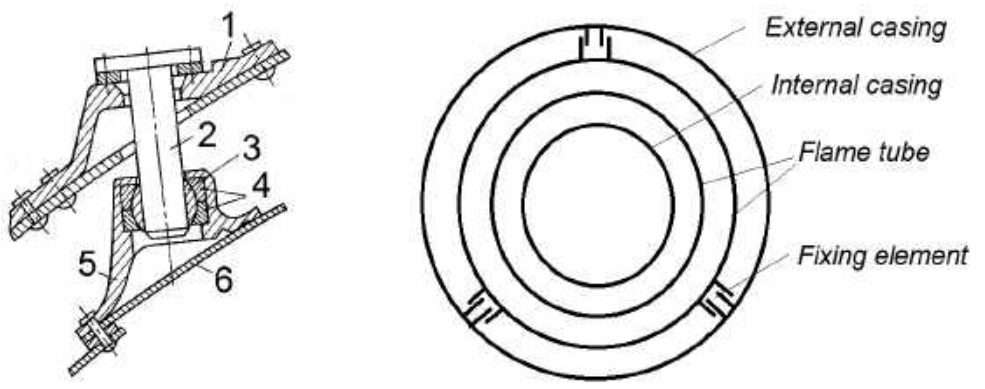


Fig. 4.25. Flame tube restraining by a flange in the rear area and movable fit on a cup of a fuel nozzle in the front area



a *b*

Fig. 4.26. Flame tube restraining by radial pins in the front area:
a – restraining member; *b* – cross-section of the mounting unit;
1 – flange; 2 – locator; 3 – spherical insert; 4 – split sleeve;
5 – flame tube casing; 6 – shell ring

4.10. Combustion initiation. Igniters

At starting, the air with low pressure and temperature enters the combustion chamber. This shortens the range of stable combustion: $0.5 < \alpha < 1.5$.

To initialize combustion, the external source of energy is required. Two types of the igniters are used in the aircraft turbine engines: spark plugs and igniters of a torch type.

Torch spark igniter (Fig. 4.27) is a miniature combustion chamber with a simple fuel control system that is optimized only for starting conditions and has short operation time.

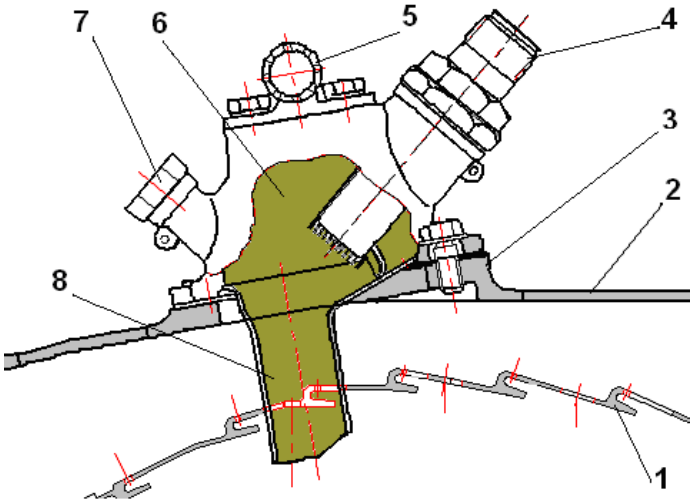


Fig. 4.27. Torch igniter:
1 — flame tube of main combustion chamber; 2 — external casing of main combustion chamber; 3 — flange for torch igniter fixing; 4 — surface discharge plug; 5 — starting fuel manifold; 6 — combustion chamber of torch igniter; 7 — starting fuel nozzle; 8 — nozzle of starting igniter

Starting centrifugal fuel nozzle of simple design and electric sparking plug are mounted inside the igniter. For ensuring a reliable starting in extremely adverse conditions, special starting fuel (gasoline) can be supplied to the igniter and the gaseous oxygen may be delivered to the burning zone. The main advantages of the torch ignition are as follows:

– high heat power (one-two orders more than the sparking plug has);

– high service life of the sparking plug and torch igniter, as all the time, besides starting, they are streamlined by the cold air that flows from the compressor and are not influenced by the flame from the flame tube;

– low consumed power (hence, low weight and cost of the power source) due to optimum design;

– relative freedom in mounting of the torch igniter in relation to a flame tube due to its high heat power;

– ability to make pulsing fuel supply and form an optimum for ignition composition of the fuel-air mixture depending on atmospheric conditions without additional accessories;

– ability to use one torch igniter for engines of all types and dimensions that significantly decreases the cost of development, equipping and servicing.

For reliability, several igniters are mounted in one combustion chamber and operate in parallel.

If the engine is equipped with combustion chamber of can or can-annular type then the igniters are placed in two or three flame tubes only. Other tubes are ignited by the flame torches that are transmitted from already operating sections of the combustion chamber through the flame propagation pipes.

Flame propagation pipes propagate flame in can or can-annular combustors from one flame tube to other and decrease pressure differential between heads of the flame tubes (Fig. 4.28).

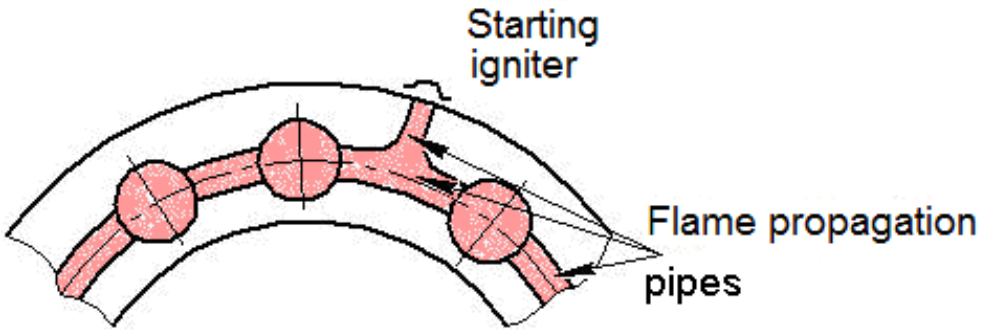


Fig. 4.28. Flame propagation pipes

Combustion chambers of the engines for low altitude of flight (the D-25V, and TV3-117) or with small volume of combustion chamber (the RD-33) may be ignited directly by a sparking plug without separate igniter.

Up-to-date engines are equipped with plasma igniters (Fig. 4.29). The working fluid for plasma generation is the air that is supplied into a corona discharge between electrodes.

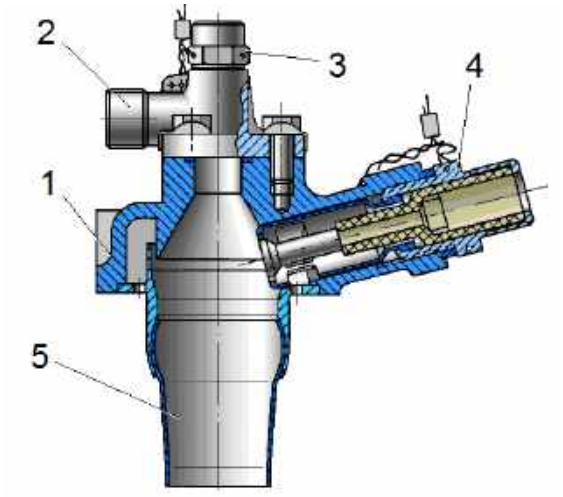


Fig. 4.29. Plasma igniter:
1 – casing; 2 – starting fuel nozzle; 3 – end cap; 4 – plasma-jet plug; 5 – pipe

4.11. Ensuring environmental performances

Standard hydrocarbon fuel contains 85 % of carbon and 15 % of hydrogen. The air is composed of 78 % of nitrogen and 21 % of oxygen; the last 1 % are neutral gases and carbon dioxide. Ideal combustion of the hydrocarbon fuel is full oxidation of carbon and hydrogen. Hence, the products of combustion are water and carbon dioxide. In the dilution zone of the combustion chamber, the secondary air is mixed with the combustion products, which oxygen does not take part in combustion. As a result, the exhaust gas contains N_2, O_2, H_2O, CO_2, and less than 1 % of inert gases. This gas is low toxic, and the carbon dioxide that is produced by the aero engines does not affect adversely the global greenhouse effect comparing to pollutions of the thermal electric stations and automotive engines.

Otherwise, a part of carbon is not oxidized during real combustion, so one more part is not completely oxidized, and the nitrogen becomes chemically active at high temperature and is partially oxidized. This results in formation of dangerous components in the combustion products:

– free carbon C;

– carbon dioxide CO;

– nitrogen oxides (NO_2, N_2O_3 et. al.), which are designated as NO_X.

Concentration of these components is strictly limited by the standards that are checked during the engine certification. These standards are periodically corrected towards more stringent requirements.

Intensity of emission depends mainly on the pressure, temperature and excess air/fuel ratio in the burning zone (Fig. 4.30, 4.31).

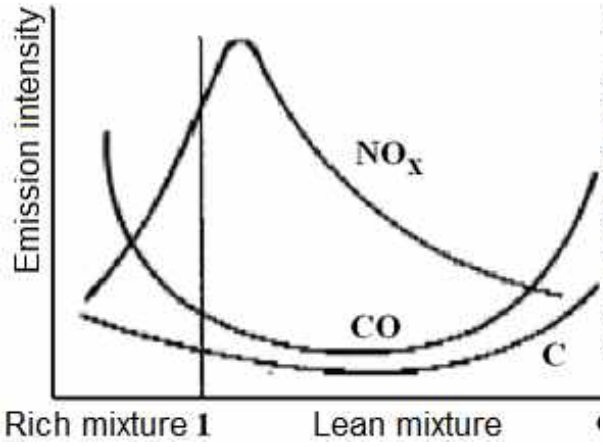


Fig. 4.30. Emissions vs excess air/fuel ratio

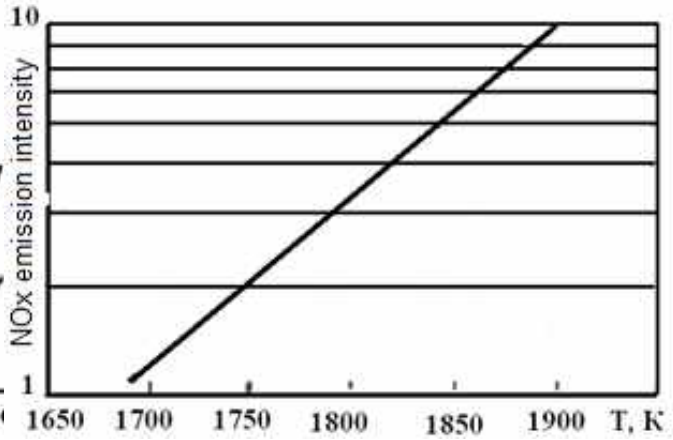


Fig. 4.31. NO_x emission vs turbine inlet temperature

Progress in the turbine engine designing is closely related to increasing of the turbine inlet temperature and compressor outlet pressure. This stimulates decreasing of the free carbon and carbon monoxide emissions, but emission of the nitrogen oxides becomes more intensive.

This problem is solved now in the aero engine industry by designing combustion chambers with burning in lean conditions (when the excess air/fuel ratio is significantly higher than one). However, in this case, we must ensure a stable burning. The combustion chamber needs in special design.

The example is a double-row combustion chamber with parallel disposition of burning zones (Fig. 4.32) that is proposed by General Electric Company.

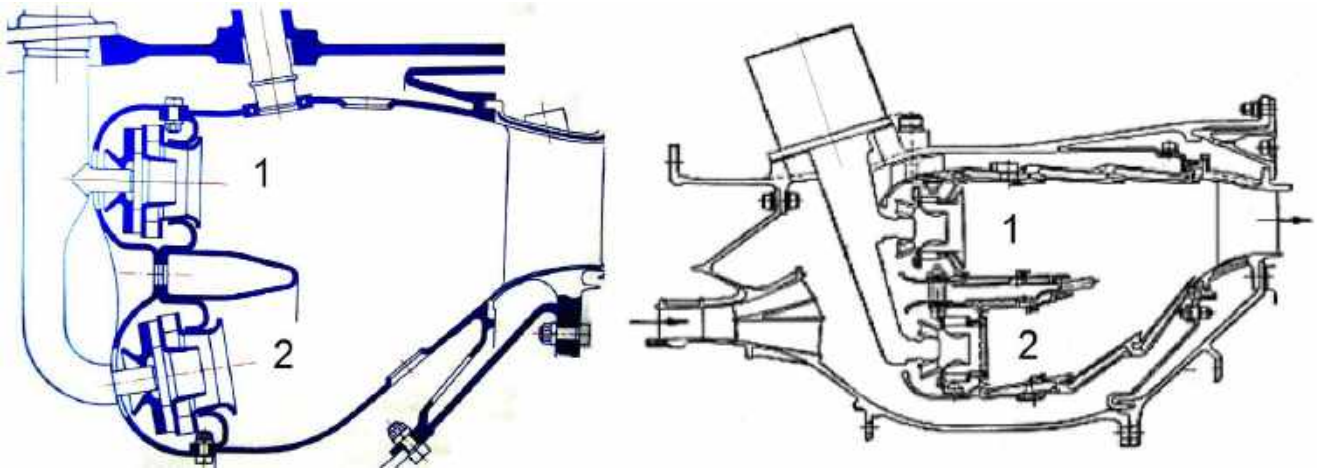


Fig. 4.32. Double-row combustion chamber:
1 – pilot zone; 2 – main zone

The external zone is a pilot one. During engine starting and idle, only this zone operates. The air is supplied in stoichiometric amount, so generation of CO and C_nH_m will be negligible.

The inner zone is initiated when the power rating increases. The automatic control system maintains a lean mixture composition in this zone, thus ensuring low emissions of the nitrogen oxides.

Another example of double-zone combustion chamber with consequently displaced zones is designed by Pratt&Whitney Company (Fig. 4.33).

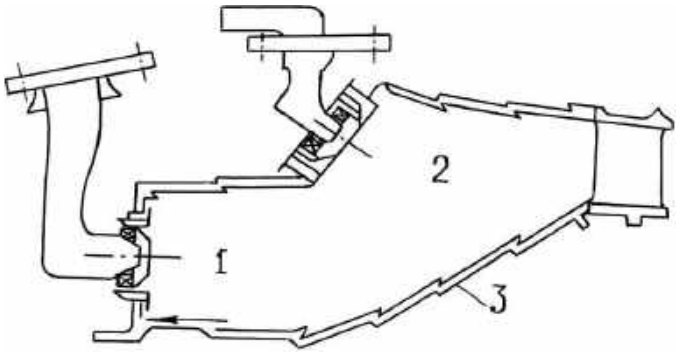


Fig. 4.33. Diagram of flame tube with burning zones that are separated by radius and length (PW-4000 turbofan):
1 – pilot zone; 2 – main zone; 3 – flame tube

The first zone in a flame tube is a pilot one. Emission of CO and C_nH_m in this zone is low, because all of fuel is supplied into this zone during starting and idle, thus providing the stoichiometric composition and high temperature of the flame.

The second zone is displaced by the flow after the first zone. It is equipped with its own flame stabilizers and fuel nozzles. This zone is the main one. Combustion in this zone is lean with temperature of flame of 1800 to 1900 K, and the nitrogen oxides in these conditions are formed less intensively.

Some alternative technologies of designing of the low-emission combustion chambers are included now into the State and International programs and are intensively developed by the leading engine designing companies.

The examples of these technologies are:

- Lean Premixed Prevaporized (LPP);
- Rich-Burn Quick-quench Lean-burn (RQL);
- Double Annular Combustor (DAC);
- Twin Annular Premixing Swirler combustors (TAPS);
- Lean Direct Injection (LDI);
- NASA multi-point LDI;

- Lean Premixed Prevaporised (LPP);
- Axially Staged Combustors (ASC);
- Variable Geometry Combustors (VGC).

4.12. Faults of main combustion chamber design structures and constructive methods that provide their reliable operation

The most of the combustion chamber damages and faults are related to the flame tubes. These faults usually are not cause of the premature removal of engine from service; they are detected during engine overhaul after expiry of the engine service life or when the engine was rejected by other reasons. Burnouts of the flame tubes resulted in the engine failure, were caused by the gas flow destruction with simultaneous improper fuel supply due to damage of fuel manifolds, or leakage of the fuel nozzles, or the flambeau affecting on the casing.

Characteristic faults of combustion chambers are as follows:

1. *Cracks close to the mixing holes of the flame tubes*. The reason of these cracks is temperature gradient combining with the thermocyclic loading. Temperature of the hole edge is less than that of the adjacent wall. In this case, tensile stresses affect the hole edge (Fig. 4.34, *a*).

Temperature stresses in the edges of holes are decreased if holes of small diameter are provided before and between the main holes (Fig. 4.34, *b*); these small holes create a protective air veil. The edges of the mixing holes may be chamfered outside or inside the flame tube (Fig. 4.34, *c*) or provided with special bushings (Fig. 4.34, *d*).

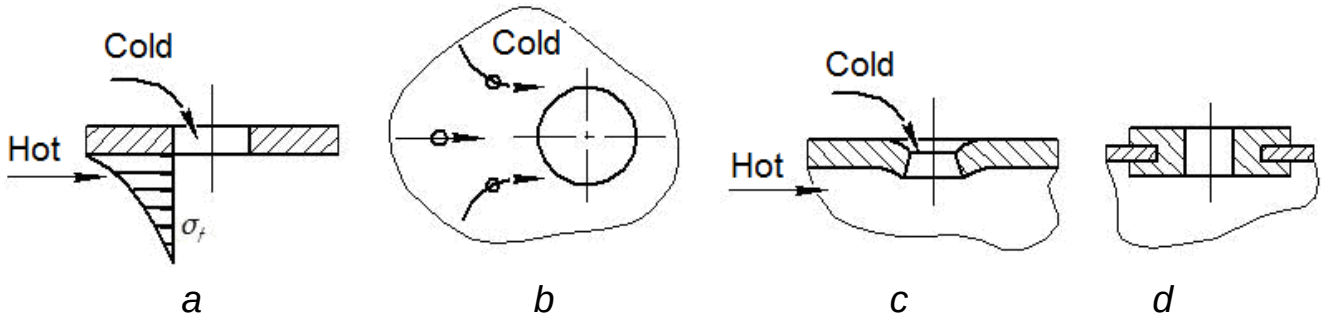


Fig. 4.34. Thermal stresses decreasing in edges of flame tube holes:
a – thermal stress distribution close to the edge; *b* – small holes before the main hole; *c* – hole with chamfered edges; *d* – hole with special bushing

2. *Burnouts of combustor domes* (domes, diffusers, perforated front walls). Typical propagation of such fault is buckling and bending of edges with subsequent burning. This fault is propagated due to leakage of fuel nozzles,

variation of the secondary airflow in flight (that is not detected at the test bench), nonobservance of procedures used for manufacture of the flame tube.

Temperature of the flame tubes reaches 1100 to 1250 K. Oxygen at such temperature and high pressure has increased chemical activity; this may initiate gas corrosion of the flame tube wall. Majority of the flame tubes overheating and burnouts is caused by incorrect position of the flame torch or by poor cooling. The flame tube walls are protected by ceramic or heat resistant enamel coating and are cooled from the outside by the secondary air, which velocity is 80 to 100 m/s, and from inside – by the protective air film.

3. *Buckling of the flame tubes walls* is usually result of non-uniform heating in circumferential direction or wall touching by a flame; the latter is because of incorrect secondary air supply or carbon deposition on fuel nozzles (usually results in the combustion chamber flaring).

Temperature stresses at non-uniform heating decrease if the flame tubes are manufactured of the heat resistant material of small thickness (0.8 to 1.2 mm).

4. *Chipping of material on the flame tubes and casings* is usually related with vibrations (oscillatory combustion or kinematic transmission of oscillations from other sources). It takes place in relatively cold parts where thermal stresses are not available. Fatigue cracks and chipping are characteristic for places of joining of heavy components to thin-walled structures or close to the local thickenings of walls, for example, in weld seams.

5. *Cracks in places of joining of two sections* are characteristic for differently heated sections. Tensile stresses appear in less heated section; they can initiate longitudinal cracks. Vibration accelerates growth of such cracks.

Compensating cuts (Fig. 4.35) are providid in section to decrease thermal stresses close to the weld seams.

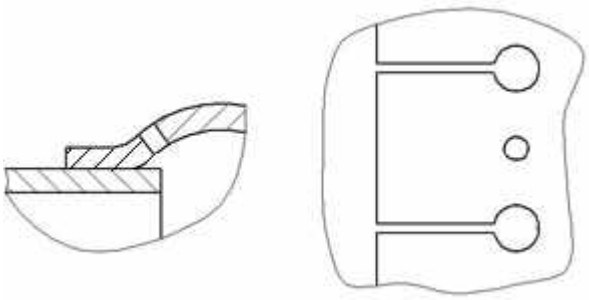


Fig. 4.35. Compensating cuts in section of a flame tube

Decreasing of stress concentration in the combustion chamber design structures increases their life time. Therefore, they are electrically polished, holes are reamed, and edges are polished and chamfered. The combustion chamber components are pressed in several steps, with annealing after each step for relaxation of the internal stresses.

4.13. Structural materials of main combustion chambers of GTE

Materials of combustion chamber components are chosen depending on their heating temperature during operation of the combustion chamber.

External casing is heated up to 300 to 400 ºC; it may be manufactured of carbon steel 10. If the operating temperature is higher, then steels Х18Н9Т (Я1Т), ЭИ417, ЭИ435, ЭИ602, ЭИ652, ЭИ703, ЭИ385, and ЭИ-868 are used.

Flame tube is heated up to 800 to 1000 ºC. Its manufacturing needs in heat protective materials that meet the following requirements:

– material at operating temperature must have high mechanical properties – ultimate strength, long-term strength, durability limit, yield limit and creep limit;

– the material must be resistant to the gas corrosion and not enter in chemical reactions with combustion products;

– the material must be resistant to temperature variation, resistant to cracking and swelling (these properties are characteristic for the materials with low thermal expansion factor);

– the material must be enough manufacturable – it must be plastic and easy for pressing, drawing, bending, and welding.

Flame tubes and diffusers that operate at temperature up to 900^0 C, may be made of alloys ЭИ-417, ЭИ-435 (ХН78Т), ЭИ-602 (ХН75МБТЮ), and ЭИ-703 (ХН38ВТ). The flame tubes that operate at temperature up to 950 ºC may be made of alloy ЭИ-894; if the temperature is higher, alloys ЭИ-868 (ХН60В), and ВЖ-102 are used.

Vortex generators are made of alloy ЖС-6М, gas collectors – of ЭИ-602.

Promising materials for manufacture the flame tubes are powder alloys based on the intermetallic structures Ni_3Al, NiAl, FeCrAl; they are operable at a temperature of 1 200 to 1 300 ºC. High thermal resistance, resistance to carbide forming, hydrogen and sulfide cracking at high temperature, high strength at high temperature and low density of these materials are their advantages comparing to the traditional structural materials.

Now ceramic materials are researched with operation temperature of 1 500 ºC and more.

4.14. Check questions

1. What is a designation of the GTE combustion chamber?
2. What is the difference between transmissions of heat to the propulsive mass in the GTE from similar process in the reciprocating engine?
3. Explain sense of terms “fuel”, “oxidizer”, “fuel-air mixture”, “combustion-mixture”, “products of combustion”.

4. What is a difference between lean, rich and stoichiometric combustion mixtures?

5. What specific parameters characterize perfection of the combustion chamber?

6. What are the main requirements to the combustion chambers?

7. How is the main combustion chamber arranged?

8. What is the reason of different design diagrams of the existing combustion chambers?

9. Why practically all GTEs of the last generations are equipped with the annular combustion chambers?

10. What for the two-zone combustion chambers are used?

11. What main loads affect design structures of the combustion chambers?

12. What is the reason of application of different power diagrams of the combustor casings?

13. Why the flame tube is excluded from the engine power diagram?

14. What design diagram decisions provide a freedom of the flame tube thermal expansion?

15. Name designing means directed on prevention of buckling and burnout of the flame tubes.

16. What are the functions of the combustion chamber diffuser?

17. Why the dump diffusers are used in the combustion chambers of the modern turbine engines?

18. What means are used to provide a specified service life of the flame tube?

19. What design structures of the combustion chamber need an enforced cooling and how is it implemented?

20. Name tasks solved by the combustor domes.

21. What design means are used for flame stabilization in the combustion chamber?

22. Why the majority of the combustion chambers of the up-to-date gas turbine engines are equipped with the swirler vanes?

23. What are the main advantages and disadvantages of the evaporative combustion chambers?

24. What type of fuel nozzles is the most propagated in the up-to-date aero engines and why?

25. What designing means provide the required turbine inlet temperature field?

26. How does the combustion chamber inflammation to be implemented?

27. When the oxygen replenishment is used?

28. What structural materials are used for manufacture of the combustion chambers?

5. EXHAUST SYSTEM DESIGN

5.1. Purpose and composition of the exhaust systems

The exhaust system of the gas turbine engine is a part of the gas turbine power plant, which is located downstream of the turbine. The exhaust systems play several functions, which are significant for the engine operation:

- efficient transforming of the gas potential energy (heat drop) into the kinetic energy;
- forming the exhaust gas flow of the high impulse and the specified direction;
- maintaining the engine required operating conditions by varying of the jet nozzle area;
- transporting the gas in the fuselage or engine nacelle;
- reducing noise level of the power plant;
- shielding the engine direct infrared radiation to decrease the aircraft infrared perceptibility;
- integration the engine with the aircraft, etc.

These multiple functions that are to be implemented in a wide range of flight altitudes and velocities, transform simple jet nozzle of the first-generation engines into the complex system, which quality affects the aircraft performance, especially for the supersonic and maneuverable aircraft.

In general case, the exhaust systems of the gas turbine engines include the following:

– post-turbine diffuser;

– gas discharging device (exhaust pipe) that supplies the exhaust gas from turbine to the jet nozzle;

– mixing chamber, which is used in the turbofans for mixing flows of the main duct and bypass duct to provide a uniform temperature of the exhaust gas at the jet nozzle inlet, thus decreasing losses of the output impulse;

– jet nozzle (constant geometry or variable, non-cooled or cooled);

– thrust reverser, thrust deviator (the device for controlling thrust vector);

– noise suppressor.

Exhaust systems of the gas turbine engines operate under heavy loading conditions:

– high temperature of the exhaust gas (under non-afterburning conditions, a turbine discharge temperature is 1000 to 1200 K and at afterburning this temperature reaches 2100 to 2200 K);

– high velocity of the gas flow (a nozzle discharge velocity under non-afterburning conditions is 600 to 750 m/s and at afterburning reaches 1100 m/s);

– the high-temperature gas that flows from the turbine is chemically reactive, because it contains a lot of oxygen, which does not take part in burning of kerosene in the main combustor;

– significant axial, radial and circumferential irregularities of the temperature, velocity and pressure.

Requirements to the exhaust systems of the gas turbine engines are as follows:

– the minimum losses of effective thrust under wide range of the flight altitudes and velocities;

– the minimum heat losses through the walls and the minimum heating of the aircraft structural members;

– reliable operation in the chemically reactive high-temperature gas medium;

– low weight and overall dimensions (not more than 4 to 10 % of the engine total weight).

5.2. Design of structural members of the exhaust systems

The simplest exhaust system of the **turbojet engine** consists of the turbine disc cowl and retained taper outlet (Fig. 5.1). The turbine disc cowl prevents abrupt expansion of flow and vortex formation downstream of the turbine, and also protects the turbine disc from overheating by the hot gas.

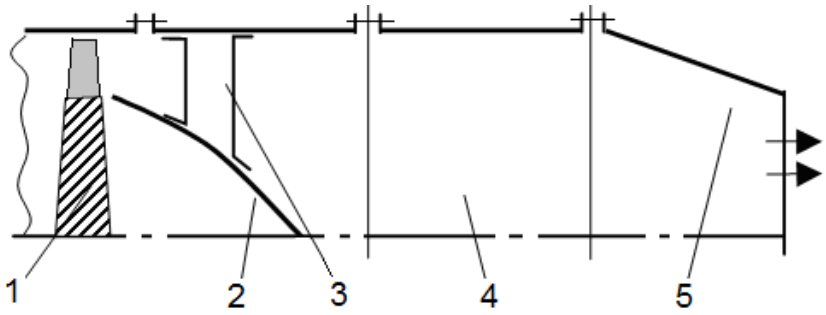


Fig. 5.1. Fixed jet nozzle of turbojet:
1 – turbine disc; 2 – turbine disc cowl; 3 – strut;
4 – extension pipe; 5 – taper outlet

Angle of the internal taper at the tip is 35 to 50º. This taper is joined with the outer casing by the radial struts or rods that are protected from overheating by cowls. The struts are cooled by the air; their design allows free thermal expansion of the joined members.

If the turbine outlet gas flow has non-axial direction, then the cowls of struts are made twisted for the gas flow straightening and decreasing hydraulic losses in the remaining parts of the exhaust nozzle.

Taking into account conditions of the engine mounting in the aircraft, design of the exhaust system may contain a gas-escape extension pipe (Fig. 5.1) made by welding of the heat resistant sheet steel. Its diameter must provide the gas velocity higher than 150 to 200 m/s, thus decreasing hydraulic losses. Joint of the extension pipe with the gas generator must allow displacement to compensate for the engine and airframe manufacturing and mounting errors, and to decrease the loads caused by deformations of the fuselage or engine nacelle.

Fig. 5.2 shows versions of design of the extension pipe attachment flanges.

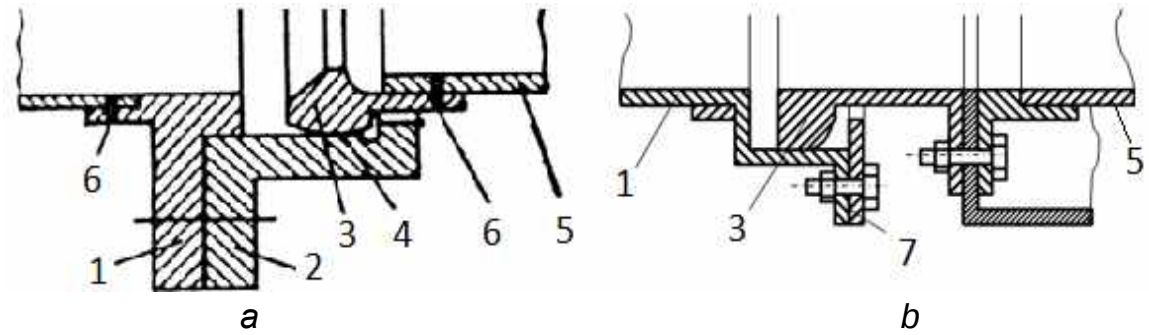
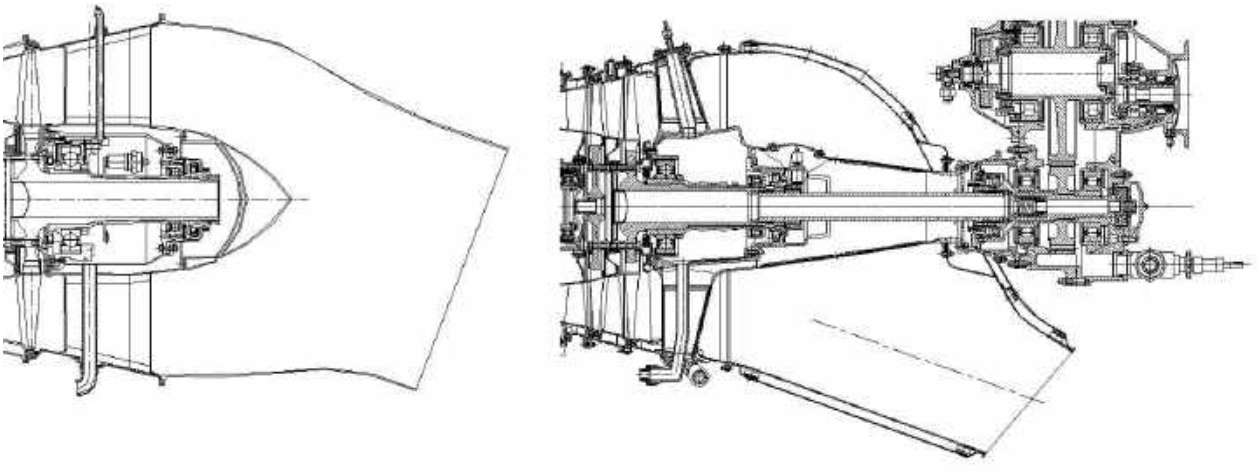


Fig. 5.2. Methods of attachment of extension pipe:
a – by spherical ring; *b* – by spherical flange;
1 – engine casing; 2 – flange of extension pipe; 3 – spherical flange; 4 – spherical ring;
5 – extension pipe; 6 – weld; 7 – connecting bar

Spherical ring 3 is joined with flange 2, which has a long groove for the ring and allows the ring axial displacement and simultaneously small turning. The rear side of the extension pipe is joined by the rollers with eccentrics, which can move by guiding channel bars when the pipe and the engine itself take the thermal deformation.

To decrease heating of the airframe structural members, the extension pipe is covered by the heat insulation and is equipped with a screen, under which the cooling air is supplied.

Exhaust system of the turboprop engine (Fig. 5.3) does not change the gas parameters essentially, because the main thrust of the turboprop engine is generated by the propeller, and jet thrust is only 10 to 15 % of the total thrust. The exhaust system of the turboprop engine provides discharge of the exhaust gas without its essential expansion. So, the exhaust gas velocity is smaller than in the turbojet engine. Low velocity allows the gas discharging under small angle to a flight line (up to 20º), taking into account engine integration with aircraft.



a *b*

Fig. 5.3. Exhaust systems of turboprop engines:
a – single-shaft turboprop; *b* – free-turbine turboprop

In the **helicopter turboshaft engines**, the gas is discharged sideways (Fig. 5.4). Available heat energy of the gas is converted into mechanical energy of the free turbine. Therefore, these engines are designed with the use of the maximum temperature differential at the free turbine, which needs the maximum possible pressure difference. As a result, a turbine discharge static pressure may be less than the atmospheric pressure, and the exhaust stack is designed not convergent, but divergent one.

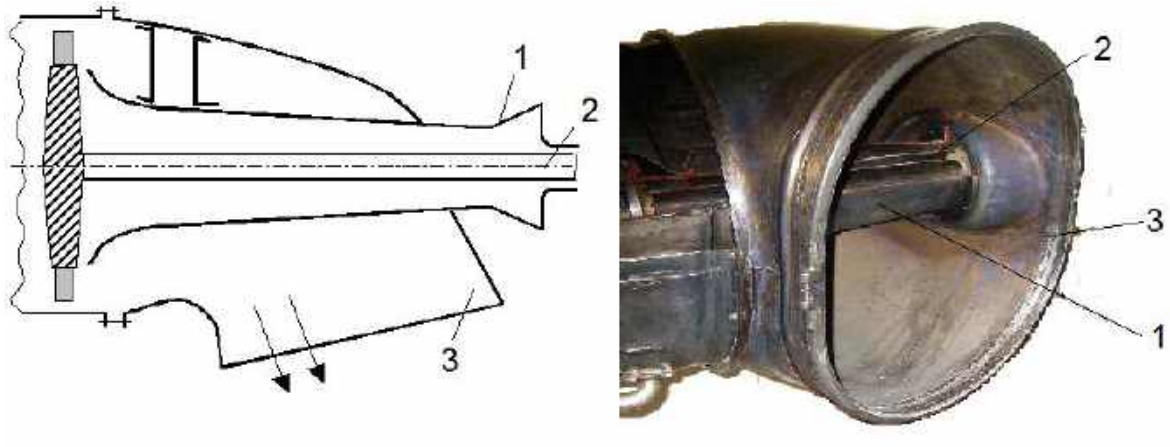
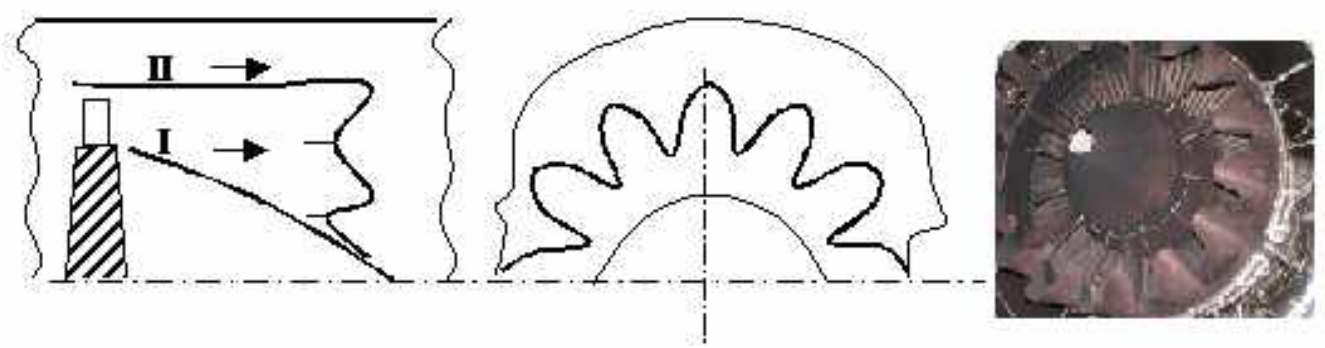


Fig. 5.4. Exhaust system of helicopter turboshaft engine:
1 – shaft shroud; 2 – free turbine output shaft; 3 – exhaust stack

Mixing chamber is used in the TFE for mixing the gas that flows from the primary duct, with the air that flows from the bypass duct. Mixer, which is located at the mixing chamber inlet, separates the air and exhaust gas flows in separate jets of small diameter, thus improving turbulent mixing and shortening length of the chamber.

The mixers are axial and radial ones. Fig. 5.5 shows the scheme and the general view of the axial (flap-type) mixer (the D-30KP turbofan), Fig. 5.6 represents the radial mixer (the RD-33 turbofan).



a *b*

Fig. 5.5. Axial mixer:
a – scheme; *b* – external view

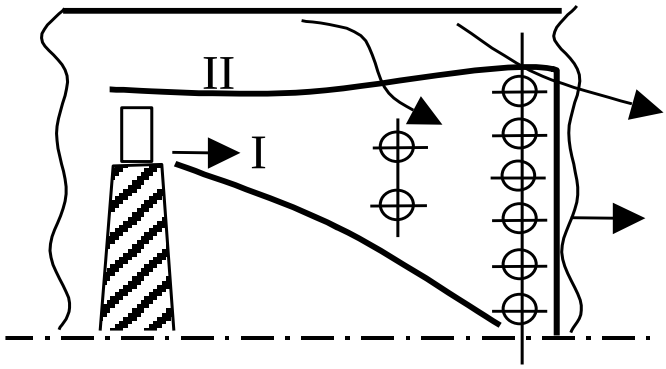


Fig. 5.6. Radial mixer

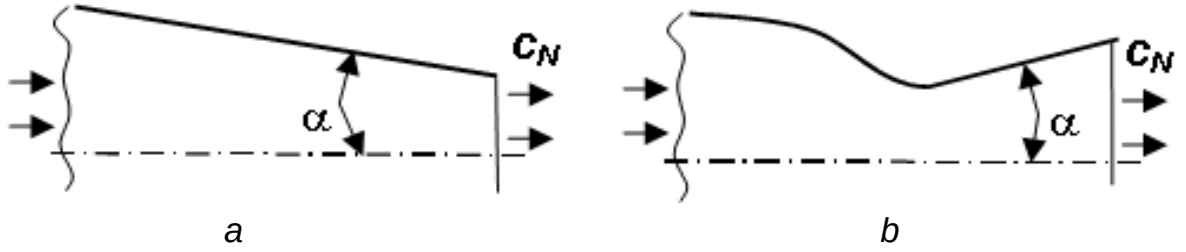
5.3. Design of jet nozzle

5.3.1. Parameters of jet nozzle

The main parameter, which determines a choice of the jet nozzle type, is available pressure ratio – ratio between the nozzle inlet stagnation pressure and the static atmospheric pressure: $\pi_N = \frac{p_T^*}{p_H}$.

This ratio for a turbojet engine at OPR ≈ 10 to 15 and TIT ≈ 1400 to 1500 K is $\pi_N \approx 6$ to 8 for M = 1, and $\pi_N \approx 25$ to 35 for M = 3.

Engines for aircraft, which flight Mach number is M ≤ 1.5…1.7, are equipped with the convergent nozzles (Fig. 5.7, *a*). Engines for the supersonic flight with Mach number M ≥ 1.7 are equipped with the convergent-divergent (Laval) nozzles (Fig. 5.7, *b*).



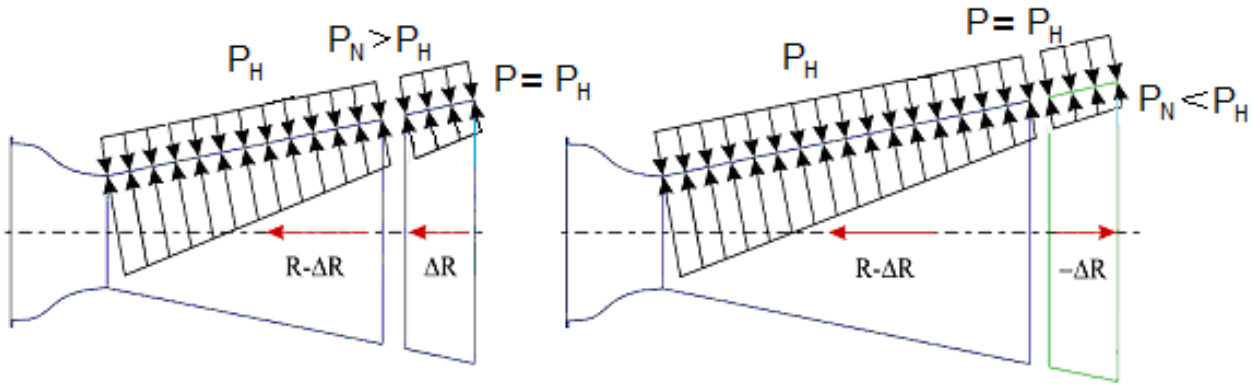
a *b*

Fig. 5.7. Nozzle profile:
a – convergent nozzle for subcritical and critical flows ($c_N \le a$);
b – convergent-divergent (Laval) nozzle for supercritical flows ($c_N > a$)

Output velocity c_N in the real nozzle is less than theoretical (adiabatic) velocity $c_{N\,ad}$ due to losses. This decreasing is characterized by velocity factor $\varphi_N = c_N / c_{N\,ad}$, which value is 0.97 to 0.99.

5.3.2. Jet nozzle operation modes

The jet nozzle has the minimum base drag at full expansion mode, when $p_N = p_H$. In case of partial expansion or an overexpansion, the thrust decreases (Fig. 5.8). Increase in a supersonic part of the nozzle at the partial expansion ($p_c > p_H$) or decrease in it at the overexpansion ($p_c < p_H$) can get the additional thrust.



a *b*

Fig. 5.8. Nozzle operation at partial expansion (*a*) and overexpansion (*b*)

Losses in the nozzle at off-design power ratings are also depend on the gas flow downstream of the nozzle. For example, the flow is compressed to pressure p_H at overexpansion. In this case, the compression shock originates in a flow core, the pressure at its outlet increases, the flow expands and the process continues with damping (Fig. 5.9).

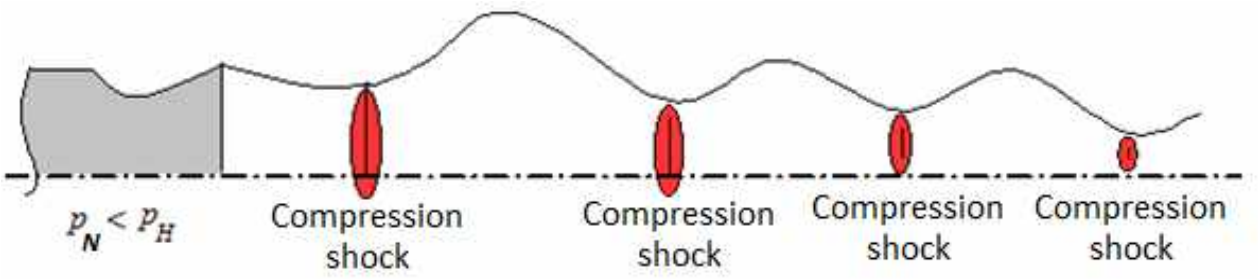


Fig. 5.9. Origination of compression shocks when nozzle operates at overexpansion mode

At partial expansion mode, the gas expands abruptly upstream of the nozzle, and a portion of the heat energy is transformed into a radial thrust (Fig. 5.10). If the nozzle is streamlined by a supersonic flow, then a compression shock originates at the jet boundary. After that, the jet is compressed, and then the process is similar to the previous case.

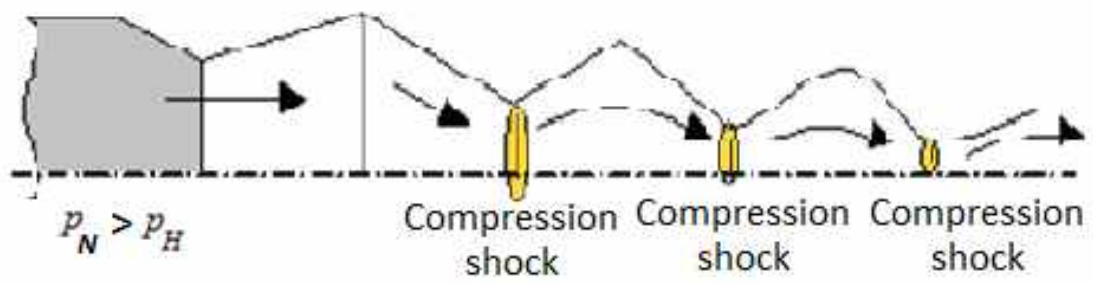


Fig. 5.10. Origination of compression shocks when nozzle operates at partial expansion mode

5.3.3. Controlling nozzle area

Hence, the nozzle that operates in off-design mode worsens the engine performance. Effective operation of the engine at all power ratings and flight conditions of the aircraft is provided by the nozzle automatic control. The variable nozzle also facilitates the engine starting, improves stability of the compressor, decreases specific fuel consumption at cruise modes, and provides invariable operation of the gas generator at afterburning and non-afterburning modes of operation.

The nozzle is controlled by variation of its output section (for supersonic nozzles, two sections are varied simultaneously: critical and output ones). This may be done in three ways:

– by turning the flaps that create a movable rim of a round cross-section; a kind of the flapped nozzle is a flat nozzle of a rectangular cross-section, which is formed by two horizontal and two vertical flat plates;
– by axial motion of a profiled central body;

– by pneumatical variation of a flow area by using the compressed air jet, which is supplied to the output cross-section and creates a “liquid” shape of the nozzle.

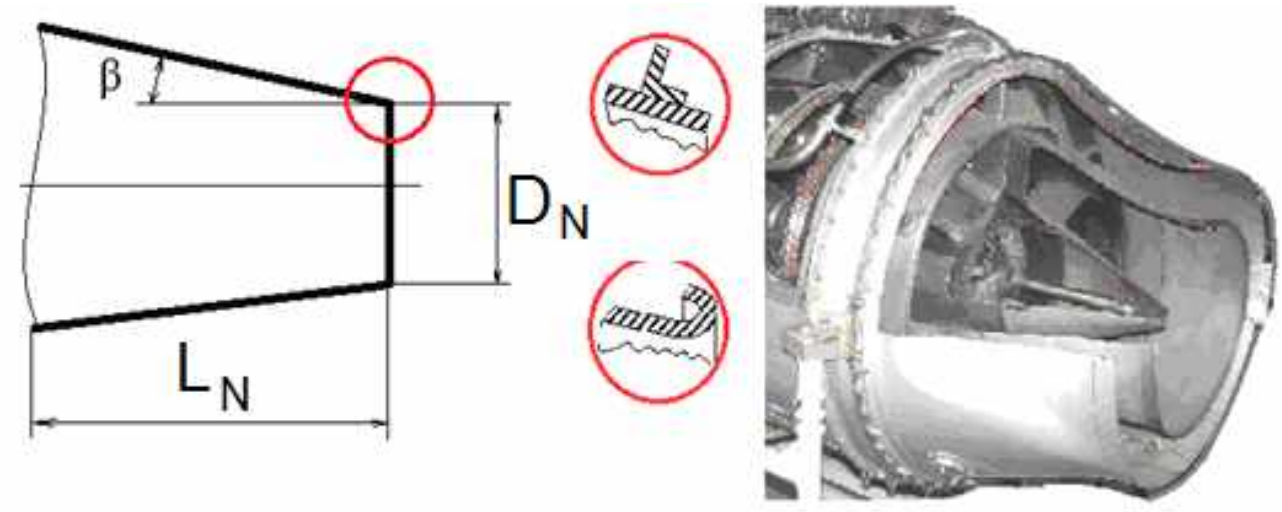
5.4. Design of the TJE and TFE jet nozzles

As it was explained above, the main parameter on which depends a choice of the nozzle type, is available pressure ratio – ratio of the nozzle inlet stagnation pressure to the static atmospheric pressure: $\pi_N = \frac{p_T^*}{p_H}$. This ratio for the turbojet engine at OPR ≈ 10 to 15 and TIT ≈ 1400 to 1500 K is $\pi_N \approx 6$ to 8 for M = 1, and $\pi_N \approx 25$ to 35 for M = 3.

Depending on the aircraft flying speed and the gas outflow velocity, convergent subsonic and convergent-divergent supersonic nozzles are used. These nozzles can be non-controlled and controlled. Engines for the aircraft, which flight Mach number is M ≤ 1.5 to 1.7, are equipped with the convergent nozzles. Engines for supersonic flight with Mach number M ≥ 1.7 are equipped with convergent-divergent (Laval) nozzles.

5.4.1. Fixed nozzle

Non-controlled fixed nozzles have angle β no more than 10º–12° and length/diameter ratio $L_N / D_N \approx 0{,}15…0{,}4$ (Fig. 5.11).



a *b*

Fig. 5.11. Diagram of non-controlled subsonic jet nozzle:
a – conical tip, *b* - nozzle of the AI-25 turbofan

Exhaust section of a nozzle is a circular one, sometimes it is of elliptical shape. Design rigidity is improved by welding profiled rings to the trailing edge or by flanging the edge.

5.4.2. Controlled subsonic nozzle

Variable (controlled) subsonic nozzle gives possibility to maintain optimum operation of the gas generator, to facilitate engine starting, to improve fuel consumption at off-design power ratings. The nozzle is made of separate flaps that are retained in the front section by means of hinges. Area of the exhaust cross-section is changed by a power ring with the hydraulic cylinder (Fig. 5.12).

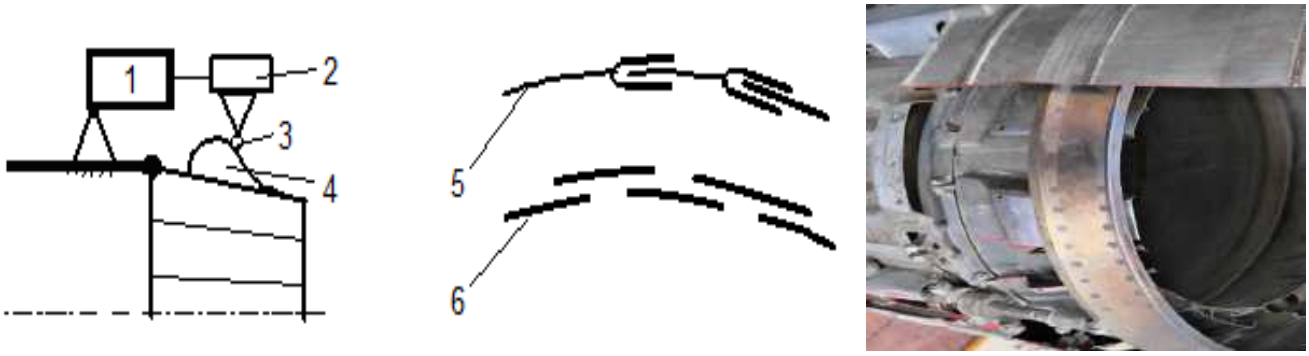


Fig. 5.12. Arrangement of subsonic variable nozzle:
1 – hydraulic cylinder; 2 – power ring; 3 – roller; 4 – profiled cam;
5, 6 – variants of flaps design in position of the minimum area; 5 – seam connection;
6 – peripheral flaps

A law of the exhaust area variation is determined by the profile cam. A leak-proofness is provided by the slot-type connection or by peripheral flaps. The number of flaps in known designs is z = 6 to 36. A shape of the cross-section becomes more circular when the number of flaps increases. The flaps are cooled by the air.

Fig. 5.13 shows design of a multi-flap convergent nozzle. Flaps 3 are of the box-type to improve rigidity and air cooling. The flaps are sealed between themselves by platform 4, which enters fork-type channel 5 of the adjacent flap. All flaps are retained by the hinges to the flange of the outer pipe. They try open under the action of the gas pressure and to press to the external ring 6. This ring controls the flaps, driven by three hydraulic cylinders 1. When the ring moves counter-clockwise (Fig. 5.13) the flaps are closed, when it moves clockwise the flaps are open.

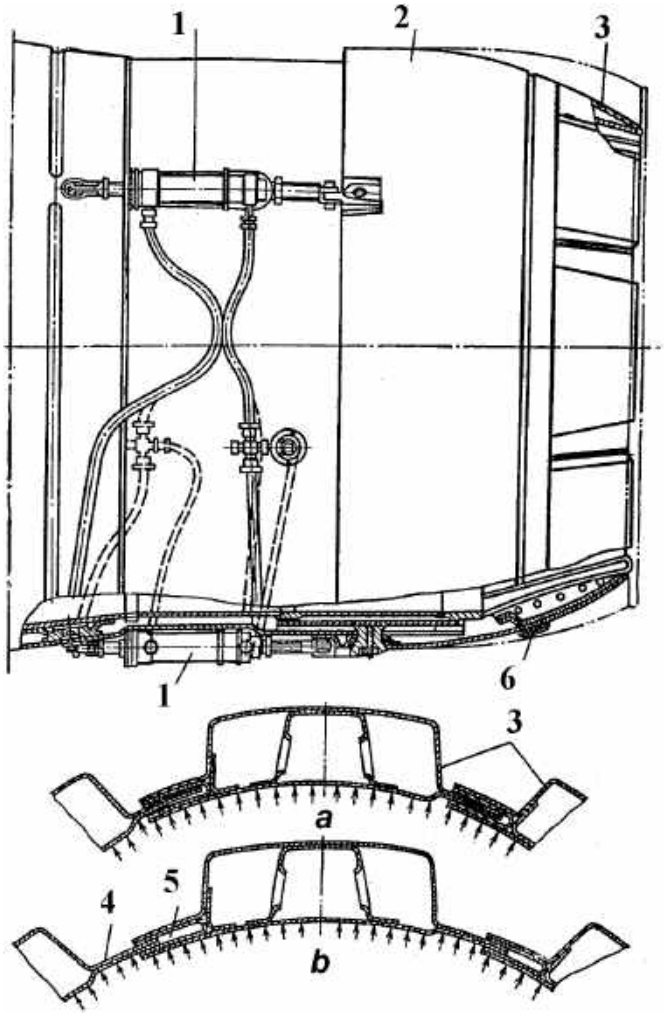


Fig. 5.13. Variable multi-flap convergent nozzle:
1 – hydraulic cylinder; 2 – variable nozzle; 3 – flaps; 4 – platform;
5 – fork-shape channel; 6 – ring; *a* – the minimum position of exhaust area flaps;
b – the maximum position of exhaust area flaps

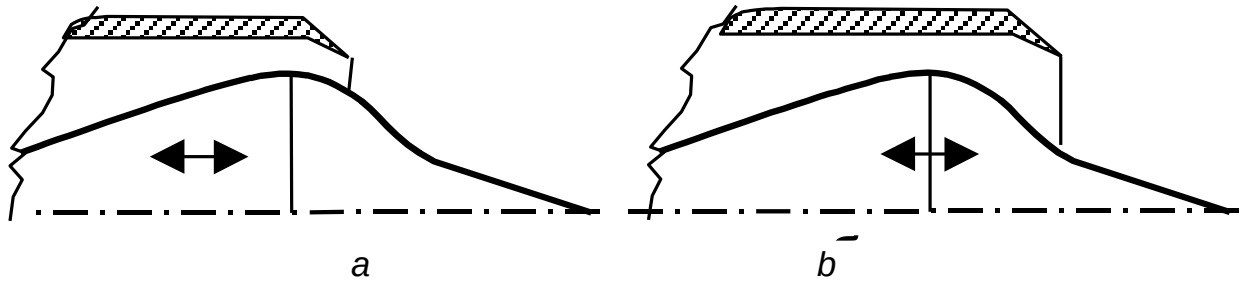
5.4.3. Controlled supersonic jet nozzle with central body

The supersonic jet nozzle with the central body is controlled aerodynamically. There are differed nozzles with the external expansion and the combined nozzles that have partial internal and partial external expansion. They are controlled due to axial displacement of the central body (Fig. 5.14). The nozzles with the central body have simple structural design, but they are not widely used because of difficult cooling of the central body and its driving mechanism.

5.4.4. Ejector nozzle

Ejector nozzle is a flapped single-row nozzle equipped with the external ejector flaps (Fig. 5.15). In this design, a solid wall of the nozzle supersonic

portion is substituted by the liquid wall, which is created by a jet of the bypass air flowing from the ejector flaps.



a *b*

Fig. 5.14. Jet nozzle with central body:
a – with external expansion; *b* – combined

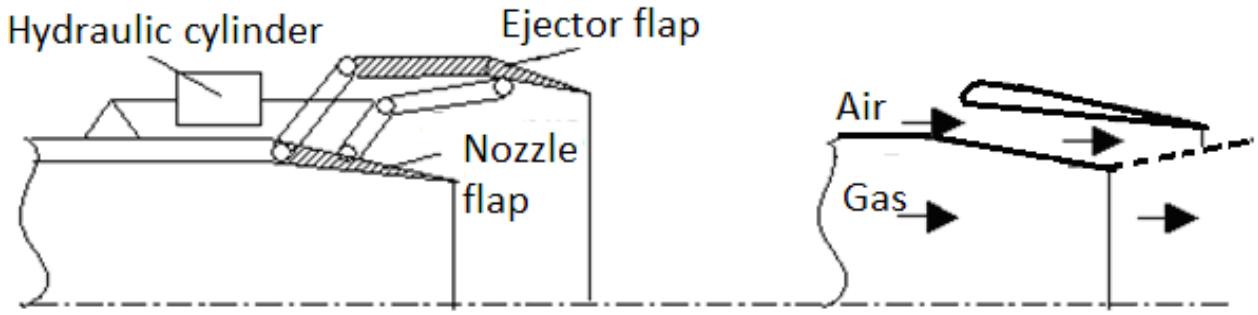


Fig. 5.15. Ejector nozzle

The ejector nozzle operates as follows. At supercritical operating mode, exhaust jet of the gas flowing from the convergent portion, expands in a concurrent subsonic flow and takes shape of a divergent portion of the Laval nozzle. This stimulates further acceleration of the flow and decreasing of the gas temperature and pressure.

Essential thrust increase and simple control are attractive features of this nozzle. So, it is widely used in the afterburning engines (for example, the ATJE R-15B of the MiG-25 aircraft). Ejector flaps may be feathering (without mechanical drive), then they retain themselves in the flow under the action of pressure differential p_N and p_H (for example, the ATJE R-29F-300 of the MiG-23 aircraft).

5.4.5. Lobe double-row nozzle

Lobe double-row nozzle is a variable convergent–divergent (Laval) nozzle. It has two rows of flaps – subsonic flaps retained by hinges in the inlet section, and supersonic flaps, which are hinged to the subsonic flaps (Fig. 5.16).

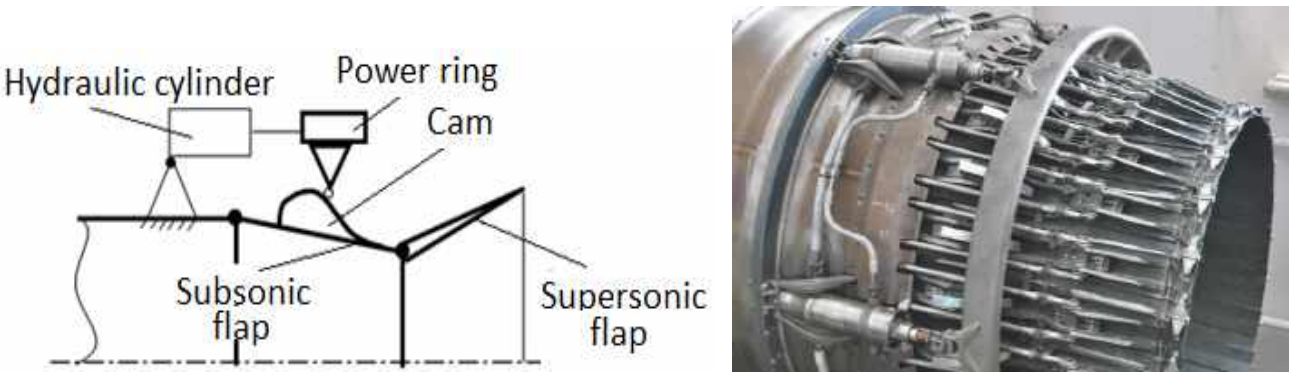


Fig. 5.16. Lobe double-row multi-mode controlled nozzle

The supersonic flaps may be driven by the special rods (the ATJE AL-21F of the aircraft Su-17 and Su-24) or using their placement in feathering position under action of the pressure differential (the ATFE RD-33 of the MiG-29 aircraft).

5.4.6. Driving mechanism of variable nozzle

Power drive of the variable nozzle consists of several hydraulic cylinders and a flap driving mechanism. The hydraulic cylinders are two-, three-position or multimode. Mounting units of the cylinders are placed as close to the hinges of the flaps as it is possible, to exclude the influence of the axial thermal deformations on the nozzle area.

The working fluid of hydraulic cylinders is kerosene with a pressure of 15 to 20 MPa. To prevent heating of the kerosene, the cylinders have circulating design, they are heat-isolated by asbestos and protected by a heat-reflecting screen.

Pistons of the power cylinders are synchronized to exclude skewing of the power ring in relation to the nozzle axis. Hydraulic, electrohydraulic or mechanical synchronizing may be used. The hydraulic synchronizing system contains constant flow valve in a drain line of the cylinder. In the electrohydraulic system, this valve is electrically driven. During mechanical synchronizing, the rods of the cylinders are connected by the flexible shafts and warm-and-warm pair or semi-revolving mechanisms.

The driving mechanism transmits the forces from the hydraulic cylinders to the flaps through a power ring that transforms the linear motion of the piston rods into the angular motion of the flaps. The power ring drives the flaps through cam mechanisms or hinged polyarticular mechanisms.

The jet nozzles are developed by the way of their integration with the aircraft. Thus, different types of flat nozzles for multi-mode manoeuvrable

aircraft have been appeared. Diagram of the flat nozzle is similar to that of the axisymmetric nozzle (Fig. 5.17).

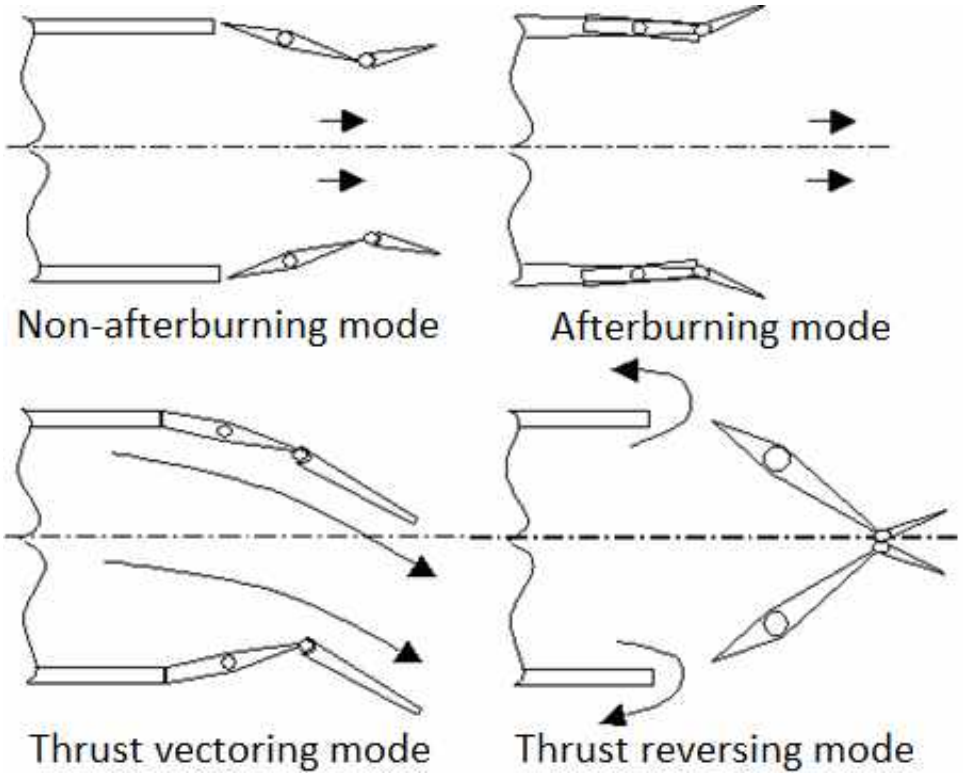


Fig. 5.17. Operation of a flat nozzle at different modes

Design of a flat controlled nozzle is shown in Fig. 5.18.

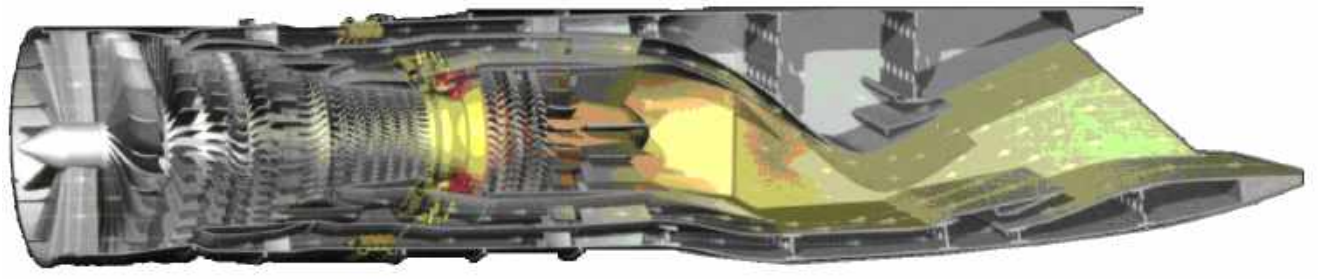


Fig. 5.18. Controlled flat nozzle of adaptive engine ADVENT

Advantages of the flat nozzles are as follows: simple design implementation of various functions (thrust vector control, reversing), good aerodynamic coordination of the exhaust jet stream with streamlining of the aircraft tail portion, improvement of the aircraft lift-and-landing performance due to generation of the vertical thrust.

Main disadvantages of the flat nozzle are increased weight as compared with the axisymmetric nozzle, higher level of losses, and difficult cooling of large flat panels.

5.5. Thrust reversers and deviators

5.5.1. Thrust reversers

Thrust reversing is used during aircraft landing for breaking and during taxing. Some military aircraft use thrust reversing for the inflight maneuvers. The thrust reverser functions by obstructing exhaust by blocker doors, which may be turned into the flow. This diverts the jet radially outwards making forward velocity component. Turning exhaust flow to a forward direction results in a forward thrust component, which acts as a brake.

The main parameter of the reverse device is the reversing factor K_r – the ratio of the reverse (negative) thrust to the maximum direct thrust:

$$K_r = \frac{P_r}{P}.$$

Experimental thrust reversers reach values of reverse factor of minus 0.85 to to minus 0.9). Commonly used thrust reversers with gas turn of 120º to 140º have $K_r \approx$ minus 0.5 to minus 0.6).

Requirements to design of the thrust reverser:

– no influence of the thrust reverser (during its activation or de-activation) on operation of the gas generator;

– the minimum loss of positive thrust when the reverser is not activated;

– exclusion of entry of hot gas into the engine intake when the thrust reverser is activated;

– fast (within 1 to 2 s) changing thrust direction from the positive to the negative one, which is necessary to accelerate aircraft after balked landing);

– synchronizing of the thrust reversers in the multi-engine power plant.

There exist a lot of diagrams of the thrust reversers, but today two of them are widely used:

– with turning a flow before the exhaust nozzle (pre-exit clamshell reverser, Fig. 5.19);

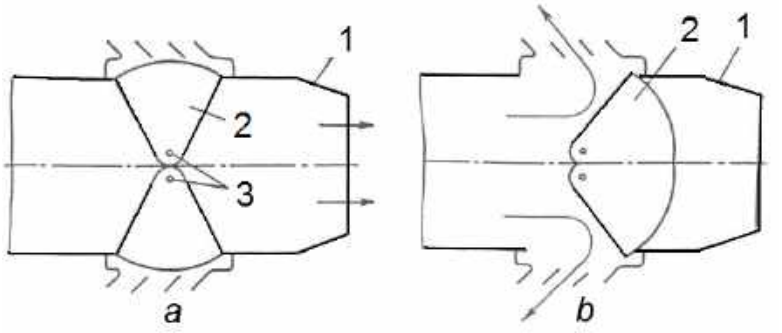
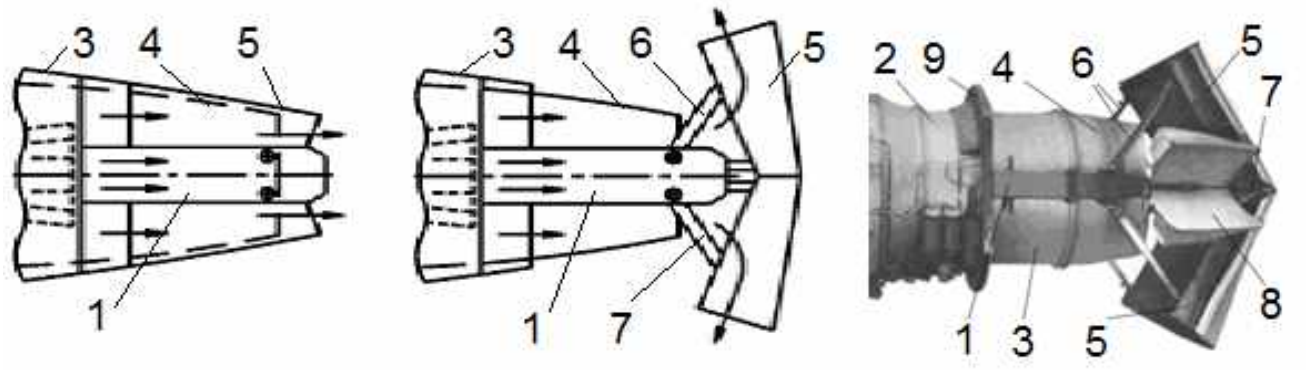


Рис. 5.19. Pre-exit clamshell reverser:
a – normal position; *b* – reverse position;
1 – common jet nozzle; 2 – blocking doors; 3 – hinges of doors

– with turning a flow after the exhaust nozzle (post-exit bucket target reverser, Fig. 5.20).



Normal position Reversing position

Fig. 5.20. Post-exit bucket target reverser:
1 – load-bearing beam; 2, 3 – casing; 4 – jet nozzle; 5 – buckets; 6, 7 – rods;
8 – fearing; 9 – fire protection partition

The first diagram is more complicated and needs special cascades for flow turning and needs sealing between the buckets and gas discharging pipe. But in this diagram less driving force is required, so the pneumatic cylinders may be used.

In the second diagram, the bucket doors, which turn flow, are the structural members of a cowl. This diagram has increased losses because turns the high-velocity flow; the bucket doors must have high strength and rigidity, because they take more loads than in the previous diagram.

Turbofan engines, which bypass ratio is high, are designed without mixing flows of the primary and bypass ducts. Therefore, the thrust reverser is mounted in the bypass duct. This duct is accomplished by the vanned cascades arranged as single members around the engine circumference. In their retracted position they are shrouded at both sides in order not to disturb the interior and exterior flows (Fig. 5.21, *a*). The shroud, together with the rear nacelle, forms convergent nozzle for the fan jet. When extended into the reverse position, the cascade shroud slides backwards, then individual blocker doors swing into the bypass nozzle duct and direct the bypass flow through the retained cascades. The shape of the shields allows turning the flow in forward direction thereby providing reverse thrust (Fig. 5.21, *b*). The value of the reversing factor is 0.22 to 0.25. The examples of this design are thrust reversers of the D-18T, D-436T, and CF-6 turbofans.

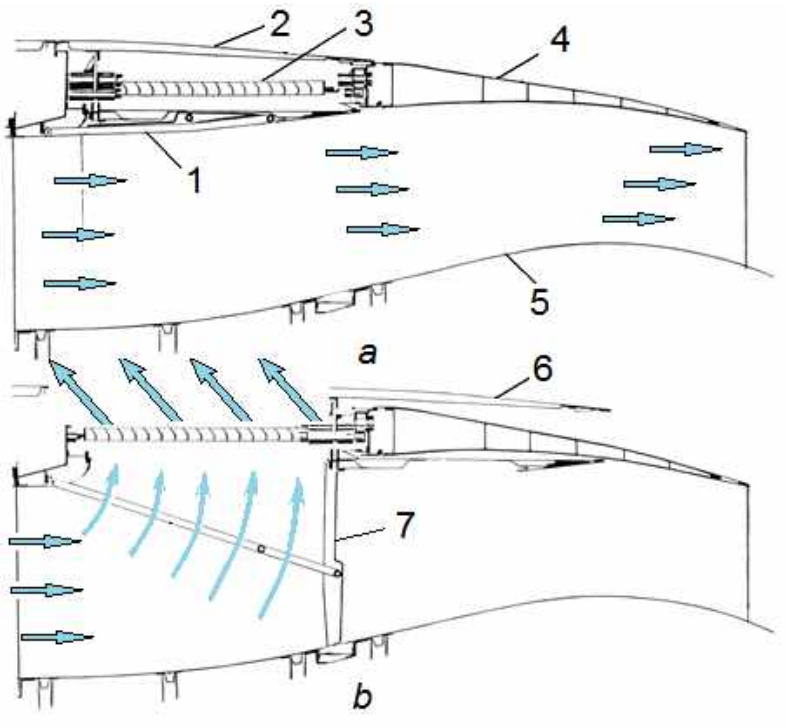
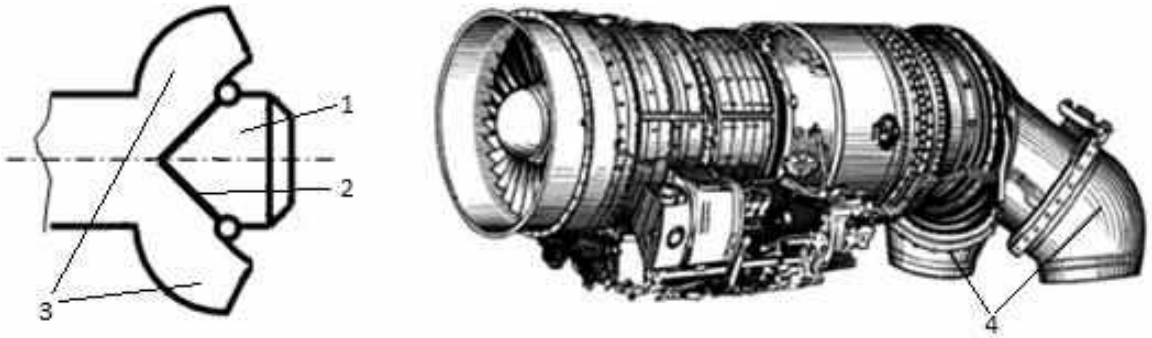


Fig. 5.21. Turbofan thrust reversing in bypass duct:
a – normal position; *b* – reverse position; 1 – blocker door in normal position;
2– cowl in normal position; 3 – cascade; 4 – cowl; 5 – cowl of engine core;
6 – cowl in rearward position; 7 – blocker door extended

5.5.2. Thrust deviators

Thrust deviators are used for the vertical or short takeoff and landing (VSTOL) and maneuverable aircraft. They create vertical component of the thrust and control thrust at the aircraft maneuvers.

There are differed deviators, which design is independent of the main nozzle, and deviators combined with the main nozzle (Fig. 5.22). The first diagram contains deviator nozzles and shuttles, the second one shows the vectoring nozzles.



a *b*

Fig. 5.22. Thrust deviators:
a – with deviator nozzles and shuttles; *b* – with vectoring nozzles; 1 – main jet nozzle;
2 – shuttles; 3 – deviator nozzles; 4 – vectoring nozzles

Fig. 5.23 shows the thrust deviators of the “Pegasus” lift-thrust engine.

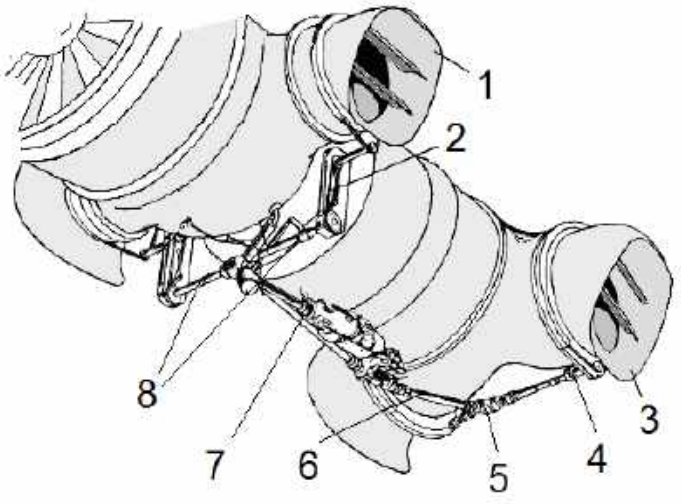


Fig. 5.23. Nozzle control system of the “Pegasus” turbofan:
1 – front nozzle; 2 – intermediate chain drive; 3 – rear nozzle;
4 – universal hinge; 5 – rear conical gear; 6, 7 – shafts of longitudinal transmission;
8 – shafts of transversal transmission

Fig. 5.24 represents composition of the power plant of the vertical-short takeoff and landing aircraft (VSTOL) Lockheed Martin F-35 with lift-thrust engine and lift fan.

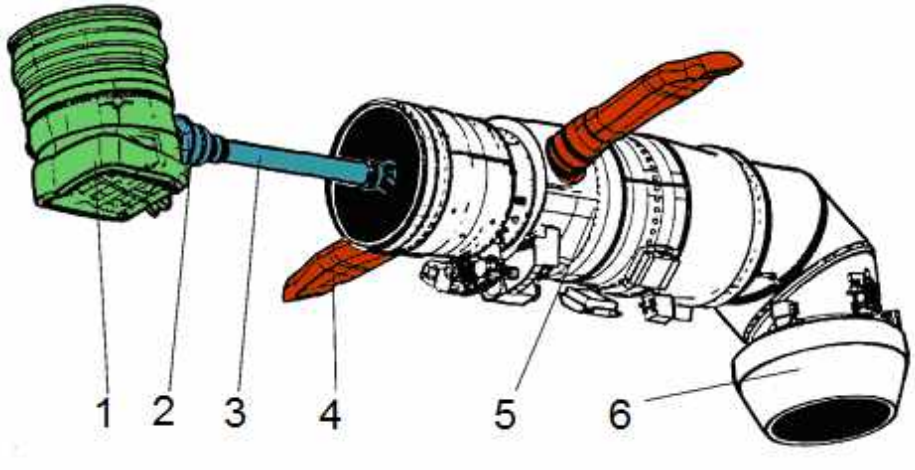
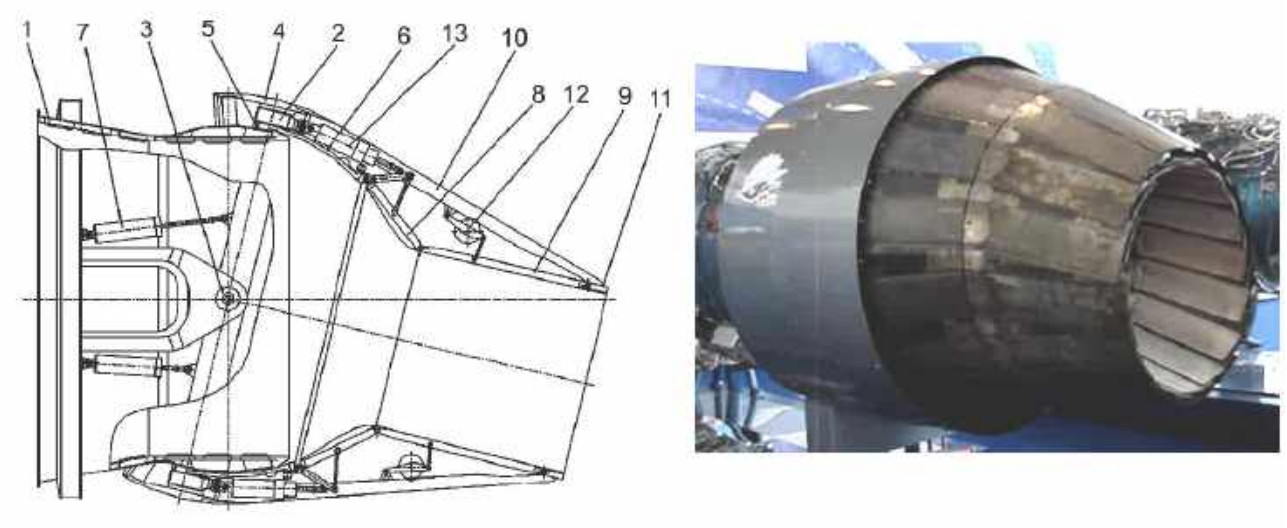


Fig. 5.24. Power plant of VSTOL with Pratt & Whitney F135 engine:
1 – lift fan; 2 – clutch; 3 – transmission; 4 – hose bleeding the air to the aircraft stabilization system; 5 – lift-thrust engine; 6 – vectoring nozzle in a vertical thrust position

Nowadays, are developed and widely used two methods of a nozzle turning: «sphere in sphere» (Fig. 5.25) and individual mechanical driving of all nozzle flaps (Fig. 5.26).

Position of the thrust deviators must provide the thrust vector passing through the aircraft gravity center.



a *b*

Fig. 5.25. Diagram (*a*) and external view (b) of the AL-31FP turbofan jet nozzle:
1 – stationary casing; 2 – movable casing; 3 – axes; 4 – spherical ring;
5 – sealing ring; 6 – nozzle casing; 7 – hydraulic cylinders of thrust vectoring system;
8 – subsonic flaps; 9 – supersonic flaps; 10 – outer flaps;
11 – guides of supersonic flaps; 12 – hydraulic cylinders for exhaust section control;
13 – hydraulic cylinders for critical section control

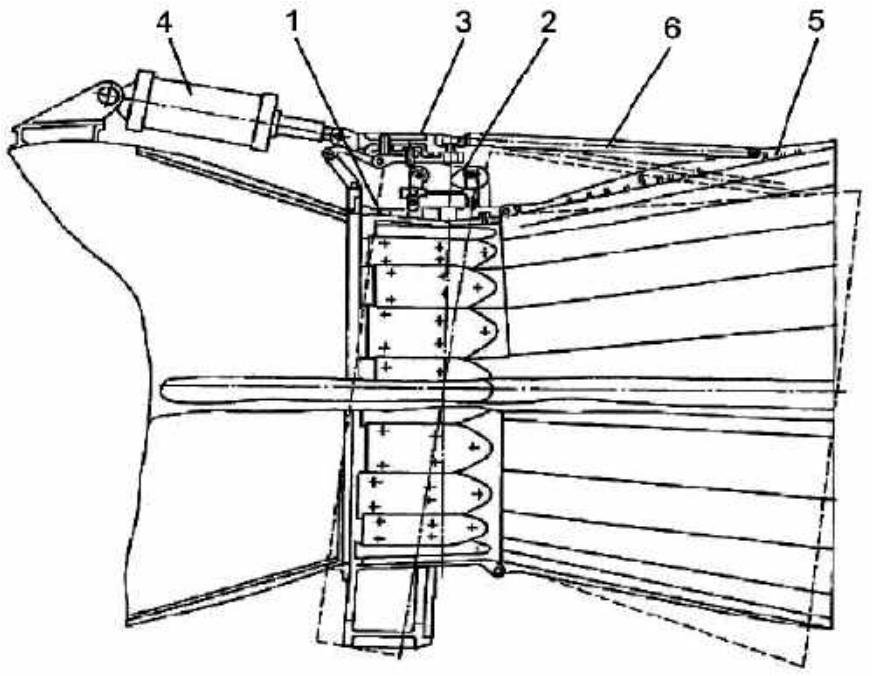


Fig. 5.26. Diagram of the KLIVT (KLImov Vectoring of Thrust) nozzle:
1 – subsonic flaps; 2 – hydraulic cylinders of critical section control; 3 – control ring;
4 – hydraulic cylinders of thrust vector control; 5 – supersonic flaps;
6 – rods for driving supersonic portion

5.6. Power plant as a source of noise and vibration

Modern aircraft engine is a complicated heat machine that consists of many systems, assemblies and parts that are interconnected. Some of these component parts are predisposed to generation of engine vibrations, which are propagated and excite multi-frequency vibrations in other component parts of the engine. The oscillations are transmitted through the engine mounts to the aircraft and cause additional alternating stresses in its structural parts, thus causing fatigue fracture of the aircraft structural members.

Power plant also generates a broadband noise, which can initiate oscillations both in the engine structural members and in the aircraft structure; this is harmful as for strength as for commerce. Acoustic oscillations in the supersonic aircraft can break wing fuel tanks; for example, this fact was taken into account at designing of the MiG-31 aircraft; the prototypes were tested at acoustic load that was generated by the power loud speaker.

The engine vibration as a reaction of the system on action of periodic exciting forces is characterized by a spectrum of the combined structure (Fig. 5.27), which is a combination of a broadband vibration noise (background) and linear spectrum (harmonic components of a set of frequencies f_i).

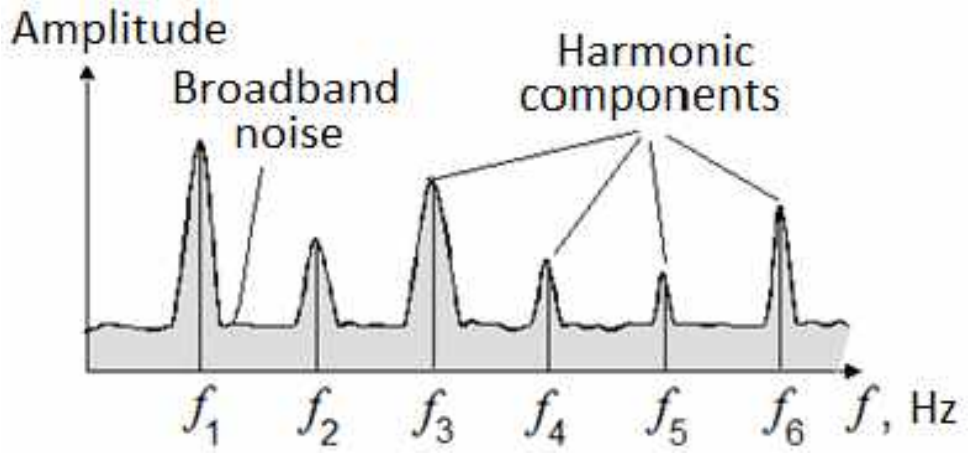


Fig. 5.27. Spectrum of noise and vibrations of gas turbine engine

The main sources of the power plant noise are aerodynamic exciting factors, while the harmonic component is caused by rotation of the engine parts.

The following sources of vibrations are characteristic to the aircraft turbine engine:

– rotor vibration;
– vibration of aerodynamic origin;
– vibration that is excited by processes in the gas flow duct;
– vibration that is excited by the gears;

– vibration of bearing assemblies;
– oscillations of blades, discs, shells (casings of the compressor, turbine, combustion chamber, jet nozzle, etc.).

Aerodynamic vibrations are strong enough. They are generated by the blade-containing component parts: propeller, fan, compressor, and turbine. This vibration is caused by two reasons:

– by non-identity of aerodynamic characteristics of the propeller, fan, compressor or turbine blades;
– by non-uniformity of the air (gas) flow that flows over the blade.

The non-identity of the aerodynamic characteristics gives different thrust and drag forces. When these forces are summarized, besides a thrust force, the non-equalized aerodynamic moment and non- equalized aerodynamic force originate, which are applied to the shaft. Their total action excites the engine vibration, which frequency is equal to the rotor rotational frequency.

Under the real conditions, a propeller (fan) rotates in the non-uniform air flow, which is caused by the aerodynamic members – wing, fuselage, struts of the engine casing, etc. In this case, the vibration is excited with frequencies f that are multiple to the number of blades z:

$$f = i \cdot z \cdot n_{bl} .$$

The total range of these vibrations is broad enough. For example, eight harmonics of the four-blade propeller take 10 to 160 Hz. Vibration of this type is multi-harmonic one. It means that the total vibration signal is a sum of the harmonic functions with different frequency, and more than one of these functions are meaningful.

The less intensive but also enough dangerous is a vibration that is excited by processes in the gas flow duct. This vibration is not rigidly related to the rotor rotational speed and has a wide frequency range – from ($0.3n_s$ to $0.6n_s$) to (500 to 5000) Hz.

The compressor rotated stall, vibration combustion and acoustic oscillations of the gas volumes are the sources of this vibration.

The intensity of vibrations can exceed that of the rotor vibrations under the adverse conditions.

The engine acoustic noise, as a rule, has aerodynamic origin. Among them, the most intensive are noise of propeller (fan), compressor, combustion chamber, turbine, and jet.

The noise of the bladed machines (propeller, fan, compressor, and turbine) have continuous spectrum with the multiple discrete components (Fig. 5.28).



Fig. 5.28. Noise intensity of bladed machines

Noise of continuous spectrum is excited by turbulence near the boundaries of the blades, by vortexes downstream of the blade trailing edge, by a random non-uniformity of the flow at the rotor inlet (the latter may be caused by the air turbulence, by on-board armament shooting or rocket firing, etc.). In the multi-stage bladed machine, these processes are complicated due to a multiple attraction of the discrete noise.

The engine air inlet section generates noise due to interaction between the turbulent jet and walls of the intake duct, and also due to a flow stall when flowing around the struts (Fig. 5.29).

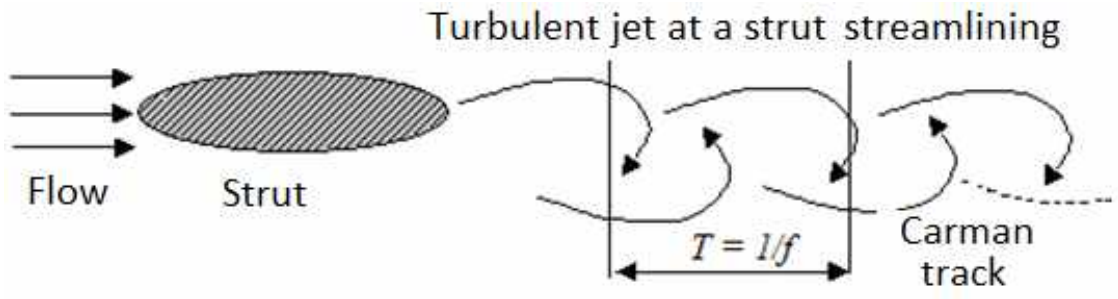


Fig. 5.29. Stall origination at struts and blades streamlining

The noise frequency at a stall is determined as

$$f = 0.212\left(1 - \frac{21.2}{Re}\right)\frac{w}{d},$$

where Re is Reynolds number;
w is flow relative velocity;
d is characteristic diameter.
The characteristic diameter for struts and blades is determined as

$$d = \sqrt{\frac{2.8\delta}{\pi}},$$

where b is chord;

δ is the maximal thickness.

Noise of the exhaust system is generated when the exhaust gas jet is mixed with the ambient air (Fig. 5.30).

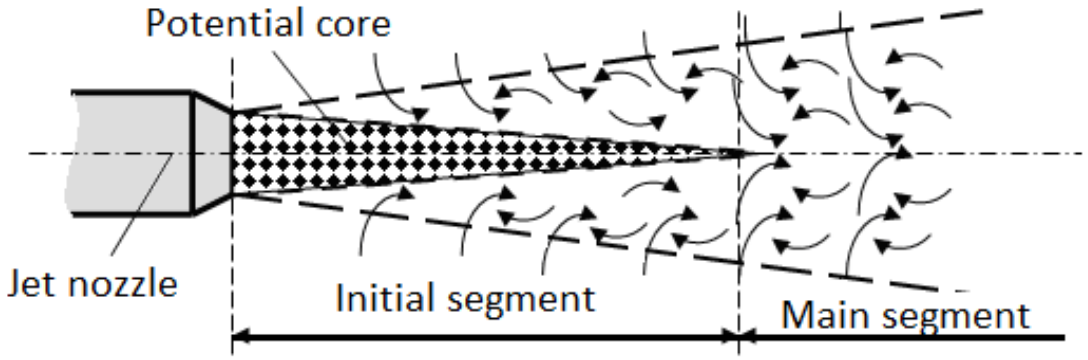


Fig. 5.30. Noise of jet origination

The noise intensity depends on a diameter of the outflowing jet (diameter of the jet nozzle) and its velocity. An acoustic power of subsonic jet W can be determined as

$$W = k\frac{\rho C_N^8 d_N^2}{a^5},$$

were $k \sim (0.3 \text{ to } 2.0)\ 10^{-4}$ is experimental constant;

d_N is diameter of the nozzle exit section;

C_N is average velocity of the gas outflow;

a is velocity of sound.

Frequency range of this noise is broad enough – 50 to 100 kHz, the maximum power depending on the jet outflow velocity is within a frequency range 1.5 to 15.0 kHz.

At normal operation, the combustion chamber generates a broadband noise, which is generated by the vortexes in a reverse flow zone. At off-design power ratings, the noise is supplemented with components of the gas oscillations due to vibration combustion, self-oscillations, and non-uniform fuel supply.

Acoustic noise of the engine is propagated in the air substance mainly in the front sector from the side of the intake duct and in the rear sector downstream of the jet nozzle (Fig. 5.31).

The noise is also propagated through the engine design structure away from the engine; this is related to the partial attraction and absorption of the sonic waves by the structural members (casing, bypass duct, and nacelle).

The irritant effect of the aircraft noise on a human depends mainly on the frequency performances and duration of the noise action.

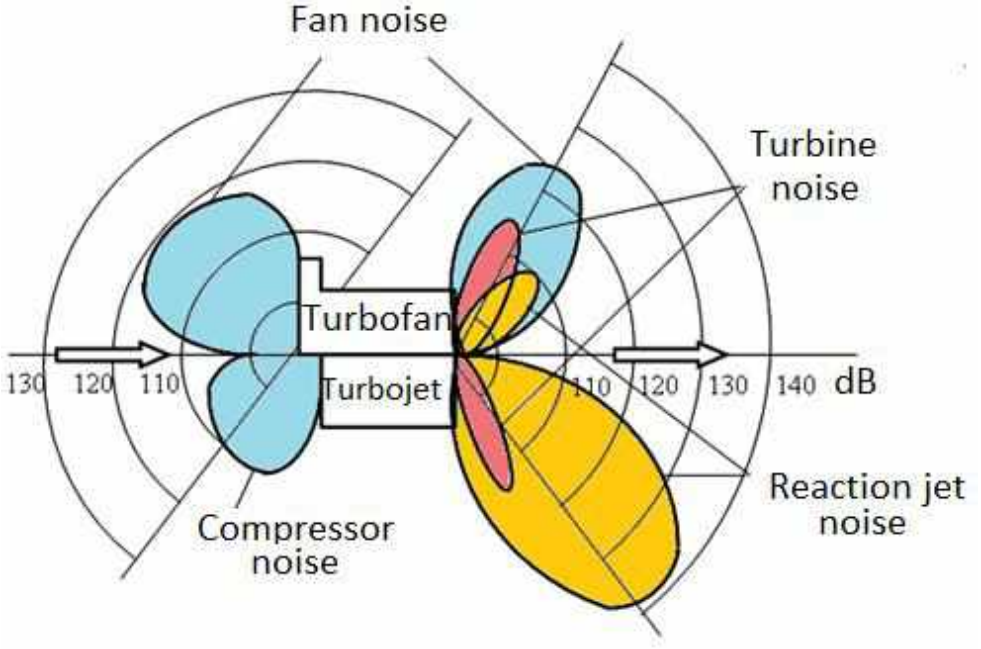


Fig. 5.31. Engine noise propagation

The aircraft noise is usually estimated by the following criteria: perceived noise level (PNL), dB, and effective perceived noise level (EPNL), dB. The most adverse for human is the noise at a frequency 3000 to 5000 Hz. The PNL criteria estimates by one number the irritant effect of the noise taking into account its frequency composition; besides, the EPNL criteria takes into account duration of the noise.

The noise performances of the engine in the aircraft can be estimated numerically, but experimental methods are preferable. The sound level meters with filters A, B, C and D are applied. The filter A is the best suited for measurement of acoustic sound for perception by a human. Performance of the filter B is widened to an area of low frequencies. Performance of the filter C is smoothing dependence of acoustic signal level on a frequency in the audible frequencies area. Performance of the filter D provides frequency correction for the aircraft engine noise measurement. For example, when the filter A is applied, a level of perceived noise is PNL = L_A + 13 dB; when the filter D is applied, then PNL = L_D + 7 dB, etc.

The measure of the aircraft noise duration is a time of the noise action from maximum level to a level on 10 PN dB lower than the maximum value.

The noise level is regulated by the National Standards or ICAO Standards depending on the aircraft takeoff weight, number of engines, takeoff thrust etc. The limits of the above-mentioned standards are almost similar, but the requirements of the National Standards are some more tough as compared with the ICAO or FAR (USA) standards.

According to the National Standards or the Limits of ICAO, engine noise in an aircraft is estimated in three checkpoints (Fig. 5.32).

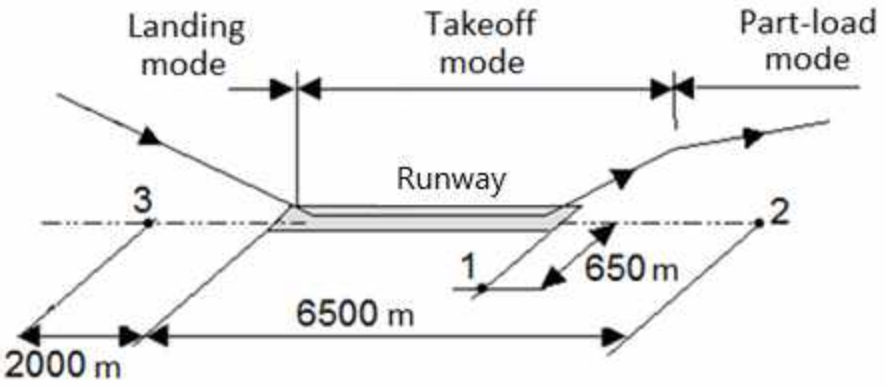


Fig. 5.32. Checkpoints for measurement of the aircraft noise

According to National Standard these points are located:

1) at a distance of 650 m from the runway axis;

2) at a distance of 6500 m from the line of the aircraft running during takeoff;

3) at a distance of 2000 m from the runway landing end.

The rated noise levels depend on the aircraft takeoff weight; according to ICAO Standard, they are as follows:

– at a takeoff (checking point 1) is 95 to 105 dB;

– at a climbing (checking point 2) is 90 to 100 dB;

– at a descending (checking point 3) is 95 to 105 dB.

The standards describe working methods of calculation, measurement and experimental data processing and also advices on the maintenance of old aircraft that not satisfy modern requirements to the engine noise.

There is tendency of toughening of the existing limits to the newly developed engines and aircraft (the applied noise limit is 4 to 10 EPN,dB less than the current norm). The fundamentally important is the decision of ICAO about upgrading of the aircraft aimed at noise abatement of the aircraft that are in service.

Nowadays, the noise abatement and norming of the auxiliary power units (APU) are under investigation. The APU is a power source of a high-frequency noise. Two types of limits are established for them:

– limits to protect the service personal and the persons that are working in the close proximity to the aircraft;

– additional norms to determine areas of impact on the population that is living in close proximity to the airdrome.

The noise level should not exceed 85 dB in places occupied by the servicing personal (luggage hatches, doors, entrance stairs, etc.); the noise of auxiliary power plant should not exceed 85 dB; in other places at a distance of 20 m from the aircraft axis – up to 90 dB.

The problem of the aircraft noise suppression needs in a comprehensive solution that takes into account correlation between members of a system ‘aircraft and engine structure – airport – maintenance conditions’. Therefore, a complex of building and planning procedures is used: planning of directions of the airfields, restriction of buildings near the airport, planning of flight routs above the living areas, etc. Rational organization of the air traffic and special methods of piloting play a significant role: high gradient of climb, high glide angle with optimization of landing profile; throttling of the engines during takeoff; lower power ratings of the engines when flying in waiting area; late extending of the landing gear and full extending of flaps during landing; turning away after takeoff, etc.

Since the main source of the aircraft noise is its engine, the main means on a noise suppression are related to the engine perfecting.

The problem of the noise level decreasing at the engine airdrome testing is enough simple for solving. For this purpose, orientation and disposition of testing areas are determined, airdrome suppressors and screening shields are applied, and methods of engine inspection are improved that decreases the engine running time. Nevertheless, the main role play designing methods that are aimed at reduction of the engine noise level. In the first order, these methods include a choice of the main thermodynamic parameters and program of control.

The main thermodynamic parameters are as follows: engine bypass ratio BPR; compressor pressure ratio CPR; turbine inlet temperature TIT; peripheral circumferential velocity of the first stage of the fan (low pressure compressor). The high bypass ratio (m = 4 to 8) in combination with the moderate circumferential velocity (u = 330 to 350 m/s) decreases the noise level. Engines with high bypass ratio are the most efficient at high degrees of heating, i.e. at high TIT, but the TIT increasing causes high velocity of the jet stream outflow, i.e. to the noise of the jet stream intensification (when temperature increases on 100 K, the noise increases on 3 to 5 dB). The low-noise engine must have limited TIT: T_g^* = 1450 to 1600 K.

High efficient performance of the turbofan engine needs in increased CPR; optimum pressure ratio that corresponds to the minimum fuel

consumption reaches 30 to 50. CPR influences acoustic performances due to the influence of pressure on velocity and density of the gas flow in the jet nozzle, and also on the circumferential velocity and loading of the compressor stages. The low-noise engine must have limited CPR: $\pi^*_{C\Sigma}$ = 20 to 30.

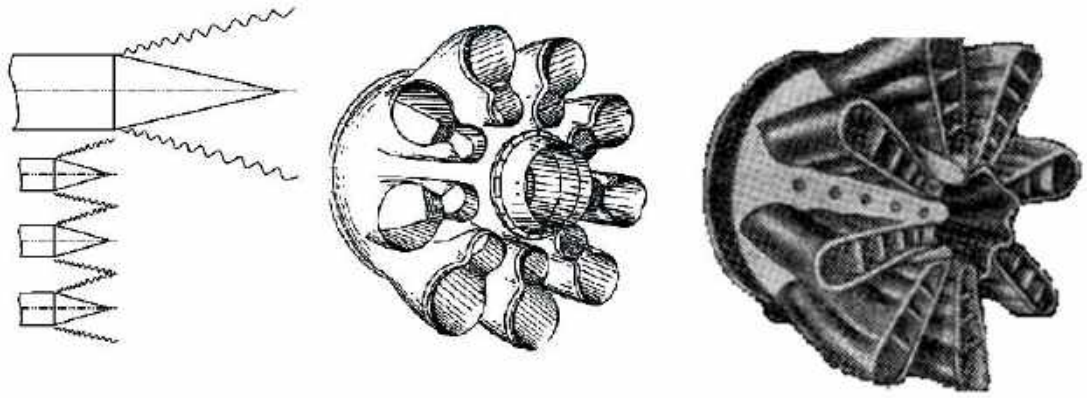
As it is clear from the above consideration of the main parameters, the problem of lightweight, efficient and low-noise engine has not a single solution and needs in compromise solutions.

The noise is also decreased due to the design solutions, in particular, by providing stall-less flow in the intake duct, by increasing the axial clearances between stationary and rotary parts, by optimum choice of the number of the compressor guide vanes and turbine nozzle guide vanes, by using a single-stage fan without the inlet guide vanes, by optimum profiling of the outlet duct. Special noise suppression members are included into the design, such as noise absorbing panels of a nacelle and the engine stator, noise suppressors in exhaust systems.

The major source of noise in the pure jet engine and low bypass ratio turbofan is high-velocity jet stream of the exhaust gas, which mixes with the atmospheric air. Power of noise is proportional to the nozzle exhaust area and to velocity in eights power. Therefore, reduction in noise level takes place if the mixing rate is accelerated or if the velocity of the exhaust jet relative to the atmosphere is reduced.

This is achieved by increasing the contact area of the atmosphere with the exhaust gas stream by using exhaust nozzle incorporating several corrugated or lobe-type noise suppressors.

In the lobe-type exhaust nozzle (Fig. 5.33), the exhaust gases are divided to flow through the lobes and small central nozzle. This forms a number of separate exhaust jets that rapidly mix with the air entrained by suppressor lobes. This principle can be extended by the use of a series of tubes to give same overall area as the basic circular exhaust nozzle.



a *b*

Fig. 5.33. Operation principle (*a*) and general view (*b*) of noise suppressors

In the corrugated exhaust nozzle, free stream of the atmospheric air flows down the outside corrugations and into the exhaust jet to promote rapid mixing. Principle of noise suppression in the high-bypass ratio turbofans with separate flows is the same as for the pure or low-bypass ratio engine. Both exhaust nozzles of these engines are equipped with chevron-shape trailing edges, which improve mixing (Fig. 5.34).



Fig. 5.34. Corrugated (chevron-type) nozzles of high-bypass turbofan

Naturally, this jet nozzle has less noise at takeoff, but the fuel consumption at cruise is somewhat higher. Therefore, there are attempts to design the noise suppressors that are moved off the gas flow duct at cruise power ratings (Fig. 5.35).

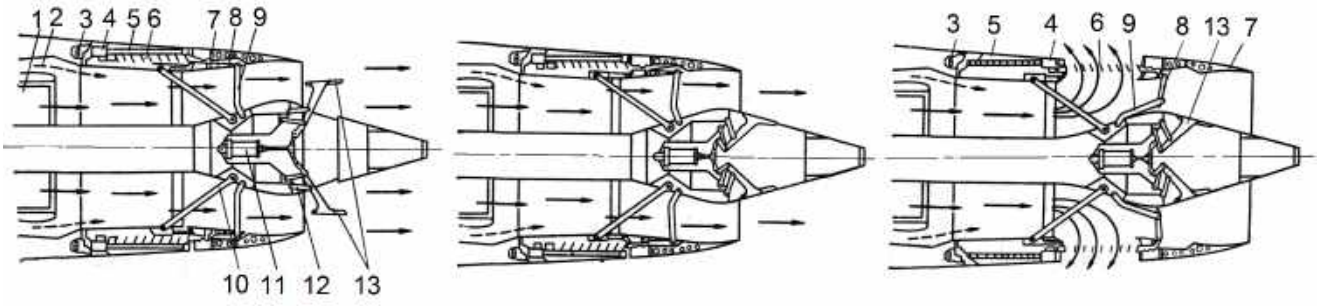


Fig. 5.35. Combined reverser-noise suppressor of SNECMA Company:
a – takeoff power rating, noise suppression; *b* – cruise power rating;
c – landing, thrust reversing;
1, 2 – flows of the internal and external air; 3 – attachment of cascade and exhaust nozzle driving mechanism; 4 – mechanism attachment nut; 5 – lead screw; 6 – reverse cascade; 7 – exhaust nozzle; 8 – reverse doors ; 9 – doors driving lever; 10 – central body driving rods; 11 – pneumatic cylinder of noise suppressor blades driving mechanism; 12 – control rods; 13 – vane

Unfortunately, noise suppression leads to some worsening of cost and maintenance qualities of all the aircraft. For example, the noise level of one airplane with takeoff weight 78 tons was 100.4 to 101.2 dB at takeoff and climbing, and 108.2 to 109.9 dB at approach and landing. After designing of the noise suppression system, the noise level became 90.5…92.5 dB at takeoff and climbing, and 96.0…97.5 dB at descending and landing. This is perfect. But the takeoff weight had increased by 2000 kg, flight distance became 510 km less (17.5 %) and cost of the airplane became 800 thousand dollars more.

5.7. Infrared radiation suppressors

Modern tools for air targets detection use infrared radiation of engines as a signal to identify the aircraft, that makes aircraft attackable by the rockets equipped with the self-direction heat heads.

The major members influencing the intensity of the engine heat radiation are as follows:

– blades of the last turbine stage;
– internal surfaces and structural members of the afterburner and jet nozzle located in the gas flow duct;
– jet of the high-temperature nozzle exhaust gas.

Infrared perceptibility may be decreased by various methods that are implemented in the exhaust system design:

– shielding of the direct IR-radiation of engine hot structural members (turbine blades, struts of exhaust duct, etc.) by the cooled central body with curved exhaust duct;
– mixing of the exhaust gas flow with cold atmospheric air (for the ATFE at non-afterburning power ratings) or with the air of bypass duct (for the ATFE);
– cooling of hot surfaces of the engine gas flow duct to a temperature that is close to that of the aircraft surface, by using air film cooling;
– covering of hot internal and external surfaces of the exhaust system by materials with low radiating capacity.

Figs 5.36, 5.37 represent diagrams of the exhaust duct with the IR-radiation suppression systems.

Efficient decreasing of the IR-radiation at non-afterburning power ratings is given by the flat nozzles with screening hot members of the gas flow duct and intensive mixing of the flat exhaust stream with atmospheric air.

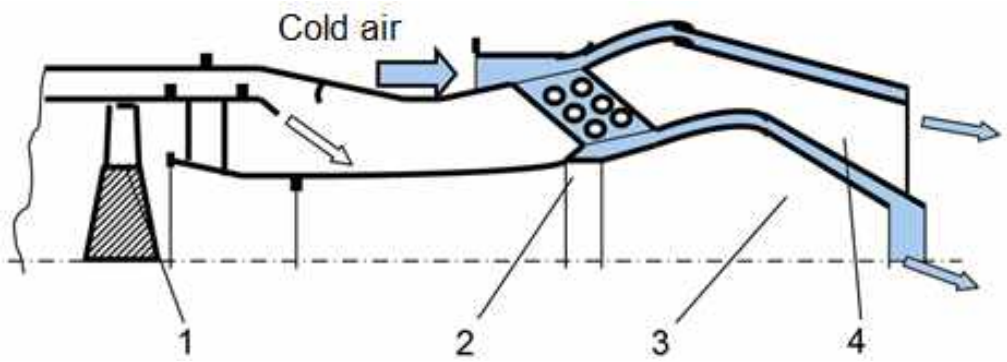
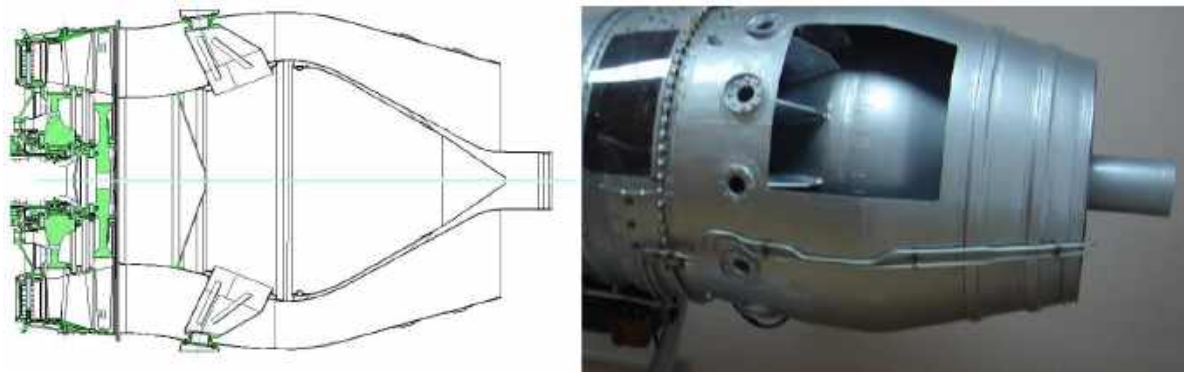


Fig. 5.36. Exhaust system with low IR-radiation:
1 – turbine blade; 2 – cooled struts; 3 – cooled central body;
4 – cooled external cowling



a *b*

Fig. 5.37. Exhaust system with IR-radiation suppression
(the R-195 turbojet of the attack plane Su-25):
a – longitudinal section; *b* – external view

Fig. 5.38 shows diagram of the F-404-GE-402 turbofan for «unobtrusive» aircraft Lockheed F-117A. In this system, traditional circular jet is converted into a flat jet of rectangular shape and flows away at high velocity through a slot in the tail portion of the fuselage, i.e. directly through the airframe design. This decreases noise and IR-perceptibility.

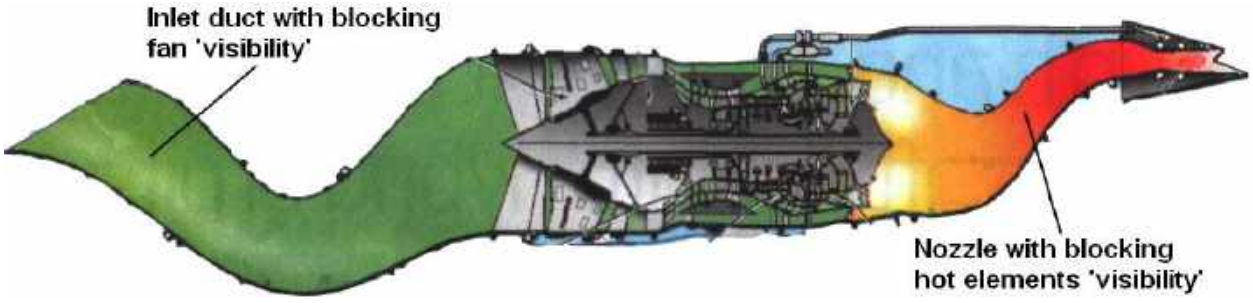


Fig. 5.38. Scheme of the F404-GE-F1D2 General Electric turbofan
of the «unobtrusive» aircraft Lockheed F-117A

Some nozzle component parts are honeycomb panels made of the nickel alloy. This material has high strength and resistance for acoustic and heat loads.

5.8. Structural materials

Materials for component parts of the exhaust systems operate at temperatures of 650 to 900 ºC. Therefore, the component parts for operating temperature 650 to 750 ºC are made of heat resistant steel 12Х18Н9Т or the heat-resistant steel cast with niobium Х18Н11Б (ЭИ-402); for higher operating temperature nickel heat-resistant alloys ХН78Т (ЭИ-435), ХН75МБТЮ (ЭИ-602), and ХН60БТ (ЭИ-868, ВЖ-98) are used. The external shields are made of the titanium alloys, for example ОТ4-1.

5.9. Check questions

1. Types of the exhaust systems, their purpose and requirements to them.
2. Structural members of the exhaust systems.
3. Specific features of the exhaust systems for the turboprop engines.
4. Specific features of the exhaust systems for the turboshaft engines.
5. What is function of the mixer? What types of the mixers do you know?
6. What is the differential between convergent and Laval nozzles? Name areas of their application.
7. What methods are used for nozzle area variation in the variable nozzles?
8. What is a principle of ejector nozzle operation? Name advantages of these nozzles.
9. How are synchronized the nozzles driving mechanisms?
10. What is the reverse factor?
11. Describe types of the thrust reversers.
12. How does the thrust reverser of high bypass ratio turbofan operate?
13. Function and types of the thrust deviators.
14. Name main principles of the engine noise suppression.
15. Types of the noise suppressors and their operation.
16. Name main principles of improvement of the engine infrared perceptibility.
17. Name cooled structural members of the exhaust systems and methods of their cooling.
18. What materials are used in the exhaust systems?

6. AFTERBURNERS OF THE AERO ENGINES

Turbojet engines of supersonic airplanes need in significant thrust increasing (45 to 60 % over maximum non-afterburning thrust at takeoff and 130 to 170 % at supersonic flight). This allows sound barrier overcoming, takeoff distance shortening, acceleration time shortening, climbing capacity improving. This thrust increasing is provided due to implementation of the afterburner.

Afterburning is the best method of thrust augmentation because provides significant thrust increasing at moderate increasing of dimensions and weight.

Afterburning mode is uneconomical, but significantly improves the aircraft performances.

6.1. Functions of the afterburners

The afterburner is located downstream of the last stage of turbine and provides additional burning of fuel, thus increasing the gas heat capacity and velocity for thrust augmentation.

Flow entering afterburner is a mixture of the gas flowing from the turbine and air flowing from the bypass duct. The fuel/air mixture in the afterburner is close to the stoichiometric one, the air/fuel ratio α_{Σ} = 1.1 to 1.3; therefore, the temperature in the burning zone is high and reaches 2050 to 2200 K.

Design of the afterburner must ensure:

- operation at high temperature in contact with the chemically active gas;
- stable combustion at all power ratings (required range of stable operation by a mixture composition is from $\alpha_{\Sigma\,min}$ = 0.7 to 0.9 to $\alpha_{\Sigma\,max}$ = 2.0 to 2.5);
- reliable afterburning starting at all allowable altitudes and speeds;
- no influence on the gas generator operation;
- prevent turbine rotor blades overheating at afterburning starting, operation and deactivation;
- minimum hydraulic and heat losses;
- minimum weight.

6.2. Design of afterburners

Afterburner consists of the combustor dome and combustion chamber (Fig. 6.1).

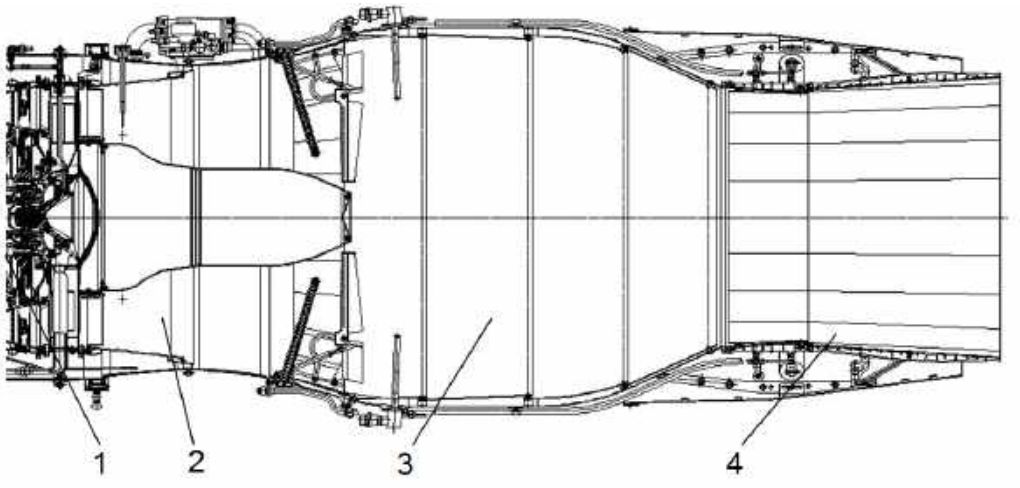


Fig. 6.1. Afterburner and jet nozzle of the ATFE:
1 – turbine; 2 – combustor dome; 3 – combustion chamber; 4 – variable jet nozzle

6.2.1. General information

Afterburner turbofan engines can be designed by different diagrams: with afterburning in the bypass duct (ATFE-II); with separate afterburning in the bypass and primary ducts (ATFE-I+II); with mixing flows of the primary and bypass ducts and common afterburner (ATFEmix). The last diagram is most widely used. The examples are the engines AI-322 ("Ivchenko-Progress" DB, the L-15 trainer-combat airplane), RD-33 ("V. Klimov" DB, the Mig-29 fighter), AL-31F ("A. Lulka" DB, the Su-27 fighter), D-30F6 ("Aviadvigatel" DB, the Mig-31 fighter), NK-25, NK-32 ("N. Kuznetsov" DB, the Tu-22M, and Tu-160 bombers).

Fig. 6.2 shows diagrams of parameters variation along the whole length of the afterburner.

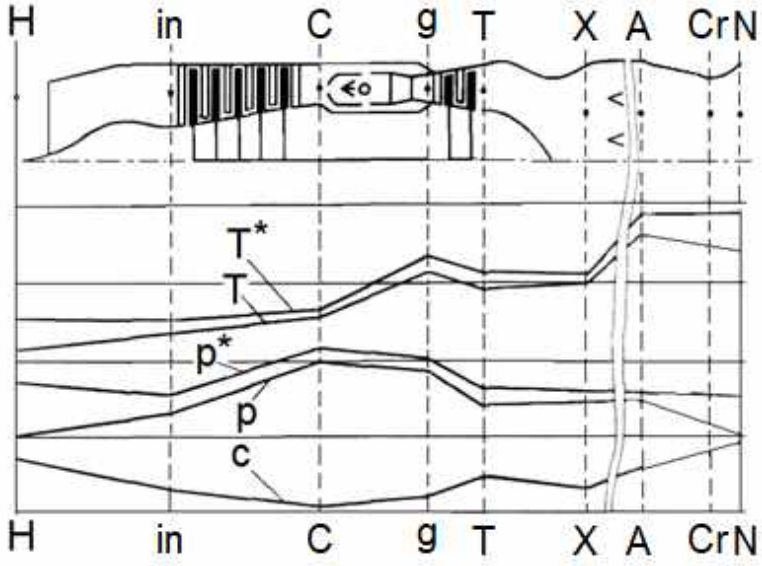


Fig. 6.2. Variation of parameters in the gas flow duct of a single-shaft afterburner turbojet

Three afterburning modes are differed: full, partial and minimum. The full afterburning mode is applied to accelerate the aircraft and reach maximum supersonic velocity. The partial afterburning is used at intermediate supersonic velocities. The minimum afterburning is used as the afterburning idle – the mode with the minimum afterburning fuel flow and minimum afterburning thrust.

All afterburning modes are higher than the maximum mode; therefore, they are harder. Duration of the continuous operation at these modes is similarly to the maximum one.

6.2.2. Why the afterburner is not provided with the flame tube?

The afterburner is an additional combustion chamber. It follows the same physical laws and principles of operation as the main combustion chamber. Therefore, to answer the question about absence of the flame tube, we must remember why the main combustion chamber needs the flame tube. And may be, the main reason of its application in the main chamber is not available in the afterburner.

Look at the Chapter 4 about the main combustion chamber, and you will understand that the purpose of the flame tube is providing a stable combustion.

The combustion is stable within a certain range of the excess air/fuel ratio:

$$0.5< \alpha <1.7.$$

The temperature of combustion within this range is very high (higher than 2200 K). Therefore, for ensuring operability of the turbine, we supply to the combustion chamber excess amount of the air, and actual air/fuel ratio is 2 to 3. This is out of the range of stable combustion.

For providing stable combustion in the main combustion chamber and specified value of the turbine inlet temperature, we separate the air that enters the combustion chamber into two portions and supply into the burning zone only primary air, thus supporting α in this zone close to one.

The design member that makes this separation is the flame tube. Of course, it significantly increases total weight of the combustion chamber and makes its structure more complicated.

In the afterburner, we combust the fuel in the gas that goes from the turbine. This gas contains less amount of oxygen, because a part of the oxygen is already used in the main combustion chamber. Therefore, the air/fuel ratio at the inlet to the afterburner is approximately by one unit less than in the main combustion chamber. Therefore, we do not need separation in the burning zone.

This is the main reason than makes possible to exclude the flame tube from the afterburner design structure. It becomes simpler and lighter.

6.2.3. Combustor dome of the afterburner

The combustor dome includes diffuser, flame stabilizers, fuel supply system, and igniter (Fig. 6.3).

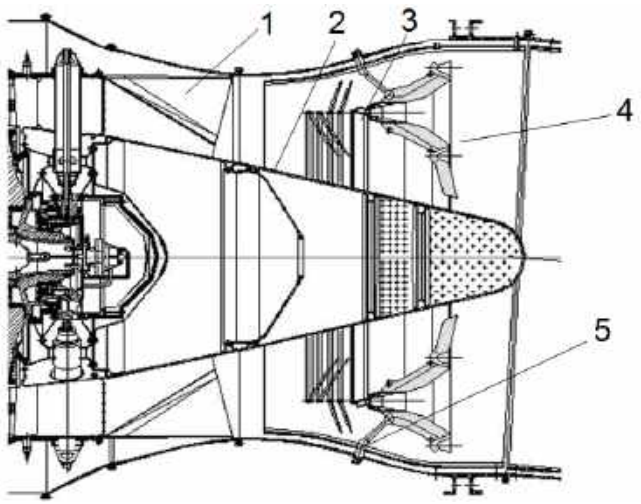


Fig. 6.3. Combustor dome of TFE afterburner:
1 – mixer; 2 – turbine disc cowl; 3 – fuel nozzles; 4 – flame stabilizer;
5 – diffuser outer cowling

Diffuser decreases the gas flow velocity for stable combustion of the afterburning fuel. It is located directly at the turbine outlet. Exhaust area and length of the diffuser decrease the flow velocity from 300 to 400 m/s to 150 to 200 m/s at optimum combination of the hydraulic losses, dimensions and weight. The optimum angle of diffuser opening is 8º to 12º, ratio of the inlet and discharge areas is within a range of F_2/ F_1 = 1.3 to 2.3.

Ring-shaped channel of the diffuser is created by a turbine disc cowl and outer cowling that are interconnected by the struts (Fig. 6.4) or hinged rods (Fig. 6.5).

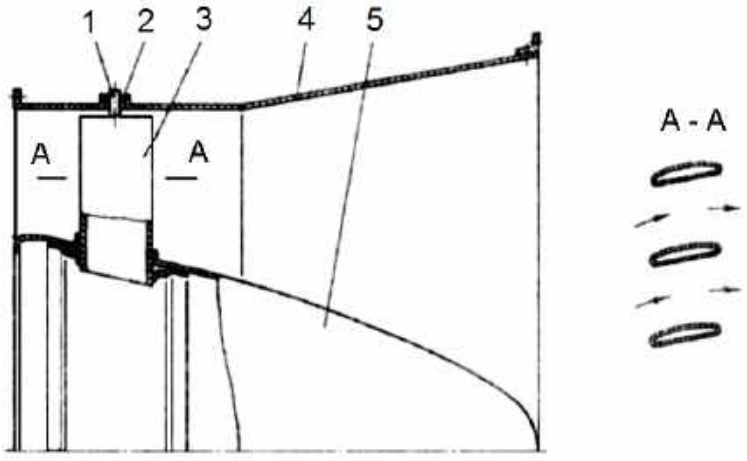


Fig. 6.4. Diffuser with restraining turbine disk cowl by struts:
1 – pin; 2 – spherical sleeve; 3 – strut; 4 – external cowl; 5 – turbine disk cowl

The junction must provide freedom of thermal deformations. Generating lines of the diffuser walls are profiled to minimize the hydraulic losses at the minimum length. To satisfy this condition, the inner wall is sometimes designed truncated, thus making a stall diffuser with sudden expansion (Fig. 6.5).

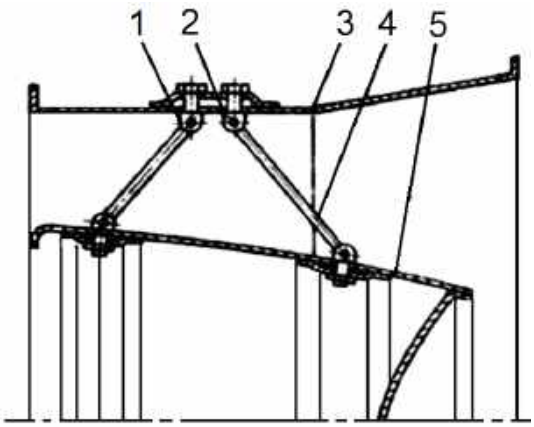


Fig. 6.5. Diffuser with restraining turbine disk cowl by hinged rods:
1 – binding band; 2 – rod fixing hinge; 3 – external cowl; 4 – rod; 5 – turbine disk cowl

Turbulent velocity of flame propagation is 10 to 15 m/s, flow velocity at diffuser discharge is 150 to 200 m/s. Therefore, a stable combustion in afterburner is impossible without special devices named as **flame stabilizers.** They provide a stable position of the flame front in the chamber preventing its drifting by the gas flow.

The most widely used are flame stabilizers made as a bluff body – chute of V-shape profile made of sheet material. They have angle of 30º to 60º directed upstream. Zone of reverse flows originates after the flame stabilizer in which products of combustion circulate at a temperature of 1500 to 2000 ºC. The zone of reverse flows has high-temperature and is a source of heat for continuous burning of fresh portions of the fuel-gas mixture that enters the afterburner. Wall of the stabilizer is cooled from outside by the flow of cold gas and afterburning fuel.

The flame stabilizers have a shape of ring, radial or radial-ring (Fig. 6.6).

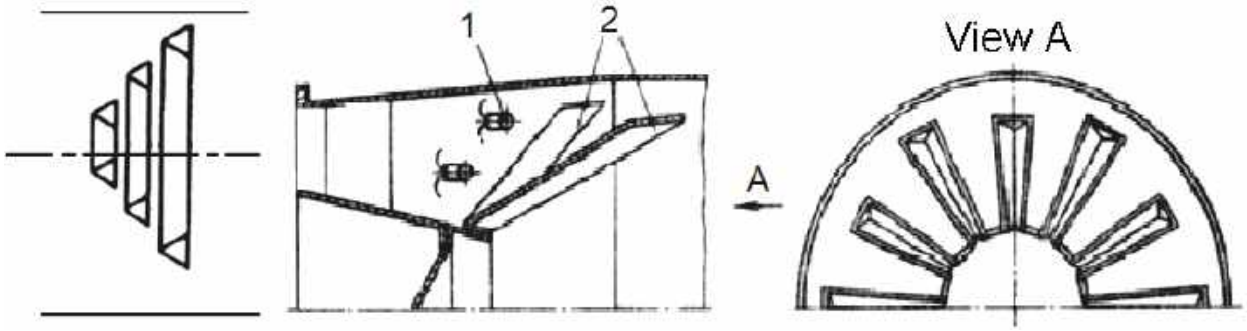
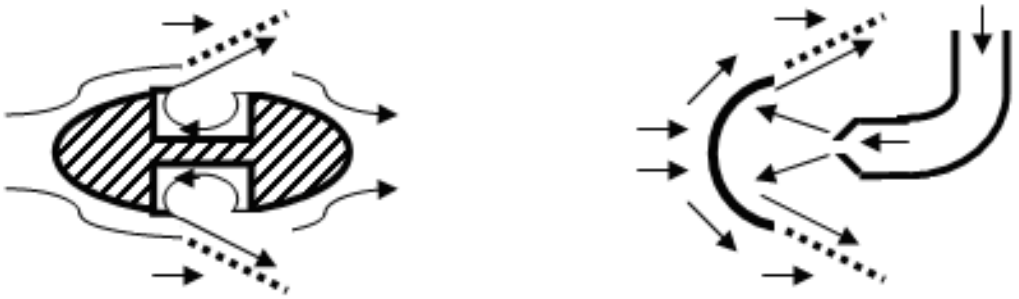


Fig. 6.6. Flame stabilizers:
1 – fuel manifolds with fuel nozzles; 2 – V-shape stabilizers

Shape of the stabilizers depends on specific feature of the engine and its afterburner, but also on a requirement of prevention of a dangerous vibration combustion.

Flame stabilizers significantly overcharge section of the afterburner (up to 20 to 25 % of its area). Hydraulic losses are decreased if the stabilizers are displayed one to another streamwise. Stabilizers with streamlined shape may be used; these stabilizers are pocket and aerodynamic ones (Fig. 6.7).



a *b*

Fig. 6.7. Pocket (*a*) and aerodynamic (*b*) stabilizers

It is difficult to provide stable inflaming and combustion of the fuel in the afterburner by using simple stabilizers. Therefore, special pre-combustion flame stabilizers may be used. The pre-combustion chamber is a small combustion chamber with low-velocity flow – approximately 10 to 20 m/s (Fig. 6.8). It provides good inflaming and stable combustion. The hot gas from the pre-combustion chamber is supplied to zones of the afterburner with complicated inflaming and combustion.

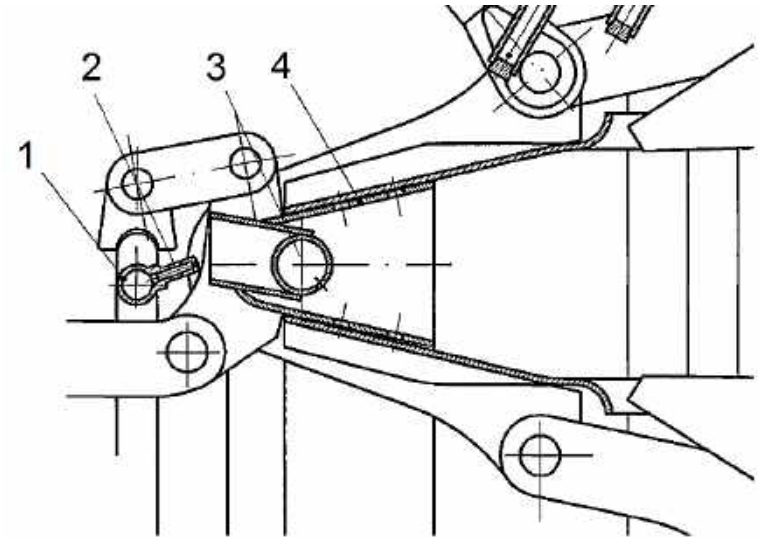


Fig. 6.8. Pre-combustion flame stabilizer:
1 – fuel manifold; 2 – fuel nozzle; 3 – vapor gutter; 4 – pre-combustion chamber

6.2.4. Fuel supplying and combustion

System of fuel supplying and mixing supplies the liquid fuel into the afterburner, where it is sprayed and partially evaporated to create a flammable mixture and to create required fuel distribution in the chamber. The mixing system includes supplying pipes and fuel manifolds, fuel spray nozzles and vapor gutters (carburetors).

Liquid fuel is sprayed by the centrifugal or jet nozzles welded to the fuel manifold. The centrifugal nozzles are oriented upstream, jet nozzles – crosswise or under an angle to a flow. The fuel is fragmented on small droplets by the gas stream.

The fuel manifolds are usually located upstream of the stabilizers at a distance 100 to 150 mm. Their restraining provides freedom of thermal deformations. The restraining members actually are the radial pins or hinged links (Fig. 6.9).

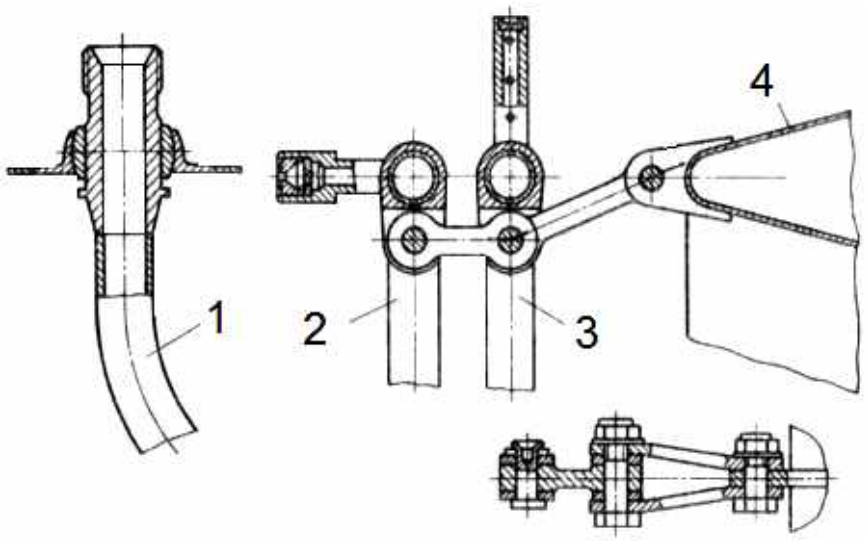


Fig. 6.9. Flame stabilizer with two cascades of fuel manifolds:
1 – pipe for supplying fuel to manifold; 2 – fuel manifold of the first cascade;
3 – fuel manifold of the second cascade; 4 – flame stabilizer

Such position of the nozzles ensures mixing of fuel with the maximum amount of the gas and vaporizing a lot of liquid droplets before the mixture reaches stabilizers, and also provides the maximum width of flame. Non-vaporized fuel droplets enter a surface of the stabilizer and create a liquid film, which flows from its rear walls and provides more rich mixture in a zone of the reverse flows. This improves stability of combustion in the afterburner.

Final choice of the stabilizers dimensions and disposition, number and disposition of the fuel nozzles is determined experimentally during afterburner development.

Devices for vaporizing liquid fuel (vapor gutters) are placed inside the stabilizer (Fig. 6.10). They provide stable operation of the afterburner with lean mixtures at $\alpha_{\Sigma} \geq 3$.

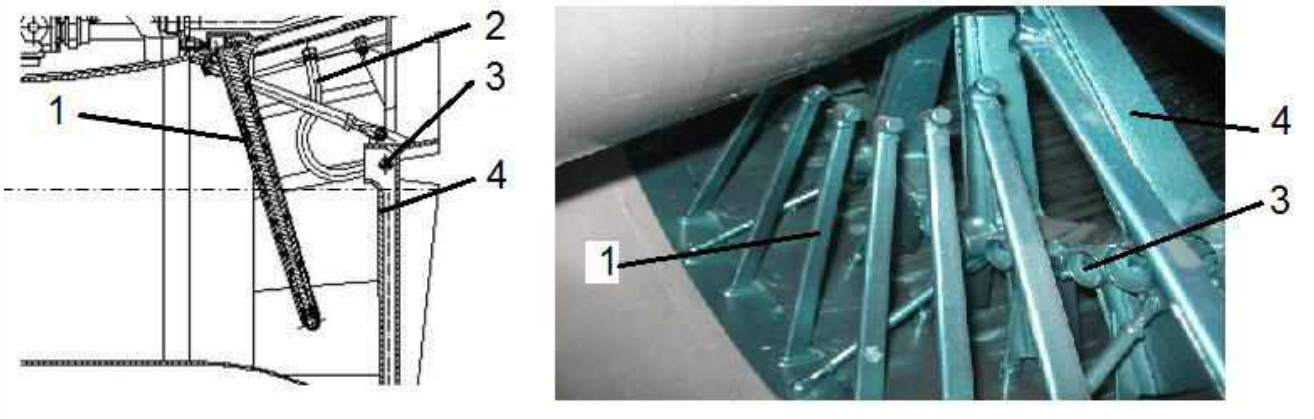


Fig. 6.10. Stabilizer with vapor gutter:
1 – fuel jet nozzle; 2 – fuel supply pipe; 3 – fuel manifold of stabilizer;
4 – flame stabilizer

The mixture is i**nflamed** in the afterburner by the igniter that is located on the axis of the combustor dome (Fig. 6.11), or by a special starting igniter that is located on the outer casing (Fig. 6.12).

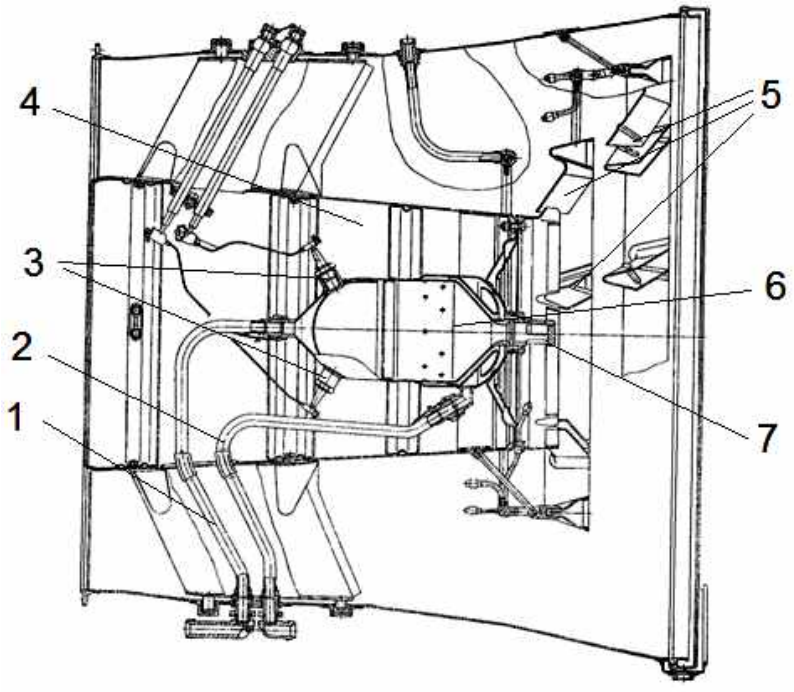


Fig. 6.11. Igniter of afterburner:
1 – air supply pipe; 2 – premixed fuel-air mixture supply pipe;
3 – electric sparking plug; 4 – turbine disc cowl; 5 – flame stabilizers;
6 – combustion chamber; 7 – flame spreader

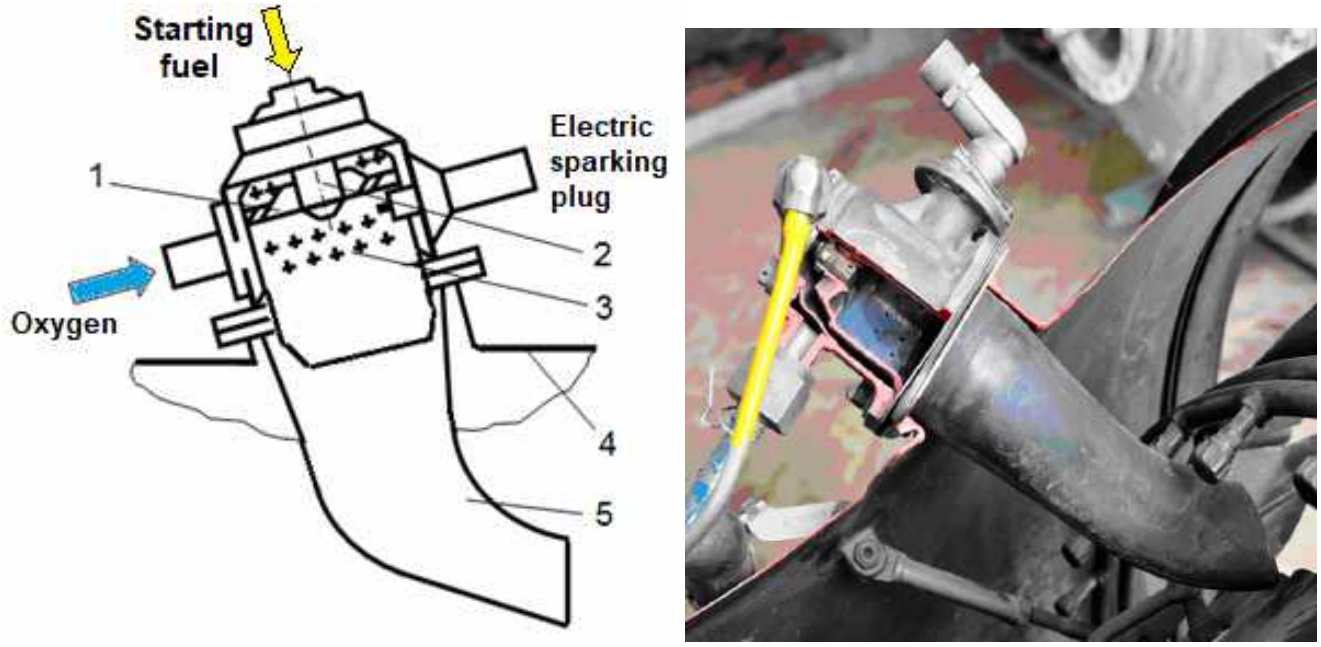


Fig. 6.12. Starting igniter of afterburner:
1 – vortex generator; 2 – starting fuel nozzle; 3 – oxygen supplying holes;
4 – combustor dome casing; 5 – flame propagation tube

The starting fuel is ignited in the igniter by an electric sparking plug. The air taken from the engine compressor or the oxygen from on-board pressure vessels is supplied to the igniter and facilitates ignition. Special branch pipe directs a flame into a zone of the maximum intensive swirling of flow where the energy of ignition is the minimum one.

Simple but high thermal power system is used in modern ATFE; this system is named the **'hot-shot' ignition system** (Fig. 6.13).

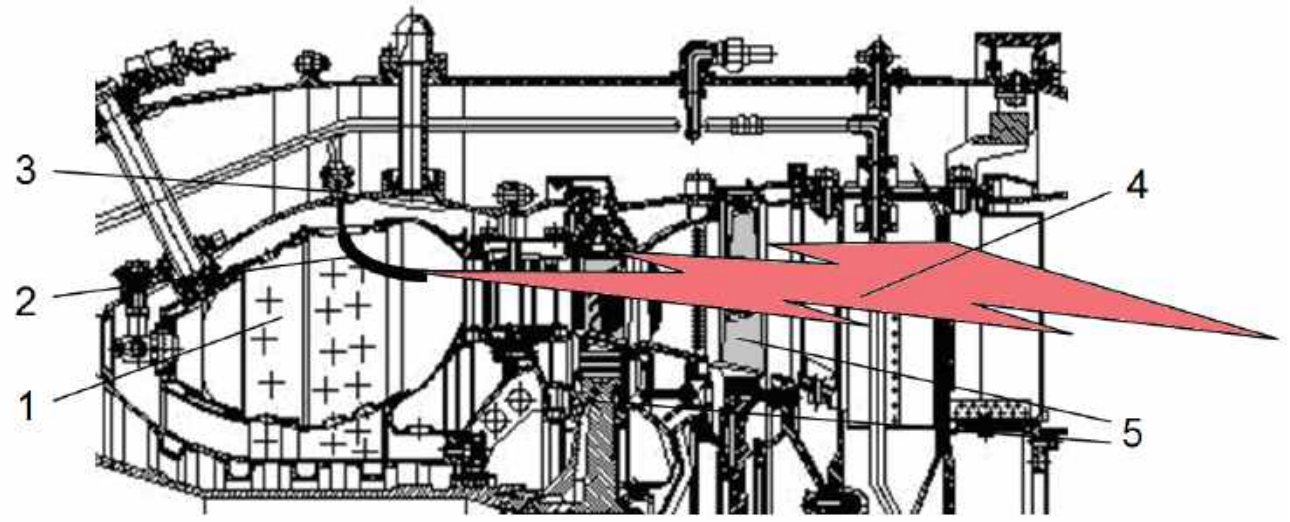


Fig. 6.13. Starting afterburner by 'hot-shot' ignition system:
1 – flame tube of the main combustion chamber; 2 – fuel jet;
3 – starting fuel nozzle; 4 – flambeau; 5 – turbine stages

This system contains a starting fuel jet nozzle that is located at the end of the main combustion chamber and is directed aside a turbine. When the starting fuel flows through the turbine, it is vaporized under the action of high temperature, thus creating a power flambeau at the turbine discharge. This system operates during the afterburner starting for a short period of time (0.2 to 0.5 s), thus preventing significant overheating of the turbine blades.

In the engines of the fifth generation, the afterburner is activated by the plasma igniters without supplying additional oxygen.

Afterburner actuation at low inlet temperature is facilitates by using **catalytic igniters** and nozzles with ultrasonic spraying (Fig. 6.14).

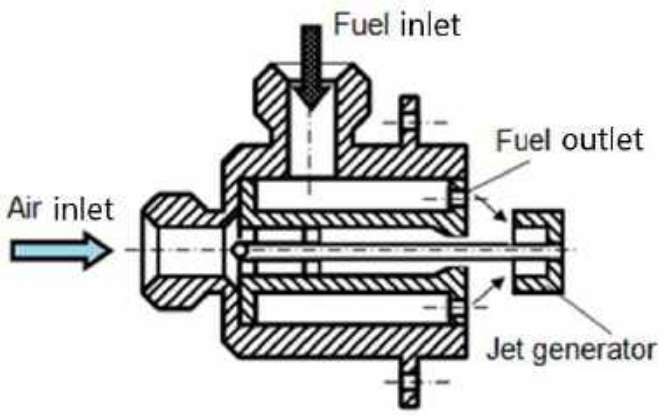


Fig. 6.14. Ultrasonic nozzle

Combustion chamber is cylindrical, conical or spherical envelopes welded of a heat resistant sheet material (Fig. 6.15). The chamber begins directly after the stabilizers of the combustor dome and is ending by a jet nozzle attachment flange. Its geometrical dimensions satisfy conditions of the maximum combustion efficiency.

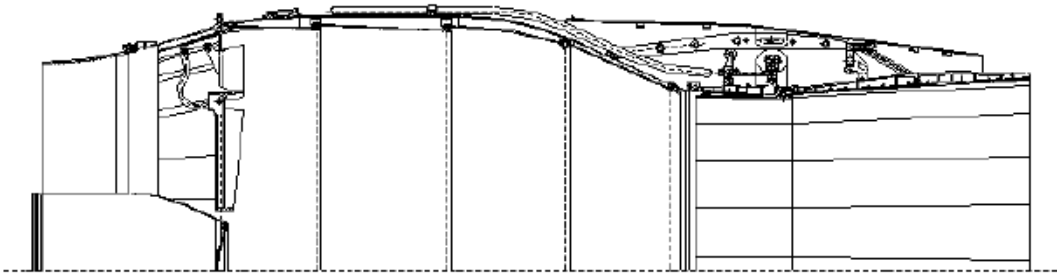


Fig. 6.15. Spherical afterburner of the fourth generation

Welds have a shape of spiral line, thus improving static and vibration strength. The chamber is attached to the combustor dome by a telescopic or flange-bolt joint, which provides a freedom of thermal deformations at non-uniform heating of the structural members. Outer surface of the chamber is cooled by the air flowing between the wall of the chamber and the casing.

6.2.5. Oscillation (vibration) combustion

Combustion processes generate a band-limited pseudo-random sound that is often referred to as “combustion roar.” In addition to the “roar” sound, which almost always exists in any confined combustion, on occasion a very intense, narrow-band (frequently single-frequency/tonal) noise is generated in the combustion chamber resulting in a high-amplitude, self-sustaining pressure oscillation. This phenomenon originates from a coupling between the flame’s heat release dynamics, the combustor acoustics, as well as transient fluid dynamics in the combustor and is referred to by many names including, but not limited to, “combustion-driven oscillation", “combustion dynamic instability", and “thermo-acoustic instability". The excited acoustic oscillation causes large pressure fluctuations (high combustor noise levels), poor combustion, increased emissions and even catastrophic combustor failure (structural damage).

Under favorable conditions, a flame in a confined space (combustion chamber) can couple with an acoustical mode of the combustor and produce strong combustion oscillations. This coupling mechanism becomes self-sustaining, resulting in high amplitude pulsations, if a favorable phase between the unsteady heat release and acoustic pressure is maintained over the whole oscillation cycle.

Combustion in the afterburner is characterized by the gas oscillations with pressure amplitude Δp up to 0.05 MPa and frequency from 50 to 5000 Hz. This mode is named “**vibration combustion**”; it is characterized by the longitudinal and transverse (radial and tangential) acoustic oscillations. The oscillation combustion is detected by characteristic “squeal” and fast destruction of the afterburner structural elements.

The **acoustic liner** is mounted along a wall inside the chamber for dumping of oscillations (Fig. 6.16).

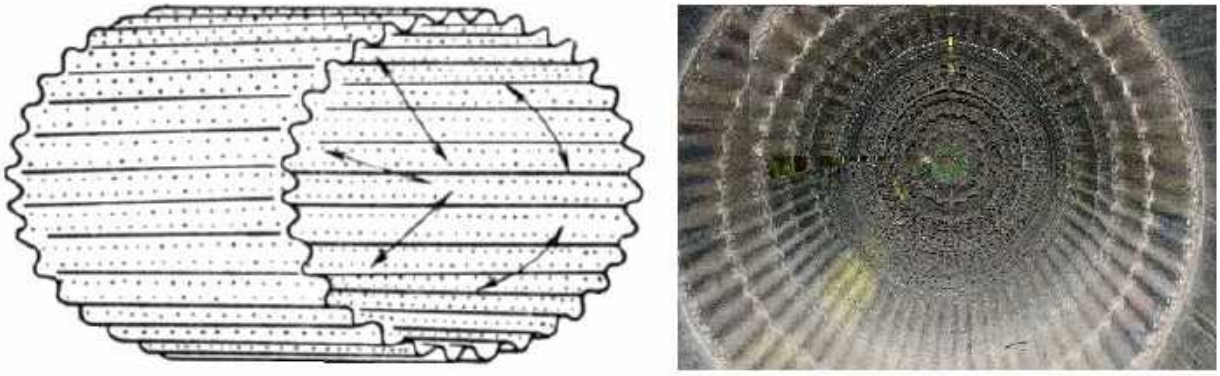


Fig. 6.16. Acoustic liner

The acoustic liner is of a corrugated perforated design. It operates like an acoustic resonant absorber, which is adjusted at dumping of oscillations of the specified frequencies. Efficiency of this system at low-frequency oscillation combustion is low; therefore, dumping this kind of oscillations at experimental development is a difficult task. Methods of this dumping are as follows:

- changing of acoustic volume (for example selecting shape and size of the turbine disc cowl);
- changing of fuel distribution in the chamber cross-section;
- changing of shape and position of flame stabilizers;
- changing of velocity of the gas flow, etc.

Inner surface of the afterburner is cooled by the gas flowing from the turbine, in case of turbofan engine – by the air flowing from the bypass duct. In this case, the acoustic liner is used as acoustic thermal shield that decreases a wall radiant heating and provides convex and film cooling.

Method of joining of the acoustic liner to the casing must compensate for a difference of the thermal expansion of its component parts relative to the casing. This compensation in radial direction is ensured by the longitudinal lobes, which are deformed within the limits of material elasticity; the compensation in axial direction is provided by the out-of-round holes in the liner that are made for coupling bolts, or by telescopic supporting on adjacent section of the liner.

6.3. Structural materials of the afterburners

Diffuser is made of sheet heat resistant material, for example, ХН60В (ЭИ868), by using contact welding and fusion welding. Outer shell ring of the diffuser that is intensively cooled by the air of the bypass duct, may be made of titanium alloys ОТ4-1 and ВТ-20.

Supply pipelines and manifolds are manufactured of the solid-drawn pipes made of steel 1Х18Н9Т (Я1Т) or ХН60В (ЭИ868). They are joined by welding or brazing. Thread joints are not used inside the afterburner because of low leak-tightness at variable thermal loading.

Casings of the combustion chamber and acoustic liner that operate at a temperature 900 to 1100 ºС, are made of heat resistant alloy ХН60В (ЭИ868). The outer casing of the TFE afterburner has low operating temperature (approximatly 300 to 400 ºС); thus, it may be made of titanium alloys ОТ4-1 and ВТ-20. Bolts for restraining the acoustic liner are made of high-melting material, for example of alloy Х20Н80Т (ЭИ435).

Stabilizers and liners are covered with high-melting enamels for the corrosion protection.

6.4. Check questions

1. Which aircrafts need engines with afterburning?
2. Main purpose of the afterburner and requirements to it.
3. Name main structural members of the afterburner and describe their functions.
4. Purpose, shape of gas path and construction of afterburner' diffuser.
5. Why the afterburner is not equipped with the flame tube?
6. How is the burning zone in afterburner stabilized?
7. Name means improving the fuel vaporizing and mixing with the air and gas flow in the afterburner.
8. How the afterburner starts? Name methods of afterburner starting.
9. Describe the 'hot-shot' ignition system.
10. What is oscillatory combustion and how is it prevented in afterburners?
11. Name cooled parts of afterburner and methods of their cooling.
12. What materials are used in the afterburners?

7. POWER SYSTEMS OF GAS TURBINE ENGINES

GTE power system is a combination of joined GTE parts, which takes and transmits loads that effect on the design members.

The GTE power system includes power systems of the stator (casing) and rotor. Both systems interact between themselves through the bearings.

7.1. General information about power system of casing

The casings of the compressor, combustion chamber and turbine are rigidly joined between themselves and compose the main load-carrying frame of the engine, which bears a rotor and contains the engine mounting assemblies, transporting assemblies and accessory gearbox.

The system of load-carrying connection between the casings of the compressor, combustion chamber and turbine is named as the power system of the engine casing.

The main load-carrying member of the turbojet engine casing usually is a rear frame of the compressor; in the turbofan this member is the separating casing of the compressor. It bears main mounting assemblies that transmit the engine thrust to the aircraft. The power system of the turbofan casing is more complicated than that of the turbojet, due to a presence of walls of the bypass duct, especially if it extends the full length of the engine.

The power system of turboprop engine includes also a propeller gearbox and front casing.

The power system of casing takes all loads that affect the engine. The portion of these loads is generated inside the casing, the other portion is transmitted from the attached members (rotor, air intake duct, propeller, afterburner, and accessories).

Magnitude and distribution of the forces and moments that load the casing are changed within a wide range due to different operating conditions.

Members of the casing operate under various temperature conditions. They may be non-uniformly heated; this causes thermal stress. The heating results in a significant expansion, which must be free for avoiding thermal stresses, which can cause buckling and cracking. Some loads change cyclically, thus generating vibrations of the casing.

The operation conditions determine the design philosophy of the power systems of casings, which must be strong at enough rigidity and minimum weight, have high maintainability and repairability; they also must provide faults isolation and the engine survivability.

7.2. Loads that affect power system of the GTE casing

Casing is affected by the loads that originate due to engine operation and due to evolutions of the aircraft in flight.

The loads that are generated by the engine operation include the following:

– torques that are generated by stationary vanes of the compressor and turbine;
– axial gas dynamic forces of the casing and rotor;
– radial gas dynamic forces of the gage pressure in the gas flow duct;
– thermal loads;
– vibration loads.

The loads that originate during the aircraft evolutions:

– mass inertial forces of the casing itself and the attached assemblies and accessories;
– gyroscopic torque of the rotor that loads the casing by additional supporting responses.

In the turboprop engines, these loads are added by weight inertial forces, gyroscopic and reactive moments of the propeller and gearbox.

Some of these loads, for example radial forces and thermal loads, are localized inside the casing causing its stress state; they are not transmitted to the engine mounts. Other loads, for example gyroscopic moment and axial gas-dynamic forces, are equalized by responses in the engine mounts.

Let’s consider action of different loads on the engine load-carrying casing.

Weight forces of the own structural members of the casing are distributed by its volume, weight forces of the joined assemblies and component parts load the casing by concentrated responses of the supports.

Gyroscopic moment of the rotor loads the casing by responses of supports.

Weight forces and gyroscopic moment generate transversal forces and bending moments in the casing as in a beam.

Thermal loads originate due to a non-uniform heating and a difference in thermal expansion factors of the joined portions of the casing.

Radial forces of a gage pressure in the engine gas flow duct may be external or internal in relation to different walls of the casing. For example, the outer casing of the combustion chamber is loaded by the internal pressure; the same pressure for the inner casing is external.

The internal gage pressure causes tensile stresses in the shell, the external pressure may cause loss of stability of the shell.

Let’s consider distribution of the axial forces and torque in engine casing taking into account balance of forces and moments that act the casing.

By summing up the axial gas forces of the casing portions and the axial gas force that affects the rotor and are applied to the casing in a plane of the thrust bearing, we take the resultant force. This force affects upstream and is equal to the engine thrust force. This force is equalized by responses in the engine mounting assemblies (Fig. 7.1).

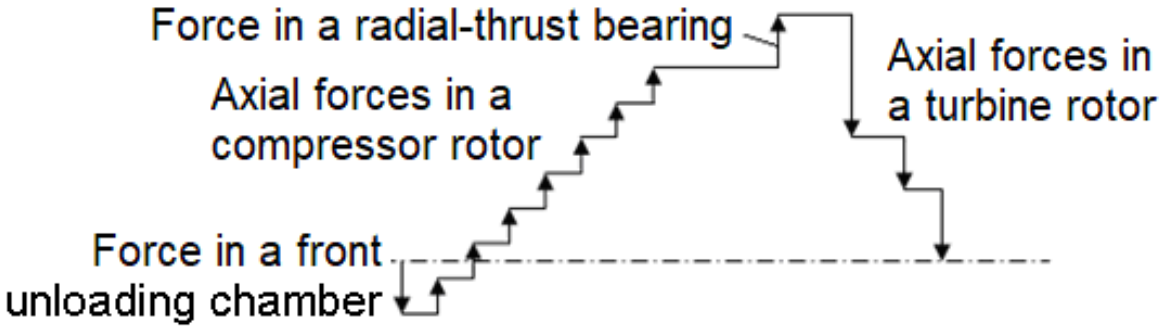


Fig. 7.1. Axial forces that are transmitted from the turbojet rotor to casing

Let’s consider action of the torque on the power casing. At axial air inlet into the compressor and axial outlet from the turbine, the torques that act the compressor and the turbine casings, are equal but they are acting to the opposite directions (Fig. 7.2). They are localized inside the engine casing and are not transmitted to the mounting assemblies and to the aircraft.

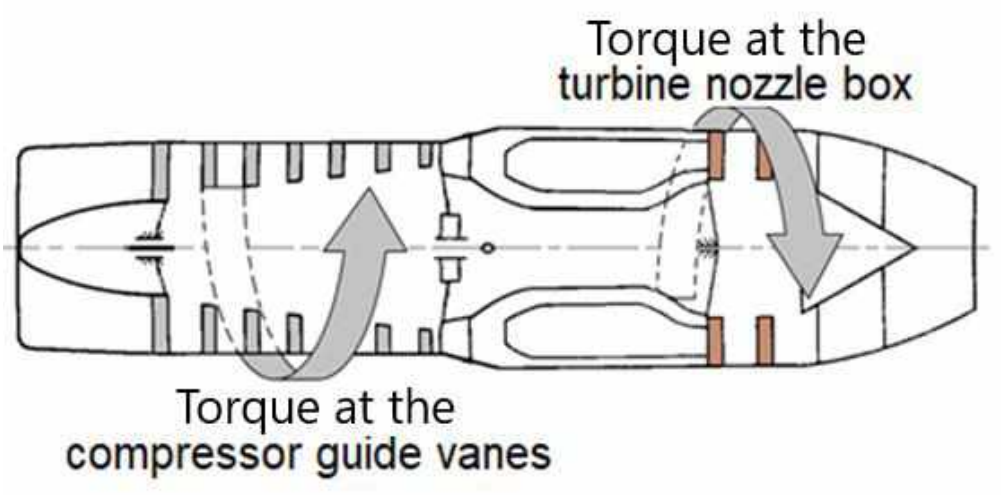


Fig. 7.2. Torque that originates at stationary vanes
of the compressor and turbine

If the output gas stream is not axial (for example, the struts of the exhaust system do not provide full straightening of the flow from the turbine) then the

torque at turbine casing will be less than that at the compressor casing (Fig. 7.3). The difference of torques is transmitted to the mounting assemblies and to the aircraft.

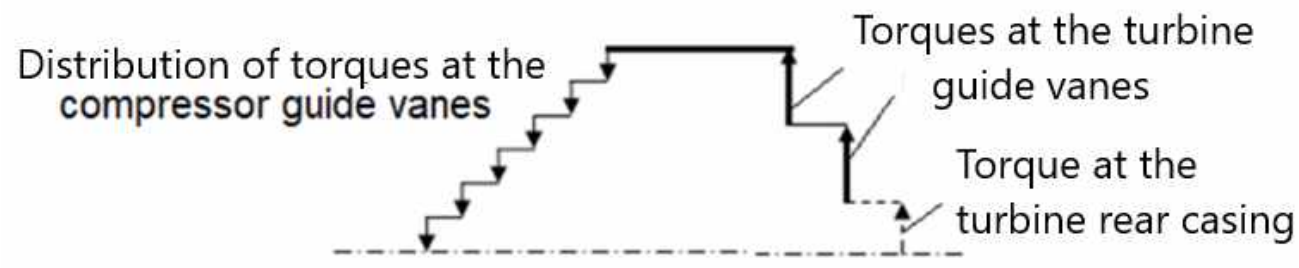


Fig. 7.3. Distribution of torques with the flow straightening at struts of turbine rear casing

In the turboprop, the turbine torque is higher in the absolute value than the compressor torque. This difference is the torque that is transmitted to the gearbox output shaft. The torque that is transmitted to the propeller is increased proportionally to the gear ratio of the gearbox (Fig. 7.4).

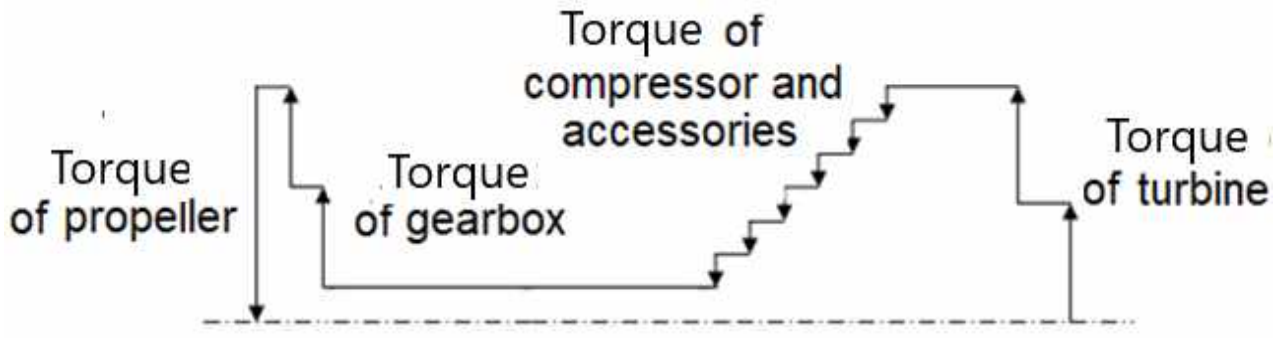


Fig. 7.4. Distribution of torques by a single-shaft turboprop rotor

The same torque with opposite signs will affect the engine stator.

The stator of the turboprop engine takes the reactive torque from the gas flow, which is equilibrated in the engine-mounting assemblies by the reaction forces. It is equal to the torque, which rotates the propeller, but has opposite sign. Thus, the mounting assemblies take a torque that is equal to a difference of the torques, which affect the turbine and compressor casings.

7.3. Methods of transmitting loads in the structural elements of power casings

The power link between the compressor and turbine casings is the basic feature of classification of the power casings. Depending on a type of this power link, the following diagrams of the power casings are differed.

7.3.1. Diagram with the internal power link

The examples of this diagram are the VK-1, RD-45, RD-500, Walter M-701 gas turbine engines (Fig. 7.5).

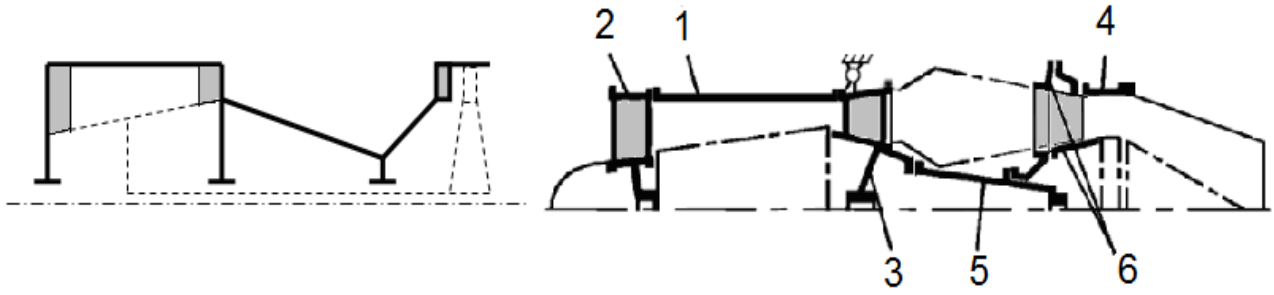


Fig. 7.5. Power frame of turbojet with internal power link:
1 – compressor casing; 2 – compressor front frame; 3 – compressor rear frame;
4 – turbine casing; 5 – rear bearing casing; 6 – combustion chamber outlet duct

Compressor and turbine casings are linked by the casing of the turbine shaft. This power link is internal in relation to the gas flow duct.

The casing of turbine shaft is loaded by the forces and torques applied by the turbine casing, intake duct and engine rotor. This diagram is a typical for the turbojet with individual (can) combustion chambers, which are not included into the power diagram of the casing, but are joined to it and load the casing additionally.

The disadvantage of this diagram is higher weight of the casing as it has thick walls and additional ribs for providing a required sagging rigidity at comparatively low diameter.

7.3.2. Diagram with the external power link

The examples are the engines AL-21F, TV2-117, TV3-117, and D-136 (Fig. 7.6).

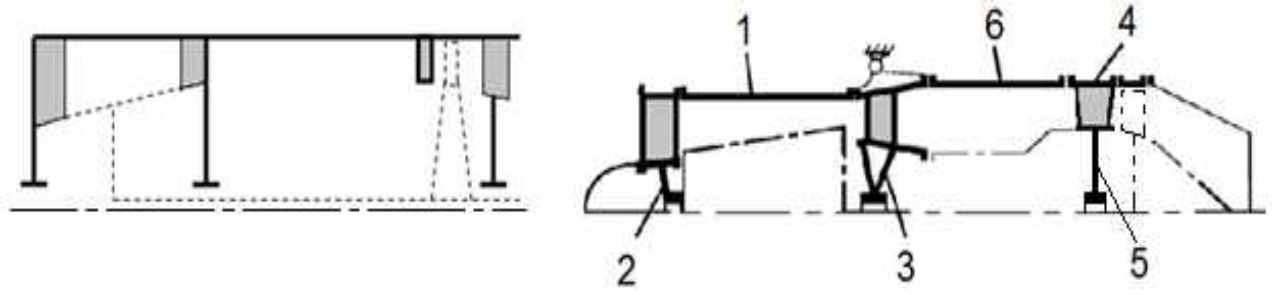


Fig. 7.6. Diagram of power system of turbojet casing with external power link:
1 – compressor casing; 2 – compressor front frame; 3 – compressor rear frame;
4 – turbine casing; 5 – rear bearing casing; 6 – combustion chamber casing

Compressor and turbine casings are linked by the combustion chamber external casing. This power link is external in relation to the gas flow duct.

The external casing of the combustion chamber has higher rigidity due to its higher diameter. This casing takes forces and torques from the turbine casing, intake duct and engine rotor. However, for transmission of loads from the turbine rotor supports, this diagram needs in load-carrying members, which cross the gas flow duct. This complicates design of the turbine rotor support and is the disadvantage of this diagram.

The diagram with the external power link allows having the maximum useful volume of the combustion chamber. It is also used in the two-spool and three-spool engines when the rear support of a rotor is located downstream of the turbine.

7.3.3. Diagram with the branched (open) double power link

The examples are the engines AI-20, AI-24, AI-25 (Fig. 7.7).

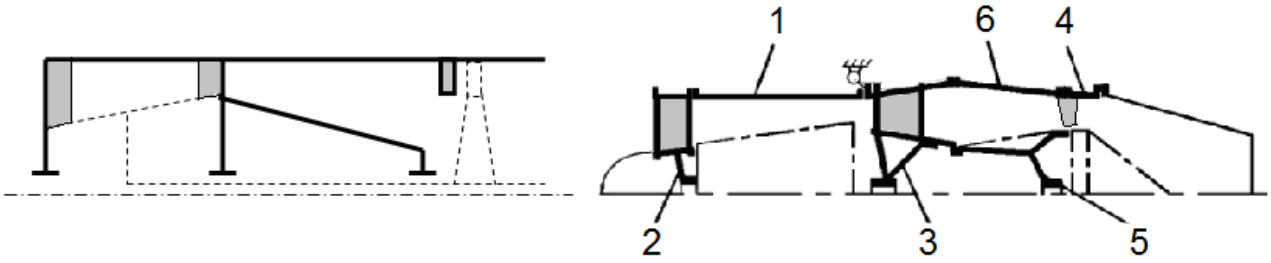


Fig. 7.7. Diagram of power system of turbojet casing with branched (open) double power link:
1 – compressor casing; 2 – compressor front frame; 3 – compressor rear frame; 4 – turbine casing; 5 – rear bearing casing; 6 – combustion chamber casing

The external casing of the combustion chamber is loaded by the forces applied by the turbine external casing, nozzle guide vanes and the exhaust system only. The forces and torques of the turbine rotor are transmitted to the compressor rear frame through the casing of the shaft. The power link in a plane of the turbine rotor support is absent, so this diagram does not need load-carrying members crossing the gas flow duct.

This power diagram is most rational for the engines with the annular combustion chamber and multistage turbine.

7.3.4. Diagram with the closed double power link

The examples are the turbojets R-11F-300, R-95Sh, R-29F-300, and AL-7F (Fig. 7.8).

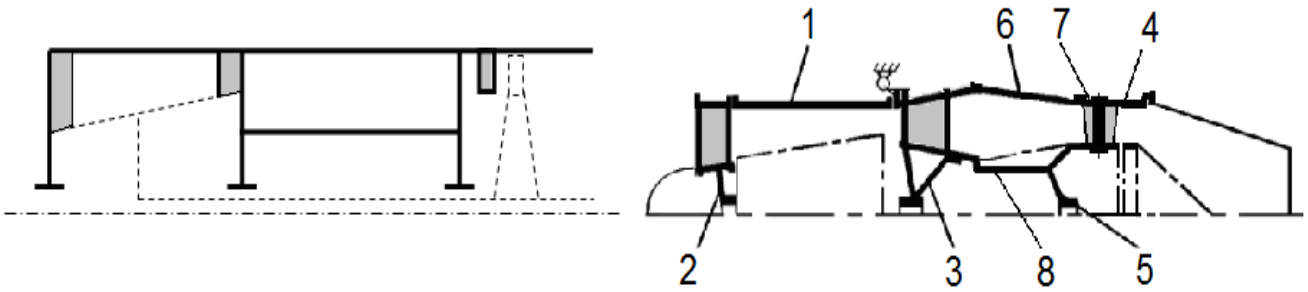


Fig. 7.8. Diagram of power system of turbojet casing with closed double power link:
1 – compressor casing; 2 – compressor's front frame; 3 – compressor's rear frame;
4 – turbine casing; 5 – casing of the rear bearing; 6 – combustion chamber casing;
7 – load-bearing rods inside nozzle vanes; 8 – casing of shaft

The turbine and compressor casings have both the internal and external power links with their bearings. This diagram uses carrying capacity of shells in full. The power link between the outer and inner contours in a plane of the turbine rotor support is provided by the struts or diaphragms that are located in the spaces between the flame tubes of the can-annular combustion chamber (the D-20P, D-30, VD-7, and D-25V), or by spokes passing through the hollow nozzle guide vanes (the R-11F-300). These power members are intensively cooled.

This diagram is widely used.

The outer and inner shells take the torque from the nozzle guide vanes. The torque is distributed between the shells proportionally to their torsion rigidity. The axial forces are distributed proportionally to tensile rigidity of the shells. Distribution of the bending moments and shearing forces follows the conditions: displacements and turning angles at the ends of the shells shall be equal.

7.3.5. Power frames of turboprop engines

In the power diagrams of turboprop casings, one of the above-considered diagrams or its version is usually used. However, the power diagrams of the turboprops have some specific features related to the method of linking the gearbox casing with the main load-carrying members of the gas generator.

Some typical diagrams are implemented:

1. The power diagram in which the casing of the gearbox is linked only by flanges with the compressor rear frame or with the front casing (the AI-20, Fig. 7.9).

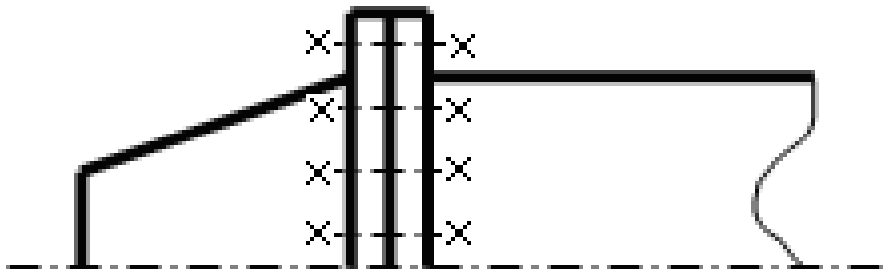


Fig. 7.9. Flange attachment of turboprop gearbox

The flange attachment is performed by the bolts or studs.

2. The power diagram, in which the casing of the gearbox is linked with the compressor rear frame by a flange or is centered by a rib, and additional axial link with the engine casing is implemented by the pipe-like rods, which transmit the axial force from the gearbox to the engine mounts (Fig. 7.10).

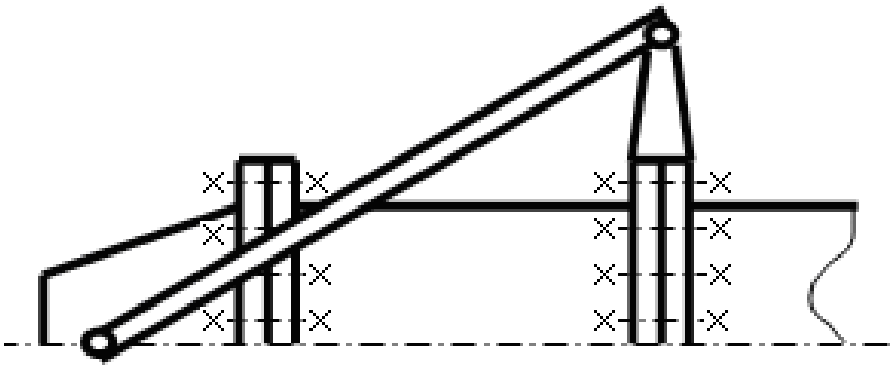


Fig. 7.10. Attachment of gearbox by pipe-like rods

3. The power diagram, in which the external gearbox may be linked with the engine by a space rod-type frame or be joined to the aircraft independently from the engine.

7.4. Engine attachment to the aircraft

The engine is attached to the aircraft by special assemblies that are located on the engine power casing. The aircraft is equipped with space rod-type frames for engines mounting.

The engine mounting assemblies are affected by the following:

– force of the engine weight;
– inertial forces of the engine and its assemblies, which are originating during maneuvers of the aircraft;
– gyroscopic torque of the rotor;
– inertial forces related to the rotor out-of-balance;

– reactive torque of the gas flow, if its velocity has a circumferential component;

– the engine thrust.

The turboprop has additional gyroscopic and reactive torques of the propeller. If the coaxial double-row propellers are used, which rotors are counter-rotating ones, then the gyroscopic and reactive torques of the propellers compensate each other, and total torques are close to zero.

The engine mounts must satisfy the following *requirements:*

- attachment diagram shell ensure easy replacement of the engine in service and its maintainability;
- mounting points must be located so that the engine will be attached in directions of all six degrees of freedom: in the axial, vertical and lateral directions and around the longitudinal, vertical and horizontal axes. The mounting system must be statically determined: the double mounting in all above mentioned directions and around all axes in inadmissible. In this way, the engine casing is isolated from deformation of the aircraft structure and the mounting assemblies are protected against the high off-design loads;
- the mounting points must ensure free thermal deformation of the engine casing under all flight conditions and engine power ratings;
- the main mounting points must be located on the compressor power casing in a plane that is close to the engine center of gravity. As a rule, this plane goes through the compressor rear support;
- additional mounting points must be located on the turbine casing and in a plane that goes through the turbine supports;
- the afterburner has additional mounting point in a plane of the variable jet nozzle casing. To make the mounting statically determined, the afterburner must be attached to the turbine casing through a hinged joint;
- in case of the thin-walled casings, to prevent large local radial deformations and touching of the rotor blades against the casing, high radial forces at the mounting points are not allowed;
- the engine rigging, mounting and transportation need in additional mounting points that satisfy requirements to the main mounting points. At the engine mounting in the aircraft, the engine suspension and supporting in arbitrary points is inadmissible.

The engine is attached to the aircraft by a power casing, as a two-support beam (Fig. 7.11). The mounting assemblies are dislocated in two planes that are perpendicular to the engine axis. One of planes is places as close to the engine center of gravity as possible. The other plane is located as far from the

first plane as it is possible, thus decreasing response forces in the mounting assemblies that are initiated by the inertial forces and torques during the aircraft maneuvers.

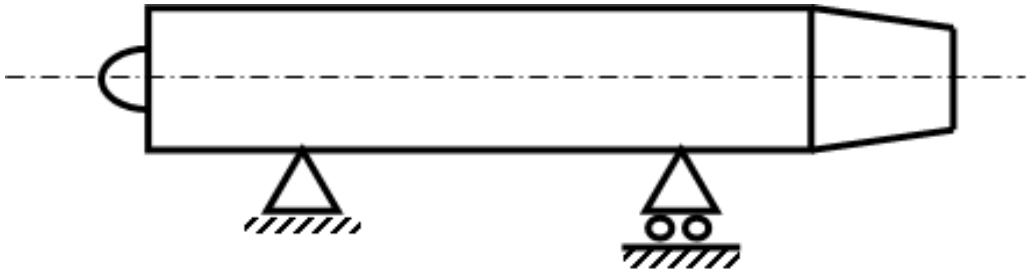


Fig. 7.11. Engine attachment to the aircraft

The engine casing is reinforced near the mounting assemblies to prevent local deformations. This is ensured by the bosses and ribs (Fig. 7.12), which distribute the loads in a volume of the casing. The mounting assemblies may be located on the rigid flanges of the power casing.

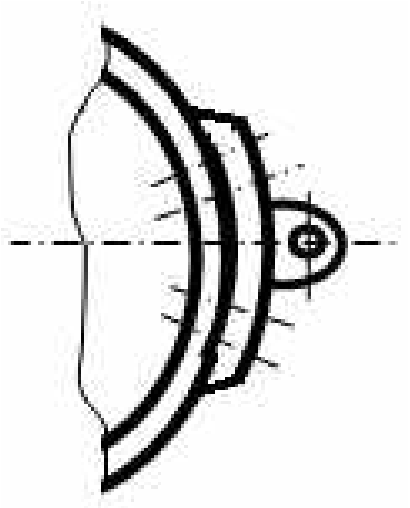


Fig. 7.12. Attachment of bracket to rigid flange

The mounting assemblies must allow free thermal expansion of the engine casing during its operation. This is done by restraining the engine to the aircraft in the axial direction in one plane only. The remaining mounting assemblies allow a linear displacement of the engine in relation to the aircraft.

The mounting assemblies contain hinges, which prevent loading of the engine casing during elastic deformations of the aircraft.

Design and disposition of the engine mounting assemblies are determined by the specific features of the aircraft. Therefore, the same engine may have some versions of mounting: for example, port and starboard engines of one aircraft. The same engine may be mounted in the different aircraft.

Variant of turbojet mounting

The turbojet may be mounted in the aircraft by the trusses made of the rods. If the engine is attached to the underwing pylon or to a tail portion of the airplane, then the fork-type assemblies that are located above the engine casing are used. Specific feature of the turbojet mount is a presence of the power loops (Figs 7.13 – 7.15). The minimum number of the power loops is two, one of which is the main one. The main power loop contains the nodes that take forces P_x, P_y, P_z, and torques M_x, M_y; the additional power loops contain nodes that take force P_y and torque M_z. Casing of the turbojet engine operates at high temperature conditions and perceives significant thermal expansions. Therefore, the engine must be attached so that thermal expansions of the casing will be compensated.

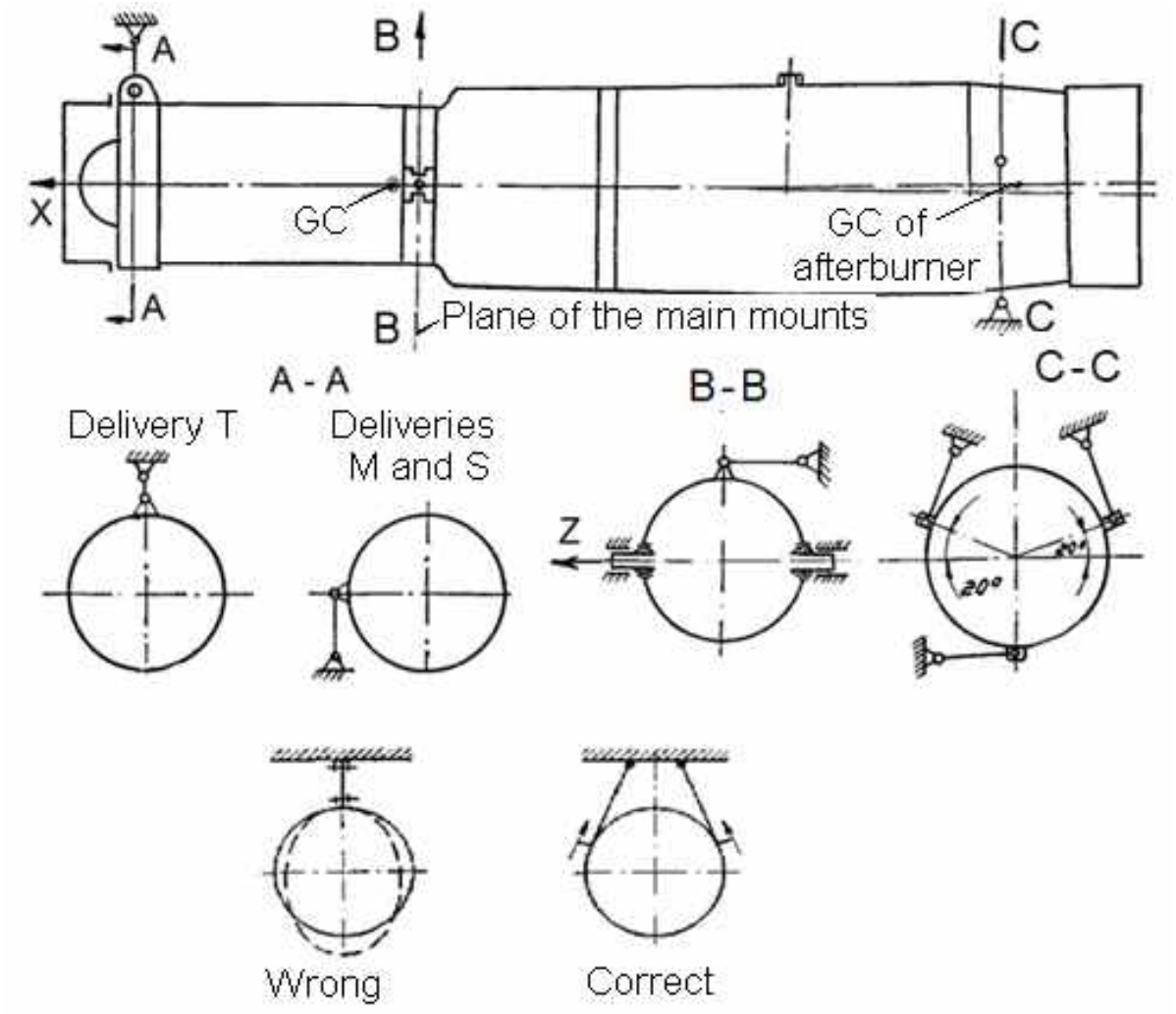


Fig. 7.13. Attachment of the AL-21F turbojet to the aircraft:
Su-24 (delivery T), Su-17M (delivery S), and MiG-23B (delivery M)

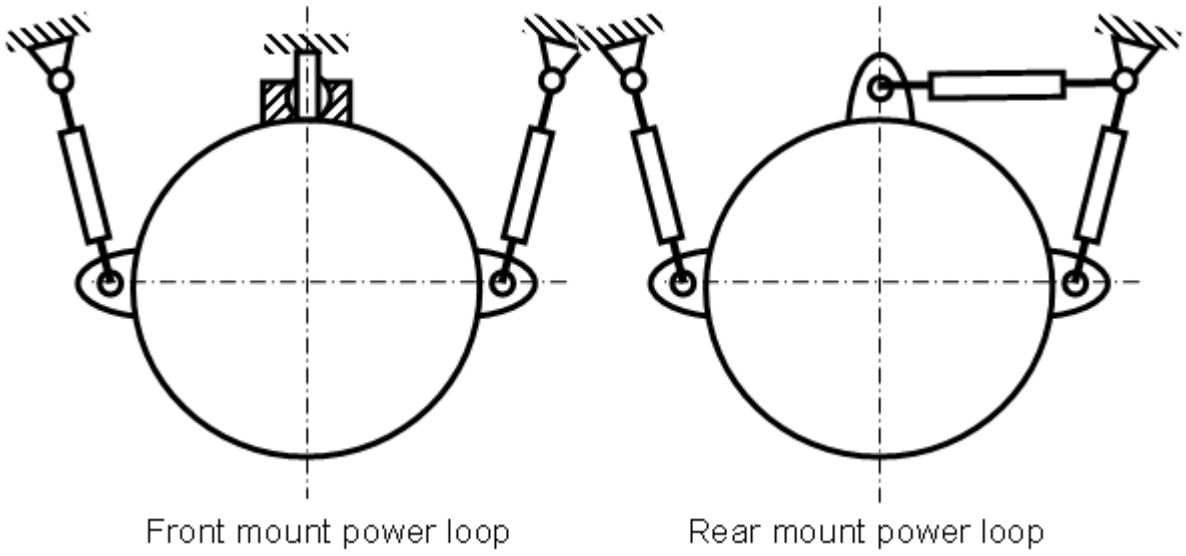


Fig. 7.14. Version of attachment of the R-95Sh turbojet to the Su-25 aircraft

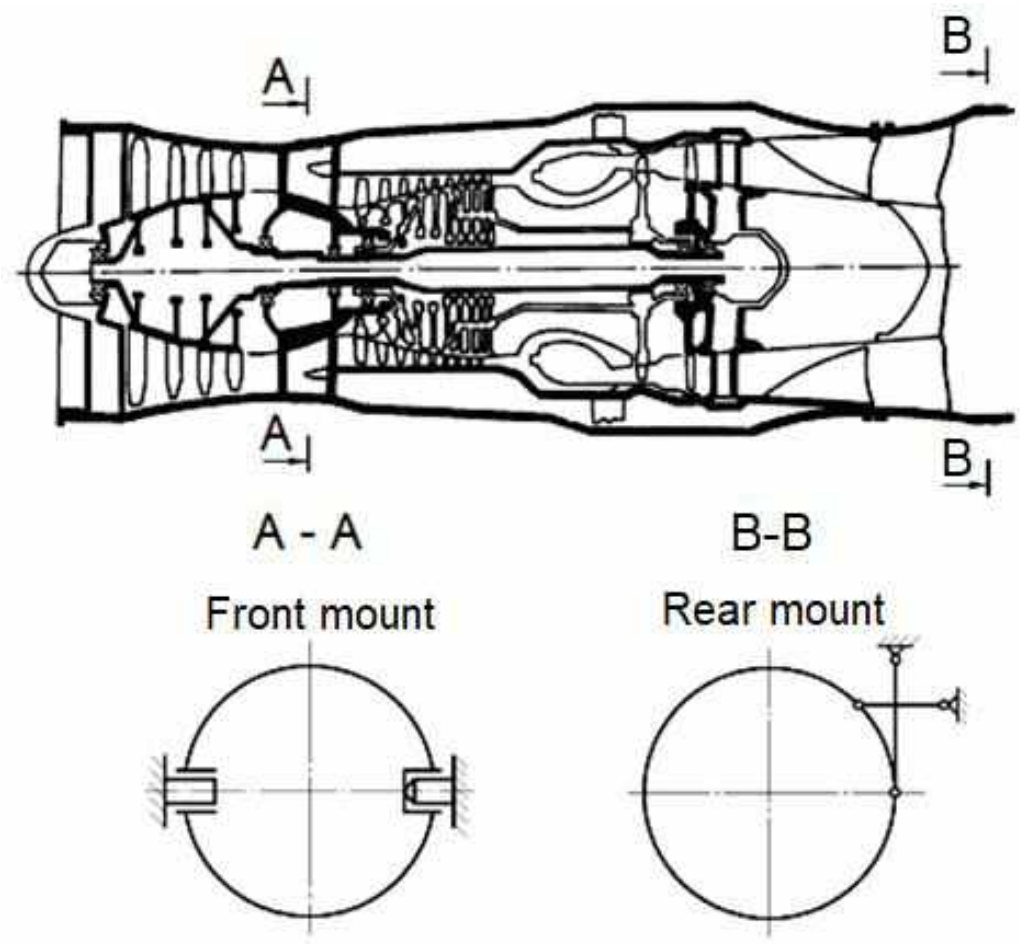


Fig. 7.15. Version of attachment of the AL-31F turbofan to the Su-27 aircraft

The compressor casing is unloaded if the mounting system contains hinged rods (Fig. 7.16). This structural design makes it possible to transmit the loads from the engine mounting loop to the casing and not to limit thermal deformations of the engine casing.

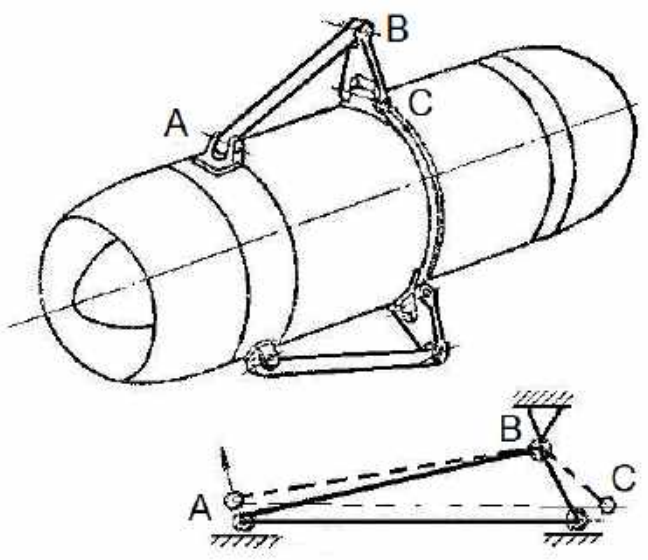


Fig. 7.16. Strengthening by the rods

Fig. 7.17 shows diagram of attachment of the Trent-800 turbofan. The system has provided for the front and rear mounting areas with cantilever brackets for attachment of the engine junction to the aircraft pylon. The inclined rod, which is mounted between the cantilever rod of the rear area and the power casing, unloads casings of the gas generator.

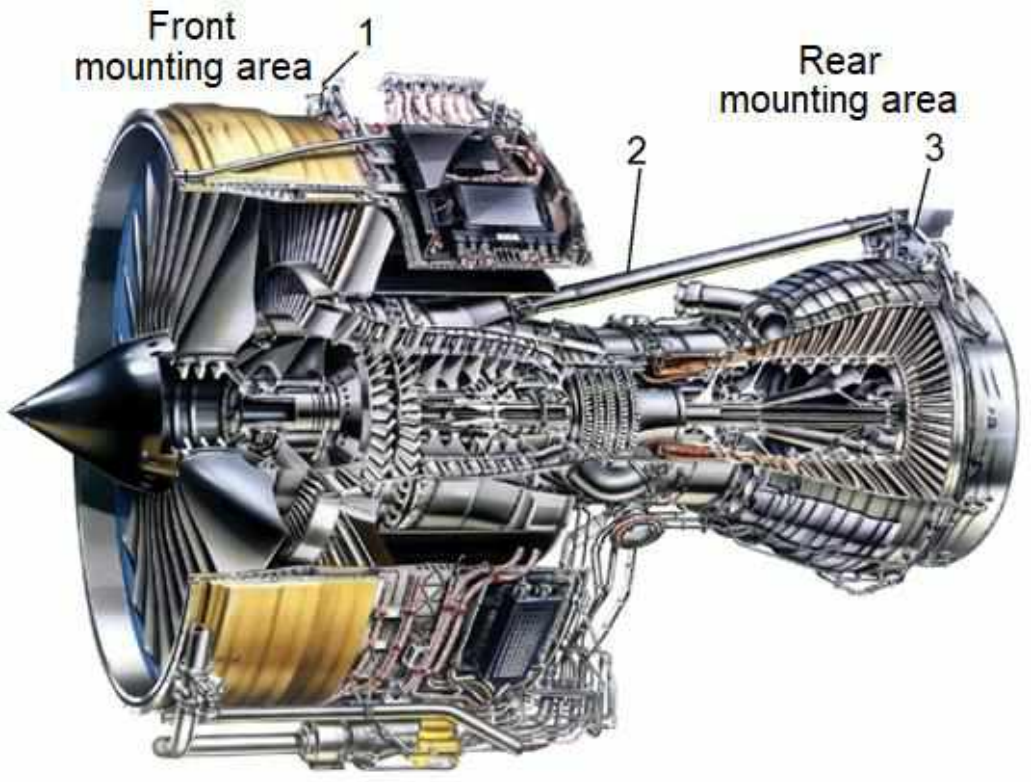


Fig. 7.17. Diagram of attachment of Rolls-Royce Trent-800:
1 – cantilever rod of the front mount; 2 – inclined rod;
3 – cantilever rod of the rear mount

Mounting assemblies of the turboprop engine (Fig. 7.18) are additionally affected by a reactive torque from the propeller that is directed oppositely to its rotation. If the power plant is equipped with two counter-rotating propellers, then the reaction torque is equal to the differential between the torques of the propellers. When determining the inertia forces and torques, it is necessary to take into account the presence of the gearbox and propellers.

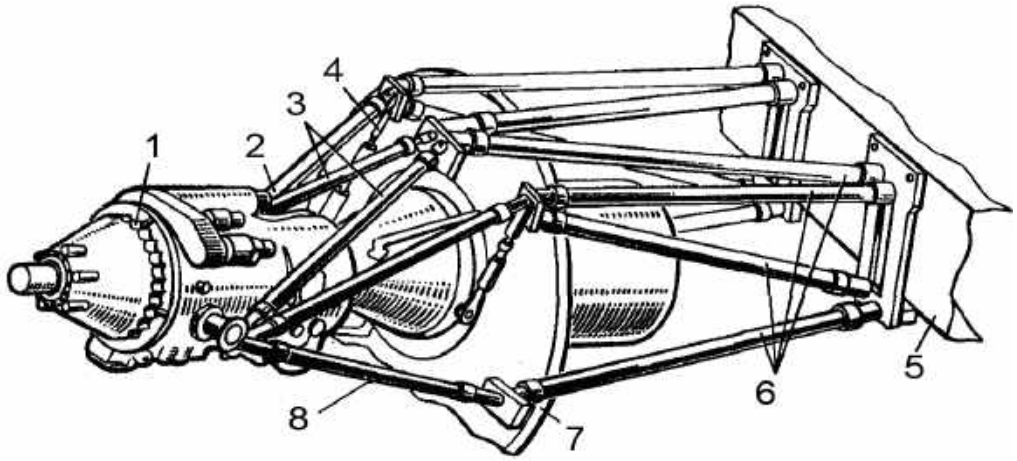


Fig. 7.18. Truss design of turboprop attachment:
1 – engine; 2, 3, 8 – side, head and lower supporting struts; 4 – strut-dumper;
5 – wing center section spar; 6 – power truss; 7 – firewall

The turboshaft engine (Fig. 7.19) is installed in the helicopter as a two-support beam.

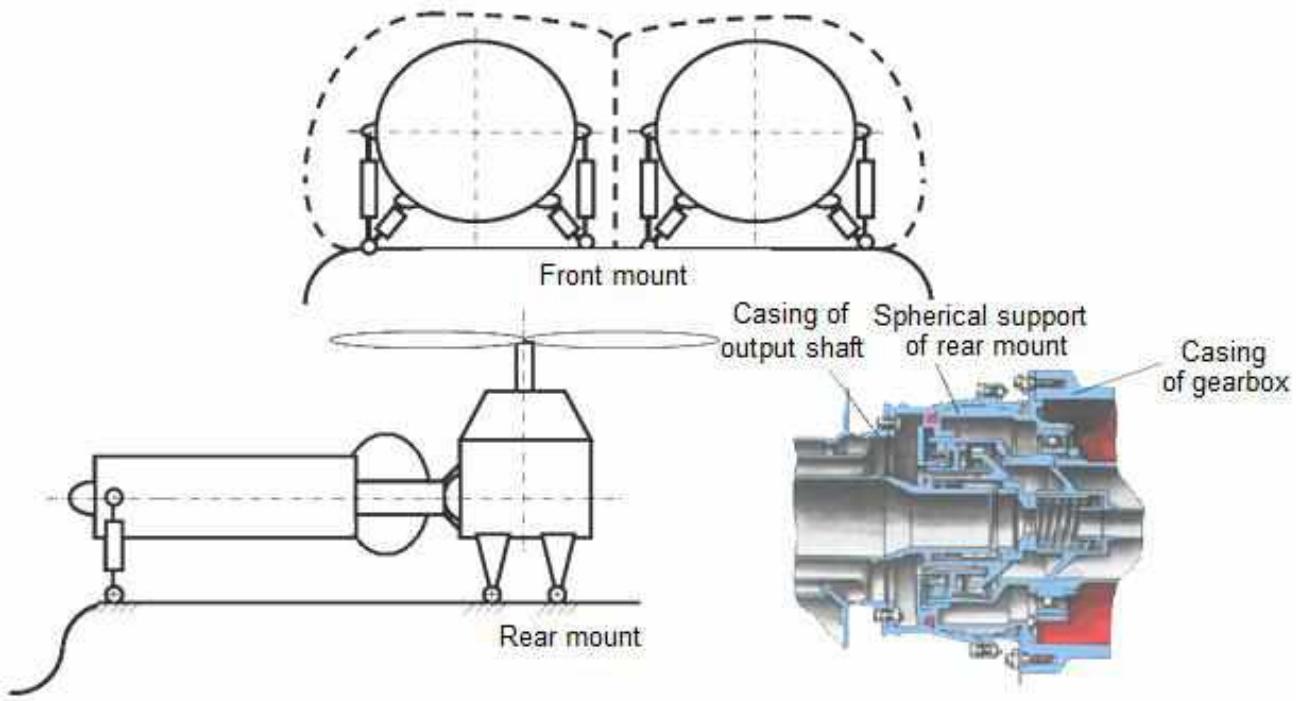


Fig. 7.19. Variant of mounting of the TV3-117 turboshaft
in the Mi-24 helicopter

The casing of the output shaft is rigidly supported by the rear mount on a spherical mounting surface of the gearbox. In the front area, the engine is attached by means of the adjusted trusses that ensures axial displacement of the design.

7.5. Strength of engine mounts

The engine mounts are strongly loaded. They must ensure a stable position of the engine at different external forces and moments. In general, the mount equilibrates components of forces that act along three axes of coordinates, which origin is a gravity center, and moments related to these axes.

Parts of the mounts fix the engine to load- bearing elements of the aircraft or the frame and ensure a required number of degrees of freedom. In general, the following forces and moments act the parts:

- axial force (thrust force);
- the engine weight;
- inertial loads caused by the engine rotor imbalance;
- non-equilibrated part of a torsion torque that acts parts of a stator;
- inertia forces of the engine mass that originate at evolutions of the aircraft;
- gyroscopic moment that acts the engine rotor and is determined by angular velocity of the rotor ω and angular velocity of the aircraft evolution Ω.

Action of the gyroscopic moment at different evolutions is shown in Table 7.1.

Table 7.1

Action of gyroscopic moment at the aircraft evolutions

Rotor's rotation (by flight)	Evo-lution				
Left	Action of M_{gyr}				

Choice of the mount construction depends on the engine type, its arrangement in the aircraft and on magnitudes and directions of the acting forces. Choice of the mount construction depends on the engine type, its

arrangement in the aircraft and on magnitudes and directions of the acting forces. Nowadays, the fast-mounting power plants take a growing application in the aircraft. This mount ensures mounting and demounting of the engine with all accessories and parts that are arranged therein. In doing so, the mounted engine may be tested preliminary.

Strength properties of engine mounts must meet the following requirements:

- perceive all loads that originate in all flight conditions;
- be strong and rigid at minimum weight;
- damp vibrations of engine and air propeller and not transmit them to the aircraft construction.

Engine casing must not belong to the aircraft power scheme; the mount must ensure interchangeability of engines, easy and free access to all units that need in periodic inspection and adjustment in maintenance. Convenient maintenance was always in the center of attention, but now a simplicity of maintenance is considered on the same level as the most significant performances of the power plant, such as reliability, weight, specific fuel consumption, etc.

7.6. Power systems of the GTE rotors

Rotor of the gas turbine engine consists of the compressor and turbine rotors and parts that join them. Besides, the rotor of the turboprop engine includes also the gearbox rotated parts.

The system of the supports, links, joins and axial restraining of the compressor and turbine rotors is names as a power system of the engine rotor.

The rotor power system must meet the following requirements.

1. *The load-carrying parts of the system must be enough rigid* to keep the shape under the action of loads. This requirement is satisfied due to corresponding profiling of the shafts and by choosing the required number of supports, which provides a stable and reliable operation of the rotor under all maintenance conditions of the engine.

2. *The shape and joints between the load-carrying parts* must be so to minimize that stresses in them. This condition provides the minimum weight of the rotor. It is satisfied due to a rational profiling of the load-carrying parts (shafts, disks), by excluding stress concentrators, by using smooth shapes without abrupt bends in the parts, by application of hollow shafts with sufficiently high external diameter and small relative thickness of the wall.

3. *The design and joining of the parts* that are heated to different temperatures must allow a freedom of thermal deformation and the minimum thermal stress. With this goal, the rotor is restrained with respect to the casing by a single radial-thrust bearing that is located in a place, which ensures the minimum variation of the axial clearances in the engine gas flow duct.

The load-carrying parts, which operate in the gas flow, must be smooth and have a streamlined shape. They must be protected against overheating.

7.6.1. Schemes of the GTE rotor power systems

One of the principal problems concerning the engine rotor design is rotor supports type, their number and location. Depending on the number of supports, the rotors are classified as two-, three- and four-support rotors.

Two-support rotors are usually used in case of small number of the compressor and turbine stages, and also if the compressor is a centrifugal one and the combustion chamber is short one. The main advantage is design simplicity. Thus, the rotor wheels of the compressors and turbines may be mounted between the supports, in cantilever or one − between the supports and other − in cantilever.

A common feature of all two-support rotors is a presence of one radial-thrust bearing and the other is radial one, thereby ensuring freedom of temperature deformation and axial relative displacement of the rotor and stator.

The radial-thrust bearing takes both axial and radial loads that originate in the turbine and compressor. Desirable value of the axial force that affects the radial-thrust bearing is provided by sealing backs of the rotor from the gas flow duct, thus creating front and rear unloading chambers. The front chamber is pressurized and the rear chamber is vented.

The bearing is located inside the rotor drum-and-disk assembly; supports are arranged as close as possible to a centre of gravity. This allows:

- reducing the design length;
- reducing the rotor sagging, caused by the sagging torque of the inertial forces;
- increasing the natural frequencies of the rotor bending oscillations (rotor becomes more rigid).

Diagram with supports located downstream of the compressor and upstream of the turbine is shown in Fig. 7.20. Advantages of this diagram are as follows: low variation of the axial clearances in the turbine; free air entry into

the compressor that is not blocked up by the load-carrying members, which transmit load from the support to the casing; small length and weight of the shaft; simple lubrication of supports and the oil tapping from the common oil sump.

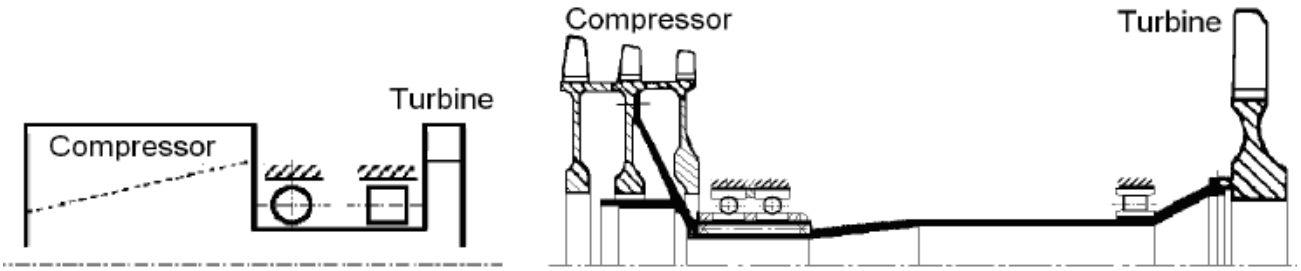


Fig. 7.20. Two-support rotor with supports downstream of the compressor and upstream of the turbine:
a – diagram; *b* – design

The main disadvantage is a difficulty in increasing the rotor rigidity because the bearings limit increasing of the shaft diameter.

Diagram with front support located upstream of the compressor and rear support upstream of the turbine is shown in Fig. 7.21.

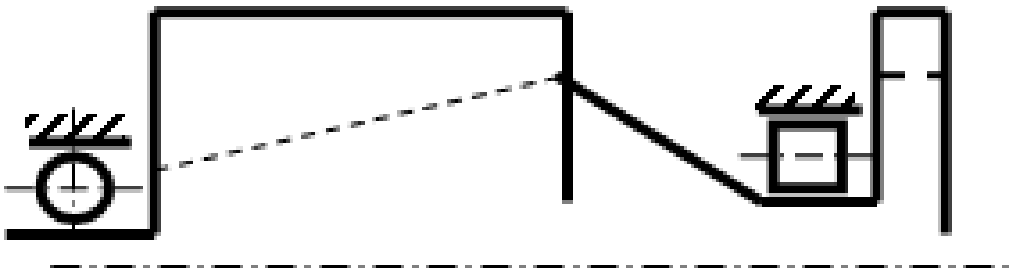


Fig. 7.21. Two-support rotor with supports upstream of the compressor and upstream of the turbine

Advantage of this diagram comparing to the previous one is as follows: it allows increasing rotor rigidity due to increasing shaft diameter.

Disadvantages are:

- significant variation of the axial clearances in the turbine;
- compressor inlet is overcharged by the load-carrying members of the stator;
- complicated oil lubrication system.

Diagram with front support located upstream of the compressor and rear support located downstream of the turbine is shown in Fig. 7.22.

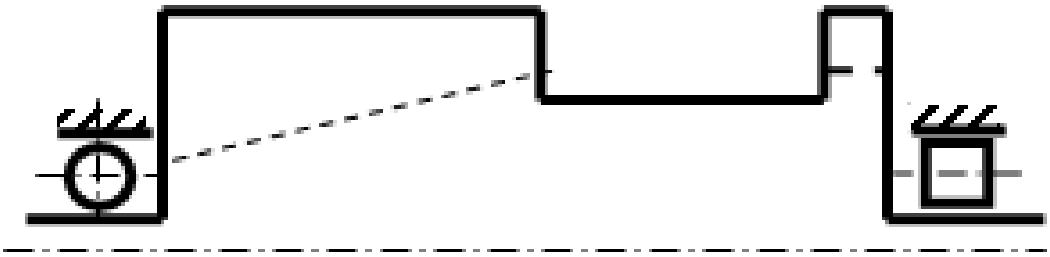


Fig. 7.22. Two-support rotor with supports placed upstream of the compressor and downstream of the turbine

This diagram also has advantages comparing to the first one:

- rotor rigidity may be increased due to increasing shaft diameter;
- simple assembling and repairing due to modular design of the front and rear supports.

Disadvantages of this diagram are:

- complicated design of the casing;
- significant variation of the axial clearances in the turbine;
- inlet to compressor is overcharged by the load-carrying members of the stator;
- complicated lubrication of the supports and cooling of the rear support.

Three-support rotors are used when the turbine and compressor rotors have high weight and low rigidity.

This diagram cannot contain common shaft of the compressor and turbine, because it is difficult to make all supports coaxial. To prevent sagging of the shaft, caused by the axial misalignment, the turbine and compressor shafts are designed as separate ones; they are linked by a special unit – **coupling**. The shaft coupling provides movable joint of the shafts. It transmits a torque from the turbine shaft to compressor shaft, restrains rotor in axial direction and, due to hinge, allows misalignment of the axes within 0.5 to 2 degrees, thus unloading the shaft from the additional sagging. The hinge of coupling is located close to the intermediate support, thus decreasing influence of one shaft on the other when their axes are not aligned.

Three-support diagram is characteristic for the single-shaft turbojets and afterburner turbojets. Some versions of location of the supports are possible.

The diagram with the **radial-thrust bearing located downstream of the compressor** (Fig. 7.23) is the most widely used one. In this case, the radial-thrust bearing operates in a zone of moderate temperatures; the radial clearances in the turbine are not varying to large extent.

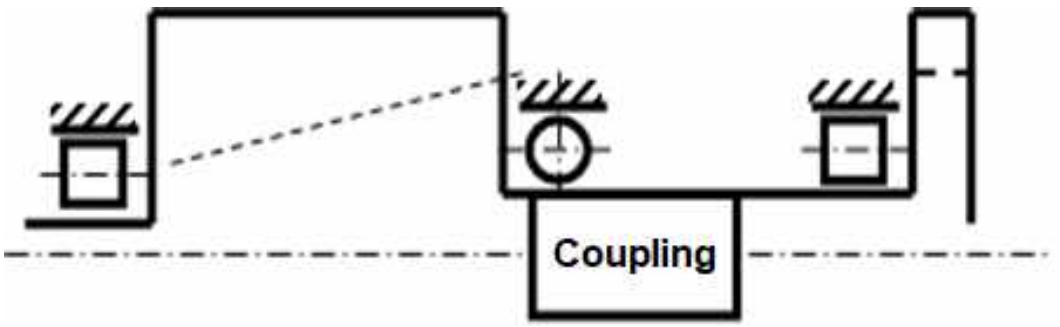


Fig. 7.23. Three-support rotor with displacement of the cantilever turbine

This scheme is usually used when the turbine has small number of stages.

Fig. 7.24 shows a diagram of the three-support rotor with the **radial bearing located downstream of the turbine**. This diagram is used when turbine has large number of stages (the AL-21F).

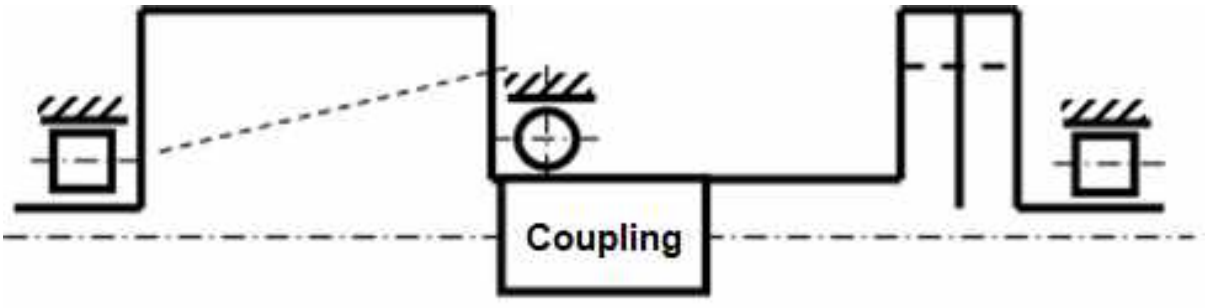


Fig. 7.24. Three-support diagram with radial bearing located downstream of the turbine

The radial-thrust bearing may be located upstream of the compressor (Fig. 7.25). In this case, a highly loaded ball bearing operates in a low-temperature zone. This facilitates its cooling, but the turbine axial clearances are varied significantly.

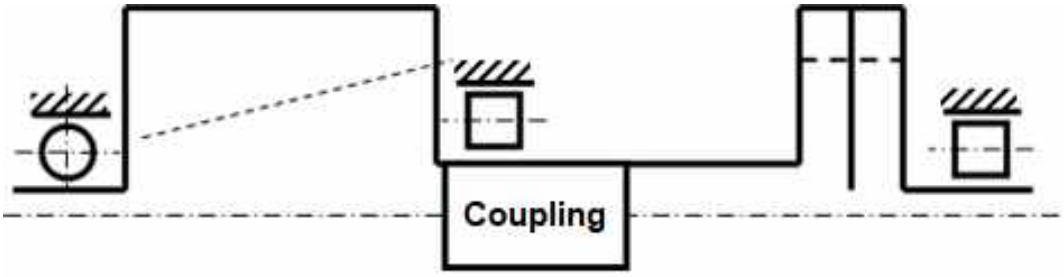


Fig. 7.25. Three-support diagram with the radial-thrust bearing located upstream of the compressor

Four-support rotors are used when the compressor and turbine rotors are long and not rigid, and the turbine has more than three stages. The supports and radial-thrust bearing may be located by several versions.

Fig. 7.26 shows the four-support rotor with one radial-thrust bearing that is located downstream of the compressor.

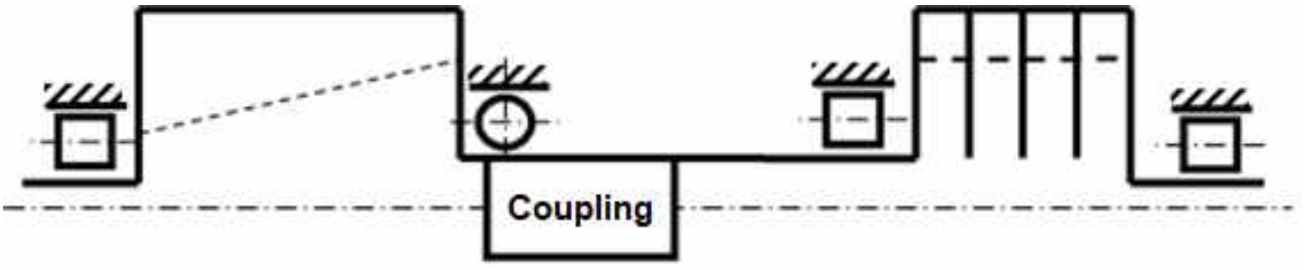


Fig. 7.26. Four-support diagram with one radial-thrust bearing
(the NK-12 turboprop)

In this diagram, the radial-thrust bearing takes a difference of the axial loads, which affect the compressor and turbine. The coupling must provide more than one degree of freedom, as in the three-support diagram, but two degrees of freedom, taking into account the axes misalignment and axes displacement. The other version of design includes a coupling with one degree of freedom, but one of the rotor supports is designed with the radial compliance.

Power diagram with two radial-thrust bearings is also applicable (the TR-1, and RD-20, Fig. 7.27).

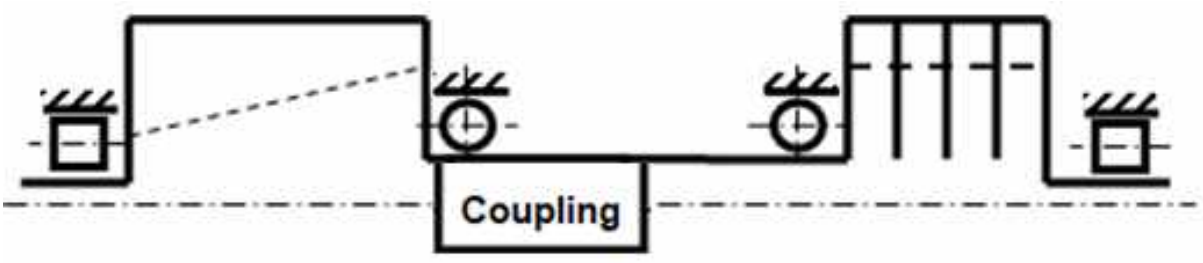


Fig. 7.27. Four-support power diagram with two radial-thrust bearings

The coupling in this diagram transmits only torque from the turbine shaft to the compressor shaft. It is simple in design and represents hollow cylinder with the inner splines at the ends. In this diagram, each radial-thrust bearing takes all loads; therefore, both bearings and load-carrying members, linking rotor and casing, must be forced.

The diagrams with four-support rotors simplify improvement of the compressor and turbine separately; thus, the engine improvement is also

simplified. Nevertheless, the fourth support increases the engine weight and complicates its design.

Multi-support rotors are specific feature of the turbofans and double-rotor turbojets and turboprops.

Each rotor of the double-rotor engine may be located and restrained on its own supports (Fig. 7.28), or some of the supports may be common for both rotors (the R-11F-300, Fig. 7.29).

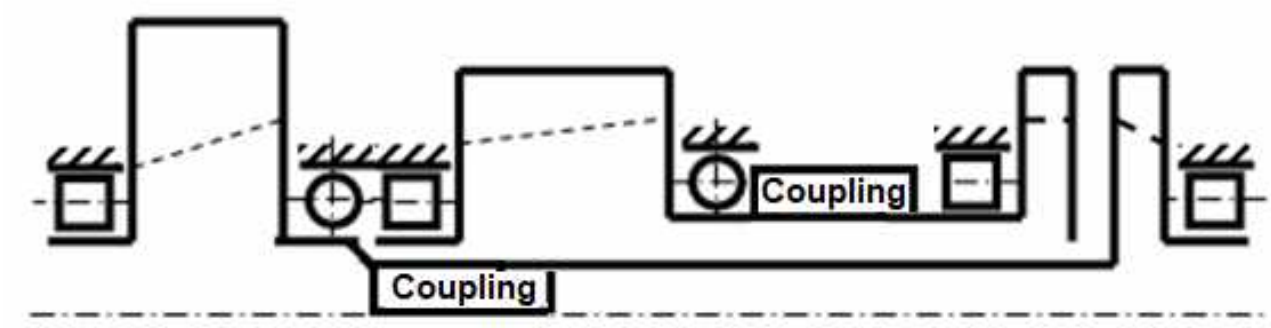


Fig. 7.28. Power diagram of the double-spool rotor with separate three-support rotors

This diagram has independent external supports. It is simple in development. The rotors are restrained in the casing independently. Lubrication system is simple. Otherwise, if the number of supports housings is increased, the engine has large axial dimensions and weight.

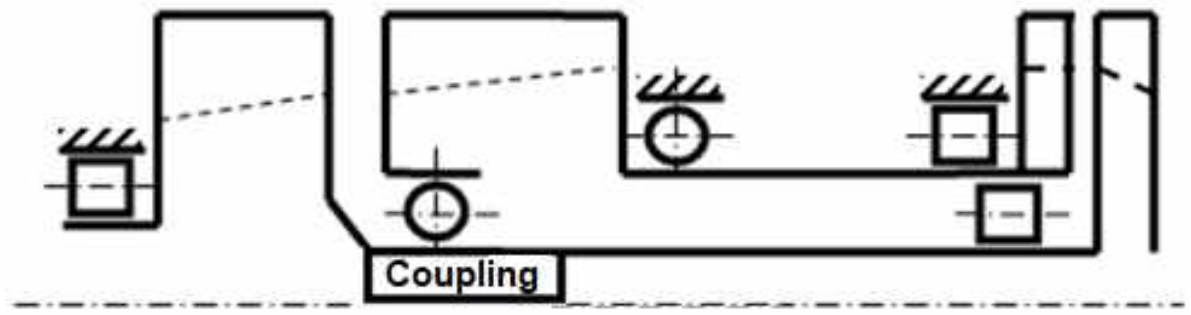


Fig. 7.29. Power diagram of the R-11F-300 two-spool afterburner turbojet

The diagram with the internal inter-shaft supports significantly decreases the engine length and weight. In this diagram, some supports of the low-pressure rotor are located inside the high-pressure rotor; the loads from the low-pressure rotor are transmitted to the casing through the high-pressure rotor. The low-pressure rotor is restrained axially by the radial-thrust bearing that is located downstream of the low-pressure compressor. This bearing transmits the axial and radial loads to the high-pressure rotor; then the total load of the low-pressure and high-pressure rotors is transmitted to the engine

power casing by the radial-thrust bearing, that is located downstream of the high-pressure compressor.

Disadvantages of rotors with inter-shaft bearings are:

- complicated arrangement;
- complicated lubrication and cooling of the inter-shaft supports.

Turboprop engines have increased number of supports because they have a lot of shafts and supports of the gearbox in addition to the rotors of the gas generator.

7.6.2. Loads that act the rotor of the gas turbine engine

Irrespective of the design diagram the rotors take the loads that are the result of the engine operation and aircraft maneuvers.

The torque is transmitted from the turbine rotor to the compressor rotor. The torque causes torsion stresses τ_{tors} in the shaft segment between the turbine and compressor. The torque of the TPE is equalized by the support torques of the compressor and propeller.

The axial gas-dynamic forces originate on the rotor blades and side surfaces of the disks as the result of interaction between the rotor wheel and the air or gas flow. These forces are caused by the axial response of the substance.

The pressure differential between the front and rear unloading chambers of the compressor gives the resulting axial force that affects downstream. The axial forces directed upstream, affect all sections of the compressor rotor. The total axial force of the compressor rotor affects towards thrust force. The total axial force of the turbine rotor affects downstream.

In the presence of the axial link between the rotors of the compressor and turbine, the resulting force of the engine rotor is equal to a difference between the forces of the compressor and turbine rotors, affects towards a thrust force and is taken by the radial-thrust bearing.

The axial force causes shaft tensile stresses σ_t.

The weight forces include the weight and inertial forces, which appear during the aircraft maneuvers. In general, they give transversal, longitudinal and lateral components, directed opposite to the respective component of acceleration. These forces are applied at the gravity centers of assemblies; their values are proportional to the overloads. The axial inertial forces cause

additional tensile or compressive stresses; transversal and lateral inertia forces cause bending stresses σ_b.

The gyroscopic torques originate when the aircraft rotates around one of side axes, and cause sagging torques that affect the rotor. These torques initiate responses of the supports and additional sagging stresses in the shaft.

The centrifugal forces and torques appear only **in case of the** rotor unbalance. Each rotor has permissible static and dynamic unbalance. These forces and torques initiate additional responses of the supports and sagging stresses in the shafts. They may cause abnormal vibration of the rotor and engine as a whole, which results in a fatigue failure of the design members. Only internal centrifugal forces affect the ideally balanced rotor and they do not result in additional loading of the rotor supports and its sagging.

The thermal internal forces originate in the rotor as the result of the non-uniform thermal expansion of the parts with the limited freedom of thermal deformation. The non-uniform thermal expansion is result of different temperature or different thermal expansion factor of the parts. They cause thermal stresses σ_T in the rotor.

7.6.3. Design of the GTE shafts and couplings

The shaft as a member of the rotor design is intended to transmit the torque from the turbine to compressor.

The shaft shall be made as strong, rigid and light part, to transmit the torque reliably, to take the axial forces and sagging torques, to decrease sagging and to improve vibrational resistance. Therefore, the GTE shafts are hollow, with high external diameter. The shafts, which external diameter is less than 120 mm, have ratio of the external diameter to the internal one of 1.14 to 1.17; this ratio for the shafts with the external diameter up to 300 mm is 1.04 to 1.1. The maximal hub diameter is limited by the bearing dimensions.

The shafts of the compressor and turbine in the two-support rotors are joined rigidly by the flange-and-bolt or tightened splined joint.

The shafts of tree- or multi-support rotors are joined by using hinged-movable joints by special connecting couplings. Three types of couplings are used:

– telescopic movable joining by the shaft splined tail extensions;
– telescopic movable joining by the single-row splined bushing;
– joining by the two-row splined bushing.

Diagram of the *telescopic movable joining by the shaft splined end extensions* is shown in Fig. 7.30.

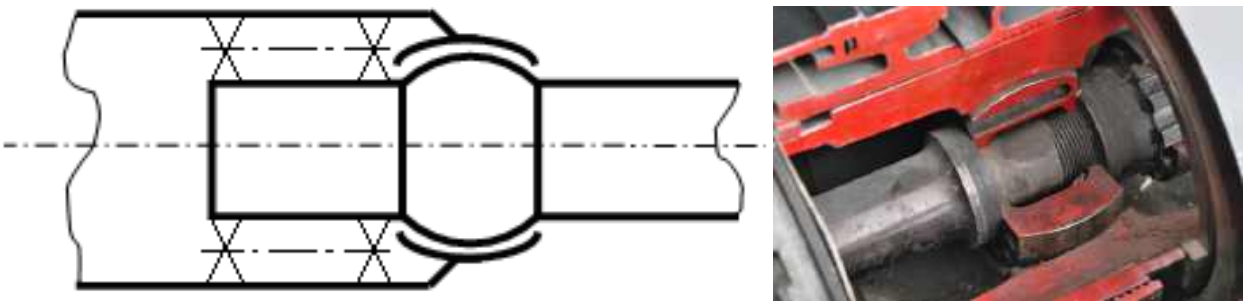


Fig. 7.30. Joining by the shaft splined end extensions

In this joint, the end of one shaft with the external splines enters that of the other shaft with the internal splines. The hinged joint transmits the axial force and ensures operation of the shafts, which are mounted with some axial misalignment.

This diagram may be implemented in various structural designs.

The teeth of the splines have backlash; this is done to compensate for the axial misalignment of 0.5 to 2.0 degrees. The axial force may be transmitted by the screw, retaining sleeve or flexible bar, which do not jam the joint. The spherical washers are installed instead of the complete spherical hinge.

These junctions are simple in design and widely used (the AI-20, AL-7F, RD-9B, D-25V, etc.).

Disadvantage of this design: the shaft has small diameter, so splines shall be long, with increased side clearances; therefore, in case of misalignment of shafts floating contact spot and teeth overloading takes place.

The telescopic movable splined joining by the single-row splined bushing. The design diagram of this joint is shown in Fig. 7.31 (the VK-1, AM-3, and RD-3M-500).

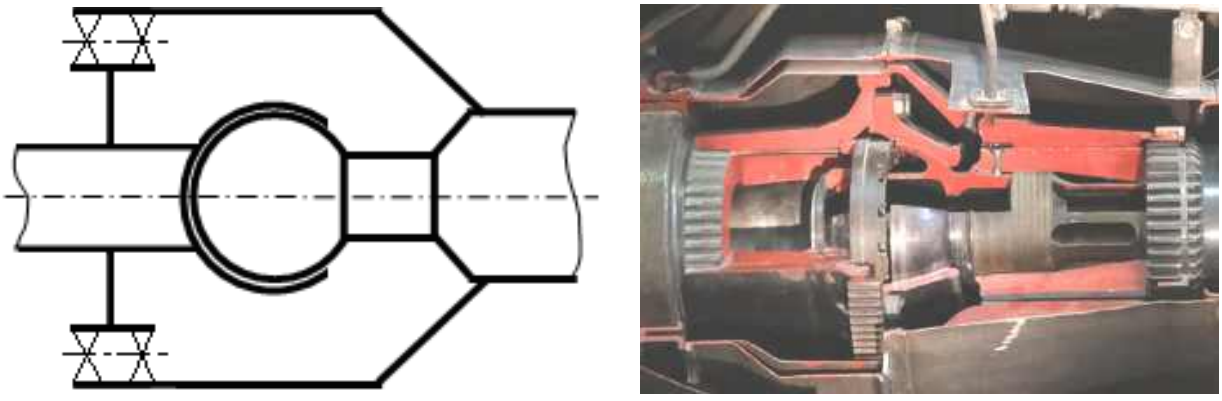


Fig. 7.31. Diagram of coupling with a single-row splined bushing

The diameter of intermediate splined bushings exceeds that of the shaft; this increases the number of teeth and decreases the length of splines. In case of misalignment of the shafts, short splines operate more reliably.

The hinge provides an axial link and unloads the shafts from additional sagging in case of misalignment, restrains the turbine rotor in axial direction and transmits the radial support response of the turbine rotor to the compressor shaft.

Joining by a two-row splined bushing. The design diagram of this joint is shown in Fig. 7.32 (the VD-7 turbojet).

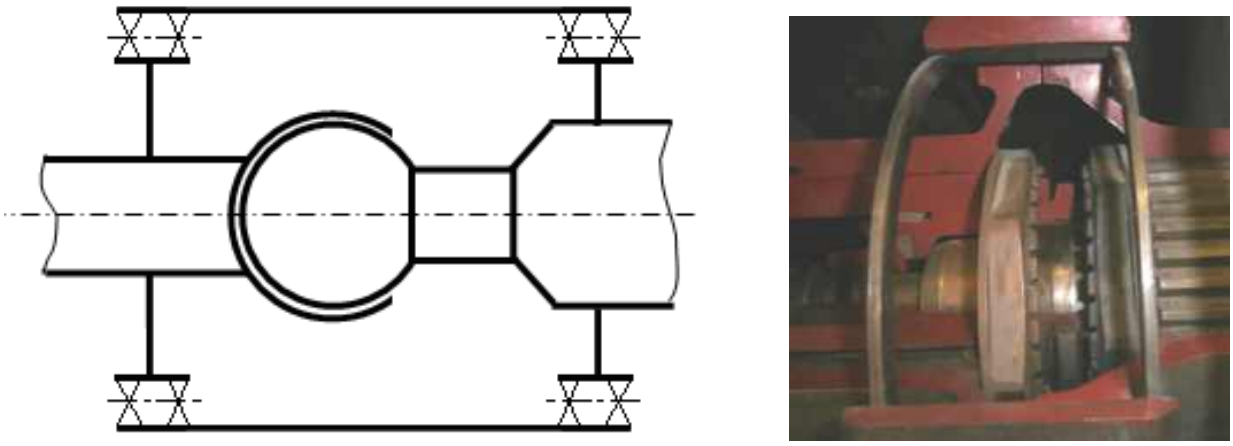


Fig. 7.32. Diagram of coupling with double-row splined bushing and single hinge

Each splined teeth joining with short splines and small clearances is like a hinge, and a two-row bushing as a whole is like a double hinge. Therefore, the shafts in the three- and four-support rotors do not jam. The axial link of the shafts is provided by a flexible rod (low-pressure rotor of the AI-25, Fig. 7.33).

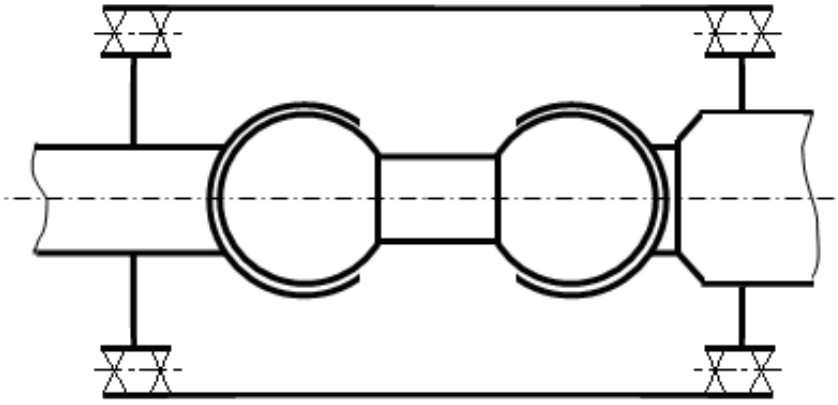


Fig. 7.33. Diagram of coupling with double-row splined bushing and two hinges

The compressor and turbine shafts of the four-support rotor (the TR-1 and RD-20 turbojets) are restrained in the axial direction each by its own radial-thrust bearing. The bushing transmits the torque only when the shafts operate with misalignment. Therefore, the hinge joint is excluded and the bushing design is simplified.

Design of the coupling must ensure single and restrained positional relationship of the assembly parts when the engine operates, simple assembling-disassembling, simple checking of the assembly parts for proper position, lubrication and cooling of movable splined joints. Non-observance of these requirements may cause disengagement of the shafts, rotor unbalance, and worsening of operation of the splined and hinged joints.

The splines are covered with copper to reduce their wearing.

7.6.4. Bearings of the GTE rotors

Support of the rotors includes the bearing with restraining parts, labyrinth and contact seals, members of lubrication and cooling. Design of the supports depends on their purpose and position in relation to the rotor.

At present, roller bearings are used in the aero engines. Their advantages are as follows:

– low friction during starting and operational power ratings;
– reliable operation at high rotational speed;
– simple design and maintenance.

The radial-thrust ball bearings can take combined load with dominating axial component. Three-point and four-point ball bearings can take high loads.

The roller radial bearings can take high radial loads mainly.

The axial force that affects the radial thrust bearing is decreased due to unloading. Total unloading force must exceed the maximum permissible load (i.e., the total force at all operation conditions affects forward, streamlined with a force approximately of 10 to 30 kN, for example, during aircraft acceleration). This excludes shock loading of balls and races and helps for the ball running-in to one side of the races.

In the aero engines, the bearings of the light and super-light series, high accuracy class, with precisely balanced cage are used. The cages are aligned by the inner surface of the bearing outer racer. This design improves heat removal from the bearing due to oil supply under the cage. Balancing of cage is also improved due to its running-in.

The GTE bearings, in accordance with operation conditions, are classified as highly-loaded high-speed ones.

Temperature of the bearings, especially turbine bearings, may reach a temperature of 200 to 250 ºC, rotor rotational speed – from 5000 rpm in the high-power GTE to 60000 to 120000 rpm in the auxiliary power units. The bearings can operate reliably if temperature of the outer racer is 40 to 50 °C less than the tempering temperature of the material. For example, steel ШХ15, which is widely used for manufacture of the bearings, has the tempering

temperature of 175 °C; therefore, such bearing operates reliably at temperature not higher than 120 to 130 °C. Operating temperature may be increased to 225 to 250 °C by improvement of the thermal processing and by using special hardened steels. The engine service life and reliability depend substantially on the bearings.

The alloyed by tungsten steel ЭИ-347Ш (8Х4В9Ф2-Ш), which is made by the electro slag remelting, is less technologic and more expensive than the ШХ15-Ш steel; but it provides bearing operability up to 450 ºС. Sometimes, high-chromium steel 95Х18-Ш is used. Below the low-temperature tempering, it provides operating temperature of 150 to 160 ºС, below the high-temperature tempering – 400 to 420 ºС. These bearings are often used in the supports with the grease, for example in PLA.

Molybdenum-alloyed steel M50 of vacuum-arc remelting has operating temperature up to 320 ºС. However, this steel has limitation at the maximum rotational speed. If $d \cdot n > 2.4 \cdot 10^6$ mm·rpm, then the circumferential tensile stresses originate, which magnitude is higher than 190 MPa.

The outer races are mounted in rigid housings with small clearance (0.02 to 0.04 mm) to allow bearing thermal expansion during heating; the inner race is press-fitted on the shaft with small tightness (0.005 to 0.03 mm), to prevent joint opening when heated. This mounting of bearing aligns the rotor and prevents jamming of the rolling members when the support is heated. Bearing heating is decreased by the following methods:

- special heat throttles are mounted;
- bearing is mounted not on the shaft directly, but on a special intermediate sleeve, with the cooling air supplying into the clearances of this sleeve;
- the bearing is highly lubricated.

The axial clearance between the rotor and stator is controlled by the adjusting ring, mounted in the radial-thrust bearing.

If the rotor is located on three or more supports, then misalignment of axes of these supports causes redistribution of the loads that affect the supports: load on one bearing increases, and the load that affects the other bearing decreases. Both bearings may be destroyed. The overloaded bearing may be destroyed when the round shape of rolling bodies is changed to the oval one. The overloaded bearing may be destroyed due to increasing of friction between the rolling bodies and cage, the rolling bodies begin to slip on the bearing race and initiate vibration and shock loads. Therefore, supports design must guarantee supports to be loaded at all operating conditions. For example, the self-aligning bearing may be used (Fig. 7.34).

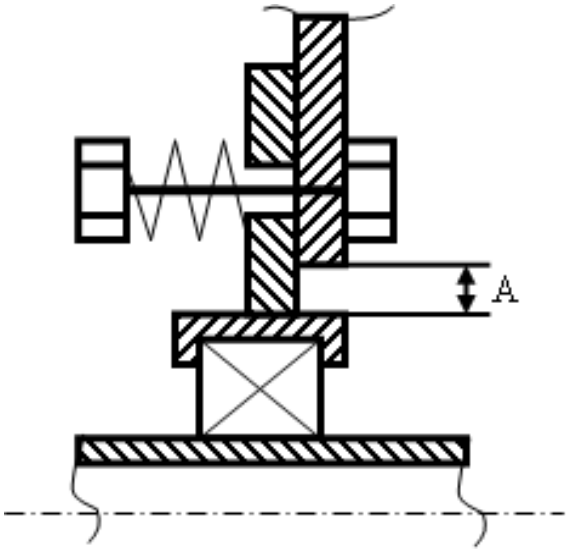


Fig. 7.34. Self-aligning bearing

In a self-aligning support, spring tightening is chosen taking into account the following conditions:

- under the normal conditions, the support operates as a rigid one;
- in case of supports misalignment, the forces of friction between the housing flanges and diaphragm are equalized by the force of shaft elasticity, and the center of bearing displaces to a new position at a distance «A».

The rotor is axially restrained in the casing by the radial-thrust bearing, which races are restrained in the casing and in the shaft (Fig. 7.35).

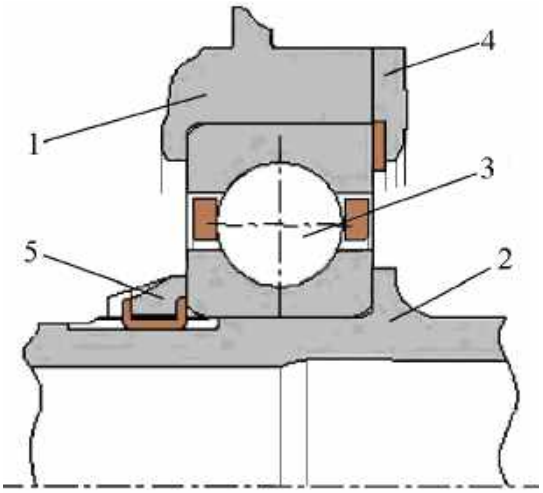


Fig. 7.35. Ball bearing of the rotor support:
1 – stator; 2 – rotor; 3 – bearing; 4 – flange; 5 – thrust nut

If the axial force is too high, a double radial-thrust bearing is used (the AM-3, and R-11F-300). This complicates support design; parameters of the bearings must be identical with high precision; axial clearances in the assembly

must be also identical. Adjustment of this support is done by the special inner and external distance rings.

As it was mentioned above, special unloading chambers are designed to decrease the axial force that affects a radial-thrust bearing. Design of the unloading system must provide one-side action of the axial force under all operation condition. Value of the axial force is 10 to 30 kN. It must exceed the permissible axial inertial force that affects the rotor, for example, during aircraft acceleration. This prevents shock loads on the balls and rolling path, and improves running-up of the ball to one side of the rolling path.

The roller radial bearings (Fig. 7.36) can take high radial loads.

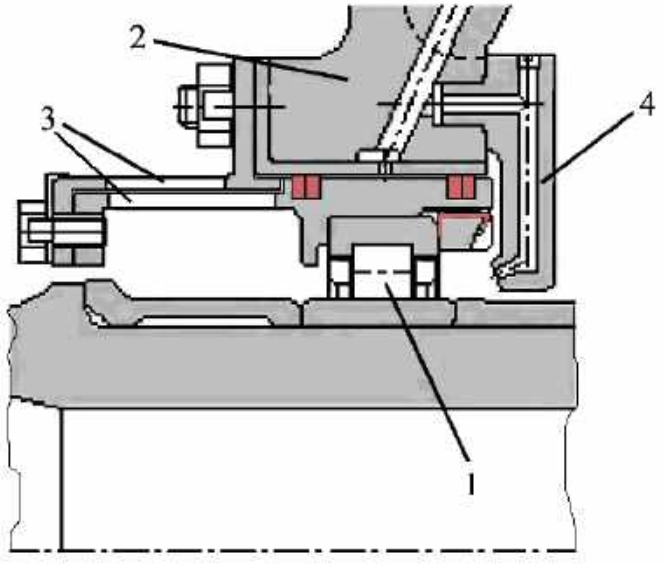


Fig. 7.36. Roller bearing of the rotor support:
1 – bearing; 2 – casing; 3 – elastic members with oil damper; 4 – oil jet

The bearings are lubricated for cooling and decreasing wearing. Lubrication oils are the mineral oil (the МК-8, and МС-20, transformer oil, etc.) or the synthetic ones. The oil takes the heat and small particles of wear from the bearing, protects the surface from corrosion, decreases contact stresses, and decreases noise level. Required oil consumption depends substantially on thermal condition of the bearing. The roller bearings need oil flow of 1 to 3 liters per minute, turbine roller bearings and radial-thrust ball bearings need oil flow of 4 to 12 liters per minute. The oil is supplied by the oil jets (6 to 8 jets for each bearing), arranged circumferentially. The oil is supplied to the inner racer under the cage; then the centrifugal force rejects it to the rolling bodies and the outer racer. Poor oil supply causes temperature rising of the inner race and rolling bodies; clearances are decreased, up to the bearing seizure.

To improve oil circulation and to exclude overfilling of the support chamber and oil foaming, the oil is scavenged from the oil chambers. Thus,

capacity of the scavenge pumps is 3 to 4 times more than that of the feed pump.

Main tasks of bearing designing are:

– determining bearing durability;
– determining the maximum rotational speed;
– determining static load-carrying capacity;
– determining bearing assembly thermal condition and required oil consumption.

The GTE bearings operate at varied loads and varied rotational speed; therefore, their analysis is made for some equivalent operating mode, which is characterized by the equivalent rotational speed at the most durable operating mode. The real axial and radial loads that affect the radial-thrust bearing are reduced to the equivalent load.

Durability of the bearing (ISO 251–90) is determined as follows:

$$L_{design} = (C_r / P_r)^{\alpha} \cdot 10^6 / (60n),$$

where n is rotational speed, rpm;
C_r is radial dynamic load-carrying capacity, N;
P_r is equivalent dynamic load, N;
$\alpha = 3$ for ball bearing, $\alpha = 3.3$ for roller bearing.

Finally, the durability safety factor is determined – ratio of the rated durability of the bearing to the engine service life. Value of this factor is 1.4 to 2.0 for the engines powering the military aircrafts and 1.5 to 3.0 for the aero engines powering the passenger aircraft.

The permissible rotational speed (which corresponds to the bearing rated durability) may be estimated by using an empirical equation:

$$n \cdot d \le (1.6 \ldots 2.0) \cdot 10^6 \text{ mm} \cdot \text{rpm},$$

where n is rotational speed,
d is bearing internal diameter.

This condition is satisfied if circumferential velocity of the inner racer does not exceed 80 to 100 m/s.

For conventional industrial bearings, this value is

$$n \cdot d \le (1.6 \ldots 2.0) \cdot 10^5 \text{ mm} \cdot \text{rpm}.$$

The bearing temperature is one of determining factors of the bearing reliability and durability. Therefore, analysis of the support thermal condition is one of required stages of the bearing designing. This analysis may be done in two versions:

– ***design calculation*** determines the required oil flow through the support;

– ***checking calculation*** estimates bearing temperature under the specified engine maintenance conditions, when the engine is already designed.

The oil circulation is determined by its main function – heat removal; all other functions require less oil consumption.

The oil circulation must be optimum one. Experimental results show that if the oil circulation is low, the bearing is overheated; in case of high circulation, some amount of oil remains in the support, hydraulic losses increase, thus increasing bearing temperature.

Significant heat is produced in the bearing by friction. The rolling friction factor is determined by the experimental equation:

$$f_r = \frac{d \cdot d_0}{2.4 d_{GC}} f_{cor},$$

where d is diameter of journal which carries the inner racer;

d_{GC} is diameter of circle of gravity centers of the rolling bodies;

d_0 is diameter of the rolling body;

f_{cor} is friction factor of the equivalent sliding bearing; for ball bearings, this factor is 0.001 to 0.004; for roller bearings, it is higher because of friction at the end faces of the roller, its value is 0.002 to 0.006.

Analysis of the highly-loaded GTE bearings needs in taking into account the additional contact-dynamic friction, because at high loading the oil film becomes hundreds times thicker, thus provoking sliding friction.

Theoretical experimentally proven researches show that the heat production is similar for the ball and roller bearings. So, criterion equations that characterize the physical process of bearing operation are same. Therefore, if the external heating is negligible, then one and the same method may be used for their heat analysis, with some little corrections. But if the external heat transfer to the bearing is significant, then the internal calculation analysis is only the first stage of bearing heating analysis. Let’s consider this first stage.

Initial data

1. Geometry :

– shaft diameter d, m;

– bearing external diameter D, m;

– diameter of rolling body d_0 (characteristic size $l = d_0$);

– diameter of circle of gravity centers of the rolling bodies $d_{GC} = \frac{d+D}{2}$, m;

– the number of rolling bodies m.

If the bearing is not chosen, then the number and diameter of the rolling bodies are unknown. They may be determined preliminary, by using the following recommendations: $m = 16$, $d_0 \approx 0.1875d$.

2. Rotor rotational speed n, rpm.

3. Load: radial load P, N; axial load A, N (for the ball bearing).

4. Specific radial clearance (radial backlash) $\bar{h} = \frac{h}{d_{GC}}$ for the roller bearing.

5. Contact angle between the rolling body and outer racer for the ball bearing γ, deg.

The absolute clearance for the roller bearings is $h \approx 0.1$ mm, for the highly loaded bearings $h \approx 0.185$ mm. The contact angle in a normally operating ball bearing is $\gamma \approx 26°$.

6. Oil inlet temperature $t_{0\,in}$, ºC.

7. Maximal tolerant temperature of inner racer $t_{bear\ max}$, ºC (for checking calculation) or required oil circulation q_0 (for design calculation).

Calculation procedure

1. Determining of cage circumferential velocity, m/s:

$$u = \frac{\pi(d_{GC} - k)}{120} n, \text{ m/s},$$

where $k = d_{roller}$ or $k = d_{ball} \cos\gamma$.

2. Determining of oil thermal parameters at specified operational temperature (if the external heating is absent, set $t_{0\,d} \approx t_{bear\ max}$, at the presence of the external heating set $t_{0\,d} \approx (0.8…0.95)t_{bear\ max}$;

– kinematic viscosity factor of oil at operational temperature ν, m^2/s;

– Prandtl criterion $Pr = \frac{\nu}{a}$, where a is thermal diffusivity factor of the oil;

– specific heat of the oil at operating temperature C_p, J/(kg K).

3. Determining of Reynolds criterion: $Re = \frac{ud_0}{\nu}$.

4. Determining of load that affects one rolling body:

– centrifugal force that affects one roller $P_c = 12.25 \cdot 10^3 \frac{d_0^3 u_2}{d_{GC}}$, N;

thus mean force that affects the generating line of one roller

$$P_{m\,roller} = \frac{2.92P + mP_c}{2m},\ \text{N};$$

– centrifugal force that affects one ball $P_{m\,ball} = \frac{A}{m}$, N.

5. Determining of Euler criterion, which is relation between the forces of pressure and inertia:

– for the roller bearing, $Eu = \frac{P_{m\,roller}}{\rho(ud_0)^2}$;

– for the ball bearing, $Eu = \frac{P_{m\,ball}}{\rho(ud_0)^2}$.

6. Determining of total resistance factor:

$$C = a\,Re^k\,Eu^i\,Pr^j + b\,Re^c\,Pr^x.$$

For the roller bearing, $b = 18\cdot10^5$, $c = -1.25$, $x = -1$ at any load.
At radial loads less than 2 kN,

$$a = 1.26,\ k = -0.5,\ i = 0.5,\ j = 0;$$

At radial load up to 50 kN,

$$a = 62.3,\ k = -0.63,\ i = 0.25,\ j = -0.4.$$

For the ball bearing at all loads,

$$b = 16.6\cdot10^5,\ c = -1.25,\ x = -1;$$
$$a = 14.7,\ k = -0.214,\ i = 0.287,\ j = 0.44.$$

7. Determining of internal heat flow, W:

$$Q_\Sigma = C\,\beta\,m\,\rho\,d_0^2\,u^3.$$

For the roller bearing, $\beta = 1 + 1.2\cdot10^3\,d(0.00125 - \bar{h})$; for the ball bearing, $\beta = 1$.

8. Then the calculation may be done in two versions:

a) design analysis – determining of required oil circulation q_0, kg/hour, which provides the set temperature $t_{bear\,max}$:

$$q_0 = \frac{3600\cdot Q_\Sigma}{C_p\left(t_{bear\,max} - t_{0\,in}\right)};$$

b) checking analysis – determining of bearing operating temperature t_{bear}, ºC, at set oil circulation q_0:

$$t_{bear} = t_{0\,in} + \frac{3600 \cdot Q_{\Sigma}}{C_p q_0}.$$

Bearing temperature t_{bear} is estimated by the iteration method. In the second item of calculation set appropriate value $t_{bear\ set}$, close to the expected one, then determine oil thermal parameters (specific heat, density, and viscosity) and execute numerical analysis up to item 8, *b*. If temperatures $t_{bear\ set}$ and $t_{bear\ calc}$ differ significantly (for example more than 5 %), then find new approximation $t_{bear\,set} = \frac{t_{bear\,set1} + t_{bear\,set}}{2}$ and repeat calculation, beginning from item 2.

If the support is heated from the outside (by the air from the labyrinth seals, from the turbine disc through the shaft, by the hot gas through the support casing, etc.), then the external heat flow is determined and additional oil circulation is added, which is enough for heat removal, or the bearing temperature is calculated taking into account this additional heating at a set oil circulation.

7.7. Design of elastic-damper supports of the engine rotors

Rotors of the up-to-date aero engines are mounted on the elastic-damper supports.

The main goal of the elastic-damper support is decreasing of rotor and engine vibrations and elimination of abnormal resonant vibrations within the engine power ratings. To solve these tasks, one must match the parameters and characteristics of the supports with the rotor system dynamic performances. This matching must be done at the stage of engine designing, because it is difficult to change the dynamic performances at the stage of development, because as a rule a significant redesign of the entire engine is required.

Designs of the elastic-damper supports are various, but all of them execute two main functions:

– to make elastic compliance of the supports that changes an elastic system of the rotor and the engine as a whole, decreases the natural oscillation frequency of the system and dynamic stresses in the parts;

– to absorb the energy of the oscillatory system and to convert it into the heat, thus preventing propagation of forced oscillations with high amplitudes

and dynamic stresses in all parts of the engine; each support has an optimum damping coefficient, which provides the maximum decreasing of vibrations.

The elastic-damper assemblies are located as a rule between the casing and outer racer of the ball or roller bearing. Their dimensions depend upon those of the journals and bearings. Rotor supports with elastic-damper assemblies are named as the elastic-damper supports.

Three types of the elastic-damper supports are most widely used now:

– with ring elastic members;

– with rod-type elastic members (‘squirrel-wheel’ members);

– hydrodynamic supports.

7.7.1. Support with ring elastic elements

The main elastic member is thin-walled elastic ring 1 (Fig. 7.37). This ring is placed between the bearing outer racer and housing with tight fit (0.03 to 0.04 mm at diameter 100 to 120 mm) and is supported by its protuberances to ring 2 that is mounted in casing 3, and to the protuberances of ring 4 that is mounted on outer racer 5.

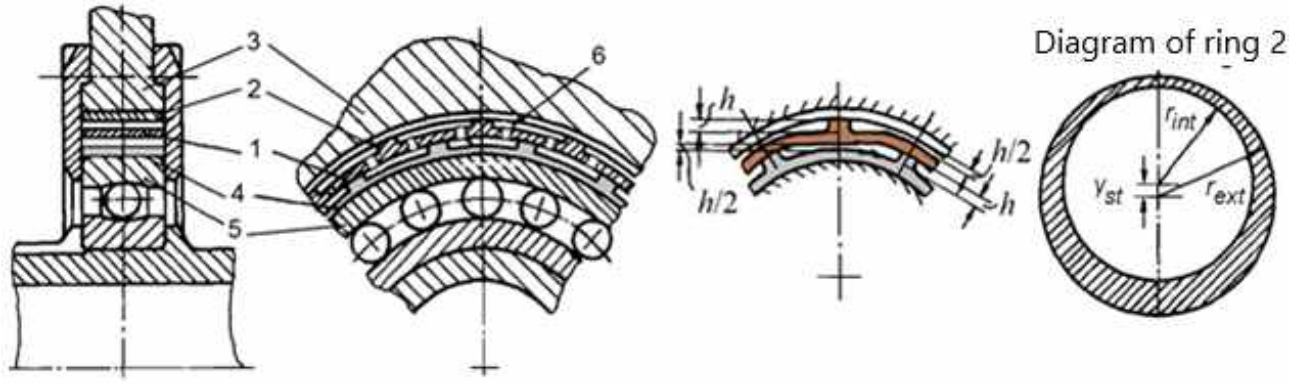


Fig. 7.37. Elastic-damper support with ring elastic members:
a – design with one elastic ring; *b* – diagram of mounting of elastic ring;
c – ring elastic members

In case of radial displacement of the bearing, the segments of the elastic ring bend, thus creating elastic response on the bearing. The elastic ring has 9 to 12 protuberances on the external and internal surfaces, and the same number of the elastic segments. The protuberances are dislocated in staggered order, and a positional relationship of the rings is restrained by a special retainer.

Thickness and width of the elastic ring determine the support rigidity, and height of protuberances determines permissible sagging of the ring segment, which is related to the strength. As usual, it is 0.10 to 0.25 mm and must be not less than a double static sagging.

The ring is mounted in the casing with tight fit by the protuberances. The negative allowance is equal to a half of the protuberance height. Ring 1 has a negative allowance of approximately 0.02 mm that prevents a backlash by the inner protuberances of ring 4.

Deformation of the ring segments causes a pumping effect; the oil is extruded or sucked through the end clearances and calibrated orifices 6. The maximum damping effect is provided due to a choice of the clearances and diameter of the orifices. Besides, the orifices 6 prevent destruction of the oil films and worsening of the support damping ability.

Fig. 7.38 shows designs of the elastic rings. The ring with a sagging limiter improves precise calibration of the ring sagging that prevents the ring overloading and loss of elasticity. To decrease a rigidity of the support, double-ring or triple-ring diagram is applied.



a *b* *c* *d*

Fig. 7.38. Designs of elastic ring:
a, *b* – single-ring diagrams; *c* – ring with sagging limiter; *d* – double-ring diagram

The main advantage of the support with the elastic ring is that this support is compact and low-weight.

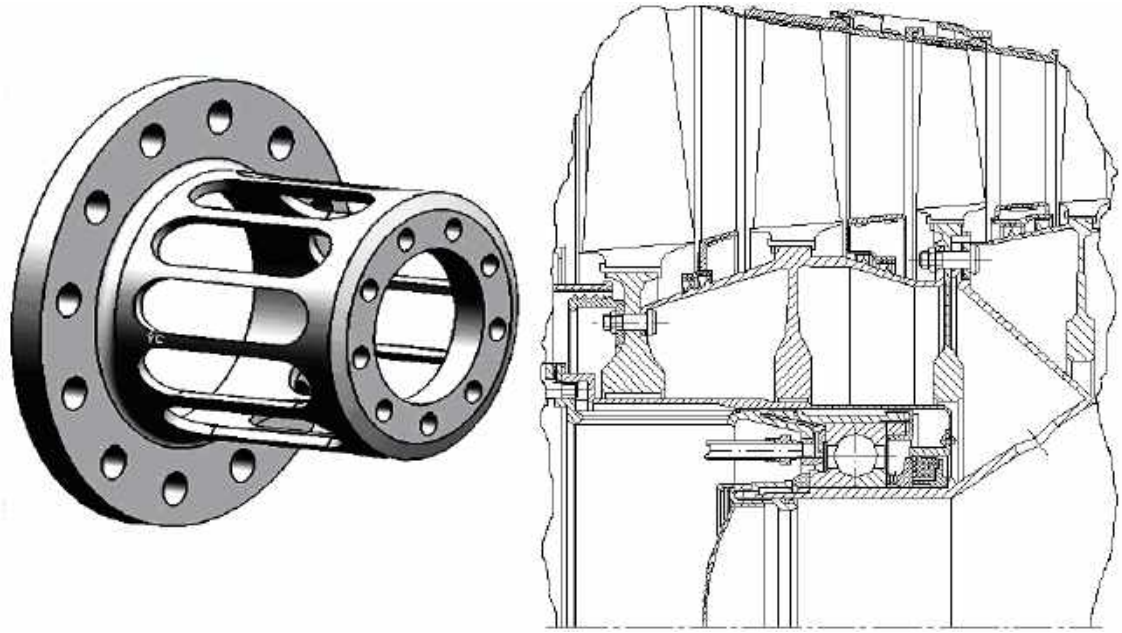
The disadvantage is tough requirements to manufacturing stability: all dimensions must be precise; development after assembling is required for reaching stable elastic-damping characteristics.

7.7.2. Support with rod elastic members of a “squirrel wheel” type

The name “squirrel wheel” is due to a superficial resemblance of the elastic element structure with the squirrel wheel (Fig. 7.39). The elastic-damper support is a sleeve with many slots. Flange at one side of the sleeve attaches it

to the casing; in the other side, the rotor bearing is mounted. Design of the casing sleeve may be different, but sometimes it is also the “squirrel wheel”. In this case, the casing sleeve is the second elastic member of the support.

Bearing and sleeves transmit the radial force from the shaft to the housing. Under action of this force, the elastic sleeves are bended, thus allowing the shaft to oscillate without high stresses.



a *b*

Fig. 7.39. Elastic-damper support of “squirrel wheel “ type:
a – elastic sleeve; *b* – design of the D-136 turboshaft LPC support

Rigidity of the support depends on the thickness of the sleeve walls, the width of slots, and the number and length of the elastic rod members (rods), which are formed by the slots.

The rod members will have the same rigidity and bending stresses in all directions if their cross-section is round. However, due to technological reasons, they are made with square cross-section.

The damping member of the support actually is thin oil layer between the sleeves. The layer thickness is 0.2 to 0.3 mm; this defines a magnitude of the elastic radial deformation of the support. The oil is supplied to the chamber from a circular groove in the housing through the radial holes that are uniformly located in the outer sleeve. Displacement of the sealing rings determines a length of the damping oil layer. Therefore, these parameters are optimized by computing or by the experimental development.

The oil layer makes not only the hydrodynamic damping effect. It also operates like a hydrodynamic bearing that perceives a rotated radial force from

the rotor. Hence, the hydrodynamic radial force is added to a rigidity force that is created by the support rods.

7.7.3. Hydrodynamic damper support

Supports with the hydrodynamic oil film without elastic members are widely used now (Fig. 7.40).

The main advantages of the hydrodynamic support are simple structure and low weight.

The disadvantage is a complicated hydrodynamic calculation that needs in the thermal state consideration.

Thickness δ and width of the oil film are determined by a hydrodynamic analysis of the oil layer, which is full load-carrying and damping.

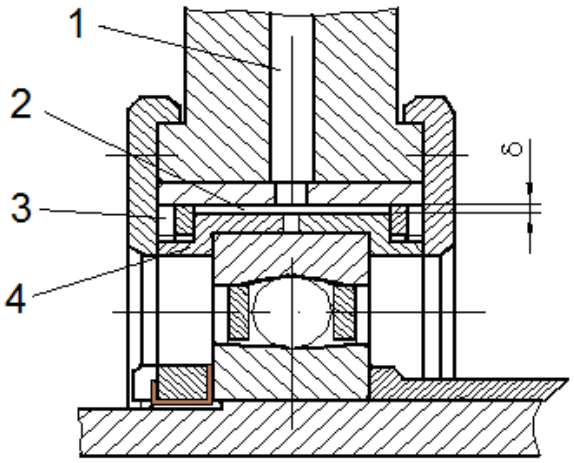


Fig. 7.40. Design of hydrodynamic damper support:
1 – oil supply from pipe; 2 – oil layer; 3 – elastic rings; 4 – floating sleeves

In the simplest designs, the load-carrying oil film is formed directly between the outer racer and the sleeve of the housing at the minimum possible end face clearance (within 0.02 to 0.04 mm).

To widen the oil film and to improve the end face seals, the design is used that is shown in Fig. 8.65. It helps to choose precisely dimensions of the oil film, to provide stability of the damping support characteristics during operation and to receive identical characteristics when assembling.

The oil layer operates at high load. So, the support is intensively heated that influences the oil viscosity. It significantly depends on the rotor rotational speed. To maintain stable elastic and damping characteristics of the support, high consumption of the oil is required. Therefore, when designing support, its thermal condition and required oil flow rate are estimated by using special numerical analysis.

7.8. Accessory drives

The accessory drives provide operation of the power plant of the aircraft accessories. Majority of the accessories are driven by the engine rotor. The accessories that are used during the engine starting usually are self-driven. Both the engine accessories (fuel and oil pumps, centrifugal breathers and de-aerators, starting units, etc.) and the aircraft accessories (hydraulic pumps, electric generators, air compressors, etc.) are mounted on the engine accessory drive gearboxes.

Reliable operation of the engine and aircraft as a whole significantly depends on a reliable operation of the accessory drives that determines the main requirements to them:

- fault-free operation at all operating conditions of the engine and aircraft;
- design of the drive with the minimum weight and overhaul dimensions must ensure the specified values of the gear ratios, powers, and sense of rotation without obstructing engine assembling and maintenance and without increasing its overall dimensions;
- the minimum weight and dimensions (very often, the engine overall dimensions depend on those of the accessory drives);
- easy assembling and disassembling of the engine and the drive itself;
- easy manufacturing and maintenance, convenient access to the places of inspection and adjustment, and easy replacement during engine overhaul.

In the up-to-date GTE, the weight of the accessories with accessory drives reaches 15 to 20 % of the engine total weight. The power used to drive the engine accessories is 0.2 to 0.5 %, and for the aircraft accessories is 0.3 to 0.6 % of the total turbine power. The lower values of the weight and power are related to the engines powering the fighters, the higher values are related to the engines powering the passenger and transport airplanes. More perfect accessories have less weight and consume less power; they also may be driven directly by the shafts of the engine or gearbox. This decreases a total weight of engine by 5 to 10 %.

The most expedient from the point of view of the maintenance the accessories shall be arranged according to their belonging. Therefore, the engine and aircraft accessories shall be attached separately.

As a rule, both the aircraft and engine accessories are located on the engine accessory drive gearboxes. Sometimes, the aircraft accessories are mounted on the special external gearboxes of the aircraft accessories. In this

case, the engine gearbox contains only a drive for the external gearbox that essentially facilitates the engine replacement in service (the RD-33, AL-31F, and F-100-PW-100).

As a rule, arrangement of many accessories in one accessory drive gearbox is not rational, because it increases engine diameter and drive power, complicates access to the accessories and makes its difficult providing a required gear ratio. Therefore, the engine is equipped with several (up to three or five) accessory drive gearboxes. The accessories are distributed between them according to their functions and specified gear rations. The task of arrangement of the accessory drive gearboxes on the engine is solved together with the aircraft designers taking into account conditions of engine location in the aircraft and accessibility to the accessories when carrying out engine maintenance in service.

Functional diagrams of the drives are usually represented as simple transmissions by using spur or bevel gears. The rolling bearings are used as the supports for the rotary parts. In a case of bevel gears, a clearance in the gearing must be controlled (that is done by placing spacer rings between the gear and radial-thrust bearing). Axial displacement of the rotor must not influence the bevel gearing (as a rule, a pair of the bevel gears is located close to the radial-thrust bearing of the engine, or by installation of the floating splined torsion shaft, the drive is located upstream of the compressor or downstream of the turbine).

Some accessories may be mounted directly in free chambers of the engine (for example, sections of the oil pumps of the AL-21F turbojet).

All gears of the drives are lubricated by splash oil (oil fog); high loaded assemblies are equipped with the oil jets to supply the oil.

7.9. Check questions

1. What is named as the engine power system?
2. Give classification of the loads that affect engine by the nature of their origination.
3. To what sides are directed the axial forces that affect the compressor and turbine?
4. What components determine the axial force that affects a radial-thrust ball bearing of the engine?
5. At what flight conditions the engine rotor is affected by a gyroscopic torque?

6. What components of the engine take an axial force that affects a rotor during aircraft retardation?

7. In what cases the inter-shaft bearing is introduced into a power system of the turbofan engine rotor?

8. Why one of the engine rotor supports contains a ball bearing, and all other supports are equipped with the roller bearings?

9. How are the radial forces transmitted from the rear support of the turbojet rotor in a power diagram with the internal power link?

10. What is the purpose of the elastic-damper supports?

11. Make a comparative analysis of designs of the elastic-damper supports with the ring-type and rod-type elastic members.

12. Name advantages and disadvantages of centering of the bearing cage by the inner and outer rings.

13. How are thermal conditions of bearings operation ensured?

14. Describe the method for calculation of thermal condition of the rolling bearing.

15. What structural members are included in the engine rotor supports and what is their purpose?

16. What loads are perceived by the engine mounting system?

17. Name requirements to the structural design of the engine mounting system.

18. Design of the engine shafts and couplings.

8. COMPRESSOR AND TURBINE RADIAL CLEARANCE CONTROL

One of the main tasks of development and manufacture of the GTE is ensuring high efficiency, especially of the last stages of the compressor and turbine.

To prevent touching between the rotor and stator at all power ratings, the radial and axial clearances are provided.

The radial clearance is a clearance between the tips of the rotor blades and casing (Δ_1) or the clearance in the labyrinth seal (Δ_2).

Relative radial clearance in the compressor last stages with long blades is changed faster than in the first stages. Increasing of the relative clearance in the compressor worsens performances of the compressor and engine as a whole (Fig. 8.1).

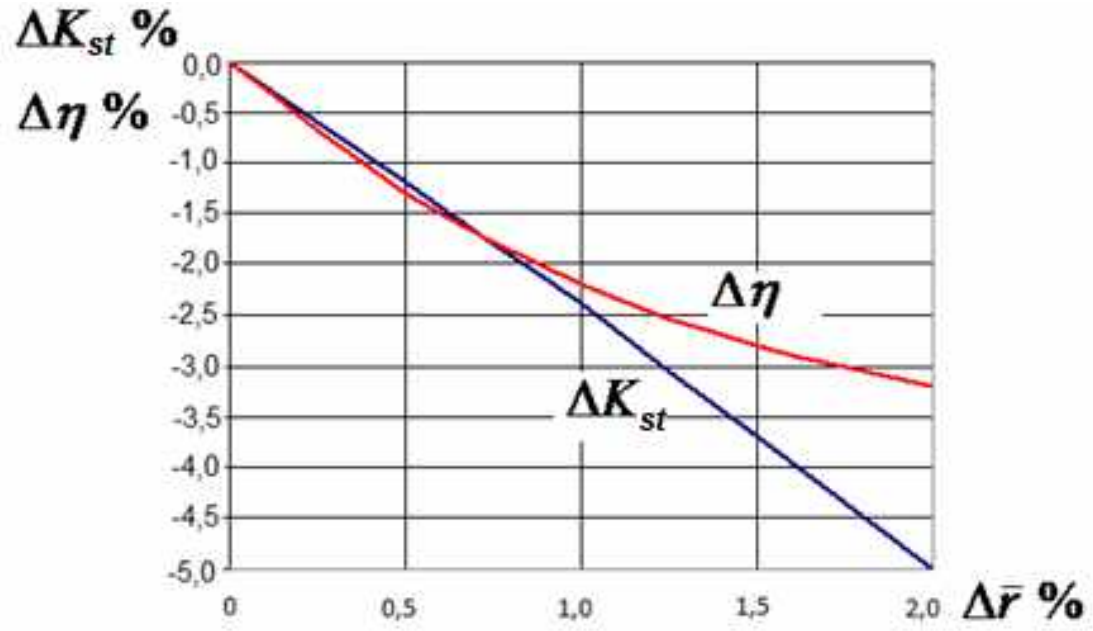


Fig. 8.1. Compressor efficiency and margin of stability vs radial clearance

Efficiency of the turbine is changed similarly: if the radial clearance changes by 3 %, then the turbine efficiency will be changed practically linearly by 5 %.

Since the significant portion of the losses in the gas flow duct of the axial bladed machines depends on the flow in the clearance and on its interaction with the main flow, so these losses are decreased by the various methods.

Several versions of the devices located above the rotor were developed to improve efficiency of the bladed machine without complicating its structure significantly. The simplest version is represented by the stator design with the annular grooves (Fig. 8.2).

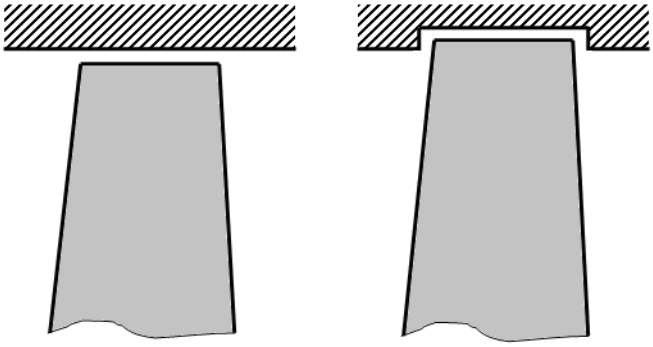


Fig. 8.2. Device located above the rotor – annular groove

At same radial clearance, the arrangement with a ring grove is essentially more efficient comparing to arrangement with smooth stator. However, this simple design not ensures optimum radial clearance at all operation conditions of the engine.

The same researches were carried out for the rectangular, triangular and saw-shape grooves that were located across the flow and at an angle to the flow (Fig. 8.3). The results are shown in Table 8.1.

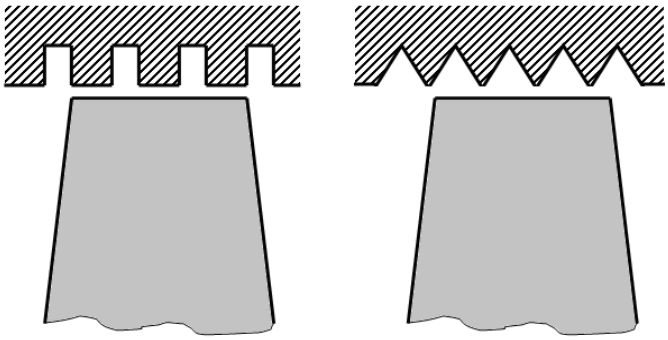


Fig. 8.3. Grooves located above the rotor

Table 8.1

Results of influence of researches of devices located above the rotor on the turbine efficiency

Casing	Turbine efficiency
Smooth casing $\overline{\delta}$ = 2.4 %	0.8484
Smooth casing $\overline{\delta}$ = 1.0 %	0.8688
Transversal grooves $\overline{\delta}$ = 2.4 %	
Rectangular	0.8474
Triangular	0.8437
Saw-shape	0.8467
Longitudinal grooves $\overline{\delta}$ = 2,4 %	
Rectangular	0.8230
Triangular	0.8348

Casing	Turbine efficiency
Screw grooves across chord of airfoil $\overline{\delta}$ = 2.4 %	
Rectangular	0.8129
Triangular	0.8225
Screw grooves along chord of airfoil $\overline{\delta}$ = 2.4 %	
Rectangular	0.8450
Triangular	0.8420
Transversal grooves $\overline{\delta}$ = 1.0 %	
Saw-shape	0.8732

Numerical analysis and testing showed that the grooves located above the rotor are not efficient at high relative radial clearance. If the relative clearance is low (approximately 1 %), then the maximum positive effect give the transversal saw-shape grooves, which depth is 2 to 3 times more than the radial clearance.

The axial clearance is a clearance between the disc rim and internal shroud of the nozzle guide vanes (mounting clearance φ) or between the trailing edges of the nozzle vanes of the nozzle guide vanes and the leading edges of the rotor blades (inter-blade clearance δ).

The axial clearances are changed during thermal expansion of the stator and rotor. The value of clearance φ in the cool and hot conditions is as follows:

$$\varphi_{cold} = L_{rot} - L_{stat};$$

$$\varphi_{hot} = L_{rot}\,(1 + \alpha_{rot}\,\Delta t_{rot}) - L_{stat}\,(1 + \alpha_{stat}\,\Delta t_{stat}),$$

where L_{rot}, L_{stat} are distances from the radial-thrust bearing to the plane of rotor and stator in a place of the radial clearance;

α_{rot}, α_{stat} are the thermal expansion coefficients of the rotor and stator parts;

Δt_{rot}, Δt_{stat} are changes of the rotor and stator temperatures in relation to the cold condition.

During starting, the stator is heated faster than the rotor. Therefore, the axial clearance upstream of the disc is decreased, and downstream of the disc is increased. During engine shutdown – vice versa, because the stator is cooled faster than the rotor.

In the known designs, the relative radial clearance is as follows:

$$\overline{\varphi} = \frac{\varphi_{cold} - \varphi_{hot}}{L} \approx 0.3 \text{ to } 0.4\ \%,$$

where

$$L = \frac{L_{rot} + L_{stat}}{2}.$$

The axial inter-blade clearance in the known designs is 10 to 40 % of the blade mean chord.

To decrease the radial clearance and to prevent rotor blades touching a casing and its break, the inserts made of the relatively soft material are used in the inner surface of the casing: for compressor – the graphite, magnesium oxide, aluminum oxide or talk; for turbine – ceramic and metal double-layer inserts (hard iron-nickel-graphite layer as a base material and nickel-graphite soft layer is a working one). If the rotor blade is designed without the shroud platform, then the trailing edge is cut.

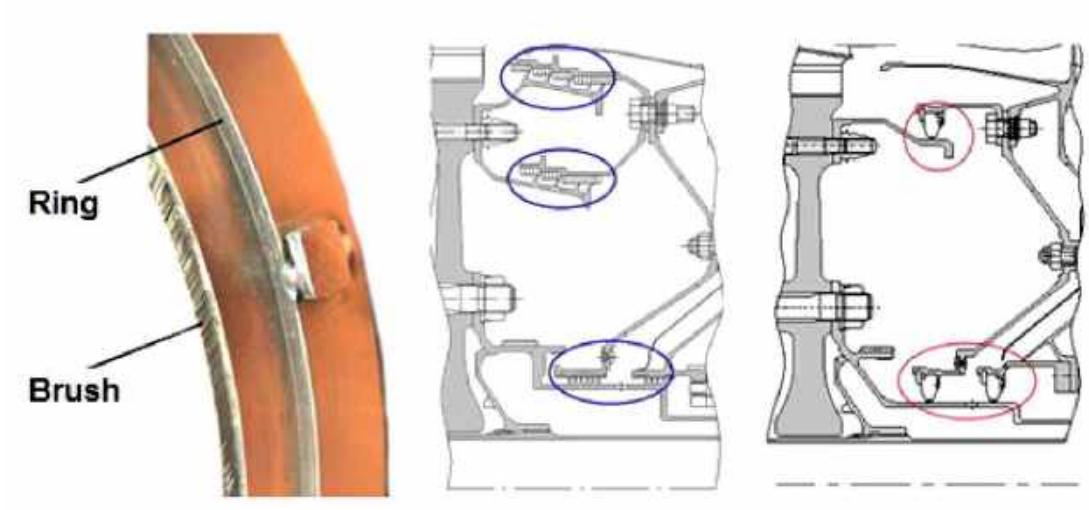
The radial clearances are decreased during engine operation within its service live.

However, the use of the devices located above the rotor (easy abradable inserts, profiled grooves, honeycomb inserts, etc.) do not maintain the minimum radial clearance at all engine power ratings.

Leading companies that design and maintain aircraft and stationary GTE are working at improvement of performances of the engines by implementing brush seals.

The brush seal is a ring-shape brush with thin wires made of nickel-chromium-cobalt-tungsten alloy or non-metallic fibers (Fig. 8.4, *a*). The angular displacement of the wires to the rotor adjacent portion decreases friction.

Fig. 8.4, *b* and *c* represent an example of the turbine arrangement, in which traditional labyrinth seals are replaced by the brush seals.



a *b* *c*

Fig. 8.4. Brush seal:
a – external view; *b* – turbine initial design with labyrinth seals;
c – turbine design with brush seals

Tests of the brush seals showed that they are 1.5 to 2 times more efficient comparing to the traditional labyrinth seals (Fig. 8.5).

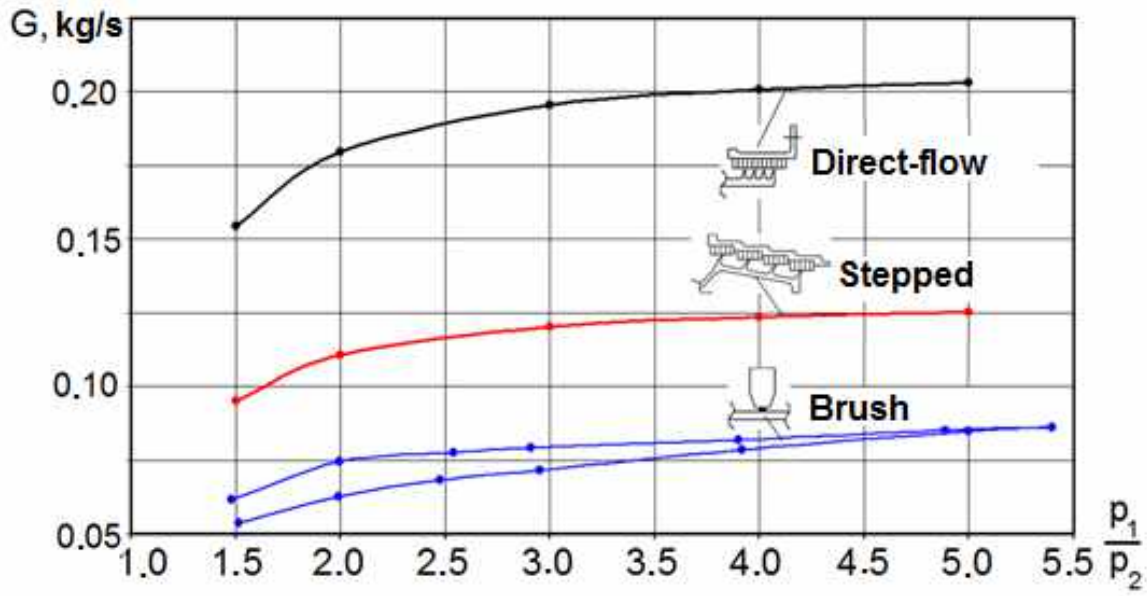


Fig. 8.5. Flow diagrams of brush and two types of labyrinth seal with four fins when radial clearance is of 0.2 mm

High efficiency of the compressor and turbine is maintained by active or passive radial clearance control at all power ratings during engine operation. The most actual task is controlling radial clearance during transient power ratings – starting, acceleration, deceleration, and engine emergency in-flight shutdown. One of the important features of the new-generation engines is availability of system of the active radial clearance control in the region of the engine compressor and turbine, which is based on information about the actual values of the radial clearances in the gas flow duct received from the sensors mounted above the rotor. Such technology of the active clearances control needs in a fast response of the actuator when the clearance changes and a feedback by direct measurements of the clearance. It ensures to take full advantage of low clearances inside the engine both at the steady and transient power ratings. According to the NASA data, the radial clearance can reach 0.125 mm; if the clearance is decreased by 0.25 mm then specific fuel consumption will be decreased by 1 %. Besides, the expenses related to engine routine maintenance and overhaul will be decreased, because high radial clearances are one of the main factors that worsen operation of structural members of the engine hot portion.

The radial clearance between the rotor blades and casing in the operating engine depends on the initial mounting clearance and a component that depends on the engine power rating. In this case, the minimum mounting clearance is chosen so that must ensure a reliable operation at all power ratings; it is determined by taking into account all mechanical, inertial and thermal loads that affect the engine.

At a steady-state power rating, the clearance is stable and it depends on the thermal deformations of the rotor and stator structural members, and also on the centrifugal elongation of the rotor. At the transient power ratings that are characterized with the rapid variations of the gas temperature and rotational speed, the clearance may be significantly increased or decreased to the abnormal values, at which the tips of the blades touch the stator inner surface. These variations of the clearances are principally axisymmetric ones. However, the non-symmetric variations of clearances may be originated due to non-uniformity of the in-flight loads that affect the engine, for example, during abrupt maneuvering, takeoff, and landing.

8.1. Methods of radial clearance control

In some engines, it is possible to control the radial clearances depending on the engine power rating. The first natural method of the radial clearance control (RCC) was a forced cooling of the problematic zones. Thermal methods of the RCC become the most developed and widespread ones. Other methods of the RCC appeared later. Their classification is shown in Fig. 8.6.

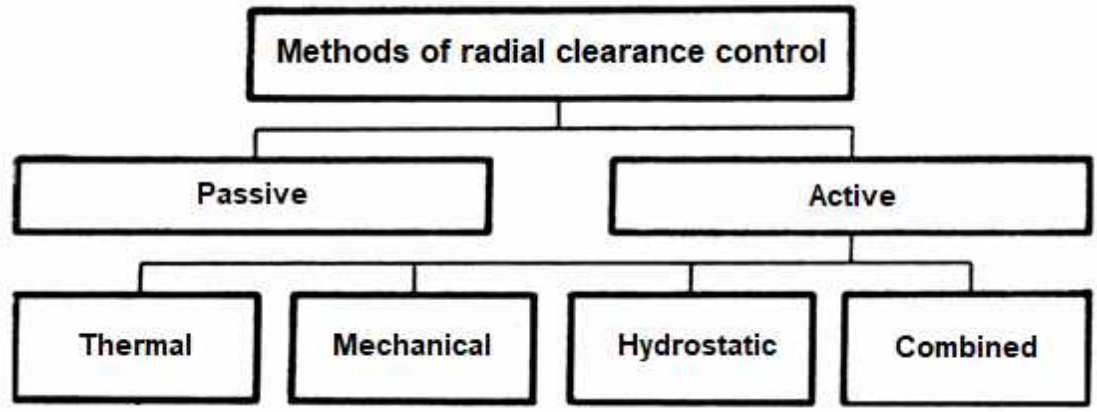


Fig. 8.6. Classification of methods of radial clearance control

Depending on the methods affecting the value of the radial clearance, there are passive and active methods of the RCC. When using the passive control, prompt action on a radial clearance is absent and controlling is performed indirectly – by matching of thermal expansion of the blades and casing due to respective distribution of weight and choosing the values of their thermal expansion; by using various shields and thermal barriers to isolate the parts from the hot gases, as well as various devices maintaining required level of the radial clearance.

The RCC makes it possible to increase the engine efficiency by 1 to 2 %, to improve matching of the stator and rotor heating rates at transient process of

the non-heated engine acceleration to the takeoff power rating (now, the takeoff with non-heated engines become a regular power rating that ensures fuel economy up to 2 to 3 %), which allows to decrease the engine wear at the transient power ratings (Fig. 8.7).

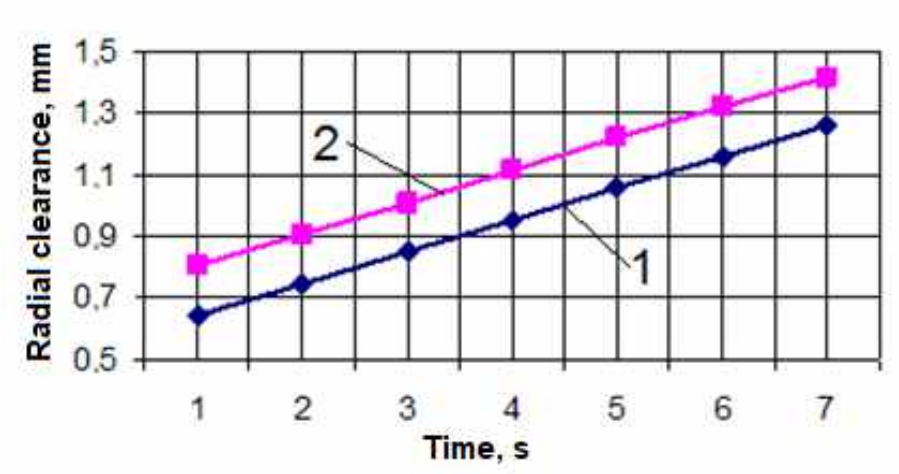


Fig. 8.7. Variation of turbine radial clearance at acceleration for heated (1) and non-heated (2) engine

The RCC is the most actual for turbine of the GTE; at high compressor pressure ratio it becomes actual also for the compressor last stages. Fig. 8.8 shows variation of the radial clearance in the first stage of high pressure turbine at various power ratings.

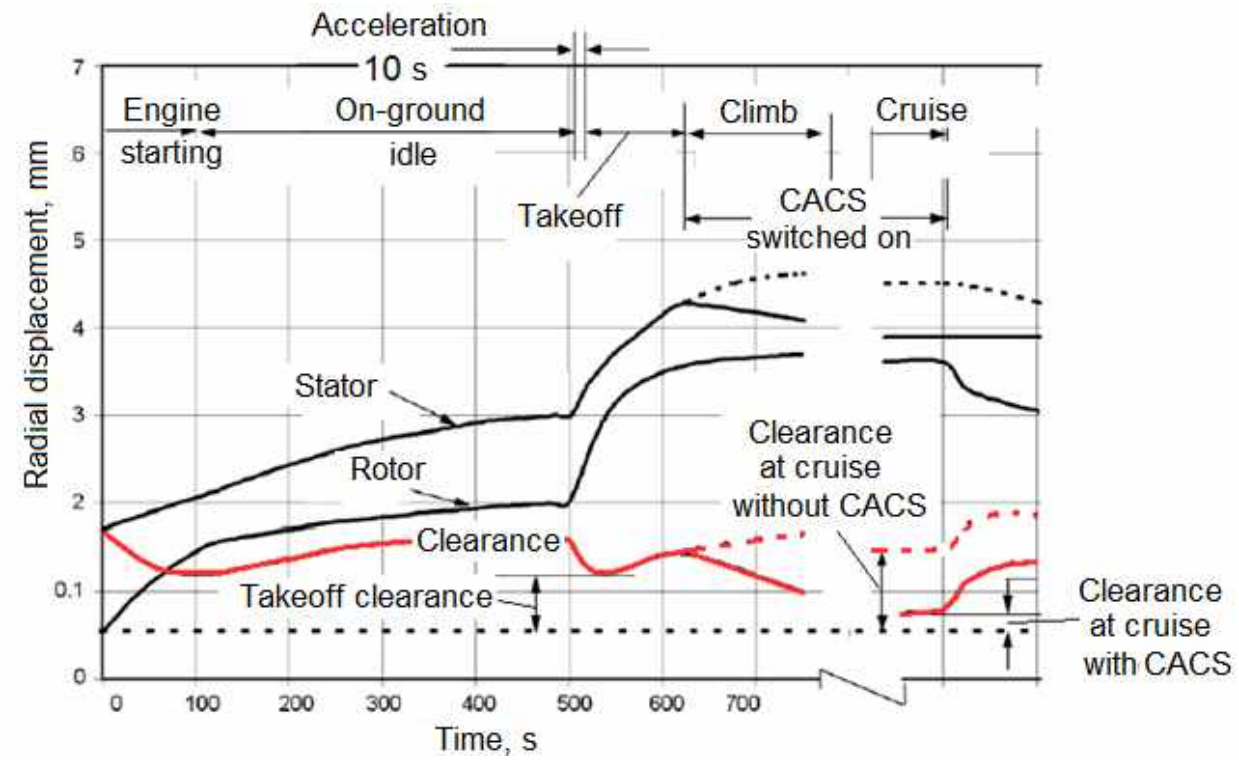


Fig. 8.8. Variation of radial clearance in turbine at takeoff, climb and cruise without and with automatic control

8.2. Methods of thermal control of radial clearances

Let the engine operates at constant corrected rotation speed $n_{cor} = n_0 = \text{const}$, when the engine inlet temperature changes. The radial clearance changes due to the thermal deformations of the assemblies (disc with blades and stator); this change may be defined as follows:

$$\Delta r_{th} = \alpha_{st} r_{st} \Delta t_{st} - \alpha_{bl} h_{bl} \Delta t_{bl} - \alpha_d r_d \Delta t_d,$$

where α_{st}, α_{bl}, α_d, are thermal expansion coefficients of the stator, blades, and disc, respectively.

Let's suppose that temperature of i-th rotor wheel rim T_{iT^*} at constant corrected rotational speed ($n_{cor} = n\sqrt{\frac{288}{T_{in}^*}} = \text{const}$) follows the law

$$T_{iT^*} = T_{i\,288}\frac{T_{in}^*}{288},$$

where $T_{i\,288}$ is design value of temperature at standard atmospheric conditions;

T_{in}^* is compressor inlet temperature.

Then

$$\Delta r_{th} = \alpha_{st} r_{st} \Delta T_{st\,288}\left(\frac{T_{in}^*}{288} - 1\right) - \alpha_{bl} h_{bl} \Delta T_{bl\,288}\left(\frac{T_{in\,288}^*}{288} - 1\right) - \alpha_d r_d \Delta T_{d\,288}\left(\frac{T_{in\,288}^*}{288} - 1\right),$$

where α is a thermal expansion factor;

Dividing Δr_{th} by the blade length, we get dependency between change of the relative radial clearance and parameters of the 'package' and the external conditions:

$$\Delta\bar{r}_{th} = \left(\frac{\Delta r}{h_{bl}}\right)_{th} = \alpha_{bl} h_{bl} \Delta T_{bl\,288}\left(\frac{T_{in}^*}{288} - 1\right)\left[\frac{1}{2}\left(\frac{2r_d + h_{bl}}{h_{bl}} + 1\right)\frac{\alpha_{st}}{\alpha_{bl}}\frac{T_{st\,288}}{T_{bl\,288}} - \frac{1}{2}\left(\frac{2r_d + h_{bl}}{h_{bl}} - 1\right)\frac{\alpha_d}{\alpha_{bl}}\frac{T_{d\,288}}{T_{bl\,288}}\right].$$

The obtained equation shows that variation of the engine inlet temperature, even if the engine operates at $n_{cor} = \text{const}$, generally is accompanied by violation of conditions of similarity of the gas flow duct. Therefore, the engine performances will be changed due to changing of the relative radial clearances.

If corrected rotor rotation speed is constant ($n_{cor} = n_0 = \text{const}$), then physical rotational speed $n = n_{cor}\sqrt{\frac{T_{in}^*}{288}}$ will be changed when the engine inlet temperature changes; the elastic deformations of blades and disc also will be variable.

The centrifugal force is proportional to the rotational speed. Thus, change of the relative radial clearance that is determined by the elastic deformations is as follows:

$$\Delta\bar{r}_e = \text{Const}\left(n_1^2 - n_2^2\right) = \text{Const}\, n_{cor}^2\left(\frac{n_1^2}{n_{cor}^2} - \frac{n_2^2}{n_{cor}^2}\right) - \text{Const}\, n_{288}^2\left(\frac{T_{in}^*}{288} - 1\right).$$

Hence, peak-to-valley value of the radial clearance consists of the thermal and elastic deformations:

$$\Delta\bar{r}_\Sigma = \Delta\bar{r}_{th} + \Delta\bar{r}_e;$$

$$\Delta\bar{r}_\Sigma = \alpha_{bl} h_{bl} \Delta T_{bl\,288}\left(\frac{T_{in}^*}{288} - 1\right)\left\{\left[\frac{1}{2}\left(\frac{2r_d + h_{bl}}{h_{bl}} + 1\right)\frac{\alpha_{st}}{\alpha_{bl}}\frac{T_{st\,288}}{T_{bl\,288}} - \right.\right.$$

$$\left.\left. - \frac{1}{2}\left(\frac{2r_d + h_{bl}}{h_{bl}} - 1\right)\frac{\alpha_d}{h_{bl}}\frac{T_{d\,288}}{T_{bl\,288}}\right] - \frac{C_d + C_{bl}}{h_{bl}} n_{288}^2 \frac{1}{\alpha_{bl} T_{bl\,288}}\right\},$$

where C_d and C_{bl} are the constants that characterize flexibility of the disc and blade.

Evidently, the wider is the operational range of the flight Mach number the higher is variation of T_{in}^*, and the higher is variation of the radial clearance of any rim at steady-state flight conditions.

Fig. 8.9 shows the influence of the compressor inlet air temperature on the radial clearance in the turbine stage that has been determined experimentally in climatic vacuum chamber.

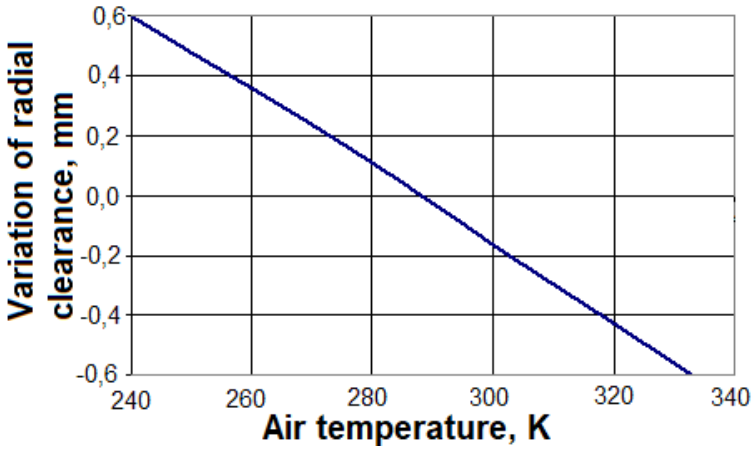


Fig. 8.9. Radial clearance vs the air inlet temperature

The radial clearance changed by 1.2 mm in the researched range of temperatures. The higher is the maximum flight velocity of the aircraft the lower is the turbine efficiency at subsonic cruise power ratings (the clearance increases). If the clearance is 1.2 mm, the losses in the turbine efficiency will

be 3.5 to 4.5 %. Intensive blowing of the stator parts by the cool air decreases these losses. This method is used in many engines, for example, the NK-86, PS-90, and D-18T (Fig. 8.10).

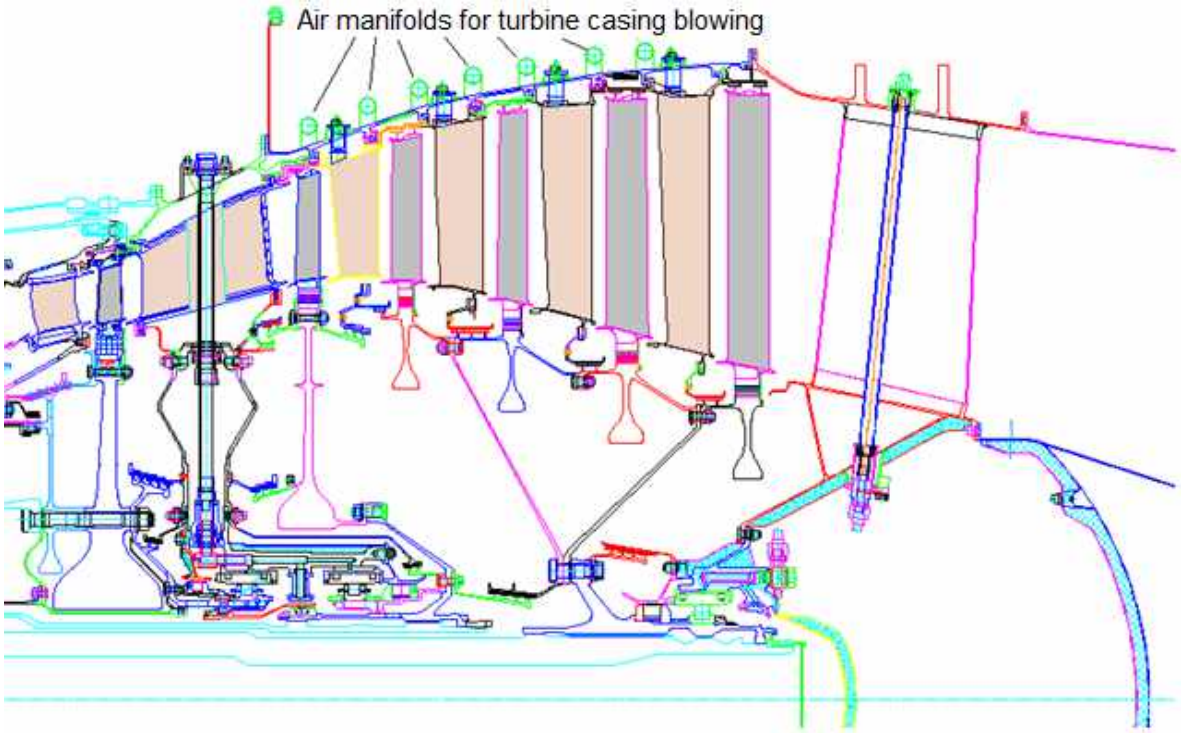


Fig. 8.10. Turbine design of the D-18T turbofan with blowing of turbine casing

Setting $\Delta\bar{r}_{\Sigma} = 0$ in the last equation, we get a relation between temperatures of the turbine parts, which determine the radial clearance:

$$\frac{T_{st\ 288}}{T_{bl\ 288}} = \frac{1+0.5\left(\frac{2r_d+h_{bl}}{h_{bl}}-1\right)\frac{\alpha_d}{\alpha_{bl}}\frac{T_{d\ 288}}{T_{bl\ 288}}+\frac{C_d+C_{bl}}{h_{bl}}n_{288}^2\frac{1}{\alpha_{bl}T_{bl}}}{0.5\left(\frac{2r_d+h_{bl}}{h_{bl}}+1\right)\frac{\alpha_{st}}{\alpha_{bl}}}.$$

According to this relation, the value of the radial clearance depends on the ratios of temperatures $\frac{T_{st}}{T_{bl}}$ and $\frac{T_d}{T_{bl}}$ in the turbine parts, linear thermal expansion coefficients of materials $\frac{\alpha_{st}}{\alpha_{bl}}$, $\frac{\alpha_d}{\alpha_{bl}}$ and geometric parameter $\frac{2r_d+h_{bl}}{h_{bl}}$. This expression demonstrates the possibility to maintain constant radial clearance when the engine power ratings (for example, the air inlet temperature) change.

The obtained relation shows that in conditions, when the corrected rotational speed is constant (n_{cor} = n_0 = const), materials and geometric

parameters of the turbine parts are known and temperatures of the blade and disc are known, the only value of the casing temperature exists, which ensures constant (design) value of the radial clearance.

Hence, the choice of materials, elasticity of the rotating parts and thermal conditions of the "package" may save the radial clearance at all Mach numbers. Therefore, we may use thermal control of the radial clearance if choosing correctly the stator material.

However, the true radial clearance never is zero. It depends on the manufacturing tolerances, arrangement of the rotor supports, elasticity of the shafts and supports, quality of the rotor balancing. Experience of Rolls Royce Company showed that three-cascade arrangement of the RB-211 turbofan maintains a radial clearance in the turbine at a level of 0.2 to 0.3 mm that is equivalent to a loss of turbine efficiency 0.8 to 1.2 % at the cruise power rating. This result was obtained not only due to choosing the physical properties of the materials (linear thermal expansion coefficients α) but also due to thermal inertia of the rotor and stator so as to prevent cutting of the blades and labyrinth seals in the stator during engine acceleration and deceleration. This task was solved at the stage of engine experimental improvement.

Previously, we solved the task of maintaining the minimum radial clearance at the steady-state power ratings, for example, at cruise power rating. It is also possible to maintain the clearance at the transient power ratings (during engine acceleration and deceleration).

Time-dependent temperature variations of the stationary and rotary parts are estimated by using the theory of regular thermal condition. According to this theory, the temperature at any point of the body is changed by the exponential law long before it reaches limit value.

Following this law, we can estimate temperatures of the stationary and rotary parts as follows:

$$T_1(\tau) = T_1 - \Delta T_1 e^{-k_1\tau}; \qquad T_2(\tau) = T_2 - \Delta T_2 e^{-k_2\tau},$$

where $\Delta T_1 = T_1 - T_{01}$, $\Delta T_2 = T_2 - T_{02}$ are differences between the temperatures at the steady-state final moment and at the initial one of the transient process;

k_1 and k_2 are the thermal inertia factors.

Then, temperature difference between the mating parts at transient power ratings determining mismatching of the radial clearances may be get from the following expression:

$$\Delta T(\tau) = T_1 - T_2 - \Delta T_1 e^{-k_1\tau} + \Delta T_2 e^{-k_2\tau}.$$

Obviously, the radial clearance will be invariable in time only if

$$T_1 - T_2 = T_{01} - T_{02},$$

i. e. when $\Delta T_1 e^{-k_1 \tau} = \Delta T_2 e^{-k_2 \tau}$.

This condition is true if $k_1 = k_2$, i. e. if the rotary and stationary parts have the same thermal inertia.

In practice, this condition is ensured by the stator redesigning. As a rule, the weight of its parts is increased (Fig. 8.11).

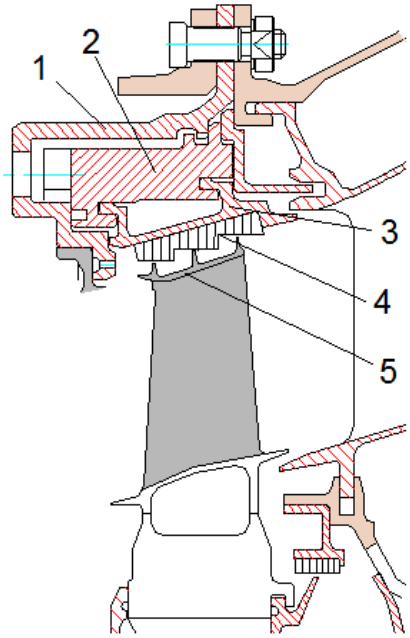


Fig. 8.11. Design of turbine stator with heavy member:
1 – casing; 2 – heavy member; 3 – shroud ring; 4 – honeycomb insert;
5 – shroud platform with labyrinth fins

The advantages of this method of maintaining the radial clearance are the reliability, simplicity and low cost. There is no need to use the specially prepared compressed air or the mechanical drives for active adjustment or control over intensive blowing of the stator parts to maintain the minimum radial clearance at the engine cruise power ratings.

Let us consider some examples of design solutions concerning the radial clearance control.

8.2.1. System of passive clearance control with heavy member of casing

The concept of minimizing radial clearance by matching of thermal state of the “package” disc-blade-stator) is the most completely implemented in the engines of Rolls Royce Company. The design of the unit for passive clearance control for the last stages of the compressor is shown in Fig. 8.12.

The unit consists of thin ring 1 that is concentrically placed in relatively massive ring-shaped members 2 and 3. The ring-shaped element 3 is a part of

compressor casing 5, and ring-shaped member 2 is a part of spacer 4 that is also joined to the heavy casing 5. At the same time, the ring-shape members 2 and 3 are used to attach compressor guide vanes 6.

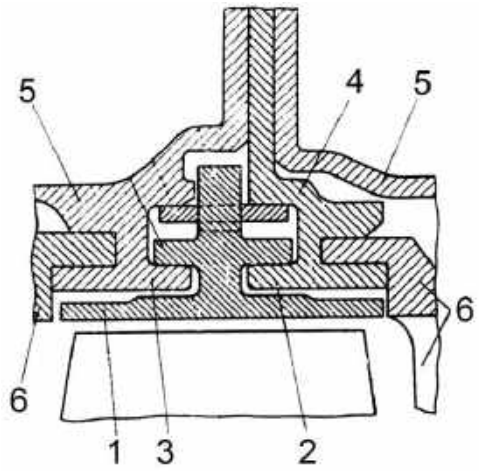


Fig. 8.12. Design of unit for passive radial clearance control in compressor last stages

8.2.2. System of passive clearance control with combination of massive casing element and blowing by the air

The above-described method of the identical thermal inertia of the stator and rotor parts increases the weight of the stator parts. Therefore, in practice, not ideal but partial equality of the rotor and stator thermal inertia is performed.

In Fig. 8.13, the method of the RCC with the partial equality of the thermal inertia is illustrated by a design of the high pressure compressor of the D-18T turbofan.

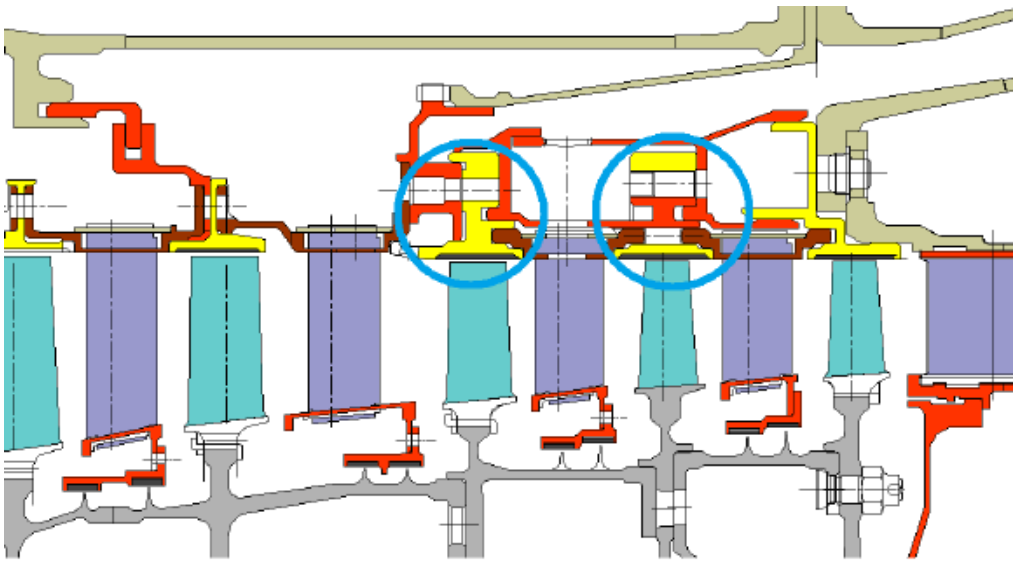


Fig. 8.13. Design with matching of thermal inertia
of the “package” (disk-blade-stator)

As it was explained above, the most dangerous power rating for the radial clearance is engine abrupt deceleration after engine operation at the maximum power rating during a long time, or in case of engine emergency shutdown without its preliminary cooling at the idle power.

Rolls Royce Company developed the combined system with “heavy body” and automatic control of the supply of the hot and cold air (Fig. 8.14).

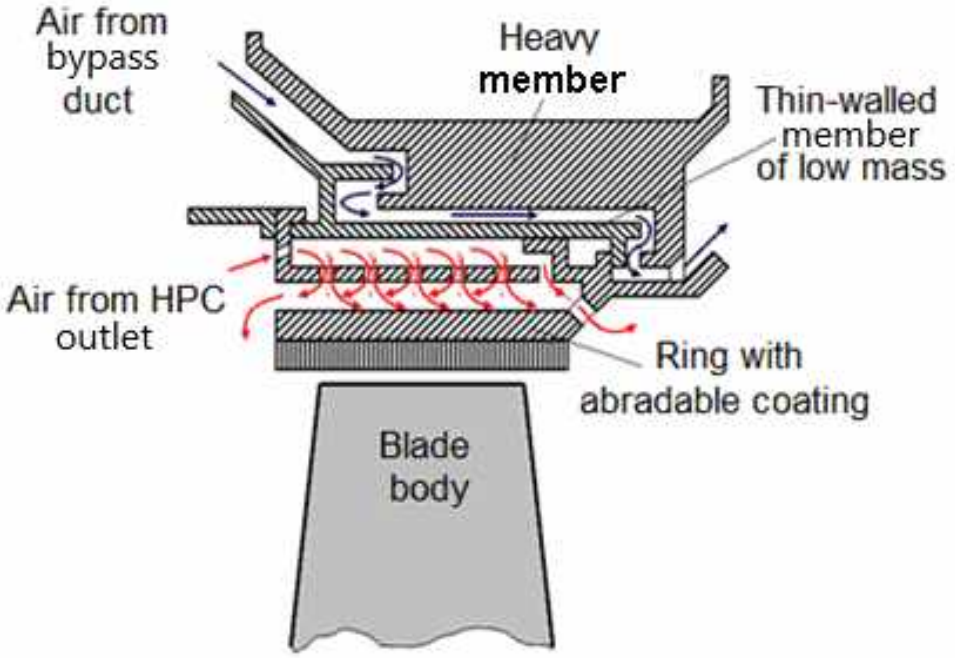


Fig. 8.14. Combined system with “heavy body” and automatic control of the hot and cold air supply

The thin-walled member bears a ring with soft abradable (for example, honeycomb) coating. When the engine power rating increases, then it expands faster than the heavy disc with blades expands. Therefore, the rotor does not touch the stator.

During expansion of the thin-walled member the channel used to supply cooling air from the bypass duct is closed. The thin-walled member touches the heavy part and the hot air from the HPC outlet heats the heavy part. Hence, the heavy part together with the thin-walled member is heated slowly, and the rate of heating is close to the rate of expansion of the disc with blades.

During engine deceleration, the thin-walled member tends to shorten, and the rate of this shortening should be higher than the heavy disc with blades has. However, shortening of the thin-walled member is restricted by the heated heavy member, which is shortening slowly because of the high thermal inertia.

The rate of variation the diameter of the system consisting of the heavy and thin-walled members is chosen by designing the weight of the heavy member and by controlling flows of the hot and cool air, which influence temperature of the parts.

8.2.3. Radial clearance control system with air blowing of stator

Systems with blowing stator parts by the air at the cruise power ratings are widely used (the NK-86, JT-9D, CF6-32, etc., Fig. 8.15).

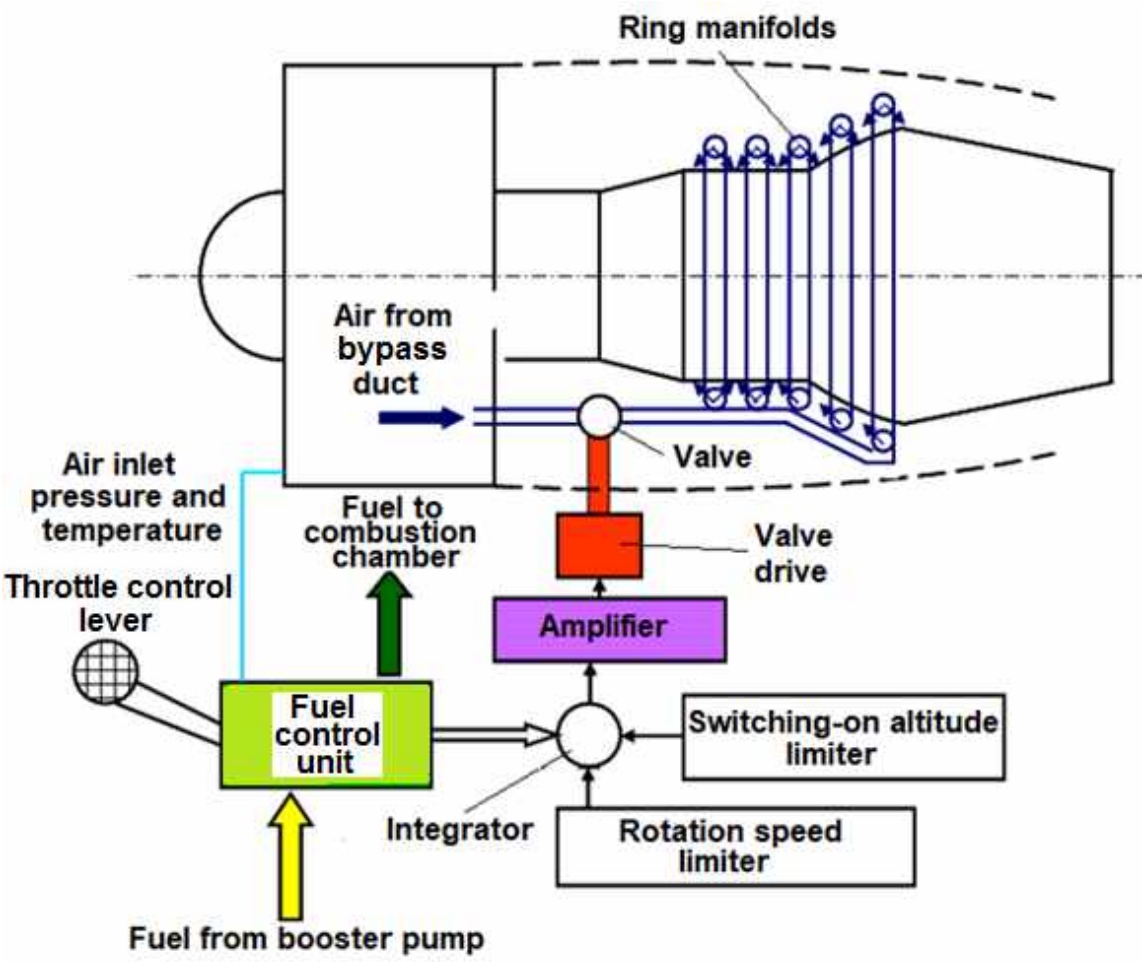


Fig. 8.15. Radial clearance control system with forced blowing of stator parts by the air

The stator of the NK-86 turbofan high pressure turbine is cooled by the air, which is bled from the bypass duct; it enters the ring manifolds and blows by air streams the surfaces subject to cooling. After that, the air flows to the bypass duct and then to the mixer and exhaust nozzle exit, thereby taking part in generation of the engine thrust.

The integrator receives a command from the altitude limiter and rotational speed limiter, and generates the valve-driving signal. The blowing is activated

at $n < n_{max}$ (at cruise power rating). The system does not operate during acceleration and when the flight altitude is less than the altitude of the cruise flight.

Variation of the blowing intensity changes the radial clearance up to 1.5 mm (Fig. 8.16).

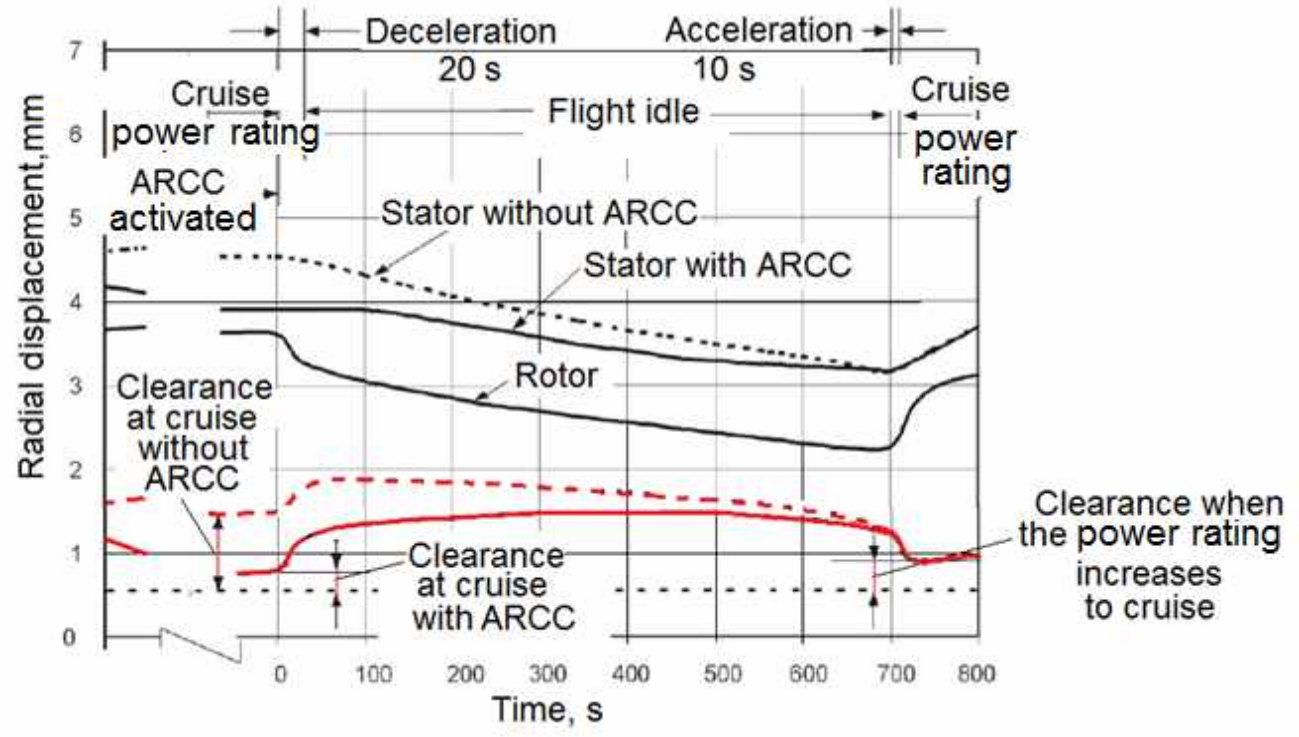


Fig. 8.16. Variation of radial clearance in turbine at cruise, flight idle, and “hot” starting

Fig. 8.17 shows manifolds used to supply the air to turbine casings of the CFM-56 (*a*) and SaM-146 (*b*) turbofans.



a *b*

Fig. 8.17. Manifolds used to supply the air to casings

Some engines are equipped with box-shape manifolds that look like thin annular ribs and complicated flanges of casings (Fig. 8.18).

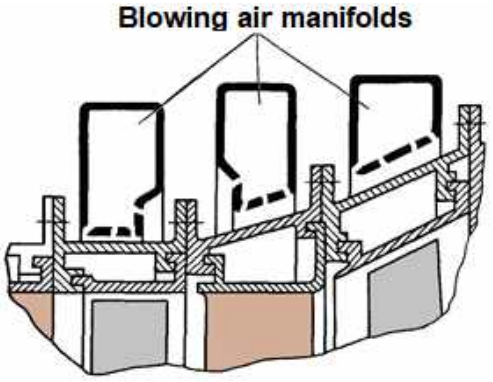


Fig. 8.18. Box-shape air manifolds

The ribs and flanges implement thermal physical and strength functions. The blowing system ensures uniform cooling of the stator both along its length and circumferentially; therefore, warping or non-concentricity of the casing do not occur at the transient power ratings.

Efficiency of this system is limited by the pressure differential. Therefore, Pratt & Whitney Company proposed the system for mixing of flows of the primary and bypass ducts. The design was developed for the last stages of the compressor and turbine of the E^3 highly efficient prototype engine. The same design was implemented in the V2500 turbofan (Fig. 8.19).

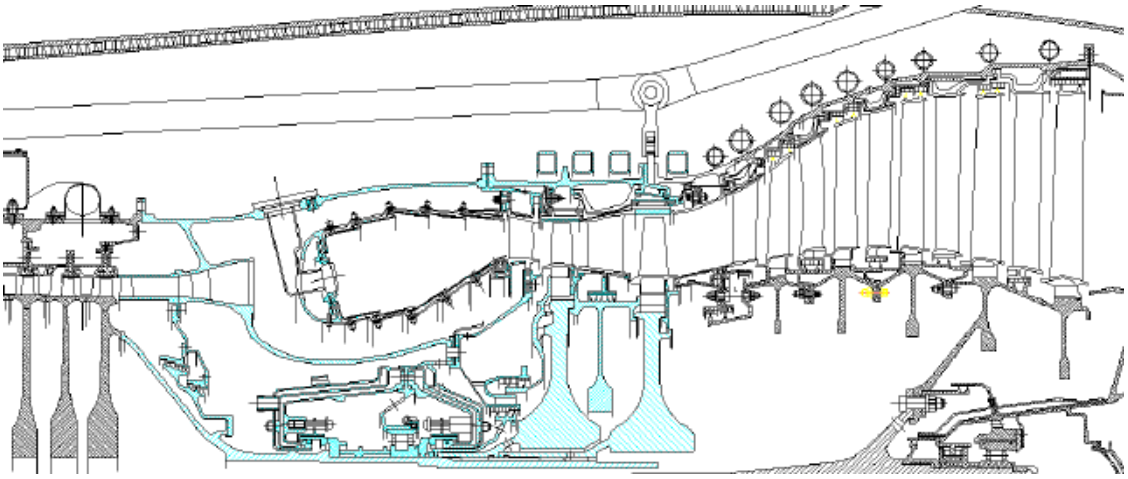


Fig. 8.19. Radial clearance control system of the V2500 turbofan

At the cruise power rating, the air is bled from the third stage of the HPC. If fast heating of the stator is required, the air bleeding is switched to the HPC outlet. This decreases efficiency but makes the system compact and finally perfect. In the design structure, the air is blown through a double-wall casing, but another version is possible – cooling by sprinkling.

In general, the method of clearance control by blowing a stator with the cold air is less efficient than the thermal control.

8.2.4. Radial clearance control with heat pipe

The original thermal clearance control method is based on application of the heat pipe that is filled with the sodium vapor (Fig. 8.20).

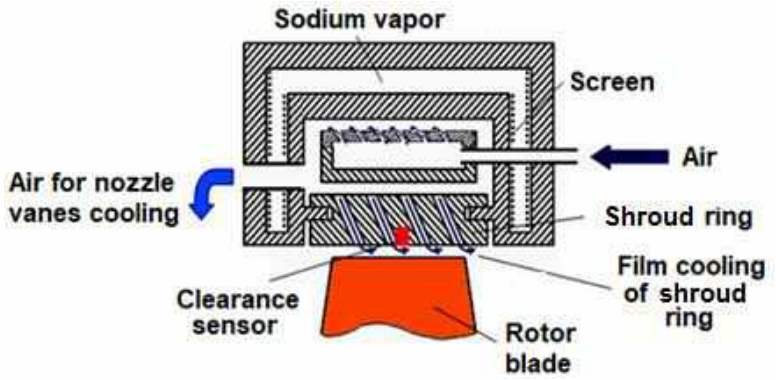


Fig. 8.20. Radial clearance control system with heat pipe

The shroud ring is a perforated metal. The use of ceramics or porous material is possible. The chamber is lined from inside by a screen made of a stainless steel, and is filled in with the sodium vapor. The air that flows from the manifold cools the vapor. The air flows through a row of orifices and then after cooling of the chamber it flows through a row of orifices provided in the shroud ring, thereby providing its protective film cooling. The remaining air is supplied to cool the nozzle guide vanes.

The shroud ring is furnished with the sensor for checking radial clearance. The signal generated by the sensor is transmitted to the system controlling air supply to the manifold.

High heat conductivity of the heat pipe ensures high response speed of the system. So, the radial clearance is controlled at all engine power ratings practically immediately.

The sensor for controlling the radial clearance is of a condenser type. It contains two electrodes: one of them is mounted on the stator and the other one is the rotor blade. When the rotor blade passes under the sensor, the capacity changes, and its value depends on the value of the radial clearance.

8.3. Mechanical control of radial clearance

It is not expedient to control the radial clearance by changing rotor radial dimensions because rotation of the rotor complicates development of the reliable system.

Therefore, there are only two ways of mechanical control of the radial clearances:

– by changing relative axial position of the design members influencing the radial clearances;
– by changing radial dimensions of the casing parts.

In this connection, the mechanical RCC is subdivided into the kinematic and collet one.

The advantage of mechanical RCC comparing to the heat control is high response speed of the system and the minimum energy consumption, because controlling mechanism need in insignificant amount of the compressed air. If the compressor or turbine blades are provided with the antivibration platforms, then then they also may be used for the RCC.

8.3.1. Kinematic radial clearance control

In case of the kinematic RCC, clearance change is ensured by correction of relative axial position of the casing parts and rotor parts having conical shape.

The active RCC system with cam mechanism is shown in Fig. 8.21.

The cam mechanism is driven by the hydraulic actuator through a fork lever. The bellows joins shroud ring to the casing. Movement of the cam mechanism displaces the shroud ring along the engine axis to the right or to the left. The system can use a feedback signal from the above-considered clearance sensor, or the cam shape can be profiled as a function of the power lever position α_{TCL}.

The weak point of this design is the bellows.

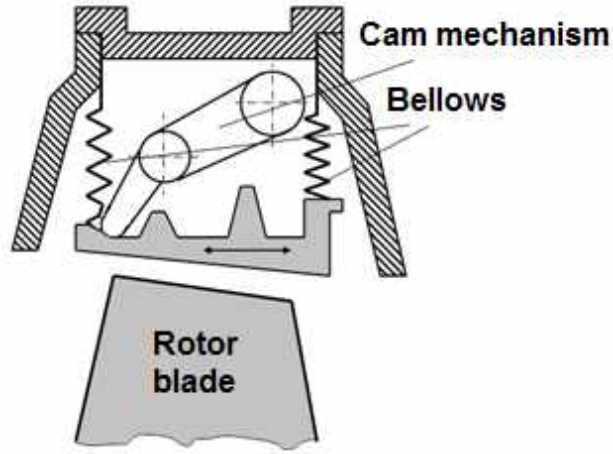


Fig. 8.21. RCC system with cam mechanism

Fig. 8.22 shows the longitudinal section of the compressor stage with the kinematic pneumatic RCC.

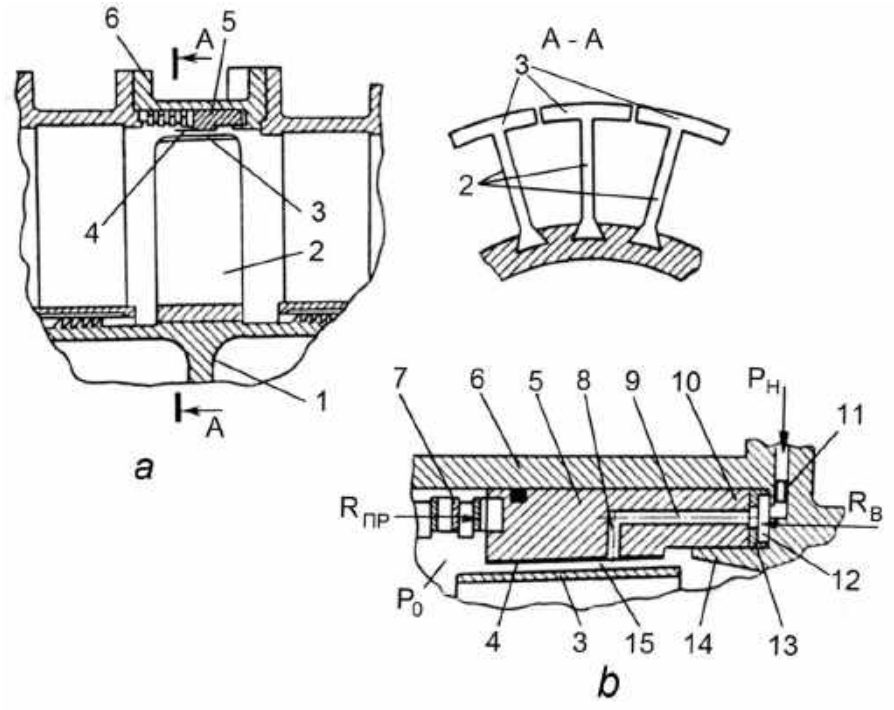


Fig. 8.22. Kinematic pneumatic RCC system

Compressor rotor 1 restrains blades 2 with antivibration platforms 3 that have a conical external shape. Conical spacer 5 is mounted above the platform; the inner surface of the spacer is covered with soft layer 4 (talk, graphite, etc.), which is easy-removed when it touches the blade. Spacer 5 is mounted in casing 6 with running fit. In Fig. 8.22, *b*, the sealing assembly is scaled. The spacer 5 is made as one part with the ring piston 10 that enters the ring-shaped chamber 12, which is machined in casing 6. Piston 10 forms a pneumatic actuator that moves spacer 5 axially. Piston 10 is furnished with sealing member 13 made of easy-deformable elastic material. Spring 7 made of plane strips presses spacer 5 at the opposite side. The air from the last compressor stages flows to chamber 12 through jet 11 at gage pressure p_H (the pressure is excessive one comparing to the pressure near spacer 5 in the engine gas flow duct). The air is blown from chamber 12 through channels 9 and 8 into radial clearance 15 between shroud platforms 3 and layer 4 of spacer 5. Thus, two opposite forces affect spacer 5 at the same time: the force of spring tension R_{spr} from the left, and the force R_{air} of the pneumatic actuator from the right. When the compressed air at pressure p_H not fed to the actuator, spring 7 pressures spacers 5 to the right and the clearance decreases to zero or (if the stop is available) to the minimum permissible value.

Mechanical control with the servo drive unit operates as follows. The air enters the pneumatic servo drive at pressure p_H, drives spacer 5 and is bled through channel 8 to clearance 15. If clearance 15 exceeds the required value,

then the air bleeding from chamber 12 will be increased, thereby decreasing pressure p_H in the chamber. Equilibrium of the forces that affect piston 10 will be disturbed, and the piston will move together with the spacer towards decreasing clearance 15 until the balance of forces is recovered. Decreasing of the clearance will increase the pressure in chamber 12, the spacer will move to the left and clearance 15 will be increased to the required value.

If channel 8 in Fig. 8.22 is not available or is contaminated, then the control depends completely on the pressure in chamber 12. If this pressure corresponds to the preset program depending on the rotor rotational speed, flight altitude, the air temperature, then we will get the closed-loop control system.

The disadvantages of the kinematic RCC are complex design, especially in multi-stage compressor, where we need to control each stage, and requirement to make the gas flow duct conical at periphery of the shrouded blades.

Numerical analysis showed that the shroud platforms of the compressor blades airfoil portion increase the hydraulic losses, which eliminates positive effect that is ensured due to decreasing the radial clearances. Finally, the shrouds decrease efficiency of compressor; therefore, the shrouded design structure in unreasonable in the compressor.

The kinematic RCC can be used in some stages of the compressor and turbine at a time. In this case, it is advisable to make the axial displacement of all rotor parts by using one actuator. This method is named as a group kinematic control.

8.3.2. Group kinematic radial clearance control system

Fig. 8.23, ***a*** shows the engine arrangement that contains compressor rotor 20, turbine rotor 8, casing 1, compressor support 16 and turbine 11 support (the front compressor support and the rear turbine support are not shown). Supports 16 and 11 are connected to casing 1 through diaphragms 18 and 10, and stator vanes 4 and 5. Shafts of rotors are joined by the splined torsion shaft 14 that transmits a torque from turbine rotor 8 to compressor rotor 20.

Supports 16 and 11 are equipped with thrust collar pivots 17 and 12 of hydrostatic end-thrust bearings 15 and 13, which axial position in relation to casings is determined by distributors 19 and 9. The distributors are linked with sensors 3 and 6 of inductive and capacity types, which measure actual radial

clearance between blades 2 and 7 and casing 1. Supports 16 and 11 have same design, so we will consider compressor support 16 as an example.

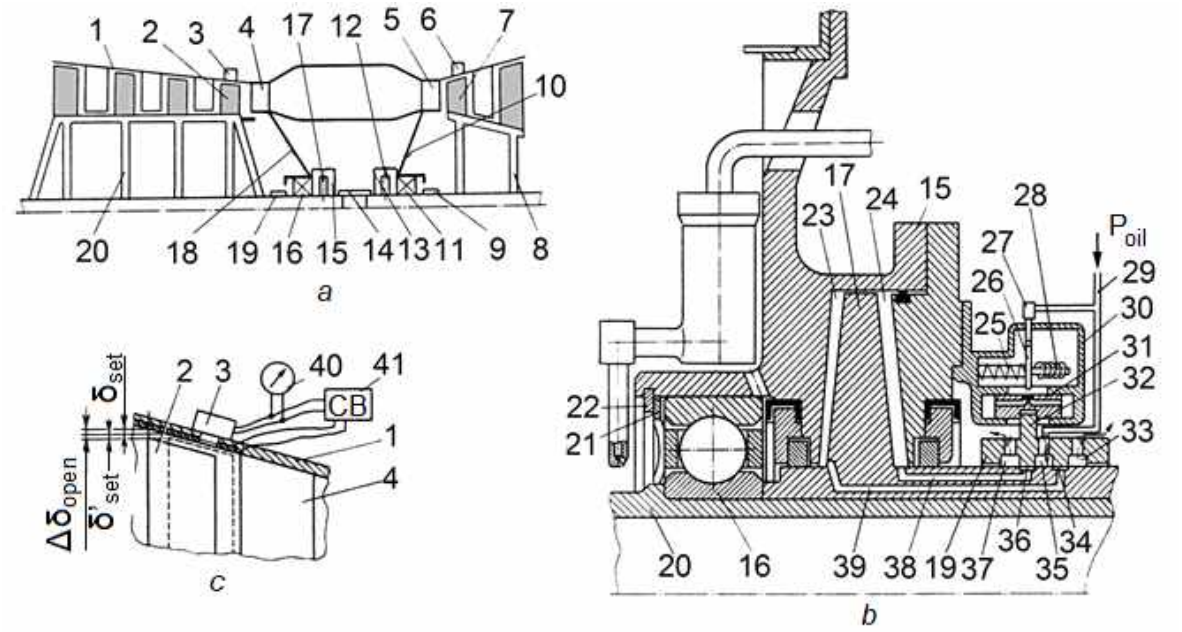


Fig. 8.23. Diagram of RCC hydrostatic system

Radial-thrust bearing 16 (Fig. 8.23) is mounted in casing 15 of the hydrostatic step bearing. Retaining ring 22 restrains ball bearing 16 in the axial direction. Annular spring 21, which is located between ring 22 and outer racer of bearing 16, prevents axial displacement of the bearing and rotor. Thrust collar pivot 17 of the hydrostatic bearing is attached to the rotor shaft and perceives the total axial force from the compressor rotor.

Pivot 17 divides a space in casing 15 into two chambers 23 and 24. The oil is supplied to these chambers from distributor 19 that is made as a four-slot slide valve with two drain grooves 37, 33, and one pressure groove 35. Grooves 36 and 34 in the shaft of pivot 17 connect channels 39 and 38 with the chambers 23 and 24.

Distributor 19 by means of pin 32 is connected to the driving mechanism 30, which is made as an electric-hydraulic actuator with piston 31 and jet pipe 26. From one side, the pipe is pressed by spring 25; from the other side, the pipe is connected to solenoid core 28, whose electric circuit includes sensor 3 that is shown in Fig. 8.23, *a*.

Pressure groove 55 of distributor 19 receives the oil at pressure p_{oil} from line 29. The same line supplies oil to jet pipe 26 through flow restrictor 27.

Command block (CB) 41 is controlling driving mechanism 30 and feedback sensor 3 (see Fig. 8.23, *a*). Adjustment of the CB is performed as follows.

The clearances in the compressor and turbine are adjusted to value δ_3 when the rotor is at a standstill. Thereto, pumps are switched on that supply the

oil to the hydrostatic step bearings and move the rotor until the blades 2 touch the parts of casing 1. One person turns the rotor to check the touching, then one marks the point on the device 40 that corresponds to a zero clearance. Then, by using command block 41, it is necessary to move the rotor from this point to position in which the radial clearance is equal to δ_{set}.

On the running engine, the radial clearance will be changed by value $\Delta\delta_{open}$ due to thermal expansions, which will result in deviation from its required value. As a result, the mismatching signal appears, and then it is amplified and processed in block 41. The block switches on the solenoid that drives core 28 (see Fig. 8.23, *b*) and deviates jet pipe 26 from the neutral position, which corresponds to requires clearance δ_{set}. Deviation of jet pipe 26 initiates motion of piston 31, pin 32, and distributor 19; pivot 17 and rotor 20 will take a new position. Displacement of rotor 20 will result in change of axial position of blades 2 until the clearance reaches the required value $\delta_{set} = \delta'_{set}$; after that, the mismatching signal of sensor 3 disappears and displacement of the rotor will be discontinued.

The axial displacement of the rotor also may be obtained by connecting pivots 17 of the hydrostatic step bearings directly to the outer racers of the ball bearings. In this case, the inner racers of the bearings must be rigidly connected to the shafts. Thus, axial displacement of the bearing will move the rotor.

The advantage of the group mechanical RCC lies in maintaining the minimum clearance by one (or two) actuators for all rotor blades in the engine gas flow duct. This is the main advantage of this system; its adjustment, refinement and maintenance become simpler, the engine reliability is increased. This makes the group RCC method more promising comparing to other methods.

However, the group control has the essential disadvantage: radial clearances at different stages of compressor and turbine are varied differently; therefore, the minimum clearances in the turbine machines with group control are higher than in the turbine machines with individual control.

Unstable temperatures of the engine parts at different operation modes and thermal deformation of the shaft will make the maximum influence on a radial clearance scatter between different stages.

8.3.3. Collet radial clearance control

The collet control method is based on application of the part that has axial slots and may be deformed radially by the collet principle. Depending on the method of deforming, there are different collet controls: with the mechanical drive and with the hydraulic (or pneumatic) drive.

The collet control with mechanical drive. Fig. 8.24, *a* shows gas flow duct of the axial compressor with RCC by using the mechanical collet. The compressor is composed of casing 1 and rotor 14 with rotor blades 16. Guide vanes 13 are retained in ring spacers 2 that are rigidly joined to casing 1. Shroud rings 12 designed as twin collets are mounted between rings 2 above blades 16.

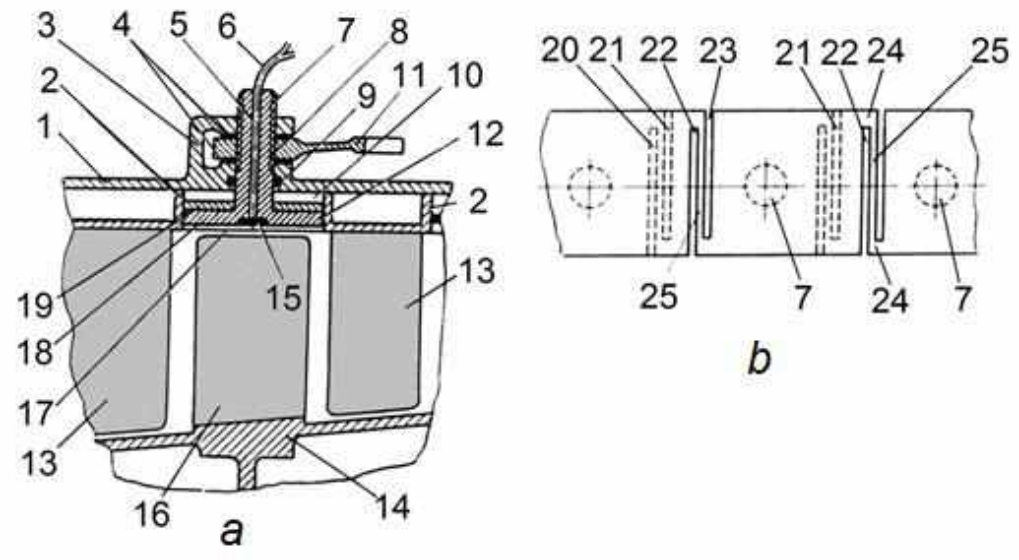


Fig. 8.24. Collet RCC system with mechanical drive

Fig. 8.24, *b* shows a scan of collet 12. The distinctive features of collets 12 from conventional collets that are used in the tooling industry are double slots 22 and 23. Narrow bulkheads between slots 22 and 23 prevent the air bleeding between the slots. This design of the collet ensures more uniform variation of its radial dimensions along all the entire length of the forming cylinder.

In a segment between slots 22 and 23, the collets have end extensions 7 with thread 8 and channel 5 that contains wire 6 connected to sensor 15, which measures radial clearance 17 between blades 16 and rings 1.

The inner surface of ring 12 is coated with a talk layer, which is removed easily when contacting rotating blade 16. Bulkheads 25 making slots 22 and 23 blind-ended axially and result in uniform deformation of the collet.

Lever 11 by thread 8 is connected to end extension 7, which is connected to the actuator similarly as it is done for changing angular position of the inlet guide vanes. Spacers 4 made of the antifriction material are mounted between casing 1, lever 11, and bracket 3; they are used as the bearings. Casing 1 is provided with seals 9 to prevent air bleeding from the compressor inner chamber.

The air bleeding through slots 22 and 23 into chamber 10 is impossible, because the design includes the sealing collets 19, which similarly to collets 12 have slots 20 and 21. These slots are displaced in a circular direction relatively

to slots 22 and 23. In Fig. 8.24, *b*, slots 20 and 21 are marked with a dotted line.

The collet system operates as follows. When radial clearance 17 between blade 16 and collet 12 increases or decreases, then sensor 15 supplies a signal to the feedback system, which generates a command to turn lever 11 so that end extension 7 under the action of thread 8 moves outward (or downward in casing 1), thereby deforming the collet and changing the radial clearance.

One command unit can turn all levers 11 of separate compressor or turbine stages. The required difference in variation of the clearances in the first and last stages can be ensured by adjusting the length of levers 11, parameters of the drive and pitch of thread 8.

Collet control with hydraulic actuator. Fig. 8.25 shows a diagram of the hydraulic drive system for radial deformation of collet 16, which design is the same as the that shown in Fig. 8.24, *b*.

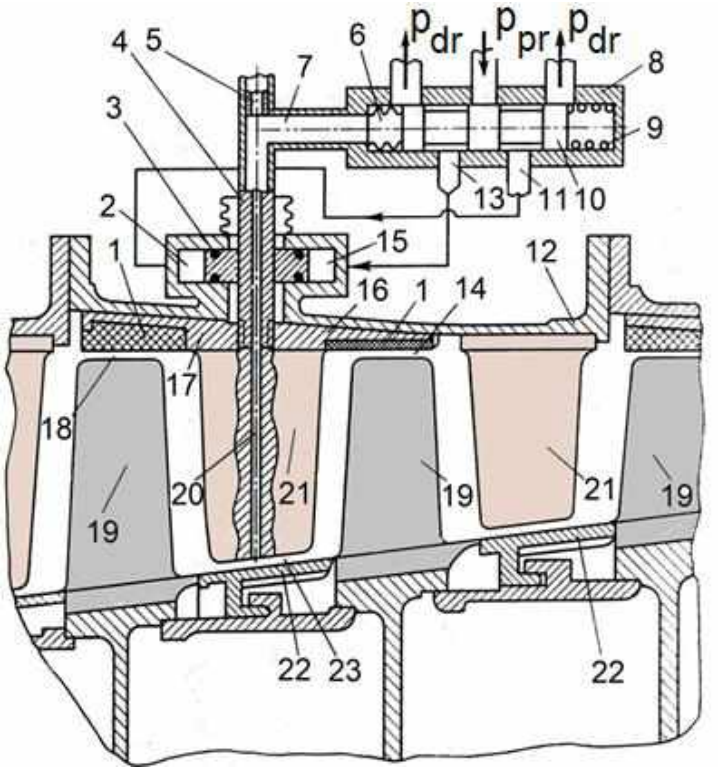


Fig. 8.25. Hydraulic drive system with radial deformation of collet

The outer surface of collet 16 has conical shape, which ensures its radial deformation. Casing 12 has the counterpart conical surface with antifriction coating. Rings 1 with abradable coating are mounted above the rotor blades on the inner surface of collet 16.

Collet 16 also restrains pins 4, which are connected to piston 3 of the hydraulic or pneumatic actuator; the latter is controlled by slide valve 10 mounted in sleeve 8 of the distributor. Channel 7 connects chamber 6 of the

valve distributor with the pneumatic feedback sensor, which consists of inlet jet 5 and channel 20 made in the guide vane.

Absence of the shroud platforms complicates measurement of the radial clearance. Therefore, in this diagram, the radial clearance is measured between vanes 21 and spacers 22.

Clearance 23 differs from clearances 18 and 14 by the value of deformation of blades 21 by centrifugal forces during rotor rotation. Nevertheless, this clearance characterizes indirectly all variations in thermal state of the rotor and stator.

The pressure differential between the inlet to jet 5 and the gas flow duct is supported constant; therefore, the RCC system is independent of the flight evaluation. With this purpose, the area of channel 7 several times exceeds that of the inlet to jet 5, and hydraulic resistance of channel 20 is equal to that of jet 5. The chamber, which contains spring 9, communicates with channels 20 in the same cross-section of the turbine machine.

The working liquid at pressure p_{pr} (discharge pressure) is supplied to the intermediate groove of slide valve 10; the used liquid is drained from two extreme grooves at pressure p_{dr}. The liquid from the valve distributor flows through channel 11 to chamber 2 of the power cylinder, and through channel 13 to chamber 15.

The system operates as follows. When radial clearance 23 increases (for example, due to changing of compressor thermal conditions), then the hydraulic resistance in the air bleeding line will be decreased, the draining flow from channel 20 will be increased, and the pressure in channel 7 and in chamber 6 will be decreased. The pressure in the line will be reduced and differential pressure at piston 3 will move it to the right. Collet 16 will also be displaced relative to casing 12, and its conical portion will interact with the conical surface of the casing. Due to this interaction, collet 16 will be compressed, and clearances 18, 14 and 23 will be decreased.

The abradable layer will perceive the difference in elongation of blades 19 and spacers 22 under the action of centrifugal forces, and the difference in thermal elongations of blades 19 and 21 will be accepted by layer 1, which is easy abradable during touching rotor blades.

8.4. Hydrostatic radial clearance control

The above-considered systems with the thermal and mechanical control need in feedback sensors that are the least reliable members in the automatic control chain. Therefore, the natural aim of designers was to find a method of clearance control that not needs in its direct measurement.

The hydrostatic principle of control consists in using of the force that originates at pumping of the working fluid into a clearance between rotor and stator elements. The force must be enough to keep the rotor at some distance from the stator.

Theory of hydrostatic bearings claims that the force in the bearing depends on the mass flow of the working fluid. The values of clearance and flow of the working fluid are related as the cubic parabola. Using this relation, we can realize a hydrostatic clearance control by two ways: at face and radial displacement of the controlling members.

8.4.1. Hydrostatic end clearance control

Fig. 8.26, *a* shows the turbine design with the end clearance control that is developed by the MTU Company (Germany).

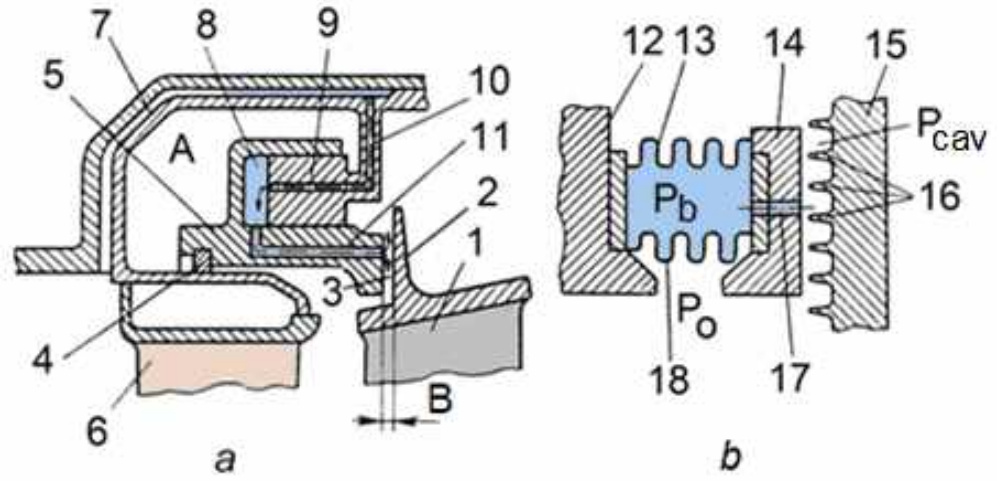


Fig. 8.26. System with end clearance control

Stationary part 5 has a row of cylinders with pistons 9. Channels 10 and 7 connect chamber 8 to chamber upstream of nozzle guide vanes 6. Channel 11 connects chamber 8 to controlled clearance B. The force that affects part 5 is a product of the pressure differential in chamber 8 and in the turbine axial clearance, and of the relation between areas of the end faces of pistons 9 and edge 3. When the clearance decreases, then the pressure in chamber 8 increases and part 5 is displaced to the left. When the clearance increases, then the pressure in chamber 8 drops and becomes less than the static pressure in chamber A. Part 5 moves to the right, and the end clearance between rib 2 of blade 1 and edge 3 is decreased.

The disadvantage of this design is that at the beginning of starting, position of part 5 is not determined; therefore, the cases of touching and wearing of edge 3 and fin 2 of rotor blade 1 are possible. Operability of this hydrostatic end seal will depend on the finish smoothness of the surfaces that

create working face clearance B, and by the co-perpendicularity of these surfaces in relation to the axis of rotation.

The most difficult is ensuring a high precision of perpendicularity of the face surfaces that form clearance B. The perpendicularity of the face of fin 2 to the axis of rotation is influenced not only by the errors of manufacture but also by the turbine disc misalignments caused by the shaft sagging, its oscillations and other types of the thermal, forced and dynamic deformation.

All of these factors stimulate some lack of squareness along the end seal in clearance B and cause intensive wearing of parts 2 and 5. When the air flow through the channels 10, 7 and 11 is increased, then the end clearance will be increased and the engine efficiency will fall down due to increase air escape.

The advantage of the system shown in Fig. 8.26, *a* is that there is no need to carry out direct measurement of the clearance.

Fig. 8.26, *b* shows another design with controlled end clearance that decreases wearing of the end faces due to implementation of a labyrinth seal.

In this design, the above-described piston-based principle of the movable part motion is replaced with the bellows-based principle. Part 14 moves by pressure p_b in the internal chamber between two corrugated shells 13 and 18. Rotating shroud 15 of the rotor blades is equipped with end face fins 16 that form a seal with ring 14, which is connected to the corrugated shells on casing part 12.

The air from the inner chamber of the bellow drive flows through holes 17 into the end clearance between stationary part 14 and rotary part 15 and fills the space between fins 16 of the labyrinth seal. Ringing 14 is in the equilibrium state under the action of two pressures: $(p_b - p_0)$ from the left and p_{cav} from the right. If the clearance decreases, then pressure p_{cav} in the chambers of the labyrinth seal will be decreased and ring 14 will be displaced to the right until the equilibrium of the pressure forces will be recovered. When the clearance increases, then pressure p_{cav} will be increased and the pressure recovering process will be inverse one.

8.4.2. Hydrostatic radial-type clearance control

The design of the above described hydrostatic clearance control with the end face slot is similar to that of the axial hydrostatic step bearings. Besides, the class of the hydrostatic bearings with the radial working slot is known, and its operating principle may be used for the clearance control.

Fig. 8.27 shows the longitudinal section of the axial compressor. Rotor 11 has rotor blades 8. Guide vanes 7 are placed between them and are attached to compressor outer casing 10.

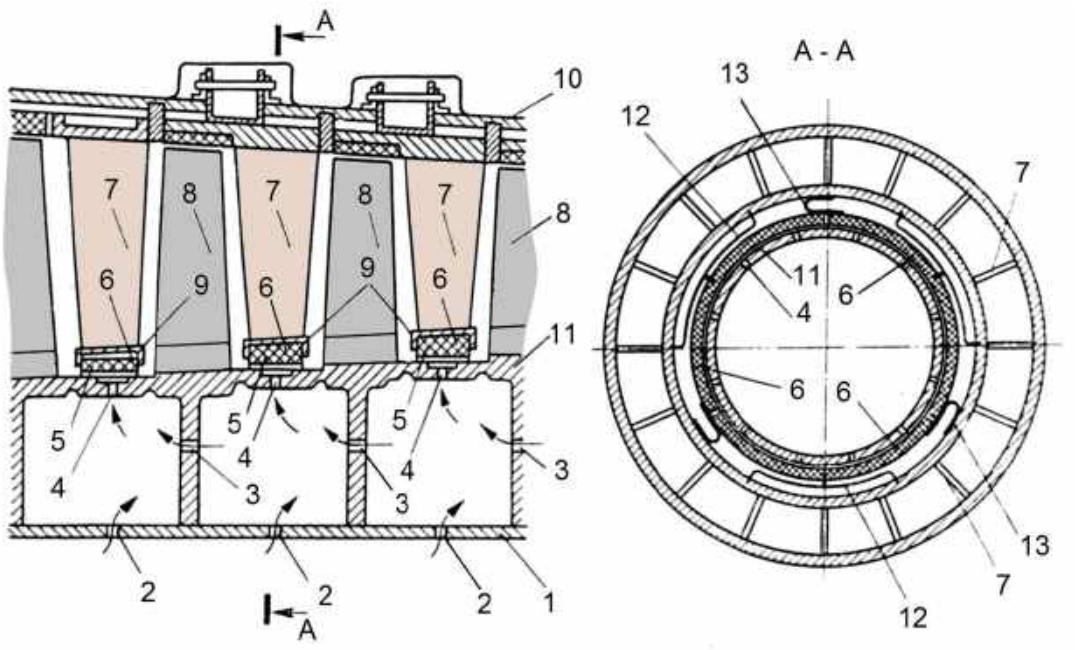


Fig. 8.27. System with radial working slot

The inner chamber of rotor 11 is pressure-tight and it is connected to the last compressor stage by channels 3 and pipe 1 with holes 2. Channels 4, provided in the outer wall of rotor 11, supply the air to radial clearance 5 between this wall and radial sealers 6 made of the anti-friction material. The number of the radial sealers must be not less than three to ensure the clearance circular uniformity. The sealers are mounted with some clearance in solid ring 9 that is rigidly joined to the ends of guide vanes 7; so, the sealers are fixed to the compressor casing. Springs 12 and 13 press the segments of sealers 6 to the outer surface of the rotor; the springs also are used to seal joints between the segments.

The system operates as follows. The compressed air is supplied through channels 4 and creates the air cushion, which presses sealers 6 from the rotor surface. The value of clearance 5 is determined automatically by the equilibrium of forces that are applied by the springs and the compressed air. Thus, the clearance is self-controlled and the compressed air supplying system does not need in the feedback with measurement of the actual clearance.

8.5. Combined radial clearance control

In case of the combined radial clearance control, two or more methods of the RCC are applied in one design. Combination of the thermal and mechanical methods is the most widespread.

Fig. 8.28, *a* shows a stage of the axial compressor that consists of guide vanes 1 and rotor blades 12. Thermal deformations of electrically heated pipe 8

(Fig. 8.28, *d*) are transformed into the radial deformations of collet ring 3, which design is similar to the above-considered collet 12 (see Chapter 1.3.3 and Fig. 8.24).

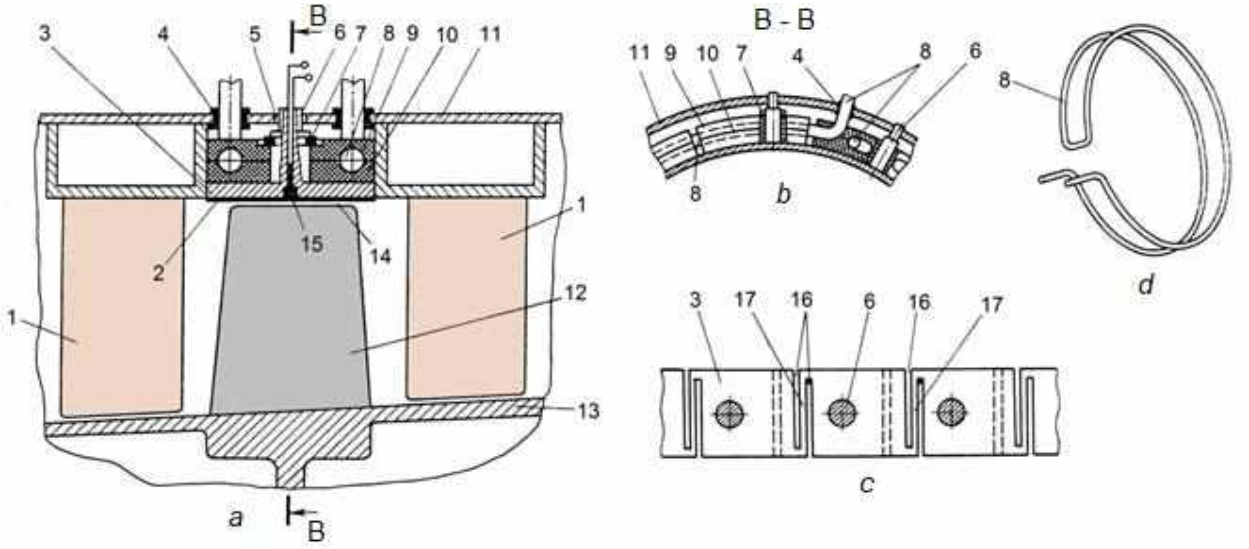


Fig. 8.28. System with electromechanical clearance control

Through slots 16 provided in ring 3 (Fig. 8.28, *c*), due to deformation of bulkheads 17, ensure a uniform radial deformation of the ring along all the length of the generating cylinder. Cylindrical end extensions 6 are uniformly placed on the outer surface of ring 3; they center the ring relative to rotor blades 12 and create clearance 14 between their tip edges and abradable coating 2. The ends of end extensions 6 are brought out of casing 11 through holes 5.

Electric heater 8 is pressed between blocks 9 and 10 (Fig. 8.28, *b*) made of dielectric material, which are pressed by spring ring 7. The ends of electric heater 8 are brought out of casing 11 through insulators 4.

When rotor 13 is rotated, the clearance is controlled by sensor 15. If the clearance is decreased lower than the permissible value, the electric current is supplied to heater 8, thereby ensuring thermal expansion. Diameter of collet ring 3 will be increased, thus increasing clearance 14. When the clearance exceeds the permissible value, the current is switched off, the length of heater 8 decreases and ring 3 will be compressed.

Combined radial clearance control with gear driving eccentrics 10 (Fig. 8.29) is designed by Rolls Royce Company for the turbine of promising engine. Located above rotor blades 1 are segments 2, which in case of turning of eccentric 10 by means of lugs 4 and 15 may move towards the tips of the blades or from the tips thereby changing radial clearance. To drive the eccentrics, intermediate casing 9 with heavy ribs 7 and 13 is attached to the main turbine casing by bolts 17. Rib 13 is provided with retainer 11, which

restrains ring 19 to flange 14. This flange has support 22 for mounting journal of eccentric 10. Other journal 5 is located in support 3 that is mounted on rib 6.

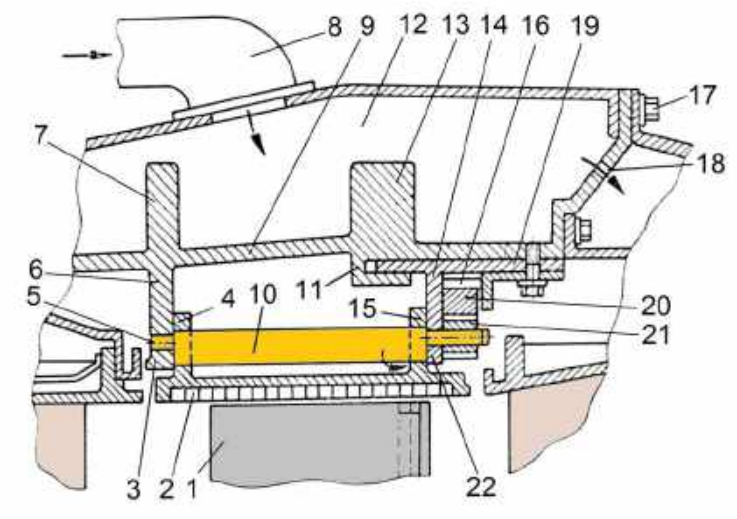


Fig. 8.29. System with eccentric clearance control

The right journal of eccentric 10 has gear 21, which is engaged with toothed quadrant 20, whose one end is attached to ring 19 by means of retainer 16. The other end of toothed quadrant 20 is loose for its thermal expansion. The controlling factor in this method is the airflow that cools the turbine casing. Variation of this flow changes the length of sector 20 that turns gear 21, thus moving sector 2.

The controlling air is supplied from the compressor outlet through branch 8 into the closed space 12 wherefrom it is discharged downstream of the turbine through holes 18.

Knowing the regularity of the turbine radial clearance variation at various engine power ratings, we can maintain the radial clearance between segments 2 and rotor blades 1. This is ensured by choosing thermal expansion coefficients of the parts, thickness of ribs 7, 13 and walls 9, 6, eccentricity of segment 2 driving mechanism, gear ratio of gears 21, 20, and also by varying the air flow in branch pipe 8.

The advantage of the considered method of RCC is small overall dimensions of the eccentrics driving mechanism. The essential disadvantage is a presence of movable parts in the drive that operate at high temperature (exceeding 1000 °C), which decreases reliability of the drive.

8.6. Efficiency of radial clearance control methods

As it was mentioned above, the methods of thermal control take the major part of known engineering solutions. The reason is that the thermal processes make maximum influence on variation of the radial clearances.

The thermal processes act thin-walled parts of the casing and rotor, initiate their thermal deformations and influence the radial clearances. Therefore, controlled heating or cooling of the casing component parts is the most expedient method of the RCC. In turbines, heating and cooling are natural processes that are related to normal operation of the assembly.

Hence, the problem of maintaining minimum clearances in the turbine is controlling of these processes to ensure the required thermal deformation. Solving of this problem becomes easier by simple and convenient supplying of the cooling substance (as usual, the cold air from the compressor) and of the heating substance (usually, the hot gas from the gas flow duct).

Specifics of the compressor structure complicates a direct transfer of the experience of the thermal control from the turbine to the compressor. So, supplying of the hot air from combustion chamber for heating of the compressor casing is inexpedient, as it needs in routing dual lines: for the gas supplying to the compressor and for its bleeding to the turbine exhaust flow duct. Bleeding of the gas to the air flow duct of the compressor is inadmissible, because it decreases efficiency and stability. Sealing of the compressor air flow duct from the hot gas complicates design of the lines and increases their weight.

Cold air, which is taken from the first stages of the compressor, is not efficient for the radial clearance control, because its pressure is less than in the subsequent stages. Therefore, this air may be used only for blowing the casing from the outside. Besides, the blowing from the outside will have increased inertia that worsens a processing speed of the RCC system. The blowing from the outside is also extremely inefficient, because needs in huge amount of the air that is taken from the flow duct (1.5 to 2 % of the total airflow and higher). Such expenses are reasonable if the blowing air is reused for some other purposes, for example, for cooling component parts of the turbine or jet nozzle, etc.

In the turbofans, the air from the bypass duct may be used for cooling of the compressor casing. However, this system has high inertia that complicates reliable maintaining of low clearances in the engines with fast transient power ratings.

Thus, the radial clearance control in the compressor differs from that in turbines. At the same time, low temperatures in compressor make favorable conditions for application of new structural materials in the systems with non-thermal (for example, mechanical) method of the clearance control.

Nevertheless, the experience in the field of thermal control in turbines may be used in the compressor. For example, seems to be real the version, in which the radial clearance is changed in the required direction by two factors: cooling by the air from the bypass duct, and heating by the electric current. The cool air decreases the clearance; the electric current increases it. During

engine starting, at takeoff and at transient power ratings, the electrical heating is switched on. At cruise, the temperature gradient decreases, and the forced cooling is the only factor that can control the system.

As it was shown above, the radial clearance control may be used at each stage individually or in a group of stages. The individual systems are expedient only in the turbine machines with low number of stages. The group systems do not ensure the minimum clearances at all stages. Nevertheless, they are attractive due to simplicity, especially in a driving part of the automatic control system.

The hydrostatic RCC is expedient in the compressors that need in very small clearances (approximately some tenths of millimeter). The essential advantage of the hydrostatic method is the effect of self-control, which excludes the feedback sensors of radial clearance and makes the system simpler. The system reliability may be high, but it will be dependent on continuity of the air supply to the working clearance of the end face or radial types.

8.7. Estimation of disc and blade deformation at steady-state power ratings

When the rotor is rotating, then centrifugal forces initiate tension stresses in the disc and rotor blades.

Radial and circumferential elastic deformations of disc under the action of centrifugal forces is determined as

$$\Delta r_{e\,d} = \frac{D_m - h_{bl}}{2} \frac{1}{E_d} \left(\sigma_r - \mu\sigma_\tau\right),$$

where D_m is mean diameter of the gas flow duct;

h_{bl} is blade length;

E_d is Hook modulus of disc material at working temperature;

σ_r is radial stress in the disc;

σ_τ is circumferential stress in the disc;

μ is Poisson factor.

Then the coefficient of a disk rigidity is determined as $\tilde{N}_d = \frac{\Delta r_{e\,d}}{n^2}$.

The blade elongation is determined in the same way:

$$\Delta r_{e\,bl} = \int_0^{h_{bl}} \frac{\sigma(r)dr}{E_{bl}} \approx \frac{\sigma_{bl} h_{bl}}{E_{bl}},$$

where σ_{bl} is a tensile stress of the blade body that is averaged on its length.

Then $C_{bl} = \frac{\Delta r_{e\,bl}}{n^2}$.

8.8. Mathematical model of the radial clearance control system

Mathematical model of the radial clearance control is formed on the basis of the incremental model of thermal condition of the casing and rotor, and on the basis of model of power loading. It is a system of differential equations and constraint equations:

$$\begin{cases} \delta = r_{st} - r_{rot}; \\ r_{st} = r_{rot}^0 + \delta_{mount} + \alpha_{st}\left(T_{st} - T_{st}^0\right) + k_1\left(p - p_c^0\right); \\ r_{rot} = \left[r_{rot}^0 + \alpha_{rot}(T_{rot} - T_{rot}^0) + k_2\left(\frac{n}{n_{max}}\right)^2 \right] + \left[h_{bl} + \alpha_{bl}\left(T_{bl} - T_{bl}^0\right)\right] + \left[h_{root} + \alpha_{root}\left(T_{root} - T_{root}^0\right)\right]; \\ T_{st}^0 = T_{rot}^0 = T_{bl}^0 = T_{root}^0 = T_l^0 = 293\ \text{K}; \\ p_c^0 = p_l^0 = 101325\ \text{Pa}; \\ \dot{T}_{st} = \frac{1}{\tau_{st}}\left[\dot{T}_g - \Theta_{st}\left(\dot{T}_g - \dot{T}_{cool}^{st}\right) - \dot{T}_{st}\right] b; \\ \dot{T}_d = \frac{1}{\tau_d}\left[\dot{T}_g - \Theta_d\left(\dot{T}_g - \dot{T}_{cool}^{d}\right) - \dot{T}_d\right] b; \\ \dot{T}_{bl} = \frac{1}{\tau_{bl}}\left[\dot{T}_g - \Theta_{bl}\left(\dot{T}_g - \dot{T}_{cool}^{bl}\right) - \dot{T}_{bl}\right] b; \\ \dot{T}_{root} = \frac{1}{\tau_{root}}\left[\dot{T}_g - \Theta_{root}\left(\dot{T}_g - \dot{T}_{cool}^{root}\right) - \dot{T}_{root}\right] b; \\ b = \left(\frac{p_c}{p_{c\,max}}\right)^{0,6}, \end{cases}$$

where b is coefficient of time constant correction to a maximum mode;

δ is radial clearance;

δ_{mount} is mounting clearance (for example, for HPC, $\delta_{mount} \approx 1$ mm, for HPT $\delta_{mount} \approx 0.7$ mm, for LPT $\delta_{mount} \approx 0.8$ mm);

r_{st}, r_{rot} are radii of stator and rotor;

T_{st}, T_d, T_{bl}, T_{root} are average temperatures of the stator, disc, blade and root (index ^{0} means the mounting temperature);

p_C is compressor discharge pressure;

n is rotor rotational speed (n_{max} is rotational speed at maximum power rating);

h_{bl}, h_{root} are length of the blade body and root;

$\tau = \frac{mc}{\alpha F}$ is time constant (the order of the time constants is $\tau_{st} \approx 30$ s; $\tau_d \approx 60$ to 100 s; $\tau_{bl} \approx 4$ to 10 s; $\tau_{lock} \approx 4$ to 20 s);

α is heat transfer factor;

c is heat capacity of the part material;

m is mass of the part;

F is surface area of heat transfer;

$\Theta = \frac{T_g - T_{met}}{T_g - T_{cool}}$ is cooling efficiency of the part;

T_g is gas temperature;

T_{met} is temperature of the part (metal);

T_{cool} is temperature of the cooling air;

α_{st}, α_{rot}, α_{root}, α_{bl} are coefficients of linear thermal expansion of the stator, rotor, root, and blade;

k_1 is pressure influence coefficient ($k_1 = (1.0…1.5)\cdot 10^{-1}$ mm/MPa);

k_2 is rotation speed influence coefficient ($k_2 \approx 0.27…0.33$ mm/rpm).

Simulation (Fig. 8.30) showed that increasing of HPC stator overall dimensions at the initial leg of acceleration (10 to 20 s) is dependent on the pressure load.

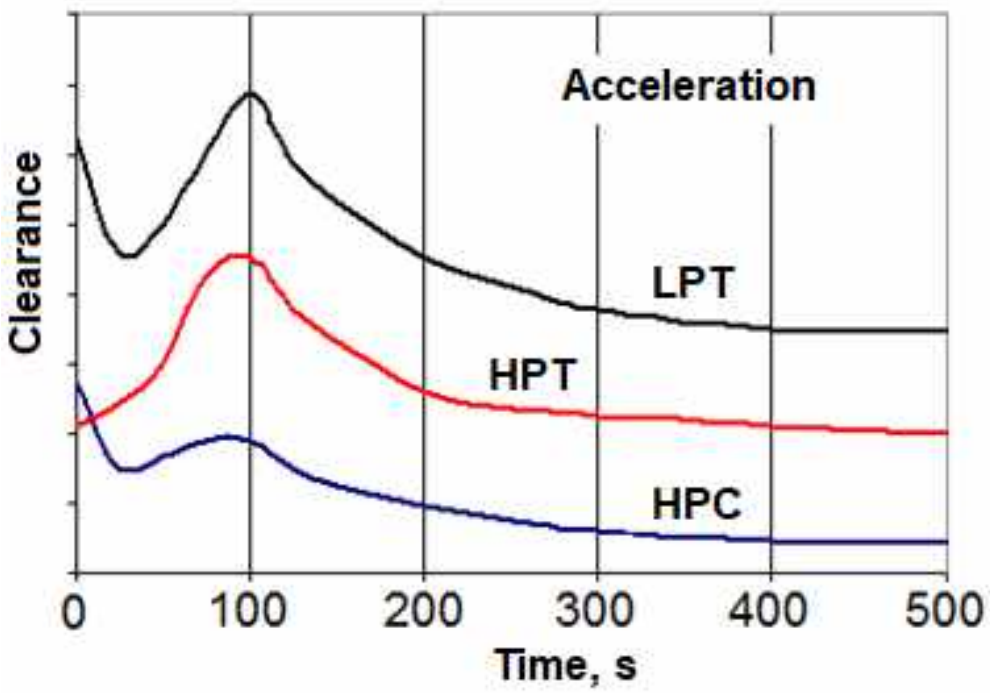


Fig. 8.30. Radial clearance simulation results

The rotor diameter increases due to the action of the centrifugal forces and compensates increase of the casing diameter by the pressure. Therefore, the radial clearance changes slowly. The further variation of the radial clearance depends on the thermal expansion of the rotor and stator.

In turbines, especially in the LPT, the radial clearance depends significantly on the thermal expansion of the rotor blades, so the radial clearance decreases significantly.

8.9. Requirements to members of radial clearance control systems

The main components of RCC systems are sensors of the clearance, control units and actuators.

The radial clearance sensors measure the actual clearance between the tips of blades and the inner surface of the stator (seal). They ensure reliability and precision of the control system, because they are the sources of information.

Sensitive member of the sensor is mounted in the engine gas flow duct and it operates in the extreme conditions (chemically active gaseous substance with temperature of up to 1500 ºC, varied composition and dielectric properties of the media, high vibrations, high velocity of the blade tips, etc.). The sensor casing is mounted on the compressor or turbine stator and it also operates under heavy-load conditions.

The radial clearance sensor shall meet the following requirements:

– range of radial clearance variation is 0 to 250 μm;
– precision of the radial clearance measurement must be not worse than 2.5 μm;
– temperature range is up to 1400 ºC;
– sample rate is not less than 50 Hz;
– failure-free time of the sensor must be comparable with the engine service life (5 to10 thousand operating hours).

The radial clearance sensors may be based on different physical principles: capacity, eddy current, ultrasonic, optical, and X-raying. The existing systems are preferably based on capacitance sensors; however, they have some disadvantages: temperature drift, influence of parasitic capacitance on the measurement results. Random component of the capacitance sensors is approximately 6 μm.

Microwave sensors are researched during the last years. They are not sensitive to composition of the gas flow and can operate at temperatures up to 900 ºC without cooling and up to 1200 ºC with forced cooling. However, the microwave sensors have low sensitivity near the lower boundary of the measured clearance that corresponds to the most dangerous power rating of the engine operation, when the rotor blades touching to casing is possible. The first generation of the microwave sensors with working frequency of 5.8 GHz ensures acceptable sensitivity only within a range of radial clearance of 2 to 13 mm. The sensors of the second generation have working frequency of 24 to

34.4 GHz, their waveguides are mounted in the holes having diameter of 6 to 16 mm and are made in the stator. They will be able to operate at a temperature of up to 2000 ºC and to measure clearance of 0 to 3 mm with error 10 μm within a whole range of the rotor rotational speed.

The analysis of the developments shows that the existing sensors do not meet all requirements, and they are not ready for application in the active clearance control systems.

The actuators change the radial clearance when the engine is running. They are based on various principles: electrohydraulic, piezoelectric and other drives, and drives that use materials with shape memory (smart materials). The main problem is high temperatures.

Electrohydraulic actuator has high response speed (approximately 1.8 ms), it does not need in complicated maintenance, but is cumbersome and its operating temperature is not higher than 315 ºC.

Piezo-ceramic actuators have perfect linear characteristics, high power and time response, but the Curie point (approximately 204 ºC) limits their operating temperature.

Examples of materials with shape memory are nitinol (Ni-Ti) alloy and electrostriction polymers (polymer muscles) that have high power ability. However, these materials have non-linear characteristics that depend on the temperature.

Controlling unit generates commands to actuators for the radial clearance control.

The control may be group or individual. In case of the group control, all actuators take one controlling signal and ensure the same symmetric displacement of the sealing members circumferentially. At the individual control, the unit generates individual signal for each actuator and ensures individual displacement of each sealing member of the stator, thus compensating asymmetric variations of the clearances.

The controlling unit implements algorithm of control. On a principle of action, it can be relay, opened or feedback.

The relay control is the most simple: the controlling signal is switched on at some range of power ratings, and is switched off out of this range. It is understand that this system ensures the optimum radial clearance only at one point of the engine performance. Therefore, its application for the multi-power rating engines is inexpedient.

The opened system has not the feedback and is a model-based. The model relates the clearance with the measured parameters of the engine. It determines the clearance indirectly, by using such parameters as the rotational speed, pressure and temperature at the engine inlet and at different stations of the gas flow duct, temperature of the stator, throttle control lever position, etc.

The most acceptable for the systems of active control of the radial clearance is the feedback system, which ensures continuous measurement of the actual radial clearance at all engine power ratings. However, this system needs in high precision of measurements, which is problematic now.

8.10. Check questions

1. Reasons that are necessitating performing radial clearance control in the compressor and turbine of the gas turbine engine.
2. Name main methods of the radial clearance control.
3. Essence of the radial clearance thermal control.
4. Principle and system of the radial clearance control with blowing of the turbine casing.
5. Kinematic systems of the radial clearance control.
6. Principles of the hydrostatic radial clearance control.
7. Mathematical model of the radial clearance control.
8. Diagrams of the automatic control systems for adjustment of the radial clearances.
9. Radial clearance sensors, their comparative estimation.
10. Estimation of deformations of the disc and blade and stator at steady-state power ratings of the engine operation.

BIBLIOGRAPHY

Boyce, M. P. Gas turbine engineering handbook [Text] / M. P. Boyce. – 3-rd ed. – Gulf Professional Publishing. – 2006. – 936 p.

Hunecke, K. Jet engines. Fundamentals of theory, design and operation [Text] / K. Hunecke. – 6-th ed. – Osceola : Motorbooks IP&W, 2003. – 241 p.

MacIsaac, B. Gas turbine propulsion systems [Text] / B. MacIsaac, R. Langton. – John Wiley & Sons Ltd. – Chichester, West Sussex, United Kingdom. – 2011. – 328 p.

Shoshin, Yu. Basic technical data of Soviet, Ukrainian and Russian cruise engines of aircraft [Text] / Yu. Shoshin, F. Sirenko. – Kharkov : National Aerospace University “Kharkov Aviation Institute”, 2015. – 65 p.

The Jet engine [Text] // The Technical Publications Department of RR plc. – Derby, England. – 1996. – 278 p.

Treager, I. E. Aircraft gas turbine engine technology [Text] / I. E. Treager. – 3-rd ed. – Glencoe / McGraw-Hill. 2001. – 677 p.

Yepifanov, S. Afterburners and exhaust systems [Text] : tutorial / S. Yepifanov, Y. Shoshin, V. Chygryn. – Kharkov : National Aerospace University “Kharkov Aviation Institute”, 2013. – 28 p.

Yepifanov, S. Major units of aircraft gas turbine engines [Text] : tutorial / S. Yepifanov, Y. Shoshin, Y. Gusev. – Kharkov : National Aerospace University “Kharkov Aviation Institute”, 2013. – 99 p.

Авдеев, А. В. Проектирование силовых схем как необходимый этап общего процесса проектирования изделий [Текст] / А. В. Авдеев, А. М. Хомяков // Справочник. Инженерный журнал. – М. : Изд. дом «Спектр». – 2016. – № 9 (234). – С. 1–23.

Берне, Л. П. Отечественные авиационные двигатели – 20 век [Текст] / Л. П. Берне, Д. А. Боев, Н. С. Ганшин. – М. : АВИКОПРЕСС, 2003. – 206 с.

Білогуб, О. В. Допоміжні силові установки і пускові системи газотурбінних двигунів [Текст] : навч. посіб. до лаб. практикуму / О. В. Білогуб, С. В. Безуглий, В. С. Чигрин. – Харків : Нац. аерокосм. ун-т ім. М. Є. Жуковського «Харків. авіац. ін-т», 2018. – 92 с.

Бондарчук, П. В. Методика расчета радиальных зазоров по обобщенному полетному циклу двигателя [Текст] / П. В. Бондарчук, А. Ю. Тисарев // Авиационно-космическая техника и технология. – Харьков : ХАИ. – 2012. – № 8 (95). – С. 208–211.

Бондарчук, П. В. Моделирование процессов и проектирование системы управления радиальными зазорами в турбине ГТД [Текст] / П. В. Бондарчук, А. Ю. Тисарев. – Самара : СГАУ, 2012. – 105 с.

Боровик, С. Ю. Активное регулирование радиальных зазоров в проточной части ГТД (обзор зарубежных публикаций) [Текст] / С. Ю. Боровик,

Ю. Н. Секистов, В. П. Данильченко // Газотурбинные технологии. – 2011. – № 2 (93). – С. 36–40.

Грановский, А. В. Влияние канавок над рабочей лопаткой на КПД турбинной ступени [Текст] / А. В. Грановский, М. К. Костеж, Н. А. Ломакин // Газотурбинные технологии. – 2012. – № 7 (108). – С. 18–23.

Иноземцев, А. А. Основы конструирования авиационных двигателей и энергетических установок [Текст] : учебник : в 5 т. / А. А. Иноземцев, М. А. Нихамкин, В. Л. Сандрацкий. – М. : Машиностроение, 2008. – Т. 1. – 201 с.

Иноземцев, А. А. Основы конструирования авиационных двигателей и энергетических установок [Текст] : учебник : в 5 т. / А. А. Иноземцев, М. А. Нихамкин, В. Л. Сандрацкий. – М. : Машиностроение, 2008. – Т. 2. – 368 с.

Иноземцев, А. А. Основы конструирования авиационных двигателей и энергетических установок [Текст] : учебник : в 5 т. / А. А. Иноземцев, М. А. Нихамкин, В. Л. Сандрацкий. – М. : Машиностроение, 2008. – Т. 3. – 227 с.

Иноземцев, А. А. Основы конструирования авиационных двигателей и энергетических установок [Текст] : учебник : в 5 т. / А. А. Иноземцев, М. А. Нихамкин, В. Л. Сандрацкий. – М. : Машиностроение, 2008. – Т. 4. – 201 с.

История конструкций самолетов в СССР 1951 – 1965 гг. [Текст] / Е. В. Арсеньев, Л. П. Берне, Д. А. Боев и др. – М. : Машиностроение, 2000. – 842 с.

Конструкция и проектирование авиационных газотурбинных двигателей [Текст] / под ред. Д. В. Хронина. – М. : Машиностроение, 1980. – 368 с.

Конструкция авиационных газотурбинных двигателей [Текст] : учебник / А. В. Штода, С. П. Алещенко, А. Я. Иванов и др. – М. : Воениздат, 1961. – 412 с.

Крюков, А. И. Некоторые вопросы проектирования ГТД [Текст] : учеб. пособие / А. И. Крюков. – М. : МАИ, 1993. – 336 с.

Кузменко, М. Л. Конструктивно-компоновочные схемы авиационных ГТД [Текст] : учеб. пособие / М. Л. Кузменко, В. С. Чигрин, С. Е. Белова. – Рыбинск : РГАТА, 2005. – 44 с.

Кузменко, М. Л. Конструкция компрессоров и газовых турбин ГТД [Текст] : учеб. пособие / М. Л. Кузменко, В. С. Чигрин, С. Е. Белова. – Рыбинск : РГАТА. – 2005. – 67 с.

Нерубасский, В. В. Турбореактивные двухконтурные двигатели для магистральных пассажирских и транспортных самолетов [Текст] : справ. пособие : в 4 ч. / В. В. Нерубасский. – Харьков : ХАИ, 2006. – Ч. 1: Двигатели большой тяги. – 261 с.

Нерубасский, В. В. Турбореактивные двухконтурные двигатели для магистральных пассажирских и транспортных самолетов [Текст] : справ. пособие : в 4 ч. / В. В. Нерубасский. – Харьков : ХАИ, 2007. – Ч. 2: Двигатели средней тяги. – 378 с.

Нерубасский, В. В. Турбореактивные двухконтурные двигатели для магистральных пассажирских и транспортных самолетов [Текст] : справ. пособие : в 4 ч. / В. В. Нерубасский. – Харьков : ХАИ, 2008. – Ч. 3: Двигатели малой тяги. – 217 с.

Нерубасский, В. В. Турбореактивные двухконтурные двигатели для магистральных пассажирских и транспортных самолетов [Текст] : справ. пособие : в 4 ч. / В. В. Нерубасский. – Харьков : ХАИ, 2011. – Ч. 4: Двигатели с форсажной камерой. – 284 с.

Нечаев, Ю. Н. Авиационные турбореактивные двигатели с изменяемым рабочим процессом для многорежимных самолетов [Текст] / Ю. Н. Нечаев, В. И. Кобельков, А. С. Полев. – М. : Машиностроение, 1988. – 176 с.

Никитин, Ю. М. Конструирование элементов деталей и узлов авиадвигателей [Текст] / Ю. М. Никитин. – М. : Машиностроение, 1968. – 324 с.

Пономарев, Б. А. Двухконтурные турбореактивные двигатели [Текст] / Б. А. Пономарев. – М. : Воениздат, 1973. – 133 с.

Пономарев, Б. А. Настоящее и будущее авиационных двигателей [Текст] / Б. А. Пономарев. – М. : Воениздат, 1982. – 240 с.

Павленко, В. Ф. Силовые установки с поворотом вектора тяги в полете [Текст] / В. Ф. Павленко. – М. : Машиностроение, 1987. – 200 с.

Попов, К. Н. Сопла ВРД с ОВТ [Текст] / К. Н. Попов, В. Д. Соколов, Н. И. Хвостов. – М. : Машиностроение, 1979. – 144 с.

Поляков, В. В. Реверсивные устройства ВРД [Текст] / В. В. Поляков, В. А. Голубев, О. В. Бондаренко. – М. : МАИ, 1990. – 48 с.

Пчелкин, Ю. М. Камеры сгорания газотурбинных двигателей [Текст] : учеб. для вузов / Ю. М. Пчелкин. – М. : Машиностроение, 1984. – 280 с.

Развитие авиационной науки и техники в СССР. Историко-технические очерки [Текст] / А. С. Яковлев, А. М. Изаксон, Ю. С. Воронков и др. – М. : Наука, 1980. – 496 с.

Скибин, В. А. Работы ведущих авиадвигателестроительных компаний по созданию перспективных авиационных двигателей (аналитический обзор) [Текст] / В. А. Скибин, В. И. Солонин, В. А. Палкин. – М. : ЦИАМ, 2004. – 424 с.

Скубачевский, Г. С. Авиационные газотурбинные двигатели, конструкция и расчет деталей [Текст] / Г. С. Скубачевский. – М. : Машиностроение, 1981. – 552 с.

Трушин, В. А. Математическая модель расчета радиального зазора между рабочими лопатками и корпусом турбины [Текст] / В. А. Трушин, А. Ю. Чечулин // Вестник УГАТУ. – 2012. – Т. 16, № 2 (47). – С. 82–86.

Трянов, А. Е. Особенности конструкции узлов и систем авиационных двигателей и энергетических установок [Текст] : учеб. пособие / А. Е. Трянов. – Самара : СГАУ, 2011. – 202 с.

Фалалеев, С. В. Современные проблемы создания двигателей летательных аппаратов [Текст] : учеб. пособие / С. В. Фалалеев. – Самара : СГАУ, 2012. – 106 с.

ЦИАМ 2001 – 2005. Основные результаты научно-технической деятельности [Текст] : в 2 т. / под общ. ред. В. А. Скибина, В. И. Солонина, М. Я. Иванова. – М. : ЦИАМ, 2005. – Т. 1. – 472 с.

ЦИАМ 2001 – 2005. Основные результаты научно-технической деятельности [Текст] : в 2 т. / под общ. ред. В. А. Скибина, В. И. Солонина, М. Я. Иванова. – М. : ЦИАМ, 2005. – Т. 2. – 462 с.

Чигрин, В. С. Конструкция и прочность авиационных двигателей [Текст] : консп. лекций / В. С. Чигрин. – Харьков : Нац. аэрокосм. ун-т им. Н. Е. Жуковского «Харьков. авиац. ин-т», Запорожье : изд. АО «МОТОР СИЧ», 2017. – 420 с.

Чигрин, В. С. Конструкция камер сгорания и выходных устройств авиационных ГТД [Текст] : учеб. пособие / В. С. Чигрин, С. Е. Белова. – Рыбинск : РГАТА, 2007. – 84 с.

Чигрин, В. С. Конструкція компресорів авіаційних газотурбінних двигунів [Текст] : навч. посіб. до лаб. практикуму / В. С. Чигрин. – Харків : Нац. аерокосм. ун-т ім. М. Є. Жуковського «Харків. авіац. ін-т», 2021. – 44 с.

Шошин, Ю. С. Трансмиссии и силовые системы авиационных газотурбинных двигателей [Текст] : учеб. пособие / Ю. С. Шошин, В. С. Чигрин. – Харьков : Нац. аэрокосм. ун-т «Харьков. авиац. ин-т», 2011. – 40 с.

Штода, А. В. Конструкция авиационных газотурбинных двигателей : учебник [Текст] / А. В. Штода, В. А. Секистов, В. В. Кулешов. – К. : КВВАИУ, 1982. – 436 с.

Шульгин, В. А. Двухконтурные турбореактивные двигатели малошумных самолетов [Текст] / В. А. Шульгин, С. Я. Гайсинский. – М. : Машиностроение, 1984. – 168 с.

CONTENTS

LIST OF DESIGNATIONS……. 3
LIST OF ABBREVIATIONS AND INDICES……..... 4
INTRODUCTION……..... 7
1. GENERAL PROBLEMS OF AERO ENGINE DESIGNING…… 9
1.1. Generations and main trends in designing of turbine engine.. 9
1.1.1. *Turbine engine generations*……..... 9
1.1.2. *Main trends in engine designing*…… 12
1.2. Types, main parameters and areas of application of air-breathing engines…….. 20
1.3. General engineering requirements to the aero engines…….. 37
1.4. Role of strength analysis, experimental researches and similarity theory in engine development ……. 42
1.5. Forces and moments affecting assemblies of gas turbine engine…… 47
1.5.1. *Classification of loads that affect the gas turbine engines*…… 48
1.5.2. *Force of the gas static pressure*…… 49
1.5.3. *Force of the flowing gas dynamic action*…….. 49
1.5.4. *Gas forces that affect the different assemblies of the gas turbine engine*……..... 50
1.5.5. *Distribution of gas forces between engine assemblies*…… 57
1.5.6. *Inertial forces and moments in the gas turbine engine*…… 58
1.6. Check questions…….. 60
2. COMPRESSOR DESIGN…… 62
2.1. GTE compressor purpose and main design parameters…….. 62
2.2. Compressors classification by a type of bladed machine……. 65
2.3. Axial compressor design arrangement…… 68
2.4. Requirements to compressor design and their implementation…… 70
2.5. Design of rotors of axial compressors……. 71
2.5.1. *Drum-type rotors*…….. 71
2.5.2. *Disc-type rotors*…… 72

2.5.3. *Drum-and disc rotors*……... 74
2.6. Rotor blades. Design and attachment to rotor…… 79
2.6.1. *Blade structure and requirements*…….. 79
2.6.2. *Blades retaining*……... 81
2.6.3. *Blade axial retaining*…… 84
2.7. Loads that affect axial compressor rotor……. 86
2.7.1. *Forces and moments*……... 86
2.7.2. *Compressor rotor axial unloading*…….. 88
2.8. Stators of axial compressors……. 90
2.8.1. *Main components of compressor casing*…….. 90
2.8.2. *Front frame*……... 91
2.8.3. *Casing of guide vanes*…… 93
2.8.4. *Rear frame*…… 95
2.9. Clearances between rotor and stator…….. 96
2.10. Sealing of compressor gas flow duct and oil chambers…… 98
2.10.1. *Contact seals*…… 98
2.10.2. *Non-contact seals*…… 101
2.10.3. *Brush seals*……... 103
2.11. Compressor controls ……. 103
2.12. Compressor structural materials…….. 106
2.13. Centrifugal compressors…… 108
2.13.1. *Classification of centrifugal compressors*…… 108
2.13.2. *Design of centrifugal compressors*…… 109
2.13.3. *Design of rotor wheel*……... 110
2.13.4. *Design of casing*……... 111
2.13.5. *Materials for centrifugal compressors*……... 112
2.14. Compressor rotor balancing…….. 112
2.15. Check questions…….. 113
3. DESIGN OF GAS TURBINE…… 115
3.1. Gas turbine purpose and operating conditions. Main requirements to the gas turbine structure and their implementation……. 115
3.2. Design diagrams and parameters of aircraft gas turbines…… 118
3.2.1. *Design diagrams*……... 118

3.2.2. *Parameters of gas turbines*…… 119
3.3. Rotor blades……. 122
3.3.1. *Design of turbine rotor blades*…… 122
3.3.2. *Rotor blades attachment*…… 124
3.4. Turbine disks…… 126
3.4.1. *Structure of turbine disk*…….. 126
3.4.2. *Joint of the turbine discs interconnected and connected with the shaft*…… 127
3.5. Axial force that acts turbine rotor…….. 129
3.6. Gas turbine stators……. 131
3.6.1. *Gas turbine casings*…… 131
3.6.2. *Nozzle boxes: operating conditions, load-carrying structures and methods of vanes-to-casing attachment*…… 133
3.7. Clearances between rotor and stator. Sealing of turbine gas flow duct…… 137
3.8. Gas turbine cooling……. 141
3.8.1. *Cooling of turbine rotor blades* …….. 142
3.8.2. *Cooling of turbine discs and casings*…… 150
3.9. Structural materials for turbine parts……. 153
3.10. Check questions…….. 154
4. DESIGN OF MAIN COMBUSTION CHAMBERS…… 156
4.1. Particular features of the combustion process in gas turbine engines…….. 156
4.1.1. *Requirements to the fuel*…….. 156
4.1.2. *Stoichiometric, rich and lean mixture*…… 157
4.1.3. *Temperature of combustion*……... 158
4.1.4. *Physical aspects of the combustion in flow*…….. 159
4.2. Combustion chambers purpose. Operation conditions and requirements to combustion chambers……. 162
4.3. Design diagrams of the main combustion chambers and problems that are to be solved when designing combustion chamber…….. 164
4.4. Decreasing velocity at the inlet to the combustion zone in relation to the compressor outlet flow velocity. Diffuser…… 165

4.5. Ensuring stable combustion. Flame tube…… 167
4.5.1. *Structural arrangements of flame tubes*……... 167
4.5.2. *Relation between secondary and primary flows in the combustion chamber*…… 169
4.6. Stabilizing combustion zone. Combustor dome……. 171
4.7. Fuel supplying. Fuel nozzles……. 172
4.8. Cooling of combustion products. Dilution zone…….. 175
4.9. Ensuring operability of design structures…… 176
4.10. Combustion initiation. Igniters……... 178
4.11. Ensuring environmental performances…… 180
4.12. Faults of main combustion chamber design structures and constructive methods that provide their reliable operation……... 183
4.13. Structural materials of main combustion chambers of GTE…. 185
4.14. Check questions…….. 185
5. EXHAUST SYSTEM DESIGN……. 187
5.1. Purpose and composition of the exhaust systems…… 187
5.2. Design of structural members of the exhaust systems……. 188
5.3. Design of jet nozzle……. 191
5.3.1. *Parameters of jet nozzle*…….. 191
5.3.2. *Jet nozzle operation modes*……... 192
5.3.3. *Controlling nozzle area*……... 193
5.4. Design of the TJE and TFE jet nozzles…….. 194
5.4.1. *Fixed nozzle*…….. 194
5.4.2. *Controlled subsonic nozzle*…… 195
5.4.3. *Controlled supersonic jet nozzle with central body*… 196
5.4.4. *Ejector nozzle*……... 196
5.4.5. *Lobe double-row nozzle*…….. 197
5.4.6. *Driving mechanism of variable nozzle*…….. 198
5.5. Thrust reversers and deviators……. 200
5.5.1. *Thrust reversers*……... 200
5.5.2. *Thrust deviators*…… 202
5.6. Power plant as a source of noise and vibration……. 205
5.7. Infrared radiation suppressors…….. 214

5.8. Structural materials……. 216
5.9. Check questions…….. 216
6. AFTERBURNERS OF THE AERO ENGINES……. 217
6.1. Functions of the afterburners…… 217
6.2. Design of afterburners…… 217
6.2.1. *General information*…….. 218
6.2.2. *Why the afterburner is not provided with the flame tube?*..... 219
6.2.3. *Combustor dome of the afterburner*……... 220
6.2.4. *Fuel supplying and combustion*…….. 223
6.2.5. *Oscillation (vibration) combustion*…….. 227
6.3. Structural materials of the afterburners……... 228
6.4. Check questions…….. 229
7. POWER SYSTEMS OF GAS TURBINE ENGINES…… 230
7.1. General information about power system of casing…….. 230
7.2. Loads that affect power system of the GTE casing……... 231
7.3. Methods of transmitting loads in the structural elements of power casings…….. 233
7.3.1. *Diagram with the internal power link*…… 234
7.3.2. *Diagram with the external power link*…… 234
7.3.3. *Diagram with the branched (open) double power link*……... 235
7.3.4. *Diagram with the closed double power link*…….. 235
7.3.5. *Power frames of turboprop engines*……... 236
7.4. Engine attachment to the aircraft…….. 237
7.5. Strength of engine mounts……. 244
7.6. Power systems of the GTE rotors……. 245
7.6.1. *Schemes of the GTE rotor power systems*……... 246
7.6.2. *Loads that act the rotor of the gas turbine engine*….. 252
7.6.3. *Design of the GTE shafts and couplings*…….. 253
7.6.4. *Bearings of the GTE rotors*…….. 256
7.7. Design of elastic-damper supports of the engine rotors…….. 264
7.7.1. *Support with ring elastic elements*…… 265
7.7.2. *Support with rod elastic members of a “squirrel wheel” type*……... 266
7.7.3. *Hydrodynamic damper support*…….. 268

7.8. Accessory drives…… 269
7.9. Check questions…….. 270
8. COMPRESSOR AND TURBINE RADIAL CLEARANCE CONTROL.. 272
8.1. Methods of radial clearance control……. 277
8.2. Methods of thermal control of radial clearances…… 279
8.2.1. *System of passive clearance control with heavy member of casing……* 283
8.2.2. *System of passive clearance control with combination of massive casing element and blowing by the air……...* 284
8.2.3. *Radial clearance control system with air blowing of stator……..* 286
8.2.4. *Radial clearance control with heat pipe……* 289
8.3. Mechanical control of radial clearance…… 289
8.3.1. *Kinematic radial clearance control……* 290
8.3.2. *Group kinematic radial clearance control system…...* 292
8.3.3. *Collet radial clearance control……* 294
8.4. Hydrostatic radial clearance control……. 297
8.4.1. *Hydrostatic end clearance control……..* 298
8.4.2. *Hydrostatic radial-type clearance control……..* 299
8.5. Combined radial clearance control……... 300
8.6. Efficiency of radial clearance control methods…….. 302
8.7. Estimation of disc and blade deformation at steady-state power ratings…… 304
8.8. Mathematical model of the radial clearance control system… 305
8.9. Requirements to members of radial clearance control systems……. 307
8.10. Check questions…….. 309
BIBLIOGRAPHY…….. 310

Навчальне видання

Єпіфанов Сергій Валерійович
Чигрин Валентин Семенович

КОНСТРУЦІЯ АВІАЦІЙНИХ ГАЗОТУРБІННИХ ДВИГУНІВ

(Англійською мовою)

Редактор перекладу Ю. Г. Муренець
Технічний редактор Т. В. Савченко
Підготовка до друку: Г. М. Гушаіл

Зв. план, 2021
Підписано до видання 26.02.2021
Формат 60×84 1/8. Папір офс. Офс. друк
Ум. друк. арк. 17,8. Обл.-вид. арк. 20.
Наклад 50 пр. Зам. №

Видавець
Національний аерокосмічний університет ім. М. Є. Жуковського
«Харківський авіаційний інститут»
61070, Харків-70, вул. Чкалова, 17
http://www.khai.edu

Видавництво АТ «МОТОР СІЧ»
м. Запоріжжя, 69068, Україна, пр. Моторобудівників, 15

Свідоцтво про внесення суб'єкта видавничої справи
до Державного реєстру видавців, виготовлювачів і розповсюджувачів
видавничої продукції сер. ДК № 4213 від 22.11.2011